SSCL-SR-1208

SSCL-SR-1208

Superconducting Super Collider Laboratory

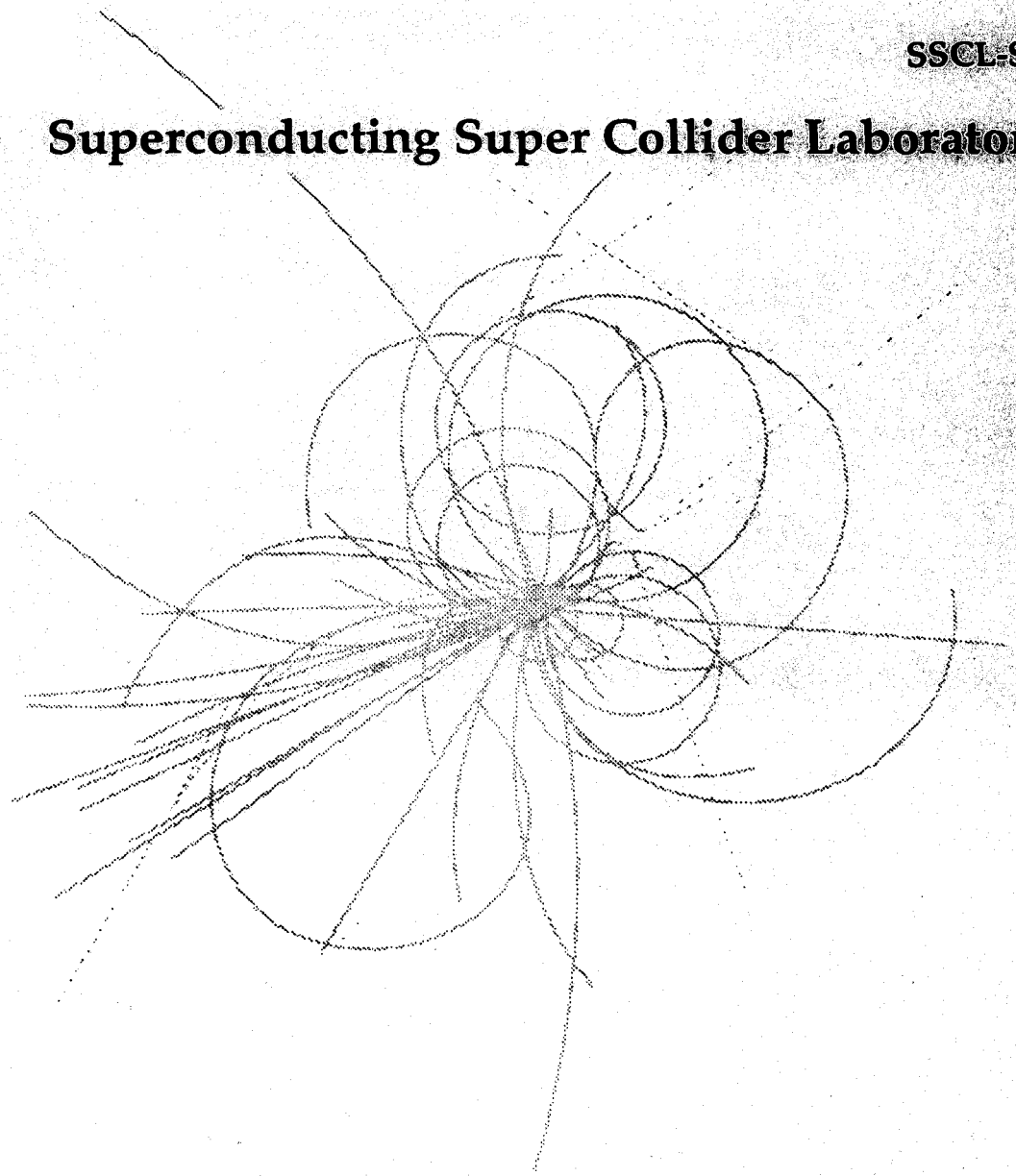

Proposal from the SSC Laboratory Physics Research Division to the Department of Energy Division of High Energy Physics

April 1992

SSCL-SR-1208

Proposal from the SSC Laboratory Physics Research Division to the Department of Energy Division of High Energy Physics

Superconducting Super Collider Laboratory†
2550 Beckleymeade Ave.
Dallas, TX 75237

April 1992

†Operated by the Universities Research Association, Inc., for the U.S. Department of Energy under Contract No. DE-AC35-89ER40486.

TABLE OF CONTENTS

1.0 Overview 1

2.0 Objectives and Strategy 2

2.1 SSC Physics 2

2.2 The SSC Experimental Physics Program 7

2.3 Physicists in the SSC Research Program - Long Range Goals 9

2.3.1 Overview 9

2.3.2 SSCL Physicists 10

2.4 Strategy 16

3.0 Current Status 21

3.1 Current Staff Physicists 21

3.2 Physics Research Division Organization 24

4.0 Current Program 25

4.1 Introduction 25

4.2 GEM 27

4.2.1 Computing/Simulation 28

4.2.2 Muon Systems and TTR 33

4.2.3 Tracking and Beam Line 42

4.3 SDC 48

4.3.1 Computing/Simulation 48

4.3.2 Muon Systems 49

4.3.3 Calorimetry 55

4.3.4 Tracking and Beamline Design 67

4.4 Common Efforts 68

4.4.1 Tracking 68

4.4.2 Electronics, Triggering and DAQ for Experiments at the SSCL 74

4.4.3 Computing 77

4.5 Research Activities Outside SSCL....79
4.5.1 CDF....79
4.6 Theoretical Physics....91
4.6.1 Introduction....91
4.6.2 Progress....91
5.0 FY 1992 AND FY 1993 PROGRAM....95
5.1 Introduction....95
5.2 GEM....96
5.2.1 Computing/Simulation....96
5.2.2 Muon Systems....97
5.2.3 Central Tracking and Beam Line....97
5.2.4 Test Beam Coordination and Support....98
5.2.5 New Efforts....98
5.3 SDC....100
5.3.1 Computing and Simulation....100
5.3.2 Muon Systems....100
5.3.3 Calorimetry....101
5.3.4 Tracking....101
5.4 Common Efforts....103
5.4.1 Tracking....103
5.4.2 Electronics....103
5.4.3 Other Physics at SSC....105
5.5 Outside Research....106
5.5.1 CDF Plans....106
5.5.2 Additional Outside Physics Efforts....109
5.6 Theoretical Physics....111
6.0 FY 1994 Plans....113
6.1 FY 1994 GEM Program....113

6.2 FY 1994 SDC Program 113
6.3 Common Efforts in FY 1994 114
6.4 Outside Activities 114
6.5 Computing 114
7.0 Funding 115
7.1 Introduction 115
7.2 Experimental Physics 116
7.3 Theoretical Physics 118
7.4 Computing 118

Table of Contents
Appendices

Appendix A Vitae 1

Appendix B Bibliography 36

Appendix C Results of Spring '91 Liquid Argon Beam Test 40

Appendix C-1 Design Studies for SDC Liquid Argon Calorimetry 59

Appendix D Progress on Scintillator Calorimetry 73

Appendix E Progress in the Use of Avalanche Photodiodes for Readout of Calorimeters 95

Appendix F A Study of Avalanche Photo Diodes in Geiger Mode 96

Appendix G Involvement of the SSC Tracking Group with Visible Light Photon Counters 99

Appendix H Progress on Tracking Detector Simulations 103

Appendix I Front End for Gas Microstrip Detectors 106

Appendix J Tests of TMC1004 Time to Digital 120

Appendix K Data Collection Studies for the Superconducting Super Collider 134

Appendix L Outline of SSCL Trigger Studies 144

Appendix M DAQ design 153

Appendix N Evaluation of VxWorks Real-Time Kernel 160

Attachment 1 DOE Report on SSC Cost and Schedule Baseline

Attachment 2 SDC Letter of Intent

Attachment 3 GEM Letter of Intent

Attachment 4 Calorimeter Conceptual Design Liquid Argon Option

SECTION 1

OVERVIEW

1.0 OVERVIEW

The Superconducting Super Collider (SSC) represents a giant step beyond existing high energy research facilities. The research opportunities reach well into the next century, when the SSC Laboratory will be the premier high energy physics research laboratory in the world. First and foremost, creating such a laboratory requires attracting and recruiting excellent scientists and support staff.

The SSC construction project has naturally absorbed considerable energy and attention during the past years. During that time it has moved from conceptual design to actual construction. The first buildings have been completed in Ellis County, Texas and work has begun on other facilities, including the magnet delivery shaft at N15 in preparation for boring the first section of tunnel for the collider this coming summer. Concurrently, the initial experimental program is being defined. The first Expressions of Interest for SSC experiments were received in May, 1990. The 21 EOIs received so far represent a broad range of potential experiments including major detectors that address the physics available at the SSC at the highest energies and momentum transfers. Now, with the acceptance of Letters of Intent from the two major collaborations, representing over 1400 physicists from almost 200 institutions, it must be recognized that the SSC physics program has begun. As part of that physics program there is an urgent need to increase the scientific research staff at the SSC. The two large projects underway (GEM and SDC) need physicists to focus on the key activities centered at the SSC; physicists to perform liaison functions which can only be done by host laboratory staff; and physicists and staff to provide expertise in the continued planning and evaluation of the rapidly developing laboratory scientific program. This document is the proposal for support of physics research groups at the SSC Laboratory.

In the following sections we review the long-term plans for Physics Research at the SSC Laboratory to establish the context for our proposal for FY 1992 and FY 1993. These are the same plans as those presented to the 1992 HEPAP Subpanel chaired by Michael Witherell. Emphasized is the crucial need for in-house physics research groups at the SSC Laboratory if there is to be successful design, construction, and commissioning of the major detectors and therefore ultimate success of the SSC itself. As discussed in the DOE's Report on the Superconducting Super Collider Cost and Schedule Baseline, the costs of these Laboratory physics research groups are to be provided from high energy physics program funding. (Attachment 1)

While the specific division of tasks will change with time as the specific needs change, the overall requirement for a smooth and steady ramp-up of physicists is required if we are indeed to construct the centerpiece of the US high energy physics program for decades to come. The situation with regard to physics research staff and activities at the SSC Laboratory is evolving very rapidly. Visible changes occur month by month. Our previous proposal of November 1991, is obsolete due to the addition of new staff and new projects. Nevertheless, we attempt in this document to not only present a summary of specific progress and a snap-shot of the current program, but to describe what we see for the remainder of FY 1992 and for FY 1993, as well as the anticipated FY 1994 program. The particular tasks undertaken by these physics research groups will be guided by the overall SSC physics program and by the talents of those who are recruited to the scientific staff. While the details will evolve the overall envelope of effort can be set forth now.

SECTION 2

OBJECTIVES AND STRATEGY

2.0 OBJECTIVES AND STRATEGY

2.1 SSC Physics

The SSC will have available a factor of 20 increase in center-of mass energy over any existing machine and a luminosity of $10^{33}/cm^2$ sec. This will facilitate a broad exploration of what lies beyond our current understanding of particle physics, as represented in the Standard Model. It will allow incisive measurements of many aspects of the Standard Model itself.

While a resounding success in describing physics accessible to experiments until now, the Standard Model leaves central questions unanswered -- questions that the SSC can answer:

Electroweak Symmetry Breaking

A central aim of the SSC physics program is the exploration of the mechanism that generates particle masses. In the minimal Standard Model, the masses of the W and Z bosons and the charged fermions result from their interaction with a fundamental scalar field whose vacuum expectation value is not zero. Associated with this field is the Higgs boson. The expected cross section for producing the Higgs boson at the SSC is shown in Fig. 2.1-1 for various top quark masses. For Higgs masses below the Z pair threshold, the most promising decay channels are ZZ* (where Z* denotes a virtual Z) and $\gamma\gamma$.

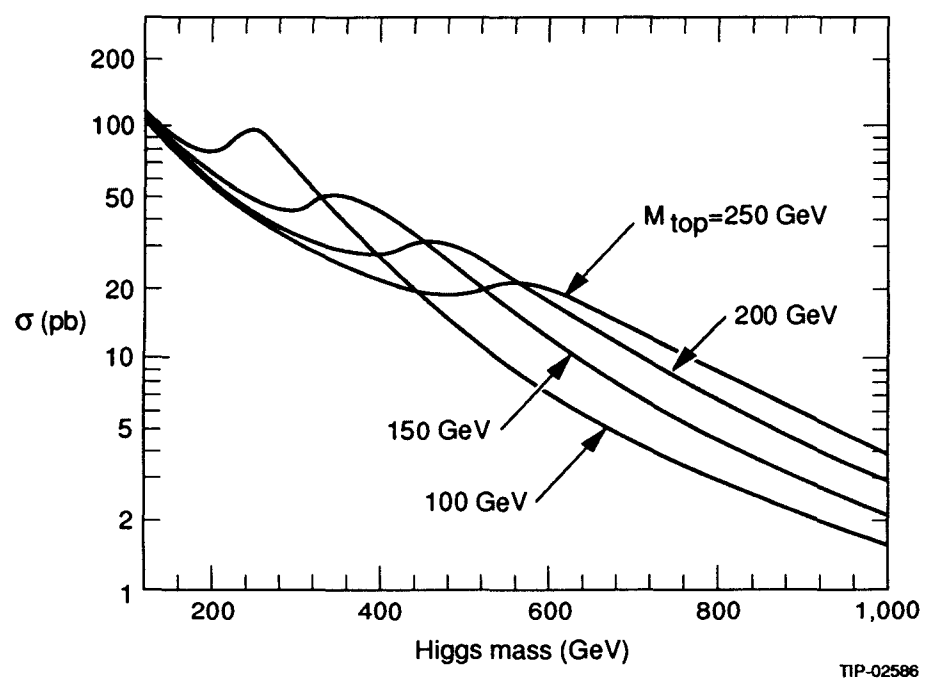

Figure 2.1-1 Expected Cross Section for Producing the Higgs Boson

Fig. 2.1-2 is representative of the possibilities at the SSC and shows in particular the capabilities of the SDC detector (see Attachment 2) to see a Higgs boson in this mass range in one year at design luminosity using the decay into four charged leptons (originating from the decay into a real and virtual Z).

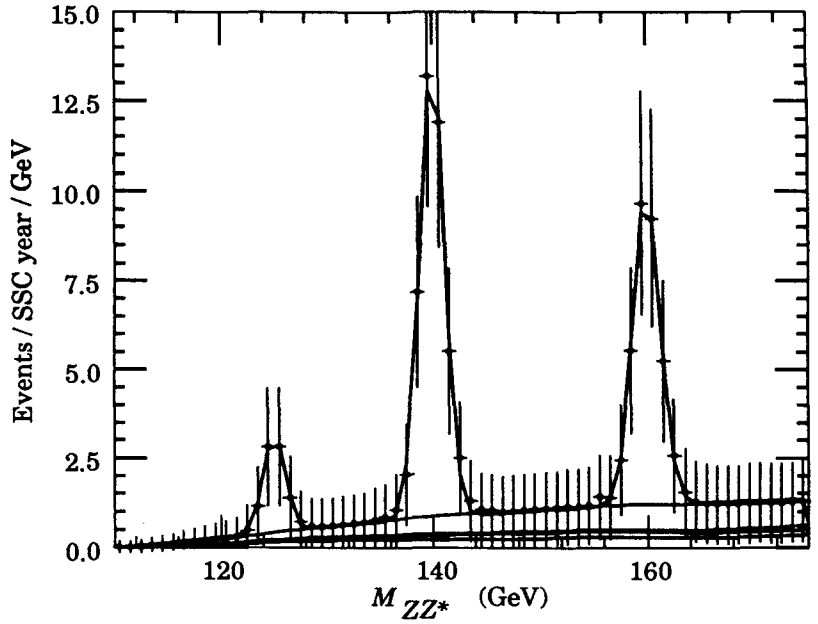

Figure 2.1-2: Signals for H $\rightarrow e^+e^- e^+e^-$, $\mu^+\mu^- e^+e^-$, and $\mu^+\mu^-\mu^+\mu^-$ using the SDC detector and Higgs masses of 125, 140, and 160 GeV.

At the lower end of the intermediate mass range, the four lepton decay has a very small branching ratio that makes this mode too small to detect. Here the decay into $\gamma\gamma$, although small, may be particularly relevant, and Fig. 2.1-3 — from the Letter of Intent for the GEM detector (Attachment 3) — shows the signal at the SSC in one year of running for various resolutions of the electromagnetic calorimeter.

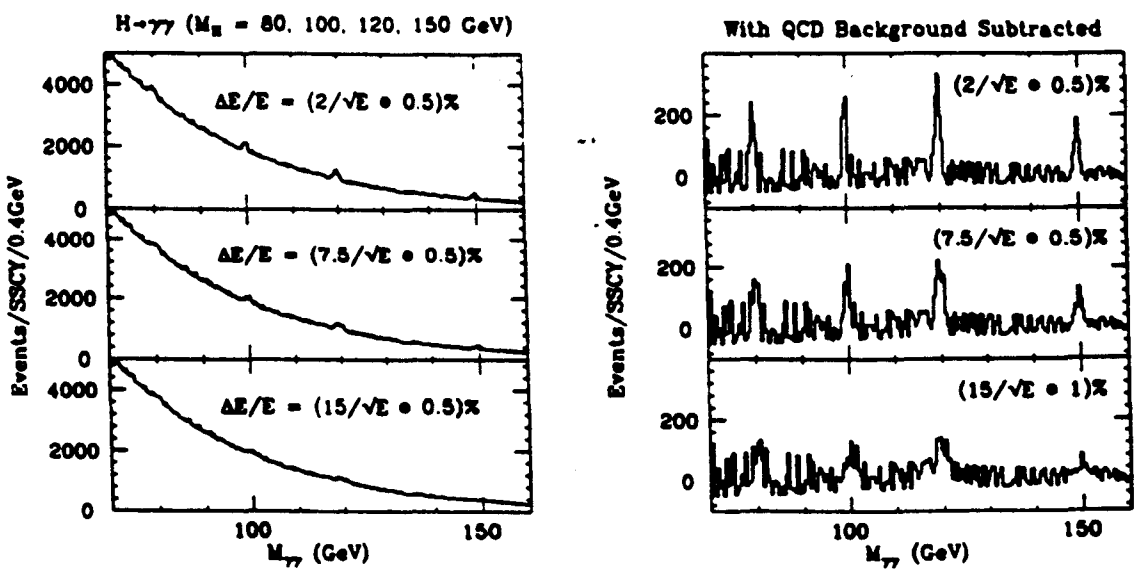

Figure 2.1-3: Signals for H $\rightarrow \gamma\gamma$ with three different calorimeter resolutions.

For $M_H > 2M_W$, a high mass Higgs boson, the signals resulting from $H \rightarrow ZZ \rightarrow$ four leptons are appreciable, as shown in Fig. 2.1-4. It should be possible to pursue the Higgs boson up to masses of about a TeV in several years of running at design luminosity, especially with the larger signal obtained by the use of other decays such as $H \rightarrow ZZ \rightarrow \ell^+ \ell^- \nu \bar{\nu}$.

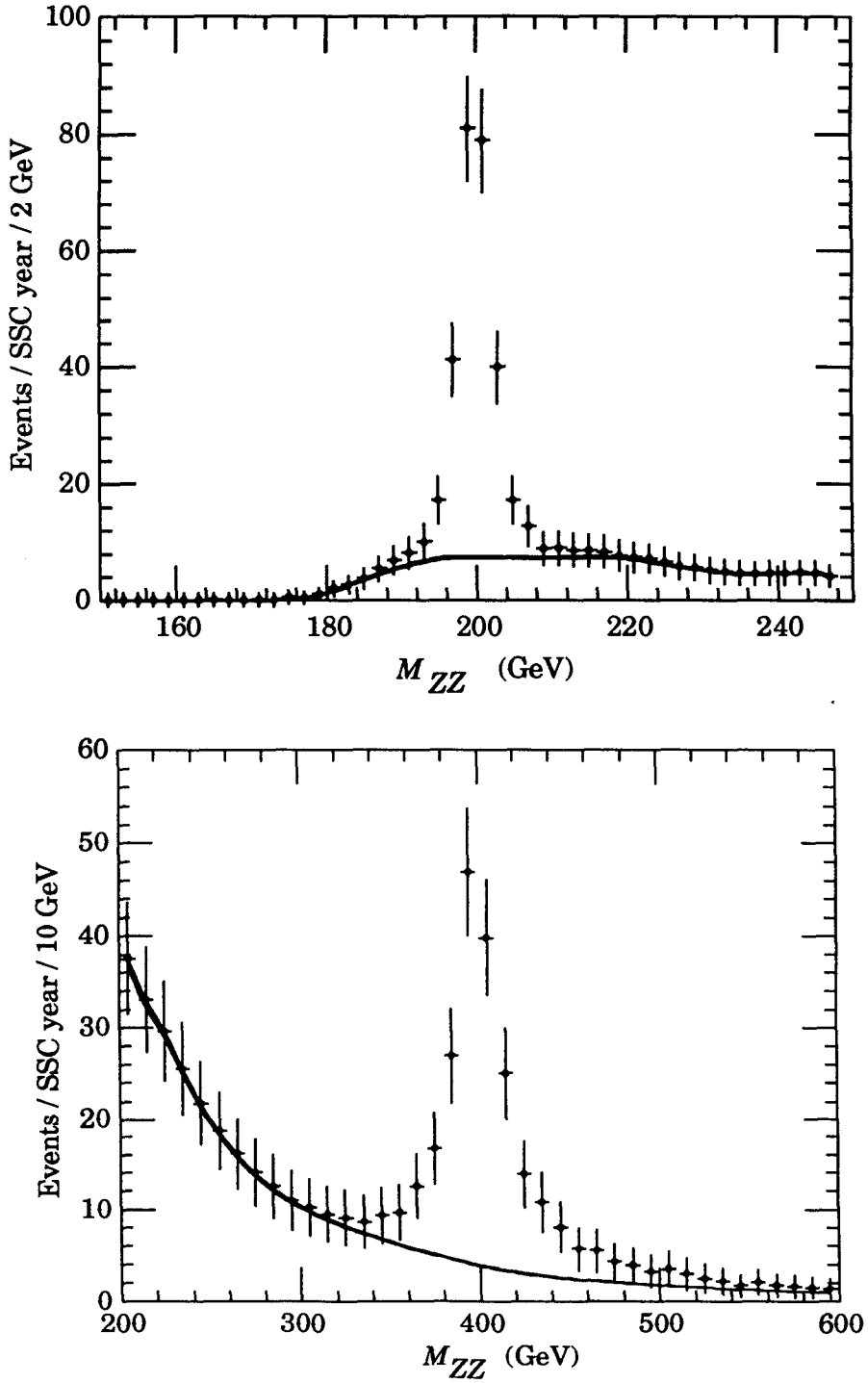

Figure 2.1-4: Signals for $H \rightarrow ZZ \rightarrow 4$ charged leptons for a high mass Higgs in the SDC detector.

If no Higgs is observed below 1 TeV, strong interaction effects are expected in the scattering of longitudinally polarized W and Z bosons at high energy. In this case, resonances may occur in the 1-2 TeV mass region for ZZ and WW pairs. Expected event rates for these high mass processes in the purely leptonic decay modes containing electrons and muons are at the level of 10 to 20 events per year for ZZ and WZ, and 50 events per year for like-sign W pairs.

Some theories alternative to the minimal standard model, such as technicolor, replace the fundamental Higgs field with a condensate of new, strongly interacting fermions. In such theories, new particle states are expected to decay to ZZ, WW, WZ or γZ pairs. The study of gauge boson pair production is generally a promising avenue for investigating electroweak symmetry breaking in many alternative theories.

Quark and Lepton Substructure

The existence of numerous, seemingly "fundamental" particles leads to the speculation that the observed particles are composite systems of other, more fundamental, entities. If quarks are composed of other particles bound by some new strong force, then at high enough energies deviations from the QCD expectation for quark-quark scattering will appear. An excess of hadronic jet events at high transverse momentum is one indication of quark compositeness. Tests for compositeness using jets of energies up to about 10 TeV are possible at the SSC.

New, Heavy Gauge Bosons

New fundamental gauge interactions may exist, mediated by massive bosons similar to the W and Z. Detection of heavy, charged bosons will be based on searches for events with energetic, isolated leptons and a large missing transverse momentum. Heavy neutral bosons decay to charged lepton pairs and can be pursued in these leptonic decay modes up to almost 10 TeV, or 100 times M_W or M_Z.

Supersymmetry

Supersymmetry postulates a relationship between fermions and bosons and predicts a rich spectrum of new particles. One example is the gluino, the supersymmetric partner of the gluon. This particle is expected to be produced copiously at SSC if it exists with a mass less than 2 TeV. The decay chain of the gluino ends in at least one stable, presumably neutral particle which does not interact with matter. The resulting transverse momentum imbalance is one of several typical signatures of the production of supersymmetric particles; another is same-sign dileptons originating in the Majoran nature of the gluino.

Top Quark

The t quark has not been found despite careful searches at CDF and elsewhere. Detection of the t quark and measurement of its mass will provide one more clue in the puzzle of the fermion mass spectrum. The cross section for t-quark production at the SSC is very large, with the yield of t quarks being tens of million per year. Even if found at the Tevatron collider, this yield will provide an opportunity for detailed measurements of t quark properties. Indeed, the leptons from t quark decays will be an important background for other particle searches at the SSC.

Bottom Quark

Literally millions of bottom quarks will likely be produced per second at the SSC. There are unique capabilities for studying rare decay modes of hadrons containing b quarks and the study of CP violation.

Not withstanding world-wide experimental effort over the last two decades by which the Standard Model has been tested with increasing accuracy and energy, no violations have been found. More than ever, if we are to find answers to what lies beyond the Standard Model, it is clear that we need to address the TeV scale directly at the SSC. Moreover, the energy and luminosity of the SSC were chosen to ensure that the nature of electroweak symmetry breaking will be revealed — in other words, there must be new physics found at the SSC.

2.2 The SSC Experimental Physics Program

The SSC experimental program should match both the physics potential and the investment in such a discovery machine. Review by the Laboratory's Scientific Policy Committee (SPC) and the Program Advisory Committee (PAC) has resulted in consistent, strong recommendations that the initial SSC experimental program should include;

- Two major detectors aimed at the physics opportunities opened by the SSC at multi-TeV energies and momentum transfers
- Several smaller experiments to add diversity to the program and especially to take advantage of the unique capabilities with respect to B-physics and "low" transverse momentum phenomena at the very high energies that the SSC brings.

Two major detectors with over 300 US physicists each, have been selected to be supported to prepare Technical Design Reports, which are the formal proposals to be considered for inclusion in the initial scientific program.

- SDC, whose design goals emphasize charged particle tracking, hermetic calorimetry, lepton energy measurement and identification, and vertex detection, is shown in Fig. 2.2-1. There are presently 101 institutions, 17 countries, and over 750 collaborators in SDC. (See Attachment 2)

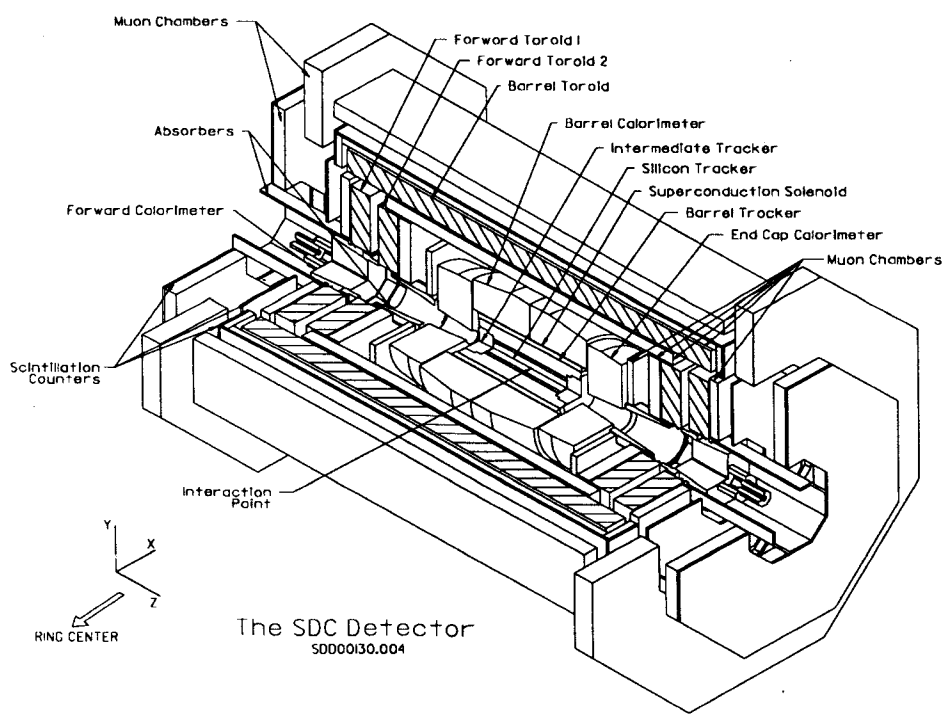

Figure 2.2-1: SDC Detector

- GEM, whose design goals emphasize identification and precision measurement of gammas, electrons, and muons, with capabilities for higher luminosity, is shown in Fig. 2.2-2. There are presently 85 institutions, 15 countries, and over 650 collaborators in GEM. (See Attachment 3)

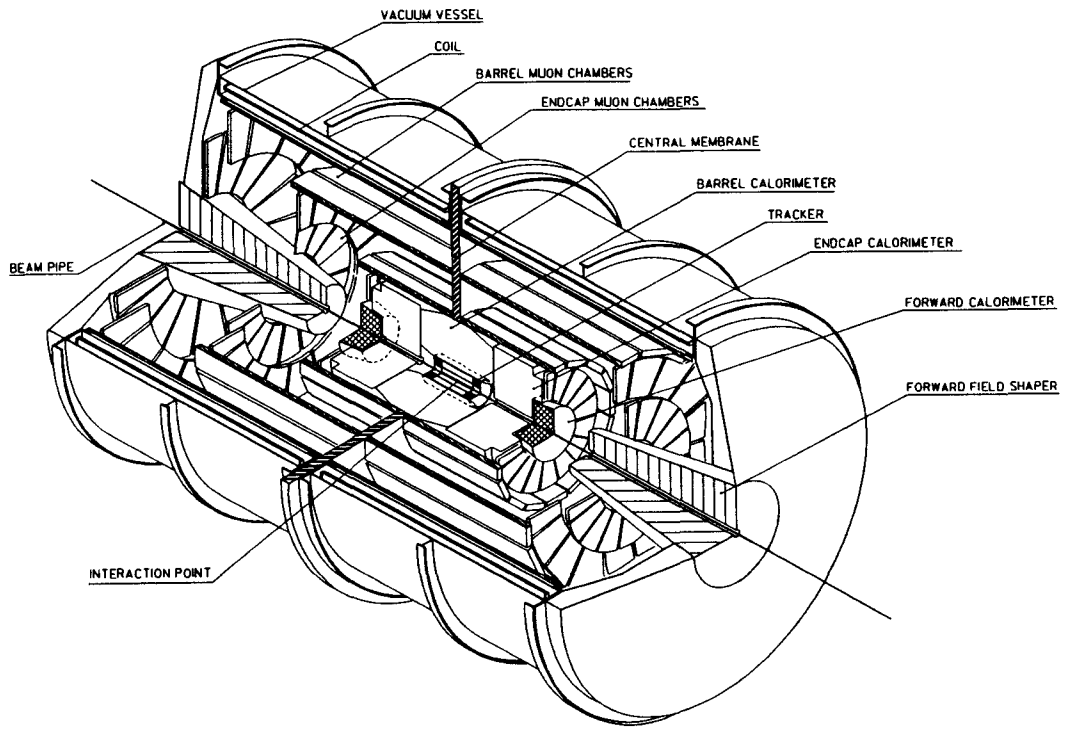

Figure 2.2-2: GEM Detector

These two major detectors are designed with complementary strengths, inasmuch as any single detector necessarily makes compromises on some detector subsystems with respect to others. Correspondingly, the two detectors jointly have significantly increased capability to both find and explore different aspects of physics discoveries. They compete to make each other better and more productive, as well as allowing a cross-check of discoveries. Furthermore, a broad international community is excited by the physics prospects and, as seen directly in the Letters of Intent, is already committed to the design, construction, and operation of GEM and SDC.

GEM and SDC herald a new era of high energy detectors. Each of these major detectors is unprecedented in scale, cost, participation, and physics opportunities and should be considered as a laboratory in itself. Each has the added complication of being world-wide in nature and being embedded in the overall SSC Project.

Technical Design Reports for these detector-laboratories are due this year (for SDC on April 1, 1992, and for GEM in the fall of 1992). With the approval of the Laboratory and the DOE of a technical, cost, and schedule baseline, construction would begin in 1993 and installation in the experimental halls in 1996.

2.3 Physicists in the SSC Research Program - Long Range Goals

2.3.1 Overview

The success of the SSC physics program requires the most crucial resource of all - many talented, creative physicists. Over 700 US physicists are currently in the major detector collaborations, with a total of 1400 scientists worldwide. Based on this scale of worldwide and US participation in the SSC experimental program, we have planned on 195 experimental physicists (staff and paid visitors) to be at the SSCL by the start of collider operations.

These SSCL physicists act as a spearhead for those in the collaborations, providing support for the collaborations, forming liaison with the other parts of the SSC project that involve technical facilities and the accelerator, helping shape the scientific program, and making their own contributions to research now. Similarly, an excellent theory group is an essential part of the Laboratory's research program, directly in terms of its own research contributions and in providing connections between experimental and theoretical physics at the SSC. Accelerator physicists provide a similar crucial resource in the construction of the injection chain and the collider itself. As construction of these machines is completed, accelerator research activities will be very important and will form the subject of separate proposals.

For several years a large fraction of the US high energy physics community has participated in detector R&D related to the SSC. Fig. 2.3-1 shows the geographic distribution of scientists who were involved in the SSC Detector Subsystems R&D program during FY 1991. This program has continued on a reduced scale in FY 1992, with most of the effort now focused by and funded from the detector-specific SDC and GEM R&D/Engineering activities.

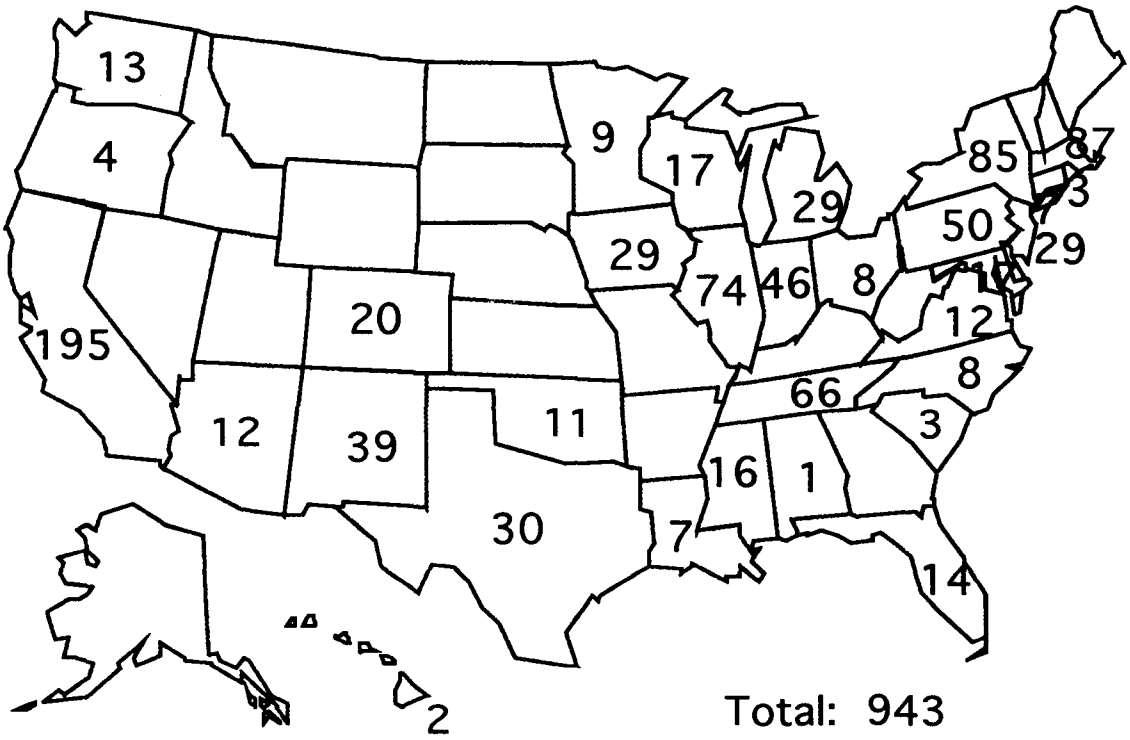

Figure 2.3-1: SSC Detector Subsystem R & D Program: Participating Scientists

There are now more than 1400 total participants in the SDC and GEM collaborations, half of them from the US. More than any previous US high energy physics laboratory, the SSC has from the beginning had a large international involvement in its physics program. Several hundred others submitted Expressions of Interest in smaller experiments.

The total involvement, actual and projected, in the SSC experimental program is shown in Fig. 2.3-2. The actuals for the total and the participating US physicists are based on the collaborators in GEM and SDC. Beyond that, jumps in FY 1993/FY 1994 of 100 physicists (50 US, 50 non-US) for each of two smaller experiments are assumed, together with a 2% yearly growth through the end of the decade. The total participation then approaches 1800 physicists at the beginning of the next century, roughly 1000 of them from the US. Also shown are the plans for experimental physicists (including long-term, paid visitors) at the SSC Laboratory, to be discussed below.

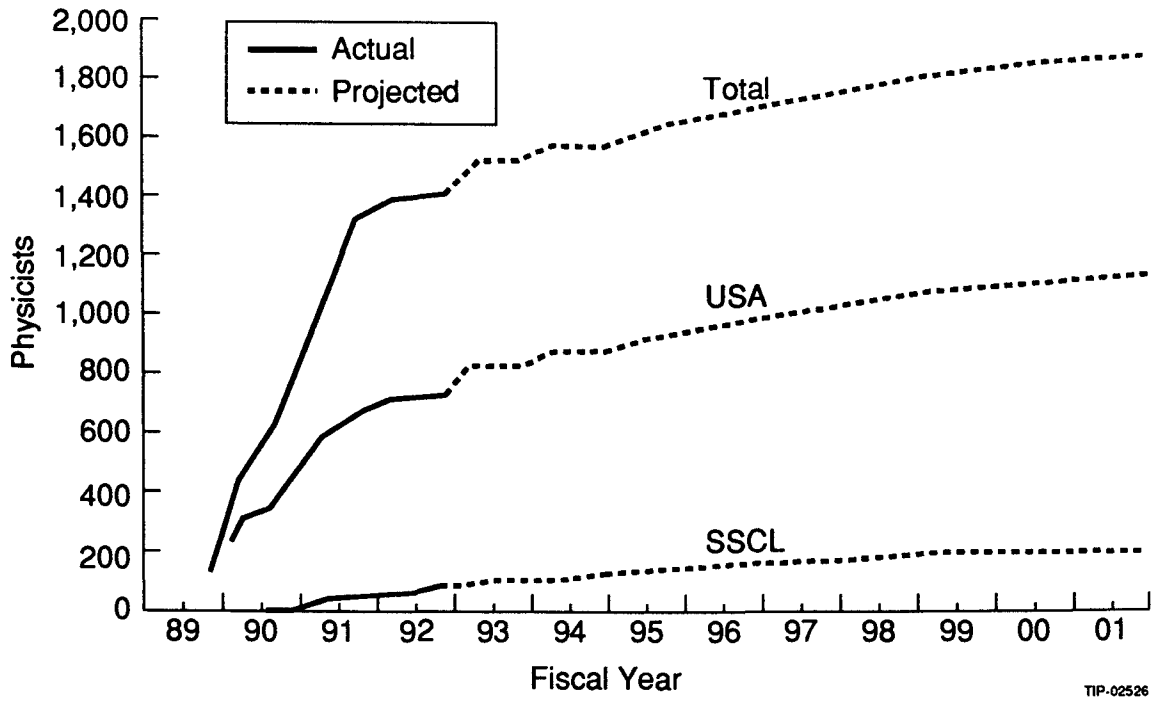

Figure 2.3-2 Physicist Involvement in the SSC Experimental Program

2.3.2 SSCL Physicists

Experimental Physics

Strong in-house groups of physicists are needed at the SSC Laboratory in order to successfully carry out the design, construction, and operations of the major detectors. The role of these groups is both to support the international collaborations and to make significant contributions to high energy physics. In more detail:

- Laboratory physicists are essential to participate in the continuous tasks associated with design and integration of the experiments.

- Laboratory physicists have a unique role in forming the liaison between the collaboration and the conventional construction, magnet, accelerator, and support parts of the of the SSC Project. Specific items that require such liaison are experimental facilities (interaction halls, assembly buildings, control rooms), beam pipes, IR magnets/optics, radiation/machine associated backgrounds, test beams and computing/simulation.

- Laboratory physicists provide for coordination/commonality between detectors

- Laboratory physicists have a special role in liaison to lab resources, integration, installation, and commissioning of subsystems built elsewhere

And last, but hardly least,

- Laboratory physicists are needed for their contributions to research, including development and construction of parts of some subsystems

Moreover, we are operating at a new scale of detectors. Specifically, this scale requires that the fabrication of the GEM magnet (that will be the largest ever built), and the fabrication and alignment of the muon modules for both SDC and GEM be done at the SSCL. Obviously, final assembly and commissioning of all systems is done in the interaction hall at the SSCL. Inasmuch as many important activities listed above are already underway, strong in-house participation is required starting now.

At the start of collider operations, we envisage 195 experimental physicists within the Physics Research Division (including paid, long-term visitors). Given the size of the detector collaborations noted above, this translates to in-house groups associated with each of the major detectors that are about 10% of the total collaboration. Others would be associated with the smaller experiments.

This size was arrived at primarily by top-down arguments, i.e., comparison with previous history, but is consistent with bottom-up estimates as well. In Fig. 2.3-3 data are gathered from the recent US "large" collider detector collaborations CDF, D0, and SLD. All show a substantial component (16% - 25%) coming from the host laboratory starting at the earliest stages of the experiment. The sum of these three collaborations, totalling 700 scientists, or approximately the size of one SSC major detector collaboration, has 130 to 150 associated experimental physicists inside the Laboratory. Based on a total of over 1400 collaborators and US HEP community involvement numbering over 700 already (which we expect to grow to around 1800 and 1000, respectively, by the time of collider operations, 195 experimental physicists at the Laboratory in FY 2000 is a minimal basis on which to plan. In the discussions below we take as a concrete model, a target of 85 SSCL physicists involved with each major detector and 25 in all the smaller experiments in FY 2000.

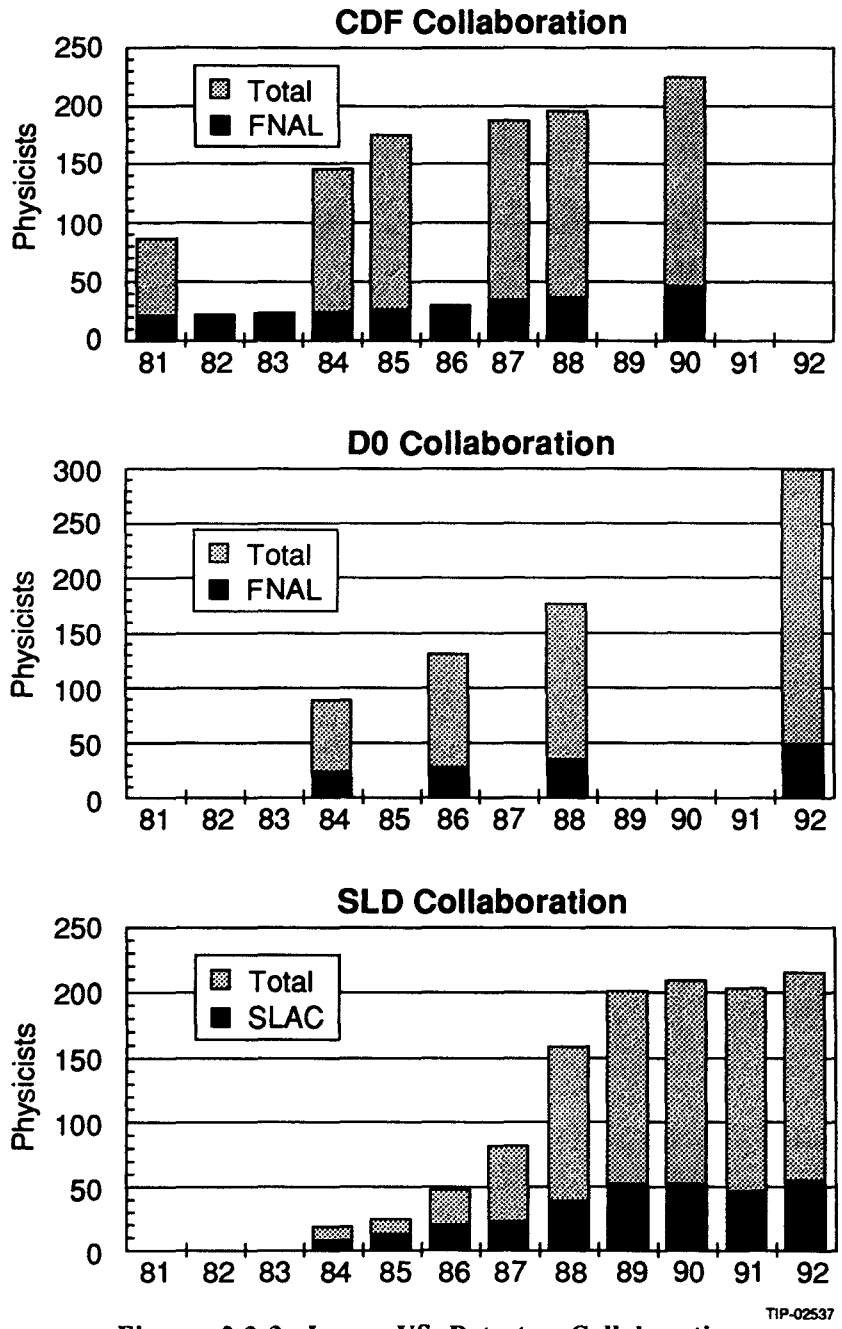

Figure 2.3-3 Large US Detector Collaborations

In-house scientific collaborators are expected to be involved in all of the subsystems of the large experiments. It is likely that there will be approximate proportional participation depending on the size and complexity of the system, as well as the amount of effort required on-site to assemble and install that system. However, even those systems that can be delivered complete to the SSC, will require a number of in-house liaison physicists to insure smooth integration with the rest of the detector, proper allocation of local resources, and to insure compliance with SSC safety and other requirements.

We do not plan to have in-house dominance of the collaborations-- this is prohibited in any case by the sheer size of the collaborations. Nor do we plan weak, almost purely service oriented groups. Collider experiments by their nature require strong in-house groups as illustrated by the present generation of large detectors at SLAC, Fermilab, and LEP.

Finally, the importance of the participation of SSC physicists in on-going experiments during the SSC construction phase must be emphasized. This is a critical element in attracting the best and most motivated physicists to the SSC. Excellent people bring with them involvement in on-going physics. For the scientific health of the SSC it is important to keep them involved and current in physics relevant to the SSC mission, for example in collider physics at FNAL, so that they can bring this expertise to bear on the SSC program. It is also highly desirable to foster a program of detector R&D to develop techniques which may be applicable to current and future experiments at the SSC and elsewhere. Their participation in experiments and R&D activities during SSC construction also ensures that their talents and creativity are not lost to the field during this lengthy period.

Experimental Physics Support

During the construction phase of the SSC experiments, the staff size of these projects will peak at over 300 people. Most of these people are engineers and technicians devoted to project design and fabrication. During this phase the physics staff will also be increasing as discussed. Physicists will draw on project support staff for many of the project-related activities; however, there is a need for a small, but critical, technical support staff, who are devoted to the research activities of the in-house physicists. This technical support staff plays the same role as the "captive" engineers and technicians found at all major high energy physics research groups at either laboratories or universities, as differentiated from that staff funded on the equipment budgets of the projects. This staff is utilized for those activities not directly associated with the project of construction of the detectors.

Experimental Physics Support staff functions include R&D activities, test beam activities, development of laboratory research infrastructure and instrumentation. The level of this support is expected to reach 35 FTEs, supporting the 195 FTE experimental physicists at SSC turn-on.

Theoretical Physics

An excellent theoretical physics group is an essential component of a high energy physics laboratory. Not only does such a group contribute directly to the research goals of the laboratory, but it plays a key role in establishing the intellectual, atmosphere that exists at a great research institution.

The theory group not only contributes to research and as host to visiting theorists, but will keep experimentalists at the Laboratory informed of the latest theoretical developments. This is of great importance, for the program of the Laboratory is to explore the nature of fundamental interactions and of matter at energies never before probed, and it is only through the interaction between theory and experiment that this program can be fully successful. The latest avenues suggested by theory can be used to tailor experiments or the analysis of experiments so as to explore new directions.

The theory group may also play a role in education, an area where the SSC Laboratory has important programmatic goals as well. Graduate students in experimental particle physics who are required to spend large amounts of time at a laboratory away from their parent institution often miss the opportunity to take any but the most basic graduate courses. Theorists can alleviate the situation by organizing short courses at the appropriate level.

In order to achieve these goals, it is important that the composition of the group be dictated primarily by quality and diversity rather than by the extent to which the research of each individual is directly and immediately relevant to specific experiments to be performed at the Laboratory. Of course, it is expected that much of the research would be concerned with aspects of theory that could conceivably be tested experimentally in the not too distant future.

We see a group of 25 theoretical physicists at the start of collider operations in FY 1999, including permanent appointees, term appointees, and long-term paid visitors. Based on experience at other national laboratories there might be approximately equal numbers in these three categories.

Computing Support

At this stage in the Laboratory's development, scientific computing efforts related to the detectors and to the research program are found in the Computing Department of the Physics Research Division. Long-range policy calls for the establishment of an SSCL Computing Division that would house scientific computing and much of the activity described below would move to that Division.

Computer activities for Physics Research have been focused on developing resources to support work on physics simulations to guide detector design. To accomplish this, the Physics Detector Simulation Facility was designed and implemented taking advantage of the RISC/UNIX environment to obtain maximum price/performance providing "super computer like" capabilities at relatively low cost. This facility which has a present capacity of 2000 VAX 11/780 computers was developed with project funds and has been operational since April 1991. As computing systems, such as the Physics Detector Simulation Facility (PDSF) become operational, they are a major resource to the physics community for the experimental program. As such, while computing hardware development and commissioning costs come from project funds, the operational support for these systems moves to HEP funds. It is projected that 46 computer operations support personnel will be needed by FY 1999 to support a 24-hour, 7-day/week program.

The usage of this PDSF has steadily grown to its current level of 60-80% saturation. There are presently an average of 50-60 physicists from both collaborations using the system 24 hours/day, 7 days/week performing detector physics simulations. The PDSF is accessible from any InterNet location and up to 80% of its user base resides outside the SSCL. Specific physics studies which are currently being performed using this resource are outlined in the SDC, GEM, and outside research programs described later in this document.

Work has begun by GEM and SDC in collaboration with Physics Computing to develop conceptual models of computing environments necessary to meet the needs of the experimental program in the operational phase of the Laboratory. The projected requirements of a single detector establishes the criteria for these systems with a data rate from Level 3 trigger of 100-MBytes/sec of raw data. At this rate it is anticipated that a minimum of 10^6 VAX Equivalents of the computing will be required for local data reconstruction and data analysis. Storage requirements of 10^{15} Bytes of storage for raw, reconstructed and analysis data will be required, at the start of detector operation in 1999.

Using this criteria, conceptual design models are being developed [Fig. 2.3-4] to study potential architectures using RISC/UNIX technologies which are anticipated to be available in the marketplace by 1997/98.

The teams working on these problems at the SSC are a homogeneous mix of physicists and computer scientists providing expertise to integrate the physics criteria and requirements to state-of-the-art computing and software development techniques. Students are working with physicists/computer science teams running and maintaining simulation codes. Student programs will include training on physics applications and UNIX distributed computing environments.

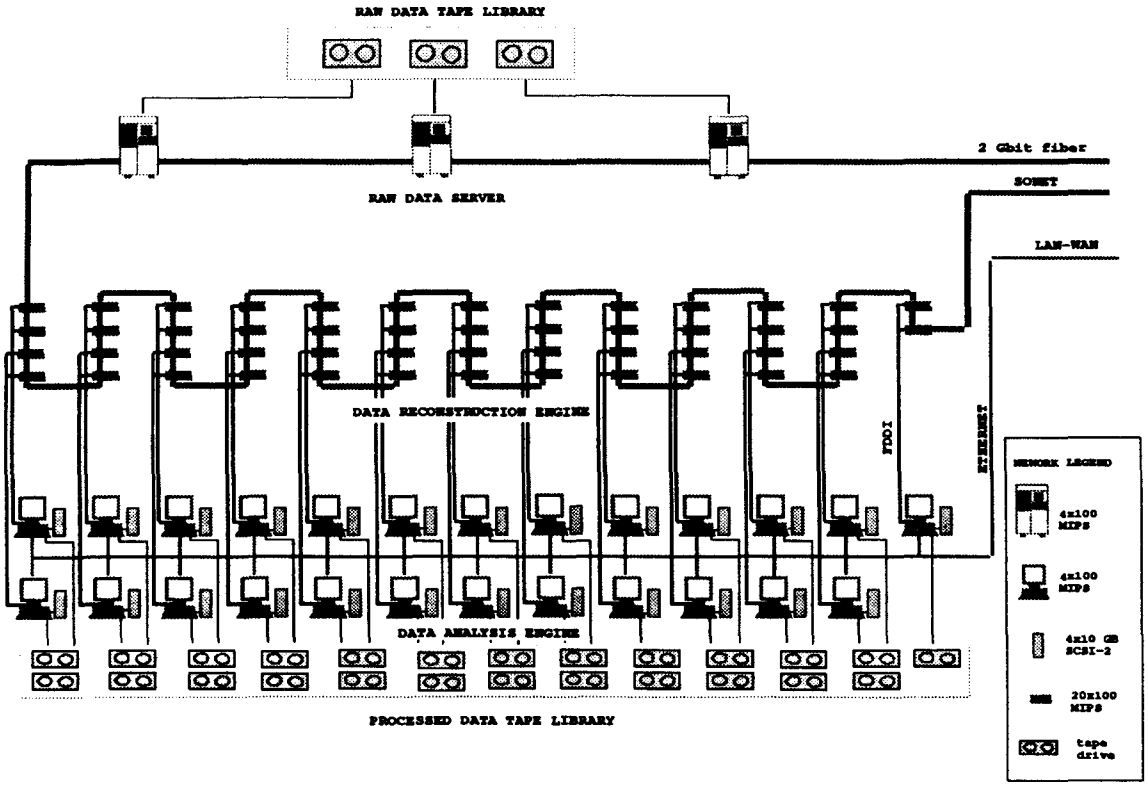

Figure 2.3-4: Conceptual Design - SDC Off Line Computing

2.4 Strategy

To achieve the goals given in the previous subsection, our overall strategy is to have a steady growth in people over this decade and to make a smooth transition from the period of the SSC Project to that of the fully operating Laboratory in FY2000. In doing so, we would phase out outside research as the SSC detectors start being assembled in 1996. In this same time-frame, experimental facilities and test beams become part of the operating Laboratory. Similarly, accelerator physics research, not dealt with directly here, becomes a high priority as accelerator operations begin.

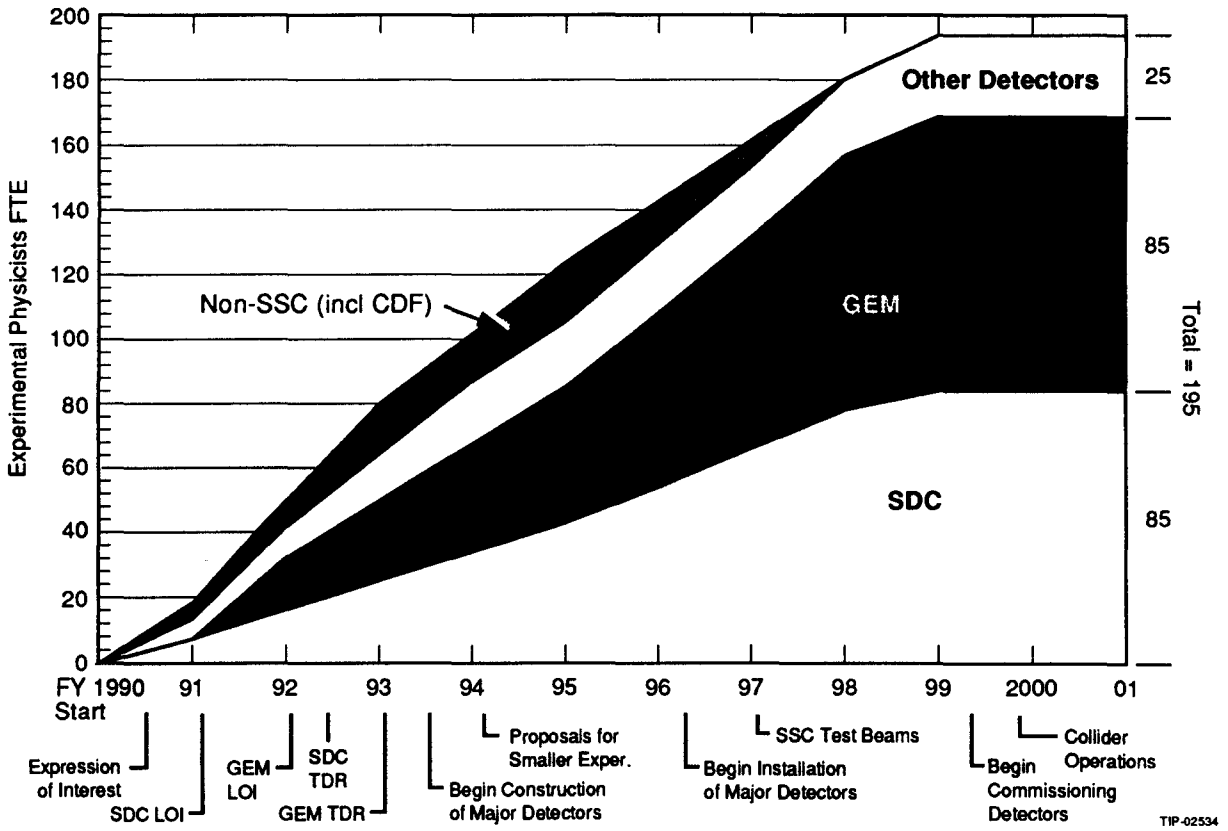

Figure 2.4-1 SSCL Experimental Physics Program Staff

The envisioned ramp-up in experimental physicists is shown in Fig. 2.4-1. The 195 experimental physicists (FTEs on the Laboratory payroll) in FY2000 are divided into 85 on SDC, 85 on GEM, and 25 on other, smaller experiments. The associated dates within the experimental program that drive this ramp-up are shown at the bottom of the figure.

Given the urgent need to have initial staffing by a core of physicists now to participate in the program already underway, and the final levels of staffing required to insure the vitality and intellectual health of the laboratory after it begins operations, one must justify the ramp-up that connects the initial to final staffing levels. There are two primary reasons for the growth shown in Fig. 2.4-1. The first is to satisfy the requirements for tasks which must be accomplished at the SSCL during the project period. These include the major assembly jobs which must be initiated during detector fabrication. Examples include the SDC muon system beginning in 1995 and the GEM magnet in 1993. Underground installation of both detectors is slated for 1996. SSC test

beam operations are scheduled to start in 1997. A major influx of visiting and commuting physicists are expected during this time, and their effectiveness will rely to a large extent on the existence of an established in-house host group.

The second reason for an almost linear growth is the large effort to recruit a staff of excellent physicists. Over the period between now and commissioning of the SSC it is necessary to hire an average of 2 physicists per month -- a daunting task. Delaying the ramp-up to later years makes it a task that much more difficult to accomplish, especially while keeping the quality high. Most of these people will come from other parts of the current high energy base program, with some small influx of new PhD's and foreign scientists. If one is to assemble the first rate staff consistent with the mission of SSC, one must seize all opportunities to hire established and mature physicists, as well as to continually sift the applications of younger candidates to select those with the requisite scientific potential.

Experimental physicists are part of a larger picture shown in Fig. 2.4-2 showing the staff in the whole SSCL Research Program. In addition to experimental physicists there are associated technical support people, theoretical physicists and computing support personnel. In FY2000 all these categories combined total 301.

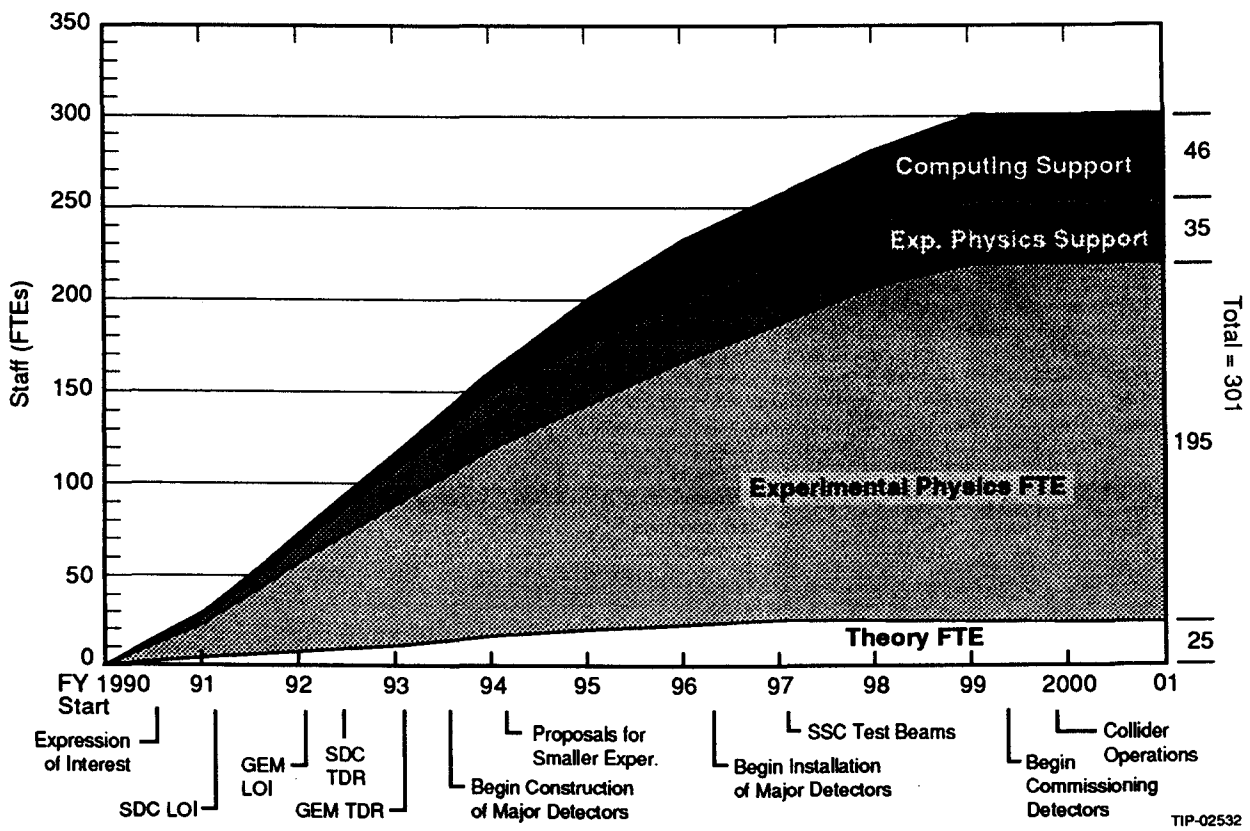

Figure 2.4-2 SSCL Research Program Staff

Finally, Fig. 2.4-3 shows all the staff in Physics Research, including the parts inside the SSC Project. In particular, there is the primarily engineering and technical (plus some management) staff associated with the detector projects that end by FY2000. Note that the technical and managerial staff associated with these projects at the SSCL is only a small fraction of

the worldwide effort. The ramp-up of Research Program personnel is identical to that in Fig. 2.4-2, and there is a corresponding growth in Experimental Facilities Operations after 1995 and in Detector Support (again, almost entirely engineering and technical personnel) after 1999. Out of the 680 FTEs in the Research Division in FY2000, the number of engineers and technicians is approximately double that of experimental physicists.

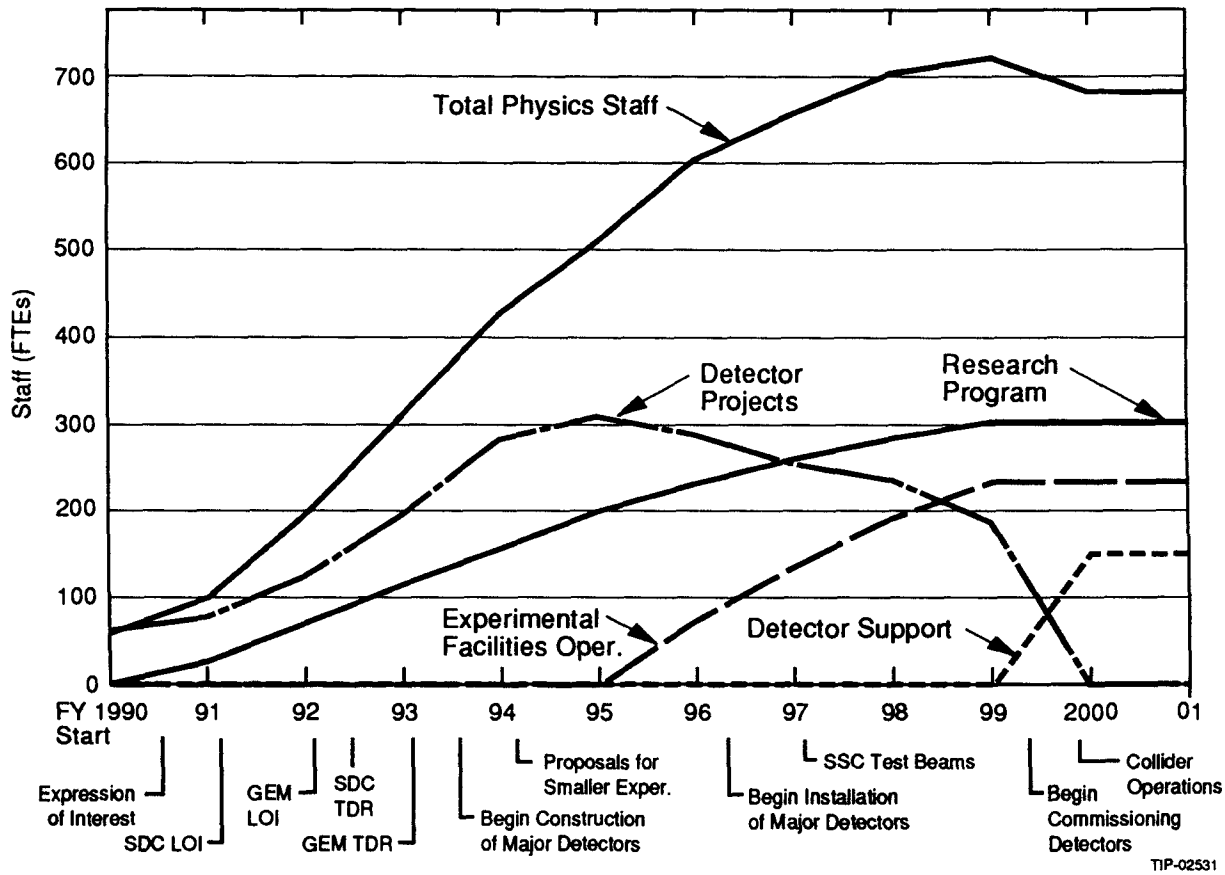

Figure 2.4-3: Physics Research

Engineers, technicians and management of the detector projects is paid for out of the SSC Project. The cost associated with the SSC research program, made up principally by physicists, is shown in Fig. 2.4-4, and is the subject of this proposal for HEP base program funding. The same totals, broken down into budget categories are shown in Fig. 2.4-5. Tables that correspond to these figures are found in Tables 2.4-1 - 3, given in FY 1991 dollars.

The SSC Total Project Cost (TPC) includes the costs of relocating physicists to the SSC and providing them with personal infrastructure (e.g. workstations). The base program is being requested to provide these physicists with salary, materials and services, research related travel, and equipment directly related to establishment of research infrastructure at the SSC, e.g. scopes, test equipment, tools, etc. These needs are typical for physicists at other US institutions, and are to be distinguished from equipment directly chargeable to the detector projects.

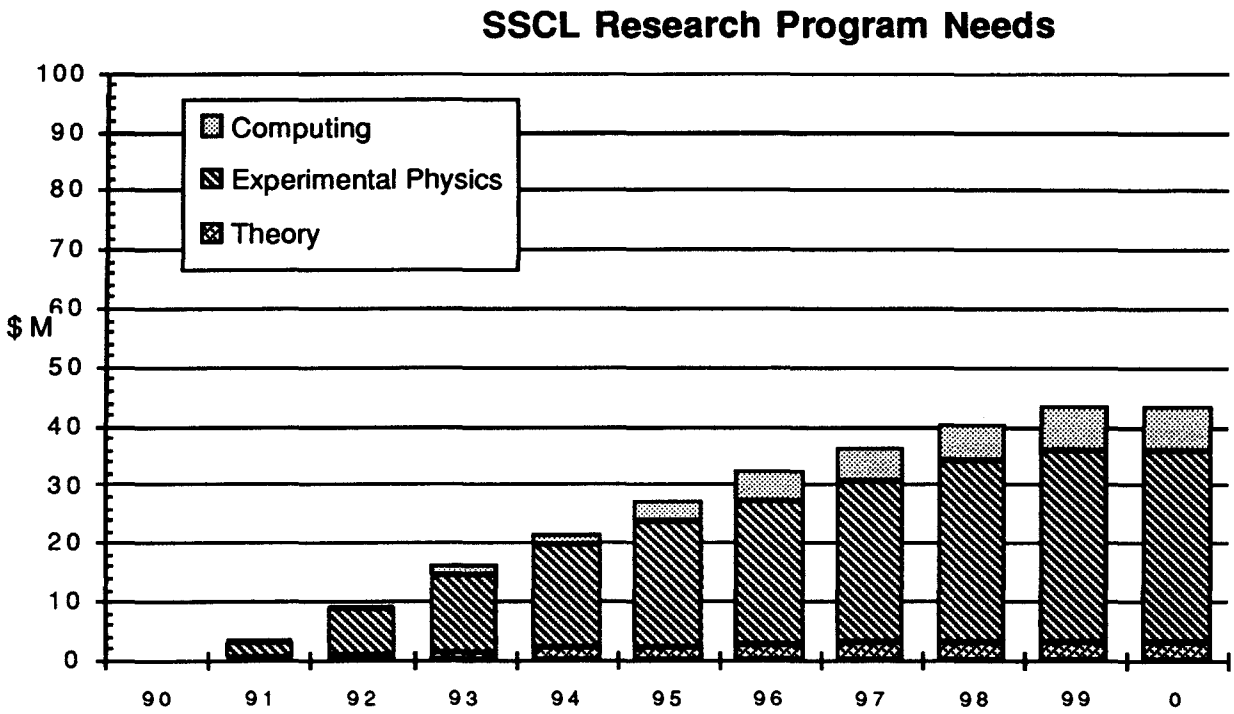

Figure 2.4-4: Physics Research Program Needs

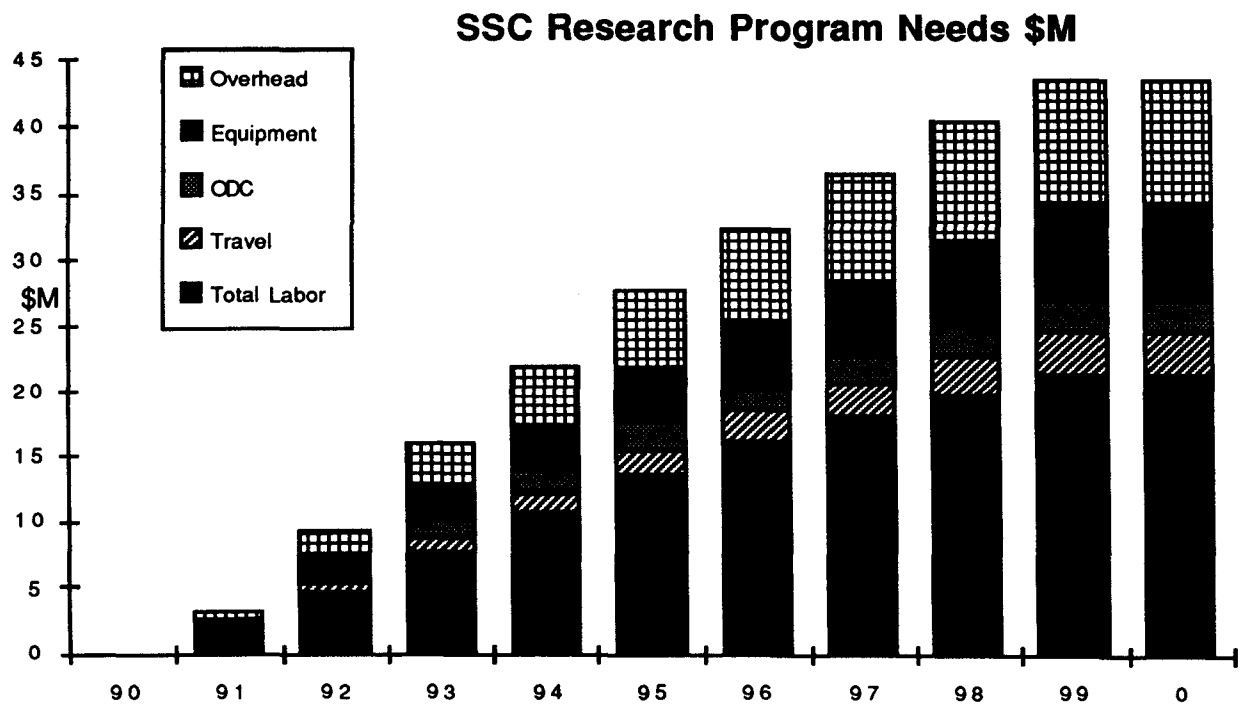

Figure 2.4-5: Physics Research Program Needs by Budget Categories

Table 2.4-1: Experimental Physics Program FTE

Fiscal Year	90	91	92	93	94	95	96	97	98	99	00
SDC	0	7	16	25	34	43	54	66	79	85	85
GEM	0	0	16	25	34	43	54	66	79	85	85
Other Detectors	0	6	10	15	20	20	22	23	25	25	25
Non-SSC (incl. CDF)	0	5	8	15	15	18	13	8	0	0	0
TOTAL	0	18	50	80	103	124	143	163	183	195	195

Table 2.4-2: Research Program Staff FTE

Fiscal Year	90	91	92	93	94	95	96	97	98	99	00
Computing	0	2.0	6.0	8.0	12.0	24.0	33.0	36.0	39.0	46.0	46.0
Exp. Physics Support	0	4.0	8.0	18.0	28.0	31.0	33.0	34.0	35.0	35.0	35.0
Experimental Physics FTE	0	18.0	50.0	80.0	103.0	124.0	143.0	163.0	183.0	195.0	195.0
Theory	0	3.4	7.0	9.0	15.0	19.0	23.0	25.0	25.0	25.0	25.0
Total	0	27.4	71.0	115.0	158.0	198.0	232.0	258.0	282.0	301.0	301.0

Table 2.4-3: SSCL Research Program Needs (FY 1991 $M)

Fiscal Year	90	91	92	93	94	95	96	97	98	99	00
Theory	0.0	0.4	0.9	1.2	2.0	2.3	2.8	3.0	3.1	3.1	3.1
Experimental Physics	0.0	2.5	7.9	13.4	17.8	21.3	24.4	27.6	30.9	32.9	32.9
Computing	0.0	0.3	0.7	1.3	1.9	3.8	5.3	5.8	6.3	7.5	7.5
Total	0.0	3.2	9.4	15.9	21.6	27.3	32.4	36.4	40.3	43.5	43.5

SECTION 3

CURRENT STATUS

3.0 CURRENT STATUS

3.1 Current Staff Physicists

We have already attracted to the Laboratory more than 30 experimental physicists and the first permanent theoretical physicists. A list is given in Table 3-1, that also contains the year of their Ph.D., their previous institutional affiliation, and their area of physics research activity. About a third came from institutions outside the US, although several of these are young Americans returning to the US after a postdoctoral period working in Europe. This list includes physicists in the Division Office and Computing that are supported by SSC Project funds and includes term appointees as well as permanent staff. Vitae are found in Appendix A and a selected bibliography is found in Appendix B.

Table 3-1 Physics Research Division

Physicist	Year of Ph.D.	Previous Institutional Affiliation	Research Activity
Bintinger, David	1975	LBL	SDC
Bird, Fred	1988	CERN	SDC, Tracking
Blocker, Craig	1980	Brandeis University	SDC, Calorimetry
Botlo, Michael	1987	CERN	DAQ/Electronics
Cormell, Laird	1975	Industry	GEM, Computing
Coupal, David	1985	SLAC	SDC, Tracking
Dingus, Peter	1987	Ecole Polytechnique	GEM, Muons
Dorenbosch, Jheroen	1977	CERN	DAQ/Electronics
Fenker, Howard	1978	Fermilab	Tracking
Frederiksen, Soren	1987	Ohio State University	SDC, Computing
Fry, Alan	1985	University of Rochester	SDC, DAQ
Fuess, Theresa	1988	FNAL	CDF, DAQ
Fukui, Toru	1990	KEK	SDC, Muons
Gilman, Fred	1965	SLAC	Division Office
Grinstein, Benjamin	1984	Harvard University	Theory
Johnstad, Harold	1967	Fermilab	SDC, Computing
Luth, Vera	1973	SLAC	Division Office
Lynch, Harvey	1966	SLAC	Division Office
McBride, Patricia	1984	Harvard University	Arrives 4/92
McFarlane, Ken	1964	Temple University	GEM, Computing
Milner, Cas	1985	LANL	DAQ/Electronics
Mitselmakher, Guenakh	1974	JINR (Dubna)	GEM, Muons
Paige, Frank	1970	BNL	Theory, GEM
Pal, Trivan	1983	CERN	SDC, Muons
Roberts, Lee	1986	Fermilab	GEM, Computing
Sheer, Irwin	1988	UCSD	GEM, Tracking
Siegrist, Jim	1979	UC Berkeley	SDC, Calorimetry
Stefanski, Raymond	1968	Fermilab	Division Office
Stocker, Francois .	1986	SUNY-Stony Brook	GEM, Muons
Takashima, Makoto	1988	MPI - Munich	SDC, Calorimeter
Thomas, Jennifer	1983	MPI - Munich	GEM, tracking
Turcotte, Marc	1986	University of Victoria	SDC, Calorimetry
Villasenor, Luis	1988	University of Michoacan	GEM, Muons
Wang, Edward	1984	LBL	DAQ/Electronics
Wu, Jin Chu	1985	New York University	Computing
Yarba, Julia	1990	Moscow State University	SDC, Calorimetry
Yost, George	1969	LBL	GEM, Computing

An experimental physics recruiting committee, now consisting of J. Ballam (SLAC), C. Blocker, W. Chinowski (LBL), F. Gilman, M. Marx (Stony Brook) and J. Siegrist meets periodically to review applications and suggest recruiting strategy and actions.

There are hundreds of applications (more than 200 since September, 1991) from experimental physicists interested in coming to the SSCL. This has allowed us to stay on the desired ramp-up of people (Fig. 3-1), during these first years of the Laboratory while at the same time getting the high quality people in 3-1. Some of the hiring pressure has been relieved by paid, long-term visitors, listed in Table 3-2. They have played an important role in bringing physics research activities to the Laboratory at a very early stage.

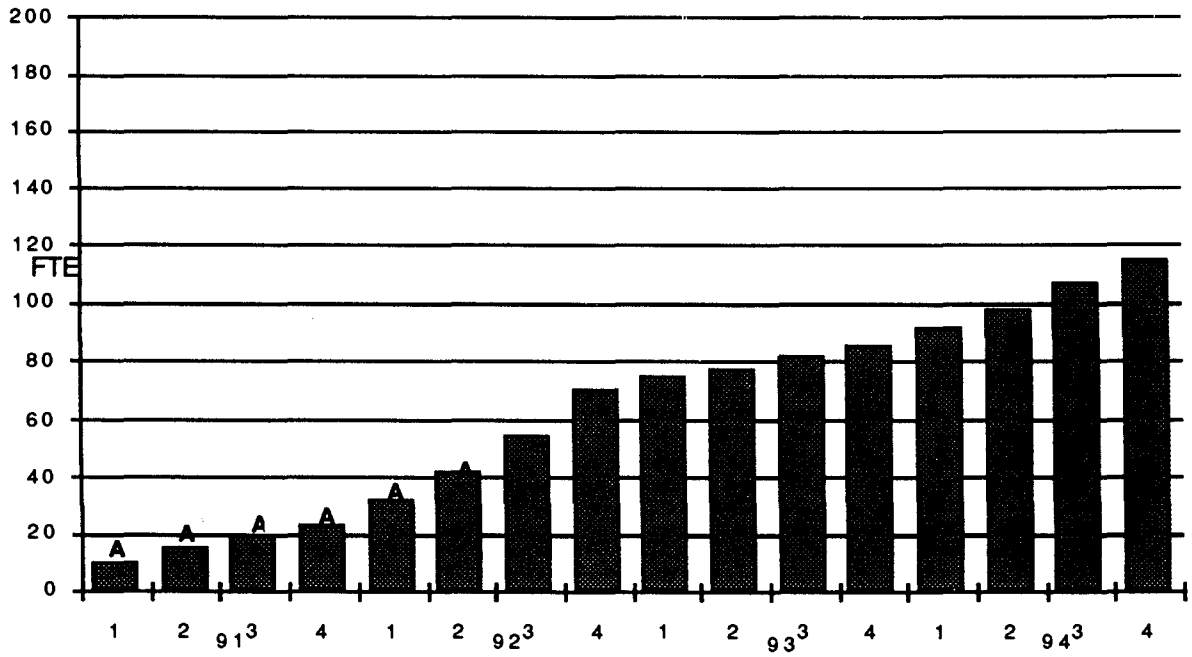

Figure 3-1: Planned and Actual Research Program Experimental Physicists at the SSCL A = Actual

Table 3-2: Physics Research Division Guest Scientists

Name	Institution	Term	Research Activity
FY1991			
Abrams, Gerald	LBL	12 mos	SDC, Calorimetry
Bensinger, Jim	Brandeis	6 mos	SDC, Muons
Chinowski, William	LBL	12 mos	Computing/CDF
Gornushkin, Yuri	Dubna	2 mos	E/T, Muons
Kane, Gordon	U. Michigan	3 mos	Theory
Korytov, Andrey	JINR	12 mos	E/T, Muons
Kubarovsky, Valery	JINR	2 mos	SDC, Muons
Kulik, Alexei	IHEP	2 mos	SDC, Muons
McFarlane, Ken	Temple	10 mos	GEM, Simulation
Meshkov, Sid	NIST	10 mos	Theory
Molchanov, Vladimir	IHEP/Serpukhov	2 mos	SDC, Muons
Paige, Frank	BNL	4 mos	Theory
Sanda, Tony	Rockefeller	6 mos	Theory
Tsyganov, Edward	JINR	3 mos	SDC, Muons
White, Andrew	UT Arlington	2 mos	SDC, Simulation

Name	Institution	Term	Research Activity
FY1992			
Barabash, Leonid	JINR	3 mos	GEM, Muons
Bensinger, Jim	Brandeis	6 mos	SDC, Muons
Bonushkin, Yuri	JINR	6 mos	GEM, Muons
Budagov, Julian	JINR	8 mos	SDC, Calorimetry
Danilov, Michael	ITEP	3 mos	Other
Fisyak, Yuri	Moscow State U.	7 mos	GEM, Tracking
Fridman, Alfred	CERN	9 mos	B Physics
Golutvin, Igor	ITEP	3 mos	GEM, Muons
Golutvin, Andrey	ITEP	5 mos	GEM, Muons
Lubatti, Henry	U of Washington	12 mos	SDC, Muons
Lynn, Bryan	Stanford	6 mos	Theory
Marx, Michael	SUNY/Stony Brook	12 mos	GEM, Physics, Integration
Meshkov, Syd	NIST	12 mos	Theory
Ogren, Harold	Indiana U.	6 mos	SDC, Tracking
Ostapchuk, Andrey	ITEP	5 mos	GEM, Simulation
Roe, Byron	Michigan	9 mos	SDC, Tracking
Sarantsev, Viktor	St. Petersburg	6 mos	GEM, Simulation
Shang, Ren-chen	Tsinghua	12 mos	GEM
Skuja, Andris	U. of Maryland	6 mos	SDC, Muons
Tchistilin, Vladimir	ITEP	6 mos`	GEM, Muons
Tichomirov, Igor	ITEP	6 mos	GEM, Muons
Timofeev, Viatcheslav	JINR	9 mos	SDC, Muons
Tsyganov, Edward	JINR	3 mos	SDC, Muons
Vanyashin, Alexandre	MEPI	11 mos	GEM, Simulation
Wang, Angel	U. of S. Carolina	3 mos	Tracking
Williams, Brig	U. of Penn.	6 mos	SDC, Electronics
Wu, Dan-Di	Beijing	10 mos	Theory
Xia, Song-jiang	Beijing	12 mos	GEM
Yu, Xiao-qi	U of S&T, China	7 mos	GEM, Tracking
Zalewski, Janusz	SW Texas S U	3 mos	DAQ
Zhukov, V.	Moscow St. U.	3 mos	GEM, Muons

There are 44 FTE experimental physicists currently at SSCL, including staff and visitors. We expect that we will reach the goal of 50 FTE by the end of FY 1992 through new hires and more visitors.

We are also very pleased to have already attracted about 10 students to the SSC Laboratory at this early stage of detector design, research, and development. They come from universities in Texas and are associated with research efforts in electronics, data acquisition and computing.

3.2 Physics Research Division Organization

The present organization of the Physics Research Division is shown in Fig. 3-2. SSC project activities, such as those responsible for construction of the detectors, are shown on the bottom line, reporting to the Associate Director. These detector projects finish in FY 1999. On the middle line is the Physics Research Program and its component activities, which continue as the dominant part of the Physics Research Division in FY2000 and beyond.

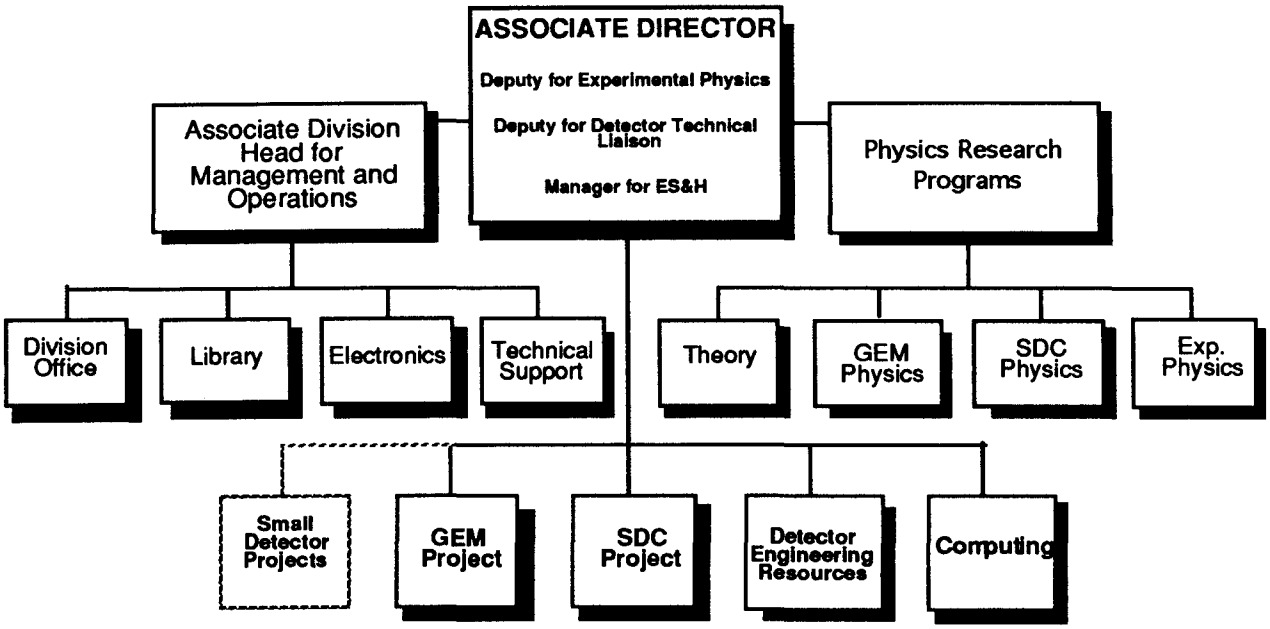

Figure 3-2: Physics Research Division Organization Chart

The Physics Research Program has already started several different activities described in detail in Section 4.

With the two major detectors proceeding toward Technical Design Reports, SDC and GEM physics groups, led by James Siegrist and Michael Marx, respectively, have formed within the Physics Research Division. These groups are participating as full scientific partners in the respective collaborations and are carrying out physics activities that are unique to their location at the Laboratory.

On-going research outside the SSCL is based in the Experimental Physics Group and started in FY 1991 with participation in CDF. Involvement has grown this year with the recruitment of additional staff and the preparation for the up-coming collider run at Fermilab. We plan to increase the effort in on-going physics by participating in another experiment. Common efforts and work towards smaller SSC experiments are also based in this group.

SECTION 4

CURRENT PROGRAM

4.0 CURRENT PROGRAM

4.1 Introduction

The current program at the SSC Laboratory has changed dramatically even since the submission of the last proposal in November 1991. These changes reflect the dynamic growth of the SSC itself, the shaping of the experimental program, and the flow of new personnel, especially physicists, to the SSC as long– and short-term visitors. This period has marked the time for submission of the SDC Technical Design Report (TDR), approval of the GEM Letter of Intent (LOI), and preparations for the imminent CDF run at the Tevatron.

In FY 1991, support was obtained from the DOE high energy base program for on-going research activities in experimental physics, theoretical physics, and related computing. Significant progress has been made in implementing research in on-going experiments and in beginning serious detector R&D activities in newly created laboratory space in Dallas. In particular, an SSC group joined the CDF collaboration. SSCL physicists are engaged in upgrading the forward muon system for the run that starts in April. New hardware for HV distribution and systems diagnostics has been constructed. Extensive work by SSCL physicists and staff has been carried out at FNAL to install the upgraded system. Code for analysis of the forward muon system performance has been generated, and on-line diagnostic systems implemented. Physics topics to pursue have been selected by the group. The details of progress on this research, and the analysis plans fo the group are presented in Sections 4.5.1 and 5.5.1 Plans for establishing another outside research effort are also evolving.

For SDC, this time has seen choices of technology made for calorimetry and muons. Both have significantly affected the efforts at the SSC. The calorimetry choice of scintillating tiles over liquid argon resulted in a redirection of the local effort. For muons, the choice of the Washington/SSCL drift tubes has focused the effort at the SSCL. A muon facility has been brought into operation and a full-length prototype of the selected technology is undergoing tests. Another major activity is physics performance simulation in support of the design development of SDC. Detailed progress is reported in Section 4.3, and plans for the remainder of FY 1992 and for FY 1993 are presented in section 5.3.

The GEM LOI was submitted at the end of November culminating a concerted effort which was centered at the SSCL. With its approval there has been a dramatic increase in GEM physicist presence with the addition of many visitors and top management spending time at the SSCL. A significant new direction is the construction of the "Texas Test Rig" (TTR) which will provide a cosmic ray test facility for evaluation and comparison of competing muon chamber technologies. This will also provide the impetus for the first significant large scale user facility at the SSCL, and will be operational by the summer of 1992. The SSC GEM group is coordinating efforts on detector simulation in support of the design report. Progress reports on establishing the GEM SSC physics groups are reported in the following section, and plans for FY 1992/93 are given in Section 5.2.

Common efforts at the SSC have focused on R&D for tracking (Sections 4.4.1 and 5.4.1) where the emphasis has been on readout devices for scintillating fibers — avalanche photodiodes (APD) and visible light photon counters (VLPC); and for electronics (Sections 4.4.2 and 5.4.2), where the emphasis has been on issues common to all major detectors — front end chip design, testing and interfaces, data acquisition, and trigger implementation studies.

The theory effort at the SSC has been blossoming. The first permanent staff has been augmented with a steady stream of visitors, and the groups has established a seminar and colloquium series for both theory and experimental topics. The theory efforts, past and future, are described in Sections 4.6 and 5.6.

Taking advantage of current computer technologies has resulted in the commissioning of the Physics Detector Simulation Facility, which has become a valuable resource for physicists, at the SSC and elsewhere, working on the development of the SSC detectors, and also preparing to do analysis of CDF data. Progress and plans for computing is described in Sections 4.4.3 and 6.4.

In this same time-frame the surface and underground facilities for both GEM and SDC are under final scrutiny before embarking on Title 1 design work. Planning for the start of fabrication for the major detectors, integration of the detectors with the machine and IR, development of the rest of the SSC physics program, planning for the start of test beams at the SSC, development of the SSC infrastructure for both experimental and theoretical physics - all those activities which will turn the SSC construction project into a forefront physics laboratory have begun, and involve the physicists of the SSC- staff and visitors.

4.2 GEM

From the beginning, it was clear that the SSC and its physicists were critical to the success of GEM. In contrast to SDC, GEM has no other HEP base in the US. BNL is a major contributor, but does not have sufficient resources to provide such a base, and the non-HEP laboratories in GEM do not have strong enough physics groups to direct such efforts. Thus an early strategic decision was to build a very strong effort at the SSC, with groups involved in all key activities in GEM. These groups will provide the project with liaison to and coordination with activities outside the SSC, as well as contributing to research and design of many subsystems. Because of the scale of GEM, certain systems (e.g. the magnet) must be built here. Others, like the calorimetry and muon modules, will have final assembly done here. However, even for systems like the central tracker which could be built completely off-site, we expect that strong in-house groups will be needed to provide the liaison critical for successful integration and commissioning within the detector. It is expected that the coordination of computing and simulation will be done from the SSCL, and that physicists here will be responsible for the integration of both mechanical and electronic aspects of the detector, including trigger and data acquisition.

The GEM experiment stresses the precise measurement of leptons - electrons, muons, and to a lesser extent neutrinos - and photons, and the need to have a robust detector capable of running at luminosities beyond the design luminosity of 10^{33}. This philosophy is based on the belief that these are the fundamental signatures for most of the standard list of physics opportunities which might be opened up by the SSC energy and luminosity - electroweak symmetry breaking, supersymmetry, extensions of the standard model, top and other new quarks or leptons. GEM will have moderate capabilities in tracking and hadronic calorimetry which will round out the physics program through QCD and compositeness studies. The current baseline detector is shown in Fig. 2.2-1.

The experiment grew out of the rejected L^* and EMPACT/TEXAS groups, with the addition of significant new groups in both the US and abroad. The group first met and organized in June 1991, and drafted an Expression of Interest (submitted in July) that was then encouraged by the PAC. An interim organization was established to facilitate the R&D program and also to formulate the LOI. The myriad of technologies which the collaboration inherited because of its mixed pedigree were winnowed quickly to several key options in each area, forming the basis for the LOI and the subsequent positive recommendation by the PAC in December. GEM grew from 300 physicists (244 US) from 51 institutions at the EOI stage, to over 650 (340 US) from 86 institutions now.

Much of the effort in creating the LOI was centered at the SSC. All major meetings are held here, and a pattern of presence here by top management has already been established. The total SSC contingent has grown from 12 at the EOI stage, to 31 now including 12 visitors. The program that these physicists are involved in is described below. Although it is described in terms of subsystems, there is much overlap between efforts - for example, between hardware systems and simulation or trigger efforts.

4.2.1 Computing/Simulation

Research Program Personnel:
L. Cormell, P. Dingus, Yu. Fisyak, K. McFarlane, F. Paige, A. Ostapchuk, V. Sarantsev, J. Thomas, A. Vanyashin, G. Yost

The computing/simulation effort includes work on simulation, computing R&D, slow control, on-line (Level 3), off-line (simulation, reconstruction and analysis), data base/calibration, data storage, networking, teleconferencing and coordination. Eventually physicists will be needed to work in each of these areas to participate, as well as to oversee and coordinate, the work done at participating institutions. Significant work has begun in areas described below, but other areas, though urgent, await the addition of new physicists. Particularly important is work directed towards the writing of the GEM TDR, which is planned for November 1992.

Detector simulation is one of the early tasks begun at the SSCL. This work includes performance appraisal through simple parameterizations of subsystems, which will be replaced where needed, by detailed simulation of all aspects of GEM. In early March, a first detector baseline was adopted, expanding and iterating the detector described in the LOI. This baseline is being subjected to intense engineering design and evaluation, detailed costing, and physics performance evaluation through simulation efforts at the SSCL and elsewhere. These efforts are being coordinated at the SSC by K. McFarlane with the help of F. Paige, to test the simulated detector against key physics processes. This effort is facilitated by the PDSF at the SSC.

Physicists at the SSCL have been actively involved in studying the physics performance of GEM. Vanyashin carried out the analysis of the signature for a 400 GeV t' quark for the LOI. The major problem is to separate the signal from the larger cross section for $t\,\bar{t}$, assuming a t mass of 150 GeV. Events were selected having one isolated lepton with $p_T > 150$ GeV and $|\eta| < 2.5$, $\not{E}_T > 100$ GeV as measured by a detector whose coverage was from $\eta_{max} = 3$ to $\eta_{max} = 5$, and four jets with $p_T > 50$ GeV in a cone R = 0.7. The $W \rightarrow \ell\nu$ momentum was reconstructed using the measured $\not{E}_T$ and was required to satisfy $p_{TW} > 200$GeV. The t' mass was reconstructed using $\vec{p}_{TW}$ plus the momentum of the nearest jet satisfying $\cos(\phi_W - \phi_j) > -0.8$. (Direct reconstruction of the other three jets was also considered.) The main conclusion of this analysis is that the η coverage of the detector is not crucial for this process because $\not{E}_T$ is not being used to reject a large background; Fig. 4.2.1-1 shows a clear t' peak even for $\eta_{max} = 3$.

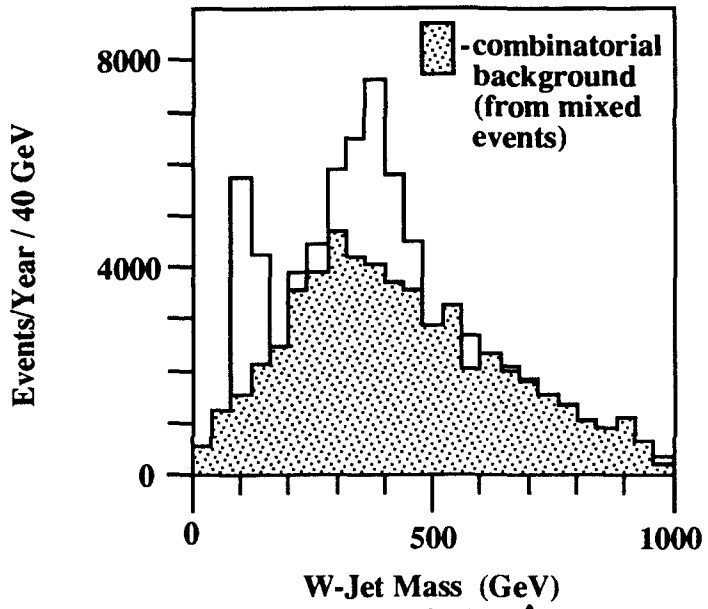

Figure 4.2.1-1: Reconstructed mass of $W \rightarrow \ell \nu$ plus an additional jet showing well separated t and t' peaks.

$\not{E}_T$ plays a more central role in the search for gluinos in the minimal supersymmetric model (MSSM). Paige (with Kahn and Murtagh at BNL) carried out the LOI analysis for a 300 GeV gluino with the full cascade decays of the MSSM, which tend to reduce the signature compared to the simplest decays. The standard model backgrounds are from heavy quarks produced at high p_T and from W and Z production. All of these were generated, and the detector response was simulated using the expected liquid-argon calorimeter resolutions, including degradations of response from the cryostat walls at $|\eta| \approx 1.5$. Events were selected having at least five jets with $p_T > 75$ GeV and $|\eta| < 3$, no muons or isolated electrons with $p_T > 20$ GeV and $|\eta| < 2.5$, and a transverse sphericity $S_T > 0.2$. The $\not{E}_T$ cross sections after these cuts for the signal and backgrounds are shown in Fig. 4.2.1-2. The signal for $\not{E}_T \approx 100$ GeV is about five times the heavy quark background, and the W and Z backgrounds are negligible. To believe such a signal one would have to measure all the QCD background processes, including t and b production as a function of p_T. This could be done by measuring the inclusive muon cross section and the $\not{E}_T$ cross section with fewer cuts. The ability of GEM to measure non isolated muons well should be valuable here.

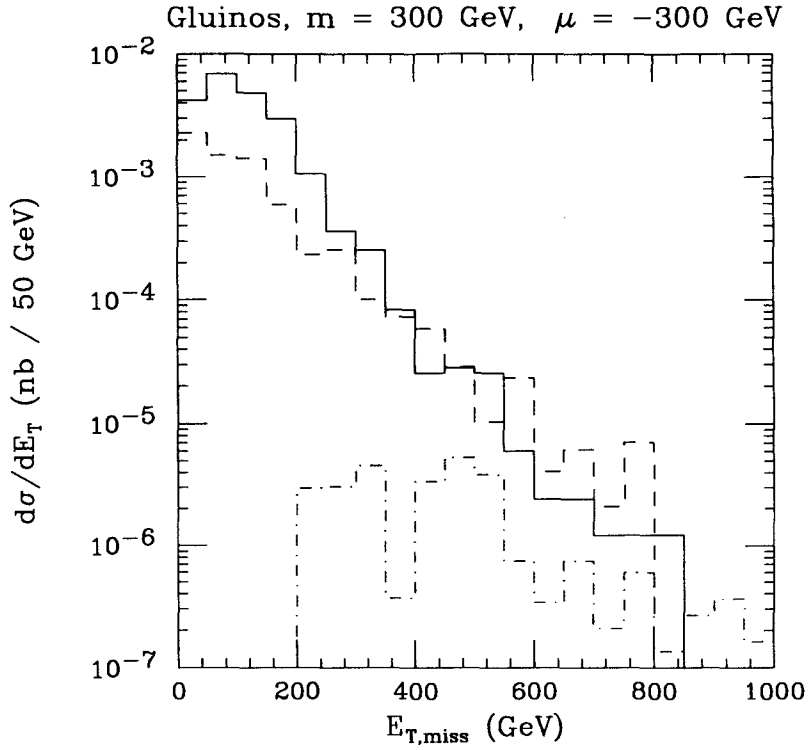

Figure 4.2.1-2: $\not{E}_T$ cross sections for backgrounds (dashed) and signal from a 300 GeV gluino

Since the gluino is a Majorana fermion, gluino pairs can give like-sign dileptons. Any gluino signature could be checked by looking for this mode, which would also help to separate the signals for the gluino and the squarks. GEM can do a good job on this in the $\mu^{\pm}\ \mu^{\pm}$ channel, which is sufficient since the gluinos are strongly produced with a large cross section. The GEM central tracker is adequate to measure the charges of about 90% of the $e^{\pm}\ e^{\pm}$ from 300 GeV gluinos, and this might provide a useful confirmation.

The LOI detector simulation for the gluino signatures did not treat performance of the forward calorimeter in much detail. The treatment has now been improved significantly. A full GEANT simulation of a proposed geometry for the GEM forward calorimeter has been carried out by the Arizona group (Rutherford, Forden, and Shupe). They find a resolution $\Delta p_T \approx 10\%$ for $|\eta| > 3$, corresponding to a fixed angular resolution. This makes sense, since the showers approximately have a fixed size and hence a fixed angular spread. This p_T resolution was then incorporated into the simplified detector simulation by Paige and Vanyashin and used to analyze a large sample of QCD jet events. These give $\not{E}_T$ both from real neutrinos coming from the heavy quarks and from mismeasurement.

The ratio

$$\mathcal{R} = \frac{\left.\frac{d\sigma}{d\not{E}_T}\right|_{\text{obs},\eta<\eta_{\max}}}{\left.\frac{d\sigma}{d\not{E}_T}\right|_{\upsilon}}$$

of observed to true $\not{E}_T$ is a measure of the detector's performance; one wants

$$\mathcal{R} \approx 1 \text{ for } \not{E}_T \approx 100 \text{ GeV}.$$

It is found that this is mainly sensitive to $\eta_{\max}$, and from Fig. 4.2.1-3 one needs $\eta_{\max} \geq 5$. The requirements are much less stringent if one makes the other cuts in the gluino analysis, but measuring the *inclusive* $\not{E}_T$ cross section is an important step in understanding the backgrounds.

If there is no Higgs or other new physics, then WW scattering will become strong at the 1 TeV scale. All charge channels will show effects of this, but the $W^\pm W^\pm$ channel is particularly interesting because there is no $q\bar{q} \rightarrow W^\pm$ background. The rates are extremely small, of order 50 events per year in the combined $\mu^\pm \mu^\pm$, $\mu^\pm e^\pm$, and $e^\pm e^\pm$ channels, so it is essential to include all of them. Thomas and Wang have carried out a GEANT simulation of the current GEM tracker design to test its ability to measure electron signs. They estimate that 6.6% of electrons with $p_T = 400$ GeV and 1.8% of electrons with $p_T = 275$ GeV are found to have the wrong sign, producing large backgrounds from mismeasured $t\,\bar{t}$ events compared to the signal. The possible solutions are to improve the tracker or to use only muons, losing a factor of four in the number of events.

Several small calculations have also been carried out. For example, when the central membrane support was proposed, Paige calculated the loss of acceptance for $H \rightarrow \mu^+\mu^-\mu^+\mu^-$. This was found to be acceptable for the required thickness. Having a local group which can carry out such calculations quickly in response to discussions at the Laboratory is imperative.

A related effort underway is the development of codes to simulate the intense radiation environment expected at the SSC, in order to evaluate the impact of this radiation on performance of and access to the detector. We have helped move the hadronic cascade code system LAHET from Los Alamos to the SSC, and are negotiating to bring the ORNL code CALOR89 to make it available to GEANT. Such codes are needed to fully simulate the neutron fluxes and radiation damage and activation, and to obtaining better estimates of calorimeter resolutions.

There are several computing R&D projects that we are involved in. The first is one initiated by SDC and SSCL on applying database techniques to HEP data; we are participating at the physicist level providing GEM-specific needs, which differ from SDC in physics driven requirements like the high data rate for the Higgs to gamma-gamma search. We are specifically interested in the development of a physicist-oriented Query Language, but are currently manpower-limited. We are involved with E-Systems, a large aerospace/defense computer company, to model and analyze the overall GEM computing system, from on-line to analysis; and in a joint project with Kung of UT Arlington, we are engaged in an examination of software development methodologies.

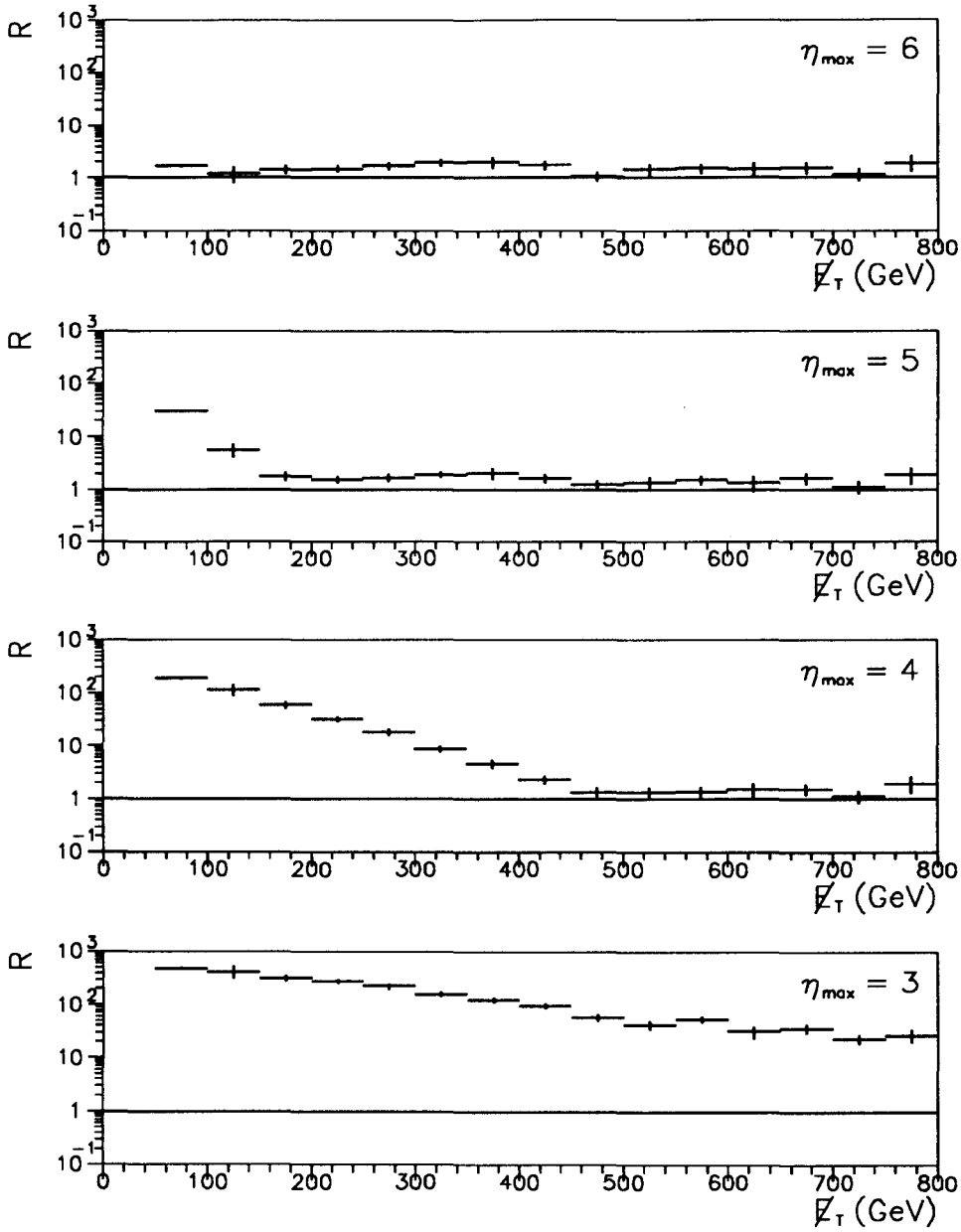

Figure 4.2.1-3: **Ratio of the Observed $\not{E}_T$ Cross Section with η_{max} = 6, 5, 4, 3 to the $\not{E}_T$ Cross Section from Real Neutrinos**

4.2.2 Muon Systems and TTR

Research Program Personnel

L. Barabash, Yu. Bonyushkin, M. Botlo, P. Dingus, Yu. Fisyak, A. Golutvin, I. Golutvin, K. McFarlane, C. Milner, G. Mitselmakher, V. Sarantsev, F. Stocker, V.Tchistilin, I. Tichamiroff, A.Vanyashin, L. Villasenor, G. Yost, V. Zhukov

4.2.2.1 Introduction

The detection and momentum analysis of muons provide important access to rare and potentially important physics at the SSC. Reactions where the muon system is essential include: Higgs scalar production, production of new heavy Z bosons, gauge boson scattering, the high mass Drell-Yan process, technicolor, and supersymmetry. The expectation is that all of these processes, if real, will occur at a low rate.

To access this important physics, the GEM Muon System will furnish the following:

(1) muon identification,

(2) charge assignment,

(3) p_T trigger - both Levels 1 and 2,

(4) beam crossing time marker, and

(5) muon momentum determination from a few GeV/c to a few TeV/c.

Muons are unique in their great penetrating power, providing a distinct advantage in carrying out searches for new physics at the SSC. With sufficient material in the electromagnetic and hadron calorimeters, particle rates in the muon system are low enough to enable triggering and momentum measurements to be made reliably with luminosities at the 10^{34} cm^{-2} s^{-1} level. The GEM muon system will detect muons with 98% solid angle coverage and with high precision measurements of the momenta.

Our design goal of a muon system with large background rejection and good momentum resolution, which can be triggered selectively on large transverse momentum, requires that the detection elements be placed outside the hadron calorimeter. Figure 4.2.2.1-1 shows a schematic of the GEM muon system. Chambers are located in three superlayers between the calorimeter and the magnetic coil or endplate in both the central and endcap regions. The amount of material within the muon tracking system is kept to a minimum so that multiple scattering is small. A trigger based on transverse momentum of the muon is generated by trigger chambers located in each of the three superlayers.

Momenta are reconstructed by measuring the sagitta S(m) given by $S = 0.3\ B\ L^2/8p$ for a trajectory at 90° to the beam, where L (m) is the length of magnetic field B (T) traversed, and p (GeV/c) is the momentum. In order to achieve good momentum resolution, the sagitta must be made as large as practically possible. Thus, $B \cdot L^2$ is the term to maximize and a large radius magnet of moderate field can provide a cost effective high resolution muon system.

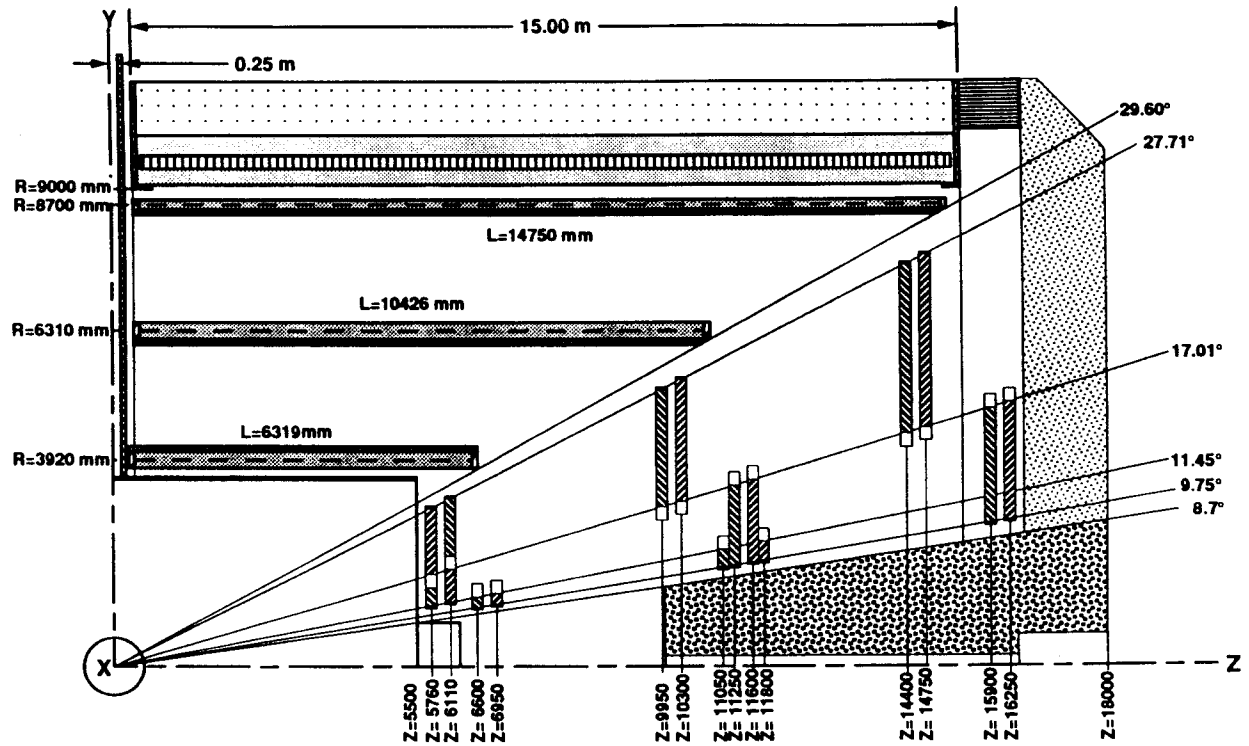

Figure 4.2.2.1-1 Overview of the GEM Muon System.

4.2.2.2 Description of Technologies

This section describes the technology options considered for the final design of the GEM muon system. For the barrel region, pressurized drift tubes (PDT) and limited streamer drift tubes (LSDT) are being investigated for the muon momentum reconstruction and Level 2 trigger. In the barrel region the Level 1 trigger and the beam cross tagging will be provided by resistive plate counters (RPC). For the endcaps cathode strip chambers (CSC) operated in the proportional mode seem to be the most attractive candidate technology. These chambers can be adapted to the radial geometry of that region, and will provide both the muon reconstruction as well as the beam tagging and Levels 1 and 2 trigger signals.

(a) Pressurized Drift Tubes. Precise tracking is possible with cylindrical tubes, operated with axes parallel to the magnetic field, due to the simple electric field configuration and the independence of the time-to-distance function on the angle of incidence. The cylindrical geometry of tubes enables improvement of resolution through pressurization as $1/\sqrt{\text{Pressure}}$ by the reduction of the diffusion coefficient, and improved statistics of cluster formation [1].

The GEM PDT's will be aluminum tubes with 300 μm wall thickness, and about 3 cm diameter. A possible configuration of the tubes is for the inner and middle modules each to consist of 8 layers of staggered tubes, and the outer to have 4 staggered layers. The number of radiation lengths in the central modules would be 8.5% X_0. The PDT alignment is based on accurate placement of wire ends relative to end plate fiducials. This can be achieved with precision machined reference end plates, and precision fabricated end plugs, pins and ferrules. It is believed

[1] Z. Zhou *et al.*, NIM A287, 439, (1990). S. Ahlen, *et al.*, Part. World 1, 168, (1990), Bing Zhou, *et al.*, IEEE Trans. NS-37, 1564 (1990), A. Tomesch, *et al.*, NIM A241, 265 (1985)

that the required precision is achievable by calculating wire position from resonant frequency measurements. Such measurements can be made non-invasively with current-magnetic field excitation, and phase shift analysis. Wire holding through crimp and solder techniques will enable long term stability. Measurements have demonstrated that wire position can be predicted correctly within a few μm. (For 4m wires tensioned at 80% of the yield strength, the sag will be about 230 μm.) At the sector level, alignment will be achieved with straight-line monitoring techniques such as those used successfully in L3.

(b) Limited Streamer Drift Tubes System. The chambers of this technology are envisaged to be rectangular boxes containing 4 layers of wires, each running through its own U-profiled cathode operated in the limited streamer mode. The positioning of the wires is achieved by supporting them on accurately machined insulating bridges running across the width of the chamber and through slots in the cathode at this support point. The bridge in turn is held against a reference point on the wall of the chamber which can be monitored or aligned from outside. The cathodes are to be made of thin aluminum, possibly coated to minimize secondary electron emission. The cathodes are held in place by a mechanical system separate from the bridges[2].

The chamber design has the flexibility of being made to any length with wire supports chosen at any point of choice to minimize sag, and thus not rely on calculating a large correction. The wires can be laid down in multiples (as is done with Iarocci tubes), inspected, and tested for position and tension before being covered. All chamber parts can be manufactured by state of the art machine shops.

The wires will be operated in limited streamer mode. It has been demonstrated that the combination of large and fast pulses give good drift time measurements [2]. The use of aluminum cathodes makes the tube itself a good transmission line that preserves the rise time of the streamer pulse for drift time measurement and gives a coarse spatial measurement along the wire using instrumentation at both ends of the wire. Because the wires lie in cathodes which are open at the top, instrumented strips can be placed over this open side to obtain a measurement of position orthogonal to the drift time measurement and correlated with it by the common timing signal. In this way an x-y coordinate for each track can be obtained all in one chamber. The chambers have been tested using Laser beams, cosmic rays, and the 0.5 TeV/c muon beam at Fermilab.

(c) Resistive Plate Counters. Resistive Plate Counters (RPC) work at a uniform electric field of about 40 kV/cm between parallel electrode plates, 2 mm thick, with a resistivity about 10^{11} Ω cm [3]. The electrode plates can be made of plastic phenolic (bakelite) or resistive glass. The field electrodes are formed by graphite varnish (~ 500 kΩ per square) painted on the outside surface of the 2 mm plates. The readout of the chambers is achieved by means of pick-up strips insulated from the field electrodes by a 0.3 mm thick polyethylene film. The voltage induced is about 0.5 V into 50 Ω with timing characteristics fast enough to tag the 16 ns beam crossings.

RPCs with dimensions up to 0.5×0.6 m^2 have been used in many experiments. It is planned that the GEM RPCs will have dimensions of up to 3.3×4.0 m^2.

The RPC system will be employed in all three superlayers of the barrel and will completely cover the precision muon measuring components as seen from the interaction point. RPCs will furnish three-dimensional space points for particles passing through the system. Short RPC strips running perpendicular to the magnetic field lines will give the x-coordinate, while long RPC strips running parallel to the magnetic field lines will give the y-coordinate.

---

[2] L. S. Osborne *et al.*, Toroidal Spectrometer Group Progress Report, SSC Prog. Rep. No. 218, September 15, 1991

[3] R. Cardarelli *et al.*, NIM A263, 20, (1988), M. Bertino et al., NIM A283, 654, (1989)

(d) Cathode Strip Chambers. The high rate environment of the endcap region makes considerable demands on the triggering and tracking technology. Hence, cathode strip chambers (CSC) are being considered. These have a high flexibility in terms of channel segmentation, pattern recognition capability, and trigger speed [4].

The chambers will be deployed in 3 superlayers at $z = 6$, 10, and 14 m. Each superlayer features modular construction with trapezoidal modules, each of which spans 22.5° of azimuth, resulting in a structure with 16-fold symmetry. The superlayers have modules containing four chambers. In the outermost superlayer only three planes will be instrumented at startup.

Each chamber consists of two cathode planes (only one segmented) with an anode plane between them. The anode wires have a pitch of 2.5 mm and the distance between the cathodes is 5 mm. The precision azimuthal coordinate is obtained by charge interpolation between neighboring strips. Measurements made with this configuration indicate a resolution of order 50 μm per strip, insensitive to anode wire placement, gas gain, pressure, temperature, and magnetic field nonuniformities.

4.2.2.3 Texas Test Rig

High precision measurement of muons is one of the fundamental goals of GEM. Achieving this goal requires construction of the world's largest magnet, a superconducting device, that must be wound and assembled on-site. High precision chambers will be built at institutions around the world, and must be brought to the SSCL, where they will be assembled into modules with extremely tight alignment and stability requirements. The scale of these projects requires the presence of a large and highly skilled group here at the SSCL. As an impetus to the formation of this group, it was proposed in November to build a cosmic ray test facility here at the SSCL - the Texas Test Rig (TTR) - to evaluate the various competing technologies proposed for use in the GEM muon system for measurement and triggering. In addition to providing a focus for GEM physicists at the SSCL, bringing together various hardware, software and data acquisition skills, this program will involve for the first time SSCL staff and visitors with a community of commuting university and laboratory physicists from outside the SSC. These physicists will come to the SSC, bringing prototypes of the various technologies for evaluation in the TTR. The TTR, shown in Figures 4.2.2.3-1 and 4.2.2.3-2, consists of an iron toroid, two planes of triggering scintillation counters, two layers of Iarocci tubes above and two below the magnet, and several compartments to place the chambers under test. The chambers to be tested include pressurized drift tubes (PDT), Limited Streamer Tubes (LSDT), Cathode Strip Chambers (CSC), and Resistive Plate Chambers (RPC) discussed above. The largest prototypes will be 4m x 1m x 0.3m, but the compartments will be 5m x 2.1m x 0.35m, to accommodate larger chambers in the future. Each chamber system will require its own gas mixture. Information from 1000 channels of TDC and ADC will be read by a data acquisition system developed here at the SSC, and processed by local off-line computers.

---

[4] R. Debbe *et al.*, BNL-45402, (presented at the Symp. on Det. Res. for SSC, Forth Worth, TX, 1990), B. Yu *et al.*, BNL-44748, (presented at 1990 IEEE Nucl. Sc. Symp. Arlington, VA (1990)

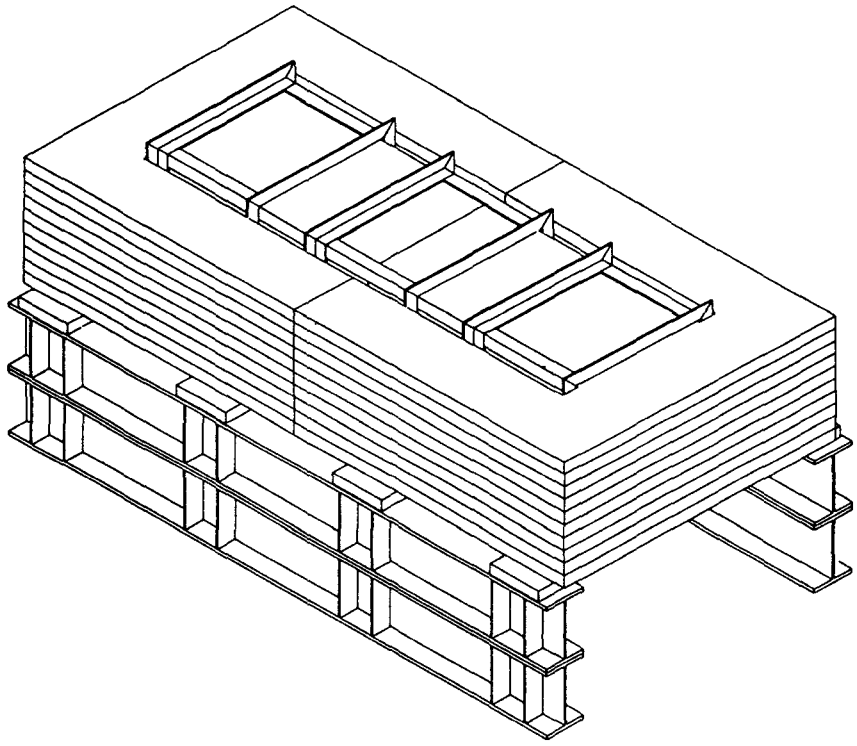

Figure 4.2.2.3-1: Perspective View of the TTR

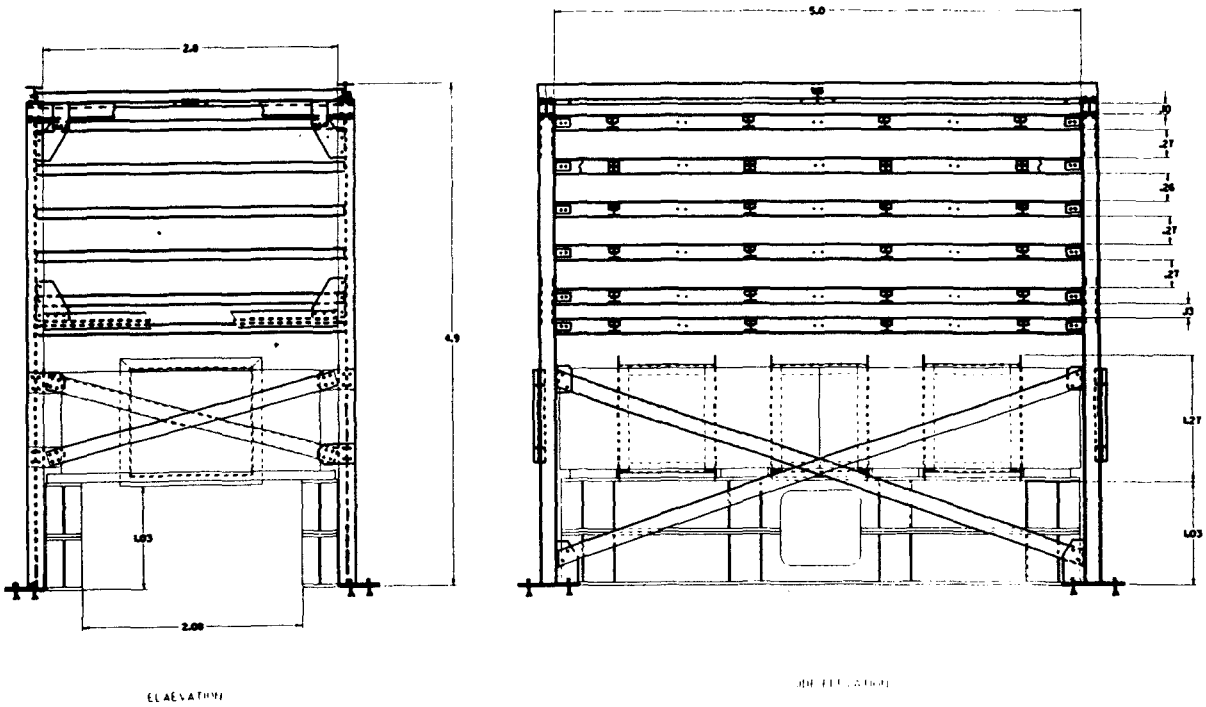

Figure 4.2.2.3-2: Muon Test Rig Structure

Building of such a system on a tight schedule, shown in Fig. 4.2.2.3-3, is a nontrivial problem, due to the lack of experience at SSCL to support experimental activity of comparable scale. As such, it has been a very valuable source for development of needed infrastructure at the SSC, particularly of the kind found at most operating HEP facilities. A small, but non-trivial example is the requirement for the use of flammable gases, and the attendant safety problems and review.

Currently we have acquired a large space in Building 4 and construction of the required foundations and clean room spaces has been completed. We have received iron from FNAL, which was sent to a local firm for machining. The magnet coils are complete, as are the support structures for the magnet and chambers, designed at the SSC. A photograph of the installed toroid and some of the physicist and support team is shown in Fig. 4.2.2.3-4. The scintillation counters are ready. Data acquisition has been designed and is functional with software being debugged, and off-line software is under development by the local group. A calculation of the accepted TTR cosmic ray muon spectrum is shown in Fig. 4.2.2.3-5.

We fully expect that the TTR will begin operations on schedule this summer, will provide critical input to the final design choices for GEM, and then will provide a critical facility for continuing development of technology for the muon system, and the laboratory that is being developed will provide the infrastructure to foster chamber work for the central tracker and test beam activities.

PRD/TTR

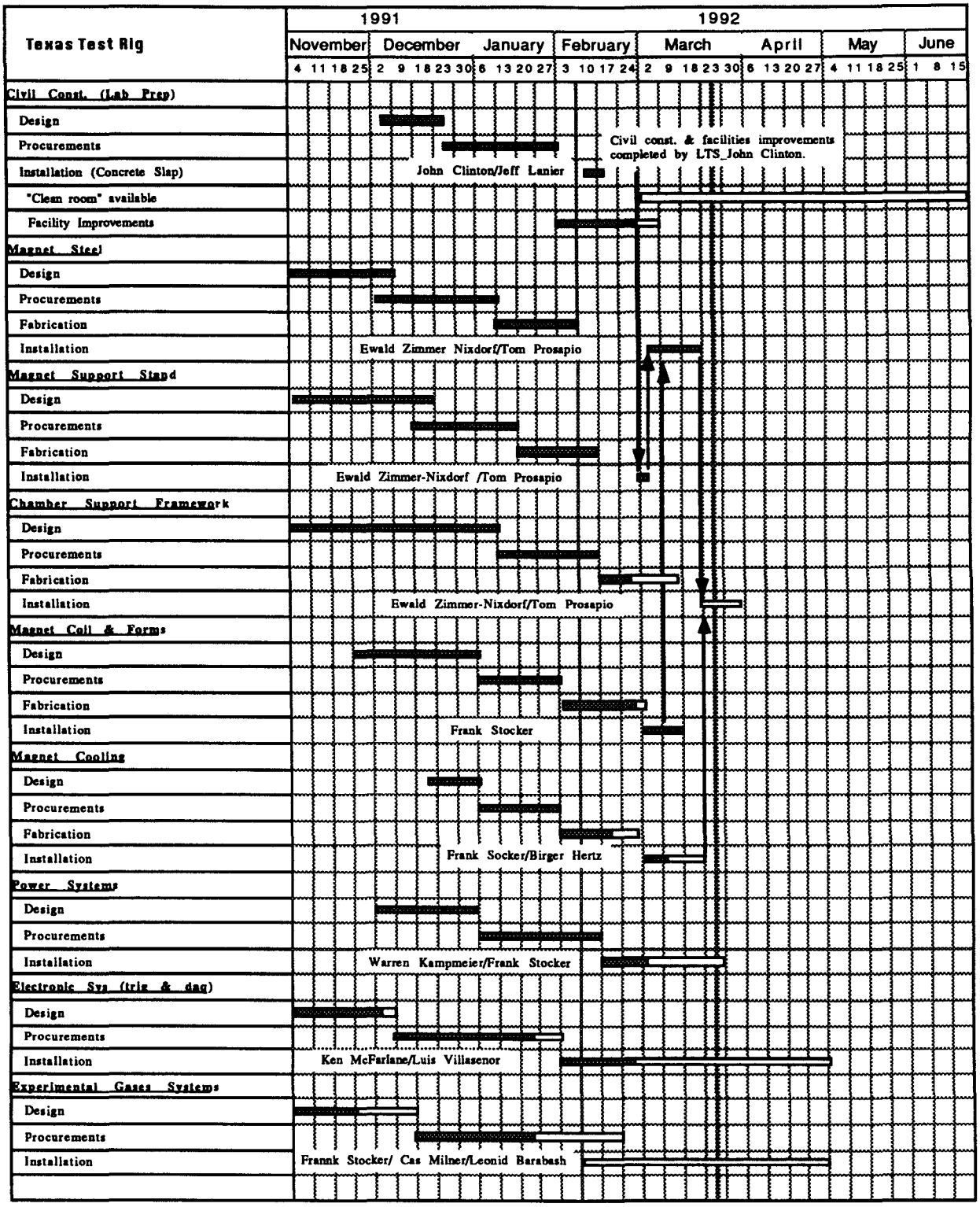

ZNX

Thursday, March 26, 1992

PRD/TTR

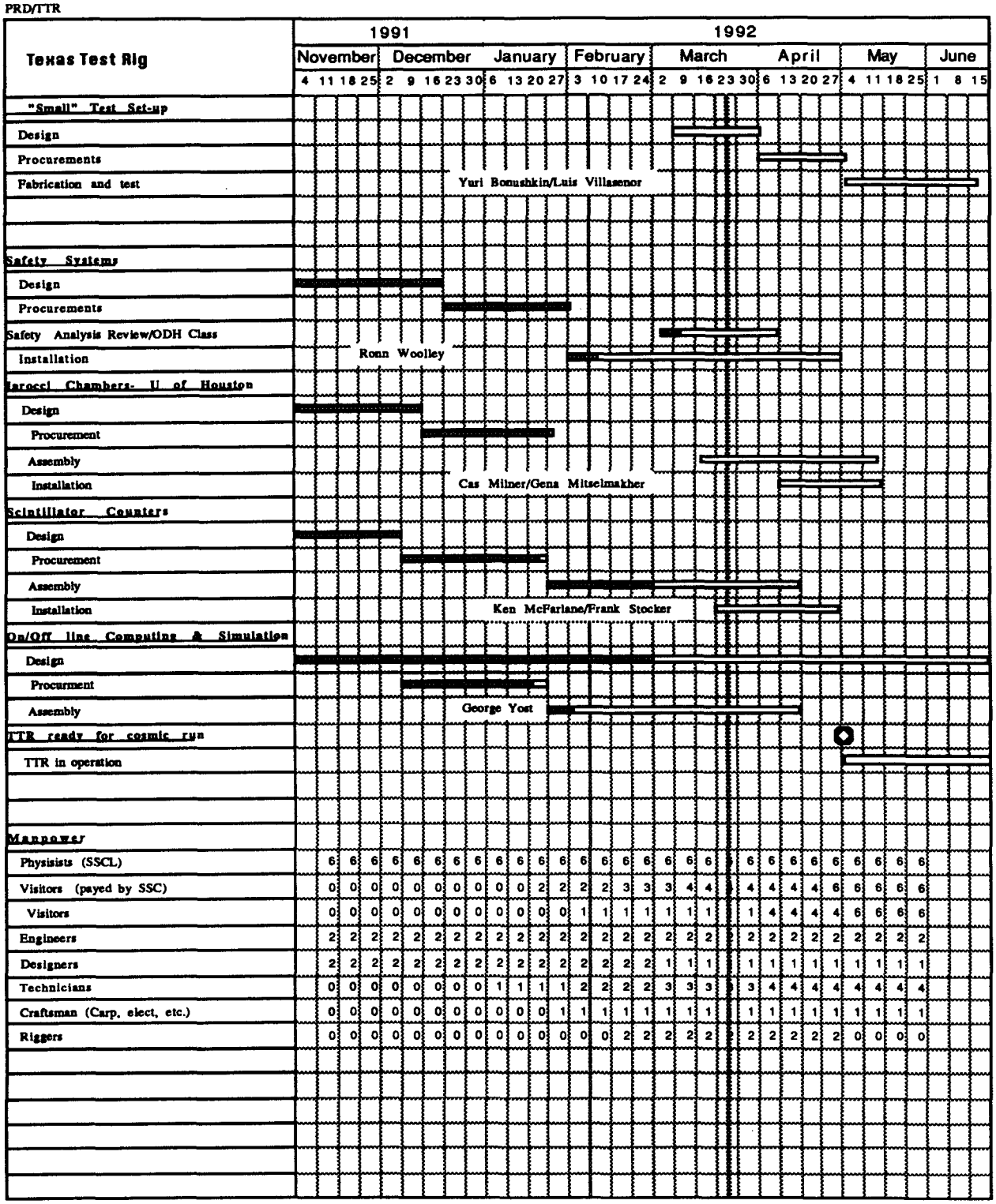

Figure 4.2.2.3-3: Texas Test Rig Schedule

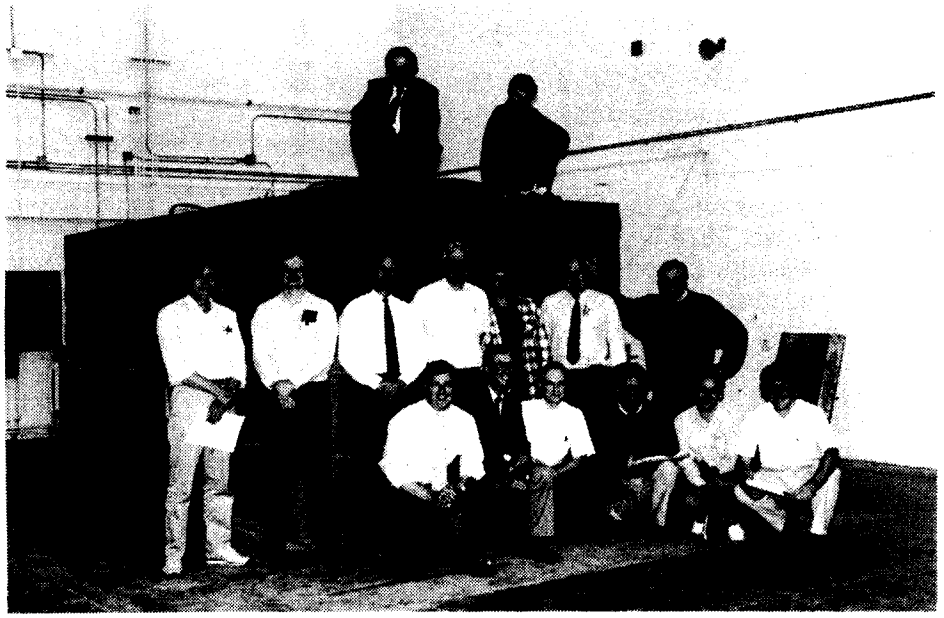

Figure 4.2.3.3-4: Photograph of TTR Magnetized Iron and some of the TTR SSC Team

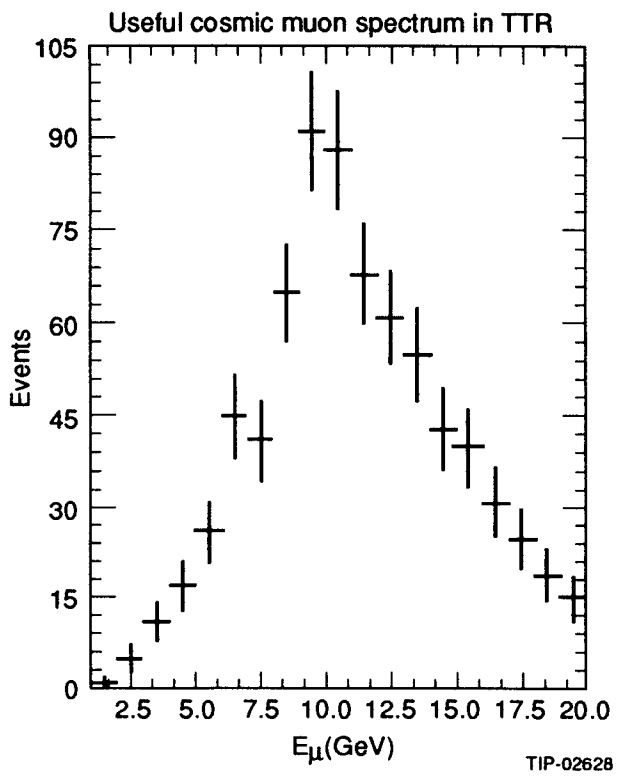

Figure 4.2.2.3-5: Useful Cosmic Muon Spectrum in TTR

4.2.3 Tracking and Beam Line
Research Program Personnel
Yu. Fisyak, K. Morgan, I. Sheer, J. Thomas, X. Yu

The Central Tracker of the GEM detector is designed to operate in the 0.8 Tesla magnetic field of the large GEM superconducting solenoid. The tracker is compact, with a 75 cm outer radius and a total length of 300 cm. It covers a pseudorapidity range of $\pm$ 2.5 units.

Since the submission of the GEM Expression of Interest, a variety of technologies were considered for use in the GEM Central Tracker. For the inner tracker silicon microstrips, silicon pixels and long drift length silicon detectors were discussed. Silicon pixel and long drift silicon detectors were considered to be too immature, with large uncertainties of performance, radiation resistance, and costs, to be a sensible choice at this time. Silicon microstrip detectors were chosen as the baseline design for the following reasons:

1. The very fine segmentation possible combined with proven high radiation resistance make this detector ideal as the element closest (10cm) to the interaction point.

2. Very high spatial resolution allows very precise vertex position and track impact parameter measurement.

3. It is a mature technology, which is presently in use in a number of fixed target and collider experiments with relatively well understood performance, radiation resistance and cost properties.

Silicon detectors were considered to be too expensive for the outer tracker. Technologies under serious discussion for outer tracker were straw tubes, scintillating fibers and interpolating cathode pad chambers. The interpolating pad chambers were chosen for the baseline design for the following reasons:

1. Pad sizes of the order of a few cm^2 in area are quite natural. This allows for a low occupancy even at a luminosity of 10^{34} $cm^{-2}s^{-1}$. Thus, this technology is suitable even at the highest luminosities of the SSC. The other technologies would result in considerably higher occupancies.

2. The pads, in some approximation, approach 3 dimensional points, which is important for good tracking in the high rate and multiplicity environment of the SSC. The two other technologies produce stereo images; i.e., all tracks projected onto a plane, which make pattern recognition more difficult in this environment.

3. Interpolating Pad Chambers are not a new technology; they have been demonstrated to have the resolution needed with chamber sizes similar to those required for the GEM tracker design.

The present baseline design consists of a Silicon Microstrip (SM) inner tracker and an Interpolating Pad Chamber (IPC) outer tracker. The geometry of the Central Tracker in this design is shown in Figure 4.2.3-1.

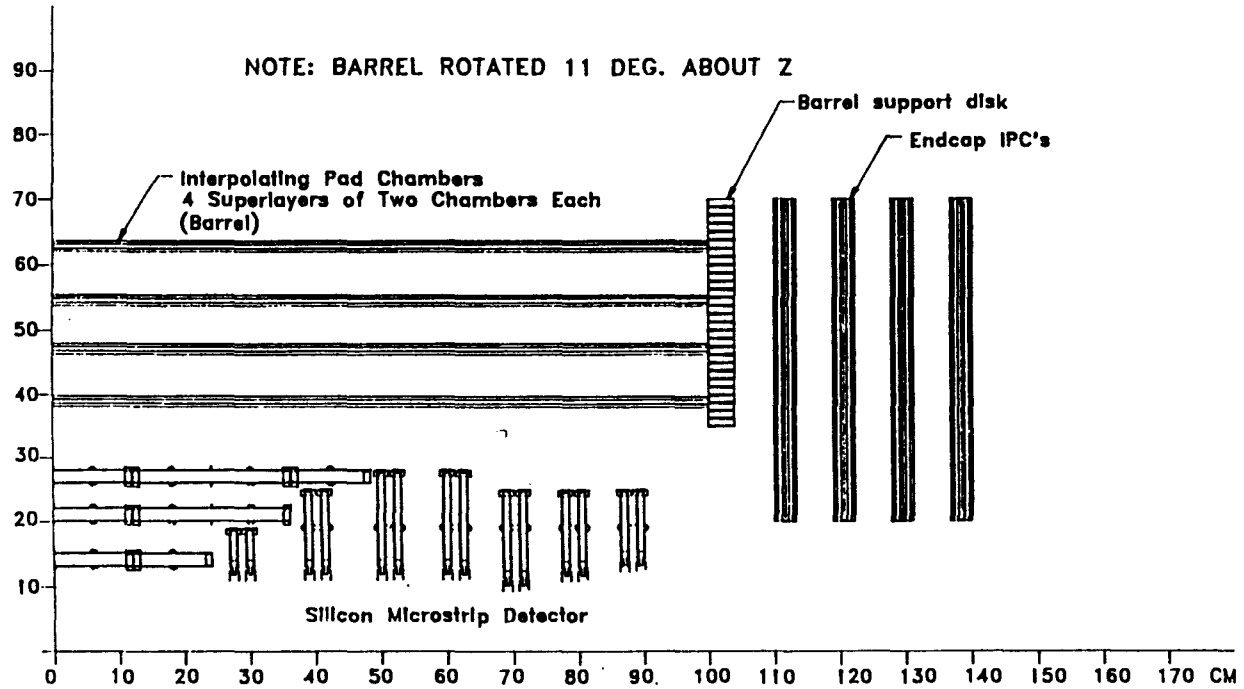

Figure 4.2.3-1: GEM Central Tracking Quadrant View

The Silicon Microstrip inner tracker consists of six layers of silicon strip ladders. Each ladder is composed of two back-to-back single sided silicon sensors with a 5 mrad stereo angle between the two sensors. Each sensor is 300μm thick with a strip pitch of 50 μm. Each pair of sensors provides a space point with a resolution of 10μm in the $r - \phi$ plane and 3mm in the $r - z$ projection. The six layers of ladders are organized into three superlayers, each of which provides a track stub to a track finding algorithm. In the forward region, the silicon sensors are mounted into disks with the strips projecting radially inward toward the beam axis. The SM is 200cm long and extends in a radius from 10 to 35cm. The total area of silicon ladders in the detector is about 7 m^2 with about 3.5×10^6 strips to be read out. The read out will be highly multiplexed, with 1028 strips to one fiber optic readout channel, for a total readout channel count of 3500.

The outer tracker consists of 8 layers of IPCs, both in the barrel region at radii between 35 and 70 cm, and in the forward region which extends from 20 to 70cm in radius. The 8 layers are arranged in 4 superlayers with 2 layers each. Each barrel layer will consist of 20 chambers, each covering 18° in azimuth, with the largest chamber being 30cm wide x 200cm long. The forward layers will be disks divided into ten trapezoidal chambers about 50cm x 50cm each. The IPCs in this system will be very similar in concept and performance to chambers with chevron shaped cathode pads which have been constructed and are now taking data in experiment E-814 at the Brookhaven AGS. These chambers have various sizes up to 50cm x 200cm and have obtained a resolution of ~50μm, or ~1% of the pad size, which is what the GEM design calls for.

Each of the chambers will be tilted in azimuth by the Lorentz angle of the gas (~6 to 9°) so that the E x B effect in the 0.8 T field does not degrade the resolution. This tilt also allows the chambers to be overlapped, eliminating dead regions due to electronics and structural elements (see Figure 4.2.3-2).

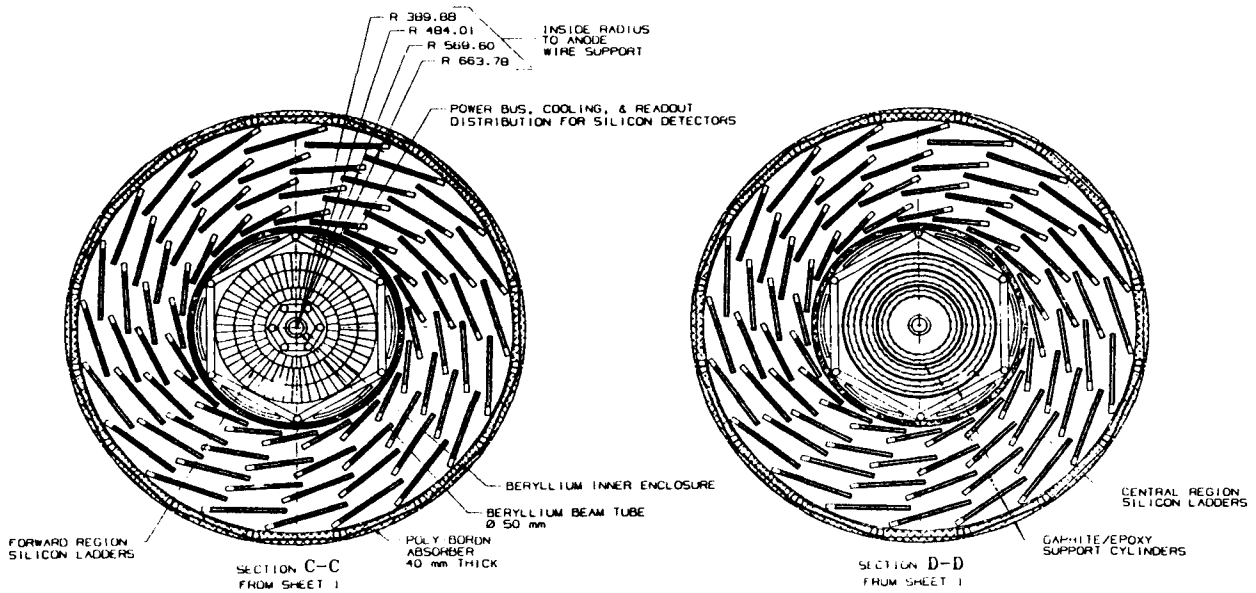

Figure 4.2.3-2: GEM Central Tracker Sections showing Silicon and Barrel IPC

The direction of good resolution in these chevron pad chambers is along the anode wire. Thus, the wires in the barrel chambers will run across the chambers, in the "ϕ direction", keeping the wire length between 15 and 30cm. In the forward chambers the wires will run in the "ϕ direction", with wire length between 10 and 40cm, as seen in Fig. 4.2.3-3.

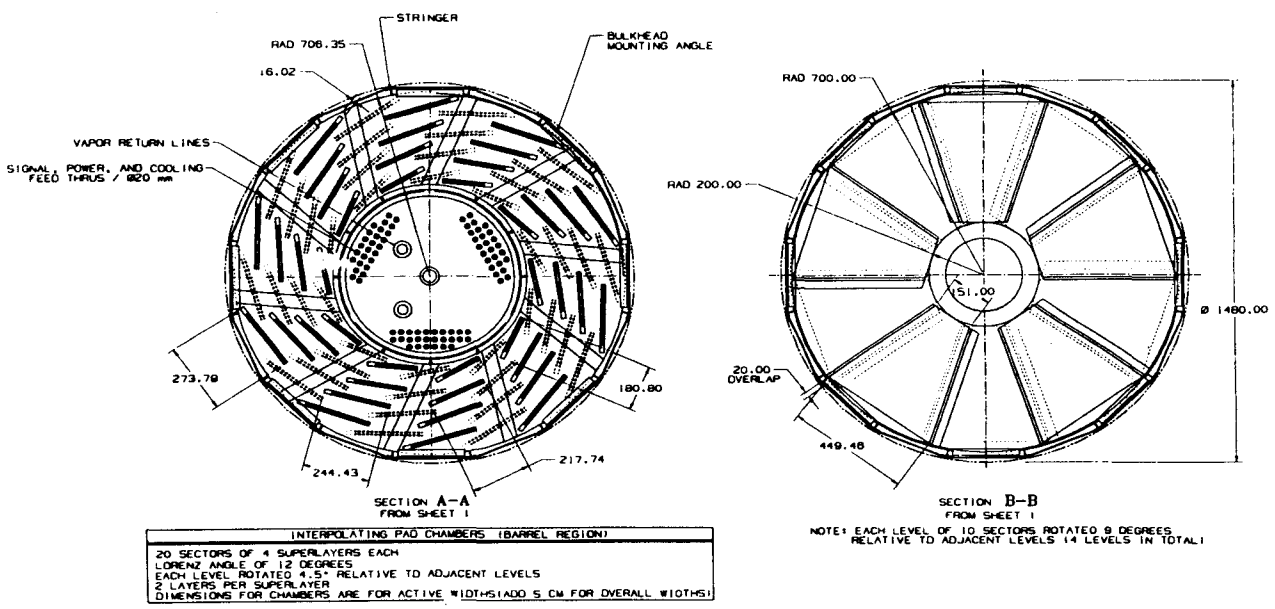

Figure 4.2.3-3: Gem Central Tracker Section showing Electronics and End IPC

In the present design pad sizes are a uniform $\Delta\eta \times \Delta\phi = 0.0007$ in all parts of the tracker. This results in a total of just under 400,000 pads for the entire device.

The anode wires will be spaced at 2.0 mm intervals. To obtain precision better than the pad size in the "Θ direction", readout of the anode wires is expected in at least one layer in each superlayer. A digital readout would provide a precision of ~600μm in this direction. This precision in each of the superlayers will provide the required $\delta \sim 1$ mm to separate event vertices at a luminosity of $10^{34}cm^{-2}s^{-1}$, when the silicon tracker may be inoperable. This would require about 100,000 wires to be read out digitally, which will be multiplexed at a level that satisfies the occupancy requirements.

The IPC readout electronics for each pad include a fast front end amplifier and shaper feeding into an analog pipeline which is multiplexed at the output by a factor of 256, giving a total of 1600 channels. The present design calls for the multiplexed analog outputs to be input to Mach-Zehnder electro-optic modulators, each of which is connected by a fiber optic cable to a remote 9 bit flash ADC system. The readout of the IPC wires can be accomplished with a simple comparator on each of the instrumented wires, followed by a multiplexed digital pipeline.

SSC Role

Previous efforts at the SSC were concentrated on developing a tracking system with Scintillating Fibers. These efforts focused on evaluation and comparison of readout devices for the fibers. These included avalanche photodiodes, multi-anode photomultipliers, and a cryogenic facility for Visible Light Photon Counters (VLPC). These efforts are still of interest to SDC, and are described later in Sec. 4.4.1.

Currently the group is concentrating on three efforts. The first is a re-evaluation of the limited goals of the GEM tracker to understand its capabilities in electron sign selection for processes like W^+W^+ scattering, which is a key signature for strong interactions in the WW sector, or a confirmation of the Standard Model nature of a light Higgs, and measurement of the asymmetry of a new heavy Z'. Fig. 4.2.3-4 shows the measured curvature distribution for high momentum tracks. We also expect to coordinate simulation activities at the SSC for the tracking, combining efforts on the SM and IPC done elsewhere.

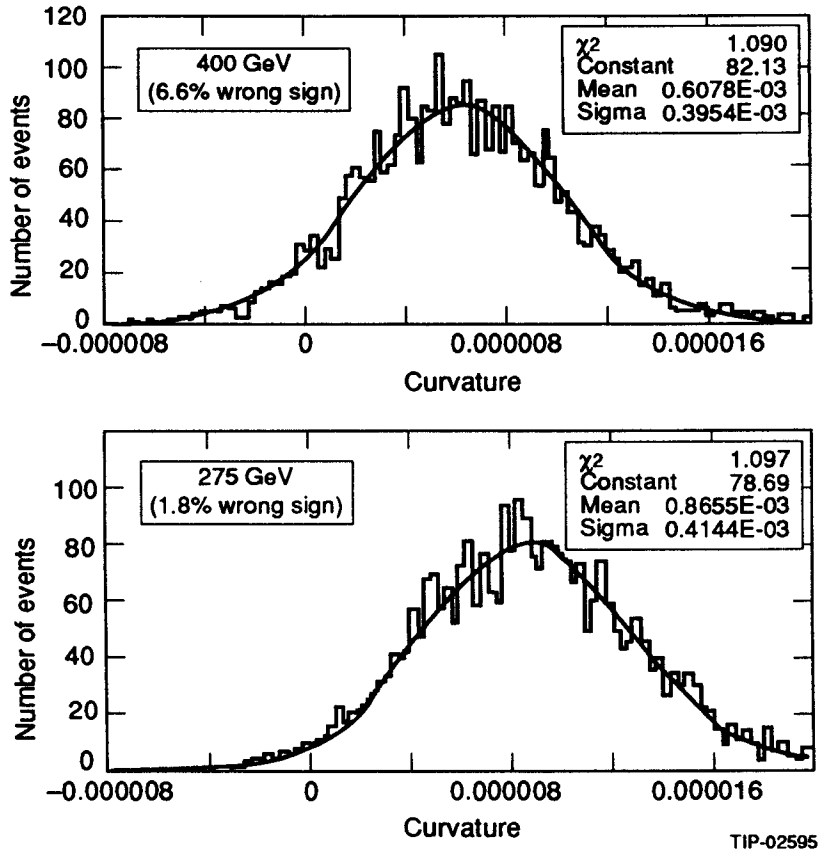

Figure 4.2.3-4: Measured Curvature in GEM Tracker

The group is also charged with integration issues for the tracker in the overall GEM design. This is particularly critical since the tracker fabrication schedule has a major impact on the order of installation of the detector, and provisions must be made in the design of GEM for tracker access during shut downs of the SSC.

A related effort is the study of issues related to the interaction of GEM with the machine. This group provides the liaison to the Accelerator Department, and is discussing issues like the final design of the Interaction Region (IR), including position and shielding of the final focus quads, machine radiation environments, and the beam line and beam pipe. The latter issue is critical because of its impact on detector assembly and the constraints of installation and vacuum may have a large effect on both tracker and forward calorimeter performance. Preliminary studies have resulted in a beam pipe concept shown in Fig. 4.2.3-5, and vacuum simulation studies are helping to determine positioning of vacuum pumping elements, so as to optimize vacuum while minimizing interference with the detector. This group is also considering issues related to the alignment of the beam pipe, detector and the machine, with a particular view to the requirements of determining vertex positions and then relating them to the external muon system - a challenging task.

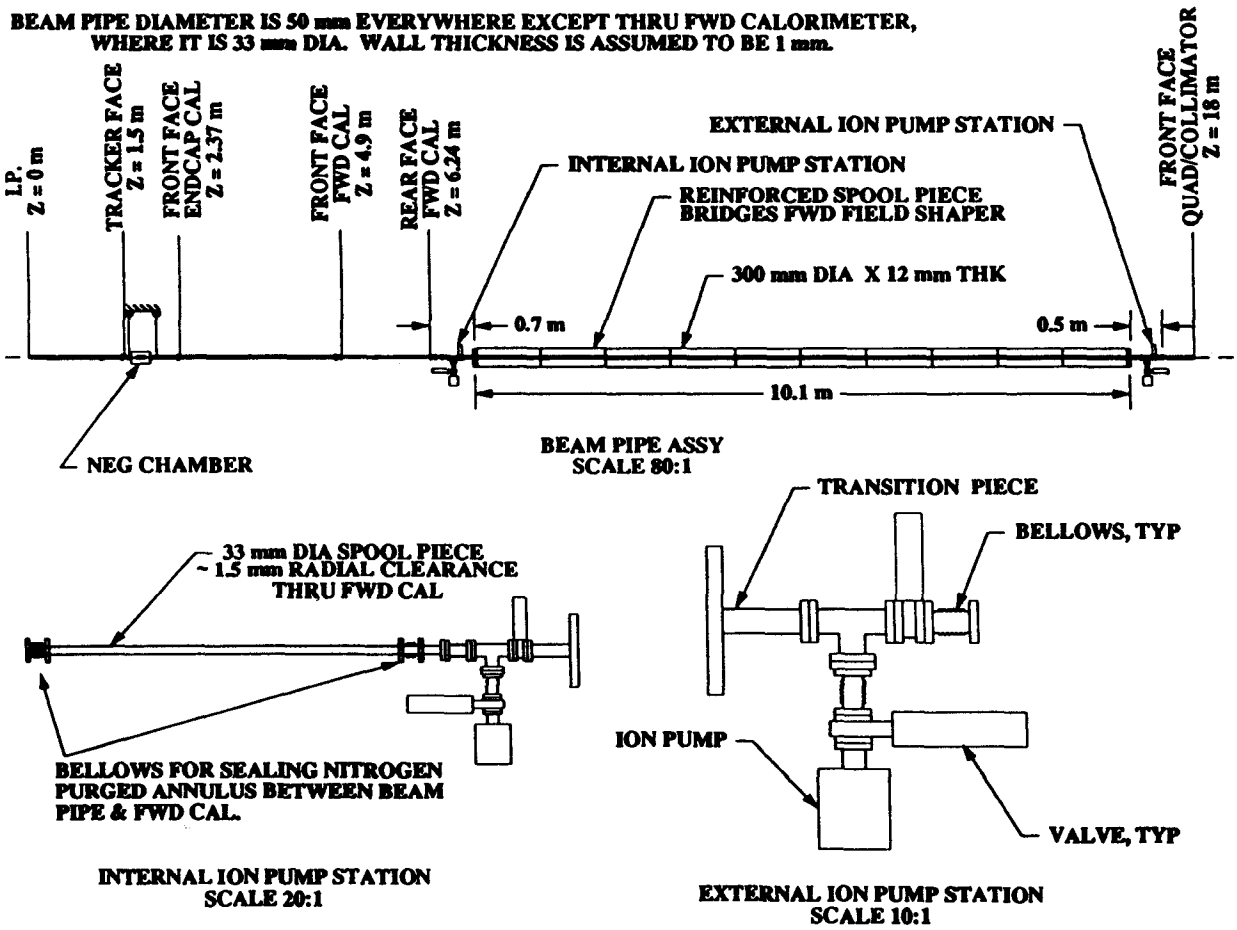

Figure 4.2.3-5: GEM Beam Pipe Concept

4.3 SDC

The Solenoidal Detector Collaboration (SDC) grew out of several initially independent US efforts concentrated at LBL, ANL, and FNAL, all of them with strong university participation, and the simultaneous activities of a number of Japanese high-energy physicists who organized and participated in a series of workshops in Japan. All of these studies were aimed at the design of a solenoidal detector for doing high-p_T physics at the SSC. At a workshop held in Fermilab in September 1989, the various groups, finding much commonality in their designs, decided to combine their activities and form a single collaboration to prepare an Expression of Interest (EOI) for submission to the SSC Laboratory. A governance document was drafted, discussed and modified at the first collaboration meeting in December 1989, and ratified shortly thereafter.

The SDC submitted its EOI in May 1990, presented its design concept to the SSCL PAC in June, and responded to ensuing PAC questions in July. The SSCL responded by requesting proponents of large high p_T detectors to combine forces where appropriate and to submit Letters-of Intent (LOI) by the end of November. The SDC submitted its Letter-of-Intent, and made its verbal presentation to the PAC in December. In January 1991, the SDC detector was approved to proceed to a full Technical Proposal.

When the SDC was initially formed in 1989, it sent out a letter to the international HEP community inviting interested collaborators to join. Since the birth of the Collaboration, a large number of new institutions have joined from both inside and outside the US, including a group at the SSC Laboratory.

The last two years have seen increasingly intense efforts by the SDC to design a detector adequately matched to the physics opportunities opened by the construction of the SSC. Activities of the SDC group at the SSC lab have included both detector construction project tasks and detector development work related to the SDC design. Among the project tasks accomplished are the completion of the LOI, numerous drawings of the overall detector concept stored in the central SDC document center at SSCL, design work on the detector facilities including the experimental hall and beam line, safety analyses of the detector design, work on the plan for test beam activities and design of the test beam facilities, and work on the DAQ system design. In addition to the direct work performed by paid staff and visitors, numerous collaboration and subgroup working meetings have been held at SSCL, with active participation by Lab staff. The SSC Lab SDC contingent has grown from two staff members at the time of the EOI to 11 FTE now.

4.3.1 Computing/Simulation

The SDC computing effort includes work on detector simulation, data storage, and on-line systems. Detector simulation work is particularly important at this stage to help guide the engineering design work. Physics studies of Z' charge asymmetries, field uniformity under various solenoid designs, calorimeter performance, track pattern recognition capability, charge identification efficiency in the tracker, and muon system performance have been carried out by SDC group members over the past year. Details of these studies are contained in the sections on detector subsystems which follow.

In addition, lab staff have supported the work of the local group and the SDC organization as a whole by maintaining and the PSDF computing facility where most of the detailed calculations are carried out.

4.3.2 Muon Systems
Research Program Personnel:
J. Bensinger, T. Fukui, V. Kubarovsky, A. Kulik, H. Lubatti, V. Molchanov, T. Pal, Skuja, A. Tsyganov

An SDC muon group was established at the SSCL at the end of FY 1991. The mission of this group is to work in collaboration with university groups to design, prototype and build the SDC muon detector and to evolve into the group which will provide for the day to day operation of the SDC muon system and provide the stable group structure into which visitors (short and long term) from the university groups can integrate. It also provides physicists with whom the university students can interact on a continuing basis while resident at the SSC. In short this mode is similar to the prevailing modus operandi at Fermilab and SLAC. Perhaps the closest model to which one can look for comparisons is the current CDF or D0 structure where a group of laboratory scientists provide the resident core of physicists, engineers and technicians which help interface the university groups as well as provide a focal point for the resident students. In establishing the SDC muon group we decided to begin our efforts by collaborating with university groups already working in the SDC muon system.

Thus we began a fruitful collaboration with H. Lubatti and the University of Washington to design the SDC central and intermediate muon system. Lubatti has organized this activity in a sabbatical at the SSCL starting in September, 1991. The Seattle-SSCL drift tube was one of four different design options which were pursued to the fabrication of prototype modules. In March 1992, the SDC Technical Board accepted the recommendation of an evaluation panel to proceed with the Seattle-SSCL option as the design of the muon system. In the following we describe the design and the contributions of the SSCL muon group to the design effort.

Description of the SDC Muon System

The muon system has three distinct functions: to trigger the detector on a muon above a threshold p_T; to identify a charged track as a muon; and to increase the precision of the momentum measurement by the inner tracker for very high p_T muons.

A schematic of the muon system is shown in Fig. 4.3.2-1. The system is divided into the central region, which includes the barrel and intermediate systems, and the forward region. The muon system has three main components: magnetized iron toroids, wire chambers, and fast counters. The effort at the SSC has been focused on the design and testing of the central chambers indicated on Fig. 4.3.2-1 by BW1, 2, 3 and IW1, 2, 3 for barrel and intermediate chambers, respectively.

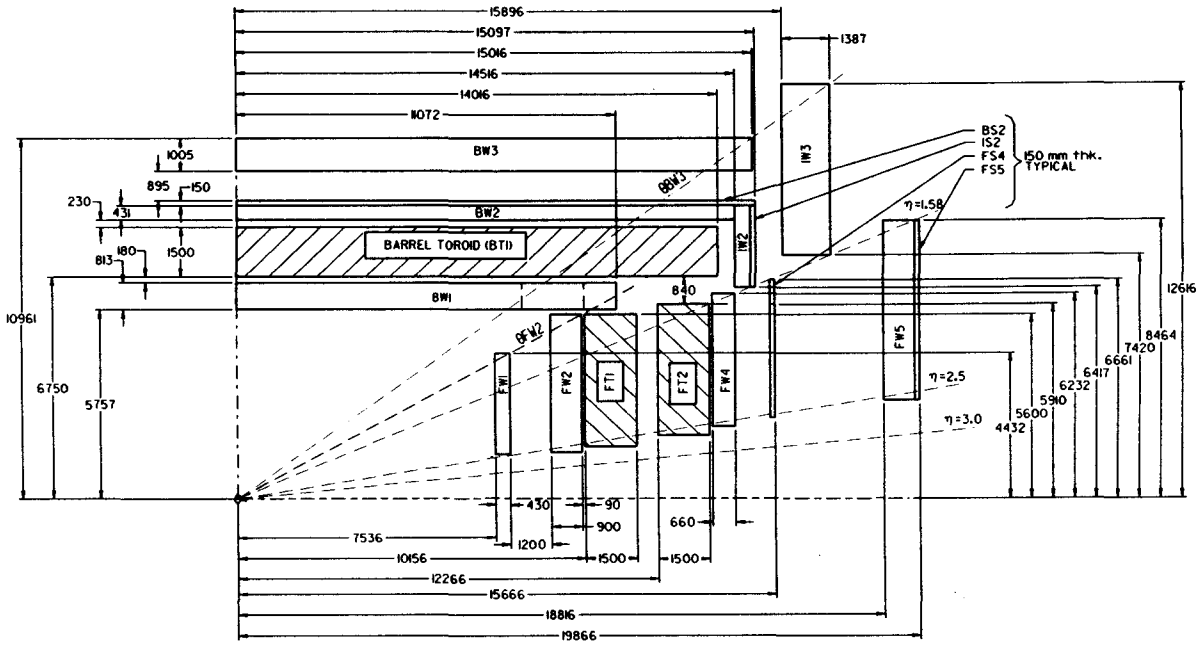

Figure 4.3.2-1: Schematic of the Muon System

Key elements of our design include field shaping to orient the drift direction in each cell to be normal to the path of a high momentum muon and the arrangement of cells in a projective geometry. Field shaping provides good resolution and the necessary two-track pair separation. The use of a projective geometry regularizes and simplifies the trigger electronics and improves the accuracy of the measurements. The timing of the signal from a drift cell in the muon detector measures the distance from the track to the anode wire. In order to make full use of that information we must know the location of the wire and of the other detectors in consistent coordinates appropriate to the physics; i.e., in the coordinates related to the interaction volume. There are several steps in getting from the wire to the physics coordinates. The first relates the wire segments to the ends of the wire, the second relates the wire ends to reference points on the module containing the wire, the third and fourth steps relate the module reference points to the central tracker reference points and relate this to the beam.

The basic approach in this design is

1. to separate the fabrication of the drift cells from that of the modules;
2. to make use of the drift tubes as structural elements of the modules; and
3. to establish the alignment and orientation of the drift cells within a module by the drift tube end caps and the module end plates.

The drift cells are aluminum drift tubes with circular cross section. Each of the cells of a module is a complete and independent, fully functional drift tube with all of the necessary passive interface components built into the end caps. The proper orientation of each tube, necessary with field shaping, is imposed during the assembly of the module by mechanical constraints (pins) which are built into the endcap support structure.

The use of round tubes in this design avoids the need for mid-span supports for the anode and so also avoids the complications which such supports incur. It allows the drift direction to be optimized for each individual tube location without affecting in any way the external configuration of the body of the tube. The homogeneity of the exteriors of the tubes makes it practical to bond all of the parts of the module together. The tubes then become structural elements of the module. This makes the module rigid without the added weight of stiffening members.

The largest modules are envisaged to be approximately 9 meters by 7.5 meters and to contain the θ, ϕ and stereo tubes. The cross-sectional view of the corners of two adjacent modules which contain four θ, four ϕ, and two stereo tubes is shown in Fig. 4.3.2-2 as an illustration. The gas manifold and gas connections as well as any electrical leads are channeled in the space between the locating end plate and protective cover. The anode wire is fixed by the end cap of the tube and located by the CNC-milled endplates.

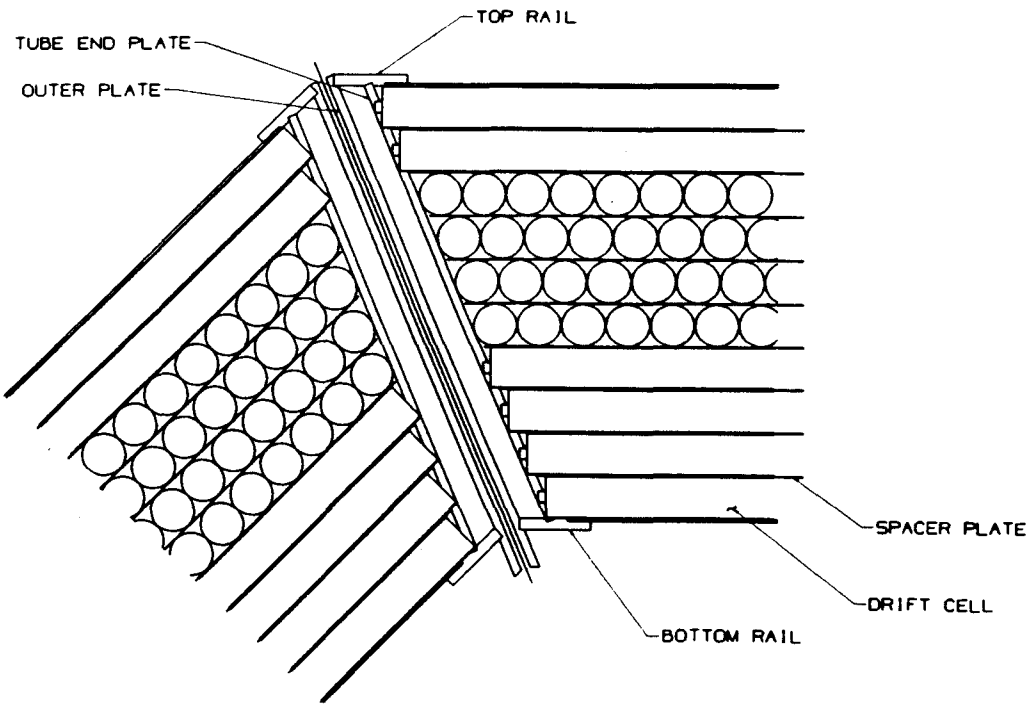

Figure 4.3.2-2: Cross Section of Adjacent Modules

Since we separate the construction of the drift cells from the module construction, the cells can be fabricated at university and national laboratories, where there is considerable accumulated experience in drift tube construction and operation. Every cell will be tested and certified before it is shipped to the module assembly sites. The mounting of the individual cells into the modules will take place at the SSCL. This allows for quality control and assurance of the alignment of the modules and location of each anode with respect to reference points on the module.

The precision inherent in this design is determined by the accuracy of a CNC mill and our ability to maintain the alignment of the modules. The position of the locating holes for one wire is related to the corresponding holes for neighboring wires and to nearby survey holes through common construction on a numerical mill, which has a precision of about 12 μm. There are several steps between the wire end location and the local survey targets on the endplate. These include the wire to endcap, endcap to mating surface of the endplate, and the endplate holes to each other and the survey targets. Since each of these will be in the 12 to 25 μm range, the overall alignment will exceed the intrinsic measurement accuracy from the drift time measurements (250 μm).

In this concept the basic sensing element is a 90 mm ID aluminum drift tube with 1.6 mm wall thickness. These tubes contain field shaping electrodes which must be oriented normal to the direction to the beam interaction point. The tubes are arranged in a projective geometry. The tubes in layers 1 and 3 and those in layers 2 and 4 form towers projecting to the vertex. Fig. 4.3.2-3 shows this geometry for the BW1 θ tubes. The projective tube layers 2 and 4 shown in Fig. 4.3.2-3 are offset from the 1 and 3 tube layers such that a particle track does not travel through the tube walls in one projective layer and the tube centers in the other. Fig. 4.3.2-4 gives an overall view of the muon modules' projective geometry for the θ and stereo layers.

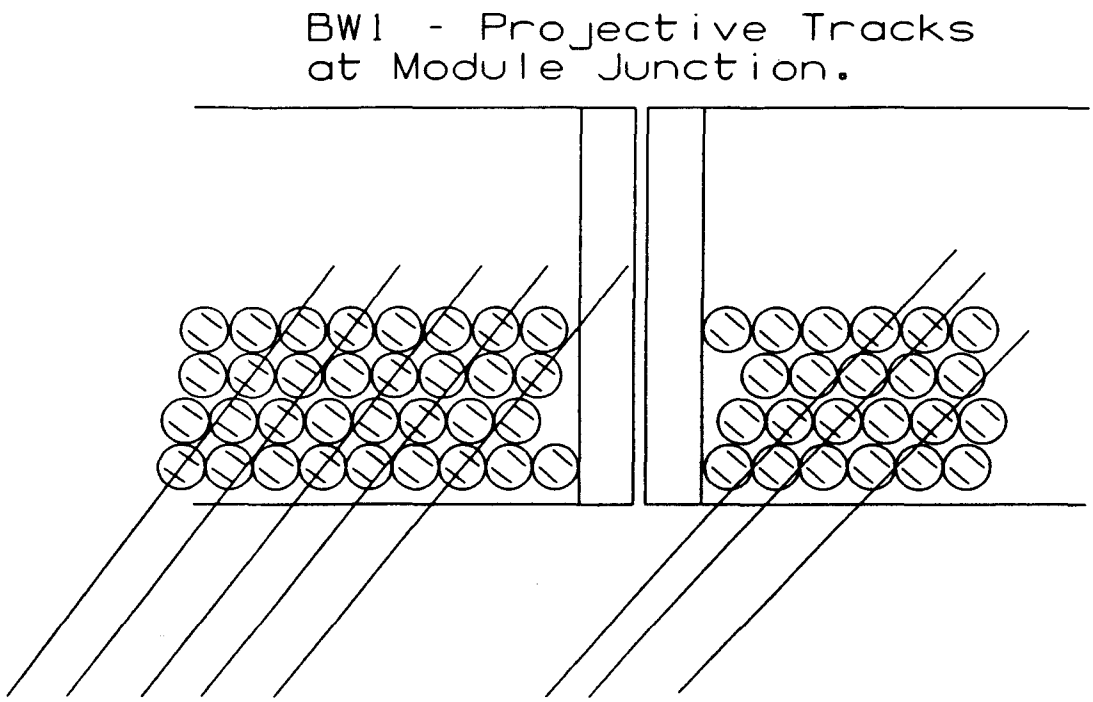

Figure 4.3.2-3: Projective Tube Layers

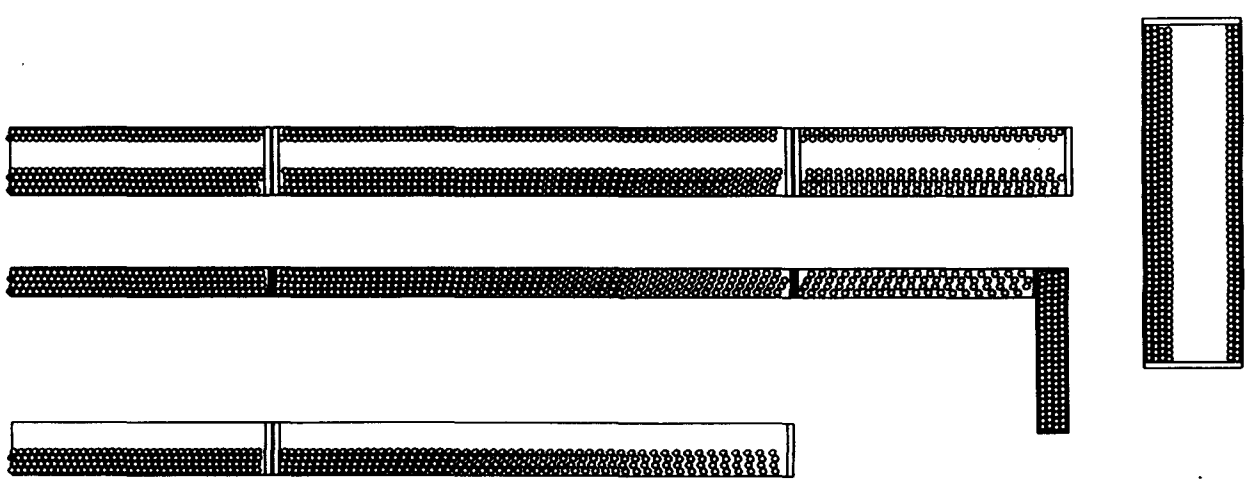

Figure 4.3.2-4: Muon Modules Overall Projective Geometry

The sense wires within the drift tubes have no support points within the tubes. They are located at their ends by crimped "feed throughs" which are located by CNC-machined holes in the end caps. In order to know the position of all points along the wires, the wire tension must be accurately controlled at assembly and the positions of the endcaps must be precisely controlled by the chamber structure. The tension of the wire is measured by pulsing the field shaping electrodes which induces a mechanical oscillation (approximately 16 Hz) and directly measures the tension. In this manner we can monitor the tension during the life time of the detector.

Table 4.3.2-1
Drift cell parameters

Inside radius	45 mm
Wall thickness	1.6 mm
Wire diameter	75 or 90 μm
Wire material	Gold plated tungsten
Wire tension	750 g or 1080 g
Electrode width	32 mm
Electrode separation	64 mm
Gas mixture	Ar-Co_2 (90-10)
Voltage at anode	6.5 kV
Voltage at electrodes	6.5 kV
Gas gain	10^5
Position resolution	250 μm
Double track separation	5 mm

Each measurement station in our chamber system consists of four layers of drift tubes which measure the muon track four times. The design goal of the single tube resolution is 250 μm. In the absence of significant systematic effects, the resolution of each station will be 125 μm. For this resolution to be fully utilized, the wire positions must be alignable to 150 μm. The mechanical design of the drift tube and chamber module are such that this should be possible.

Efforts at SSC

In FY 1992 the main activity began after the arrival of H. Lubatti from the University of Washington in September 1991. All work during this period was carried out in collaboration with the University of Washington group.

J. Thunborg and H. Lubatti worked in conjunction with lab facility engineers to develop detailed specifications for the muon lab. These included utilities, general work space, clean room, and layout tables for construction of a 9 meter prototype module. Final design was quickly achieved and by November 15, 1991 the muon lab was available for occupancy.

In parallel with effort to establish a muon lab, work was initiated with the Seattle group to finalize the design of the muon system. The description of the SDC muon system given above was the result of the collaborative effort between the SSCL-SDC muon lab and the University of Washington. The design quickly evolved into two options: one with field shaping electrodes and one without. It was decided that the prototype with no field shaping would be constructed at the University of Washington and the field shaping option would be constructed at the SDC muon lab.

The two groups worked closely to finalize the module and tube design and develop the jigging for fabrication of the tubes and prototype modules.

In November we issued a preliminary version of the Conceptual Design Report (CDR). By December we began to fabricate the no-field shaping option in Seattle and on January 10 the evaluation committee came to Seattle. On January 20 we began to assemble field shaping drift tubes and set up the jigging for the prototype at the SDC muon lab. The module was completed on the evening of January 28 and the evaluation committee arrived on January 30.

The prototypes which we constructed consisted of 30, nine meter drift tubes arranged in rows of 8,7,8,7. Fig. 4.3.2-6 shows a photograph of the prototype module. We are currently triggering on cosmic rays to study the resolution of the 75 mm drift tubes.

A data acquisition system based on CAMAC and a PC was brought on-line and is currently being used to collect cosmic ray data. We initiated a parallel effort to establish the VME/UNIX based system being developed at KEK.

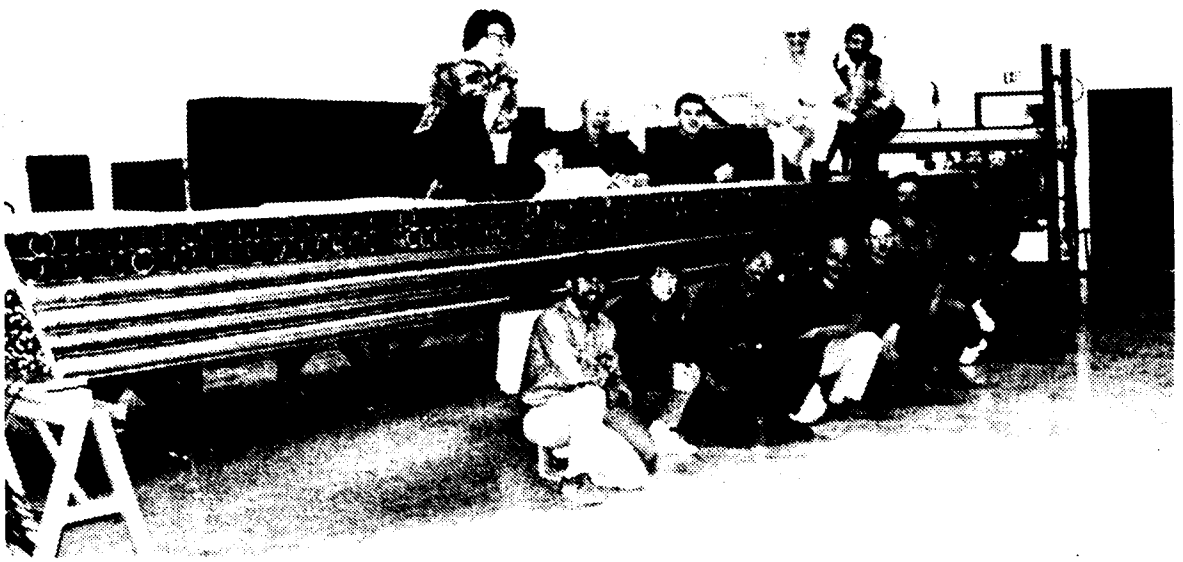

Figure 4.3.2-6: Prototype SDC muon module in SSC muon lab.

A gas mixing station was established. The heart of the station is a mass flow meter which meters up to four gases which are subsequently mixed. We are currently using this system to provide the $ArCO_2$ (90-10%) for tests of the prototype module discussed above. We plan to use this gas mixing system to study variations in the mixing ratios and the effect of small amounts of impurities such as Oxygen during the current fiscal year.

In the late fall we established a collaboration with A. White's group at the University of Texas , Arlington. This group designed and built a cosmic ray hodoscope for triggering the nine meter prototype module. They are continuing to work with us on the redesign effort which is

currently underway. We also are working with A. White and the University of Texas Automation and Robotics Research Institute (ARRI) to automate the production of the drift tube end caps.

During October and November 1991 we participated in a muon beam test at Fermilab (Fermilab T816) in collaboration with groups from U. of Arizona, U. Colorado, U. of Illinois, U. of Washington, U. of Wisconsin, U. of Maryland and groups from Japan. The test was designed to study the charged particle debris which accompanies a muon exiting an absorber. As the muon energy increases, radiative processes become more important than ionization as the energy loss mechanism. The energy at which the energy loss from radiative processes equals the energy loss from ionization (critical energy) is approximately 300 GeV in Fe. The radiative processes, e^+e^- pair production and bremsstrahlung can contribute considerable debris which exits the absorber and will register as tracks in the muon tracking chambers. In order to calibrate the Monte Carlo we designed a test to study the energy dependence of the multiplicity and angular distribution of the charged particles which accompany the muon as it leaves the absorber. The SSCL group provided some of the FASTBUS electronics, participated in the data taking, and is currently working on the analysis of the data taken at muon energies of 90, 210 , 480 and 550 GeV.

4.3.3 Calorimetry
Research Program Personnel:
G. Abrams, C. Blocker, J. Budagov, J. Siegrist, M. Turcotte, L. Villasenor, J. Yarba

The calorimeter of the SDC detector will play a pivotal role in many physics measurements at the SSC, as it is crucial for the identification and measurement of high energy electrons, photons, jets, and weakly interacting particles (such as neutrinos) via the technique of missing transverse energy. The calorimeter system must meet and maintain the level of performance necessary to do the physics anticipated at the SSC.

Since leptons will play a central role in most searches for new phenomena at SSC energies, the ability of the EM calorimeter to identify and measure electrons is a particularly important design consideration. For example, the detection of intermediate vector bosons (Ws and Zs) through their leptonic decays will be necessary for the search for new high mass particles, such as a high mass Higgs.

Another important capability of the EM calorimeter is to find and measure the mass and width of a potential high-mass Z' decaying to an electron-position pair. Since the width of such a Z' is expected to be 7%, it is important to keep the contribution of the energy resolution to the width to under 7%.

Another crucial requirement on the EM calorimeter is finding a low-mass Higgs (mass much less than twice the W mass). It is thought that the most promising signature for such a Higgs is its decay to two photons. The branching ratio for this decay is small, so it is imperative that the mass resolution be good enough to see such a signal above a substantial continuum background, even in associated production modes.

The hadron calorimeter, in conjunction with the electromagnetic calorimeter, is important for the identification and energy measurement of jets. For steeply falling cross sections, such as the single jet inclusive differential cross section, it is important to understand the energy scale of the calorimeter, since a small error in the energy scale of the jets is equivalent to a large error in the differential cross section.

Both the hadronic and electromagnetic calorimeters are important to the measurement of missing transverse energy, and hence to the detection of neutrinos and other potential weakly interacting particles such as gluinos. In particular, spatial uniformity of the calorimeter is important to prevent spuriously large missing transverse energies.

Development work on several candidate calorimeter technologies was carried out by the community in FY90 and FY 1991 through the 'generic' and 'large subsystem' SSC detector R&D programs. The SSCL group participated in research on the Liquid Argon option in FY 1991, with special emphasis on the Liquid Argon option for the SDC. This work at SSCL was a continuation of work initiated by two of us (Abrams, Siegrist) at LBL in FY90 in collaboration with KEK and BNL.

SSCL physicists participated in several important milestones during FY 1991 concerned with the SDC calorimeter decision process. The main milestones this year were the November 1990 SDC calorimeter review and document, the draft SDC calorimeter requirements document, the prototype liquid argon EM module that was designed and constructed at SSCL and tested at BNL, and the SDC Liquid Argon calorimeter conceptual design report. Elements of all of these activities were supported by this grant along with large subsystem proposal funding. The following paragraphs summarize the work and findings in each of the major activities.

In the fall of 1990, the SDC had four calorimeter technologies under consideration: warm liquids, liquid argon, 'pasta' scintillator, and tile-fiber scintillator. At the November review, two technologies were chosen to be supported by SDC to move to the conceptual design stage. In addition, a number of critical issues for the chosen technologies were identified. The need for a design requirements document was expressed, and the process to move toward a final decision for SDC was outlined.

The conclusions and material presented at the review were compiled into a report by one of us (Siegrist). The general conclusions of the review were that Liquid Argon and tile-fiber calorimetry techniques appeared to be the most promising for SDC. While a strong preference in favor of the scintillator solution was expressed, it was felt that the risk of proceeding with only one technology at that time was too high, and two technologies with complementary risks should be carried by the collaboration.

The critical issues identified at the November review for liquid argon included electron acceptance, cryostat walls at the $\eta = 3$ boundary, the value of e/h in Pb-LAr, the speed of response, the electronic noise, the impact of pileup, the location of the preamplifiers, safety, cost, and integration of the cryostat design with the rest of the SDC design. The critical issues list for the scintillator was much shorter: impact of radiation damage on the resolution, radiation hardness of the optical system, cost, and the impact and value of e/h in the design. The review guided the efforts of both the SDC Liquid Argon and tile-fiber groups for the remainder of the year. A date of September 1991 was set for the final SDC decision on the calorimeter technology.

At the November review, the collaboration realized that the design requirements on the calorimeter performance were not well enough understood. An extensive simulation effort was continued after the review and focused on generation of a comprehensive draft requirements document by August 1991 in preparation for review at the August SDC collaboration meeting. This document was edited by one of us (Siegrist) and covers work on calorimeter requirements from both inside and outside the SDC collaboration. In several areas, members of the SSCL staff made direct contributions to the document, notably in pileup and signal processing, $\not{E}_T$, and high luminosity considerations. This work continues in FY 1992 (see below).

The Liquid Argon Large subsystem proposal test beam run ended June 30, 1991. SSCL physicists contributed to the effort mainly during June 1991 while tests were performed on the EM prototype module. The data from these tests are still being analyzed, but the trend is clear: the concepts and ideas behind the Liquid Argon design work. Details of the beam test measurements are given in Appendix C and are summarized here.

A schematic drawing of the beamline setup is shown in Fig. 4.3.3-1. The calorimeter was installed inside a vacuum insulated aluminum cryostat and tested in the AGS A3 test beam line at

BNL. Two Cerenkov counters were used to separate electrons from pions and muons. A large veto counter indicated beam halo and upstream interactions. A small counter was installed downstream of the calorimeter to identify muons. A hodoscope of 1mm scintillating fibers provided vertical and horizontal position measurements.

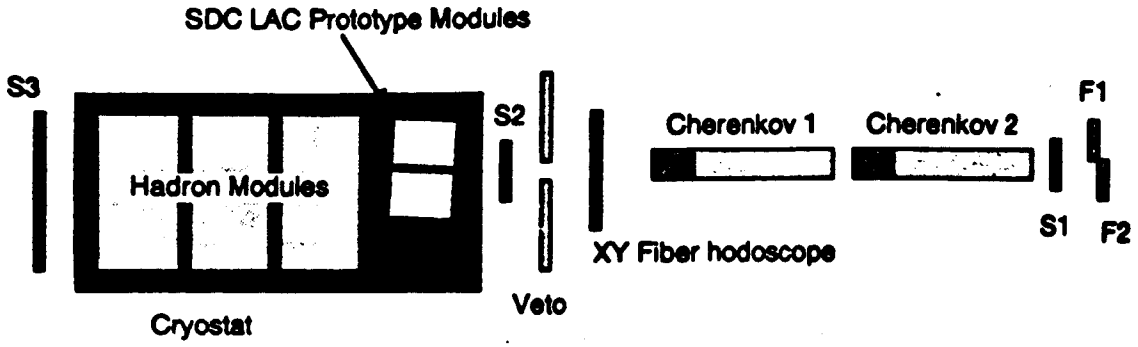

Figure 4.3.3-1: Schematic View of the BNL Spring 91 Test

The EM test calorimeter built at the SSC consists of two modules, each with six towers (Fig. 4.3.3-2). In depth, each tower consists of a massless gap layer, EM1 (5 layers), a shower max strip layer, and EM2 (19 layers). The lead thickness is 6 mm, vs 4mm for the SDC design. The signals are carried by strip lines to the back of each module, where the electronics are located. No preamp cooling was necessary for this test since any bubbles that might be formed rise harmlessly in the vertical direction. The high voltage was distributed along the top of the modules, and the strip layers were also read out on the top. The azimuthal gap between modules was set with precision calipers to 3mm, the value appropriate for SDC.

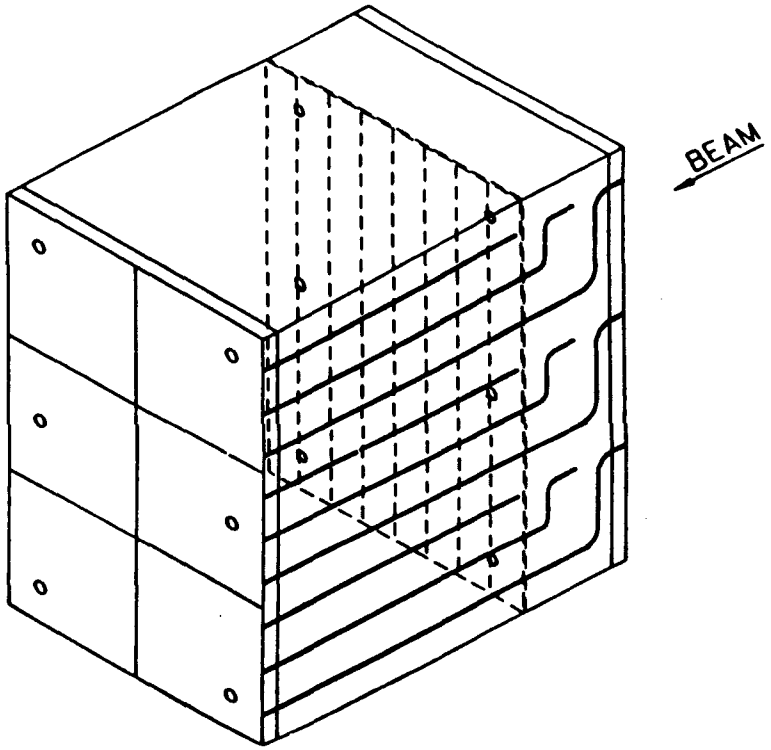

Figure 4.3.3-2: Schematic of the EM Test Module

In general, the EM prototype module behaved as expected. One of the major advantages of a Liquid Argon calorimeter is the ability to predict much of its behaviour from first principles. Fig. 4.3.3-3 shows the calibrated EM1 + EM2 energy peak for 10 GeV incident electrons. The resolution is $\sigma_E/E = 0.057$, corresponding to $10\%/\sqrt{E}$, in agreement with simulations. The spatial uniformity (which contributes to the constant term in the energy resolution) was $\pm$ 0.5%. The electronic noise was predicted, and measured to be about 17 MeV for the front EM section and 60 MeV for the rear EM section.

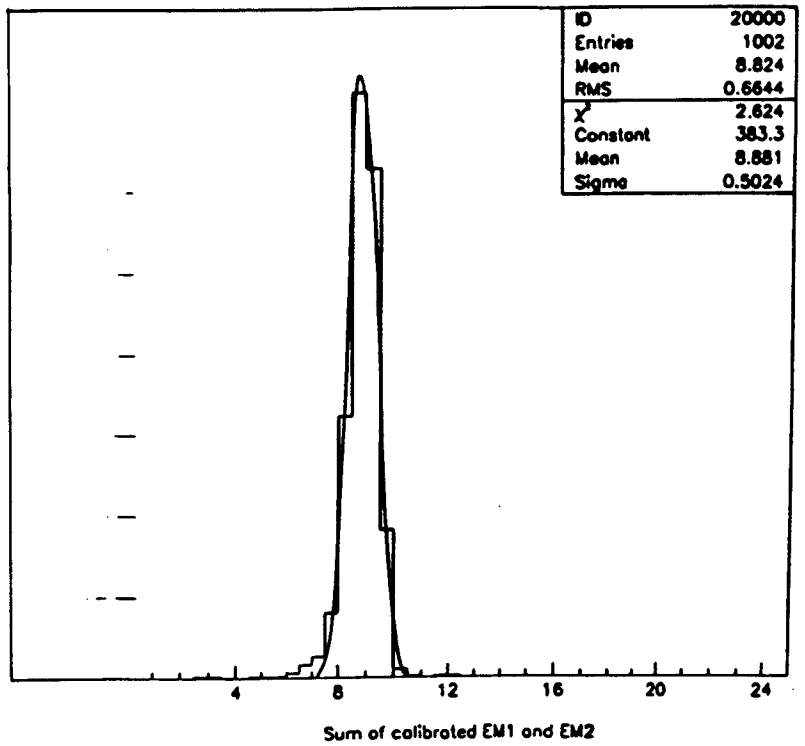

Figure 4.3.3-3: Calibrated Energy Distribution for 10 GeV Incident Electrons, Strip Energy Ignored.

One of the general worries about liquid argon calorimetry is the speed of the signal. In the BNL beam test, acceptable performance was obtained for peaking times as low as 50 ns. In addition, the timing resolution (that is, the precision to which the start time of a pulse could be measured) was 1.5± 0.2 ns. Both of these are sufficiently good for an SSC calorimeter.

Another advantage of Liquid Argon calorimetry is that the cracks between towers can be kept quite small. In the EM prototype module, the crack between towers caused less than a 3.2% dip in the response while the energy resolution rose to $24\%/\sqrt{E}$, at 10 GeV. Both of these are quite acceptable.

The hadron calorimeter was exposed to beams of momentum 0.5, 1, 2, 3.5, 5, 7.5, 15, and 20 GeV/c. The e/π ratio reaches its maximum value of 1.25 near 5 GeV and drops to a value of 1.15 at 20 GeV. Fig. 4.3.3-4 is for a nominal shaping time of 100 ns. We have also measured e/π for shaping times of 50 and 200 ns; within the precision of the existing data, we do not see any variation in the ratio attributable to a change in shaping time. the energy resolution for pions was measured online to be approximately $70\%/\sqrt{E}$.

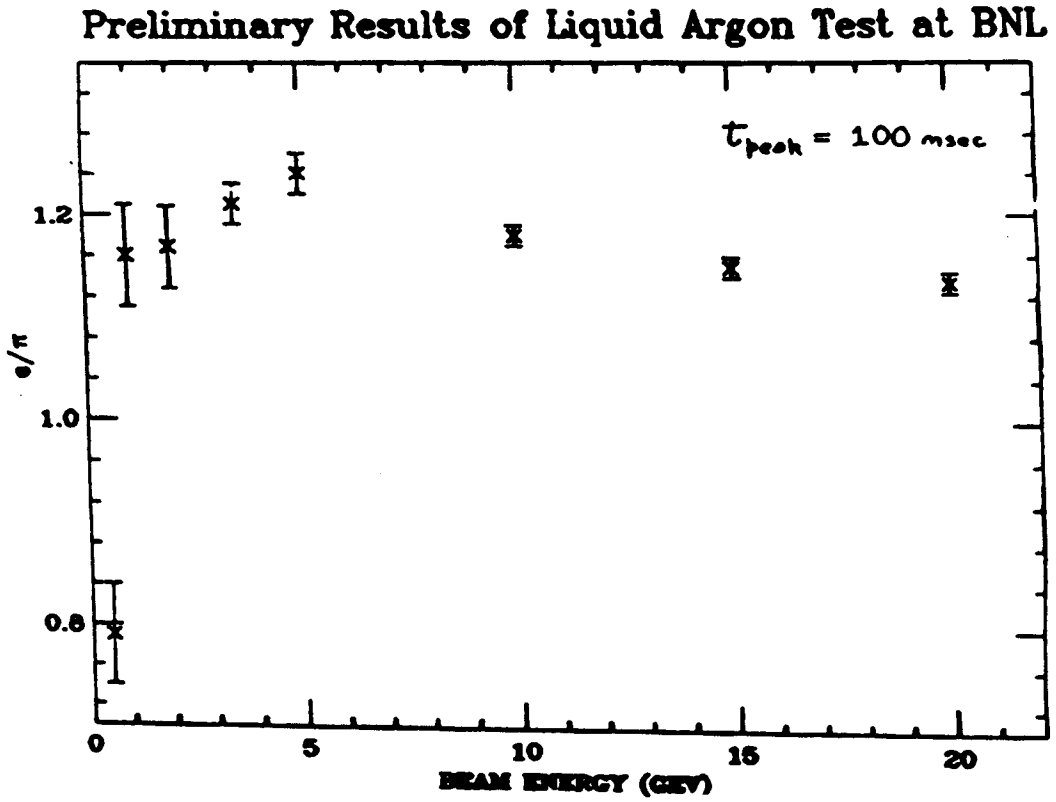

Figure 4.3.3-4: Measured e/π vs Beam Energy

Based on the test beam work at BNL, and other work, a Liquid Argon Conceptual Design Report was written. This report served as one of the documents that formed the basis of the SDC Calorimeter Decision. A summary is given in Appendix C1. The conclusion was that Liquid Argon is a workable and viable solution to the problems posed to calorimetry at the SSC.

At the September SDC technical board meeting, the decision was reached to proceed with the tile-fiber calorimeter design. Both the Liquid Argon option and the tile-fiber design were judged to be viable options for SDC. However, the list of small problems with the Liquid Argon design, and the potential for further improvement of the scintillator design with more R&D weighed in favor of scintillator.

FY 1992 Activities

SDC has selected a read-out technology based on the use of scintillating plastic for light production, wavelength shifting scintillating fibers for light capture, clear fibers for light transport and photomultipliers for light detection. We believe that by understanding the properties of the various elements of the detection system, we should be able to bring this technology to a higher level of quantitative and reliable predictability. In order to do so, a complete macroscopic physical model of the light generation, capture, transport and detection processes is being developed. Parameters of this model are being measured in the laboratory with the aim of maintaining a constant cross-check of the developing understanding. We expect this understanding to permeate the design of the calorimeter calibration system which is our major SDC responsibility. In addition, we have a strong effort in understanding the effects of the various calorimeter element tolerances on the energy resolution function. We have also studied (and plan to expand on this study) the energy response in the complicated region of the barrel-to-end-cap transition.

This work is being carried out in collaboration with university groups at UT Arlington and Purdue, and foreign groups in Dubna. The Arlington group is interested mainly in the light flasher needed for monitoring phototube stability and electronics needed for charge injection to monitor the performance of the downstream electronics and trigger chain. The Purdue group is interested in the mechanical design of the source driver system. The Dubna group is interested in radiation resistant plastics and the module test program. Our interest in the overall design of the calibration system and its performance is well matched to the needs of the collaboration. Physicists at SSC Lab will carry responsibility for the production testing of modules in the SSC Lab test beams where the performance of the calibration monitoring system will be measured. Thus, our group has a close connection to the effort needed to establish the beam test program at the SSC. In addition, the calibration system work leads to the online monitoring and constants determination needed once the detector becomes operational. Our work is summarized here and presented in more detail in Appendix D.

Preliminary Measurements

We have procured or assembled some of the basic equipment necessary to make measurements relevant to understanding the optics systems and photon detection.

A 25-layer tower of tile/fiber assemblies alternated with brass plates was built and cosmic ray signals were obtained from it. We have begun to use this to understand the time structure of pulses from the tile/fiber assemblies. In addition, we will use cosmic rays detected with this tower to study the response as a function of such factors as how the tile is wrapped and how the edges are treated (rough, polished, painted white, etc.).

We made measurements of the transmission and flouresence spectra of several scintillators, including NE110, the green fiber currently used in the SDC calorimeter prototypes, and several samples supplied by our Russian colleagues. We hope these measurements will help optimize the coupling of light from the tile to the fiber and thus increase the light output.

We are investigating the possibilities of putting a computer-controllable, neutral-density filter ("smart cookie") between the light fibers and the phototube. This would allow us to compensate for radiation damage easily. It would also allow us to do cleaner source calibration since we eliminate tile-tile cross talk from the penetration of the gamma rays through several layers of the calorimeter. We have made preliminary measurements on a candidate material based on encapsulated liquid crystal material, and the results are encouraging.

Optical Model

We have begun writing codes on a detailed optical model of light production, transport, absorption, reflection, re-emission in the fiber, and capture in the fiber of a tile/fiber assembly. We are trying to measure the various parameters that go into this model and compare the output of the model to measurement in the lab.

Each tower of the calorimeter will be a stack of absorber layers and scintillating tiles arranged in a pointing geometry. Each tile in the assembly is equipped with its own read-out fiber. The read-out fiber path is a loop in the volume of that tile (see Fig. 4.3.3-5). The captured end of the loop is polished as a mirror, while the free end protrudes out of the tile, between modules. Blue light generated from scintillation as the result of the passage of a charged particle in the tile plastic is reflected around the volume of the tile by hitting its inner surfaces. This light is sometimes absorbed in the tile plastic or sometimes crosses the loop of wavelength shifting fiber and with some probability, the material of the wavelength shifting fiber then scintillates in the green. The green light is then captured in the body of the fiber loop with some probability and is then transported to the outside of this loop through a splice to clear fiber with some efficiency. Some light will reflect off the polished end of the loop before exiting. Light will then be

transported by the clear fiber to an output equalization device before it enters the photomultiplier. This device, in its simplest form, is imagined to be a changeable neutral density filter. However, we are currently studying the possibility of using a digitally controlled liquid crystal light diffusion screen.

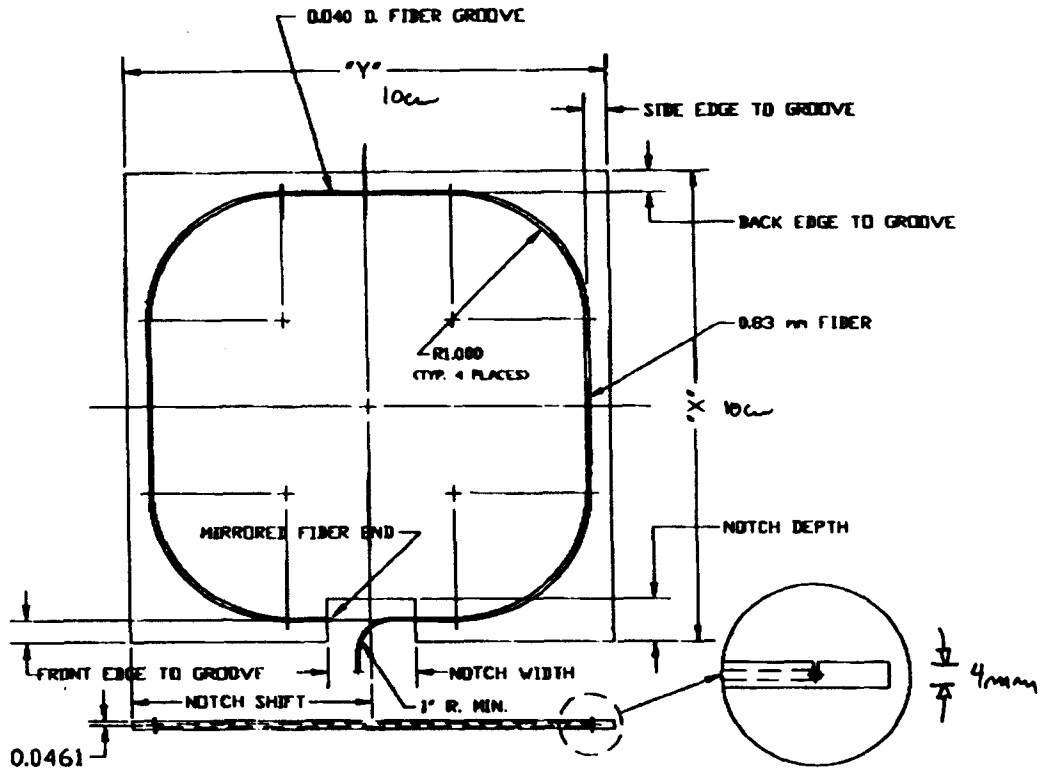

Figure 4.3.3-5: "Sigma" tile design. A 10cm X 0.4cm tile is grooved and a wavelength-shifting fiber with one end polished as a mirror is inserted. The other end exits the tile and is eventually spliced to a clear fiber.

The parameters of the optical model are therefore:

1) The number of blue photons generated per unit length along the path of charged particles traversing the plastic tile.

2) The angular distribution of these photons.

3) The light attenuation length of the photons in the tile plastic.

4) The reflection efficiency of blue light at the inner surfaces of a wrapped tile. The reflectivity of the wrapping material and the nature of the interface control both the amount of light reflection and the degree of randomization in the direction of the reflection.

5) The capture efficiency of the wavelength shifting fiber loop. This depends on the loop geometry and on the indices of refraction of the tile plastic and the fiber material. It also depends on where the wavelength shift occurs in the loop and on the attenuation length of the blue light in the green fiber.

6) The light transport efficiency of the wavelength shifting fiber. This includes the attenuation length of green light in the green fiber material.

7) The light transmission efficiency of the splice to clear fiber.

8) The light transport efficiency of the clear fiber. This includes the attenuation length of green light in the clear fiber.

9) The efficiency of transmission of the variable density neutral filter ("smart" cookie).

10) The photomultiplier transfer function including optical effects at the mating interface between the "cookie" and the entry face of the phototube.

The optical model is based on the numerical ability to count how many photons enter the photomultiplier tube as a function of the number of photons produced by the primary ionization. The amount of charge integrated at the output of the phototube is deduced from an understanding of the photomultiplier transfer function. We have decided to make use of the standard SDC simulation environment to carry through particle transport implementing our geometries with standard GEANT tools augmented with custom code to handle specific processes (light reflection, absorption and transmission). We are aware of the existence of other software that may prove to be helpful, and we are currently investigating the applicability of such code.

Fig. 4.3.3-6 shows the result of our first simulation. Plotted is the absolute number of observed photons in a perfectly absorbing wavelength shifting fiber (u -shaped) loop as a function of the distance from the tile center when a minimum ionizing particle traverses its plane in a perpendicular direction. The tile is 10cm $\times$ 10cm $\times$ 4mm while the wavelength shifting fiber has a diameter of 1mm. The minimum ionizing particle's primary ionization creates 1000 photons per millimeter emitted in random directions along its straight path. The model includes an inner surface mirror reflectivity of 0.9 for the primary ionization light and a light attenuation length of 100cm for this light in the tile plastic. The optical model is currently being refined by adding the capture efficiency of the fiber that was computed from first principles.

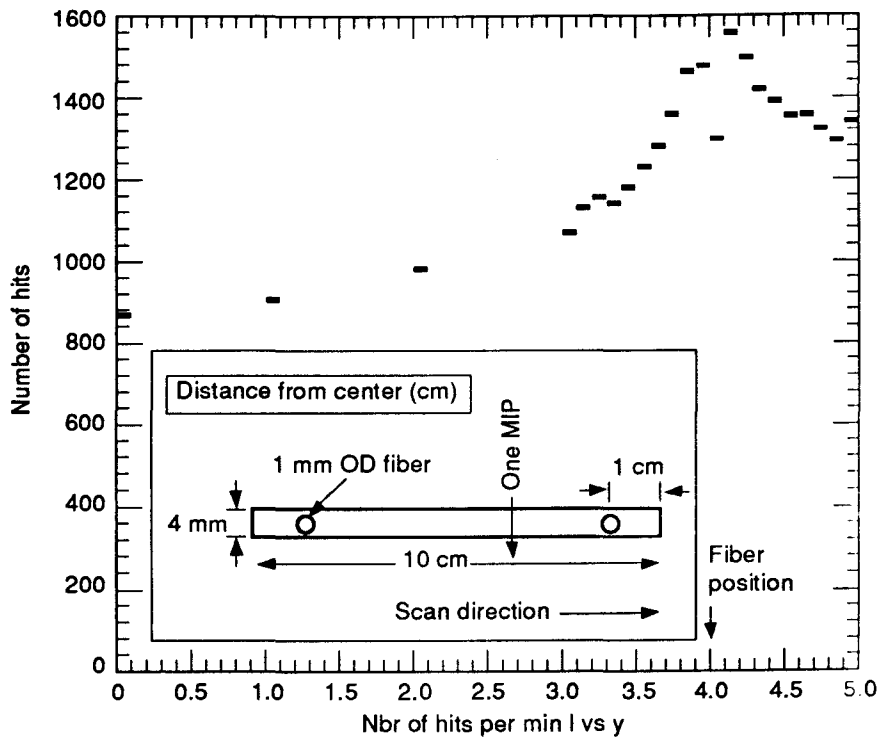

Figure 4.3.3-6: Number of hits per minimum ionizing particle versus the transverse direction from the tile center across the tile surface. The number of generated gammas per mm was 1000, the inner reflectivity of the wrapped tile was 0.9 and the attenuation length of blue light in the tile plastic was 100cm. The inset shows the geometry and scan direction.

The various parameters of the model are not all easily amenable to prediction from first principles and their measurement is currently being performed. Equipment to carry out these measurements has been procured (and is still being procured). Some relevant measurements have been presented in the section on preliminary optical measurements. In addition to the equipment used in making those measurements, we have built a dark optical test bench with photomultiplier and associated DAQ system.

Source Calibrations

The source calibration for SDC is envisaged to be monitoring the current out of the phototube when a Cs^{137} source is driven past tiles in the calorimeter. We have obtained one of the prototype source drivers designed at Purdue and are in the process of getting safety approval for the 5 mCi source.

We have a simple model, detailed GEANT simulations, and lab measurements to determine the sensitivity of the phototube current to the positioning of the source relevant to the center of a tile face. We find that the response changes by 10% for a 1mm change in the source position, indicating that some care will be needed in locating the source tubes relative to the tiles in the calorimeter.

Calorimeter Response Studies

We have done detailed GEANT simulation studies to understand the effect of calorimeter imperfections on the energy resolution. In particular, we have so far studied effects (1) tile-to-tile non uniformity, (2) light attenuation in the clear fibers, (3) response changes due to radiation damage, (4) gaps between neighboring tiles, and (5) non uniform response across a tile. For example, it is found that 10% tile-to-tile non uniformity contributes 0.6% to the constant term in the energy resolution. Similar size contributions are found for the expected size of the other imperfections.

We have also done a detailed GEANT simulation of the electron response and energy resolution in the region of the barrel-to-endcap transition in the SDC calorimeter. IN the geometry studied, two narrow but significant transition regions were found. In both regions, the energy resolution was significantly worse than the nominal resolution over a small region of pseudorapidity (Fig. 4.3.3-7).

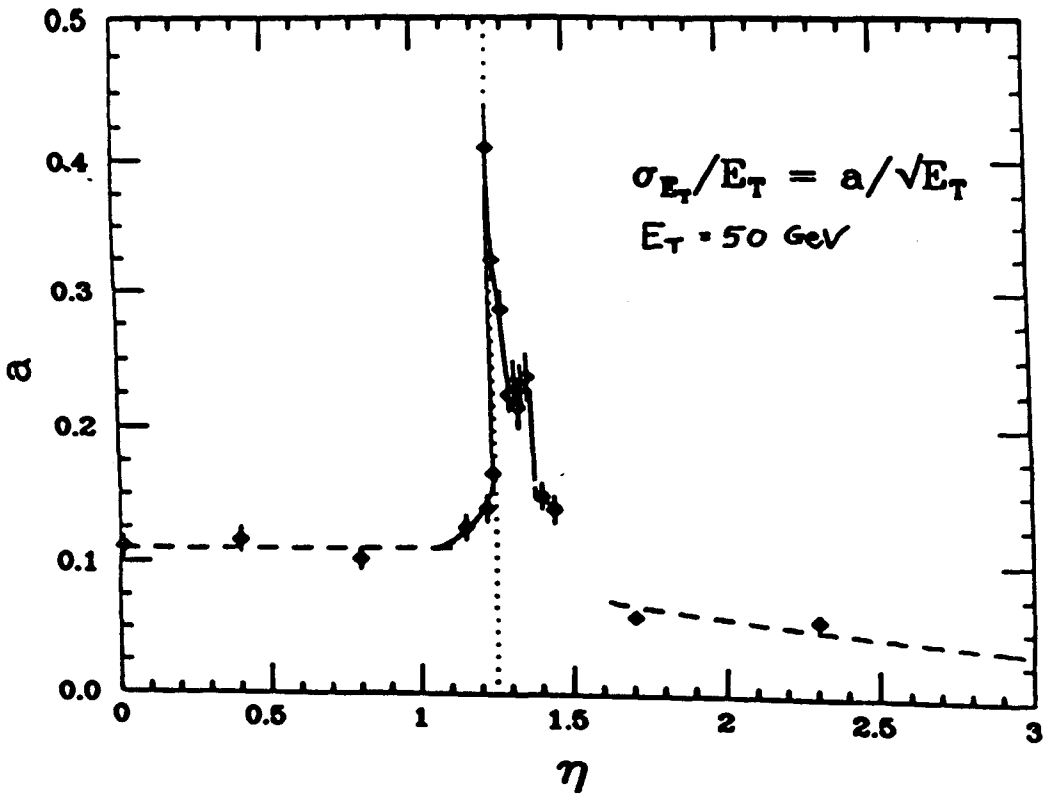

Figure 4.3.3-7: Calculated Energy Resolution for 50 GeV E_t Electrons vs η.

We have also done a detailed GEANT studies and extending them to include such things as phi cracks and effect of rotating the cracks slightly, material in the tracker, geometries closer to the current SDC design, material in the barrel-endcap transition from the tracker cables, and the solenoid support structure.

Joint Scintillator R&D Program

We have initiated a joint R&D program with physicists, engineers and chemists in the Commonwealth of Independent States. Colleagues at JINR, Dubna (Russia) have been engaged in parallel and complementary work on the optical model of calorimeter and on the simulation of the effect of various tolerances on the energy resolution function. In addition, a large scintillator R&D program exists between various institutions including the Monocrystalreactive NPO (Scientific-Industrial Complex) in Kharkov (Ukraine) and JINR in Dubna. New and competitive radiation hard scintillating plastic is being developed in the Ukraine and beam tested by colleagues in Russia. We have initiated a collaborative effort with scientists from these institutions and the Tbilisi State University, the Kharkov State University, the Moscow Engineering-Physics Institute to mount a cosmic ray test of scintillating plastic tiles read out with wavelength shifting fibers. Two modules (each 2 towers wide x 5 towers long) will rest side-by-side between scintillator trigger arrays and position chambers (MWPC's, drift chambers or drift tubes). Each module will be a stack of tiles and lead absorber layers prototyping the electromagnetic section of the SDC calorimeter. The objectives of the planned test are listed below:

1) Measure the properties (accuracy and stability of response) of 20 SDC electro-magnetic towers using the cosmic ray background of muons.

2) Study the position dependence and the accuracy and stability of response of the calibration procedure that uses sources driven through calibration tubes passing near every tile in the stacks in three different locations. These tubes are installed in grooves machined in the absober layers. The grooves thus run in the direction perpendicular to the tile layers along the long axis of the modules. The feasibility of using tubes running along the edges of modules in the direction transverse to the tile layers will also be studied.

3) To study the feasibility and properties of the concept of the "brilliant cookie" (digitally controlled variable neutral density filter or diffusive screen). This device could be installed in the optical path of each clear fiber (of a given bundle) coming to a photomultiplier tube and could be used to continually control (equalize) the amount of light delivered from each tile in a given tower thus allowing compensation of the light output due to radiation damage or other sources.

4) To study the properties of different flasher calibration systems for the photomultiplier tubes. In a variant of this system, light could be piped directly to each tile through a light delivery system to be designed.

5) To study and compare the relative properties of the HAMAMATSU-series (Japan) and FEU--series (Russia) photomultiplier / base assemblies.

6) To study and compare the response of different scintillators and fibers, damaged and undamaged by radiation. The design of the two stacks is such that it can easily be disassembled with the tile-fiber assemblies replaced.

4.3.4 Tracking and Beamline Design

Research Program Personnel:
F. Bird, D. Coupal, H. Ogren, B. Roe

The SDC central tracker design is based on a silicon inner tracker combined with an outer tracker. The outer tracker baseline design is a combination of modular straw tubes in the barrel region, and gas micro strip detectors in the endcap region. The alternative outer tracker design that appears attractive from a cost and performance point of view is a pure scintillating fiber design.

In January 1992, the SDC technical board determined that the two outer tracker technical designs should proceed on an equal R&D footing until a decision can be made in late 1992. Efforts at the SSC Lab since early 1991 have focused on understanding the design requirements on the SDC tracker, and on methods for readout of scintillating fibers. The hardware efforts on the tracker were begun as a common effort with physicists working in the GEM group. The hardware and simulation efforts are detailed in the next section under "tracking". Additional work at SSC Lab has been done on integration of the tracker design with the rest of the SDC systems.

A related effort is the study of the design of the beam vacuum pipe. Bryon Roe along with facilities people and people from the accelerator groups have taken a preliminary look (SDC-92-180) at the design. They conclude that a design with a cylindrical center section (±1.1m) of Be mated to a conical stainless section (10m) is adequate. This design minimizes backgrounds in the detector while adequate vacuum characteristics are obtained without requiring pumps in the active region.

4.4 Common Efforts

An important role of staff members at SSC Lab is to provide liaison to encourage commonalty of efforts in the two large detector designs. By this technique, we can hope to save some money on the overall experimental program costs. To this end, common efforts on charged particle tracking technique, electronics, and computing support have been initiated here. These efforts are detailed in the following sections.

4.4.1 Tracking

Research Program Personnel:
F. Bird, D. Coupal, H. Fenker, K. Morgan, J. Thomas, A. Wang

The major detectors at the Super Collider will use tracking systems of various types. These will likely include silicon micro strips and/or pads, scintillating fibers, straw tube gas chambers, planar drift or proportional wire chambers, large scale drift tubes for muon tracking, and others. Just as the laboratory physics program will benefit from consistency of design and the presence of in-house expertise in the areas of software engineering, front end electronics, and even civil engineering, it will also benefit if a group composed of experts in the field of tracking systems is available within the laboratory.

During the coming year, the group's activities will concentrate on scintillating fiber tracking. The relevance of this technique has been demonstrated by its use in previous and ongoing high energy physics collider experiments including L3 and UA2, its inclusion in the LOI for GEM, and its continuing consideration as an option for outer tracking in SDC. It also is a detector technology which has a multitude of unanswered fundamental questions. Readout techniques, pattern recognition, multi-event separation, ribbon construction, mounting and surveying, quality assurance, and optical connections are just some of the main topics. As a relatively new group we are in a position to take a fresh look at progress and problems in the field without being encumbered by our own history and inertia. We anticipate that we will contribute to the field by making side-by-side comparisons of competing readout devices (VLPCs and APDs and others), by involving the SSC engineering staff in answering questions about quality assurance, cryogenics, and systems integration, and by performing in-house detector simulations to help develop system requirements for both SDC and GEM detectors. Our work has been carried out in close collaboration with groups at UCLA, Purdue, Northeastern, Rochester, FNAL, and Saclay.

Physics Motivation

A tracking system consists of a solenoidal magnetic field and the tracking detector. The detector should provide precision momentum measurement, charge determination, good primary and secondary vertex reconstruction, and robust track triggering. As such, it improves lepton identification when used in tandem with the calorimetric and muon systems, permits photon/electron separation, improves the calorimeter calibration, helps to remove the large photon conversion background, and permits jet studies at the new SSC energies. It also allows charge selection which is very important in reducing the background to physics processes. A tracking detector must satisfy many requirements:

High resolution	Excellent momentum resolution for energetic charged tracks will be necessary to reconstruct massive final states and charge selection capabilities.

High granularity	Perhaps more important than resolution, the difficult task of finding the interesting tracks in complicated, multiple interaction events requires a high degree of segmentation in the tracking system for robust pattern recognition.
Radiation resistance	The tracking detector must survive for many years in a high dose environment.
Performance	The detector must produce coordinate points suitable for precision momentum measurements at rates comparable to the SSC interaction rate.

As mentioned above, we choose to focus on the 'outer' tracking detectors that contribute information directly to the formation of the electron trigger.

The most promising candidates for SSC 'outer' tracking detectors are 'straw' tubes, interpolating pads, and scintillating fibers. Straw tubes are a more mature technology, yet serious questions remain concerning their suitably for SSC, in particular, relating to their viability at high luminosity where straw occupancies can be many tens of percent, due simply to the tube diameter. In contrast, scintillating fibers are of smaller diameter and so promise more robust high luminosity performance. Fibers also have the advantage that stereo layer construction is much more straightforward than for a comparable straw system. Fiber technology has progressed to the point where radiation hardness is much less of a concern than it once was. For these reasons, we have chosen to concentrate on fiber tracking systems. We also intend to take part in the development of interpolating pad chambers, the chosen technology of the GEM collaboration.

Scintillating fiber tracking systems have performed successfully in contemporary high energy experiments, e.g. UA2. However, for the SSC environment, there are many unresolved technical issues. There are generic problems of pattern recognition and multiple track separation with such a detector. There are difficult construction problems with fiber ribbon technology, optical connection, positioning and quality assurance. Most importantly, a clear choice of a system for readout of the fibers has not appeared to date, and it is in this area that we propose to focus our own research efforts in the coming year(s).

Current candidates for fiber readout include silicon avalanche photodiodes (APDs) and visible light photon counters (VLPCs). There are on-going efforts here in both of these new technologies, efforts that we plan to greatly expand upon. Progress and planning for these research and development projects are described herein. Other important options for fiber readout such as hybrid photomultipliers and multi-anode phototubes are being investigated as well.

Progress to Date

Research activities in FY 1991 focused on the means of detecting the light produced in a scintillating fiber by a passing particle. This was a startup effort in which the primary activity was the study of avalanche photodiodes (APDs) operating in their linear mode (below breakdown), leading to development, installation, and testing of a 96 channel APD system used to sense the light from a pre-shower counter test and a shower-maximum detector test in a Fermilab test beam. (See Fig. 4.4.1-1 and Appendix E) The preshower detector is made of layers of scintillating fibers similar to a fiber tracker. The shower-maximum detector uses optical fibers to transmit the light from scintillating plates to the readout devices. Our contribution to this has been to develop the APD array for use in this test from concept through operation and analysis. The results are not only informative but are so interesting that the SDC is considering this form of readout for its shower maximum detector. Appendix F describes our work to date on Geiger mode readout of APDs. (Fig. 4.4.1-2)

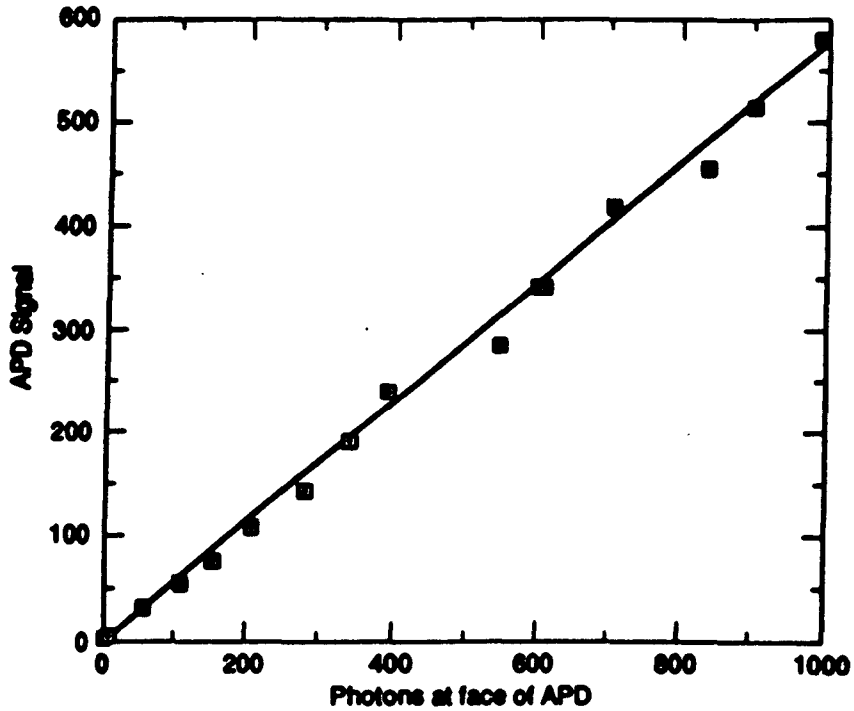

Figure 4.4.1-1: Response of an APD to varying amounts of incident light. The scatter of the data above and below the straight line was reduced by stabilizing the temperature of the APD.

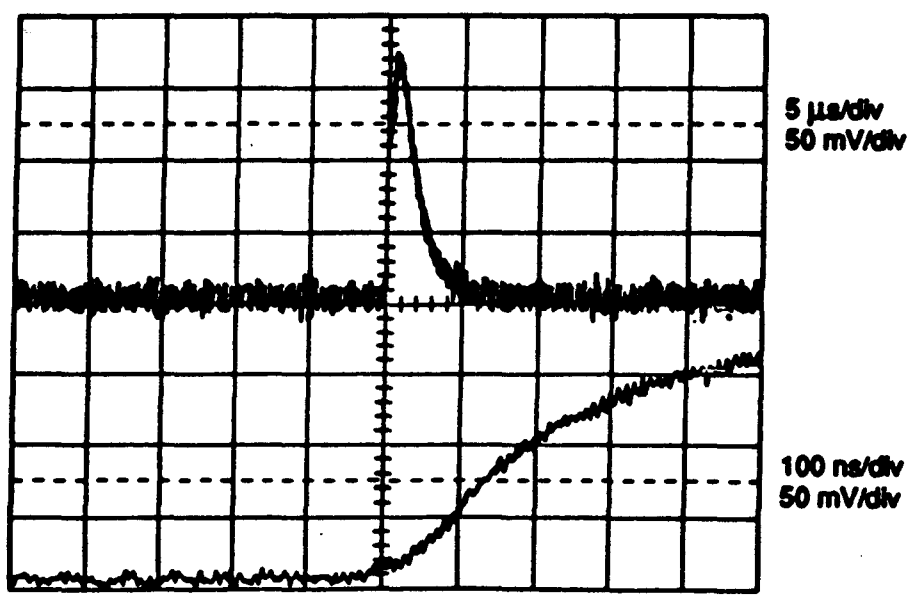

Figure 4.4.1-2: Oscilloscope trace showing the signal from an avalanche in an APD operated in Geiger mode. The same trace is shown at two different time scales. For this response the APD was discharging into 240 KΩ.

As a group we solved many problems in order to implement this experiment. A means was developed to couple the light from a scintillating or optical fiber onto the sensitive part of the APDs, and have it work effectively in a test beam environment. This requirement had to be satisfied at the same time that the APDs were maintained in a light-tight, temperature controlled environment, and were coupled via minimum lead-lengths to extremely sensitive electronics fabricated by SSCL electronics staff. Fig. 4.4.1-3 shows the solution we developed. The temperature control is necessary as the APD gain is a function of the difference between its bias and breakdown voltages, and the breakdown voltage varies with temperature. Our system was built with temperature monitors in the data stream so that gain corrections could be applied in the final analysis.

Analysis of the preshower detector data is being performed at the SSC Lab. With gain corrections applied and poorly operating channels accounted for in the analysis as of this writing, we can observe the e/π separation power of the preshower counter in Fig. 4.4.1-4, which shows the spectra of energies deposited by the two particle types in the preshower counter.

Ongoing work in the laboratory is exploring the application of APDs to scintillating fiber tracking detectors. The preliminary results are promising by showing that APDs already exhibit superior performance to conventional high-quality photomultiplier tubes for detecting pulses of light consisting of only a few photons.

Our goal towards evaluating VLPCs (visible light photon counters) was to develop a conceptual design of a test station for these devices. We have collaborated in testing prototypes of these devices in a cosmic ray fiber tracker so that we can make informed plans for our own testing station, and we have briefly operated some of them in our laboratory. (Fig. 4.4.1-5) A summary report on this experience is in Appendix G. We have accumulated a liquid helium dewar and have fabricated a "cold finger" for use in further testing VLPCs when they become available for use in our lab.

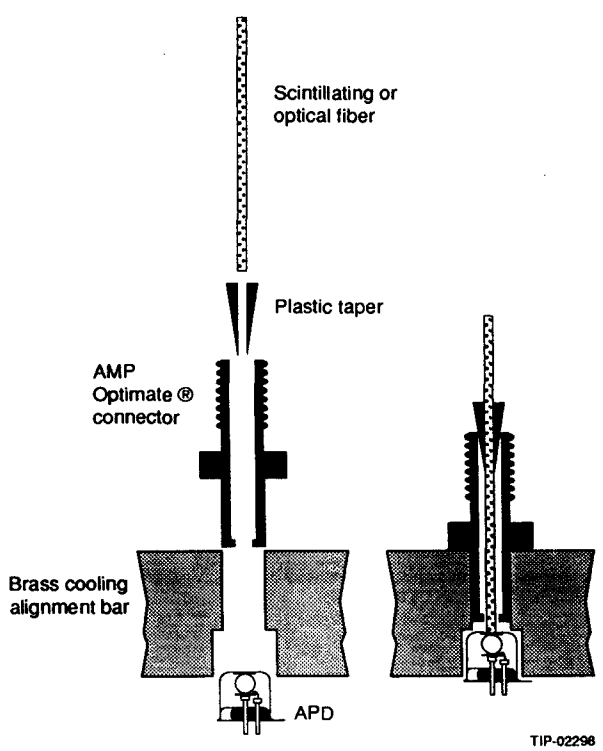

Figure 4.4.1-3: Optical Alignment Procedure. The APD is mounted in a thermally stabilized brass bar.

We have assembled a 480 channel FASTBUS ADC system in our lab for use in evaluating the various scintillating fiber readout techniques on a common test platform. This system, consisting of both hardware and software, and already oversubscribed, will find use in interpolating pad chamber tests, multichannel PMT tests, APD, and VLPC tests within the coming months. Another component of this test platform will be a scintillating fiber cosmic ray telescope and standardized optical connectors, currently being developed.

The group is also contributing to the understanding of the requirements for tracking devices by performing detailed simulations of proposed SSC detectors. (see Appendix H) This is extremely important work, as it provides guidance to the detector builders and allows suggested system designs to be tested in the context of a whole physics detector before any resources are committed to its construction. Fig. 4.4.1-6, for example, shows the results from a calculation of the channel occupancies for the silicon/outer tracking options of SDC as various ingredients in the simulation are "turned on". These initial studies will provide important information to help select between the SDC options, as they are based upon the most thorough simulation of the expected SSC environment available at present. Clearly, much work remains to develop and understand the optimal algorithms for track reconstruction and fitting, work that we intend to pursue in earnest at SSCL.

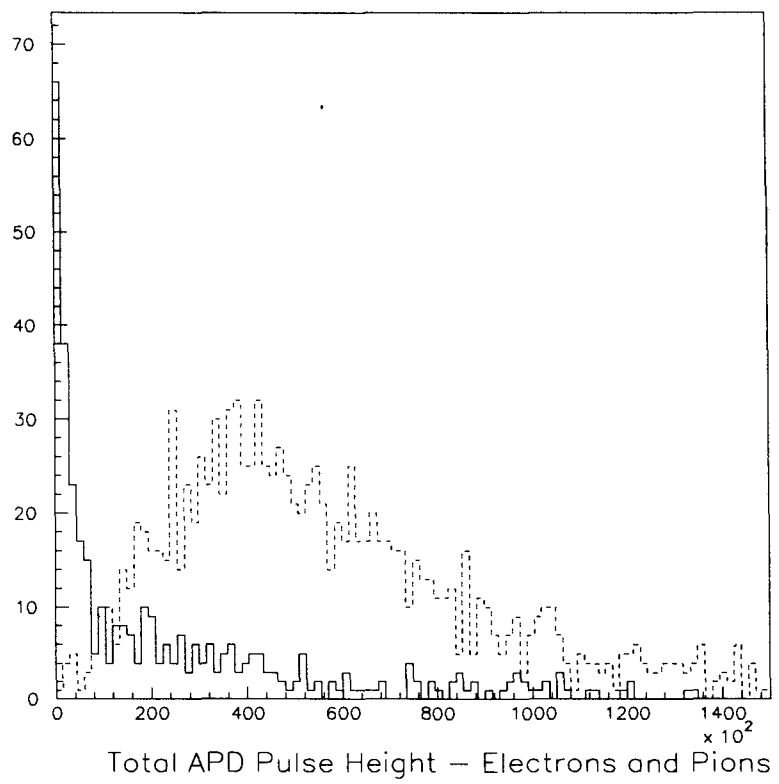

Figure 4.4.1-4: Energy deposit in the fiber preshower detector as measured by the APD array. Dotted curve is for electrons, solid is for pions. Beam energy is 35 GeV. The detector was placed at 5 radiations lengths for this run.

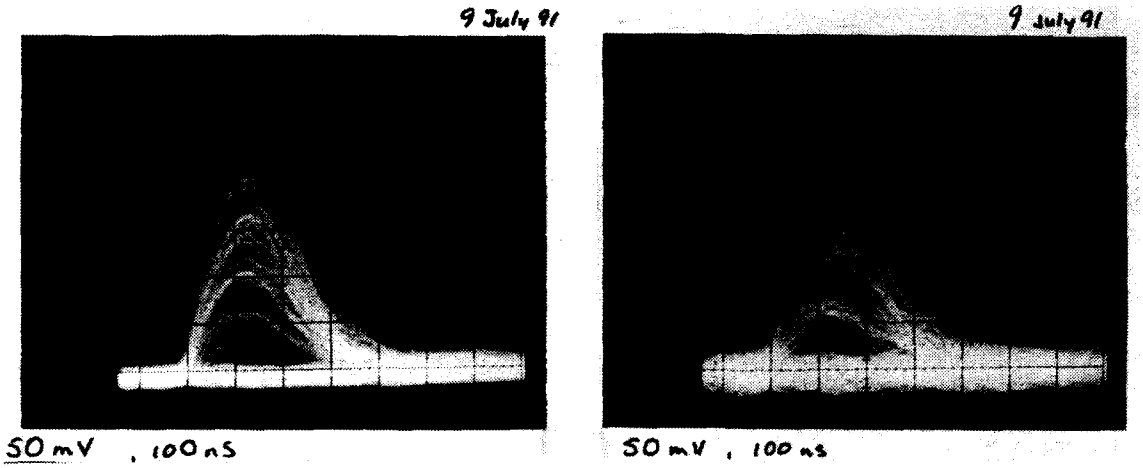

Figure 4.4.1-5: Oscilloscope Pictures of Multiple Photoelectron Pulses from VLPC

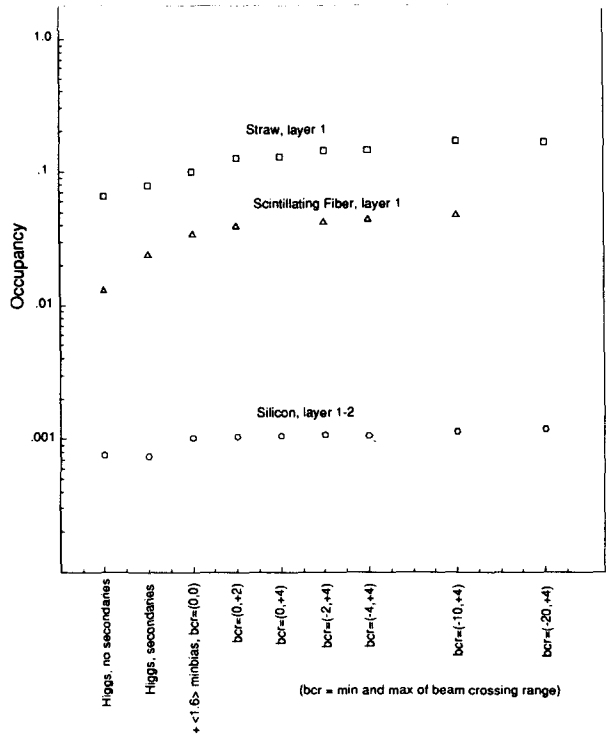

Figure 4.4.1-6: Occupancy in the SDC Inner Silicon Layer and the Innermost Layers of the Two Outer Tracker Options Under Various conditions in the simulations.

4.4.2 Electronics, Triggering and DAQ for Experiments at the SSCL

Physics Research Personnel:

The SSCL group of physicists working on electronics consists of 4 staff physicists: M. Botlo, J. Dorenbosch (group leader), C. Milner and E. Wang. Their respective activities are concentrated in the areas of DAQ, overall system design, data collection simulation and trigger studies. Presently the group has eight engineers: G. Vanstraelen, M. Abuzaid (front end design), D. Crosetto, P. Kibuule (testing), M. Bowden, S. BeiBei (front end interface), A. Booth (data collection simulation) and M. Jazelski (DAQ). Six students from different universities participate in the effort: M. Howe (Texas A&M, design), W. Yang (SMU, testing), V. Kapoor (UT Arlington, simulation), J. Lonon (U of Oklahoma, Norman, trigger), F. Zhou (UT Arlington, trigger) and J. Hayes (UNT Denton, DAQ).

Current R&D Program

A major fraction of the experimental budget at the SSC is allocated to electronics systems for capturing and collecting the data. The detector subsystems are rapidly becoming well defined. However, at present there exists no comprehensive design for the readout electronics. For this reason extensive R&D is underway in the High Energy Physics community. Because of its central position, the SSCL can naturally play a catalyzing role in this process. It is also a logical institution to play an important role in Quality Assurance (QA) for detector electronics.

Electronics design and testing at the SSCL is fully driven by the needs of the experiments. Priority is given to R&D of readout system components that have the longest lead times. Particular emphasis is given to research that may lead to electronics or readout systems useful to more than one experiment. To further simplify commissioning and maintenance of the readout, we attempt to define protocols that are common to all detector subsystems and that can be adopted by several collaborations. Work is done in close contact with physicists and engineers outside the SSCL working on similar projects such as groups at FNAL, LBL, BNL, KEK, and many universities.

Present Activities

The SSCL electronics group has chosen its main activities taking into consideration:

- the lead time required for critical designs,
- the possibility to catalyze development in the collaborations,
- the potential to share designs between detector subsystems and collaborations,
- the immediate needs of the collaborations and
- future involvement in QA for the detector electronics.

Therefore, the main efforts are directed towards:

- front end chip design,
- front end chip testing,
- the definition of the interface to these front ends,
- studies of the data collection network,
- trigger studies and
- the development of data acquisition hard and software.

Much of this work is on the leading edge of technology. Two patents have been applied for in FY 1991 by engineers working in the electronics group.

Below we give an overview of the efforts and future plans, followed by selected results from our efforts in the appendix.

Front End Chip Design

The front end chips capture, store, and digitize the analog signals from the various detector subsystems. No commercial devices are expected to be available for this purpose, due to a long list of non-standard requirements. Depending on the detector subsystem one will need devices with the following qualities: radiation-hard, low power, low noise, low mass, fast, extended dynamic range, reliable and economical. The front ends are critical electronics devices with very long design times, therefore front end development is given highest priority.

SSCL is involved in the design of two front ends: a chip to capture the small signals from gas microstrip track detectors and a very challenging current splitter / ADC system. The gas microstrip front end is a low power, radiation-hard amplifier-comparator design with local digital storage and data encoding. It is developed in collaboration with a group at Texas A&M. The design is described in Appendix I.

The current splitter / ADC will measure calorimeter signals each 16-ns beam crossing interval, with a linear dynamic range of 19 to 20 bits. The current splitter design is being done in collaboration with designers at Fermilab, UT Arlington and Texas Instruments. It targets the SDC calorimeter design, but it may also be useful to the GEM collaboration. The front end design group is equipped with professional Computer Aided Design software providing an integrated environment for design, simulation and test vector generation. Both designs are implemented as full custom VLSI.

Front End Chip Testing

As front end design has a long lead time, it significantly influences the priority scheme for work done by the SSCL group. Front end chips must be tested, their interface to the rest of the readout system must be defined, and the way they store and pass data must be optimized. Many of the SSCL electronics activities are therefore directly related to front end design.

Very few groups in the HEP community are equipped to test front ends at full speed over a wide range of conditions. To address this problem, the SSCL has set up a dedicated test facility. It will fulfill the needs of the in-house front end designers while sufficient capacity is planned to investigate many of the outside designs as well. The laboratory can play a mayor role in QA for SSC front ends. We have installed an IC verification station that allows testing of complex digital chips at frequencies well beyond the 64 MHz needed at the SSC. To test analog and mixed analog/digital designs, the system is enhanced with extensive analog Test and Measurement equipment. At present we are investigating a Time to Digital converter designed by a KEK group for SDC, a prototype of the current splitter design, and a commercial chip that may be used to complete the splitter / ADC system. A report on the TDC tests is included in Appendix J.

Front End Chip Interface

The SSCL electronics group plays a central role in the definition of the protocols that determine how the front end systems interact with the other components of the detector readout, the gating logic, the trigger, and the data acquisition network. We believe that common protocols will greatly simplify commissioning and running the experiments. They will also lower the amount of manpower needed to maintain the electronics hardware and software. At present we are concentrating on the definition of such protocols for SDC. We are establishing close contacts with all groups in SDC working on front ends, gating logic, trigger and DAQ to understand the details of their requirements. Common solutions will be sought that efficiently meet the needs of all subsystems.

Protocols must be defined at many levels: at the behavioral level one describes the signals to be used for communication and the way data are ordered and packaged, at the system level one must choose the technology used for signal transfer, at the board level one must decide on parallel or serial data transfers, at the chip level one must pick the signal shapes, and at the transistor level one must provide standardized drivers and receivers. Many of these areas are being addressed at the SSCL. We are involved in studies of various drivers and receivers, we are investigating the noise and feedback aspects of different signal options and we are doing extensive simulation at the behavioral level.

Data Collection Network Simulation

The SSCL electronics group has chosen the MODSIM language for high level behavioral simulation. We have a beta-test site agreement with the supplier, CACI. The MODSIM discrete-event simulation software package allows an object oriented description of the front ends, the gating logic, the trigger logic, and the data collection network. It allows rapid prototyping of complete data acquisition systems.

Simulated readout prototypes are used to investigate the tradeoffs between competing architectures, to optimize buffer sizes and bandwidth, and to try out different protocols. A copy of early published results is included in Appendix K. The group has coded a software tool that can be used to model different data collection networks. It is relatively straightforward to insert the actual parameters that are expected for the future data acquisition systems. A study has been made to determine the relationship between memory sizes needed at the different nodes of the network, the bandwidth of the channels between the nodes, and the overall efficiency of the system. We have also investigated several schemes to throttle events in the gating logic. Some throttling is needed to avoid data loss and to prevent overlapping event information. It is found that such throttling mechanisms can be implemented without impeding the overall transfer efficiencies.

Trigger Studies

The data acquisition system dynamics are dominated by the behavior of the trigger logic. This logic selects, in real-time, proton collisions that contain interesting physics and must be read out. The trigger logic is expected to be implemented as multi-level decision logic. At subsequent levels pattern recognition is done on increasing amounts of information to extract the relevant signatures. Each level reduces the event flow rate though the system by a certain factor. These factors combine in a multiplicative way to reduce the rate from the 64 MHz collision rate to a few Hertz. At that rate the selected events can be recorded on mass storage.

The read out system architecture is strongly coupled to the trigger logic implementation. The trigger rates determine directly the frequencies new information must be provided the next trigger levels, while the overall trigger rate sets the speed at which events are recorded on mass storage. The amount of information required by each level, combined with the rates, determine bandwidths needed for different data paths. The amount of storage needed in the data acquisition network and in the front ends is strongly coupled to the latency of the different trigger levels. Therefore a good understanding of the trigger is mandatory before a fully optimized system can be designed.

Together with physicists from the collaborations, the electronics group is involved in physics simulations to derive precise specifications for the different trigger levels. (Appendix L) An attempt is made to simultaneously optimize the trigger logic and readout electronics. In each case a careful assessment is made to identify where economic commercial solutions are expected to be available, and where in house design will be needed. Much of this work is done in close collaboration with GEM, but is applicable to both experiments.

Data Acquisition Systems

The collaborations are presently preparing tests of detector prototypes in cosmic ray setups and in test beams. These tests require simple data acquisition systems that are modular, scalable, cost effective, easy to adapt and that can be transported between different hardware platforms. They must have a flexible human interface for inspecting data on-line. (Appendix M)

Two DAQ systems are under development at the SSCL. One is a simple, low rate system using LabView, a commercial DAQ development tool for the Macintosh. It is optimized for cosmic beam test setups. The other system is designed to run at higher rates. After evaluating several commercial real-time kernels, the VxWorks UNIX operating system was selected as the software platform. (Appendix N) The real-time software currently runs on Motorola 68030 CPU's in VME. Data are transferred to a host workstation and stored on Exabyte tape. Both systems are now available for use by the GEM collaboration. The Macintosh system is already in use at BU, the VxWorks systems will be used for the "Texas Test Rig" muon chamber tests at the SSCL.

4.4.3 Computing

Requirements for off-line computing at the SSC Laboratory in support of the experimental program range from providing an estimated 4000 VAX equivalents for detector simulation early in the project, to establishing off-line computing resources in 1999 for data reconstruction and analysis which will approach 10^6 VAX equivalents.

Powerful resources to address these computing issues have been developed within the Physics Research Division and each of the major detector projects. The Computing Department in the PRD, will plan, design, procure, install, implement, and operate off-line computing systems in support of detector design and experimental programs. PRD computing is also responsible for assuring that commonality issues are addressed, software engineering, methodologies and tools are used, and quality is maintained in the development and operation of off-line systems. Hardware development and commissioning costs come from SSC project funds.

Each major detector has a computing group which is responsible for defining Physics requirements for off-line systems including simulation control, off-line (simulation, reconstruction and analysis), data base/calibration, data storage and networking.

The strategy for computing was defined early in the process of developing resources. The basis for this strategy is to take advantage of the 90's technologies of RISC/UNIX work station environments, and their resulting price/performance advantages, and develop major computing resources using these technologies to take advantage of heterogeneous open systems.

Implementation of this strategy has resulted in the development of the Physics Detector Simulation Facility (PDSF) (Fig. 4.4.3-1) which in its current phase represents the equivalent of 2000 VAX11/780 computers accessible to the physics community worldwide through wide area networks.

The majority of physicists currently using PDSF, reside outside the SSCL. Operational support for PDSF is requested from HEP funds. Operational support for the PDSF for FY 1992 includes 5.5 FTEs (system managers, operators, network support) and vendor maintenance contracts, totaling $150K. There are also several students from local universities working on computing R&D at the SSC.

CDF analysis code will be transported to PDSF to start the analysis of data from the previous CDF run. There currently is 3GB of CDF data residing on PDSF. This data will initiate the SSC participation in the analysis of CDF data.

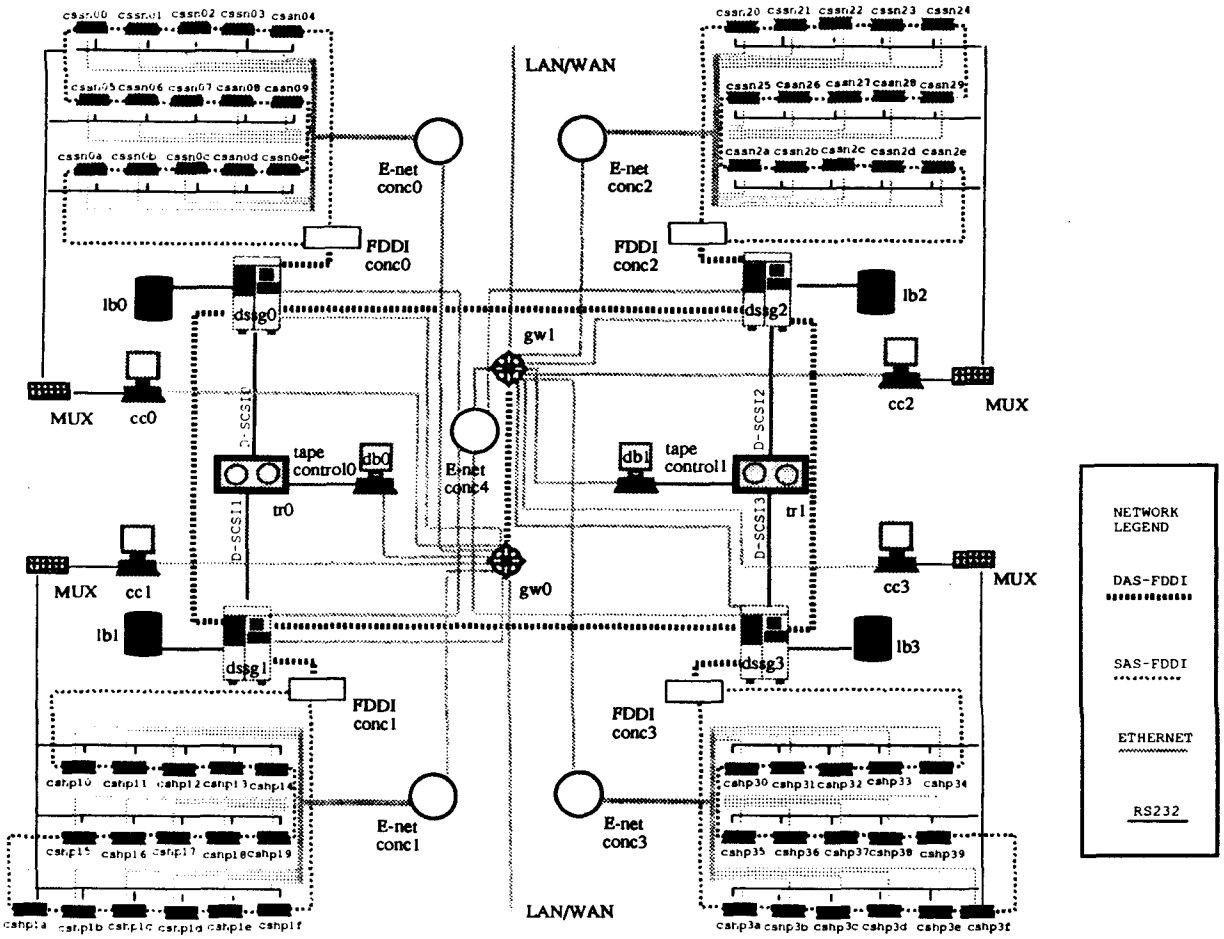

Figure 4.4.3-1: PDSF Architecture Implementation

4.5 Research Activities Outside SSCL

During FY 1991, participation in the CDF experiment by staff at SSCL was successfully initiated. Progress in FY 1991 and to date in FY 1992 on the proposed CDF work is detailed below. In addition to the CDF effort, and depending on the scientific program, support for one or two other HEP experiments outside SSCL will be initiated in FY 1992. An active search for appropriate experiments to join is being carried out now by members of the SSCL staff. When a suitable experiment is found, an addendum to this program will be prepared for consideration and review by the DOE.

Participation in the CDF experiment at FNAL seemed a particularly natural first choice for us since the collider physics being carried out there is a prototype of what we can expect to have at SSC. Since several of the senior members of the group were already members of CDF, it was relatively straightforward to start a group at SSCL. This has helped our recruiting efforts considerably, as expected.

4.5.1 CDF

Research Program Personnel:
J. Bensinger, F. Bird, C. Blocker, W. Chinowsky, D. Coupal, A. Fry, T. Fuess, J. Thomas, M. Turcotte

Introduction

The Fermilab Collider is the highest energy collider in the world and will continue as such until the SSC/LHC era. Planned luminosity upgrades promise to make it one of the best laboratories for testing the Standard Model in the coming decade. The CDF detector has been in operation since the collider turn-on, accumulating to date 4.7 pb^{-1} of data.

CDF is a solenoidal general-purpose detector well-suited for the environment. Particle tracking and momentum measurement inside the 1.5 T superconducting coil are provided by a vertex TPC and high precision drift chamber. Calorimetry has electromagnetic and hadronic sections segmented into 5000 projective towers with polar angle coverage from 2° to 178° and full azimuthal coverage. Muon coverage is provided by drift chambers in the barrel region and a large toroid system in the forward region.

The CDF upgrade plans and run schedule are presented in the first section of this report. The next section reviews CDF physics results and prospects for the upcoming runs. The next section deals with SSCL's role in CDF and reviews progress in FY 1991-92.

Run Schedule and CDF Upgrades

To date, CDF's only significant data run was in 1988-89, resulting in 4.7 pb^{-1} of data written to tape. Towards the end of the run the collider luminosity reached 2.0×10^{30} cm^{-2} sec^{-1}, twice the design luminosity. About 5500 9-track tapes were written. Some of the many physics results from this data will be presented in the next section. The current future running schedule is shown in Fig. 4.5.1-1, including a table of estimated peak luminosities. In this scenario CDF hopes to get 50 pb^{-1} by the end of runs Ia and Ib, 100 pb^{-1} in run II and 300 pb^{-1} in run III.

Fig. 4.5.1-2 shows the CDF detector configuration planned for the upcoming runs (Ia and Ib). A new level 3 trigger is required for the increased event rate. A silicon microvertex detector opens a number of physics topics involving displaced vertices, including b-jet tagging and bottom meson lifetime measurements. More iron has been added to the central muon system and rapidity coverage extended down to $|\eta|<1.0$.

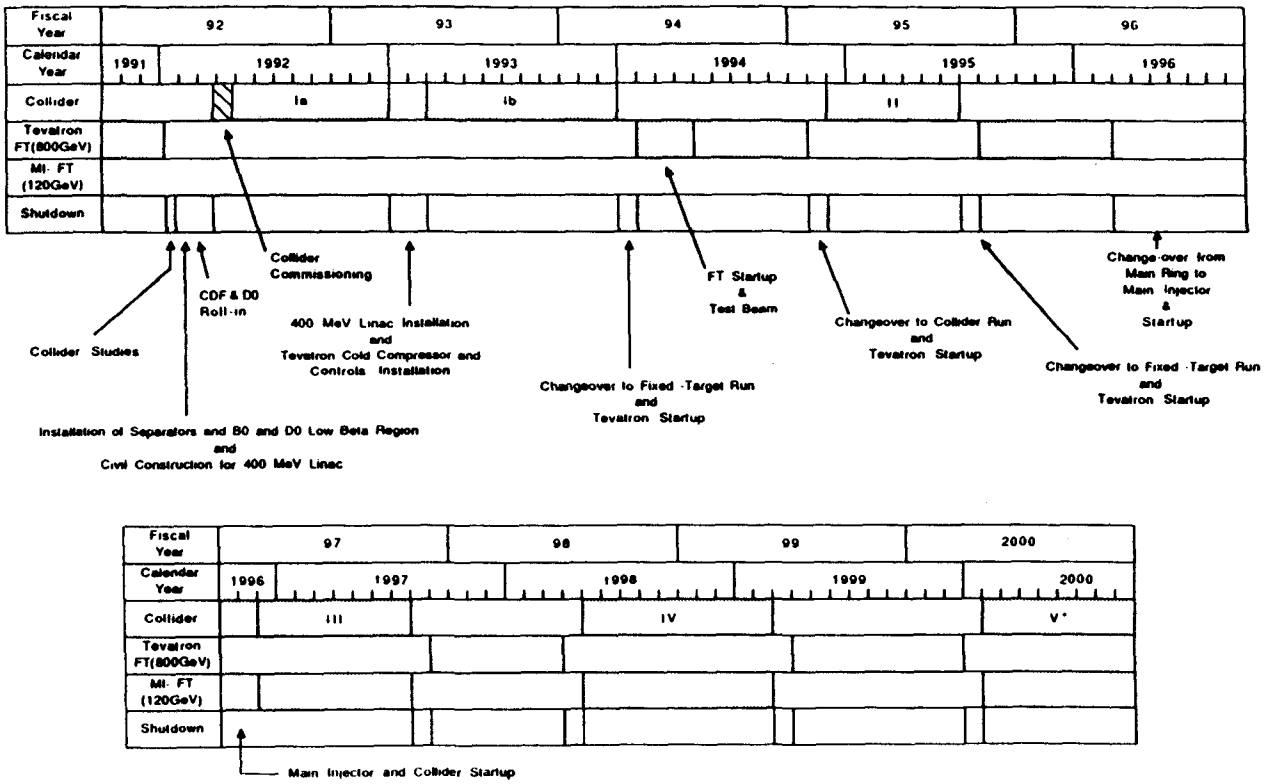

Figure 4.5.1-1: FNAL Draft Long Range Schedule

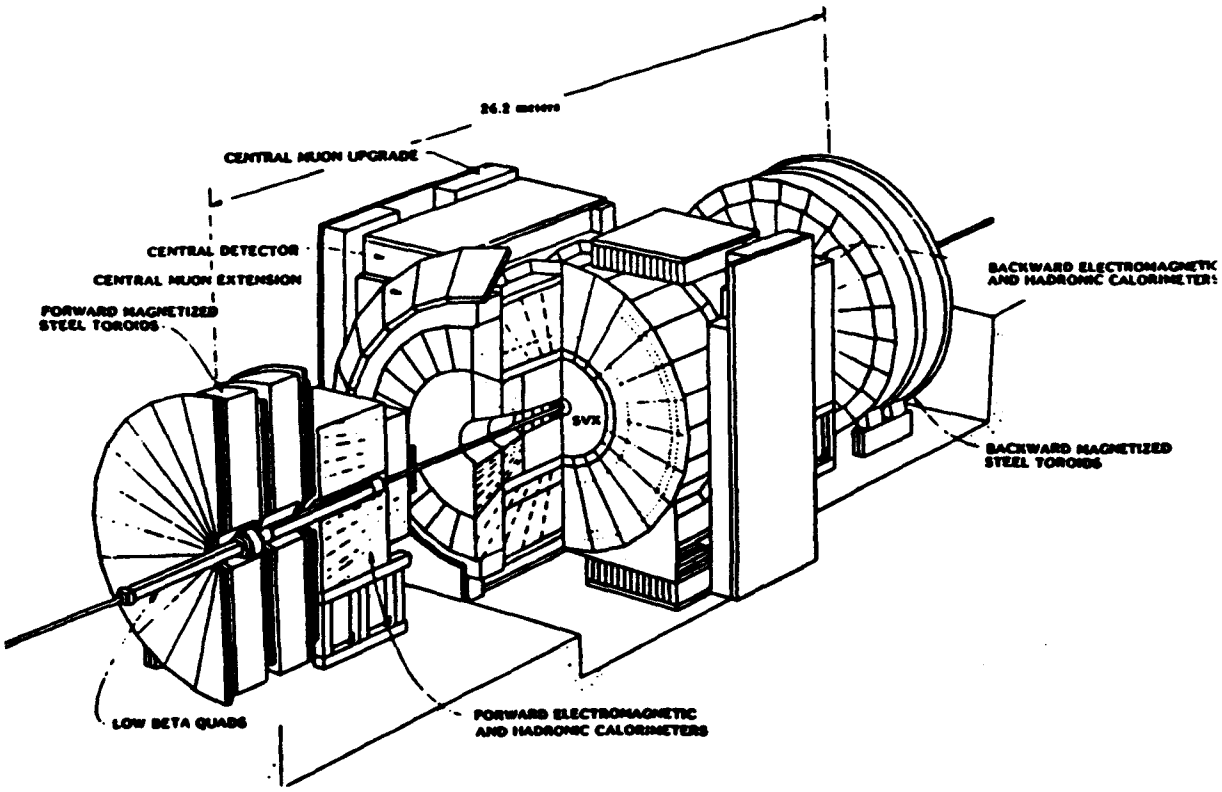

Figure 4.5.1-2: CDF Detector for the Upcoming Runs (Ia and Ib)

Fig. 4.5.1-3 shows the proposed configuration for runs II and III. A central part of this upgrade is a new plug calorimeter that, in turn, allows the forward muon system to be pushed forward, closing the hole in the muon coverage. Front end electronics and data acquisition upgrades are necessary for still higher event rates and the reduced time between beam crossings (400 nsec). A second generation silicon vertex detector will provide improved detection of primary and secondary interactions.

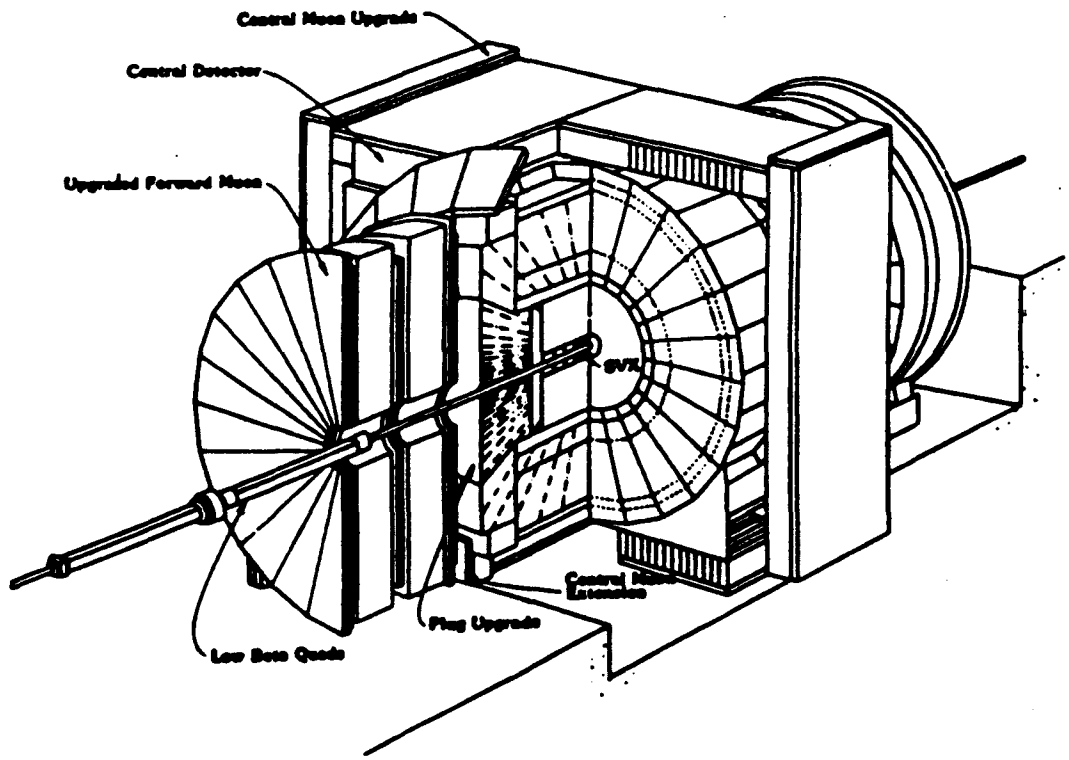

Figure 4.5.1-3: CDF Detector Proposed Configuration for Runs II and III

Physics Results and Prospects

Top Quark Physics

One primary goal of CDF remains the discovery of the elusive top quark. At Collider energies the dominant production mechanism is $q\bar{q} \rightarrow t\bar{t}$. Fig. 4.5.1-4 shows the production cross-section versus top quark mass. The decays where both top quarks decay to jets is dominated by QCD background so the CDF searches have required that at least one of the top quarks decay semileptonically to a high p_T lepton. Demanding that both top quarks decay into high p_T leptons has also been used. It has a very low background but suffers from a low rate. Based on the 88-89 data, CDF is able to set a 95% CL limit of 72 GeV/c^2 based on this $t\bar{t} \rightarrow \ell^+\ell^- + X$ mode. Another analysis that requires only one lepton plus additional jets in the event is able to set a limit of 77 GeV/c^2. The current limit is 89 GeV/c^2 based on ee, $\mu\mu$ and $e\mu$ plus e+jets events with a $b \rightarrow \mu + X$ tag.

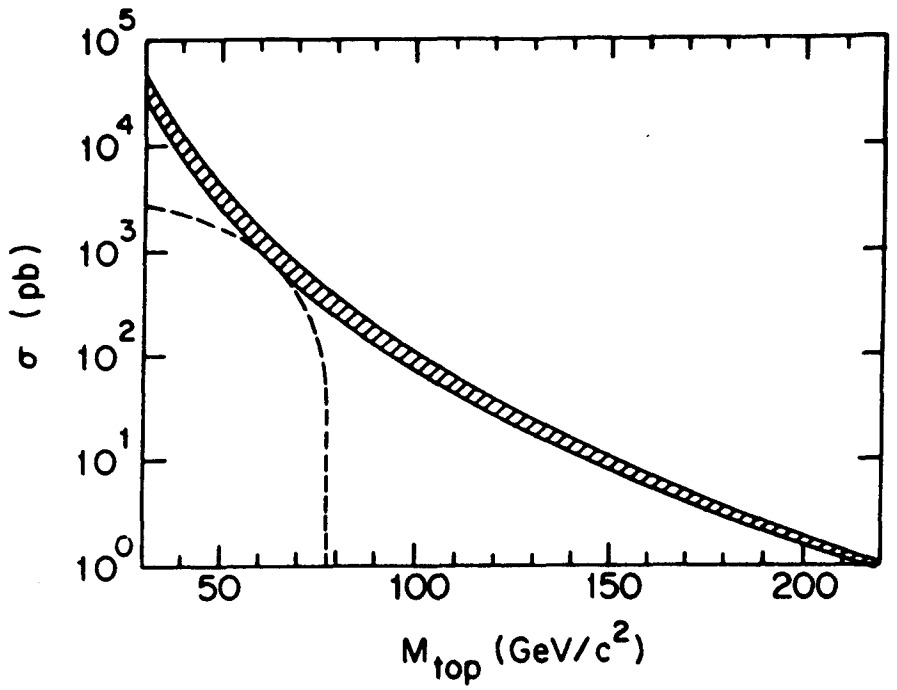

Figure 4.5.1-4: Production Cross-Section vs. Top Quark Mass

Clearly, lepton acceptance is important in searching for the top quark and drives much of the upgrade design for future runs. With the event sample expected in runs Ia and Ib and the increased muon coverage provided by the upgrade of the central muon system, it is expected that CDF will have sensitivity to top quark masses up to 150 GeV/c^2. In the proposed upgrade for runs II and III, increased coverage for electrons and, especially, muons will increase acceptance for the $e\mu$ mode by 45%, the $\mu\mu$ mode by 100% and the μ+jets by 40%. With the expected increase in data sample CDF should be sensitive by the end of run III to masses less than 200 GeV/c^2,the present limit derived from consistency of the Standard Model.

Electroweak Physics

CDF has from the 88-89 data run around 5000 $W \rightarrow \ell + \nu_\ell$ events and 500 $Z \rightarrow \ell^+ + \ell^-$ events. The Z sample has, of course, been far surpassed by the LEP experiments, but CDF will have the largest sample of W events in the world until well into LEP II running.

The W boson mass measurement is fundamental to our understanding of the Standard Model. The hadronic decay modes are again swamped by QCD, so the leptonic decay modes are used to determine the mass. Since the neutrino is not detected, the invariant mass of the missing transverse energy and the lepton p_T is used to estimate the W mass. This transverse mass distribution is shown in Fig. 4.5.1-5 for electrons and muons. Fits to data using Monte Carlo predictions for the shape yield a mass of 79.91±0.39 GeV/c^2. This measurement together with the Z mass measurement from LEP provides a measure of $\sin^2\theta_W$, which combined with low energy experiments provides a constraint on the top quark mass shown in Fig. 4.5.1-6. Estimates of how the systematic errors scale with luminosity predict an error on the mass of 70 MeV/c^2 for run II and 50 MeV/c^2 for run III. As can be seen from Fig. 4.5.1-6, this level of precision in the W mass together with a measure of the top quark mass provide a sensitive test of the Standard Model.

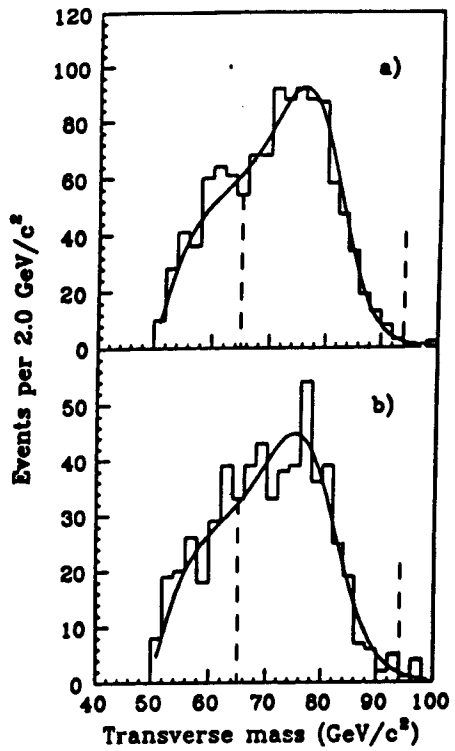

Figure 4.5.1-5: a) Transverse Mass Distribution for all W $\rightarrow e\nu$ candidates. Overlaid is the best fit to the data. Indicated with dashes is the range of transverse mass used in the fit. b) the transverse mass distribution for all W $\rightarrow \mu\nu$.

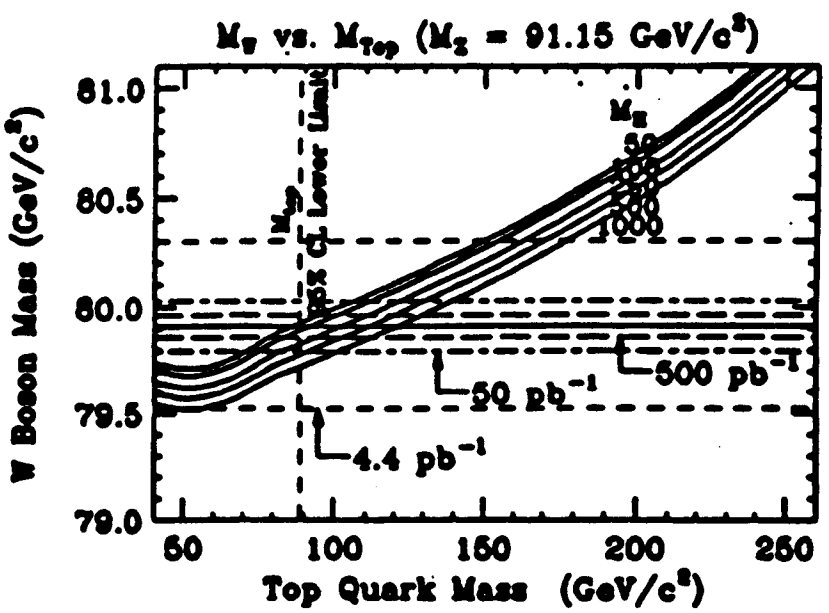

Figure 4.5.1-6: Constraints on the Top Quark Mass by measurements of M_W. Uncertainties are given for several values of integrated luminosity. Example given is for the current best measurement of M_W.

Other electroweak measurements such as the decay width of the W boson will provide additional consistency checks of the Standard Model. CDF can also look for extensions to the Standard Model in the electroweak sector, such as additional vector bosons. Based on 88-89 data CDF can rule out at the 95% CL W′ [Z′] masses below 520 [380] GeV/c^2. The mass sensitivity is expected to reach 950[850] GeV/c^2 by the end of run III.

Jet Physics

Fig. 4.5.1-7 shows the CDF results for the inclusive jet cross section versus transverse energy, showing remarkable agreement over many orders of magnitude. Quark compositeness would show up as a deviation from QCD in this plot at high transverse energy. Agreement with QCD allows CDF to set a limit of Λ>950 GeV for the compositeness scale. We expect by the end of run III to extend the sensitivity to Λ to 1500 GeV. Measurements of di-jet rates and invariant mass, 3 and 4-jet rates and jet fragmentation studies will test QCD with increased precision and provide input to the various models.

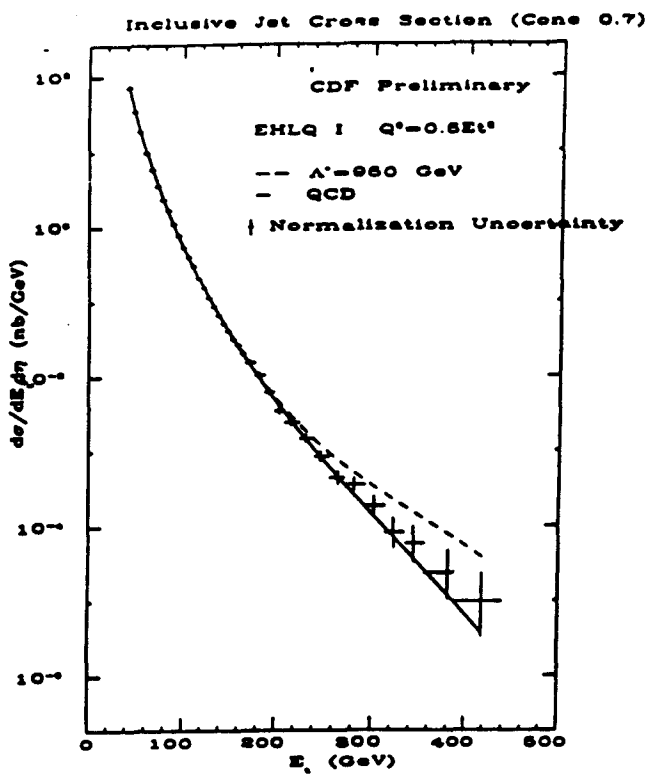

Figure 4.5.1-7: Inclusive Jet Cross Section. The solid curve is the QCD prediction and the dashed curve is for a quark compositeness of Λ = 950 GeV.

Bottom Quark Physics

The $p\bar{p}$ collisions at the Tevatron are a copious source of bottom quarks. Most of the leptons in CDF are from the semileptonic decay of the b quark. Fig. 4.5.1-8 shows the p_T spectrum of electrons in CDF with and without the electrons from W/Z decay. Also shown is the prediction from ISAJET for the charm plus bottom and charm only contributions. Fig. 4.5.1-9 shows the measured b quark production cross section based on the inclusive lepton signal. CDF also reconstructs some exclusive states. Fig. 4.5.1-10 shows the J/ψ peak from a two muon trigger. About 2/3 of these are found to come from B meson decay. Reconstructing the J/ψ and a nearby charged track assumed to be a kaon gives the peak shown in Fig. 4.5.1-11 in agreement with B meson mass measurements at e^+e^- machines.

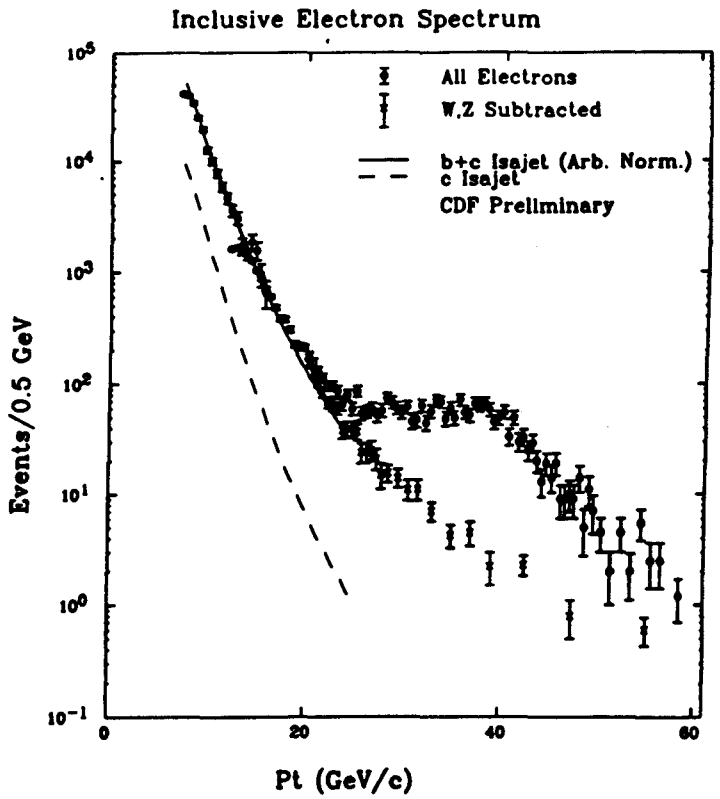

Figure 4.5.1-8: Inclusive Electron Spectrum

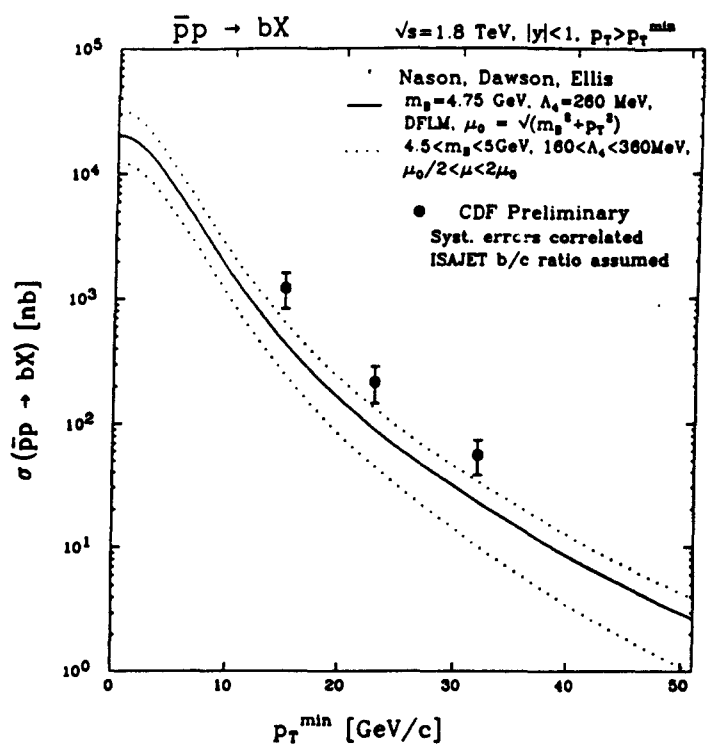

Figure 4.5.1-9: Measured Inclusive B Quark Production

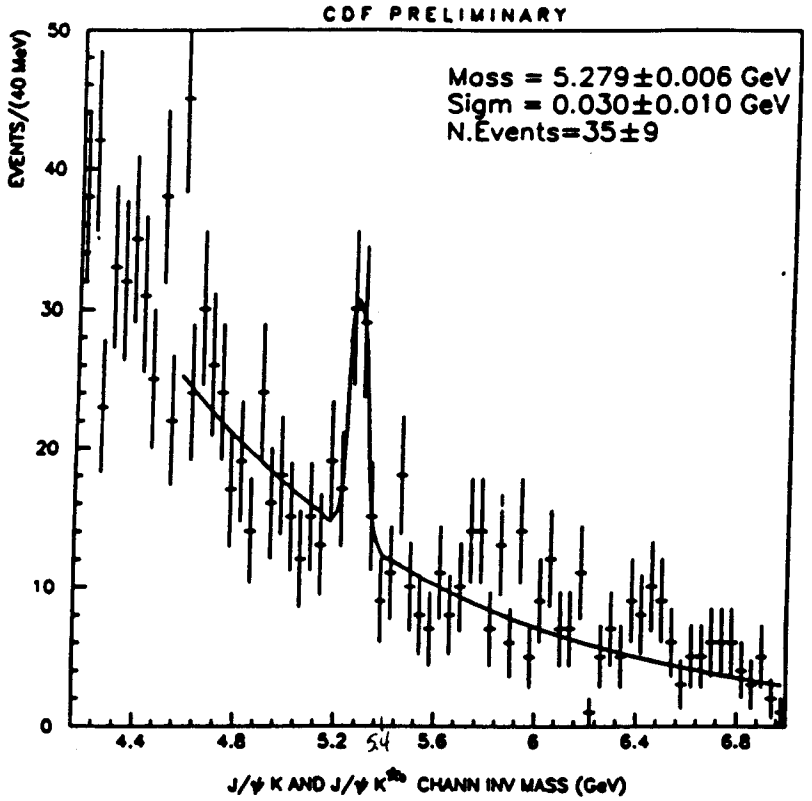

Figure 4.5.1-10: Reconstructed B Meson Peak from ΨK Mode.

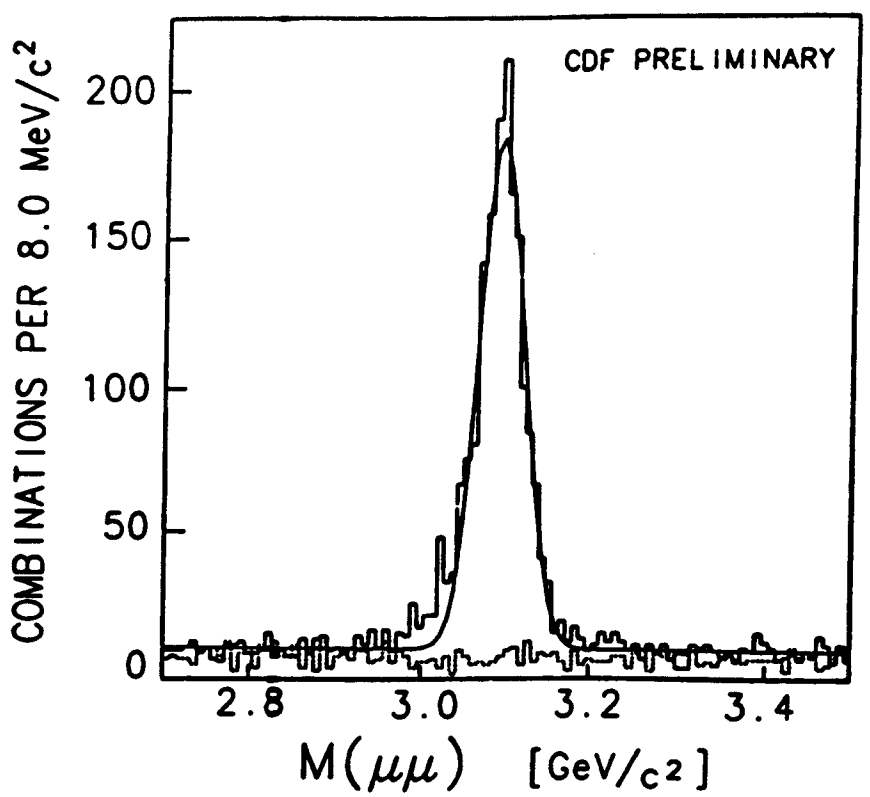

Figure 4.5.1-11: $\Psi \rightarrow \mu\mu$ Sample Collected in 2.6 pb^{-1}.

The prospects look very good for b quark physics from future runs. All the above results were done without the silicon microvertex detector that will be installed for the next run. The displaced secondary vertices will improve tagging efficiency and provide lifetime measurements for the B_u, B_d and B_s mesons. By the end of run III, CDF hopes to have 10^6-10^7 semileptonic b decay events with an identified secondary vertex and about 10^6 $B \rightarrow J/\psi + X$. This sample of events will allow a measure of the B_s mixing parameter (χ_s) up to around 10.

Other Physics

CDF has set limits on various processes beyond the Standard Model including mass limits of 150 GeV/c^2 for SUSY quarks and gluinos. The reach for these SUSY particles should extend to 250 - 300 GeV/c^2 with the data of run III. The additional data will also extend the search range for additional Higgs bosons and technicolor.

SSCL Role

The SSCL physicists on CDF have already contributed hardware and manpower to the CDF experiment and plan to take an active role in the future data-taking, analysis and detector upgrades. Besides the exciting physics of CDF, this experiment provides valuable experience as physicists work on design detectors for the SSC. The CDF group at SSCL currently consists of 8 staff physicists working 50% time on CDF. We will soon add two post-doctoral physicists at Fermilab working 100% time on CDF.

The principal task that the SSCL group in CDF has undertaken is assistance in the operation and upgrade of the forward muon system for the upcoming runs and the design and construction of new components for the "pushed-up" configuration (see Fig. 4.5.1-3) for runs II and III. Before discussing progress on our 1991 milestones we will describe in more detail the CDF forward muon system.

As shown in Figures 4.5.1-2 and 4.5.1-3, the CDF forward muon system consists of a toroid pair on each side of the detector, 11 meters from the interaction point (in the present configuration). On each side are three planes of drift chambers and trigger counters with 1.8 Tesla toroids between the planes. The drift chambers have two layers of cells. The first plane of chambers has one layer with cell sizes from 1.6 cm to 7.7 cm covering an approximately constant size in η and a second layer with larger cells to resolve the ambiguity in drift direction. The second and third planes have proportionally larger cells to form towers projecting to the interaction point. Each chamber is a wedge covering 15° in azimuth, but three chamber signals are OR'ed together to form a 45° octant. Finer azimuthal segmentation is provided by cathode pads that subtend 5° in azimuth and 3° in polar angle. Scintillating counters cover each chamber and provide a Level-0 trigger.

In the last run, the forward muon chambers experienced a number of problems. The chambers are an electrode-less design that depends on the accumulation of positive charge on the cell inner surfaces to develop the proper field shape. Although they perform well in the lab, in the high radiation environment of the last Collider run their gain sagged by as much as 50%. The current thinking is that excess space charge distorted the field, resulting in excess charge deposited on cell walls. For triggering, the rates in the scintillating counters were too high, requiring the single forward muon trigger to be prescaled to an acceptable rate for the data acquisition. Also a lack of redundancy in the chambers led to large backgrounds in the inclusive muon sample from mis-reconstructed tracks and non-guassian scattering. For studies that included a trigger in the central part of the detector, such as the top search, the chambers performed adequately.

A number of changes are to be installed for the next run to possibly improve the performance of the forward muon system. The scintillators have been cut to a smaller size (from 15° to 5° in azimuth) to reduce the rates. It is unknown whether the chambers will work at the

higher luminosities of this upcoming run. It was the performance uncertainty of the current chambers and the higher rates expected in runs II and III that led CDF to propose replacing these chambers. This upgrade was reviewed before the FNAL PAC in April 1991. The conclusion of the PAC was that, given the tight budget and the other CDF upgrades for runs II and III, CDF should do further evaluations of the current chambers as to their survivability at high luminosity. R&D on a new chamber design will continue in parallel.

The SSCL group has taken on a number of responsibilities in preparing the forward muon detectors for runs Ia and Ib. SSCL fabricated four pulse fan out modules that are part of a diagnostic system for the drift chambers. Pulses are fanned out to the cathode pads and signals induced on the wires are read back through the data acquisition. These modules are installed, tested and operational at CDF. We are also working together with University of Wisconsin physicists on the software that controls this system.

As already mentioned, the current chambers suffer from over-charging resulting in reduced efficiency. It has been known for some time that reducing the voltage to zero and applying a small negative voltage clears the excess charge. SSCL has built six HV relay boxes that allow us to switch to negative supplies between Tevatron fills (about once every 24 hours). The boxes also provide HV fan out and crowbarring of the outputs when a channel trips. They are now installed and working at CDF. SSCL has taken responsibility for the entire HV for the forward muon detector (drift chambers and scintillators). The drift chamber HV is provided by CAEN HV supplies controlled by a PC. The PC communicates with the CDF on-line through ACNET, the Tevatron accelerator network. ACNET is also used to control the HV for the scintillators. The HV system is operational and in use now to check-out the drift chambers and scintillators.

Several SSCL physicists have been spending roughly 2 weeks per month at FNAL since January working on installation of the forward muon system. Good progress has been made towards meeting the early-April deadline.

A task of prime importance in the upcoming run is to evaluate the performance of the chambers at high luminosities. We discuss in the next section plans in this regard. We have already taken some steps toward this goal, transporting CDF data to the SSCL Physics Detector Simulation Facility, (PDSF) which will be used to analyze CDF data. Fig. 4.5.1-12 shows the occupancy per minimum bias event for the 56 coordinate measuring cells for each of 3 planes of chambers, derived from a CDF tape read on a local workstation.

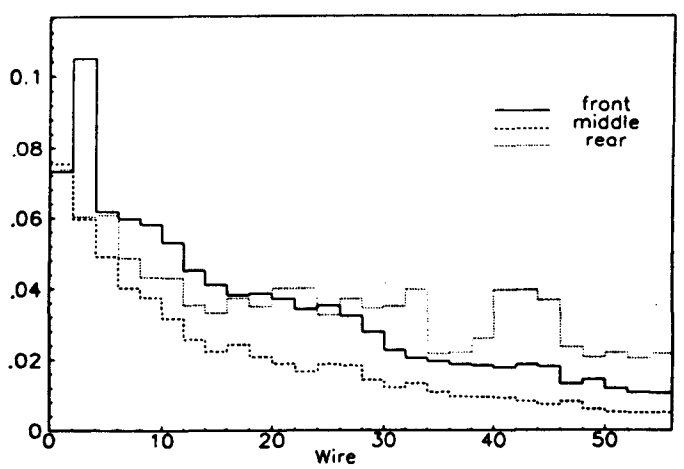

Figure 4.5.1-12: Forward Muon Wire Occupancy
muon drift chamber wire occupancy versus wire number measured from data taken in the last CDF run. The three curves are for the front, middle and rear planes of drift chambers.

Also towards understanding the behavior of an existing forward muon chamber we have obtained one of the spare chambers and are studying it in the lab here at SSCL using cosmic rays. We have also acquired a strong radioactive source in hopes of producing this overcharged state. Bringing this apparatus into operation was a challenge in that it required that the SSC laboratory define and implement its safety policies concerning use of explosive gas mixtures and intense radioactive sources in the on-site laboratories. This presented a number of hurdles that have for the most part, been surmounted. The chamber has been run with cosmic rays — Fig. 4.5.1-13 shows the drift time for one cell. The next step (now in progress) is to use the radioactive source to reproduce the conditions that over-charge the chambers in the Collider.

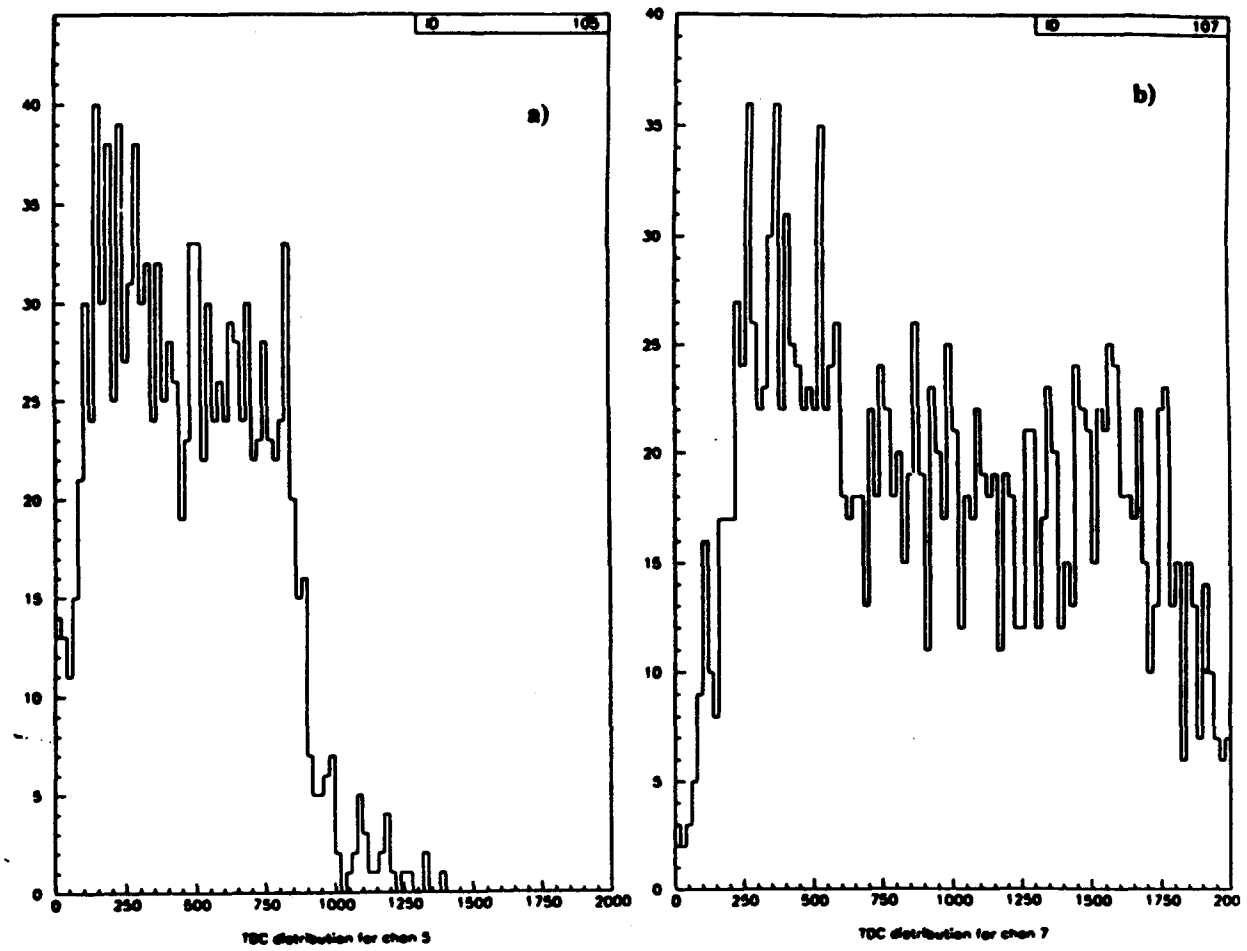

Figure 4.5.1-13: Distribution of Drift Times for a) coordinate cell and b) ambiguity cells for cosmic rays in the CDF forward muon chamber at SSCL.

In spite of the changed emphasis towards understanding the current system, R&D on new designs continue. A challenge in reconstructing muons and the reason more redundancy is desirable is the spray of knock-on electrons and muon bremsstrahlung that accompany high energy muons. Fig. 4.5.1-14 shows an example from a GEANT simulation done here at SSCL of a single muon producing associated particles as it traverses the toroids in the "pushed-up" configuration. This design has 4 layers of small cells in each plane for increased robustness against the additional "junk". This level of redundancy is found to have good rejection at the trigger level. The next step in this simulation effort is to use the current chamber design in the "pushed-up" configuration.

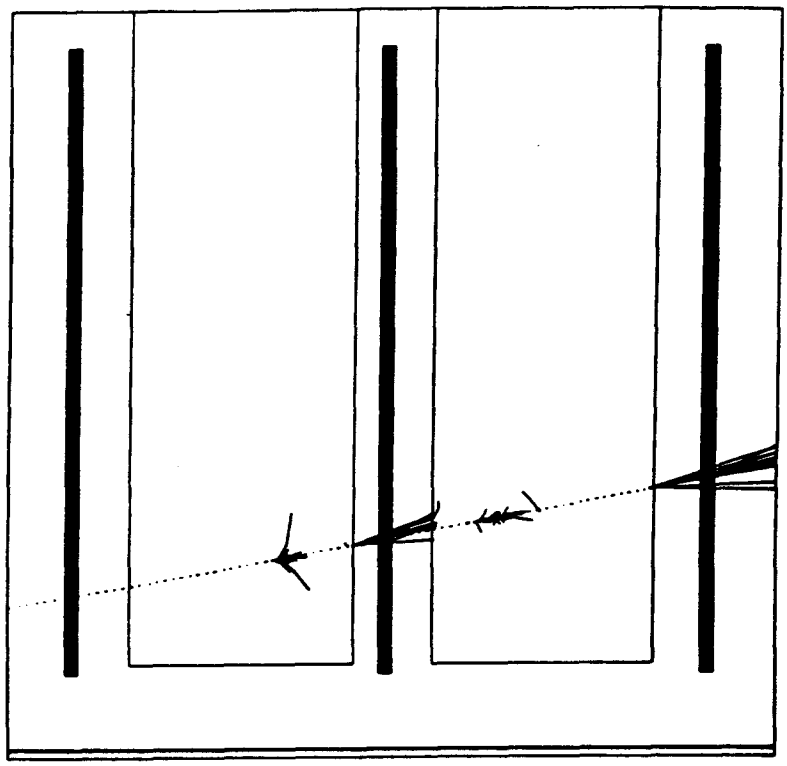

Figure 4.5.1-14: Example from a GEANT Simulation of muon bremsstrahlung-induced showers as a muon traverses two toroids of the forward muon system.

A final activity in FY 1992 was participation by SSCL physicists in the CDF test beam studies. Sections of the central, plug and forward calorimeters were mapped and recalibrated with pion and electron beams. Besides being critical to maintaining the resolution of these calorimeters, the test beam shifts give newcomers a valuable introduction to the CDF data acquisition system.

The primary goal for the rest of FY 1992 concerning the forward muon system is to evaluate the drift chamber performance versus luminosity. It is critical that we determine whether these chambers will survive the high luminosities of runs II and III. Much of the information will be obtained from the data itself, looking at occupancies and efficiencies versus run conditions. To aid in monitoring run conditions we plan to read out chamber currents from the HV system and write them to disk. In addition, sources built into selected chambers will directly monitor the sagging gain associated with overcharging. The plan is to derive a gain periodically form these sources and write the value to disk for later correlation with chamber currents and forward muon data. With this monitoring we hope to be able to isolate the source of the radiation that causes the chambers to overcharge, i.e., is it due to the steady state fluxes from continuous running or momentary bursts of radiation from partial beam loss in the Tevatron or the Main Ring.

The drift chamber operating in the laboratory here at SSCL can now be studied using a radioactive source to produce the overcharged condition. We plan to look at gain sagging versus dose using a radioactive source and study possible ways to limit the detrimental effects of the overcharging. We now have the capability of adding components such as water or alcohol to the argon-ethane gas mixture to see if they have any effect.

SSCL physicist will take shifts on CDF during the data-taking run. One member of our group (T. Fuess) is trained as a CDF "Ace", i.e., an expert in operating the CDF detector.

4.6 Theoretical Physics

Research Program Personnel:
B. Grinstein, G. Kane, B. Lynn, S. Meshkov, F. Paige, A. Sanda, D. D. Wu

4.6.1 Introduction

It is of the utmost importance to establish the presence of distinguished theoretical particle physicists at the SSCL and to do so at a relatively early stage in the life of the Laboratory. While ultimately this will be achieved through the creation of both a permanent theory group and an active visitors program, it may take some time to attract people of the highest caliber. Therefore, while recruiting permanent members for such a group should have a continuing high priority, a strong visitors program is especially critical in the early years of the Laboratory's existence. Even after a permanent theory group is in place it is important to have many visitors enlivening the SSCL with a continuous stream of new theoretical ideas and viewpoints from outside the Laboratory. This adds to the diversity of the theory group and the atmosphere of the Laboratory. It is with this in mind that the early program in theoretical physics was planned.

Advice on theoretical physics activities is provided to the Associate Director for the Physics Research Division by a Theory Advisory Committee. Present members of this Committee are T. Appelquist (Yale), W. Bardeen (FNAL), S. Drell (SLAC), D. Gross (Princeton), I. Hinchliffe (LBL), and J. D. Jackson (UCB).

4.6.2 Progress

There were two primary goals of the 1991 program: to establish a strong long-term visitors program and to hold a conference on implications of developments in electroweak and flavor physics for the SSC.

The establishment of the long-term visitors program had a noticeable effect on the atmosphere of the lab. A dialogue between those working in experiment and in theory was established, and a weekly seminar put in place. Theorists G. Kane (U. of Michigan), S. Meshkov, F. Paige (BNL) and A. Sanda (Rockefeller) spent between three and nine months at the SSCL in FY 1991.

Kane calculated Standard Model QCD predictions for the transverse polarization of a top quark produced at, for example, the SSC. This result can be used to test the standard model in SSC experiments and is reported in an SSCL preprint (SSCL-486).

Meshkov investigated the possibility that the collisions of B-mesons and protons could be studied experimentally at the SSC (SSCL-463, Phys. Rev. D44, R1903 [1991]). This would be feasible because at the SSC B-mesons are produced at very high energies and have correspondingly long lifetimes in the laboratory. The cross sections are estimated by hypothesizing a scaling law and then using it to extrapolate from K-meson collisions with protons. He also continued research on a theory of quark and lepton mass generation in which an underlying symmetry is systematically broken to produce spectra that are consistent with the observed quark and lepton mass hierarchies and those of the weak mixing angles manifested in the Cabibbo-Kobayashi-Maskawa matrix.

Sanda considered the question of how to match the theory that describes elementary excitations, i.e., QCD, to the effective theory at low energies, namely a chiral Lagrangian. There is evidence that the matching is smooth, in the sense that the renormalization point dependence of matrix elements of operators that mediate the weak transitions is similar in the full and effective theories (SSCL-373). Sanda also presented two papers at the International Workshop on the B Factory at Tsukuba, Japan: "Model Independent Test of the Standard Model" (SSCL-481) and

"The B Factory, The Superconducting Super Collider, and the e^+e^- Linear Collider: How They Stack Against Each Other" (SSCL-347). While at the Laboratory, Paige contributed to two Letters of Intent (SSCL-SR-1155 and SSCL-SR-1161) to write proposals for experiments at the SSC.

There was also an active shorter-term visitors program, with many theorists visiting for periods of up to a few weeks. The total number of visitors peaked at the time of the conference in May (see below), and included B. Grinstein (Harvard), Z. Huang (Simon Frazer), G. Martinelli (Rome), A. de Rujula (CERN) and M. Wise (CalTech). The visitors program also includes theorists from universities in the Dallas metropolitan area. V. Teplitz (SMU), P. Rosen (UT - Arlington) and now F. Olness (SMU) are present on a regular basis, adding to the activity level and atmosphere of the theory group.

The second annual SSC Spring Conference, "Electroweak and Flavor Physics: Implications for the SSC", was held May 20-23, 1991 and was organized primarily by the theory group visitors. There were seventy-three participants (including thirty-one speakers), representing fifty-one institutions, who discussed the latest developments in theory and experiment. Topics included neutrino physics, K-decays and B-physics. The Conference closed with a round table on "SSC Possibilities for B Physics", underlining the importance of the SSCL for future research in an area already established as of both current and future interest.

At the beginning of FY 1992, Benjamin Grinstein (Harvard) and Frank Paige (BNL) accepted offers to join SSCL's Theory Department. Recent work of Grinstein has focused on the development of the Heavy Quark Effective Theory (HQET) and its implications for D- and B-meson physics. He applied the canonical quantization procedure to the HQET to investigate its Hilbert Space (SSCL-Preprint-12). Using two dimensional QCD in the large N approximation as an exactly soluble model of the strong interactions, he calculated static properties of heavy mesons and compared with predictions of the HQET (SSCL-Preprint-64); (see Fig. 4.6-1). Recently a method for studying the effects of chiral symmetry breaking in the light quarks sector on properties of heavy mesons has been developed. Grinstein and collaborators used this method to calculate f_{D_S}/f_D and B_{B_S}/B_B (SSCL-Preprint-25).

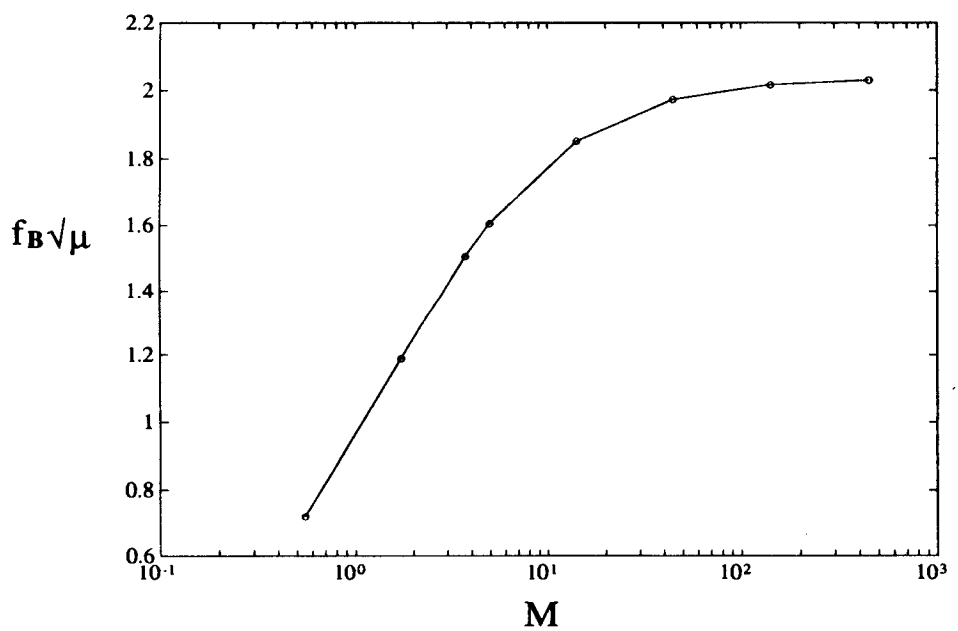

Figure 4.2.6-1: Plot of the pseudo-scalar decay constant $f_B\sqrt{\mu}$ as a function of the mass of the heavy quark. The mass of the light quark, m, is fixed throughout: $m^2 = 0.3$.

Grinstein has been invited by the editors of Annual Review of Nuclear and Particle Science to write a short review of this new field. This has appeared as publication SSCL-Preprint-34. The longer, more detailed review "Lectures on Heavy Quark Theory" appeared as SSCL-Preprint-17.

Grinstein's interests span a variety of subjects, as evidenced by his previous work which includes, among other topics, quantum cosmology and wormholes, radiative B-decays, CP-violation, neutrino physics, supersymmetry, grand unification and large scale structure of the universe. It is not unlikely that his work in the future will represent this rich background. For example, he recently investigated the effect of a heavy top quark on the QCD connections to relations between electroweak parameters (SSCL-Preprint-13).

Paige has established a worldwide reputation for expertise in the area of simulation of physics processes as "seen" in detectors. He developed in this connection the ISAJET Monte Carlo program which has been widely used for physics simulation at hadron colliders over the years. His work is of course of immediate relevance to experiments at the SSC. Paige will continue development of ISAJET. Currently ISAJET employs the branching approximation based on leading-log QCD to generate multi-jet final states. Other Monte Carlo programs are available which generate exact lowest-order matrix elements for multi-jet states, but do not generate complete events. An effort is under way to combine the two approaches. The exact matrix element will be used for the desired final state partons and the branching approximation will then be applied to generate QCD effects on all scales from those in the matrix element down to of order 1 GeV, and the resulting partons will then be hadronized. This is clearly qualitatively correct, but it is not yet clear how well it will work in practice.

Paige will continue to add new processes to ISAJET in response to theoretical developments and the interests of the experimental collaborations. He will continue working on specific calculations of signatures and backgrounds for the GEM detector, although many are also applicable to SDC. A key issue will be the development of a coherent trigger strategy, which involves an interplay between the possible signatures for new physics, the Standard Model backgrounds, the available experimental hardware, and the trigger and data acquisition electronics.

Meanwhile, the visitors program provides an essential part of the theoretical activity. As mentioned above, it is important to maintain a strong theoretical visitors program when a full, permanent theory group is established. S. Meshkov and Dan Di-Wu (Beijing) are long term visitors for FY 1992. Short-term visitors have included Z. Bern, M. Dugan, I. Dunietz, M. Golden, P. Griffin, C. Llewellyn-Smith, and T. Truong.

Meshkov organizes the weekly seminar series (including both theoretical and experimental physics topics), as well as special talks. The list of seminars so far in FY 1992 is shown in Table 4.6-1, and gives an indication of the growing physics research atmosphere at the SSC. Many of the theory speakers listed stayed for periods of several days or more, contributing to the intellectual atmosphere at the SSCL.

In addition, the theory group has been involved in several major meetings that involve the SSC Laboratory as a whole. Members of the group have helped organize the SSC meeting held in Corpus Christi in October, 1991. The SSC Laboratory will be organizing the 1992 Rochester Conference, to be held in Dallas in August, 1992. Here again, it is expected that the theory group will have a role in helping organize activities associated with that Conference. The theory group participated in the meetings at the Laboratory in November, 1991 which brought together current and former TNRLC fellows from around the country.

Table 4.6-1: Seminars at SSCL in FY 1992

Date	Speaker	Institution	Title
9/4	Z. Huang	Simon Fraser	Heavy Quarks and Strong CP Problem
9/5	P. Hurst	Fermilab	Electroweak Physics at CDF
9/6	S. Dasu	SLAC	Deep Inelastic Scattering at SLAC
9/19	N. G. Deshpande	Oregon	A Model for CP Violation Based on Higgs Exchange
9/26	H. Montgomery	Fermilab	D0-Status and Future Evolution
9/27	H. Quinn	SLAC	CP Violation in B Physics: Additional Modes
10/9	A. Fridman	University of Paris	B Physics in Proton-Proton Interactions
10/10	D. Nanopoulos	Texas A and M	Unified Theories and the SSC.
10/21	S. Brodsky	SLAC	New QCD Mechanisms for Heavy Quark Production
10/22	M. Dugan	Harvard	Decoupling of Doubler Fermions in the Lattice Standard Model
10/24	J. Schwarz	Caltech	Superstrings
10/31	F. Olness	S.M.U.	What is Really Inside a Proton?
11/1	M. Golden	Boston	Hiding the Electroweak Symmetry Breaking Sector
11/5	J. Rafelski	Arizona	Strange Antibaryons from Quark- Gluon Plasma
11/14	R. R. Shannon	Arizona	Hubble Space Telescope Optical Systems Failure Report.
11/19	U. Goerlach	CERN	Search for New State of Nuclear Matter- the Quark Gluon Plasma
11/20	R. R. Wilson	Cornell	Starting a Modest Laboratory
11/21	J. Mehra	Trieste	My Last Encounter with Richard Feynman
12/2	M. Turcotte	SSCL	Liquid Argon Calorimetry
12/3	V. N. Beljaev	Moscow	Status of the Soviet Union and its Scientific Program
12/4	J. Bensinger	SSCL	The SDC Muon System
12/5	T. Fuess	Fermilab	Search for W' and Z' at CDF
12/5	R. Adair	Yale	Are Biological Effects of 60 Herz EM Fields Possible?
12/9	J. Dorenbosch	SSCL	Electronics, Trigger and Data Acquisition
12/12	G. West	Los Alamos	Why QCD Perturbation Theory Works so Well
1/20	Z. Bern	Pittsburgh	New Perturbative Rules for QCD
1/27	E. Prebys	CERN	Results from LEP
1/28	D. Ng	North Carolina	Looking for New Gauge Bosons at the SSC
1/29	J. Kroll	Chicago	Measurement of Electron Production in Hadronic Z^0 decays, and a determination of the Partial Width of the Z^0 to b - b bar.
2/3	I. Dunietz	CERN	CP Violation with b-flavoured Baryons
2/5	G. McCartor	SMU	Introduction to Light Cone Quantization
2/6	I. Dunietz	CERN	Determining the CP Violating Phase with B-decays
2/13	A. Kunin	CERN	A search for Standard Model Higgs Boson with L3 detector at LEP
2/18	L. Naiquan	Hefei	Construction of 800 MeV Synchrotron Radiation Source
2/24	R. Settles	MPI	Progress in Linear Colliders.
2/27	D. Robertson	SMU	Light Cone Physics
2/28	A. Aeppli	BNL	Radiative Corrections to W pair production via Four Fermions
3/3	T. Truong	Ecole Polytechnique	Elementary and Composite Higgs
3/5	J. Xian	CERN	Recent Results from L3
3/12	V. Miransky	Ohio State	Origin of Particle Masses
3/13	V. Miransky	Ohio State	Why is top much heavier than bottom?
3/16	L. Frankfurt	Michigan State	Fluctuations of Color in High Energy Processes.

SECTION 5

FY 1992 AND FY 1993 PROGRAM

5.2 GEM

5.2.1 Computing/Simulation

The primary focus of work is expected to be coordination of the simulation effort in support of the TDR. It will eventually be desirable to have physicists at the SSCL familiar with the simulation activity for each subsystem, that is magnet, beam pipe, central tracking, calorimetry, forward calorimetry, muon systems, and trigger levels 1 through 3. This work will have to be matrixed with efforts directed at simulating key physics processes, and coordinated with the efforts in pattern recognition and event reconstruction, and physics analysis in general. During FY 1992/93, the SSC effort will coordinate simulations throughout the collaboration, and provide library and code management facilities to assure orderly development of the full detector simulation codes including event generation facilitated by the availability of the PDSF at SSC, definition of standards and file structures, and the general problem of the creation of software standards for GEM. We will need support for a GEM software library and software distribution system, and expect significant effort on database development. We expect the hardware for actual simulation work to be supported by the PRD Computing Support group.

Computing for the TTR will be done entirely at the SSCL. Both the on-line system and the off-line system are being constructed by SSCL staff, augmented by visitors. The DAQ is a dual effort using on the one hand a MacIntosh in a reliable system well-tested elsewhere, and on the other hand a VME-based system using a UNIX workstation which is viewed as experimental, but which will have a much greater data-taking rate capability. This second system may form the prototype for GEM DAQ systems for subsequent test beams running at accelerators. The off-line system will be capable of running on a variety of UNIX-based workstations, and will be designed to allow it to be adapted for future running with muon chamber prototypes. This system is designed to test each technology and look for problems, and that facility is well suited to the needs of prototype testing.

We need to initiate development of the GEM slow control system which will eventually provide the experimental control system. The first system that will need support is the magnet which will be complete in 1996, but the specification of its control system is an integral part of the overall procurement which is on the critical path for GEM completion. We intend to coordinate our work in this area with the accelerator controls group at the SSC. The requirements in this area are mixed - it requires hardware engineering for detailed data acquisition development, as well as software support for user interfaces, and of course physicist support to determine the user needs. The time scale is set by the magnet which requires a working control system in hand in a few years to test the first coils that will be wound. While other collaborators could provide equipment and software, we need SSC staff input to ensure compatibility with other GEM and SSC systems.

We expect to initiate local work for the on-line level 3 filter. The urgent issues are the determination of which algorithms will run in this system, which is envisaged a ranch (Texas size farm) of CPU's, and an assessment of the run times of these algorithms. This work interacts directly with work on developing the overall trigger strategy. This work requires support for design and analysis of the system architecture which will be coordinated with the joint effort with E-Systems; software support for design and simulation of demands on the level 3 is also needed. Since the level 3 system has been estimated to cost up to $20M, this is an area of large uncertainty and technical risk, requiring definition in the near future. The SSC computing group will play an integral role in this effort.

The level 3 effort is closely related to work on networking, data communication and data storage. We have chosen to have single data store, and not have local storage at the detector in case of data transmission failure. The data will come off the detector into the level 3 and then over a data link to the off-line and storage. The SSC group must understand the technical issues and the likely prognosis for future developments. The SSC computing group must also assess the specific needs for GEM data storage, which because of our interests in processes like Higgs to gamma-gamma, are likely to be significantly larger than SDC's needs.

Needs for the simulation and computing efforts include continued funding for the external contractors; funds for R&D to establish the slow control system for the magnet; funds for teleconferencing facilities to facilitate the many efforts being coordinated through the SSC. The effort will grow from 5 FTE currently, to 9.5 FTE in FY 1994.

5.2.2 Muon Systems

The GEM muon group will spend the remainder of FY 1992 utilizing the TTR for the detailed test, evaluation and comparison of muon chamber and trigger technologies. Selection of the final technologies is a key element in the progress towards the TDR in November. Representatives from 18 collaborating institutions will participate at the SSC during this time period. SSC staff have major responsibilities in the operation of the TTR, including the magnet, trigger, data acquisition and analysis. It is expected that one of the prototypes tested will be built here at the SSC, in order to develop both the infrastructure and the experience in working with large high-precision chambers. This infrastructure is critical in order to service all of the visiting groups with their attendant technologies. We expect to continue running the TTR after the decisions are made, to extract all possible useful data and experience with the chambers.

Detailed planning will also begin for the construction at the SSC of the first GEM muon module, consisting of 3 superlayers. This will most likely be a hybrid of several technologies, but will serve to begin to understand the mechanical and alignment constraints required to achieve the GEM resolution goals. Here again the SSC staff will act as host and coordinator of the activities of both US and foreign groups involved in this effort.

The muon laboratory infrastructure developed in support of the TTR and subsequent work will also likely provide support for other GEM efforts requiring wire chamber technology, namely the central tracking and test beam activities discussed below.

Major needs for the muon group include test and measurement facilities such as lasers and precision tables; specialized tooling to create an operating chamber facility, such as winding tables; scopes and accumulation of electronics and logic units needed for testing. The effort will grow from 7.25 FTE now to 8.5 FTE in FY 1994.

5.2.3 Central Tracking and Beam Line

The SSC tracking group expects to grow and diversify its efforts in the coming years. We expect to build one of the IPC prototypes at the SSC utilizing joint laboratories with the muon effort. Since the IPC technology is also shared between the central tracking and the forward muon system in GEM, this is a natural symbiosis for the local groups as well. This hardware effort will be augmented by simulation activities in support of tracking. We expect to study issues of resolution, particularly emphasizing the physics of sign selection. We will also use the radiation transport codes installed at the SSC to continue studies of the radiation environment of the tracker, particularly emphasizing optimization of the beam pipe and forward calorimetry shielding. The

group will work closely with the accelerator group, many of whom are also GEM participants in the final designs of the IR and positioning of the final focus quads.

Since the beam pipe and vacuum at the interaction point most directly affect the tracking performance, we will continue to work on these areas. Studies of the how the beam pipe is assembled and brought to a sufficiently good vacuum, and the interaction of these issues with the overall GEM detector assembly and integration are major concerns.

The tracking effort needs funding for development of the infrastructure of a precision chamber test facility. This includes data acquisition, precision table, and telescopes, fast scopes, and a gas analyzer. Also needed is a precision CNC mill which will be shared with other efforts. The tracking effort is expected to expand from 1.5 FTE now to 4 FTE in FY 1994.

5.2.4 Test Beam Coordination and Support

A critical element of the GEM project is the test beam activity related to R&D efforts in support of the detector design. This past year activities were concentrated on calorimetry measurements in the BNL and FNAL test beams. This year there will again be calorimetry tests performed, at BNL and CERN. It is also expected that tests of muon chambers and measurements of punch through will be done in association with CERN groups. In the near future possibilities exist for running at SLAC at the end of 1992, FNAL during 1993 and late 1994, IHEP (Serpukhov) in 1993 and later, and in dedicated CERN beams. Finally it is expected that beams will become available at the SSC itself by January 1996.

GEM expects to avail itself of all opportunities for testing models, prototypes, and actual detector elements, in order to ensure the success of the detector. These efforts require significant coordination and support. The group at SSC has undertaken this challenge and has begun planning for long term involvement in test beams world-wide.

The effort begins with compiling the detector subsystem needs and plans, and providing liaison and negotiations with host laboratories. The equipment for testing goes beyond the test elements themselves. It includes beam chambers and diagnostics; particle identification devices like Cerenkov counters, TRD's and lead glass; hardware trigger elements and data acquisition. Our group has begun to assemble and plan for providing such infrastructure to avoid duplication and efficiently support such efforts. The data acquisition team is designing a portable high rate system, which may first be tested on the TTR and then used for GEM test beam activities at the various sites discussed above. This system will be provided complete with diagnostic software. The muon group is planning as part of their infrastructure to have a chamber facility capable of delivering small beam chambers for such tests. These chambers will be designed to have a position resolution of 50 μm or less in order to enable precise tests of GEM inner tracking technologies. We also expect to develop a pool of electronics that will be available for tests at the SSC and elsewhere. This kind of in-house capability exists at currently operating laboratories; the challenge here at SSC for GEM, which does not have access to such resources, is to develop this capability for SSC testing by providing it earlier for tests done in the near future elsewhere. The test beam support effort needs data acquisition and front end electronics. Development of precision chambers in coordination with the muon and tracking efforts will also need support. The effort will grow from .25 FTE now to 2 FTE in FY 1994.

5.2.5 New Efforts

Despite the success of GEM in initiating a viable program at the SSC, there are significant areas which need particular attention. At the moment there is no effort directed towards calorimetry, triggering and electronics. The calorimetry group is still struggling with choosing a

technology. The choice is between a sampling liquid-ionization device or a hybrid total absorption crystal combined with a fiber scintillator hadronic calorimeter. The decision is slated for August 1992, and we expect that as soon as it is made recruitment of calorimetry people to the SSC will be facilitated. In either case, the SSC will become a focus for significant effort, but the details will depend on the particular choice and on the physicists who come. For either technology choice it is likely that the EM calorimetry will be built elsewhere; however the scale of the hadron calorimeter in either scintillating or liquid argon cases, will most likely require significant effort at the SSC. Thus we expect that this will be the focus of any near term work on calorimetry here. Final assembly of either calorimeter must be done at the SSC, and will require an expert in-house group to facilitate assembly, test (including beam test at the SSC), installation and commissioning. We expect this effort to reach 6 FTE by FY 1994.

There is also no current local effort on electronics and trigger, although the SSC has significant resources in talented engineers and some physicists in this area. In order to effectively utilize this pool we need to recruit some key personnel in this area, and expect a level of 4 FTE by the end of FY 1994. A guideline for our recruiting efforts is given by the need to draft and produce the TDR by the end of the year. Since this effort is expected to be centered at the SSC, we have set a goal to have local experts in each of the areas covered in the TDR. This includes all of the major technical subsystems and areas. While the precise level of effort is uncertain, each of these groups will need funding to establish the requisite infrastructure. The summary of current and projected effort for GEM is given in Table 5-1.

Table 5-1: Summary of Current and Projected GEM Efforts (FTE)

	Current	FY92	FY93	FY94
Computing/Simulation	5	5.5	7.5	9.5
Muons	7.25	7.5	8.5	8.5
Tracking	1.5	1.75	2.25	4
Test Beam	.25	.25	.75	2
Calorimeter	0	.5	3.5	6
Trigger/DAQ	.25	.5	2.5	4
Total FTE	14.25	16	25	34

5.3 SDC

During this period, the SDC will move from the proposal stage into active construction. Significant work on this detailed integration of the detector subsystems into the design will accelerate at the SSC Lab. The permanent SDC project manager will be appointed. Further work on beamline design, test beam facilities for SDC, and the surface and underground facilities will be proceeding during this period. While the bulk of the SDC detector will be constructed elsewhere, important in-house efforts in the muon system, calorimetry, and charged particle tracking will help tie together the offsite activities with the local infrastructure. Important efforts in the SDC DAQ system design and software and simulation will be expanded. Areas in which work has already been initiated are detailed below.

5.3.1 Computing and Simulation

Physics simulation activities at SSC Lab for SDC will concentrate, as in the last year, on detailed simulations needed to guide the engineering design. A few areas that need further physics simulation work that we plan to work on locally are signatures for non-minimum Higgs Sector models, more detailed work on trigger rates, and more concentrated work on electron signature in the SDC design. This work will largely be carried out on the PDSF, and will be supported by the PRD computing support group.

Details of the proposed design of the SDC software systems are provided in the SDC TDR. We plan for the highest level parts of the online system to be defined at an early stage by a top-down design using standard software engineering tools. The top-down design will then be used with the "bottoms-up" hardware prototypes as hardware is purchased and expertise in its operation acquired. The schedule for prototyping and testing the online system is closely linked to the DAQ installation schedule. The next major milestone is the testbeam running at Fermilab in 1994. During 92-93, parts of the online system based software will be tested as prototypes in preparation for the 1994 Fermilab test. Effort at SSC Lab is already being put into evaluating existing UNIX-based systems at KEK and from commercial vendors, as a common effort with the GEM group. This effort will grow to 6 FTE by the end of FY 1994.

5.3.2 Muon Systems

During FY 1992-93 we will continue developing the round tube design. We have now decided on 90 mm drift tubes the barrel and intermediate muon detector.

Thus we will build some short 90 mm cells to test at BNL in May and June. These tests will also include tests of 45 mm round drift cells for the forward system. We will continue our cosmic ray tests of the 9 meter prototype module in collaboration with University of Texas, Arlington and the University of Washington. We will construct some 9 meter drift tubes with optimized Al extrusions and field shaping electrodes. We are currently redesigning the end cap electrodes based on our experience with the 9 meter prototype (J. Thunborg, H. Lubatti). We will continue work on implementing a VME based DAQ system in collaboration with KEK physicists.

A major effort in this period will be to design and fabricate in the SSC-SDC muon lab a super module consisting of BW1, BW2 and BW3 layers. This will involve perfecting the manufacturing process for both the drift tubes and the module assemblies. We also will fabricate an alignment stand which will hold one super-module in order to evaluate and test our alignment procedure. The super module will be instrumented with electronics and cosmic ray triggers will be recorded by our DAQ system. This will allow us to better understand the alignment requirements and allow us to further refine our system design.

For the forward system we will continue to develop a design with the goal of providing a final design document for the forward chambers by fall 1992. Various prototypes will be constructed and tested. Detailed design of the muon-system toroid magnets will proceed (J. Bensinger). Prototype tests of the magnet system will be carried out during this period. Construction is scheduled to begin in 1994. The entire group will continue to work on specifying the surface facilities needed for super-module assembly.

The major needs for the next years will be to bring the muon lab infrastructure up to full capacity. There are needs for tooling such as layout tables; gas control equipment; electronics and data acquisition modules, as well as materials like adhesives and wire. The muon group will grow from 3.5 FTE now to 9.5 in FY 1994.

5.3.3 Calorimetry

During FY 1992-1993 SSCL physicists will continue the development efforts on the calibration system for the SDC calorimeter. The near-term schedule is driven by the need to generate a preliminary design in time for the final design of the pre-production prototype module that is to be tested in early 1994. The preliminary design of the calibration systems needs to be completed around January 1993. This includes all the details of the light flasher system, the source drivers, the current measuring electronics, the charge injection system, and the mechanical mounting and provision of power and cooling for the move. In July 1992, a review is planned of the conceptual design for the calibration system. In preparation for that review, studies of details of both the expected system performance, summarized by a calibration system requirements document, and the final conceptual design and cost, as summarized by a brief conceptual design report, will be carried out. Further work on the details of the optical model for the calorimeter system will be carried out as our understanding of the system performance improves.

Work on calorimeter simulations, particularly on the insitu calibration methods, studies of cracks, and the electron response for the full detector, will continue. Beam tests of prototype end cap EM calorimeters, and alternative EM designs will be carried out at BNL in early summer 1992 in which SSCL physicists will have some participation. A 20-tower EM stack will be constructed in collaboration with Dubna for study of the time stability of the calibration system. We hope to have the stack operational by late summer 1992, and continue studies with the stack throughout the period. Testing of front end electronics schemes for both signals and current measurement will be carried out in conjunction with the 20 tower stack test. Work on the test beam systems needed by the calorimeter will continue.

The calorimeter group is helping to organize an international conference on calorimetry to be held in Corpus Christi in October.

The estimated calorimeter budget includes funds for scopes, VME electronics, sources and source drivers for calibration studies, and items like scintillator, fibers, and photomultipliers. The calorimeter group will expand from its current strength of 3 FTE to 9 FTE by the end of FY 1994.

5.3.4 Tracking

The SDC tracking group will diversify its efforts in the coming year. Studies of what facilities will be needed here to support the installation of the silicon inner tracker, and the fiber, straw and gas microstrip options are already underway. Shortly after the SDC TDR is completed, we should have a fairly clear picture of the staff and facilities needed for the installation of the tracking package. The ongoing SDC silicon tracker effort has requested SSCL assistance with radiation damage tests at LAMPF next summer, as a way to begin collaboration with the local group. Our work on fiber readout techniques will continue through the period. This will mainly focus on the design of the VLPC readout system, including the cryogenic system and its safety analysis. Engineering work on the barrel straw design will continue. Work on track detector

simulations will also continue, and focus on the electron response of the full SDC design. The tracking effort will grow from 1.5 FTE now to 3.5 FTE in FY 1994.

Table 5-2 gives a summary of current and projected efforts on SDC.

Table 5-2: Summary of Current and Projected SDC Efforts (FTE)

	Current	FY92	FY93	FY94
Computing/Simulation	2	3	4.5	6
Muons	3.5	4.5	7.5	9.5
Calorimeter	3	4	6	9
Tracking	2	2.5	3	3.5
Electronics/DAQ	1.5	2	3	4
Test Beam	0	0	1	2
Total FTE	12	16	25	34

5.4 Common Efforts

5.4.1 Tracking

The Tracking Group will focus on the use of scintillating fibers and interpolating pad chambers during FY 1992 and FY 1993. We perceive that these are relevant, developing areas of importance in High Energy Physics not only within the context of SSC experiments, but wherever high collision rate experiments require tracking detectors.

We intend to investigate more fully the applicability of avalanche photodiodes to the readout of scintillator calorimeters, and will gain more experience with these APDs operating in linear mode to investigate fully this mode of operation of the detectors for use in tracking systems.

Initially more promising for scintillating fiber trackers, however, is the operation of APDs in Geiger mode. In this mode the output of the diodes can easily average 10^6 electrons per incident photon. As a result, the required signal processing electronics can be quite simple and cheap. On the other hand, in order to run the tracker at rates above about 10^6 sec^{-1} per fiber, circuits may be needed to be developed to recharge the pn junction quickly. We will continue forays into this line of research (Appendix F), and clearly need to pursue them more completely. Towards this end we have prepared the electronics and other systems for a Geiger mode tracking test, and plan to beam test them once the APD production problems are solved.

We will study another promising device, the visible light photon counter, or VLPC (Appendix G). While these devices are not available for in depth studies in our labs as of this writing, we anticipate their availability within the coming months. It seems prudent to experiment with these new single photon counters and to compare our results with those of Atac and Rockwell International, the developers of the device. Apart from the need for a liquid helium dewar and modest cryogenic support equipment, the facilities required for such tests are similar to those for any fiber tracking study.

In particular, one such need is for a standard multi-channel optical connector. Successful short-run prototypes of these have been developed by other researchers, but no 'standard' such device exists. We intend to convene a quorum of the researchers who are active in the readout techniques for scintillating fibers, along with expertise from the plastics molding industry and engineering talent, to develop specifications for low-loss, dense, multi-channel connectors. They would be designed with the HEP community in mind and would, among other things, put a premium on space and material budgets. These are issues which are not a concern in the communications industry where existing connectors have been developed.

Ribbons of scintillating fibers destined for use in trackers are another area which we feel needs attention. We would like to concern ourselves with the mechanical quality of the final ribbon. Since the resolution of a tracker can be no better than the alignment of its elements, it is important to understand the limitations of fiber placement accuracy. We expect that the results of this work would be applied in the future either for assuring the specified alignment of ribbons or for obtaining alignment constants for each ribbon destined for use in a detector.

To support these efforts we need funds for scopes, electronics, power supplies, a laser and a fiber polisher. We expect this effort to grow slowly from 3 FTE now to 5 FTE in FY 1994.

5.4.2 Electronics

In general work at the SSCL will closely mirror the needs of the SSC experiments. The demands from the present collaborations will increase, while new ones will be generated by the "small experiments" program. Designs may be also required for HEP experiments outside the

SSCL. They would provide a valuable opportunity to test new designs under realistic experimental conditions.

During FY 1992-93, the group will gradually become more involved in hardware implementations of design ideas. Simulation will continue to play a major role, but its focus will shift from abstract behavioral descriptions to detailed investigations at the register-transfer level. Electronics R&D and detector prototype testing will require the fabrication of prototype front ends, readout boards and crate-level systems. Some of these prototype systems will have functionalities, data rates and bandwidths approaching those required by SSC experiments.

Front End Design

In FY 1992 we expect to fabricate the first prototypes for the gas micro strip detector readout chip and for the current splitter. Depending on types of calorimeters selected by the collaborations, a fast, low power ADC with a reduced dynamic range may be needed for the shower-max detectors. SSCL could participate in such a current splitter-ADC design. It would probably be fully implemented in CMOS.

As the front end designs mature, more attention will have to be given to the circuitry that collects the data from these chips. The functionality of these Data Collection Circuits (DCC's) is currently under study (see above). Possibly commercial chips can be used. If, however, no commercial solution can be found, these digital chips will have to be designed within the HEP community. Several full custom digital chips will be required for the trigger logic. The SSCL will build up its digital VLSI design capability to satisfy this need. The efficiency of the designers will be enhanced using professional CAD methods: high-level behavioral specification and logic synthesis to design, lay out, verify and test the VLSI's.

Demand for testing will explode in the 1992-1994 period. All detector subsystems face a similar schedule requiring front end prototypes to be fabricated and tested during this period. Also, as designs mature, testing must be done with increasing precision, putting greater demands on the quality of the test equipment and on the ingenuity of the test personnel. Demand for board-level testing will also develop. This will require the acquisition of a different class of equipment and software. Given the high cost of such equipment, it makes sense to provide a central facility to the collaborations at the SSCL. If professional CAD software and of industrial test methods (like Boundary Scan) are used consistently in the HEP community, testing will faster, more accurate and more economical.

Front End Interface

By the end of FY 1992 the functionality of the interface with the front end chips must be defined. Choices will have to be made on signal levels and on data acquisition protocols. We also expect availability of prototype line drivers and receivers. In FY 1993 these protocols will be applied to all detector subsystems. General purpose software will be developed to monitor data flow and to provide error detection and correction. Special emphasis will be given to efficient diagnostics.

The use of similar hardware and software throughout the detectors will represent economies of scale, and large savings can be made in the effort needed to commission and operate the experiments.

Data Collection Network

The simulations of the Data Collection networks will become more detailed. Initially, high level models will be used with parameter values representing actual, realistic technological alternatives. Later a change in software tools will occur from the very abstract MODSIM language

to languages tailored to electronics simulation, such as VHDL and Verilog. These languages also provide a closely-linked design, simulation, test, and production environment. The simulation will extend from the front end and data collection domain to the area of event building and higher level on-line processing. More emphasis will have to be given to studies of fault tolerant and redundant systems.

Trigger Studies

Trigger studies will continue to play a central role in the design process. As the detectors become better defined, these studies will become more realistic and will shift towards implementation alternatives. By 1993 enough may be known about technologies available at turn-on to consider building the first small scale prototypes for some of the critical trigger components.

Data Acquisition

The DAQ systems developed at the SSCL will be used by the GEM collaboration in FY 1992 for muon chamber prototype tests at the SSCL and in test beams. It is expected that the LabView based system will be ported to non-Macintosh platforms. This will make it faster and enhance the portability. The UNIX based system will be implemented on different platforms. Various processors and data transfer media will be evaluated. We will also look into the use of software available in the public domain for monitoring tasks. Public domain software may also provide an affordable human interface.

The modularity of the system will be exploited to provide DAQ systems to test different detector prototypes for both collaborations. Experience gained from these tests will be incorporated in the design. Additional features, such as partitioning and dynamic segmentation, will have to be added to work towards the actual data acquisition system for the experiments. The group may also participate in the DAQ efforts of HEP experiments joined by the SSCL and in test beam preparations.

To support these efforts we need funds for test and measurement equipment, wire bonders, a wafer probe and data acquisition. The common electronics effort will grow from 4 FTE now to 6 FTE in FY 1994.

5.4.3 Other Physics at SSC

Currently A. Fridman is visiting the SSC and exploring B-physics possibilities here. We expect a low-level effort directed at small experiments to grow slowly until a call for proposals is issued in FY 1993, which will centralize activities. A summary of current and projected efforts on common and other physics is given in Table 5-3.

Table 5-3: Summary of Current and Projected Common and Other Efforts (FTE)

	Current	FY92	FY93	FY94
Tracking	2.25	3.5	5	5
Electronics/DAQ	4	4	5	6
B-Physics/Other	1	2.5	5	9
Total FTE	7.25	10	15	20

5.5 Outside Research

5.5.1 CDF Plans

By FY 1993 we should know whether we are building new forward muon chambers for runs II and III or using the current chambers. There will likely be considerable activity in this area regardless of the chosen option. If we decide to build new chambers, SSCL will undoubtedly be involved with some major portion of this construction, e.g. chamber construction, front-end electronics or trigger electronics. If we decide to stick with the current chambers, they will still need new front-end and possibly trigger electronics to deal with the higher rates.

The SSCL CDF group will concentrate its physics analysis efforts on two or three topics. The leading candidates are (1) measurement of the W mass, (2) measurement of the top quark mass, and (3) determination of the inclusive J/Ψ cross section. These analyses will begin in 1992 and continue into 1993.

W-mass Measurement

Measurements of various quantities in the electroweak sector of the Standard Model have reached the precision where it is necessary to include higher order corrections. Through virtual loops, these corrections are sensitive to heavier objects in the theory (such as the top quark and the Higgs) and to potential new physics. The most precise measurements are currently made at LEP. However, the various parameters measured there (mass, total width, partial widths, decay angular asymmetries, etc. of the Z) tend to have very similar dependence on the higher order effects, reducing the sensitivity to the top mass (or once the top mass is known, to other higher order effects). The mass of the W, on the other hand, has a distinctly different dependence on these higher order effects (see Fig. 5.5-1). Thus, although the mass of the W will not soon be measured as accurately as the mass of the Z currently is, it is still crucial for testing the Standard Model to measure the W mass as accurately as possible.

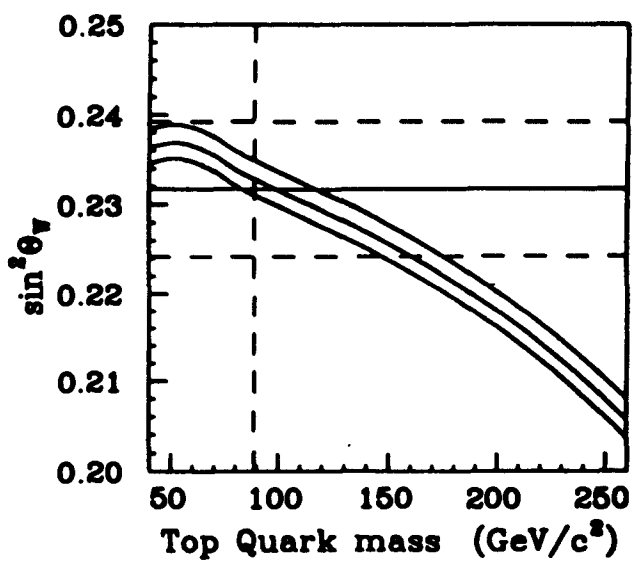

Figure 5.5.1-1: Relationship between $\sin^2 \theta_W$ and the top quark mass. The flat solid line is from the CDF W mass measurement and the dashed lines are one standard deviation errors. The vertical dashed line is the CDF lower limit on the top quark mass. The curves are $\sin^2 \theta_W$ determined from LEP Z mass for Higgs masses of 1000, 250, and 50 GeV/c^2.

In 1990, CDF published a result on the W mass of 79.91 $\pm$ 0.39 GeV/c^2. This measurement, in conjunction with a similar measurement by UA2 and measurements of other electroweak parameters, already limits the top quark mass to be less than about 200 GeV/c^2. Table I shows the contributions to the error in the current CDF mass measurement. In the electron mode, the most important single error is the statistical error of roughly 350 MeV/c^2, but the systematic error is already significant. As more data is accumulated, it is imperative to reduce the systematic errors in order to appropriately reduce the total error.

The one of the largest systematic errors in Table 5-4 is from the determination of the electron energy scale. We will work, in conjunction with the CDF analysis group doing the W mass measurement, on improving the determination of the energy scale in order to reduce this systematic error.

Table 5-4. Uncertainties in the W mass measurement

Uncertainty	Electrons	Muons	Common
Statistical	350 (440)	530 (650)	
Energy scale	190	80	80
(1) Tracking chamber	80	80	80
(2) Calorimeter	175		
Systematics	240	315	150
(1) Proton structure	60	60	60
(2) Resolution, W p_T	145	150	130
(3) Parallel balance	170	240	
(4) Background	50	110	
(5) Fitting	50	50	50
Overall	465 (540)	620 (725)	

All uncertainties are quoted in units of MeV/c^2. In parentheses are the statistical (and overall) mass uncertainties if Γ_W is determined in the fit as well. The scale uncertainties are in common with the Z mass measurement. The uncertainties which are the same for both samples are listed as common.

Presently, the electron energy scale is set by comparing the energy measured in the calorimeter to the momentum measured in the central tracking chamber (E/p - see Fig. 5.5.1-2) for a tightly selected sample of electrons from decays of W's. This method relies on understanding (1) the calibration of the momentum scale of the tracker, (2) radiative effects, particularly due to bremsstrahlung in the material surrounding the beam, (3) energy resolution, (4) possible selection biases, and (5) possible biases in the fit. For the current CDF measurement, the errors on the energy scale are 0.10% from tracking, 0.16% from statistics in the E/p plot, 0.10% from uncertainty in the amount of material surrounding the beam, and 0.11% from the other systematic effects (event selection, fitting, and resolution). When these are added in quadrature, the overall electron energy scale uncertainty is 0.24%. With an increased data sample, it should be possible to reduce most of these errors.

We would also like to explore using Z decays to e^+e^- and the well-measured Z mass from LEP to determine the electron energy scale. From a set of 65 e^+e^- pairs where both were in the central calorimeter, CDF measured a Z mass of 91.1 $\pm$ 0.3 $\pm$ 0.4 GeV/c^2, where the systematic error is primarily from the energy scale determination. Ignoring this contribution, the power of this method is comparable to the E/p determination. Also, in this case the uncertainty is dominated by the statistical error, which obviously shrinks as the data sample is increased.

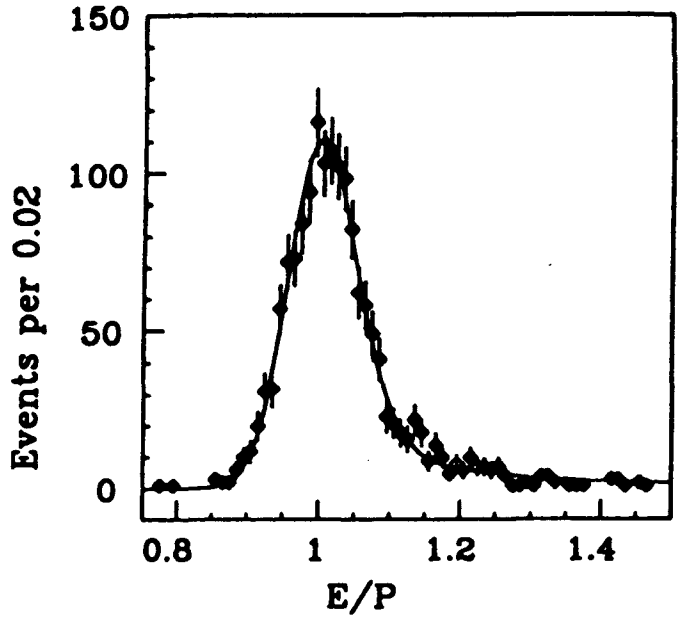

Figure 5.5.1-2: E/p distribution for W decay electrons compared to the radiative simulation. This match sets the overall scale of the central electromagnetic calorimeter.

Since a subgroup of the SSC CDF group is also part of the SDC calorimeter calibration group, working on the CDF electron energy scale is a particularly good match to our interest and expertise. In addition, some of us have experience with LEP with the radiative corrections to W and Z production and decay that are necessary to understand in both the E/p and Z mass methods.

Top-mass Measurement

One of the major aims of the CDF collaboration for the upcoming runs is the discovery of the top quark. Several groups in CDF are working on how to find the top quark in various channels (e-μ, lepton+jets, b-quark tagging, hadronic decays, eτ).

Not only is it important to find the top quark, but it is very important to measure its properties as well as possible, particularly, its mass. As discussed above, the higher order electroweak corrections depend on the top mass. Once this mass is known well, precision electroweak measurements become sensitive to other things, such as the Higgs mass, inconsistencies in the Standard Model, and potential new physics.

Since the expected top production cross section depends on the top mass (see Fig. 4.5.14) its measurement provides one measure of the top mass. It is important to try to measure the mass in other ways both to show consistency and to reduce the error on the mass measurement. At the SSC lab, we intend to study how to measure the top mass from the top events, once they are found. We are pursuing several preliminary ideas. First, the lepton spectrum in e-μ events and lepton+jet events depends on the mass. The question is how best extract the mass given what wil initially be a small number of events. Secondly, in lepton+jet events, it is possible to determine th momentum of the neutrino - the transverse component by $\not{E}_T$ and the longitudinal component by constraining the lepton and the neutrino to the W mass. There are usually two solutions to this constraint and it is important to have a strategy that optimizes the selection of the correct choice. Then, it is necessary to optimize the choice of jet to combine with the lepton and neutrino to form the top. A third possibility is to combine the three jets from a hadronic top decay, such as the top

quark in a lepton+jet event that didn't decay semileptonically or either top quark in a purely hadronic decay top event. Some of the questions here are how to optimally select the triplet of jets that came from a top decay (b-tagging could be very useful here), how to combine the jets to get the best top mass resolution, and how to optimally use the W-mass constraint.

For both methods in the lepton+jet events, combinatorics due to the presence of several jets are a serious background. This can be reduced by tagging which of the jets come from bottom quarks. One way to do this is by observing the semileptonic decay of the b. This method is limited by the semileptonic branching ratio and by the efficiency for observing the electron or muon. For the upcoming run, CDF is installing a silicon vertex detector (SVX). This will allow tagging of b jets by observing secondary decay vertices separated from the primary vertex. We are particularly interested in working on b-quark tagging by using the SVX. In addition, some of us are members of the SDC tracking group and hence have some expertise here and interest in understanding b-quark tagging in SDC.

J/Ψ Cross Section

CDF has observed a clean signal of J/Ψ's in the $\mu^+\mu^-$ channel (see Figure 4.5.1-11). We are involved in the analysis effort to determine the inclusive J/Ψ cross section from these events. Most of these J/Ψ's are expected to have come from B decays, and thus a measurement of the J/Ψ cross section is related to measurements of the b quark cross section.

A major difficulty in this is the uncertainty in the polarization of the J/Ψ's. The polarization determines the angular distribution of the muons in the J/Ψ center-of-mass frame. Due to the p_T cut on the muons, CDF does not have uniform acceptance in the center-of-mass angle, and hence, the overall acceptance has substantial dependence on the polarization. Study is underway to see if this polarization can be measured with the CDF J/Ψ sample, but it appears that once the p_T and geometrical cuts are made on the muons, the expected center-of-mass angular distribution is very similar for the various possibilities of the polarization, making a measurement very difficult. Work is continuing to resolve this issue.

Funds for this year are for continued support of the muon chamber effort. For following years, expenditures will depend on whether we are building new chambers or developing new front-ends for the current chambers.

5.5.2 Additional Outside Physics Efforts

The physics staff at the SSC is growing rapidly, and this brings with it the continuing interests of new staff in the physics that they were involved in, and interests in participation in new activities during the SSC construction. As part of recruitment, we encourage physicists to be involved in high quality research. Some negotiate the level of their participation in past activities, which is expected to decline as they become involved in the SSC physics program. In addition, the SSC aims toward organized participation in outside physics research. The criteria for such activities include excellence of the physics; timeliness of the results so that programs can be smoothly turned off as SSC physics approaches; relevance of the physics or detector challenges (e.g. high rate or similar techniques) to the SSC mission; and a critical mass of interested physicists at the Laboratory. Typically, interested physicists will organize and negotiate their prospective involvement with an experiment and then present the SSC PRD with a proposed plan. Since physicists at the SSC have research and tasks requiring their presence at the SSC, negotiation of their required presence at the outside experiment requires careful consideration.

There is currently an on-going negotiation between physicists at the SSC and the D0 Collaboration. D0 is complete and ready to take data in the upcoming run at Tevatron Collider. This run is partially exciting because of the prospect of discovery of top. There are 4 physicists at

the SSC who were previously in D0, and 10 others who have expressed an interest in participating. In addition there is a large pool of young D0 physicists who are in the process of applying to the SSC, for whom an organized and supported D0 involvement is an added inducement to come to the SSC. In addition there is a local group at University of Texas, Arlington that is actively involved in both D0 and SDC, that has an interest in local participation. The current SSC activities of physicists at the SSCL have matches to interests in D0 upgrade activities in tracking, muon triggering, simulation and analysis. Working on the tracker upgrade would represent a significant contribution from the SSC, while at the same time fitting in a timely way with R&D for the SDC tracker. Development of a muon trigger using space point wire chambers, has a natural overlap with the interpolating pad chambers selected for the GEM forward muon system. Of course, physics interests are one of the primary motivations and leads naturally to interest in involvement in analysis for the upcoming run. The existence of the PDSF at the SSC provides significant computing power for analysis of both detector simulations and physics data.

In addition to interest in D0, there is a significant community of SSC physicists who came to the laboratory by way of LEP experiments. While the SSC will not support fragmented efforts on all 4 LEP experiments represented here, there would be interest in participation in Z^0 and WW physics if a coordinated effort on a single experiment could be mounted. Finally considerable discussion among SSC physicists continues on the possible involvements in fixed target experiments in the rare K decay program and b physics. As yet these discussions have not yielded either a critical mass or satisfaction of the likelihood of timely results. Clearly the nature of funding will depend on the which outside ventures are approved.

A summary of current and projected levels of effort on outside physics research is presented in Table 5-5.

Table 5-5: Summary of Current and Projected Outside Physics Activities (FTE)

	Current	FY92	FY93	FY94
CDF	4.5	5	7	7
Other	2.25	3	8	8
Total FTE	6.75	8	15	15

5.6 Theoretical Physics

The buildup of a permanent theory group should continue in the remainder of FY 1992 and through FY 1993, with one or two more permanent appointments made. The Laboratory aims to recruit one or more theorists who can not only contribute to the theoretical physics research program but might also lead it. Although there is clearly some bias towards theorists who are not completely disconnected from experiment, the search will span the whole range of particle physics, with the hope of attracting a first rate person who has made and will continue to make substantial contributions. In addition, we hope to hire a theorist at the equivalent level of an Assistant Professor. The Laboratory believes that this approach will enable it to attract good people without unduly limiting its choices in the future. Once a permanent theory group is established and expected to grow further, it will be the time to start a postdoctoral program. This will consist of fixed-term appointments, typically of two year duration with possible extension to three years. Approximately two postdoctoral appointments are planned the first year, with a similar number planned for succeeding years to bring the total up to about six such appointments by the mid 90s. Such appointments are important not only because they establish a flow of younger people through a frontier laboratory and into the high energy physics community, but because they also bring in new ideas from the outside and, just as importantly, youthful enthusiasm.

The visitors program will be maintained at least at the previous year's level, if not expanded somewhat. Many have expressed interest in visiting the laboratory for periods of up to a year. B. Lynn has received a fellowship from the TNLRC and will spend it at the SSC. Dr. Lynn has made important contributions to the comparison of higher order electroweak calculations with LEP data, and he brings to the Laboratory a strong background in field theory combined with a lively interest in experiment.

The theory group will organize a weekly seminar. Members of the group will actively participate in workshops and symposia around the nation and overseas and will act as an information bridge between the laboratory and the rest of the scientific community.

Involvement in workshops and conferences will continue. Consideration will be given to holding an SSC Physics School during this fiscal year. There has been recent growing interest by the experimental community in the possibility of studying heavy hadrons (D, D_s, B, B_s, Λ_b, Ξ_b, etc.) at the SSC. The theory of heavy hadrons has seen enormous progress over the last year with the discovery of new approximate symmetries of QCD in the large mass limit. A meeting is being organized in October 1992 that will attempt to bring together the communities of theorists and experimentalists interested in the physics of heavy hadrons.

As a result of efforts of the theory group, the prestigious yearly Lattice Conference will be hosted by the SSCL in 1993. Preparations are well underway, and a Program Organizing Committee has been formed. At least one member of the Program Organizing Committee has agreed to spend one month at SSC as a visitor, prior to the conference.

Grinstein intends to continue to investigate the nature and magnitude of connections to the HQET predictions. He is continuing calculations within the '*t* Hooft model of the effects of finite heavy masses, in particular to form factors in heavy meson to light meson semileptonic decays. The 1/m connections to Luke's theorem are also part of his ongoing research. Borrowing from methods developed in connection with the HQET, Grinstein proved that certain heavy hadron decay amplitudes factorize. He intends to explore possible avenues to extend this result to other systems, and to investigate the size of the corrections in systems of physical import. He has also considered ways of searching for deviations from the Standard Model through precision measurements of weak interaction parameters, in a scenario which includes a moderately heavy Higgs boson. He intends to explore consequences of this scenario for hadron colliders.

Paige will continue development of ISAJET, a Monte Carlo program which simulates pp and $p\bar{p}$ interactions at high energy. It currently generates multi-parton final states based on the branching approximation to perturbative QCD, which includes all orders of perturbation theory but does not agree with any order exactly. Work has been started on interfacing ISAJET to various exact multi-parton generators such as PAPAGENO and VECBOS. The intention is to use the exact matrix element to the order to which it is known but to add higher order corrections using the branching approximation so as to get realistic events. This development will be continued and applied to understanding the W + jets background to the top search at CDF. Work will also continue on adding new physics processes of interest both for the Tevatron and for the SSC experiments. In particular, the mass and decay formulas for particles in the Minimal Supersymmetric Standard Model (MSSM) will be added in collaboration with H. Baer (Florida State). In the MSSM or any other realistic model, supersymmetric particles typically decay via complex cascades, giving significantly different signatures than just the simplest modes, so having the MSSM model in the generator is important both for supersymmetry searches at the Tevatron and for designing the SSC experiments. Finally, ISAJET and other event generators will be coupled with a fast parameterized simulation of GEM to continue the effort to understand physics signatures, backgrounds, and trigger strategies. In developing the design of the detector it will be important to be able to study the effects of any design choice on as wide range of plausible physics as realistically as possible.

Theory will grow from its current level of 4.3 FTE to 15 FTE by the end of FY 1994.

SECTION 6

FY 1994 PLANS

6.0 FY 1994 PLANS

The research program at SSCL will be guided by the pace of activities on the detectors which will be quite intense. Physics simulation efforts needed to guide the construction and design are a crucial element for a successful experimental program at the SSCL. R&D efforts will be directed at prototypes suitable for beam testing and finalization of specifications before initiating production. In FY 1994, major beam tests of detector subsystems are planned to occur at FNAL for both SDC and GEM. Lab physicists will participate in these tests, both in terms of supplying hardware for the tests and in participating in analyzing the results. The design activities carried out by the local engineering and technical staff will be guided by a combination of SSCL physicists and many visiting scientists. FY 1994 will also see intensification of work on small experiments. SSC physicists will be involved in preparation of the corresponding proposals (planned for January 1994), their defense, and in integration of these experiments into the lab program and facilities. Outside research activities will reach their peak in FY 1994/95 with work on at least two experiments.

6.1 FY 1994 GEM Program

GEM will change from design and R&D activities towards initiation of detector fabrication and test. Much of the activity will be centered at the SSC, including:

SSC physicist activities will concern issues of field mapping and mitigation of the return field of the superconducting solenoid, which will begin its construction phase with the setting up of the coil winding workshop at IR5 and the winding of the first 20m diameter coils.

Building on the TTR facilities, the SSC muon group will be involved in pilot production of chambers, and assembly and alignment of prototype supermodules. In FY 1994 the muon assembly hall at IR5 will be completed and the first module prototype assembly will be initiated.

Establishment of an SSC calorimeter test facility will be a high priority. In FY 1994 the calorimeter assembly hall at IR5 will be nearing completion and the first module prototype assembly will be initiated off-site.

Facilities for precision testing of prototype IPC and development of gas systems will occupy the tracking group.

The data acquisition design is to be completed during FY 1994. A prototype slow control for the magnet will be commissioned. Simulation of the on-line will be underway, and off-line coding will have begun. These activities will be coordinated from the SSC.

6.2 FY 1994 SDC Program

In FY 1994 the detailed design for most major systems will be complete and fabrication of final detector components will continue or begin. Tracking systems will be in the final design phase and fabrication of long lead time items will be initiated. Preparations for construction of muon chamber/counter supermodules at the muon assembly building will begin.

The tracking program at the SSC in FY 1994 depends on the choice of the outer tracker. Selection of either the straw-tube/gas microstrip tracker will affect the local effort. Work on the silicon tracker initiated in FY 1993 will continue, but at a more detailed level. We expect to establish a capability at the SSC suitable to support the outside silicon effort and provide test and repair facilities. If the scintillating fiber option is chosen, the SSC effort will collaborate on completion of large-scale systems tests of fibers coupled to VLPCs packaged in cassettes and cryostats. The design and testing of the accuracy of forming and positioning fiber ribbons will continue. Tests of a prototype cylinder with fiber ribbons will be completed.

The development of scintillators for calorimetry with improved radiation resistance will continue. At the SSC, overall calibration systems will be evaluated and overall planning for test beams and on-site assembly and installation will be in progress.

The plan for muon chambers includes continued work on chambers and systems integration with electronics systems and utilities, including gas systems. Simulation work on muon trigger designs will continue. Design and prototype work for the front-end systems will continue in FY 1994. The major focus of activity will be to test at the SSC initial production versions of the various front-end systems before starting full-scale fabrication in FY 1995. The DAQ system for use in test beams will be will be expanded and improved to support test beam work in FY 1994 at Fermilab and elsewhere.

6.3 Common Efforts in FY 1994

The common efforts in electronics, data acquisition and tracking are expected to continue in FY 1994. By this time system definitions, as well as triggering and data acquisition architectures for SDC and GEM will be specified, and the efforts will be directed towards solving common problems. Since tracking technologies will have been chosen it is likely that these efforts will also be focused on specific R&D issues for the chosen systems. Since proposals for small experiments are due in early 1994, we expect that SSC physicists will be involved in proposal preparation and their defense.

6.4 Outside Activities

In FY 1994 the CDF run will be ending and activity will move back to the SSCL and concentrate on data analysis utilizing the PDSF. The level of effort will be stable at about 7 FTEs, and it is expected that a similar size effort on at least one other experiment will also be in progress. For CDF, and D0 (if that is chosen), some SSC effort will be directed towards upgrades for future running, especially for technologies which are relevant to SSC experiments.

6.5 Computing

The PDSF will continue to support physics simulations for detector design, but as designs mature, emphasis will shift to the simulation of events and the resulting physics when collider operations begin. The PDSF, because of its open architecture, provides an excellent resource for testing computing concepts and models being developed for off-line production data analysis, storage and distribution systems. PDSF will be upgraded in FY 1994 to support these activities, mainly through the addition of network devices, storage interfaces and applicable software and hardware to support performance studies of data bases with data sets exceeding 1TB.

Support for SDC computing will continue with activities expanding in the development of the "Kernel" of the off-line data reconstruction and analysis software. Techniques and methodologies provided by the prior years studies in software engineering will be incorporated into these designs.

Continuing support will be provided for the development, maintenance and distribution of GEM codes for physics studies and detector simulation. In addition to the continuing detector simulations efforts new efforts, will begin to develop the core of GEM off-line analysis system.

Computing research and development projects will continue with the HEP database performance studies and with high speed tape storage which will include acquisition of robot-based helical scan tape systems and subsequent integration into PDSF. Advanced projects research will continue with emphasis on the needs of the experimental detector groups. Possible projects include development of networked mass storage systems, and development of advanced distributed computing networks. Support will expand from operation and maintenance of PDSF to include systems developed or acquired to support these research efforts.

SECTION 7

FUNDING

7.0 FUNDING

7.1 Introduction

As stated earlier in this proposal, the success of the SSC physics program requires the most crucial resource of all — many talented, creative physicists. They are needed in the SSC program as a whole and in particular at the SSC Laboratory. The physics program presented here is principally directed towards physics at the highest energies and momentum transfers (via groups associated with the SDC and GEM detector collaborations); it also involves other associated SSC experiments, on-going non-SSC experiments (including CDF), theoretical physics, and computing support.

The research program identified in this proposal can only be successful if the described strategies to provide a steady growth in people, both Laboratory staff and paid visitors, are implemented over this decade. It is especially important to maintain the projected ramp-up of physicists in the early years of the Laboratory's development to establish a scientific base on which to build the research program of the SSC. The High Energy Physics Base Program is being requested to provide funding to support the development of this scientific base, the core of the SSC research program. The funding requested is primarily for the support of physicists. This includes physicists' salaries, basic materials and services, research related travel, and equipment directly related to establishment of research infrastructure, including the equipment need for labs at the SSC for high energy physics research. The SSC Project will fund the costs of relocating physicists to the SSCL and providing them with basic personal infrastructure (e.g., offices, workstations). Some technical support (engineers and technicians) will come out of the SSC Project; however, all other research-related costs are requested to be funded from the HEP Base Program.

In total, the Research Program presented here requests $9.4M for FY 1992, $15.9M for FY 1993, and $21.6M for FY 1994. These figures, shown in Table 7-1a, are in FY 1991 dollars, and include overhead (growing slowly from 32% in FY 1991 to 40% in FY 1999). The corresponding requests in then-year dollars are given in Table 7-1b.

Table 7-1a: FY91 M$ with Overhead

Fiscal Year	92	93	94
Theory	0.86	1.17	2.00
Experimental Physics	7.17	11.67	15.12
Exp. Physics Support	0.69	1.68	2.64
Computing	0.67	1.33	1.89
Total	$9.39M	$15.86M	$21.65M

Table 7-1b: Then year M$ with Overhead

Fiscal Year	92	93	94
Theory	0.89	1.21	2.11
Experimental Physics	7.34	12.15	15.97
Exp. Physics Support	0.71	1.75	2.79
Computing	0.69	1.38	2.00
Total	$9.62M	$16.50M	$22.86M

Neither the subject of a physics research program at the SSCL nor the size of the associated costs of this program are new. The size of the physics research staff at the Laboratory and corresponding cost estimates have been discussed a number of times. A comparison of the present costs with those given for theoretical physics, experimental physics, and computing at the June, 1990 DOE review of the SSC Project baseline and as presented in the FTP/A for 1993 (submitted in April, 1991) is shown in Table 7-2.

Table 7-2: Estimated SSCL Research Program Costs (Theory, Experimental Physics, Computing) (FY 1991$M, Including Overhead)

	Baseline Review Presentation (6/90)	FY93 FTP/A (4/91)	HEPAP Presentation (2/92)
FY91	2.3	2.0	3.2
FY92	6.2	10.7	9.4
FY93	11.1	19.9	15.9

The figures from the June, 1990 review of the SSC Project baseline have been put in FY 1991 dollars and overhead has been added to make a more relevant comparison with the needs estimated in the present proposal.

In FY 1991 the physics research program at the SSCL was supported at the $2.0M level by the DOE Division of High Energy Physics. This funding came roughly mid-way through the 1991 Fiscal Year, and was broken down into $0.15M for Theoretical Physics, $1.65M for Experimental Physics, and $0.2M for Computing. These funds were used to carry out the FY 1991 activities described in Section 4.0 of this proposal, including support of long-term theory visitors, collaboration with CDF, calorimeter and tracking R&D programs, and operations of the Physics Detector Simulation Facility. The figure of $3.2M given in Table 7-2 would have applied if the research program had been funded from the beginning of FY 1991 and had been costed in a similar manner to that done in this proposal for all the later years.

For FY 1992 and FY 1993, DOE has indicated potential funding levels of $3M (see, for example, the President's budget message to Congress for FY 1993). Funding at a level significantly below the Research Program needs of $9.4M in FY 1992 and $15.9M in FY 1993 will cause the detector projects to lack adequate Laboratory physicist involvement during this critical period.

7.2 Experimental Physics

The experimental physics program described in this proposal identifies a steady growth profile of physicists to 195 by FY 2000. The hiring goals for this period are to fund 50 full time equivalent physicists (FTE's) in FY 1992 and 80 FTE's in FY 1993. It is projected to increase this staff to 102 FTE's during FY 1994. As outlined in this proposal, these physicists will be involved with two major detector projects (GEM and SDC) as well as outside SSC research projects such as CDF and internal common research programs. Included are the requirements to fund minimal technical support to physicists (engineers and technicians). The labor costs of the "captive" technical support for SSC physicists (shown in Table 7-1a & b) which will grow from 6 FTEs in FY 1992 to 21 FTEs in FY 1994, are not included here.

The model used for developing these budget estimates is like the models used for the SSC TPC budget. This model averages projected costs in constant FY 1991 dollars and adds appropriate escalation for each year (2.46% in FY 1992; 4.06% in FY 1993; 5.59% in FY 1994). The salaries for physicists are budgeted at an average of $66.7K/FTE; an average of $9.3K/FTE to provide for basic personnel materials and services (workstation upgrades, software, supplies etc.); a travel allotment averaging $13K/FTE to provide travel/lodging costs for research related physics conferences, workshops and meetings held outside the SSC as well as travel to outside research activities; an equipment allotment (items costing over $5K) of $26.4K/FTE which will be used to purchase resources such as computers, test and analysis equipment, shop tools etc., to support research programs and build the infrastructure of the laboratories needed at the SSC for these programs. Additionally, budget is provided to support university students working with physicists on research program. Exact allocation of resources per task depends on the need; some resources are allocated to the equipment pool to cover common needs and new initiatives. The following Tables 7.2-1, 7.2-2, and 7.2-3, identify the detailed funding requirements for each program by fiscal year.

Table 7.2-1: FY 1992 Experimental Physics Program (FY 1992 $M)

Description	Labor	Equip.	Mat'l Supplies	Travel	Over-head	Total
SDC	1.07	0.40	0.16	0.23	0.48	2.34
GEM	1.07	0.40	0.16	0.23	0.48	2.34
Common Efforts	0.68	0.25	0.10	0.14	0.33	1.50
Non-SSC (incl CDF)	0.54	0.20	0.08	0.11	0.23	1.16
Total	$3.37M	$1.25M	$0.50M	$0.71M	$1.51M	$7.34M

Table 7.2-2: FY 1993 Experimental Physics Program (FY 1993 $M)

Description	Labor	Equip.	Mat'l Supplies	Travel	Over-head	Total
SDC	1.73	0.71	0.24	0.34	0.78	3.80
GEM	1.73	0.71	0.24	0.34	0.78	3.80
Common Efforts	1.04	0.43	0.14	0.20	0.47	2.28
Non-SSC (incl CDF)	1.04	0.43	0.14	0.20	0.47	2.28
Total	$5.53M	$2.27M	$0.76M	$1.08M	$2.51M	$12.15M

Table 7.2-3: FY 1994 Experimental Physics Program (FY 1994 $M)

Description	Labor	Equip.	Mat'l Supplies	Travel	Over-head	Total
SDC	2.42	0.98	0.31	0.44	1.11	5.27
GEM	2.42	0.98	0.31	0.44	1.11	5.27
Common Efforts	1.42	0.58	0.19	0.26	0.65	3.10
Non-SSC (incl CDF)	1.07	0.43	0.14	0.19	0.49	2.33
Total	$7.34M	$2.97M	$0.95M	$1.34M	$3.37M	$15.97M

7.3 Theoretical Physics

The theory group contributes to research and as host to visiting theorists, and keeps experimentalists at the laboratory informed of the latest theoretical developments. Such a group contributes directly to the research goals of the laboratory, and plays a key role in establishing the intellectual atmosphere that exists at a great research institution. The projections for the SSC are to establish a group of 7 FTE theorists by FY 1992, growing to 15 by FY 1994. Table 7-4, outlines the funding requirements for the theory group.

Table 7.3-1: Theory Program FY 1992, 93 and 94 (Then year $M)

Description	Labor	Mat'l & Supplies	Travel	Over-head	Total
FY92	0.55	0.02	0.09	0.22	$0.89M
FY93	0.79	0.03	0.08	0.31	$1.21M
FY94	1.33	0.05	0.18	0.55	$2.11M

7.4 Computing

Computing resources for experimental physics (simulation, off-line data storage, reconstruction analysis and distribution systems) at the SSC will be developed and procured using TPC funds. After commissioning, the operational and maintenance support for these resources will be funded from the HEP. Operations and maintenance include: operators (24 hour coverage), systems managers, network support, application libraries and hardware/software maintenance.

The Physics Detector Simulation Facility (PDSF) is an example of a major computer resource in operation at the SSCL. This state-of-the-art computing resource which has the equivalent capacity of 2000 VAX 11/780's was developed using TPC equipment funds at an approximate cost of $3M. The PDSF has been operational since April 91 and serves a worldwide physicist user community; 60-80% of its users reside outside the SSC. Operation of the PDSF is being supported by HEP funds. Staff to support operations will grow from 6 FTE's in FY 1992 to 12 FTE's in FY 1994. Table 7.4-1 shows the costs for FY 1992 operations and projected funding requirements for FY 1993 and 94.

Table 7.4-1: Computing Program FY 1992, 93, and 94 (Then year $M)

Description	Labor	Equip.	Mat'l & Supplies	Travel	Over-head	Total
FY92	0.39	0.00	0.07	0.04	0.19	$0.69M
FY93	0.68	0.25	0.11	0.01	0.33	$1.38M
FY94	0.97	0.36	0.16	0.01	0.50	$2.00M

APPENDIX A

VITAE

NAME: **P. FREDERICK BIRD**

EDUCATION (DEGREE/INSTITUTION/YEAR):

1977 B.S. in Electrical Engineering, University of New Mexico

1982 M.S. in Electrical Engineering, Stanford University

1988 Ph.D. in Physics, Stanford University

PROFESSIONAL EXPERIENCE:

1988 Postdoctoral Research Fellow, CERN

1991 Staff Physicist, Superconducting Super Collider Laboratory

RECENT PUBLICATIONS:

1. Measurement of τ Branching Ratios, D. DeCamp, *et al.*, (The ALEPH Collaboration), CERN-PPE/91-186, to be published in Physics Letters B.

2. Electroweak Parameters of the Z Resonance and the Standard Model, The LEP Collaborations, CERN-PPE/91-232, to be published in Physics Letters B.

3. On Estimating the Top Quark Mass from Global Analyses of e^+e^- Collision Data, D. Levinthal, F. Bird, R. G. Stuart, and B. Lynn, CERN-TH-6094/91, July 1991, to be published in Zeit Physics C.

4. Measurement of the Absolute Luminosity With the ALEPH Detector, D. DeCamp, *et al.*, (The ALEPH Collaboration), CERN-PPE/91-129, to be published in Zeit Physics C.

5. Improved Measurements of Electroweak Parameters from Z Decays into Fermion Pairs, D. Decamp, *et al.*, (The ALEPH Collaboration), CERN-PPE/91-105, August 1991.

NAME: **CRAIG BLOCKER**

EDUCATION (DEGREE/INSTITUTION/YEAR):

1974 B.S. , University of Nebraska-Lincoln

1976 M.A., University of California-Berkeley

1980 Ph.D., University of California-Berkeley

PROFESSIONAL EXPERIENCE:

1980 Research Associate, Harvard University

1982 Assistant Professor, Harvard University

1985 Associate Professor, Brandeis University

1991 Staff Physicist, Superconducting Super Collider

RECENT PUBLICATIONS :

1. Measurement of QCD Jet Broadening in $p\bar{p}$ Collisions at $\sqrt{s}$= 1800 GeV, F. Abe *et al.*, (CDF Collaboration), Phys. Rev. D44, 601 (1991)

2. Measurement of $\sigma B(W \rightarrow e\nu)$ and $\sigma B\ (Z^{o} \rightarrow e^{+}e^{-})$ in $p\bar{p}$ Collisions at $\sqrt{s}$= 1800 GeV, F. Abe *et al.*, (CDF Collaboration), Phys. Rev. D44, 29 (1991)

3. Measurement of the W-Boson Mass in 1.8 TeV $p\bar{p}$ Collisions, F. Abe *et al.*, (CDF Collaboration), Phys. Rev. D43, 2070 (1991)

4. Top-Quark Search in the Electron + Jets Channel in Proton-Antiproton Collisions at $\sqrt{s}$ = 1.8 TeV F. Abe *et al.*, (CDF Collaboration), Phys. Rev. D41, 2330 (1991)

5. Two-Jet Invariant-Mass Distribution at $\sqrt{s}$ = 1.8 TeV F. Abe *et al.*, (CDF Collaboration), Phys. Rev. D41, 1722 (1990).

NAME: **MICHAEL BOTLO**

EDUCATION (DEGREE/INSTITUTION/YEAR):

1981 B.S. equivalent, University of Vienna

1984 M.S., University of Vienna

1987 Ph.D. in Physics, University of Vienna

PROFESSIONAL EXPERIENCE:

1987 Post Doc, UA1 and Asterix, CERN

1990 Staff Physicist, Superconducting Super Collider

RECENT PUBLICATIONS :

1. A Search for Rare B Meson Decays at the CERN SPS Collider, UA1 Collaboration, C. Albajar *et al.*, Phys. Lett. B262, 163, (1991).

2. Test Beam Performance of a Tracking TRD prototype, with J. T. Shank *et al.*, CERN-PPE-91-49, Sub. to NIM.

3. Readout of Overlapping Events, with J. Dorenbosch *et al.*, SSCL-348, (1991).

4. Anti-proton Proton Annihilation at Rest in H-2 Gas Into $\pi^+\pi^-\pi^0$ 1: Annihilation from S States, Asterix Collaboration, B. May *et al.*, Phys. Lett. B257, 459 (1991).

5. Anti-proton Proton Annihilation at Rest in H-2 Gas Into $\pi^+\pi^-\pi^0$ 2: Annihilation from P States, Asterix Collaboration, B. May *et al.*, Z. Phys. C46, 203 (1990).

6. Data Acquisition studies for the SSC, C.Milner *et al.*, IEEE 1991 Nuclear Science Symposium, to be published in IEEE Transactions on Nuclear Science (1992).

NAME: **LAIRD R. CORMELL, JR.**

EDUCATION (DEGREE/INSTITUTION/YEAR):

1970 B.S. in Physics, University of Oklahoma

1971 M.S. in Physics, University of Illinois

1975 Ph.D. in Physics, University of Illinois

PROFESSIONAL EXPERIENCE:

1989 Scientist II, Superconducting Super Collider,

1987 Principal Investigator, Bell Technical Operations

1985 Senior Scientist/Systems, Design Engineer, Merdan Group, Inc.

1983 Associate Research Professor, Arizona Research Laboratories

1975 Assistant Professor, Sloan Foundation Fellow, Physics Depart., Univ. of PS

PUBLICATIONS

1. High Energy Physics Computing at the SSCL, L. R. Cormell, Proceedings of the International Conference on Computing in High Energy Physics '91, p. 77, 1991.

2. Longitudinal/Energy Flow in Hard Proton Nucleus Collisions at 400 GeV/c, with R. C. Moore, *et al.*, Physics Letters B244, 347 (1990).

3. Physics and Detector Simulation Requirements, L. Cormell, *et al.*, AIP Conference Proceedings 209, 352, Sante Fe, 1990.

4. Evidence for Multiple Scattering of High Energy Partons in Nuclei, with M. Corcoran, *et al.*, published in Physics Letters B, May, 1990.

5. High p_T Proton-Nucleus Interactions with H. E. Miettinen, *et al.*, Physics Letters, B207, 222 (1988).

NAME: **DAVID P. COUPAL**

EDUCATION (DEGREE/INSTITUTION/YEAR):

1979 B.A. in Mathematics, University of Texas at Austin

1979 B.A. in Physics, University of Texas at Austin

1985 Ph.D. in Physics, The University of Chicago

PROFESSIONAL EXPERIENCE:

1979 Teaching Assistant, The University of Chicago

1979 Research Assistant, The University of Chicago

1984 Postdoctoral Research Associate, Stanford Linear Accelerator Center

1988 Research Physicist, Stanford Linear Accelerator Center

1990-present Staff Physicist, Superconducting Super Collider Laboratory

RECENT PUBLICATIONS :

1. Measurement of the $b\bar{b}$ Fraction in Hadronic Z° Decays with Precision Vertex Detectors, (Mark II Collaboration), (1990).

2. Measurement of the $b\bar{b}$ Fraction in Hadronic Z° Decays, J.F. Kraz *et al.*, (Mark II Collaboration), Phys. Rev. Lett 64, 1211 (1990).

3. Determination of α_s from a Differential Jet Multiplicity Distribution at SLC and PEP S. Komamiga *et al.*, (Mark II Collaboration), Phys. Rev. Lett. 64, 987 (1990).

4. Search for Long-Lived Massive Neutrinos in Z Decays, C. K. Jung *et al.*, (Mark II Collaboration) Phys. Rev. Lett. 64, 1091 (1990).

5. Measurement of the Charged particle Inclusive Distributions in Hadronic Decays of the Z Boson, G. S. Abrams *et al.*, Phys. Rev. Lett. 64, 1334 (1990).

NAME: **PETER J. DINGUS**

EDUCATION (DEGREE/INSTITUTION/YEAR):

1977 B.S. in Electrical Engineering, University of Rhode Island

1983 M.A. Physics, University of California Berkeley

1988 Ph.D Physics, University of California Berkeley

PROFESSIONAL EXPERIENCE:

1988 Postdoctoral Research Fellow, Ecole Polytechnique Paris France

1991 Staff Physicist, Superconducting Super Collider Laboratory

RECENT PUBLICATIONS:

1. Excited States of Composite Electrons in H1, T.Carli, P.Dingus, Y.Sirois,will appear in Hera Workshop spring 1992.

2. The Energy Scale Corrections in H1 for Contained EM Clusters, P.Dingus J.P.Pharabod Y.Sirois, H1-8/90-146 H1 Note 1990.

3. Study of Software Compensation for Single Particles and Jets in the H1Calorimeter, H1 Calorimeter Group, Contributed paper to the XXV International Conference on High Energy Physics, Singapore 1990.

4. Photoproduction of an Isovector $\rho\pi$ State at 1775-MeV. Slac

5. Hybrid Facility Photon Collaboration (G.T.Condo *et al.*, Phys. Rev. D43, 2787-2791, 1991.

NAME: JHEROEN DORENBOSCH

EDUCATION (DEGREE/INSTITUTION/YEAR):

1970 B.S. in Physics, University of Nijmegen, Holland

1973 M.S. in High Energy Physics, University of Amsterdam

1977 Ph.D. in High Energy Physics, University of Amsterdam

PROFESSIONAL EXPERIENCE:

1970 Student, Zeeman laboratory at Amsterdam, p antiproton in BEBC

1973 Graduate Student, Zeeman laboratory at CERN, small angle pp scattering

1977 Research Associate, Stanford Linear Accelerator Center, Mark II

1981 Staff Member, Nikhef Institute at CERN, CHARM

1984 Staff Member, Nikhef Institute at CERN, UA1

1990 Staff Physicist, SSCL, head of electronics,

RECENT PUBLICATIONS :

1. Low Mass Dimuon Production at the CERN Proton-Antiproton Collider, C. Albajar *et al.*, (UA1 Collaboration), Phys. Lett. B 209, 397 (1988).

2. A Search for Neutrino Oscillations, F. Bergsma *et al.*, (Charm Collaboration) Z. Physics. C40, 171 (1988).

3. J/Psi and Psi' Production at the CERN $p\bar{p}$ Collider, C. Albajar *et al.*, (UA1 Collaboration) Phys. Lett. B256, 112 (1991).

4. Monolithic CMOS Front-end Electronics with Analog Pipelining, F. Anghinolfi *et al.*, CERN-ECP-90/13.

5. BATS, the Readout Control of UA1, M. Botlo *et al.*, NIM A302, 331 (1991).

6. Data Acquisition studies for the SSC, C.Milner *et al.*, IEEE 1991 Nuclear Science Symposium, to be published in IEEE Transactions on Nuclear Science (1992).

NAME: HOWARD C. FENKER

EDUCATION (DEGREE/INSTITUTION/YEAR):

1973 B.A. in Math and Physics, Vanderbilt University

1978 Ph.D. in Physics, Vanderbilt University

PROFESSIONAL EXPERIENCE:

1978 Florida State University at Brookhaven Laboratory and Fermi National Accelerator Laboratory,

1981 Fermi National Accelerator Laboratory

1989 Visiting Associate Professor at Northeastern University

1990 Staff Physicist, Superconducting Super Collider Laboratory

RECENT PUBLICATIONS :

1. Progress in the Use of Avalanche Photodiodes for Readout of Calorimeters, H. Fenker *et al.*, SSCL-552 (1991).

2. A Readout System for Plastic Scintillating Fibers, H. Akbari *et al.*, NIM A302, 415 (1991).

3. Instrumentation for SSC Test Beams, H. Fenker and F. Stocker, Particle Accelerator Conference, San Fancisco, 6-9 May 1991.

4. Inclusive Charm Cross-Sections in 800 GeV/c p p Interactions, R. Ammar *et al.*, Phys. Lett. 183B, 110 (1987).

5. A High Rate Transition Radiation Detector for Particle Identification in a Hadron Beam, D. Errede *et al.*, Symposium on Particle I.D. at High Luminosity Hadron Colliders, Batavia 5-7 April, 1989.

NAME: **SOREN FREDERICKSEN**

EDUCATION (DEGREE/INSTITUTION/YEAR):

1982 Ph.D. in High Energy Physics, University of Ottawa.

1978 B.Sc. with Physics Honours, University of British Columbia.

PROFESSIONAL EXPERIENCE:

1991 Application Physicist III at Superconducting Super Collider Laboratory.

1990 System Analysit I at Superconducting Super Collider Laboratory.

1987 Research Associate at The Ohio State University.

1982 Graduate Student at University of Ottawa.

1981 Summer Research Student at the University of Ottawa.

RECENT PUBLICATIONS

1. "A Study of Semi-Muonic Charmed Particle Decays", Soren G. Frederiksen, Proceedings of The General Meeting of The Division of Particles and Fields of the American Physical Society, Jan. 1990

2. "Measurement of the relative branching fraction Gamma(D0 ---> K μ η) γ (D0 ---> μ X)", K. Kodama, *et al.*, Phys. Rev. Lett. 66, 1819 (1991).

3. "Charm meson production in 800 GeV/c proton-emulsion interactions", K. Kodama, *et al.*, Phys. Lett. B 263, 573 (1991).

4. "Charm pair correlations in 800 GeV/c proton-emulsion interactions", K. Kodama, *et al*, Phys. Lett. B 263, 579 (1991).

5. "Measurement of the form factor ratios in the decay D+ ---> $K^*(892)^0$ μ+ η", K. Kodama, *et al.*, Phys. Lett. B 274, 246 (1992).

NAME: **C. ALAN FRY**

EDUCATION (DEGREE/INSTITUTION/YEAR):

1973 Exchange Student, Keio University, Tokyo, Japan

1976 B.S. in Mathematics, University of Victoria

1981 M.S. University of Victoria

1985 Ph.D. in Physics, University of British Columbia

PROFESSIONAL EXPERIENCE:

1977 Research Assistant, University of Victoria

1975 Physics Laboratory Instructor, University of Victoria

1985 Research Associate, University of Rochester

1989 Visiting Scientist, KEK

1990 Staff Physicist, Superconducting Super Collider Laboratory

RECENT PUBLICATIONS :

1. W.X. Gao, *et al.*, "High quality muon detection for the SSC," *U. Rochester 1240; SSCL-563*, (1992).

2. M. Franklin, *et al.*, "Development of Diamond Radiation Detectors for the SSC and LHC," submitted to *Nuclear Instruments and Methods*, (1991).

3. R. Tanaka, *et al.* (AMY Collaboration), "Evidence for Hard Scattering of Hadronic Constituents of Photons in Photon-Photon Collisions at TRISTAN," Accepted in *Physics Letters,* (1991)

4. T. Sasaki, *et al.* (AMY Collaboration), "A Measurement of the photon structure function F2," *Physics Letters,* B252 (1990) 491.

5. T. Kumita, *et al.* (AMY Collaboration), "Measurements of R for e^+e^- Annihilation at TRISTAN," *Physical Review D,* 42 (1990) 1339.

NAME: **TORU FUKUI**

EDUCATION (DEGREE/INSTITUTION/YEAR):

1985 B.S.in High Energy Physics, Tokyo Metropolitan University

1987 M.S. in High Energy Physics, Tokyo Metropolitan University

1990 Ph.D. in High Energy Physics, Tokyo Metropolitan University

PROFESSIONAL EXPERIENCE:

Tokyo Metropolitan University

KEK

1991 Physicist, Superconducting Super Collider

RECENT PUBLICATIONS :

1. Measurement of R and Search for New Quark Flavors Decaying Into Multi-Jet Final States in e^+e^- Collisions Between 54.0 and 61.4 GeV C.M. Energies, 1990

2. Measurement of the Reactions $e^+e^- \rightarrow \mu^+\mu^-$ and $e^+e^- \rightarrow \tau^+\tau^-$ between $\sqrt{s}$ = 50 and 60.8 GeV, 1990

3. Determination of the QCD Scale Parameter $\Lambda \overline{MS}$ with QCD Cascade on the Basis of the Next-to- = Leading Logttarithmic Approximation, 1990

4. Experimental Limits on Extra-Z Bosonns From e^+e^- Annihilation Data With the VENUS Detector at $\sqrt{s}$ = 50 ~ 64 GeV, 1990

5. Experimental Study of Color Degree of Freedom of Gluous in e^+e^- Annihilation at $\sqrt{s}$ around 60 GeV, 1991

NAME: **BENJAMIN GRINSTEIN**

EDUCATION (DEGREE/INSTITUTION/YEAR):

1980 M.S. in Physics, Centro de Investigacion y Estudios Avanzados del IPN

1984 Ph.D. in Physics, Harvard University

PROFESSIONAL EXPERIENCE:

1980 Physics Teacher, U. Iberoamericana (Mexico City)

1981 Teaching Fellow, Harvard University

1984 Junior Research Associate, California Institute of Technology

1987 Postdoctoral Fellow, Lawrence Berkeley Labatory

1988 Associate Scientist, Fermi National Accelerator Laboratory

1989 Assistant Professor, Harvard University

1991 Staff Physicist, Superconducting Super Collider

RECENT PUBLICATIONS :

1. Review of Recent Developments in Heavy Quark Theory, Fourth Conference on the Intersections between Particle and Nuclear Physics, Tucson, Arizona, HUTP-91/A028, May 1991.

2. QCD Enhancement of $b \rightarrow s\gamma$ Decay for a Heavy Top Quark, w/Peter Cho, HUTP-91/A020, April 1991.

3. Operator Analysis for Precision Electroweak Physics, w/Mark B. Wise, HUTP91/A015 AND CALT-68-1720, March 1991.

4. Effective Hamiltonian for Nonleptonic $\overline{B}$ or Λ_b Decays to Final States with Two Charmed Hadrons, w/Wolfgang Kilian, Thomas Mannel and Mark B. Wise, HUTP-91/A005 CALT-68-1713, February 1991, revised May 1991.

5. CP Violation in K Decays, in Physics of Elementary Interactions, Proceedings of the XIII Warsaw Symposium on Elementary Particle Physics, Z. Ajduk, S. Pokorski and A.K. Wroblewski, eds., World Scientific, Singapore, 1991.

NAME: **HARALD JOHNSTAD**

EDUCATION (DEGREE/INSTITUTION/YEAR):

1964 M.S. eq. in Physics, Mathematics, and Astronomy, Faculty of Mathematics and Natural Sciences, University of Oslo.

1967 Ph.D. eq. in Nuclear and High Energy Physics, Faculty of Mathematics and Natural Sciences, University of Oslo.

PROFESSIONAL EXPERIENCE:

1989 Staff Physicist, SSC Laboratory

1979 Associate Scientist, Fermilab

1978 Senior Research Associate, Northeastern University

1976 Staff Physicist, IN2P3, Strasbourg

1975 Staff Physicist, University of Mons

1975 Visiting Scientist, Serpukhov

1974 Research Associate, Northeastern University

1972 CERN Fellow, European Laboratory for Particle Physics

1967 Scientific Associate, Niels Bohr Institute

RECENT PUBLICATIONS:

1. Proceedings, International Workshop on Physics and Detector Simulation for SSC experiments, SSC Laboratory, 1990.

2. The usage of ZEBRA data structures in HEP computing, Ettore Majorana Conference on Data Structures and Software Engineering, Erice, 1990.

3. HEP software libraries, distribution, and organization. Proposal for the HEPLIB initiative, Ettore Majorana Conference on Data Structures and Software Engineering, Erice, 1991.

4. Proceedings, First International Workshop on HEP Software for the HEPLIB User Organization, SSC Laboratory, 1991.

5. Requirements to HEP software for SSC experiments, Conference on Software Engineering and Artifical Intelligence, LaLonde, 1992.

6. Proceedings, International Workshop on HEP Data Base Systems , SSC Laboratory, 1992.

7. Plan for a joint scintillator R&D program and for the conduct of a cosmic ray test of the SDC calorimeter prototype stacks and their calibrartion system at SSCL, with C. Blocker , *et al.*, 1992.

NAME: VERA G. LÜTH

EDUCATION (DEGREE/INSTITUTION/YEAR):

1969 M. Sc. in Physics, Heidelberg University

1974 D. Sc. in Physics, Heidelberg University

PROFESSIONAL EXPERIENCE:

1971 Research Associate, Heidelberg University

1974 Research Associate, SLAC, Stanford University,

1977 Staff Physicist, SLAC, Stanford University,

1985 Senior Research Staff Physicist, SLAC, Stanford University

1984 Visiting Scientist, CERN

RECENT PUBLICATIONS:

1. "First Measurements of Hadronic Decays of the Z^0 Boson", with G. S. Abrams, *et al.*, SLAC-PUB-5045, published in Phys. Rev. Lett. 63, 1558 (1989).

2. "Measurements of the Z^0 Resonance Parameters", with G. S. Abrams, *et al.*, SLAC-PUB-5113, published in Phys. Rev. Lett. 63, 2173 (1989).

3. "Search for Decays of the Z^0 to Unstable Neutral Leptons with Masses Between 2.5 GeV and 22 GeV", with P. Burchat, M. King, *et al.*, SLAC-PUB-5176, published in Phys. Rev. D41, 3542, (1990).

4. "Precise Determination of the Lifetime of the Charmed Baryon Λ_c" with S. Barlag, *et al.*, published in Phys. Lett. B218, 374 (1989).

5. Measurement of the Masses and Lifetimes of the Charmed Mesons D^0, D^+ and D_s^+, with S. Barlag, *et al.*, published in Z. Phys. C46, 563 (1990).

6. "The Mark II Silicon Strip Vertex Detector" with G. Gratta, *et al.*, SLAC-PUB-5443, submitted to Nucl. Inst. and Meth. (1991).

7. "B-Physics at e^+e^- Factories" with David B. MacFarlane, SLAC-PUB-5419, to be published in *Proceedings of the 1990 DPF Summer Study on Physics for the Decade*, Snowmass, CO. (1990).

8. "Design of a Vertex Detector" to be published in *Proceedings of the 1990 Workshop on the Physics and Detector for a High Luminosity B-Factory*, Stanford, SLAC-373 (1991).

9. "CP Violation in the B System - Physics at a High Luminosity B Factory" SLAC-PUB 5596 (1991), to be published in *Preceeding of Les Recontes de Physique de la Vallee D'Aoste,* La Thuile (1991).

NAME: **HARVEY L. LYNCH**

EDUCATION (DEGREE/INSTITUTION/YEAR):

1961 B.S. Massachusetts Institute of Technology

1966 PhD. Stanford University

PROFESSIONAL EXPERIENCE:

1966 Postdoctoral Fellow, CERN

1968 Research Associate, SLAC

1973 Assistant Professor, SLAC

1976 Staff Physicist, DESY

1981 Visiting Professor, UCSB

1982 Staff Physicist, SLAC

1991 Staff Physicist, SSCL

RECENT PUBLICATIONS:

NAME: **PATRICIA L. MCBRIDE**

EDUCATION (DEGREE/INSTITUTION/YEAR):

1984 Ph.D., Yale University

1977 B. S. in Physics, Carnegie Mellon University

PROFESSIONAL EXPERIENCE:

1984 Harvard University

1976 Yale University

RECENT PUBLICATIONS:

1. Search for Narrow High-Mass Resonances in Radiative Decays of the Z^0. The L3 Collaboration, B. Adeva *et al.*, L3-029 (Feb. 1991).

2. Measurement of Electroweak Parameters from Hadronic and Leptonic Decays of the Z^0. The L3 Collaboration, B. Adeva *et al.*, L3-029 (Feb. 1991).

3. Measurements of $Z^0 \rightarrow b\bar{b}$ Decays and the Semileptonic Branching Ratio ($Br(b \rightarrow \ell + X)$. The L3 Collaboration, B. Adeva *et al.*, L3-029 (Feb. 1991).

4. Search for Leptoquarks in Z^0 Decays· The L3 Collaboration, B. Adeva *et al.*, L3-029 (Feb. 1991).

5. Measurement of the Inclusive Production of Neutral Pions and Charged Particles on the Z^0 Resonance. The L3 Collaboration, B. Adeva *et al.*, L3-029 (Feb. 1991).

NAME: KENNETH W. MCFARLANE

EDUCATION (DEGREE/INSTITUTION/YEAR):

Ph.D., University of Birmingham, UK

B. Sc., University of Glasgow, UK

PROFESSIONAL EXPERIENCE:

1991 SSC Laboratory

1975 Temple University

1963 University of Pennsylvania

1958 University of Birmingham UK

RECENT PUBLICATIONS:

1. New searches for the C-noninvariant decay $\pi^0 \rightarrow 3\gamma$, J. McDonough, V. L. Highland, W. K. McFarlane, R. D. Bolton, M. D. Cooper, J. S. Frank, A. L. Hallin, P. Heusi, C. M. Hoffman, G. E. Hogan, F. G. Mariam, R. E. Mischke, L. E. Piilonen, V. D. Sandberg, U. Sennahauser, R. D. Werbeck, R. A. Williams, S. L. Wilson, D. P. Grosnick, and S. C. Wright, Phys. Rev. D38, 2121-2128 (1988)

2. Preliminary Results and Status of BNL E791: Study of very Rare K_L^0 decays. K. McFarlane, XXIIIrd Recontres de Moriond, Les Arcs, France, March 6-13, 1988. In "88 Electroweak Interactions and Unified Theories," Editions Frontiere, Gif sur Yvette Cedex, France (1989)

3. New Experimental Limits on $K_L^0 \rightarrow \mu e$ and $K_L^0 \rightarrow ee$ Branching Ratios, C. Mathiazhagan, W. R. Molzon, R. D. Cousins, J. Konigsberg, J. Kubic, P. Melese, P. Rubin, W. E. Slater, D. Wagner, G. W. Hart, W. W. Kinnison, D. M. Lee, R. J. McKee, E. C. Milner, G. H. Sanders, H. J. Ziock, K. Arisaka, P. Knibbe, J. Urheim, S. Axelrod, K. A. Biery, G. M. Irwin, K. Lang, J. Margulies, D. A. Ouimette, J. L. Ritchie, Q. H. Trang, S. G. Wojcicki, L. B. Auerbach, P. Bushholz, V. L. Highland, W. K. McFarlane, M. Sivertz, M. D. Chapman, M. Eckhause, J. F. Ginkel, A. D. Hancock, D. Houce, J. R. Kane, C. J. Kenney, W. F. Vulcan, R. E. Welsh, R. J. Whyley, R. G. Winter, Phys. Rev. Lett. 63, 2181-2184 (1989)

4. Measurement of the Branching Ratio for theDecay $K_L^0 \rightarrow \mu\mu$ C. Mathiazhagean, W. R. Molzon, R. D. Cousins, J. Konigsberg, J. Kubic, P. Melese, P Rubin, W. E. Slater, D. Wagner, G. W. Hart, W. W. Kinnison, D. M. Lee, R. J. McKee, E. C. Milner, G. H. Sanders, H. J. Ziock, K. Arisaka, P. Knibbe, J. Urheim, S. Axelrod, K. A. Biery, G. M. Irwin, K. Lang, J. Margulies, D. A. Ouimette, J. L. Ritchie, Q. H. Trang, S. G. Wojcicki, L. B. Auerbach, P. Buchholz, V. L. Highland, W. K. McFarlane, M. Sivertz,

M. D. Chapman, M. Eckhause, J. F. Ginkel, A. D. Hancock, D. Joyce, J. R. Kane, C. J. Kenney, W. F. Vulcan, R. E. Welsh, R. J. Whyley, R. G. Winter, Phys. Rev. Lett. 63, 2185-2188 (1989)

5. Higher-statistics Measurement of the Branching Ratio for the Decay $K_L^0 \rightarrow \mu\mu$ A. P. Heinson, J. Horvath, C. Mathiazhagan, W. R. Molzon, K. Arisaka, R. D. Cousins, T. Kaarsberg, J. Konigsberg, P. Rubin, W. E. Slater, D. L. Wagner, W. W. Kinnison, D. M. Lee, R. J. M cKee, E. C. Milner, G. H. Sanders, H. J. Ziock, P. Knibbe, J. Urheim, K. A. Biery, M. V. Diwan, G. M. Irwin, K.Lang, J. Margulies, D. A. Quimette, A. Schwartz, S. G. Wojcicki, L. B. Auerbach, J. Belz, P. Buchholz, V. L. Highland, W. K. McFarlane, M. Sivertz, J. L. Richie, A. Yamashita, M. D. Chapman, M. Eckhause, J. F. Ginkel. A. D. Hancock, J. R. Kane, C. J. Kenney, Y. Kuang, W. F. Vulcan, R. E. Welsh, R. J. Whyley, R. G. Winter, Phys. Rev. D44, R1-R4 (1991)

NAME: **E. CAS MILNER**

EDUCATION:

1980 B.S. in Physics, The University of Texas at Austin

1985 Ph.D. in Physics, The University of Texas at Austin

PROFESSIONAL EXPERIENCE:

1985 Post-Doctoral Fellow, Los Alamos National Laboratory

1988 Staff Physicist, Los Alamos National Laboratory

1990 Superconducting Super Collider Laboratory

RECENT PUBLICATIONS:

1). E. C. Milner *et al.*, "Data Acquisition Studies for the SSC", IEEE 1991 Nuclear Science Symposium, to be published in IEEE Transactions on Nuclear Science, (1992).

2). A. P. Heinson *et al.*, "Higher-statistics measurement of the branching ratio for the decay $K_L^0 \rightarrow \mu\mu$", Phys. Rev. D44, R1 (1991).

3). J. Baciagalupi *et al.*, "Measurement of Proton-induced radiation damage to CMOS transistors and pin diodes," IEEE Trans. NS 37, 1238 (1990).

4). R. E. Chrien *et al.*, "Search for radiative transitions in the hypernucleus ${}^{10}_{\Lambda}B$", Phys. Rev. C41, 1062 (1990).

5). C. Mathiazhagan *et al.*, "New experimental limits on the $K_L^0 \rightarrow \mu e$ and $K_L^0 \rightarrow ee$ branching ratios", Phys. Rev. Lett. 63, 2181 (1989).

6). C. Mathiazhagan *et al.*, "Measurement of the branching ratio for the decay $K_L^0 \rightarrow \mu\mu$", Phys. Rev. Lett. 63, 2185 (1989).

NAME: **GENA MITSELMAKHER**

EDUCATION (DEGREE/INSTITUTION/YEAR):

1968 Research Physicist, Institute for Nuclear Research, Dubna

1974 Ph.D., Institute for Nuclear Research, Dubna

PROFESSIONAL EXPERIENCE:

1986 Head of The Colliding Beams, Physics Dept., JINR, Dubna, USSR,

1988 Vice-Director of the Superhigh Energy Physics Laboratory, JINR, Dubna, USSR

1990 Visiting Scientist at CERN, Head of The Colliding Beams, Physics Dept., JINR, Dubna, USSR

1991 Staff Physicist, Superconducting Super Collider Laboratory

RECENT PUBLICATIONS :

1. Yu. M. Antipov *et al.*, "Fe-scintillator hodoscopic hadron calorimeter" NIM A295 (1990) 81-5.

2. P. Arnio *et al.*, "The DELPHI Detector at LEP" CERN/PPE 90-128 to be published in NIM.

3. P. Abreu *et al.*, "A Study of the Reaction $e^+e^- \rightarrow mu^+mu^-$ Around the Z Pole", Physics Letters 260B (1991) 240.

4. P. Abreu *et al.*, "Determination of Z-resonance parameters and Couplings From its Hadronic and Leptonic Decays" CERN/PPE 91-95, to be published in Nuclear Physics B.

5. P. Abreu *et al.*, "A Measurement of the Lifetime of the Tau Lepton" CERN/PPE 91-115, to be published in Physics Letters B.

NAME: FRANK E. PAIGE

EDUCATION (DEGREE/INSTITUTION/YEAR):

1966 B.S. (Massachusetts Institute of Technology)
1970 Ph.D. (Massachusetts Institute of Technology), Advisor/Professor K. Huang, MIT
Dissertation: "Veneziano Model for Nucleon-Nucleon Scattering"

PROFESSIONAL EMPLOYMENT

1970 Brookhaven National Laboratory, Upton, NY11973

1970 Research Associate

1972 Associate Physicist

1975 Visiting Assistant Professor, UC/San Diego

1975 Physicist, BNL

1978 Physicist (continuing)

1984 Physicist (tenure)

1987 Senior Physicist

1991 Senior Physicist, SSC Laboratory.

RECENT PUBLICATIONS

1. SSC physics signatures
(Jan. 1992; to appear in proceedings of SSC Symposium, Corpus Christi)

2. $\ell^{\pm}\ell^{\pm}$ signature for gluino production
BNL-46959 (Dec., 1991)

3. GEM letter of intent
Technical note GEM-TN-92-49 (Nov., 1991)
(With B. Barish, W. Willis, *et al.*,)

4. Jet contributions to $\not{E}_T$ cross sections
BNL-46828 (October, 1991). 9 pp.

5. $t\bar{t}$ lepton triggers
BNL-46821 (October, 1991). 5 pp.

6. Possible $H \rightarrow W^+W^-$ signal for $2m_W < m_H < 2m_Z$
BNL-46829 (October, 1991). 5 pp.

7. An expression of interest to construct a major SSC detector SSC EOI-0020 (July, 1991). 111 pp.

NAME: **TRIVAN PAL**

EDUCATION (DEGREE/INSTITUTION/YEAR):

1975 B.Sc. (HON), A.R.C.S., in Physics, Imperial College of Science and Technology, University of London, England

1977 M.S. in Physics, University of Geneva, Switzerland

1982 Ph.D. in Physics, University of Geneva, Switzerland

PROFESSIONAL EXPERIENCE:

1983 Research Fellow, California Institute of Technology, Pasadena, CA

1986 Senior Research Associate, CERN and University of Bern, Switzerland

1992 Staff Physicist, Superconducting Super Collider Laboratory, Dallas, TX

RECENT PUBLICATIONS :

1. Recent Results on W and Z Physics from UA2 at the CERN $p\bar{p}$ Collider. T. Pal, Proceedings of the Particles and Fields 1991 Meeting. Vancouver, Canada. World Scientific (1992).

2. Study of Electron Pair Production Below the Z Mass at the CERN $p\bar{p}$ Collider. J. Alitti *et al.,* (UA2 Collaboration), CERN-PPE/91-177, November 1991. Accepted for publication in Phys. Lett. B.

3. An Improved Determination of the Ratio of W and Z Masses at the CERN $p\bar{p}$ Collider. J. Alitti *et al.,* (UA2 Collaboration), CERN-PPE/91-163, October 1991. Accepted for publication in Phys. Lett. B.

4. A Measurement of the W and Z Production Cross Section and a Determination of $\Gamma(W)$ at the CERN $p\bar{p}$ Collider. J. Alitti *et al.,* (UA2 Collaboration), CERN-PPE/91-162, October 1991. Accepted for publication in Phys. Lett. B.

5. Time of Flight Measurements with Hadronic Showers. K. Borer *et al.,* Nucl. Inst. and Meth. A311, 113 (1992).

NAME: **LEE ROBERTS**

EDUCATION (DEGREE/INSTITUTION/YEAR):

1986 Ph. D. in Physics (Elementary Particle Theory)

1982 M. A. in Physics, December 1982, State University of New York at Stony Brook

1981 B. S. in Physics & Mathematics, Iowa State University of Science and Technology

PROFESSIONAL EXPERIENCE:

1986 Systems Analyst I Physics Software Projects Group Computing Division, Fermi National Accelerator Laboratory

1990 Systems Analyst II/Applications Physicist III, Computing & Data Analysis Department, Physics Research Division, Superconducting Super Collider Laboratory

RECENT PUBLICATIONS :

1. "CZ/CPS, A Communications ZEBRA implementation using CPS," SSCL-412 (unpublished). SSCL, April 1991.

2. "BCD/CPS, An event-level GEANT3 parallelization via CPS," SSCL-413 (unpublished). SSCL, April 1991.

3. "Monte Carlo Simulation of Silicon Vertex Detector for Bottom Collider Detector, Part I," FN-488 (unpublished). FNAL, June 1988.

4. "Evaluation of the FPS-164 Computer for High Energy Physics Pattern Recognition Problems,"Computer Physics Communications 47, 1987, 195--206.

5. "Quantum electrodynamic radiative corrections to the decay π° to $\gamma\, e^+\, e^-$," Physical Review D 33 (1986), 3457--3460.

NAME: **JAMES L. SIEGRIST**

EDUCATION (DEGREE/INSTITUTION/YEAR):

1974 B.S. in Physics, University of Texas at Austin

1979 Ph.D. in Physics, Leland Stanford Junior University

PROFESSIONAL EXPERIENCE:

1975 Research , SPEAR, (SLAC-LBL Magnetic Detector)

1979 Research Associate, Stanford Linear Accelerator Center, (MARK II)

1981 CERN Scientific Associate, (UA2)

1983 LBL Division Fellow, (CDF)

1987 LBL Staff Physicist, (CDF)

1988 UC Berkeley, Associate Professor of Physics, (CDF)

1990 Superconducting Super Collider, (CDF)

RECENT PUBLICATIONS :

1. Measurement of the mass and width of the Z^0 boson at the Fermilab Tevatron, with F. Abe *et al.,* (CDF Collaboration) Phys. Rev. Lett. 63, 720 (1989).

2. Search for new heavy quarks in electron-muon events at the Fermilab Tevatron Collider, with F. Abe *et al.,* (CDF Collaboration), Phys. Rev. Lett. 64, 147 (1990).

3. Measurement of the ratio $\sigma B(W \rightarrow e\nu)/\sigma B(Z \rightarrow ee)$ in $p\bar{p}$ collisions at $\sqrt{s}$= 1.8 TeV, with F. Abe *et al.,* (CDF Collaboration), Phys. Rev. Lett. 64, 152, (1990).

4. SDC LOI, SDC Collaboration, November 1990.

5. Hadron Collider Physics, with Marge Shapiro, Annual Reviews. of Nuclear Science, Vol. 41, 1991.

NAME: **RAYMOND J. STEFANSKI**

EDUCATION (DEGREE/INSTITUTION/YEAR)

1963 B.A. in Physics, State University of New York at Buffalo

1968 Ph.D. in Physics, Yale University, December

PROFESSIONAL EXPERIENCE:

1969 Staff Physicist, Fermilab

1990 Staff Physicist, SSCL

RECENT PUBLICATIONS:

1. Charm Meson Production in 800 GeV/c Proton - Emulsion Interactions, with K. Kodama, *et al.*, (Fermilab-E653 Collaboration), CMU-HEP91-17 (Nov, 1991)

2. Charm Pair Correlations in 800 GeV/c Proton-Emulsion Interactions, with K. Kodama, *et al.*, (Fermilab-E653 Collaboration), CMU-HEP91-18 (Nov, 1991).

3. Measurement of the Relative Branching Fraction G (D^0 -> Kmn)/(D^0 -> mX),with K. Kodama, *et al.*, (Fermilab-E653 Collaboration), published in *Physical Review Letters*, Vol.66 No. 14 (1991) 1819.

4. Hybrid Emulsion Spectrometer for the Detection of Hadronically Produced Heavy Flavor States with K. Kodama, *et al.*, (Fermilab-E653 Collaboration), published in *Nuclear Instruments and Methods in Physics Research* , Vol.A289 (1990) 146.

5. A New Limit on K_L, K_S -> p^0 e^+ e^-, with A Barker, *et al.*, (Fermilab-E731 Collaboration), published in *Physical Review* , Vol.D41 (1990) 3546.

6. A Test of CPT Symmetry Through a Determination of the Difference in the Phases of h_{00} and h_{+-} in K -> 2 p decays, with M. Karlsson, *et al.*, (Fermilab-E731 Collaboration), published in *Physical Review Letters*, Vol.64 (1990) 2976.

7. A Determination of Re(e'/e) by the Simultaneous Detection of the Four K(L), K(S) -> p p Decay Modes, with J.R. Patterson, *et al.*, (Fermilab-E731 Collaboration), published in *Physical Review Letters*, Vol.64 (1990) 1491.

NAME: FRANCOIS W. STOCKER

EDUCATION (DEGREE/INSTITUTION/YEAR):

Diploma Thesis in Applied Physics, University of Bern,1973

PH.D. in Physics, University of Bern, 1985

PROFESSIONAL EXPERIENCE:

Member of the UA2 Collaboration, 1981-1986

Postdoctoral Research Associate, SUNY at Stony Brook, 1986-1990

Member of the D0 Collaboration, 1986-1990

Staff Physicist, Superconducting Super Collider Laboratory, 1990-present

RECENT PUBLICATIONS:

1. An Expression of Interest to Construct a Major SSC Detector.R. V. Steiner, et al., SSC-EOI0020, July 1991.

2. Test and Calibration Beams at the SSC, F. Stocker et al.,to be published as a IEEE Conference Record, May 1991.

3. Instrumentation for SSC Test Beams, H. Fenker et al., to be published as a IEEE Conference Record, May 1991.

4. The Central Tracking Detectors for D0, A. Clark et al., Nucl. Instr. and Methods A279, 243 (1989).

5. Measurement of the Strong Coupling Constant Alpha-S from a Study of W Bosons Produced in Association with Jets, R. Ansari et al., Phys. Lett. B215, 175 (1988).

NAME: **MAKOTO D. TAKASHIMA**

EDUCATION (DEGREE/INSTITUTION/YEAR)

1979 B.A. in Physics, University of Pennsylvania

1983 M.S. in Physics University of Wisconsin-Madison

1988 Ph.D. in Physics, Universitaet Hamburg

PROFESSIONAL EXPERIENCE:

1989 Postdoctoral Research Fellow, CERN, Guest Scientist,

1991 Max Planck Institute for Physics

1992 Staff Physicist , Superconducting Super Collider Laboratory

RECENT PUBLICATIONS

1. Performance of the ALEPH Time Projection Chamber, W.B. Atwood, *et al.,* Nucl. Inst. and Meth. A306 1991

2. Measurement of B-B Mixing at the Z, D. Decamp *et al.,* ALEPH Collaboration, Phys. Lett. B258 1991

3. Measurement of the Polarization of Leptons produced in Z Decays, D. Decamp *et al.,* ALEPH Collaboration, Phys. Lett. B265, 1991

4. Search for the Neutral Higgs Boson of the MSSM and other Two-Doublet Models, D. Decamp *et al* ALEPH Collaboration, Phys. Lett. B265 1991

5. Measurement of the Charged Particle Multiplicity Distribution in Hadronic Z Decays, D. Decamp *et al* ALEPH Collaboration, Phys. Lett. B273, 1991

NAME: **JENNIFER THOMAS**

EDUCATION (DEGREE / INSTITUTION / YEAR):

1980 B.S., Bedford College, University of London

1984 D. Phil, University of Oxford, Department of Nuclear Physics

PROFESSIONAL EXPERIENCE:

1983 Research Associate, Imperial Colledge of Science and Technology

1985 CERN Fellow, CERN

1988 Wissenchaftlicher Angestellter, Max Planck Institut, Munchen

1991 Staff Physicist, Superconducting Super Collider

RECENT PUBLICATIONS :

1. Search for a New Weakly Interacting Particle, Phys. Lett.
2. Search for a Very Light Higgs Boson, Phys. Lett.
3. Measurement of Electroweak Parameters from 2-Decays into Fermion Pairs, CERN EP/90-104
4. Search for Excited Neutrinos in Z Decay, CERN CP/90-107
5. Searches for the Standard Higgs Boson, CERN EP/90-101

NAME: MARC TURCOTTE

EDUCATION (DEGREE/INSTITUTION/YEAR):

1979 B.Sc. Physics (Honours), McGill University, Montreal, Canada

1986 Ph.D. Experimental High Energy Physics, McGill University

PROFESSIONAL EXPERIENCE:

1986 Postdoctoral Research Associate, University of Victoria-TRIUMF

1990 Staff Physicist, Superconducting Super Collider Laboratory

RECENT PUBLICATIONS:

1. Electromagnetic Resolution of a Tile-Fiber Calorimeter for the SDC. SDC-92-199 (Feb '92)

2. Status of EM Module for BNL Beam Test. Proceedings of the SDC Collaboration Meeting at KEK, Japan, SDC-91-00033 (May 1991).

3. Electronic Technology and the SLD Detector. (Dec. 1990) SLAC-PUB-5248.

4. Quality Assessment and Control in Building SLD Lead-Liquid Argon Calorimeter Modules at TRIUMF, (1989).

5. Cosmic Ray Test of an End-Cap LAC Module, (1989) SLD Note #193.

6. Test System for the LAC Daughter Boards, (1989) SLD Note #192. N. Ushida, *et al.*, Production Characteristics of Charmed Particles in Neutrino Interactions. Phys. Lett. B206:380, (1988). N. Ushida, *et al.*,

7. Cross-sections for Neutrino Production of Charmed Particles. Phys. Lett. 206B:375, 1988. N. Ushida, *et al.*, Limits to Muon-Neutrino, Electron-Neutrino ---> Tau-Neutrino Oscillations and Muon-Neutrino, Electron-Neutrino ---> Tau- Direct Coupling.

8. Fermilab E531 Collaboration. Phys. Rev. Lett. 57 (1986) 2897-2900. N. Ushida, *et al.*, Lifetime of D0 Charmed Meson Produced in Neutrino Interactions. Phys. Rev. Lett. 56 (1986) 1771-1774. N. Ushida, et al., Lifetimes of the Charmed Particles D+-, F+-, and Lambda(c)+ produced by Neutrinos. Phys. Rev. Lett. 56 (1986) 1767-1770.

NAME: **LUIS VILLASENOR**

EDUCATION (DEGREE/INSTITUTION/YEAR):

1981 B.S. in Physics and Mathematics, University of Michoacan, Mexico

1984 M.S. in Physics, CINVESTAV-IPN, Mexico City

1988 Ph.D. in Physics, CINVESTAV-IPN, Mexico City

PROFESSIONAL EXPERIENCE:

1988 Professor, Department of Physics, University of Michoacan, Mexico

1991 Staff Physicist, SSC Lab

RECENT PUBLICATIONS:

1. Two-Jet Mass Distributions at the CERN Proton-Antiproton Collider. UA1 Collaboration. Phys. Lett. B209 (1988) 127.

2. Measurement of the Bottom-Quark Production Cross-Section in Proton-Antiproton Collisions at a CM Energy of 0.63 TeV. UA1 Collaboration Phys. Lett. B213 (1988) 405.

3. Studies of Intermediate Vector Boson Production and Decay in UA1 at the CERN Proton-Antiproton Collider. UA1 Collaboration. Z. Phys. C 44 (1989) 15.

4. Topics on Experimental High Energy Physics. G. Moreno y L. Villasenor. Revista Mexicana de Fisica 36 Suplemento 1 (1990) S1-S19.

5. A Small Multiwire Proportional Chamber for Pedagogical Use. C. Avilez, G. Moreno y L. Villasenor. Proceedings of the Third ICFA School on Instrumentation for Elementary Particle Physics, Edited by J. dos Anjos et al., WORLD SCIENTIFIC 1991.

NAME: **EDWARD M. WANG**

EDUCATION (DEGREE/INSTITUTION/YEAR):

1976 B.S. in Electrical Engineering, University of Michigan

1976 B.S. in Physics, University of Michigan

1984 Ph.D. in Physics, University of Michigan

PROFESSIONAL EXPERIENCE:

1984 Lawrence Berkeley Laboratory

1991 Superconducting Super Collider

RECENT PUBLICATIONS:

1. Electromagnetic and Muon Detector at the SSC", EOI-18 and FSU-SCRI-91T-15 (1991).
2. "Test of Spin Dependence in Charm-Quark Fragmentation to D", Phys. Rev. D43, 29, (1991).
3. "Jet Response of Homogeneous Calorimeter", Proc. of Symposium on Detector R&D at the SSC, Ft. Worth, Tx (1990).
4. "A Measurement of the Total Hadronic Cross Section in Tagged 2-photon Reactions", Phys. Rev. D41, 2667, (1990).
5. "Electron Identification and Implications in SSC Detector Design", SSC-287 (1990).

NAME: **Jin Chu Wu**

EDUCATION (DEGREE/INSTITUTIONS/YEAR):

1985 Ph.D. in Physics, University of Pittsburgh.

1984 Theoretical Advanced Study Institute in Elementary Particle Physics, Ann Arbor, MI, .

1981 M.S. in Physics, University of Pittsburgh,

1980 Fudan University (Graduate School), Shanghai, China

PROFESSIONAL EXPERIENCE:

1991 Physicist, Superconducting Super Collider Laboratory

1990 Scientist, The Pittsburgh Supercomputing Center

1988 Senior Scientist, Shanghai Institute of Standards

1986 Adjunct Assistant Professor of Physics, University of Pittsburgh

1986 Data Analyst, Extrel Corporation

PUBLICATIONS:

1. "Effects of the renormalization-group equations in the $E_6XSU(3)_H$ model", J. C. Wu, Phys. Rev. D 42, 3239 (1990).

2. "Implications of the $E_6XSU(3)_H$ model", J. C. Wu, Phys. Rev.D36,1514(1987).

3. "Finite-lattice-spacing corrections to masses and g factors on a lattice", R. Roskies and J. C. Wu, Phys. Rev. D 33, 2469 (1986).

4. "Additional scalar bosons in SU(5) theories",J.C.Wu, Phys. Rev. D32,1253 (1985)

5. "Lattice studies of the magnetic moment of the electron", J. C. Wu, Ph.D. Thesis, August, 1985.

6. "Reconciling the proton lifetime and the Weinberg angle in supersymmetric SU(5) theories", J. C. Wu, Pitt-24-84, September, 1984.

7. "Proton decay due to scalar bosons in SU(5)", J. C. Wu, Pitt-22-84,July,1984.

NAME: **JULIA YARBA**

EDUCATION (DEGREE/INSTITUTION/YEAR):

1984 M.S., Moscow State University

1990 Ph.D., Moscow State University

PROFESSIONAL EXPERIENCE:

1984 Physicist, Moscow State University, Nuclear Physics Institute

1991 Physicist, Superconducting Super Collider

RECENT PUBLICATIONS :

1. Vector Meson Production in π^-p Interactions at 360 GeV/c (LEBC-EHS Collaboration) Z. Phys. C, V. 44, p. 531, M. Aguilar-Benitez, J.V. Yarba (1989)

2. Charge and Energy Flow in π^+p, π^-p , and PP Interactions at 250 GeV/c (NA22 Collaboration, Z. Phys, C., v. 43, p. 37, I.V. Ajineko, J.V. Yarba (1989)

3. Neutral Kaon Production in π^+p and π^+p interactions at 250 GeV/c (NA22 Collaboration) Z. Phys. C, v. 46, J.V. Yarba, (1990)

4. Inclusive Particle Production in 400 GeV/c pp Interactions (NA27 Collaboration) Z. Phys. C, v. 50, p. 405, M. Aguilar-Benitez, J.V. Yarba (1990)

5. Bose-Einstein Correlations in pp- Interactions at 400 GeV/c (NA 27 Collaboration, CERN-PRE/91-102, M. Aguilar-Benitez, J.V. Yarba, (1991)

NAME: **GEORGE PALMER YOST**

EDUCATION (DEGREE/INSTITUTION/YEAR):

1963 A.B. -- Princeton University, Senior thesis advisor: Pierre Piroue

1969 Ph.D. -- University of Maryland, College Park, Ph.D. advisor: G.B. Yodh
Thesis: 4-Prong Plus Neutral Vee Production in 4.25 BeV/c K-p Collisions

PROFESSIONAL EXPERIENCE:

1963 Research Assistant, University of Maryland

1968 Research Assistant, Florida State University

1971 Assistant Research Physicist, University of California, Berkeley

1974 Physicist P5, Lawrence Berkeley Laboratory

1976 Assistant Research Physicist V, University of California, Berkeley

1978 Assistant Research Physicist VI, University of California, Berkeley

1981 Specialist II, University of California, Berkeley

1982 Senior Visiting Fellow, Imperial College, London, SW7 2AZ, U.K.

1987 Specialist III, University of California, Berkeley

1989 Physicist, Superconducting Super Collider Laboratory, Dallas, Texas

RECENT PUBLICATIONS:

1. Production and Decay Properties of the $\omega\pi^0$ State at 1250 MeV/c^2 Produced by 20 GeV Polarized Photons on Hydrogen, with J. E. Brau *et al.*, Phys. Rev. D 37, 2379 (1988).

2. Coherent Production of π^+ and π^- Mesons by Charged-Current Interactions of Neutrinos and Antineutrinos on Neon Nuclei at the Fermilab Tevatron, with M. Aderholz *et al.*, Phys. Rev. Lett. 63, No. 21, 2349 (1989).

3. Detector Research and Development for the Superconducting Super Collider. Proceedings, Symposium, Fort Worth, USA, October 15-18, 1990, T. Dombeck, V. Kelly, and G.P. Yost (editors), Singapore: World Scientific (1991).

4. Photo Reproduction of an Isovector $\rho\pi$ State at 1775-MEV, SLAC Hybrid Facility Photon Collaboration (with G.T. Condo, *et al.*,), Phys. Rev. D43 (1991).

5. Averaging in the Presence of "Sliding" Errors, G. P. Yost, SSCL-485, to be published in Nucl. Instrum. Methods (1991).

APPENDIX B

BIBLIOGRAPHY

SSCL-287, 6/90, J. Bensinger, Ed Wang (LBL) and H. Yamamoto (UCLA), Electron Identification and Implications in SSC Detector Design

SSCL-332, 9/90, R. Stefanski, Status of Detectors at the SSC, Published in the *Proceedings from Workshop: Physics at UNK*, Protvino, USSR, September 25-28, 1990

SSCL-335, 11/90, G. Chartrand, L. Cormell, R. Hahn, D. Jacobson, H. Johnstad, P. Leibold, M. Marquez, B. Ramsey, L. Roberts, B. Scipioni and G. Yost , Attachment A: Physics and Detector Simulation Facility Type O Workstation Specifications

SSCL-347, 1/91, A.I. Sanda , The B Factory, The Superconducting Super Collider, and an e^+e^- Linear Collider: How They Stand Against Each Other, Presented at the Third Workshop on Asymmetric B Factory at KEK, Tsukuba, Japan, January, 1991

SSCL-348, 1/91, J. Dorenbosch, M. Botlo, A. Fry and C. Milner, Readout of Overlapping Events, 60, January, 1991

SSCL-373, 3/91, A.I. Sanda, T. Morosumi and M. Rebelo (Rockefeller Univeristy), From QCD to Chiral Dynamics, March, 1991

SSCL-375, 9/91, K. McFarlane, Benchmarks for the SSCL Physics Detector Simulation Computing Facility, 105, September, 1991

SSCL-400, 4/91, L. Cormell , High Energy Physics Computing at the SSCL, Presented at the Conference on Computing in High Energy Physics (CHEP 91), Tsukuba, Japan, March 1991, April, 1991

SSCL-412, 7/91, Lee Roberts, CZ/CPS A Communications Implementation Using CPS, July, 1991

SSCL-413, 4/91, L. Roberts, BCD/CPS An Event-level GEANT3 Parallelization via CPS, April, 1991

SSCL-455, 5/91, F. Stocker, H. Fenker, and R. Schailey, Test and Calibration Beams at the Superconducting Super Collider, Presented at the IEEE Particle Accelerator Conference, San Francisco, CA, May 6-9, 1991, May, 1991

SSCL-456, 5/91, H. Fenker, F. Stocker, and R. Schailey, Instrumentation for SSC Test Beams, Presented at the IEEE Particle Accelerator Conference, San Francisco, CA, May 6-9, 1991, May, 1991

SSCL-463, 6/91, A. Fridman and S. Meshkov, Total Cross Sections of Beauty and Charmed Mesons and Protons, *Physical Review D*, American Physical Society, June, 1991

SSCL-481, 6/91, A. I. Sanda, Model Independent Test of the Standard Model, Talk given at the 1991 International Workshop on the B Factory, KEK, Tsukuba, Japan, June, 1991

SSCL-485, 8/91, G. P. Yost, Averaging in the Presence of Sliding Errors, Published in *Nuclear Instruments and Methods in Physics Research*, A312 (1992) pp. 598-608 (North Holland), August, 1991

SSCL-486, 6/91, G. L. Kane, G. A. Landinsky, and C.-P. Yuan, Using the Top Quark for Testing Standard Model Polarization and CP Predictions, June, 1991

SSCL-498, 8/91, V. Gupta, B. McKellar, and D. Wu, The Degeneracy of the Free Dirac Equation

SSCL-502, 8/91, Bruce McKellar and Dan-di Wu, Quantum Electrodynamics with Complex Fermion Mass, August, 1991

SSCL-540, 10/91, D. Atkinson, M. Harada, and A. I. Sanda, Is There a *P*-Wave Bound State of $W_L W_L$, October, 1991

SSCL-552, 9/91, H. Fenker, K. Morgan, and T. Reagan, Progress in the Use of Avalanche Photodiodes for Readout of Calorimeters, September, 1991

SSCL-566, 1/92, M. Cannalire and A. Fridman, Dilution Effects for CP Vilation Measurement in B Decays, January, 1992

SSCL-Preprint-12, HUTP-91/A045, 11/91, M. J. Dugan, M. Golden, and B. Grinstein, On the Hilbert Space of the Heavy Quark Effective Theory, Submitted to *Physics Letters B*, January, 1992

SSCL-Preprint-13, HUTP-90/A029, 11/91, B. Grinstein and M. Wang, An Effective Field Theory Calculation of the QCD Corrections to Weak Parameters, Submitted to *Nuclear Physics B*, January, 1992

SSCL-Preprint-17, HUTP-91/A040, 12/91, B. Grinstein, Lectures on Heavy Quark Effective Theory, Presented at the Workshop on High Energy Phenomenology, Mexico City, Mexico, July, 1991, January, 1992

SSCL-Preprint-21, SFU-Preprint-91-5, 12/91, Z. Huang, K. Viswanathan, and D. Wu, Vacuum Orientations in Strong CP Violation, To be published in *Physics Letters*, January, 1992

SSCL-Preprint-23, 10/91, F. E. Paige, SSC Physics Signatures, Presented at The Project, The Progress, The Physics, 1991 Symposium on the Superconducting Super Collider, Corpus Christi, TX, October 13-17, 1991, March, 1992

SSCL-Preprint-27, 7/91, F. J. Gilman, The SSC Project and Experimental Program, Lecture given at the International School of Subnuclear Physics, Erice, Sicily, July 22, 1991, February, 1992

SSCL-Preprint-34, 2/92, B. Grinstein, Light-Quark, Heavy-Quark Systems, To appear in *Annual Review of Nuclear and Particle Science*, 42, February, 1992

PN-92-00005, H Æ $\rightarrow \mu\mu\mu\mu$ and H Æ $\rightarrow \mu\mu ee$ Acceptance, Frank E. Paige, 03/06/92

PN-91-00001, Jet Contributions to E_T Cross Sections, Paige, Frank E., 10/07/1991

PN-91-00002, $t\bar{t}$ Lepton Triggers, Paige, Frank E., 10/07/1991

PN-91-00003, Possible $H \rightarrow W+W-$ Signal for $2m_W < m_H < 2m_Z$, Paige, Frank E., 10/07/1991

PN-91-00004, Lepton Triggers at the SSC, Paige, Frank E., 09/13/1991

SDC 90-00116, Proposal for the Testing of Prototype Detectors, J. Bensinger, D. Green

SDC 91-00034, SSC Detector Muon Subsystem Beam Tests, H. Lubatti

SDC 91-115, Tracking Volume Report, M. Gilchriese

SDC 92-199, Electromagnetic Resolution of a Tile Fiber Calorimeter for the SDC, M. Turcotte

APPENDIX C

RESULTS OF SPRING '91 LIQUID ARGON BEAM TEST

LAr EM Prototype Module

The basic design concept behind the SSCL LAr EM prototype design follows closely on the work of Radeka and others. The idea is to preserve the fast intrinsic risetime of the leading edge of the Liquid Argon signal by appropriate arrangement of the signal leads and absorber plates. For SDC, peaking times in the 60 nsec range were judged adequate to our needs, so a flat geometry of absorber plates interspersed with g-10 readout boards, and connected by kapton striplines to electronics mounted in the liquid directly behind the stack could be made to work. The stack is supported by a series of through tie-rods. The next section summarizes the test setup and results obtained at the BNL test.

BNL Beam Test Results

The Liquid Argon Large Subsystem proposal test beam run ended June 30, 1991. SSCL physicists contributed to the effort mainly during most of June 1991 while tests were performed on the EM prototype module. Insufficient time has passed to fully analyze the results of the test. The basic trends are clear: the concepts and ideas behind the Liquid Argon design work. In some cases below, numbers taken directly from the on-line logbook are quoted. These numbers will be subject to change as the pedestals and other constants become better known.

Test Setup Description

A schematic drawing of the beamline setup is shown in Figure C-1. The calorimeter was installed inside a vacuum insulated aluminum cryostat and tested in the AGS A3 test beam line at BNL. The beam line was modified to provide beams of negatively charged particles with momenta from 0.5 to 20 GeV. Two Cherenkov counters operating below atmospheric pressure were installed in the beam to separate electrons from pions and muons. A large veto counter indicated beam halo and upstream interactions. A small counter was installed downstream of the calorimeter to help select muons. A Hodoscope of 1 mm scintillating fibers provided position measurements, both horizontal and vertical, for localization of shower positions. The hodoscope in combination with the finger counters F_1, F_2 give a 1/2 mm position resolution at the calorimeter front face. The interaction rate varies from a few KHZ to a few MHZ/spill (0.8 sec for extraction). A view of the cryostat is shown in Figure C-2 and the EM module fixture in Figure C-3. Horizontal motion of the cryostat was possible for position scans, but not vertical.

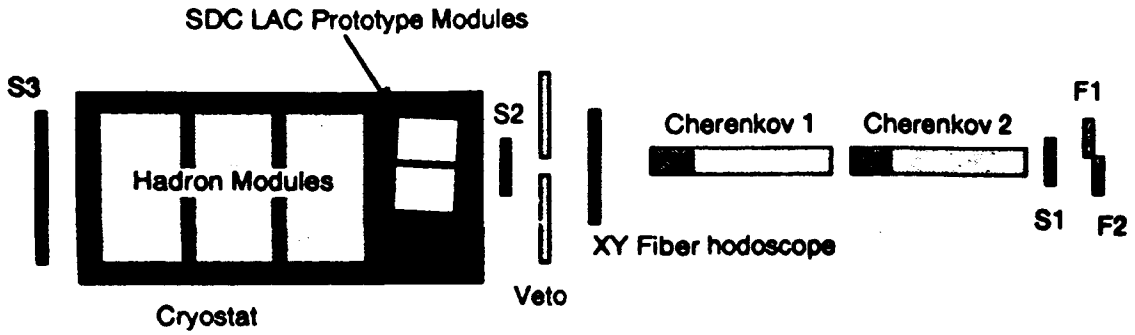

Figure C-1: Schematic View of BNL Spring '91 Test

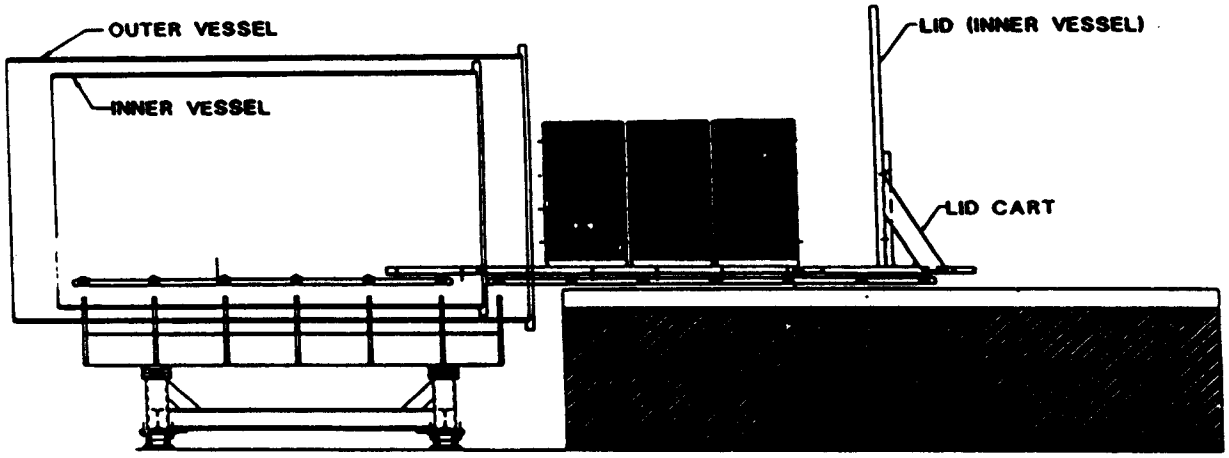

Figure C-2: Side View of BNL Cryostat

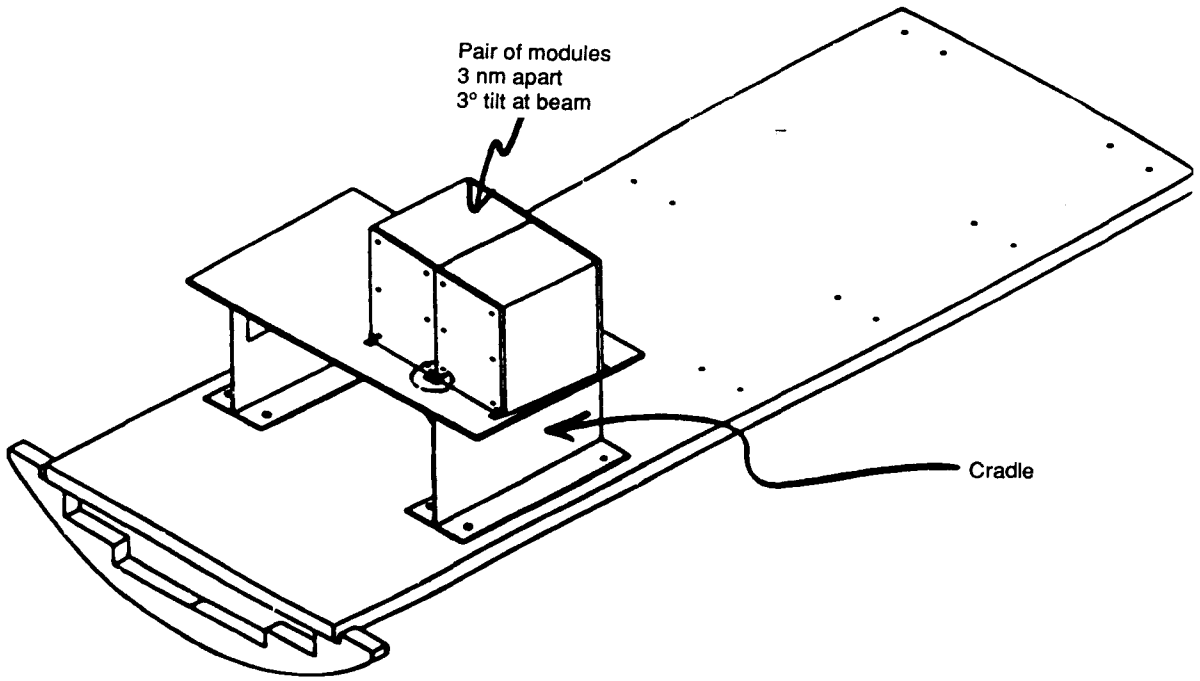

Figure C-3: Schematic of Module Support for EM Test Modules

EM Test Module Results

The EM test calorimeter consists of two modules, each with six towers (Figure C-4). In depth, each tower consists of a massless gap layer, EM1 (5 layers), a shower max strip layer, and EM2 (19 layers). The lead thickness is 6 mm, vs 4 mm for the SDC design. The signals are carried by strip lines to the back of each module, where the electronics are located. No preamp cooling was necessary for this test since any bubbles that might be formed rise harmlessly in the vertical direction. The high voltage was distributed along the top of the modules, and the strip layers were also read out on the top. The azimuthal gap between modules was set with precision calipers to 3 mm, the value appropriate for SDC.

The goals of the EM test were to establish that the SDC electrode structure gives speed of response fast enough for SSC operation, to verify that the electronic noise and timing resolution are understood and predictable, and to measure the stochastic energy resolution, the response

across the inter-module gap, and the uniformity of response away from the gap. Preliminary results on all of these subjects are presented below.

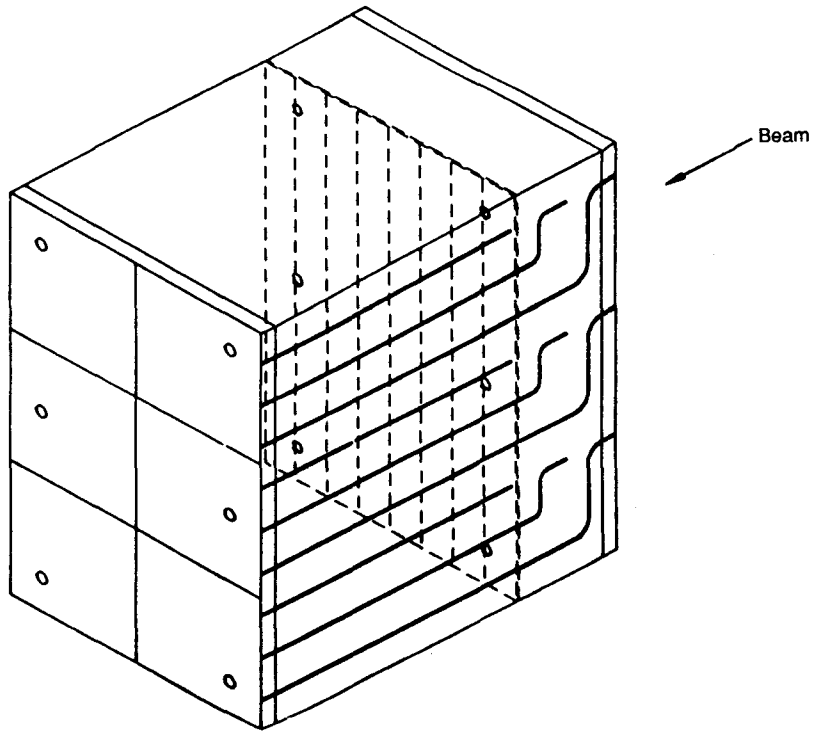

Figure C-4: Schematic of EM Test Module Showing Pads, Tie Rods, Readout Strips and Strip Layer at Shower Max

1. Speed of Response

Figure C-5 shows the signal observed in EM_1 and EM_2 for various shaping times with 10 GeV electrons incident. The curves show the dependence on peaking time that is expected if the leading edge has a risetime that is fast compared to the peaking time. (The absolute normalization of this curve is arbitrary). The good agreement shows that the charge is being transferred from the stack as expected, and that the speed is fast enough for peaking times at least as low as 50 ns.

2. Electronic Noise

The pedestal width and 10 GeV minimum ionizing peak for an EM2 channel is shown in Figure C-6. The electronic noise performance of two towers (four channels) has been analyzed. Two EM1 channels have measured noise of 16+/-2 and 17+/- 2 MeV, while the EM2 channels have noise of 50+/-7 and 67+/-7 MeV. The predicted values are 23+/-5 and 50+/-10 respectively. The agreement at the 20% level indicates that the electronic noise is predictable and that there is no significant pickup noise.

The timing resolution of EM2 for 10 GeV incident electrons (corresponding to 5.1 GeV of energy deposited in the channel) was determined by measuring the zero-cross time of a number of events with a digital storage scope. For 100 ns peaking time, the resolution was 1.5 +/- 0.2 ns, in good agreement with the predicted value.

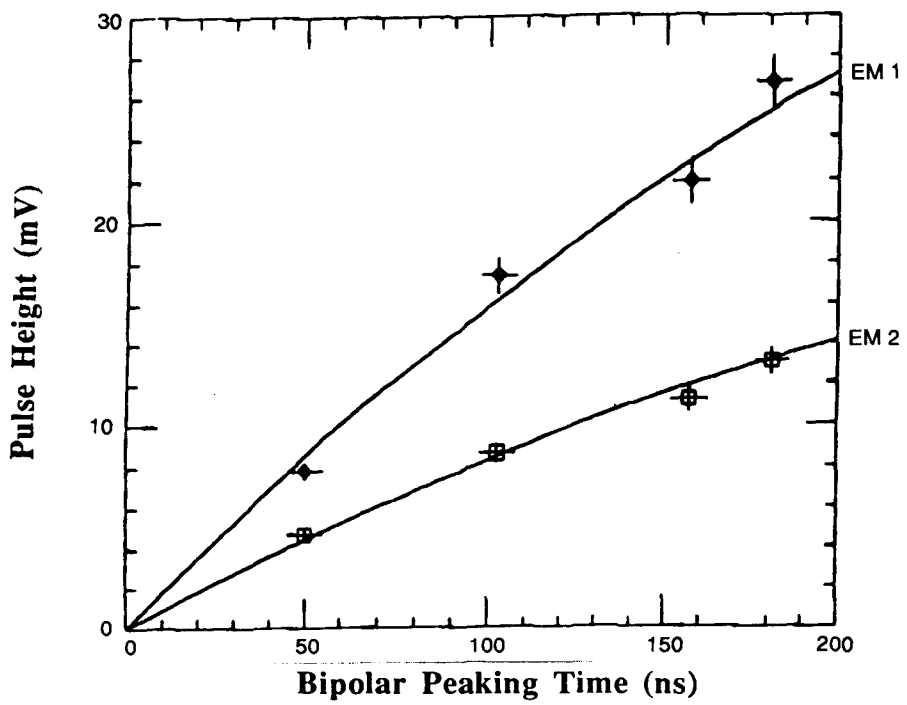

C-5: Measured Pulse Heights of 10 GeV e-, 5-200ns Bipolar Shaping. Curves are expected values for no addition ballistic deficit.

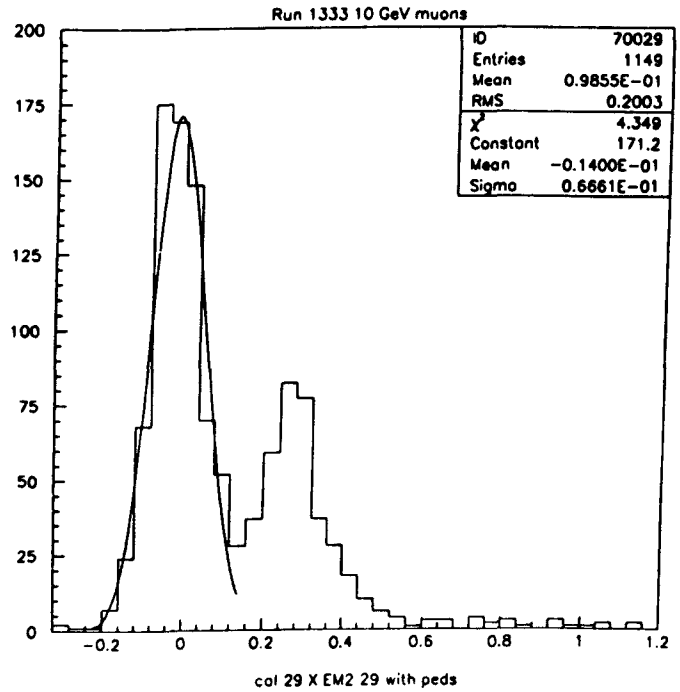

C-6: Pedestal width and minimum ionizing peak EM2

3. Energy Resolution

The charge injection circuit on the preamp boards suffered from cross-talk at the 30% level, rendering it useless for determining the calibration of each channel. It did, however, verify the stability of the response in time. There was insufficient time to repair the system before the beam test. The preliminary results presented here use calibration constants for EM1 and EM2 derived from the data; the strips and massless gaps will not be used until the full calibration is available. Events are selected to be at locations that give showers well contained in a single tower. The relative weight (w) of EM1 and EM2 is determined by optimizing the resolution sigma E/E of the quantity of EM1+w•EM2. Figure C-7 shows resolution vs w for 5 GeV and 10 GeV incident energies; the results are the same for other energies. The difference in the relative weight between EM1 and EM2 is due to the factor of two difference in transformer ratio. The overall scale is set by requiring the average of EM1+w•EM2 reconstruct the beam energy less the energy not observed in the strip layer (although the results presented here do not depend on this scale).

Figure C-8 shows the calibrated EM1 + EM2 energy peak for 10 GeV incident electrons. The resolution is sigma E/ E = 0.057, corresponding to 18%$\sqrt{}$ (10 GeV), in agreement with simulation.

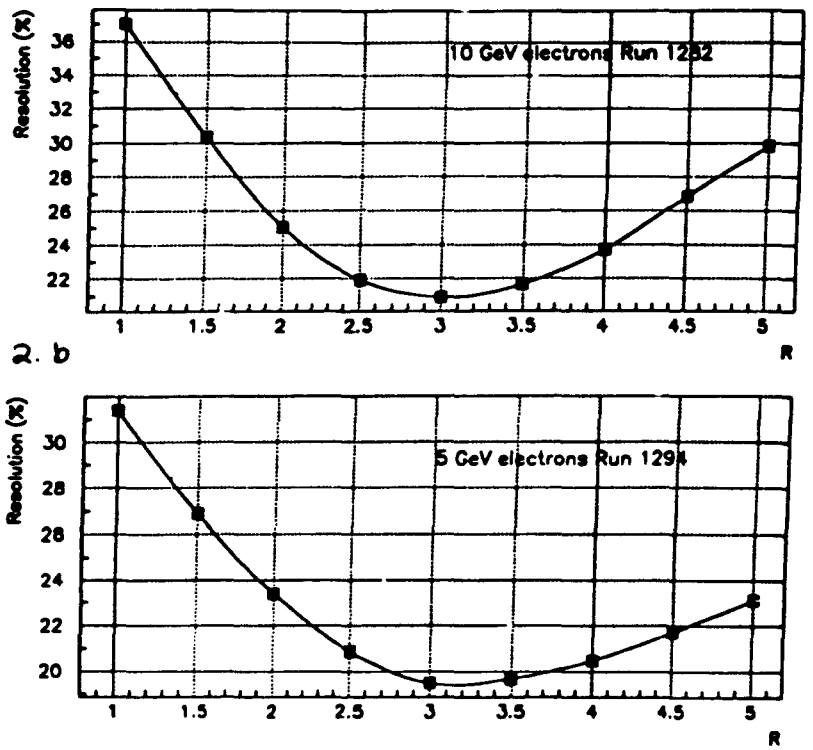

C-7: EM resolution vs weighting factor (see text).

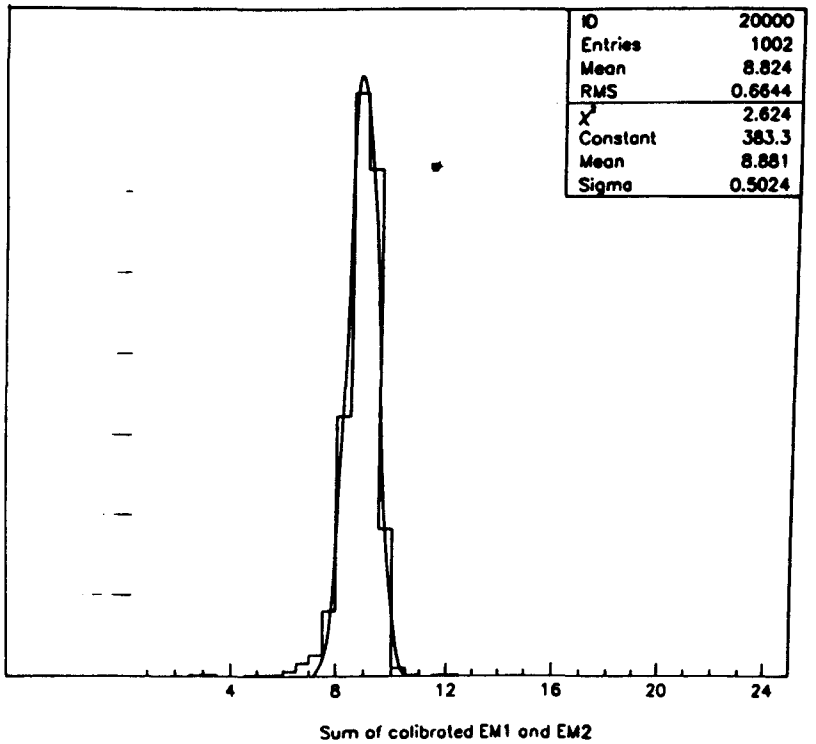

C-8: Calibrated energy distribution for 10 GeV incident electrons, strips ignored.

4. Uniformity and Crack Response

Data from 10 GeV electrons were taken at four cryostat positions to measure the response across the azimuthal crack. The location of the electron in each event was determined from the fiber hodoscope data.

A similar scan has been performed with Geant. Figure C-9 is the energy deposited in the active liquid argon, including strips, as a function of position. A small dip, < 3.2%, is observed for positions within 5 mm of the crack. The separate response of EM1, strips, and EM2 are shown in Figures C-10-12. The EM2 signal increases at the crack because the electron travels some distance into the crack before showering, resulting in later shower development. Figure C-13 is the Geant uniformity scan for EM1 + EM2 only. Note that excluding the strips and their dip results in a small bump in Figure C-13.

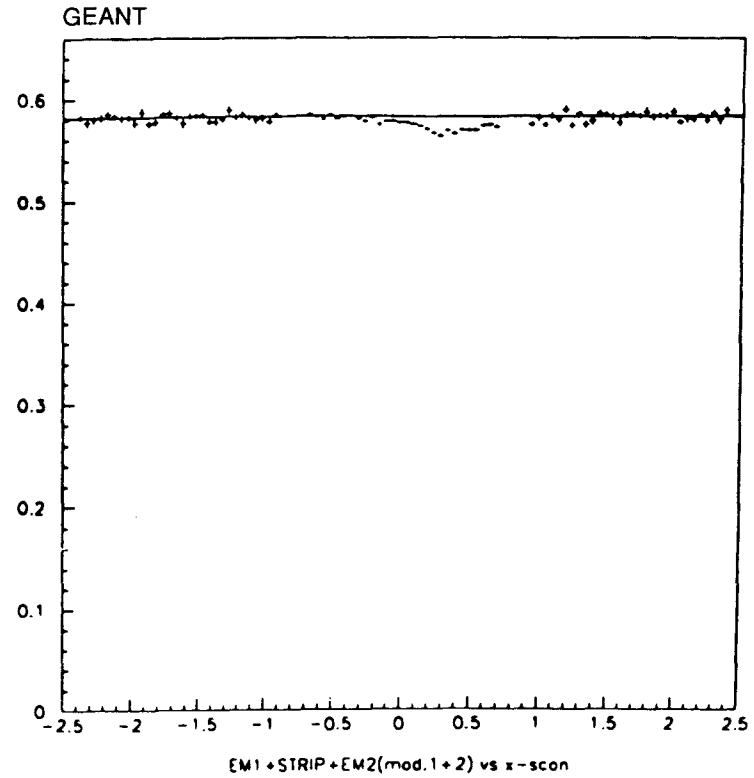

Figure C-9: Calculated energy deposited in liquid argon vs position.

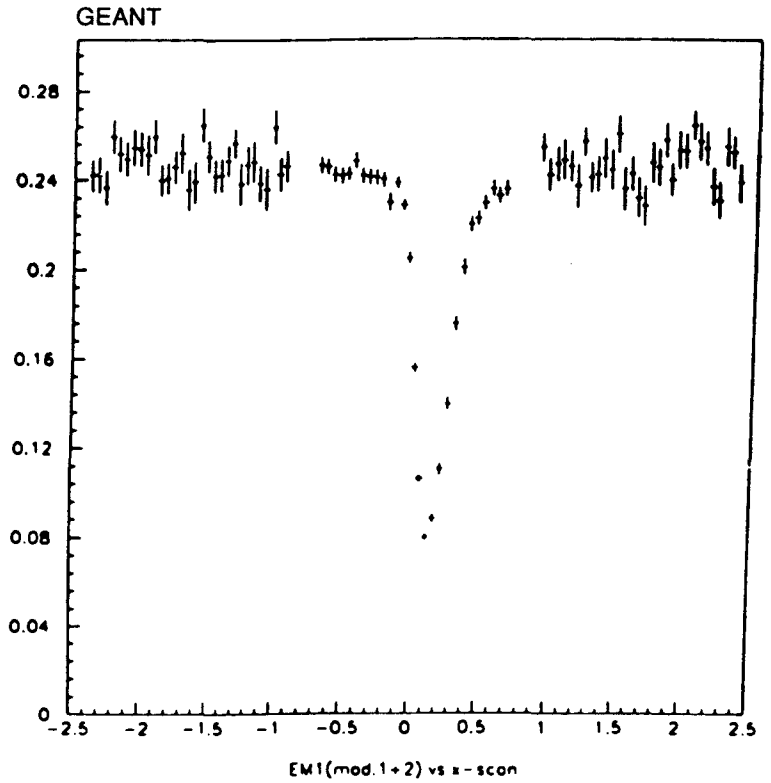

Figure C-10: Calculated energy desposited in EM1 vs position.

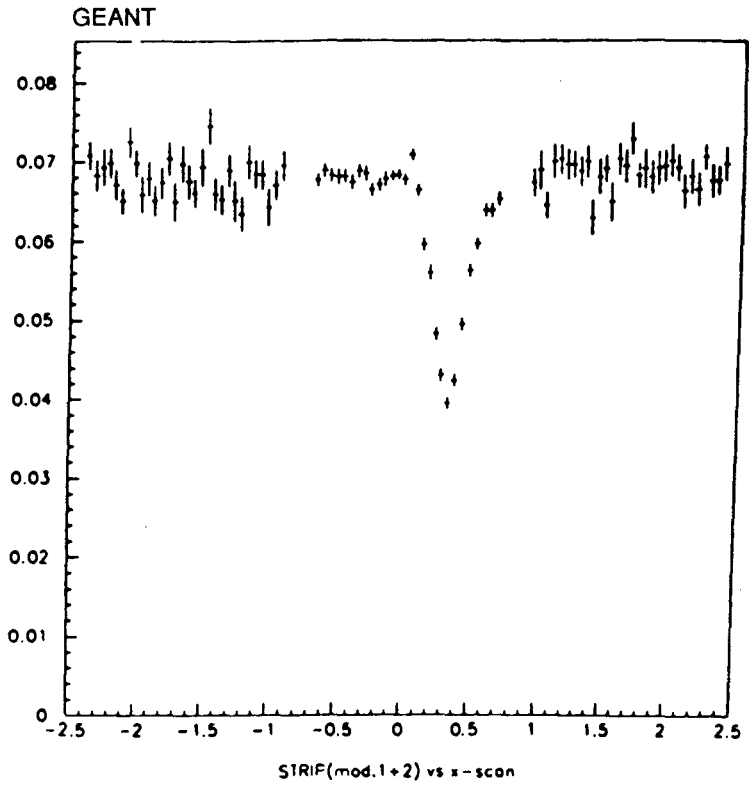

Figure C-11: Calculated energy deposited in strips vs position.

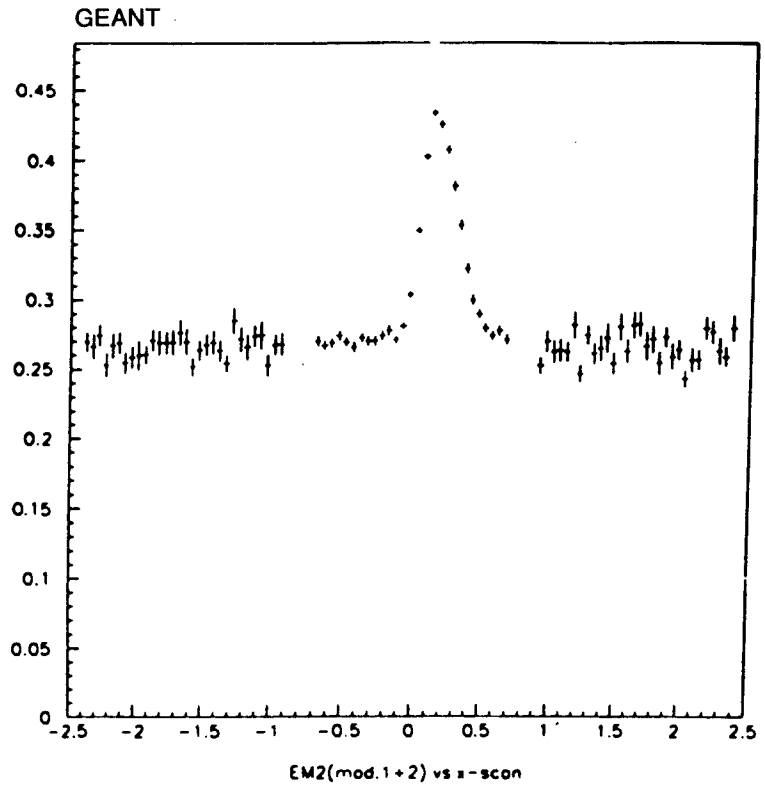

Figure C-12: Calculated energy deposited in EM2 vs position

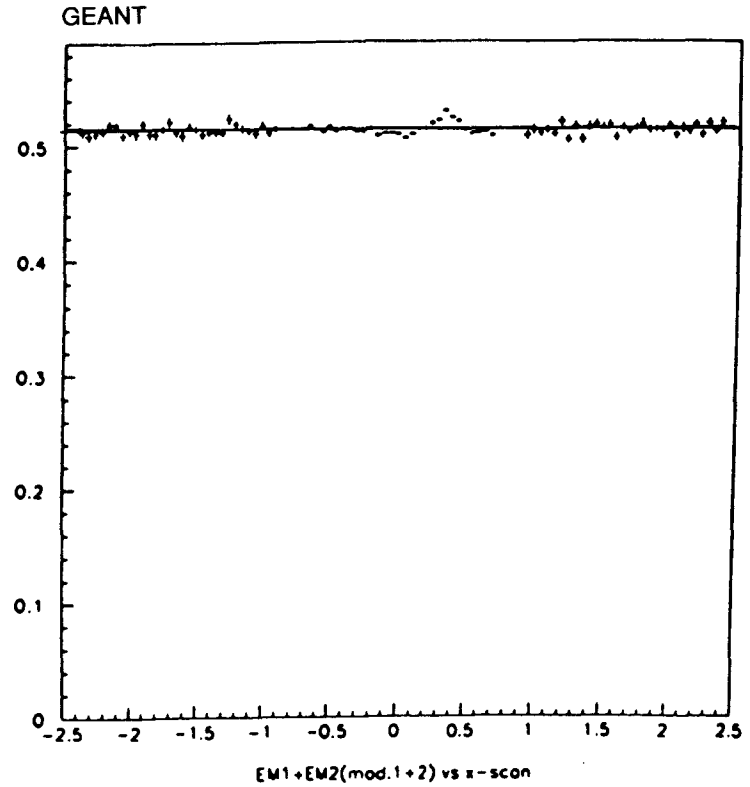

Figure C-13: Calculated energy deposited in EM1 + EM2 only vs position.

Figures C-14 and 15 are the measured EM1 and EM2 individual response and the sum EM1 + EM2 response of the EM calorimeter as a function of position. The features predicted by the Monte Carlo are present in the data, including the increase in response at the crack.

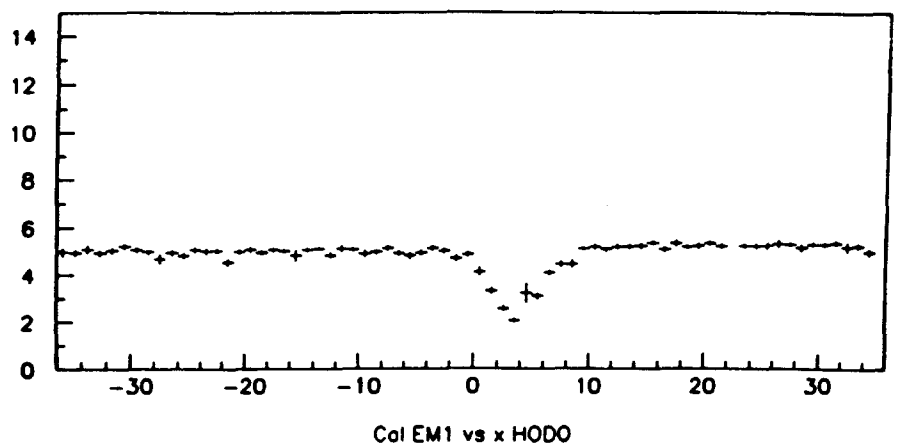

Figure C-14a: Measured EM1 response vs position

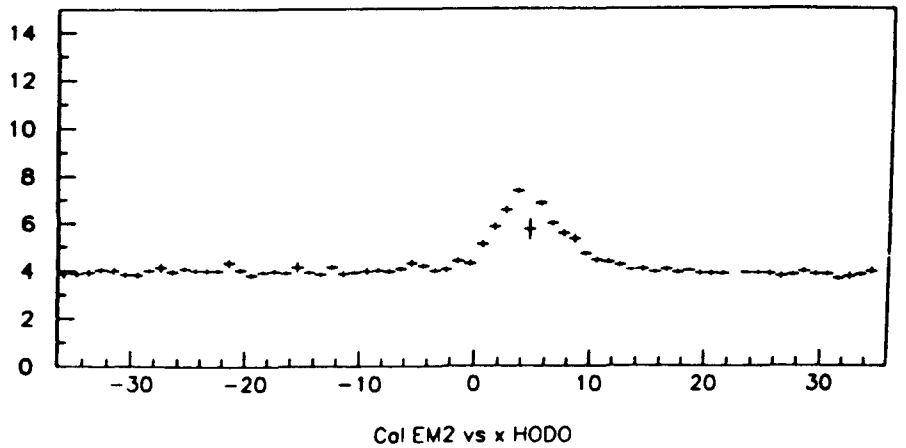

Figure C-14b Measured EM2 response vs position

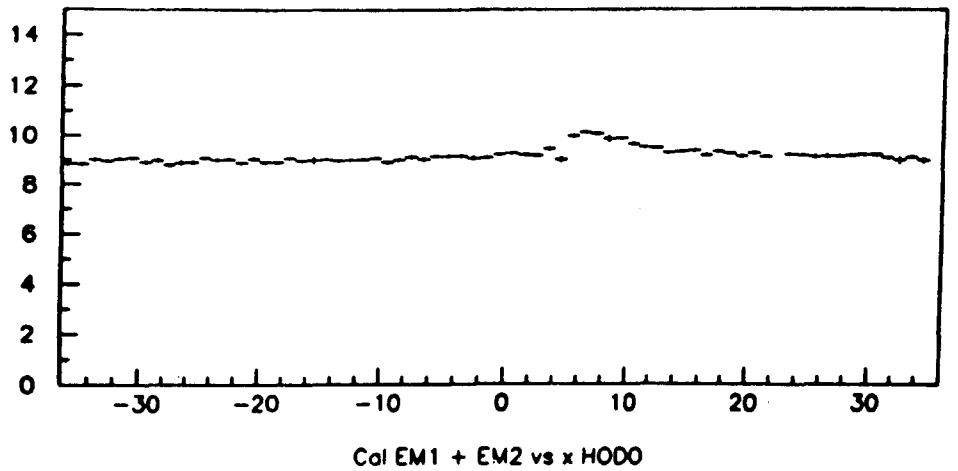

Figure C-15 Measured EM1 + EM2 Response vs Position

The uniformity of response away from the crack is found using the data with -8 < x < 16mm. As can be seen from the dashed lines in Figure C-16, which represent a +/-1% deviation from the average value, the uniformity is very good. The difference between the average observed signal in this region and the signal at each 1mm scan point, divided by the statistical error at that point, is histogrammed in Figure C-17. The fit is a Gaussian of width 1.28. Interpreting the increase above one as a measurement of nonuniformity gives a value of 0.8 sigma, or 40 MeV as the additional rms due to nonuniform response. 40 MeV corresponds to 0.5% of the average response.

The EM1 + EM2 energy peak for the crack region, -8mm < x < 16mm, is Figure C-18. The resolution corresponds to 24% Sqrt (10 GeV). Clearly, no electrons will be lost in the phi cracks of the SDC LAC.

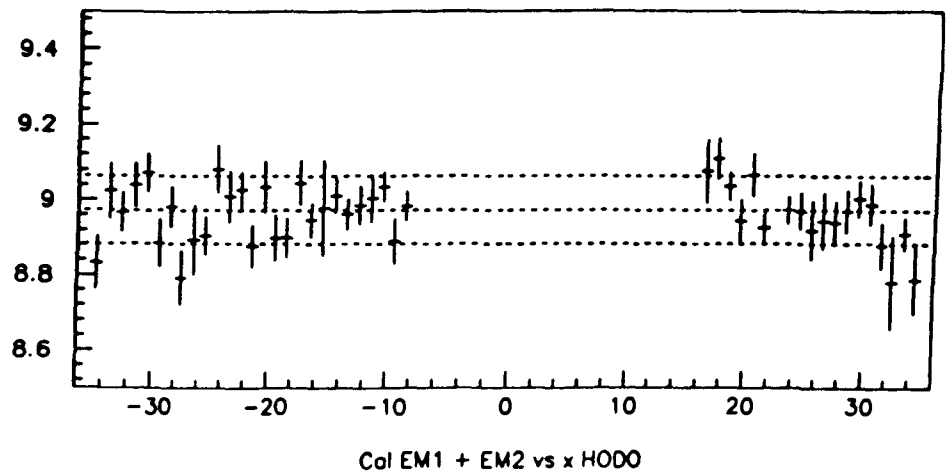

Figure C-16: Uniformity of Measured Response Away from the Crack. The Dashed Lines are at +1% Deviation.

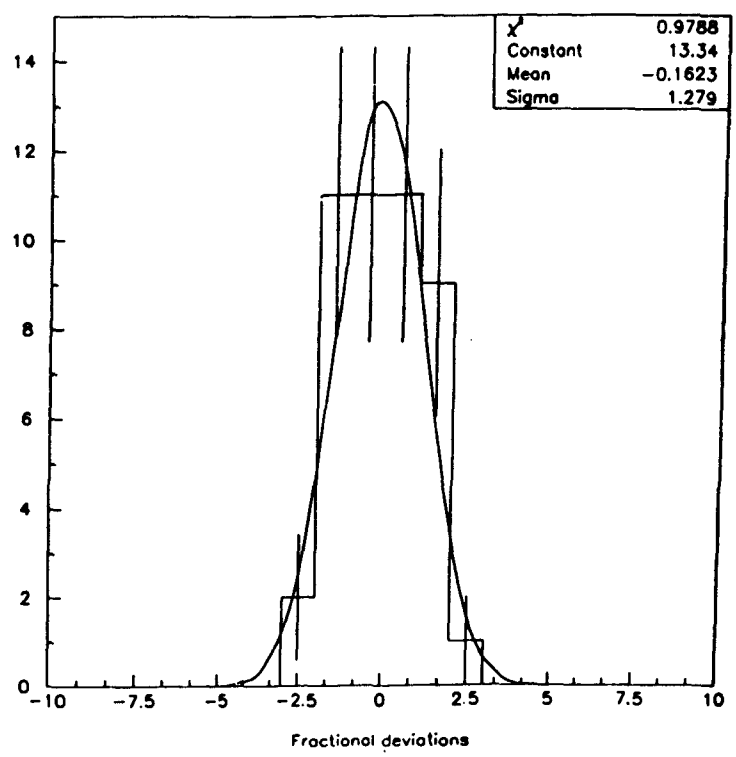

Figure C-17: Measured Difference in the Signal and Average Signal Divided by the Statistical Error

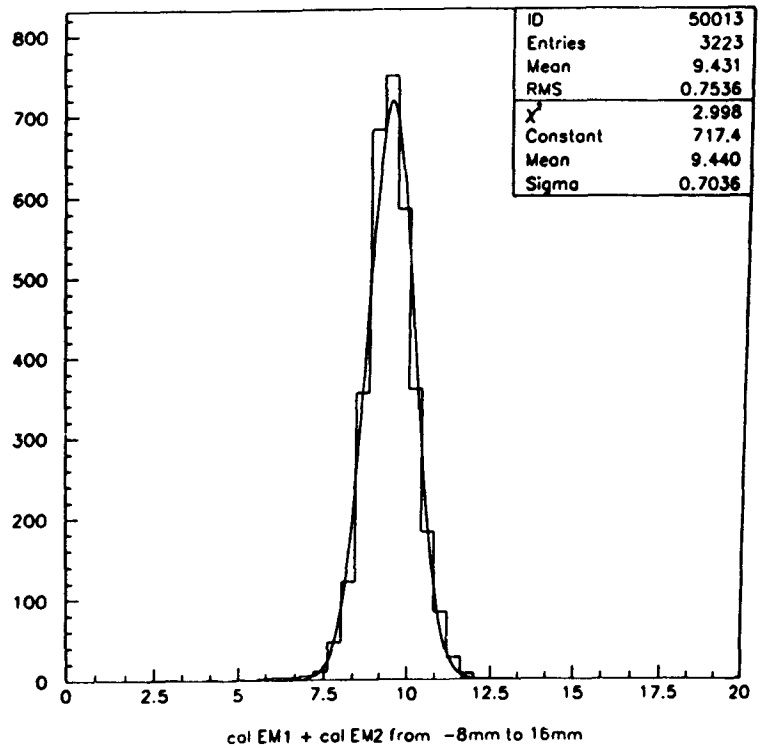

Figure C-18: Energy Distribution for Electrons Incident in the Azimuthal Crack

Hadron Module Results

The calorimeter tested this spring at BNL was built to measure performance for peaking times ranging from 50 to 200 ns and to measure the e/π ratio for 12 mm thick lead. The NA34 (HELIOS) calorimeter had previously measured $e/\pi = 1.12$ with 3.4mm uranium plates and 100ns shaping time. Calculations have suggested that the e/π can be moved closer to one with thick lead absorber plates, rather than uranium. The stack was built using 12mm X 100cm X 100cm lead plates with a total depth of 7.5 lambda. The design is very similar to HELIOS: the stack is segmented transversely into forty 2.5 cm wide x-strips alternated with forty 2.5 cm wide y-strips. It is divided longitudinally into 3 sections. Each unit cell consists of 1 lead plate followed by a 2mm argon gap followed by a 1.7mm G10 printed circuit board and then another 2mm argon gap (Figure C-19). The interleaving of the X and Y strips in depth provides information about the transverse profile of the shower and a direct measure of the sampling fluctuations.

The main design parameters of the test calorimeter are presented in Figure C-20. For comparison, the corresponding data for HELIOS calorimeter are also included in the table.

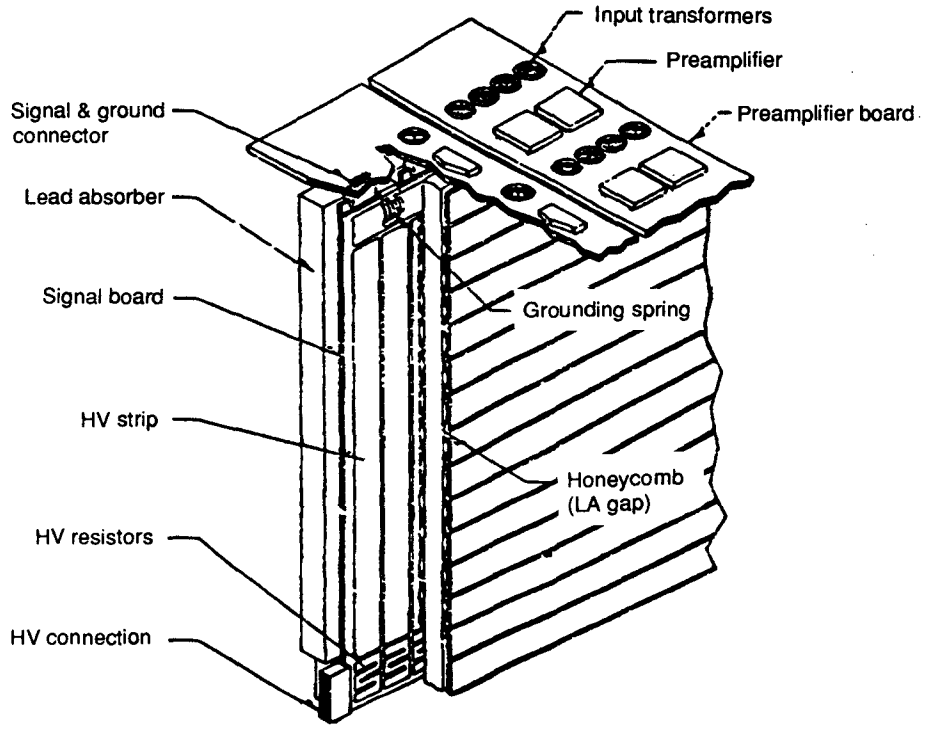

Figure C-19: Liquid Argon Test Calorimetry

1. e/π

The hadron calorimeter was exposed to beams of momentum 0.5, 1, 2, 3.5, 5, 7.5, 15 and 20 GeV/c. Figure C-21 displays the linearity of the response to electrons. Figure C-22 is the preliminary measurement of the e/π ratio as a function of energy. The data points have been averaged over several runs at the same energy. The errors plotted represent the spread of the measurements done at different times and, therefore, account for both statistical errors and systematic uncertainties related to the changes in the data-taking conditions. The e/π ratio reaches its maximum value of 1.25 near 5 GeV and drops to a value of 1.15 at 20 GeV. Figure C-22 is for a nominal shaping time of 100 ns. We have also measured e/π for shaping times of 50 and 200 ns; within the precision of the existing data, we do not see any variation in the ratio attributable to a change in shaping time.

2. Energy Resolution

The energy resolution for pions measured on-line was approximately 70% $\sqrt{E}$. Final versions of the e/π and resolution numbers will be available later.

3. Pileup

The high rate capability of the A3 beamline has been used to determine the effect of pileup on energy measurements. Figures C-23 and 24 show the energy observed in the calorimeter when it is exposed to 10 GeV pions at low rate and at 400 kHz incident rate, respectively. Peaking time

is 100 ns. The data shown are taken with an analog sum over 8 vertical and 8 horizontal strips that contains 60% of the pion shower energy. Note that the mean value is unchanged by the pileup; this is a consequence of the bipolar shape having no net area ($\int_0^\infty h(t)\,dt = 0$) where h(t) describes the signal shaping properties of the shaper and integrater. The high rate produces a non-gaussian tail in the observed energy distribution, thereby increasing the rms without substantially increasing the FWHM. The rms measured at high rate agrees with the value predicted by Campbell's theorem. Note that the size of the tail is very much larger in the test beam than will be observed at the SSC: the pileup particles at BNL have E=10 GeV, while they are typically <1 GeV for minimum bias events.

Characteristic	Helios	LAC
Absorber	3.4mm^{238}U	12mmPb
Absorbtion Length	4.5η	7.5η
Size	120cm x 120cm	100cm x 100cm
LA Gap	2.5mm	2.0mm
Readout	(48) 2.5cm Strip	(40) 2.5cm Strip
Sampling Ratio	12%	5.5%
Number of Cells	10	16
Transformer Ratio	11.1	12.5.1
Feedback Capacitor	5Pf	5Pf
Shaping Time	135.Nsec	50,100,200 N sec
mv/GeV	1.8mv/GeV	1mv/GeV
Charge Transfer Time	~35 Nsec	~25 Nsec

Figure C-20: Liquid Argon Calorimetry

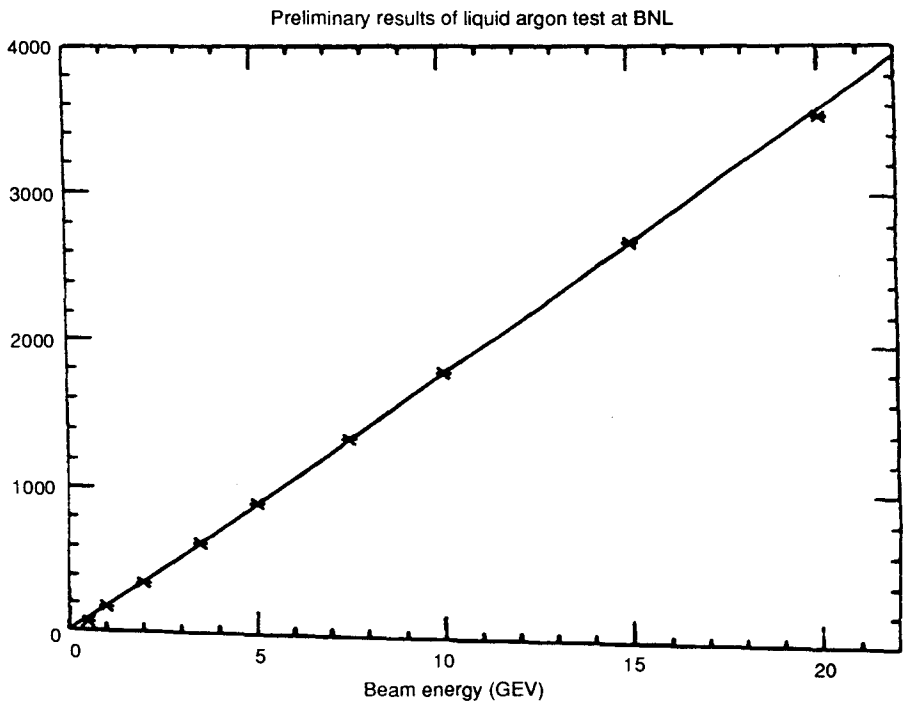

Figure C-21: Response Linearity of HAD Calorimeter for Electrons

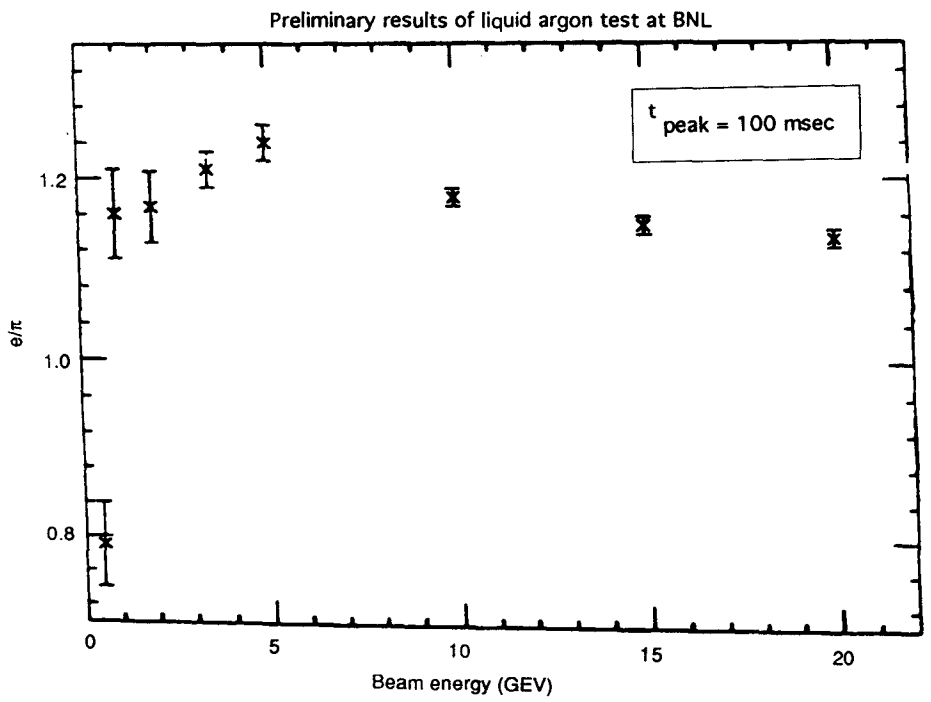

Figure C-22: Measured e/π vs Beam Energy

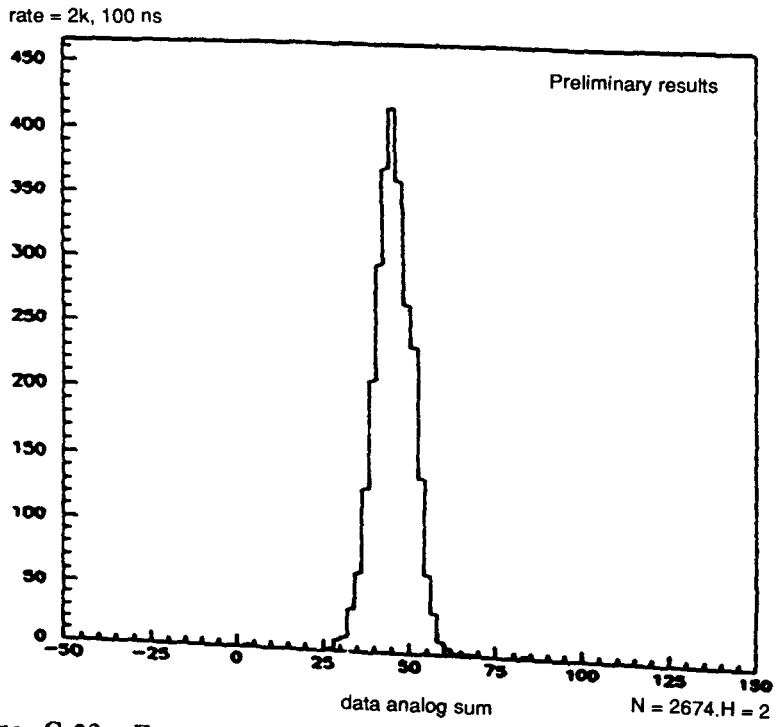

Figure C-23: Energy Distribution for 10 GeV Pions at Low Rate

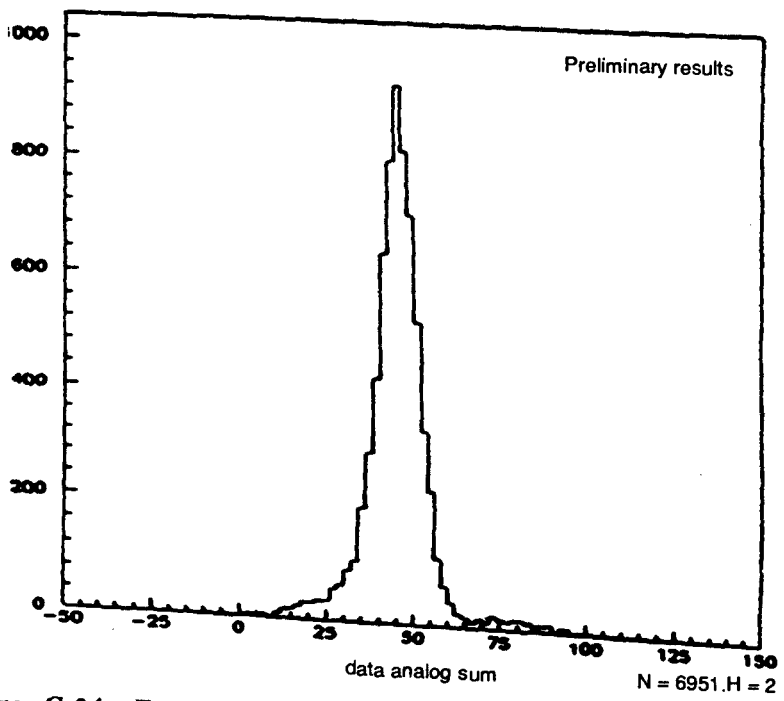

Figure C-24: Energy Distribution for 10 GeV Pions at High Rate

This work has been largely completed in FY91, but the final write-up and other details will be completed in FY92 (see below).

APPENDIX C-1

DESIGN STUDIES FOR SDC LIQUID ARGON CALORIMETRY

This section summarizes the expected performance for the SDC LAC conceptual design. Before detailing the calorimeter's performance in measuring electrons, jets, and $\not{E}_T$ in sections 1-3, a few general comments are in order.

The main strength of the liquid argon design is the inherent stability associated with the fundamental ionization process, and the consequent simple calibration. The ease of calibration results in a high quality calorimeter capable of measuring electromagnetic showers with a small constant term in the resolution. In fact, almost all aspects of the calorimeter response are calculated from simple geometrical considerations and knowledge of the parameters of the electronics readout. This means that the amount of charge deposited by showers in the liquid gaps and subsequently collected by the electronics can be calculated reliably and compares well with measured values. The capability to reliably predict performance without beam tests as design changes are made in moving from conceptual design to final design is an important feature that can lower the risks in making design changes. Given our present state of knowledge of the design requirements and budget uncertainties, this seems a particularly important capability.

1. Electrons and Photons

Angular Coverage

The LAC design has been chosen to give good electron acceptance for all $\eta<3$. The mechanical design features modules tilted at a 3° angle and secured by tie rods, with a 3mm crack between modules (Figure C1-1). The size of the gap is set by assembly tolerances due to cryostat deformation during loading; since the individual modules are small, this tight tolerance can be maintained. Acceptance losses will be associated with the crack and tie rods; a Geant calculation indicates that the observed energy will have a dip of <3.2% within 5mm of the crack at 10 GeV. Figure C1-2 shows the expected resolution for 20 GeV electrons and Figure C1-3 is the calculated electron energy distribution for electrons incident on the azimuthal crack. The small non-gaussian tail of <1% of the events (calculated for a uniform azimuthal distribution of incident electrons) is a negligible acceptance loss.

Figure C1-4 shows the calculated energy distribution for electrons incident directly on the tie rod. Again, the non-gaussian tail of <1% of the events (in the tie rod fraction of <2% of the total surface area) is a negligible acceptance loss. Finally, Figure C1-5 shows the model used for the materials in the solenoid and cryostat walls. This results in a distribution of dead material in front of the calorimeter shown in Figure C1-6. The "massless gap" in the front of the module is used to correct for the energy lost in the material in front of the calorimeter. Figure C1-7 shows the resolution vs. η with the massless gap correction. The calorimeter has a 97% acceptance for $\eta<3$ for resolutions of 25% $\sqrt{E_T}$ or better. Note that the calorimeter is still sensitive in the region around $\eta=1.3$ --- more than 50% of the energy in an incident electron is detected. Electrons incident in this region will not be lost. This level of performance exceeds SDC requirements.

Energy Resolution and Linearity

The results from the beam test and the Mark II calorimeter can be scaled to estimate the energy resolution in the proposed LAC EM calorimeter. The EM energy resolution scales with the

square root of the the absorber thickness. Scaling to Mark II [2] results of 9.5% $\sqrt{E}$ for 2.2 mm plates yields 13% $\sqrt{E}$ for our 4 mm plates. The constant term is estimated to be of order 0.5% before *insitu* calibration.

The predicted energy linearity at η=0 for the proposed design before the massless gap correction can be seen in Figure C1-8[3] . The nonlinearity is less than 4% for energies above 10 GeV and is corrected by use of the massless gap with a weight between 5 at low incident energy and 2.5 at high energy. Note that the compartment weights are constant for energies above 100 GeV.

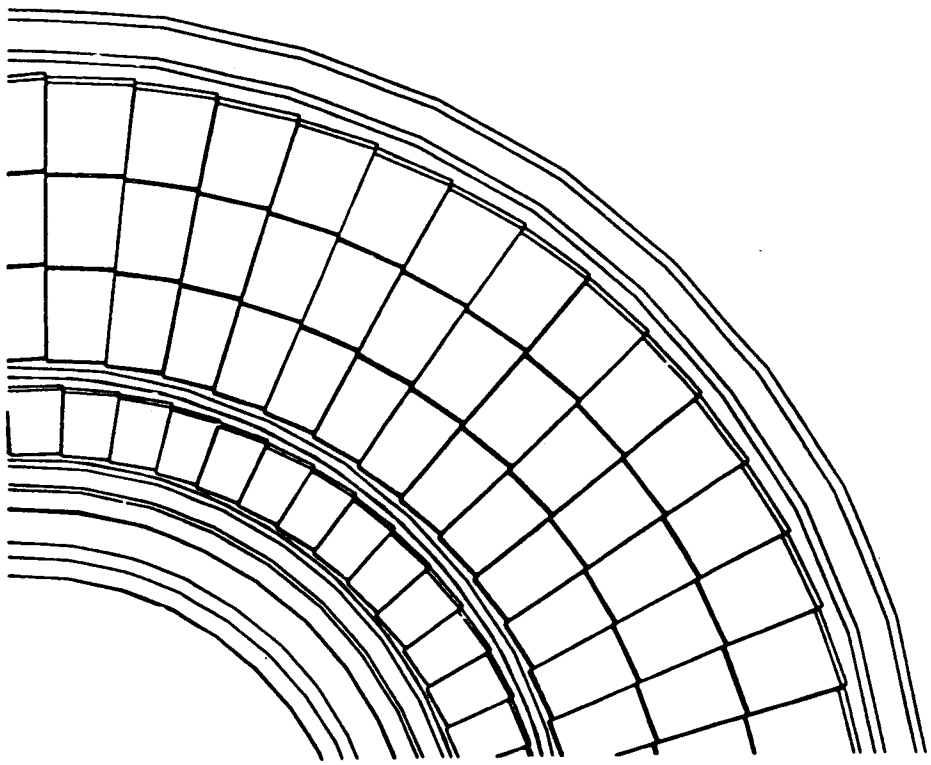

Figure C1-1: Quarter End View of the LAC Design. Note 3° Tile of Azimuthal Module Cracks.

---

2 M. Turcotte, "Estimation of the SDC LAC Energy Resolution", SDC Calorimeter Review, ed. Nodulman, Maki and Siegrist November 1990.

3 C. Hearty, "Resolution and Hermeticity of the Liquid Argon Electromagnetic Calorimeter as a function of Pseudorapidity", SDC-90-00145-Rev November 1990.

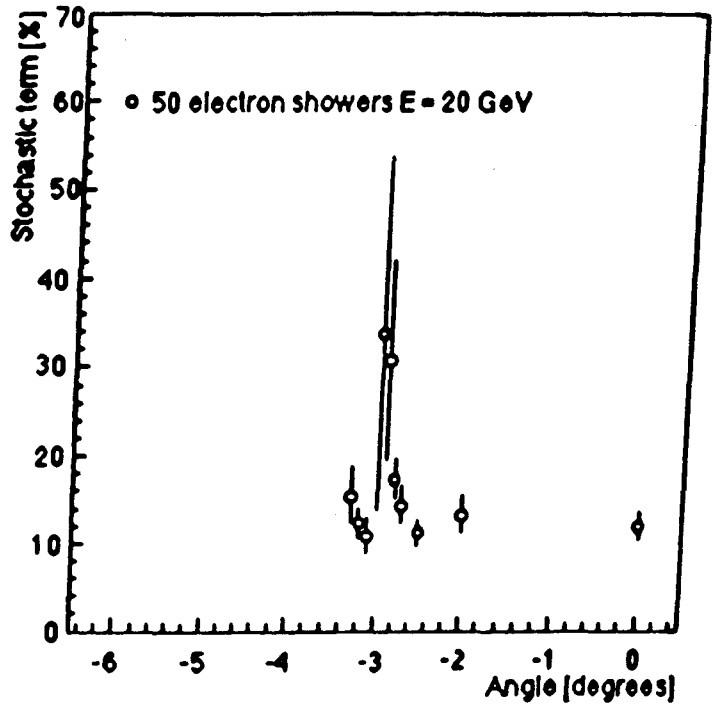

Figure C1-2: Calculated Resolution for Electrons vs Position Across the Azimuthal Crack

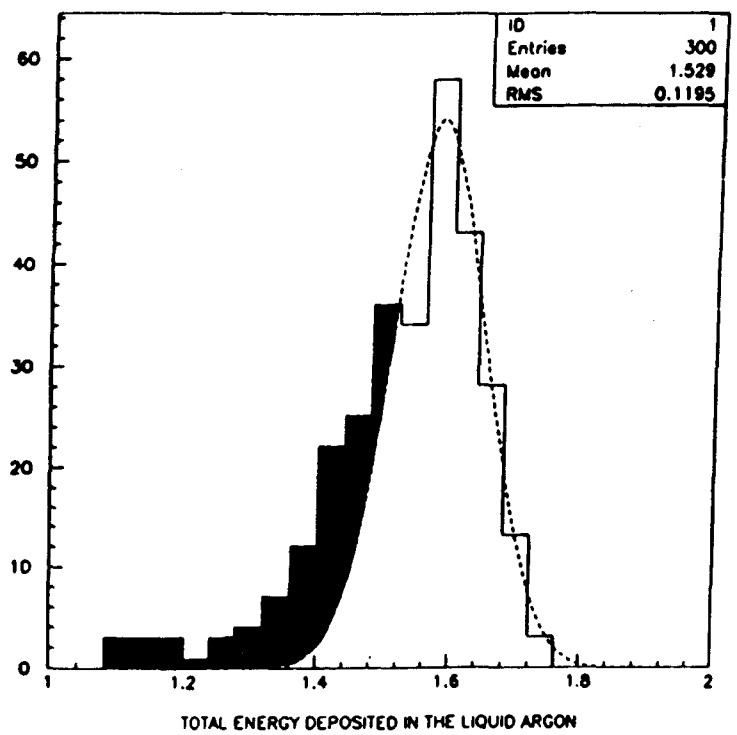

Figure C1-3: Calculated Energy Distribution for Electrons Incident on the Azimuthal Crack

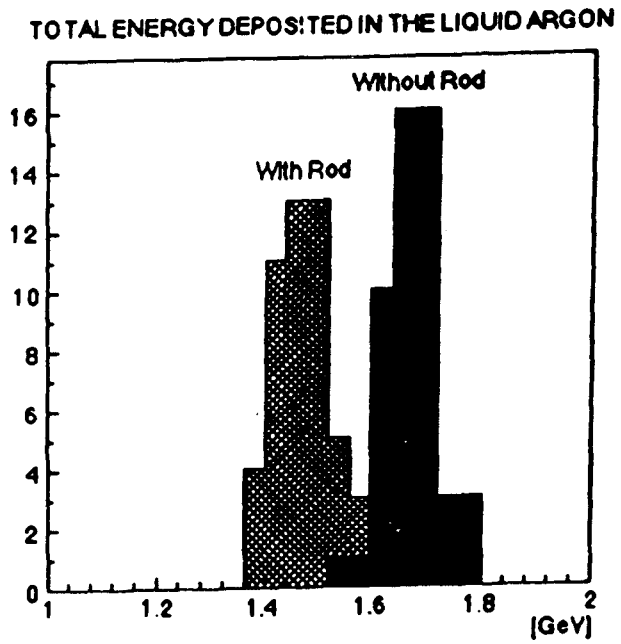

Figure C1-4: Electron Energy Distribution for Direct Impact on Support Tie Rod

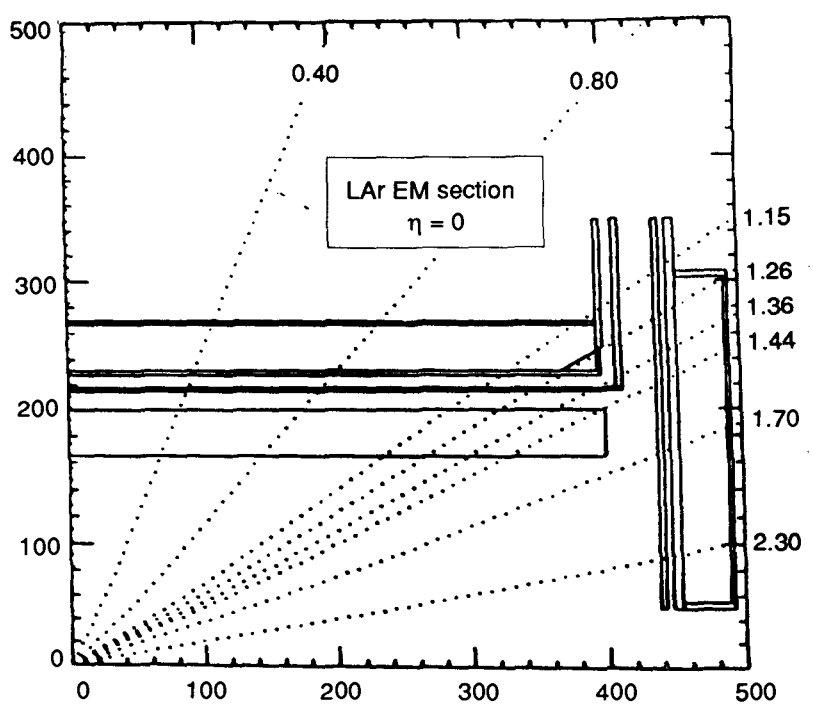

Figure C1-5: Schematic Model for Material in Front of the Calorimeter

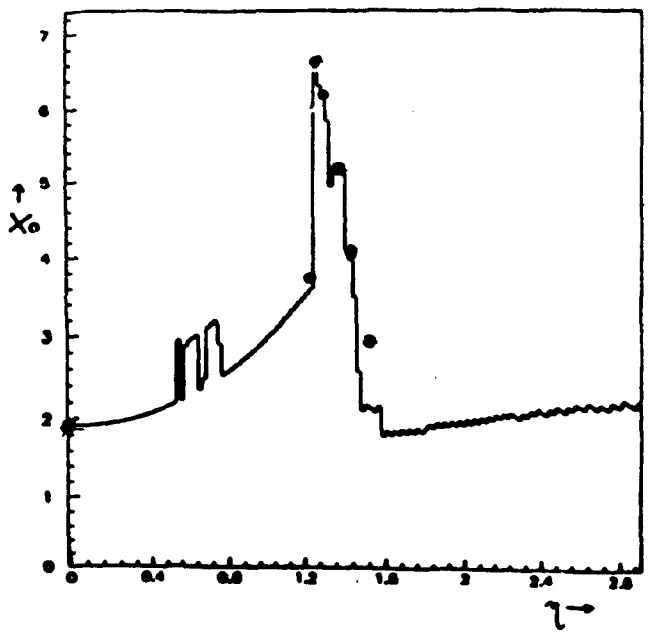

Figure C1-6: Radiation lengths of dead material in Front of the Calorimeter vs.

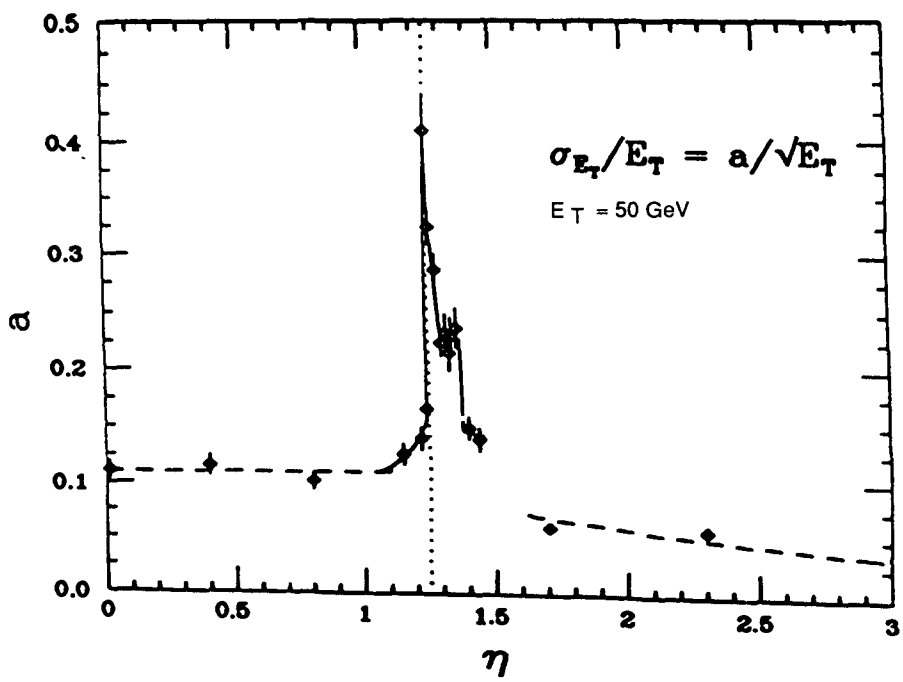

Figure C1-7: Calculated Energy Resolution for 50 GeV E_t *Electrons vs* η

Figure C1-9 shows the resolutions expected after the massless gap correction. Full resolution is recovered for energies above 5 GeV.

Position Resolution

The r-phi position resolution at 20 GeV is calculated to be 2.5 mm, based on 2 cm wide strips at η=0. Note that the chosen segmentation for the calorimeter is not necessarily optimal. As the requirements are better understood, the configuration of towers and strips can be optimized to provide maximum background rejection capability within a constant channel count budget. The lateral (0.05 x 0.05) segmentation chosen and two compartments in depth in addition to the massless gap and strip layer represent a reasonable compromise based on best information we have now.

Noise, Pileup, and Isolation

The critical problem for the design of the EM compartment of the Liquid Argon calorimeter is the measurement of the isolation for electrons. The electronic noise in a single 0.05 x 0.05 EM tower is calculated for 60 nsec peaking time to be 80 MeV; 27 MeV in EM1 and 75 MeV in EM2. With a reasonable single-compartment threshold of around 200 MeV, the contribution of the electronic noise to the isolation sum will be quite small. A direct analog sum with no discrimination in a cone of radius 0.15 would yield only 420 MeV of electronic noise.

The HAD1 compartment has 274 MeV electronic noise for 100 nsec peaking time. The analog noise without any discriminator in full depth in a cone of radius 0.15 is 2.9 GeV. Since most of the shower is contained in the first 5 λ, it may be sufficient to sum over only EM + HAD1. The 0.15 cone noise is then 1.5 GeV. With the use of the appropriate discrimination, the contribution to the energy in the isolation cone can be made quite small, while retaining sensitivity to minimum ionizing energy depositions.

The effect of multi-event pileup on the electron isolation has been studied in a series of notes by C. Blocker [4], E. Wang [5], Y. Sakai [6], and in the BNL beam test. The main results are summarized here.

---

4 C. Blocker, notes in preparation.

5 E. Wang, "Shaping Studies", July 1991.

6 Y. Sakai, "Pileup Issue of Liquid Argon Calorimeter", Proceedings of SDC Collaboration Meeting at KEK May 1991.

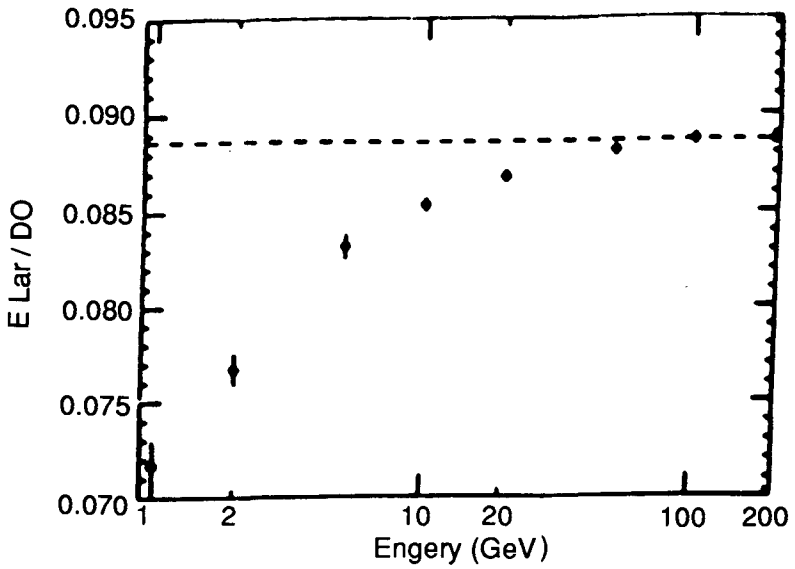

Figure C1-8: Fraction of Total Energy Deposited in the Liquid Argon vs Incident Energy, with No Massless Gap Correction. Total Energy is Incident Energy Less Leakage (~0.5%).

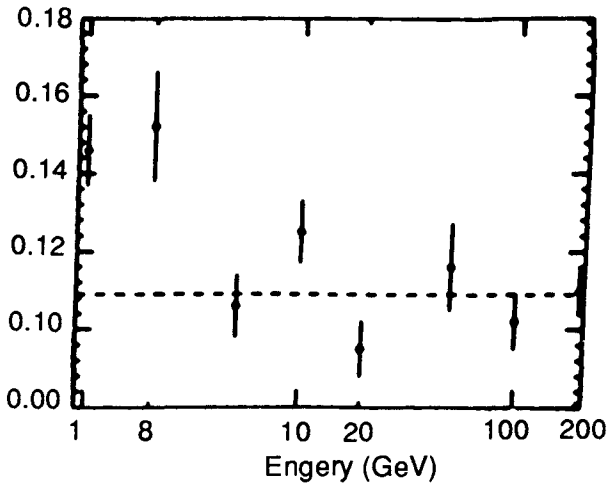

Figure C1-9: Electromagnetic Resolution vs Incident Electron Energy, with Massless Gap Correction.

The notes from C. Blocker calculated by hand the expected average energy seen in a tower due to pileup. The result is:

$$\bar{E}_{tower} = \frac{\bar{E}\,\bar{n}_p\,\Delta\eta\Delta f\bar{n}_{ev}}{2p\Delta t}\int_0^{\infty} h(t)\,dt$$

Where $\bar{n}ev$ is the average number of events per beam crossing, $\bar{n}p$ is the average number of particles per unit η, E is the average energy per particle, Δt is the time between crossings, and $\Delta\eta$ X $\Delta\phi$ is the tower size. The function h(t) describes the effect of the integrator and shaper.

If $\int_0^\infty h(t)\,dt = 0$, then there is no average energy in the tower due to pileup. Investigation of the probability distribution for particles hitting towers shows that the most likely outcome is that no particle hits a tower; the rms of the distribution is dominated by those cases when one particle hits a tower.

The rate into individual towers is only about 600 kHz at 10^{33} luminosity, which is small compared to the 100 MHz interaction rate. Wang has calculated the E_t distributions from minimum bias and two jet events (ISAJET) into 0.2 X 0.2 isolation cones (Figure C1-10). Note that the effect of the pileup is to generate a non-gaussian tail; the main part of the resolution (FWHM) is not affected. The small non-gaussian tail may cause some loss of events due to the isolation cuts. Figure C1-11 shows the fraction of events above various thresholds for various peaking times. For a 100 nsec peaking time and a relatively low 1.5 GeV threshold on a 0.2 by 0.2 cell, only about 3 percent of events are lost. The rms of the distribution is about 700 MeV, in agreement with previous calculations [6].

The time resolution for EM energy depositions, determined by the zero-cross of the bipolar output, is <5 nsec for energies of 1 GeV or above in a channel. This far exceeds SDC requirements. This predicted value is consistent with the resolution of 1.5 ns measured for 5 GeV deposited in EM2 by the EM test beam module.

2. Hadrons and Jet Response

Angular Coverage

The LAC design parameters have been chosen to give single particle hadron and jet measurements with minimal impact from support and structural members. For a design with base resolution

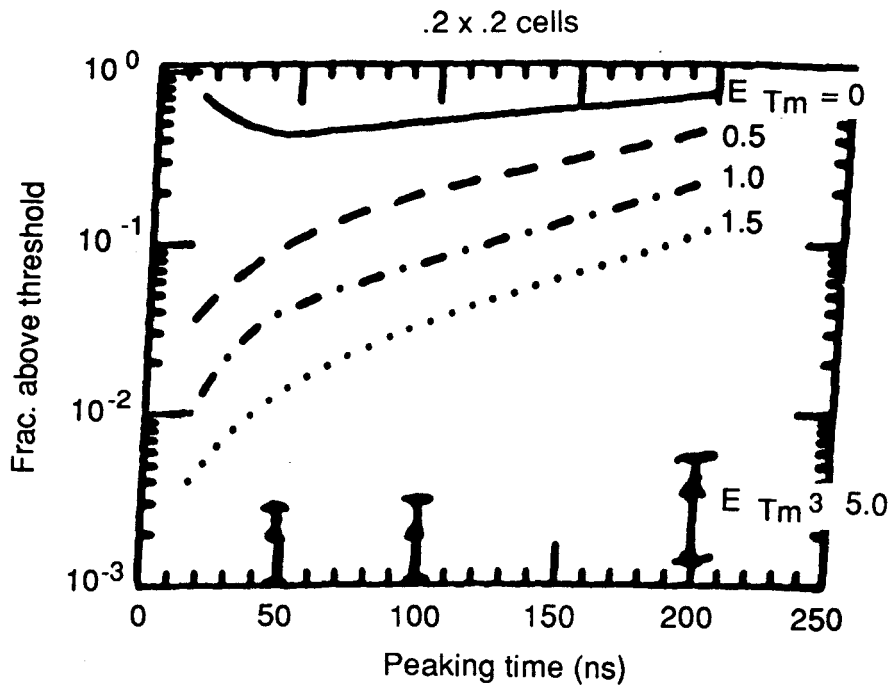

Figure C1-10: **Energy Distribution in a .2 × .2 Cone from Pileup for Various Bipolar Shaping Times.**

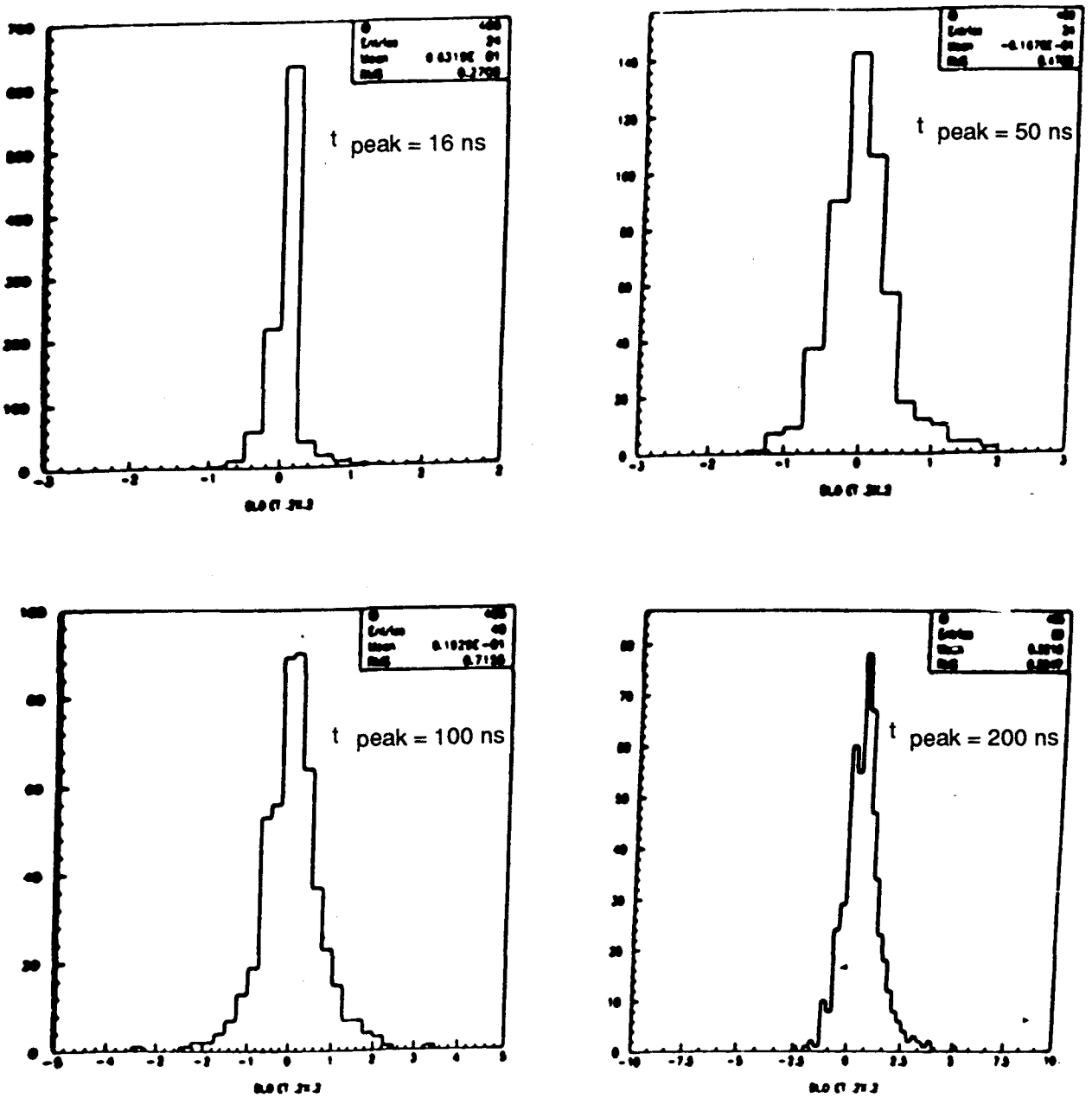

Figure C1-11: Fraction of Events Above Various Thresholds vs Peaking Time.

50% $\sqrt{E}$ + 5.2%, Figure C1-12 shows the resolution calculated via the Wormersley parameterization for this cryostat design. The region near η=1.3 has poor resolution due to the cryostat structural elements and walls. Since this region is only 0.08 wide in η it is much smaller than the intrinsic jet size — corrections can be made for jet response. The region of reduced resolution is only 3% of the solid angle and should have negligible impact on jet measurements. The situation with the η=3 boundary and the impact on $\not{E}_T$ measurements is summarized below.

Resolution and e/π

The expected resolution is obtained by scaling from the preliminary BNL beam test results. In the beam test, 12 mm lead plates were used with 2mm gaps; 14 mm plates are used in the SDC design. A resolution of 70% $\sqrt{E}$ is predicted for the stochastic term.

The intrinsic component of the hadronic resolution includes an energy independent contribution arising from the e/h ratio. Using D. Groom's anstaz [7],

$$\left(\frac{e}{\pi}\right)^{-1} = 1 - (1 - h/e)\, E^{-0.15}$$

e/h is determined to be 1.25 from the preliminary e/π value of 1.15 measured at 20 GeV. This value is translated into a constant term of $b = 0.14 \cdot |1-e/h| = 3.5\%$. A nonlinear term of <2% in pion response from 100 to 200 GeV should result, which can be reduced by energy-dependent weights in the depth compartments. A pion beam calibration will remove any remaining nonlinearity.

Time Resolution

The time resolution for the hadronic compartment is expected to be <5 nsec for energies of 10 GeV or greater in a channel. This meets SDC requirements.

3. Neutrinos and E_T

A critical design issue for the SDC LAC involves the cryostat wall thickness near the $\eta = 3$ boundary. In order for the calorimeter to have good E_T resolution, the design must feature few dead areas. The November 1990 design had put little or no work into the $\eta=3$ region, since the main concerns at the time were on the electron coverage. Since then, two approaches have been taken. The first has been to work within the general outlines of the November 1990 design to thin the walls in the $\eta=3$ region as much as possible, consistent with sound design practice. The

---

7 D. Groom, Proceedings of the Workshop on Calorimetry for the SSC, Tuscaloosa, AL 1989.

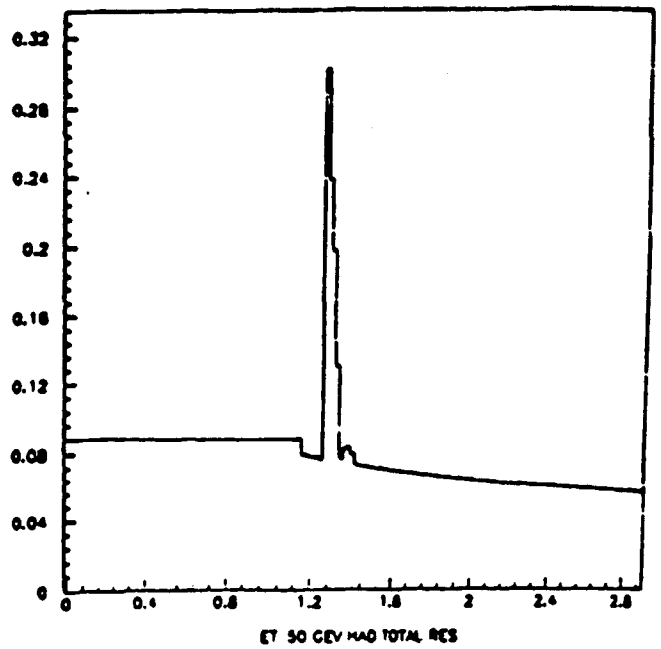

Figure C1-12: Energy Resolution for 50 GeV E_t Incident Piln vs η.

result of this effort is shown in Figure C1-13a. The walls in the η=3 region are roughly half as thick as they were at the time of the November review.

A second approach was to try completely new design ideas for the η=3 region. The best of these efforts is shown in Figure C1-13b. This design features two conical heads and a vessel stay through the EM compartment to dramatically reduce the η=3 wall thickness --- essentially to zero. Figure C1-14a shows the live and dead material vs η for this design and Figure C1-14b shows the dead material preceding the calorimeter. Complete finite element calculations have not been carried out for the new design of Figure C-37b, but hand calculations and preliminary FEA work show that wall thicknesses close to the ones shown should be achieved. Designs of this type completely alleviate the η=3 problem.

Studies are underway on the possibility of using jet clusters rather than individual towers to calculate $\not{E}_T$. There are two advantages to this scheme. Dead regions due to cryostat walls or structural members subtend angles substantially smaller than jet cones. Therefore, corrections can be applied to the energy observed in cones containing a dead region. Without the presence of a jet, such corrections are difficult to apply. The second advantage is to lessen the effect of electronic noise and pileup: the p_t of pileup particles is typically less than 1 GeV.

Wang has calculated the $\not{E}_T$ observed in minimum bias events with a 5 GeV E_t cluster threshold, where the cluster is formed from towers with energy greater than 0, 1 or 5 GeV. The calorimeter is taken to be perfect. Figure C1-15 shows the results, together with the true $\not{E}_T$ distribution. The preliminary indication is that the distribution for the cluster threshold does not appear to be significantly different.

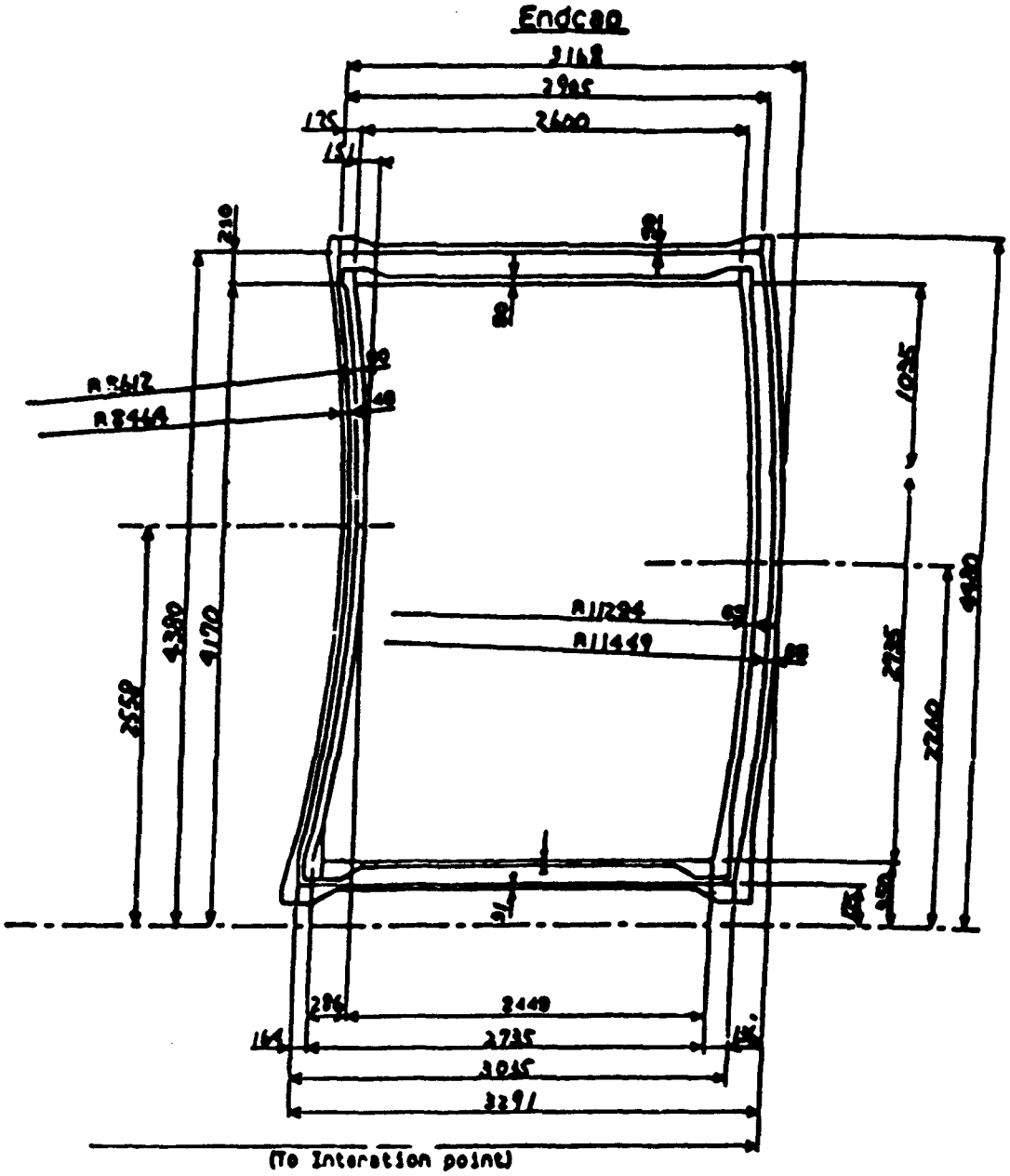

Figure C1-13a: KHI Cryostat Design in the Endcap Region.

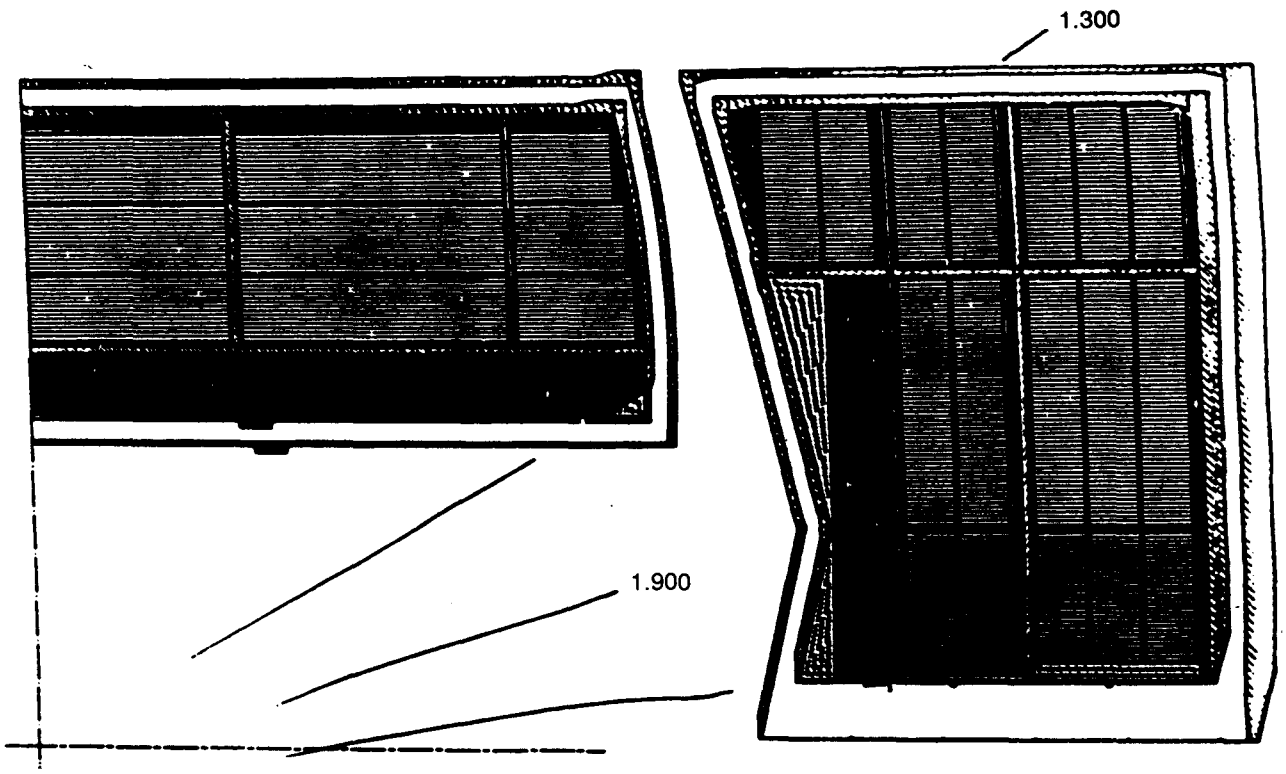

Figure C1-13b: LBL Cryostat Design

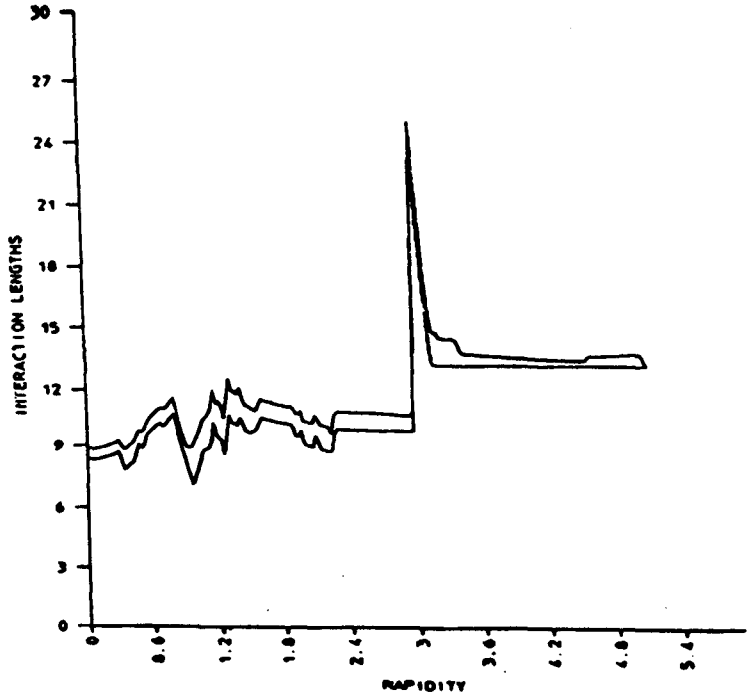

Figure C1-14a: Live and Total Interacting Lengths vs η.

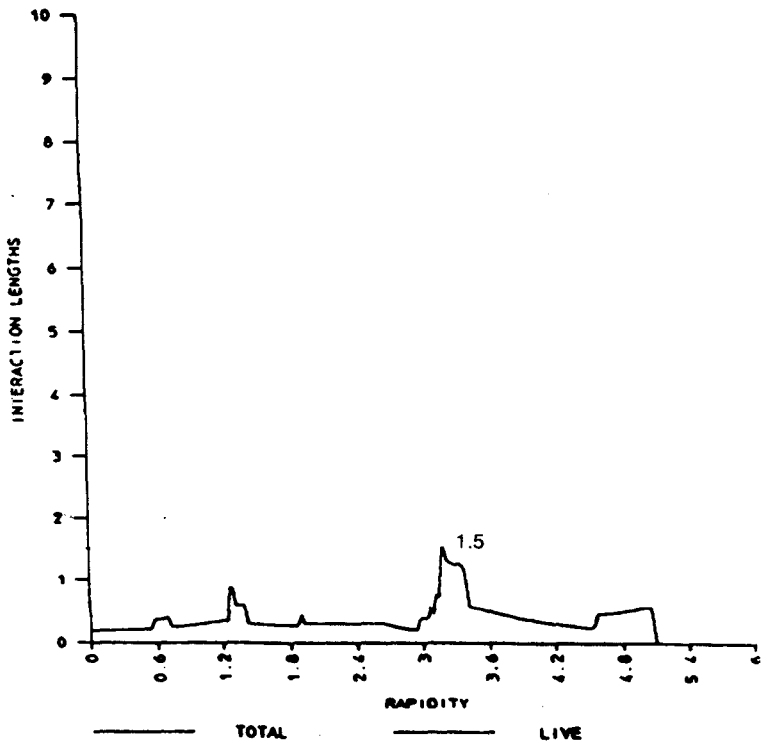

Figure C1-14b: Dead Interaction Lengths in Front of the Calorimeter vs η.

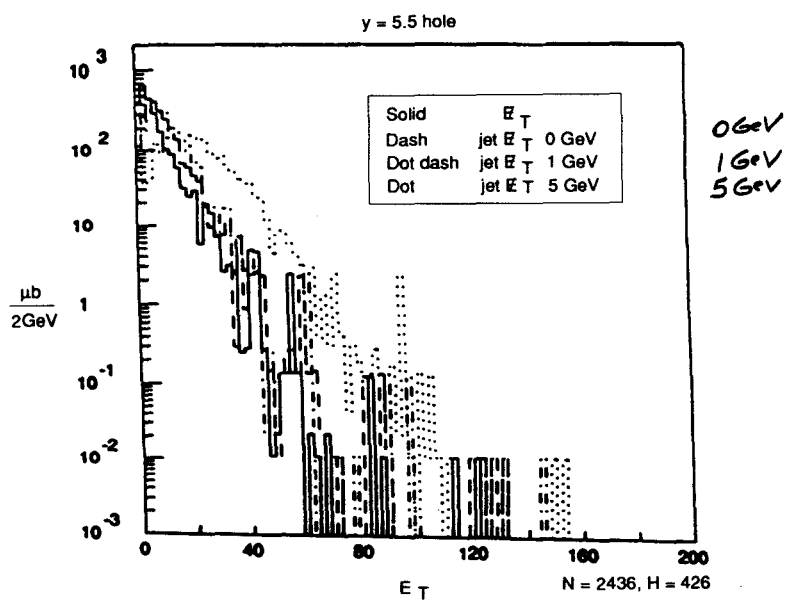

Figure C1-15: **Observed $\not{E}_t$ in Min Bias Events Calculated from Clusters with a 5 GeV Thresholds for Various Single Tower Thresholds.**

APPENDIX D

PROGRESS ON SCINTILLATOR CALORIMETRY

This appendix summarizes work done on (1) properties of scintillators, (2) an accurate optical model of light production and transport in tile/fiber assemblies, (3) source calibrations, (4) effects of calorimeter imperfections on the energy resolutions, and (5) the degradation of energy response and resolution in the barrel-endcap transition of the SDC calorimeter.

Preliminary Optical Measurements

We have procured or assembled the basic equipment necessary to make measurements relevant to advancing our understanding of the optics system and photon detection. In a preliminary assembly, we have built a single tower structure made of 25 layers of 5.2mm thick NE110 tiles and 4.8mm thick brass absorber plates. Each tile is read out by a scintillating fiber loop with two ends exiting. Fibers arethen gathered at the sides of the tower and bundled up to the cookie which mates to a HAMAMATSU R329 photomultiplier. The setup shown in Figure D-1. Figure D-2 shows the distribution of the raw data from cosmic ray muons with the characteristic Landau tail. We have used a digitizing ocilloscope to record the pulse shapes from the stack, under different conditions. Figure D-3 shows examples of these measurements.

As part of the effort to understand the properties of various samples of plastic scintillator, we have measured the transmittance of NE110 and that of many types of scintillating plastics provided to us by collegues in Kharkov, Ukraine. Figure D-4 shows examples of some of these scans. We have also made fluorescense measurements of these scintillator samples. Figure D-5 shows the experimental setup and some of the spectra obtained in different conditions, for fixed or varied excitation or emittance wavelengths. When excited by light in the UV range λ_{ex} = 240nm), one sample (Russian # 398) had a dominating emission peak at λ = 435nm (Figure D-5b). Its excitation spectrum at this emission wavelength is dominated by a peak at λ = 413 nm (Figure D-5c). We have looked at the match between the emission spectrum of this sample and that of the green wavelength shifting fiber. (Figure D-5d) shows the emission spectrum of the green fiber for an excitation wavelength of 435nm. It peaks at 496nm. However, at this emission wavelength of 496nm, the excitation spectrum actually peaks at 487nm (Figure D-5e). The slight mismatch results in some loss of efficiency which leads us to conclude that significant improvements might be obtained by better engineering the chemistry of the wavelength shifting compounds. We are continuing the systematic studies of several compounds and have initiated a collaborative R&D effort with other institutes (see section on Calorimeter Calibration and Joint Scintillator R& D Program).

In addition to studies of transmittance and fluorescence of various scintillator samples, we have made preliminary measurements of the transmittance of a digitally controlled variable density diffusive screen. Such a device could be used to equalize the light delivery of groups of tiles, if it were installed in the optical path of fibers at the "cookie" (which gathers the fiber bundle at the phototube). Figure D-6 shows the conceptual arrangement and (Figure D-7a) shows one of the transmittance measurements on a sample of the screen at 60% of the maximum capacity control bias voltage. (Figure D-7b) shows the transmittance of the screen at a fixed wavelength λ = 500 nm as a function of the % of the full capacity bias voltage.

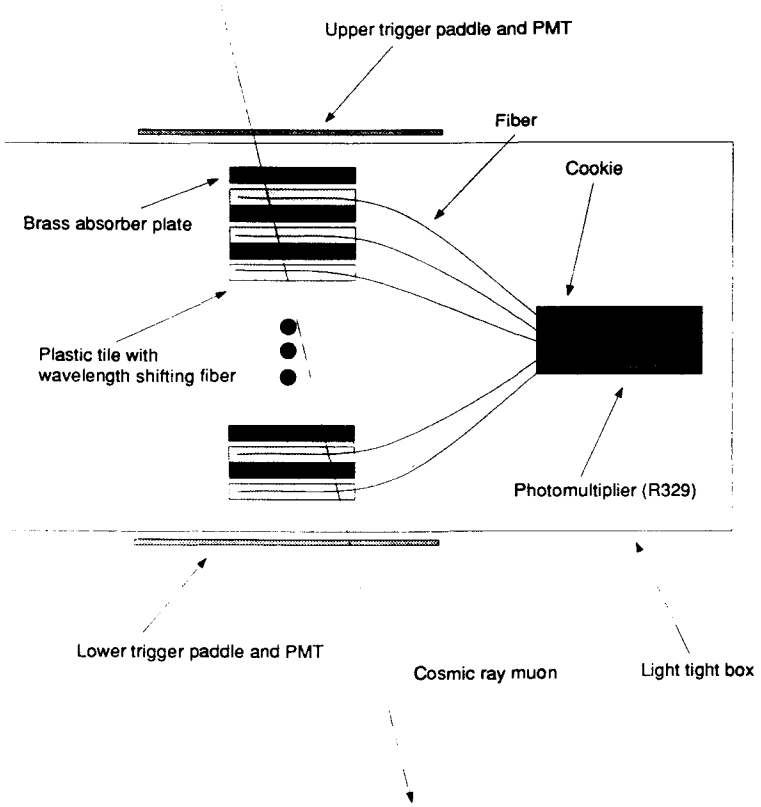

Figure D-1: Schematic diagram of the one-tower arrangement and trigger system. The data is read out using CAMAC through a GPIB interface to lab view on the MacIntosh computer

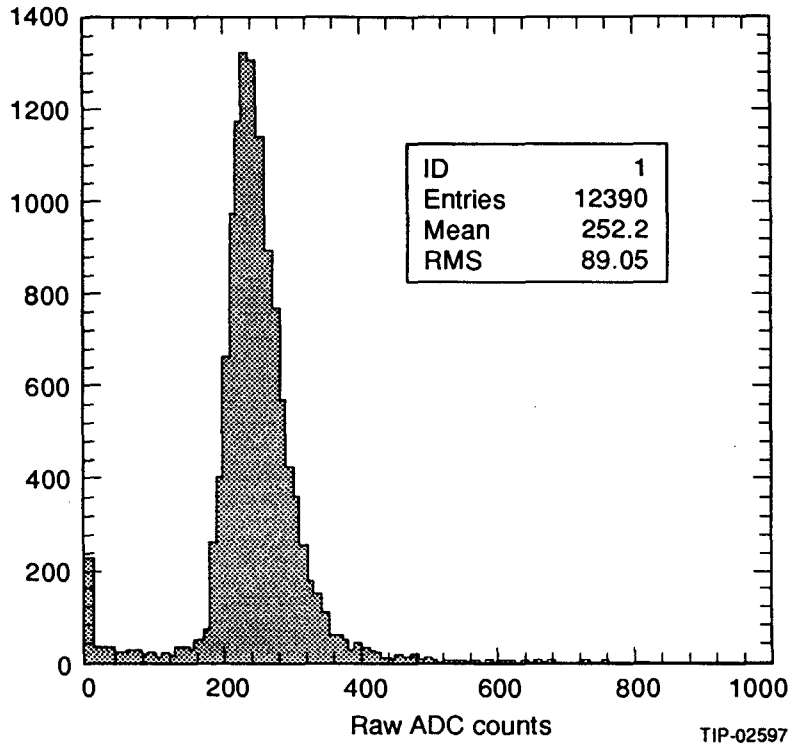

D-2: Distribution of the raw data from cosmic ray muons traversing the one-tower arrangement.

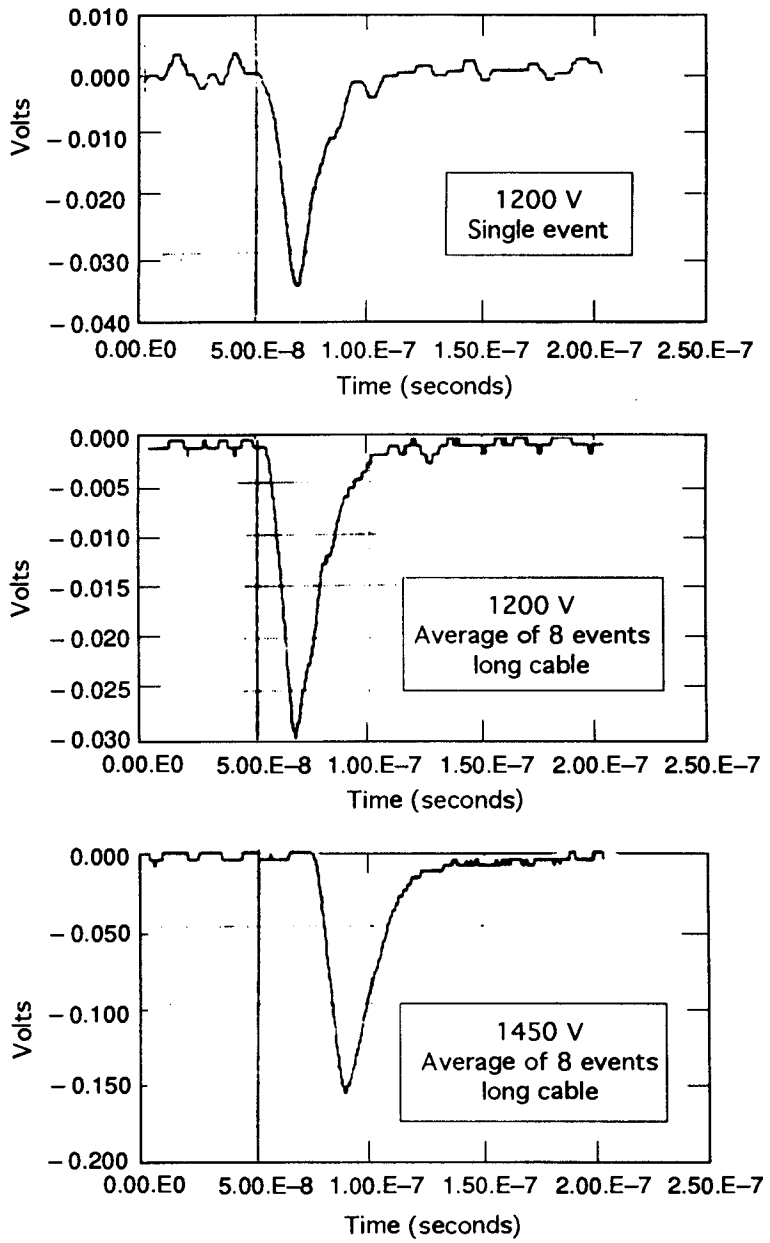

D-3: Examples of digitized pulse shapes from cosmic ray muons traversing the one-tower stack under different conditions.

NE 110 after cleaning surface with isopropyl
Transmittance at 600 nm is 90.77

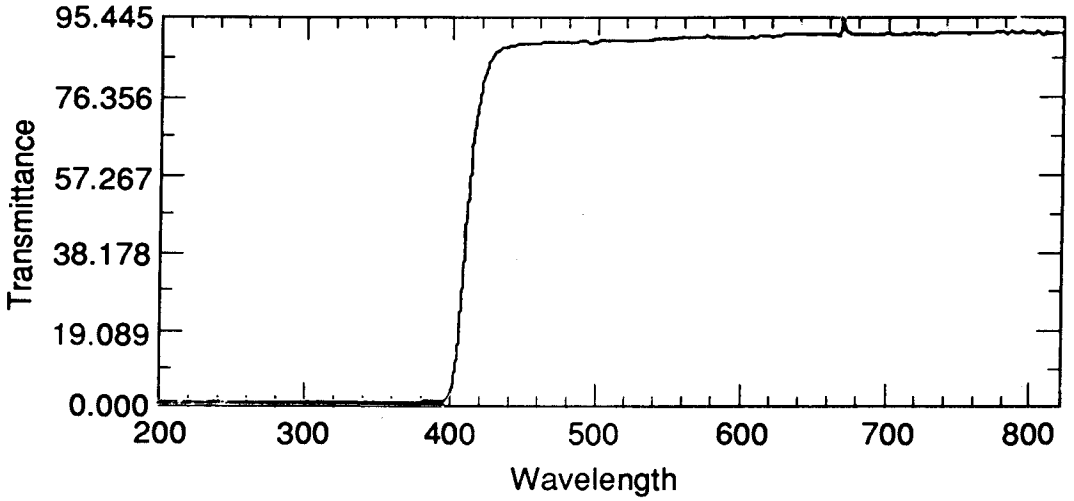

Sample 390
Transmittance at 600 nm is 100.5

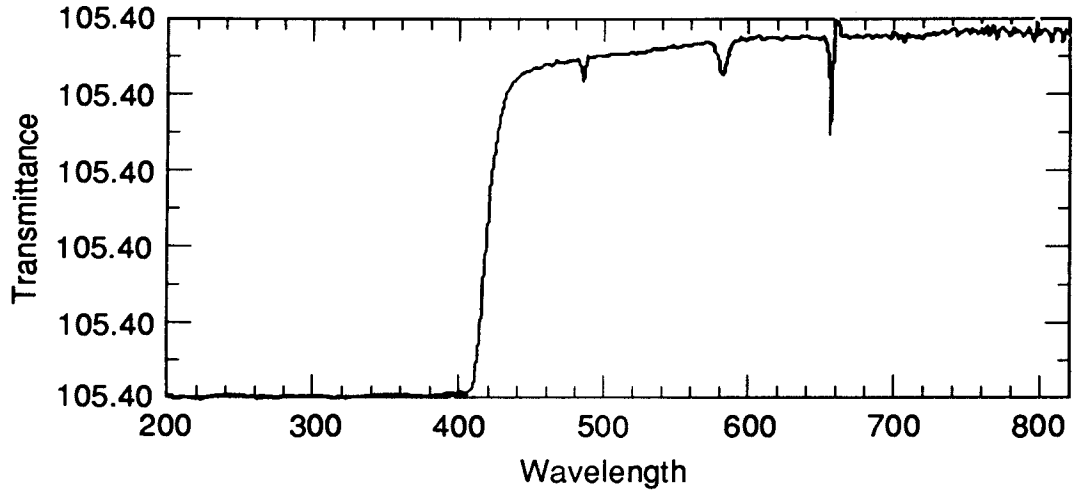

D-4a and b: Examples of Transmittance measurements of samples of NE110 and Sample 390.

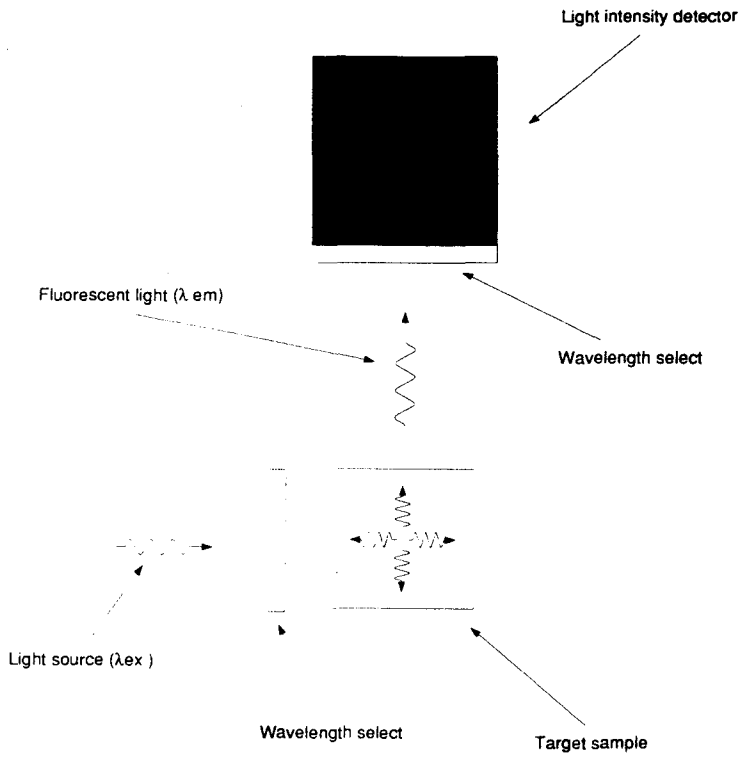

D-5a: Schematic diagram of the fluorescence measurement setup.

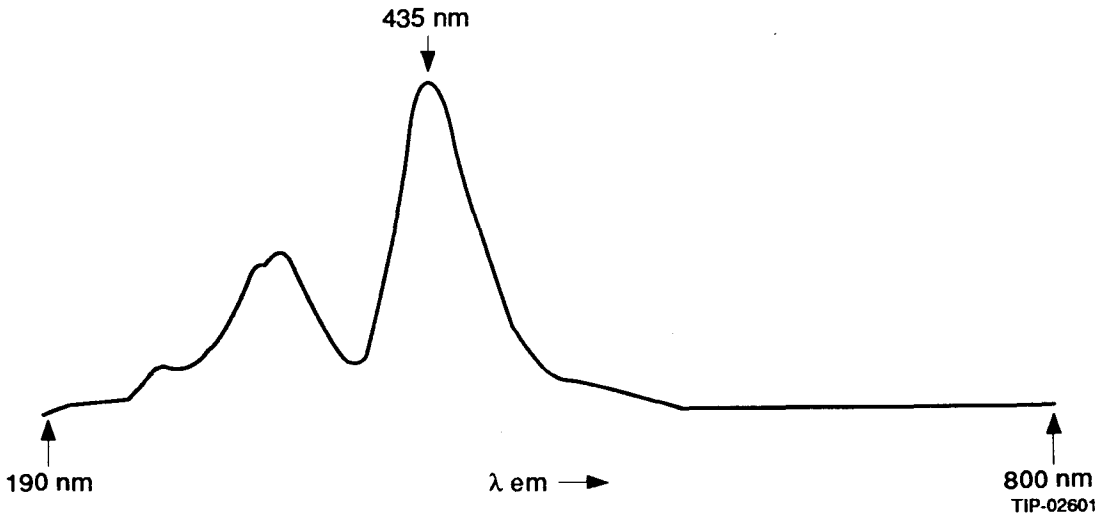

D-5b: Fluorescence spectrum for Sample 398. The amplitude of fluorescent light is plotted in arbitrary units versus the emission wavelength ranging from 190nm to 800nm. The excitation wavelength selected was 250nm.

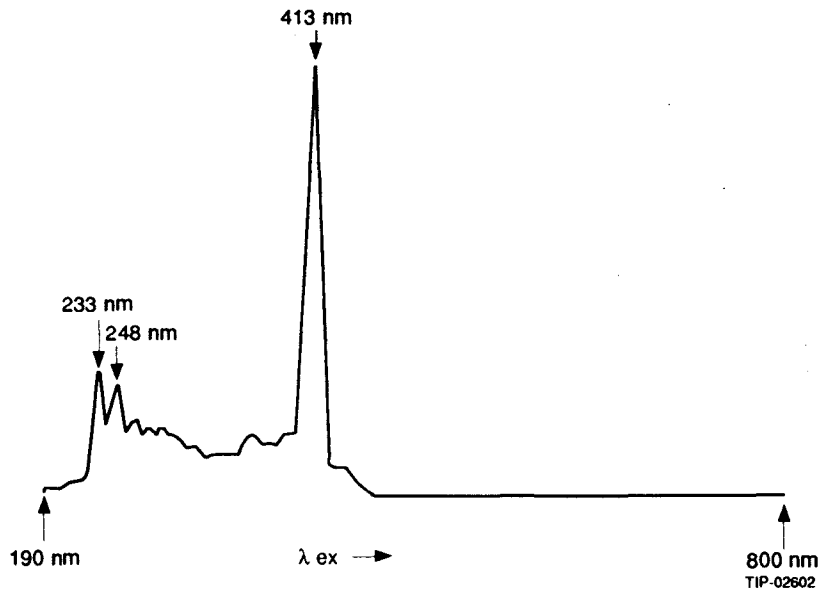

D-5c: Fluorescence spectrum for Sample 398. The amplitude of fluorescent light is plotted in arbitrary units versus the excitation wavelength ranging from 190nm to 800nm. The emission wavelength selected was 435nm.

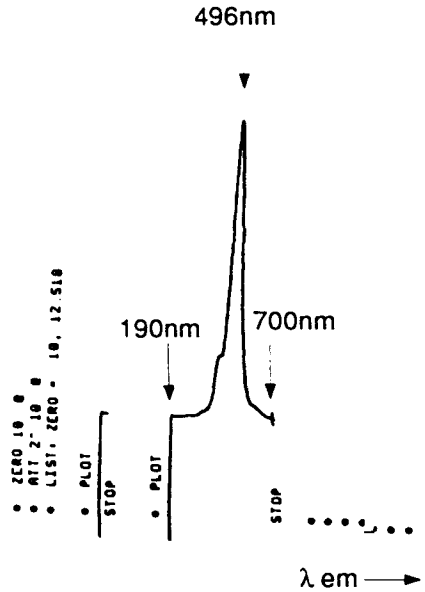

D-5d: Fluorescence spectrum for the green wavelength shifting fiber. The amplitude of fluorescent light is plotted in arbitrary units versus the emission wavelength ranging from 190nm to 700nm. The excitation wavelength was 435nm.

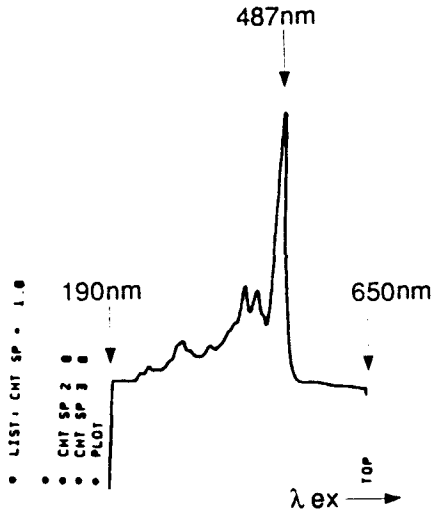

D-5e: Fluorescence spectrum for the green wavelength shifting fiber. The amplitude of fluorescent light is plotted in arbitrary units versus the excitation wavelength ranging from 190nm to 650nm. The emission wavelength was 496nm.

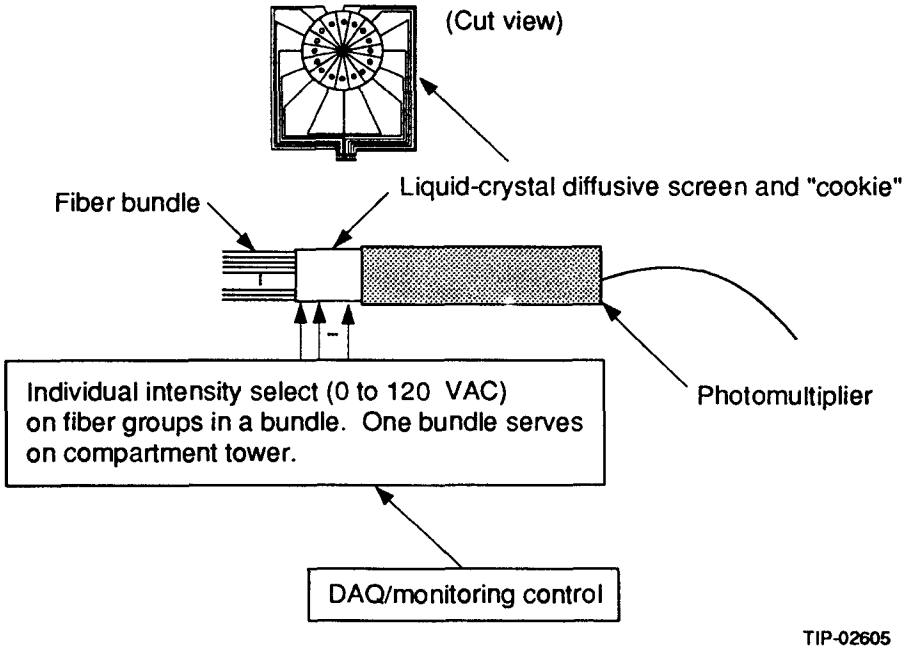

D-6: Schematic diagram of the liquid crystal diffusive screen used in e optical path of the clear fibers from a tower. The light intensity delivery of each group of tiles in the bundle is controllable by changing the opacity of the selected region on the screen.

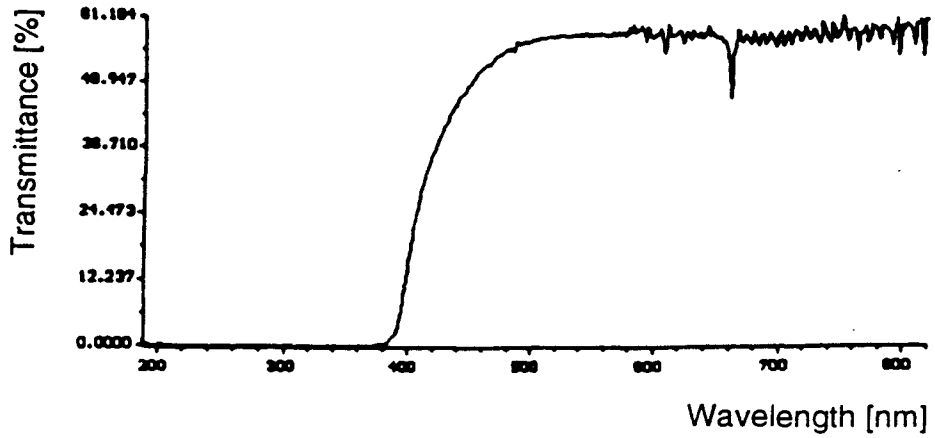

D-7a: Transmittance spectrum of the liquid crystal diffusive screen at 60% of the maximum bias AC voltage.

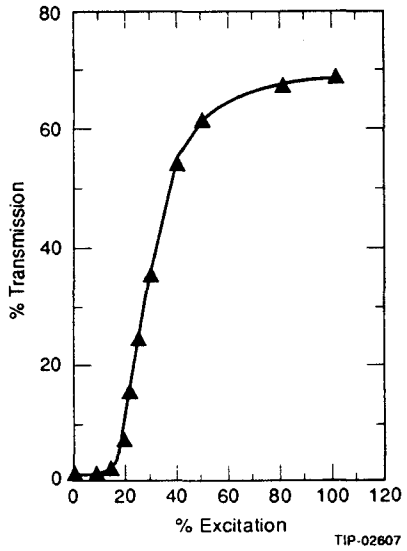

D-7b: Percentage transmittance of the liquid crystal diffusive screen at a single wavelength (500nm) versus percentage bias AC voltage.

Optical Model

Each tower of the calorimeter will be a stack of absorber layers and scintillating tiles arranged in a pointing geometry. Each tile in the assembly is equipped with its own read-out fiber. The read-out fiber path is a loop in the volume of that tile (Figure D-8). The captured end of the loop is polished as a mirror, while the free end protrudes out of the tile, between modules. Blue light generated from scintillation as the result of the passage of a charged particle in the tile plastic is reflected around the volume of the tile by hitting its inner surfaces. This light is sometimes absorbed in the tile plastic or sometimes crosses the loop of wavelength shifting fiber and with some probability, the material of the wavelength shifting fiber then scintillates in the green. The green light is then captured in the body of the fiber loop with some probability and is then transported to the outside of this loop through a splice to clear fiber with some efficiency. Some light will reflect off the polished end of the loop before exiting. Light will then be transported by the clear fiber to an output equalization device before it enters the photomultiplier. This device, in its simplest form, is imagined to be a changeable neutral density filter. However, we are currently studying the possibility of using a digitally controlled liquid crystal light diffusion screen.

The parameters of the optical model are therefore:

1) The number of blue photons generated per unit length along the path of charged particles traversing the plastic tile.

2) The angular distribution of these photons.

3) The light attenuation length of the photons in the tile plastic.

4) The reflection efficiency of blue light at the inner surfaces of a wrapped tile. The reflectivity of the wrapping material and the nature of the interface control both the amount of light reflection and the degree of randomization in the direction of the reflection.

5) The capture efficiency of the wavelength shifting fiber loop. This depends on the loop geometry and on the indices of refraction of the tile plastic and the fiber material. It also depends on where the wavelength shift occurs in the loop and on the attenuation length of the blue light in the green fiber.

6) The light transport efficiency of the wavelength shifting fiber. This includes the attenuation length of green light in the green fiber material.

7) The light transmission efficiency of the splice to clear fiber.

8) The light transport efficiency of the clear fiber. This includes the attenuation length of green light in the clear fiber.

9) The efficiency of transmission of the variable density neutral filter ("smart" cookie).

10) The photomultiplier transfer function including optical effects at the mating interface between the "cookie" and the entry face of the phototube.

The optical model is based on the numerical ability to count how many photons enter the photomultiplier tube as a function of the number of photons produced by the primary ionization. The amount of charge integrated at the output of the phototube is deduced from an understanding of the photomultiplier transfer function. We have decided to make use of the standard SDC simulation environment to carry through particle transport implementing our geometry's with standard GEANT tools augmented with custom code to handle specific processes (light reflection, absorption and transmission). We are aware of the existence of other software that may prove to be helpful tools and we are currently investigating the applicability of such code.

Preliminary Results and Plan for Measurements

Figure D-9a and b shows the result of our first simulation. Plotted is the absolute number of observed photons in a perfectly absorbing wavelength shifting fiber (u -shaped) loop as a function of the distance from the tile center when a minimum ionizing particle traverses its plane in a perpendicular direction. The tile is 10cm × 10cm × 4mm while the wavelength shifting fiber has a diameter of 1mm. The minimum ionizing particle's primary ionization creates 1000 photons per millimeter emitted in random directions along its straight path. The model includes an inner surface mirror reflectivity of 0.9 for the primary ionization light and a light attenuation length of 100cm for this light in the tile plastic. The optical model is currently being refined by adding the capture efficiency of the fiber that was computed from first principles and is plotted on Figure D-9[1] .

---

1 M. Asai and M. Turcotte "Effects of Quasi Projective Inter Module Cracks" May 1991.

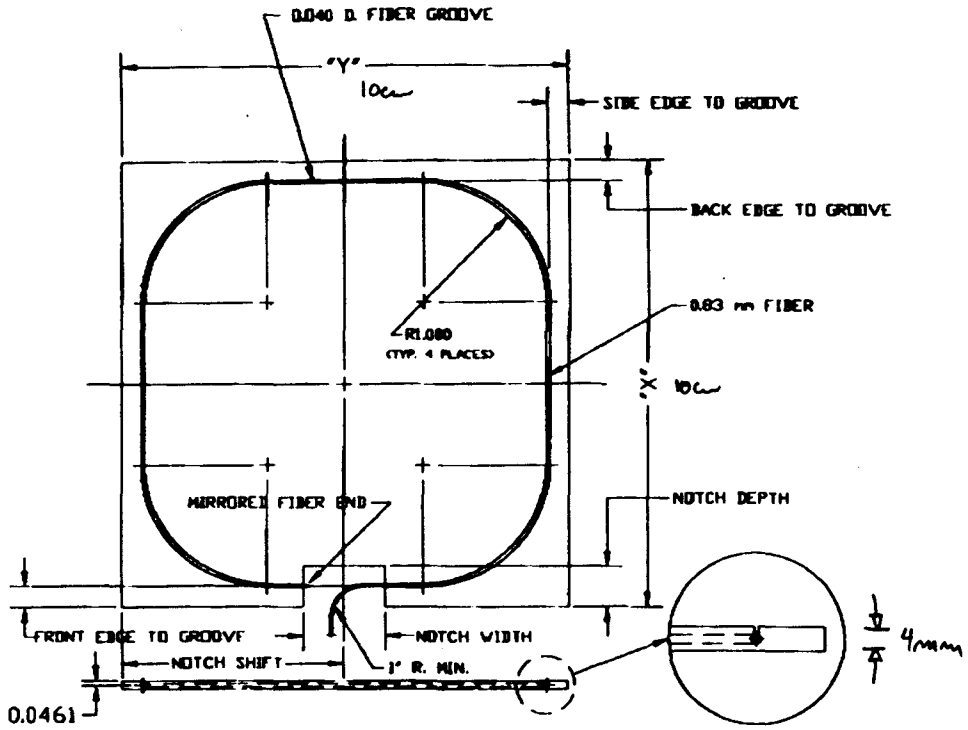

D-8: "Sigma" tile design. A 10cm X 0.4cm tile is grooved and a wavelength-shifting fiber with one end polished as a mirror is inserted. The other end exits the tile and is eventually spliced to a clear fiber.

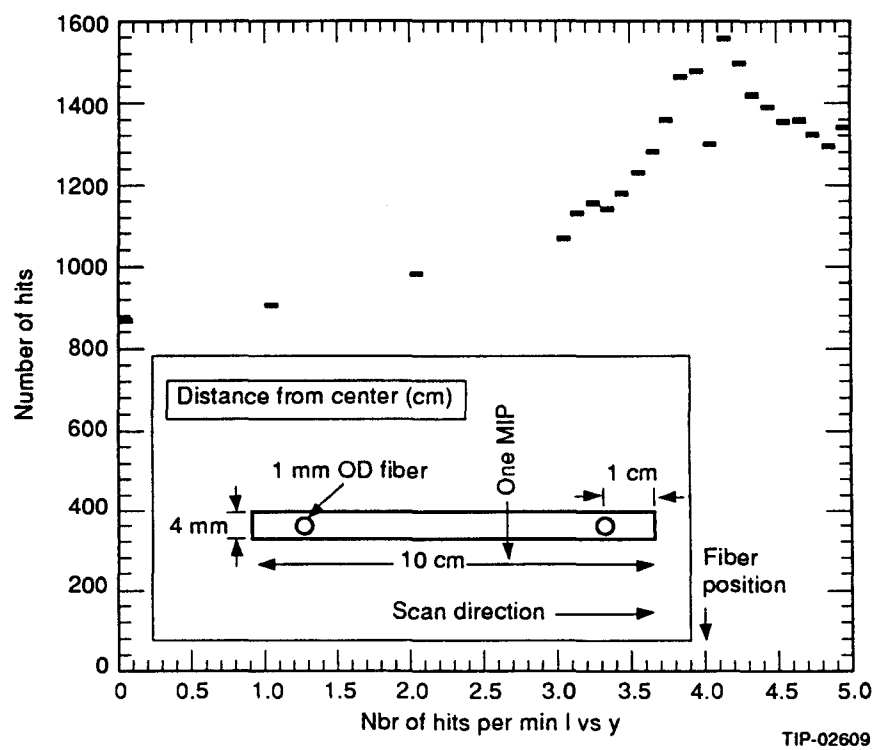

D-9: Number of hits per minimum ionizing particle versus the transverse direction from the tile center across the tile surface. The number of generated gamma's per mm was 1000, the inner reflectivity of the wrapped tile was 0.9 and the attenuation length of blue light in the tile plastic was 100cm. The inset shows the geometry and scan direction.

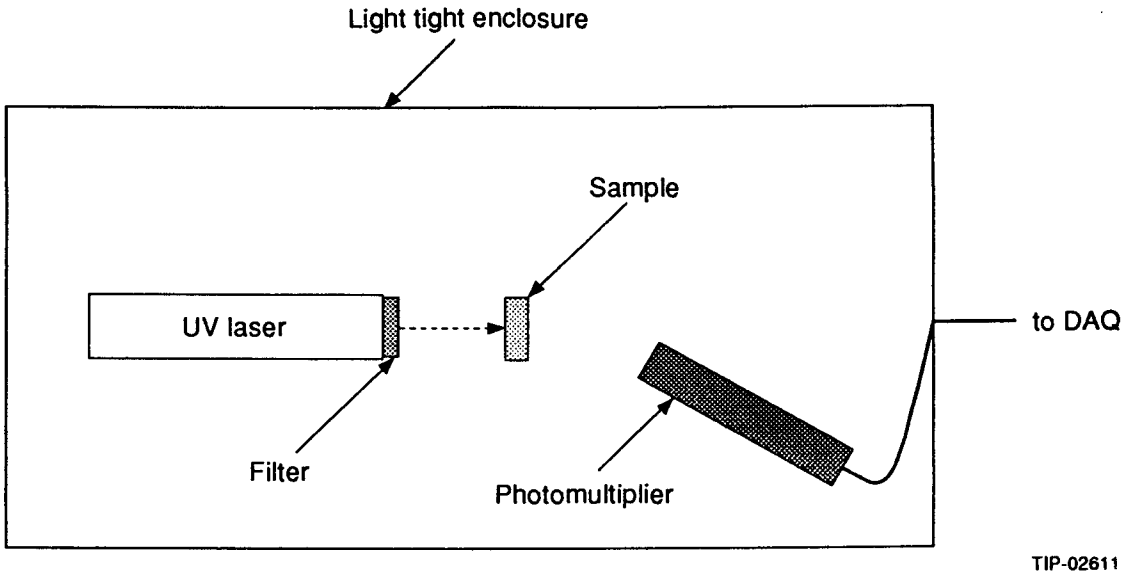

D-10: Schematic diagram of the optical test bench. The laser unit can be located outside the dark enclosure with the light piped in using a fiber.

The various parameters of the model are not all easily amenable to a prediction from first principles and their measurement is currently being performed. Equipment to carry out these measurements has been procured (and is still being procured). Some relevant measurements have been presented in the section on preliminary optical measurements. In addition to the equipment used in making those measurements, we have built a dark optical test bench with photomultiplier and associated DAQ system (Figure D-10).

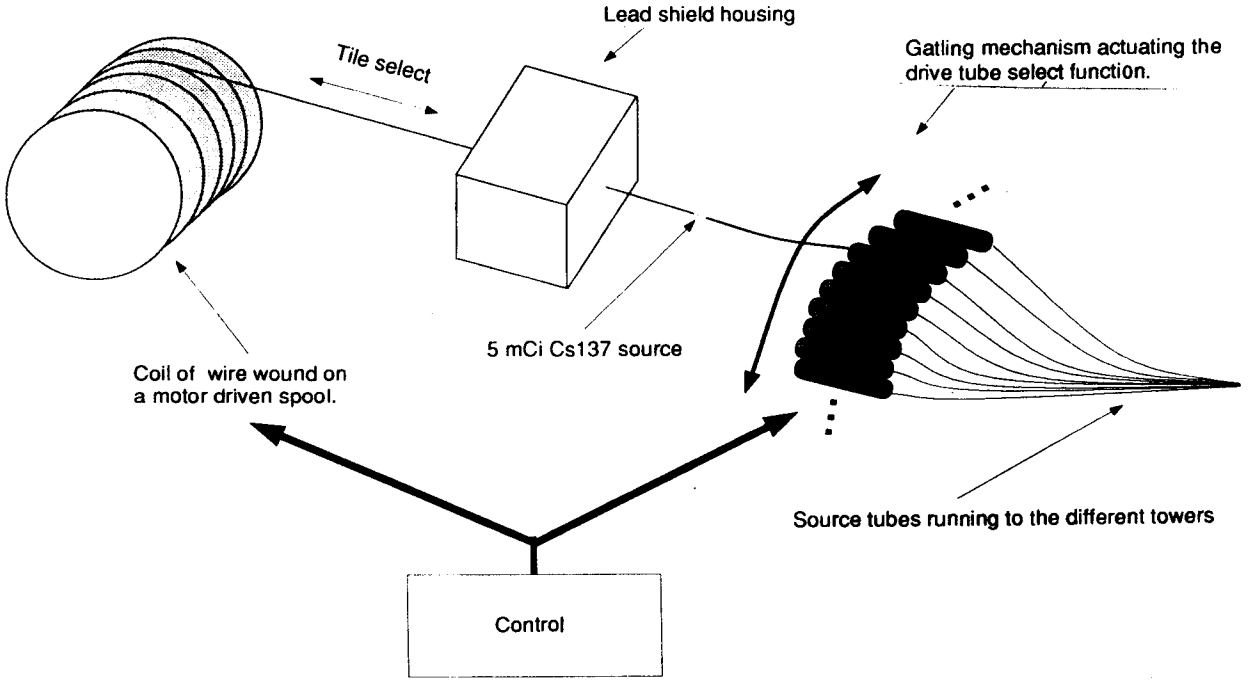

D-11: Schematic diagram of the "Gatling gun" source driver mechanism. A thin wire carrying a strong gamma source as its tip is wound/unwound on a motor driven spool. The wire can be driven at constant speed inside a guiding tube past tiles in the tile-fiber-calorimeter. The source tube selection is achieved by rotating the Gatling mechanism thus aligning the source wire with the desired tub.

Calorimeter Calibration

We have studied experimentally and confirmed with simulations some aspects of the calibration scheme currently envisaged for the SDC calorimeter. This scheme currently relies on the induced current from (5 mCi) Cs^{137} sources traveling at the end of long "wires" inside hypodermic quality stainless steel or plastic tubes past all the tiles in the stack or some significant fraction thereof. The wires are extended or retracted by coiling them up on a spool using a motor driven mechanism. Which of the many tubes traveling through the stacks get fed with a source carrying wire is determined by a "Gatling gun" mechanism whereby the desired source tube is lined up with the source wire driver. See Figure D-11. The exact positioning of the tubes and the parameters of the calibration have not been established yet. However, we expect the following items to be of importance:

1) Source type.

2) Source strength.

3) Accuracy of position with respect to the tile.

4) Scanning speed.

We have already investigated the effects originating from the accuracy of positioning the source with respect to the tiles using a simple model, a simple Monte Carlo, and a GEANT simulation. Figure D-12 show the geometry and Figure D-13 shows the agreement between the model, simple Monte Carlo, and GEANT. From this, we deduce that the sensitivity of the source-to-tile position is 10% mm. We check these calculation by comparing the position sensitivity of a disk-shaped source emitting several gamma lines from 88 KeV to 1.836 MeV to a GEANT of the same geometry and gamma energies, finding very good agreement.

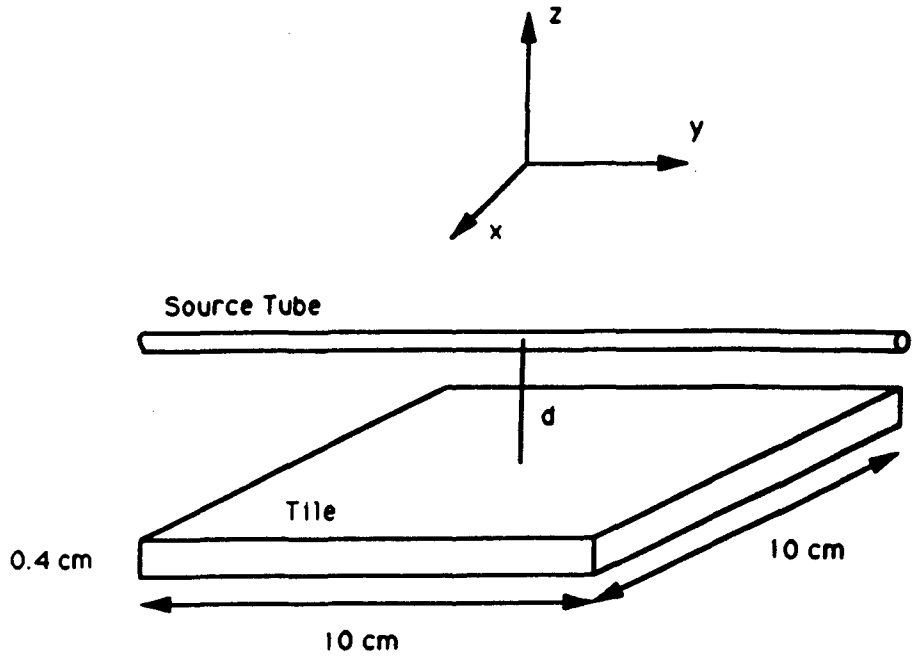

D-12: **Location of source tube relative to the tile and definition of the coordinate system.**

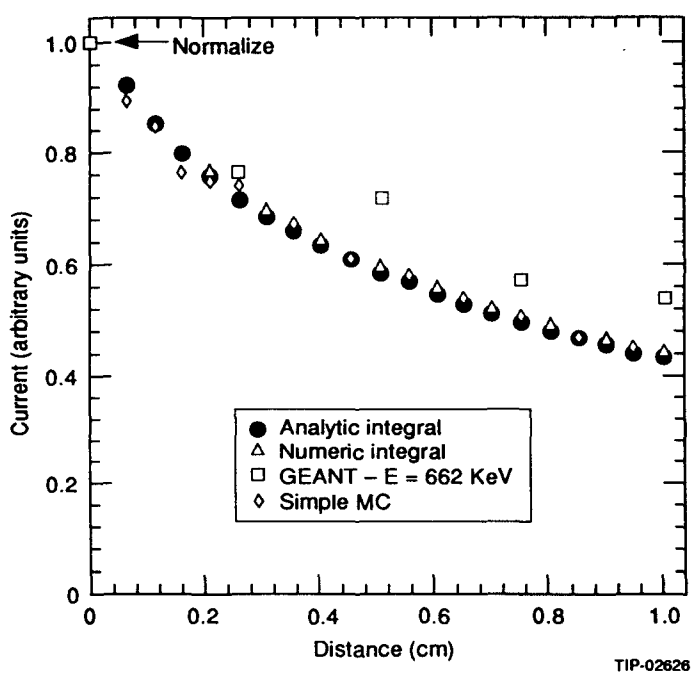

D-13: **Source current as a function of the distance normal to the face of the tile.**

Calorimeter Response Studies

We have devoted a significant effort into understanding the effects of various sources of calorimeter energy resolution worsening using full GEANT simulations of electromagnetic showers. To date, we have considered and studied the following items:

1) The tile-to-tile non uniformity originating from random differences in light output of selected samples to build towers.

2) The light output deficit originating from the finite attenuation length of green light in clear fibers running from the most radically inward tile layer to the most radically outward tile layer.

3) The effect of the light output deficit originating from radiation damage to tiles according to a radial (longitudinal) profile assumed to be proportional to that of low energy (2 GeV) electron showers.

4) The effect of the non uniform response across the tile surface.

The results of the simulation runs performed to date indicate that all the effects from the sources listed above are mostly confined to contributions to the energy-constant term of the resolution function. Figure D-14 displays how the electromagnetic energy-constant term grows with a gaussian tile-to-tile non uniformity of response indicating that a 10% variation will result in a contribution of about 0.6%. Figure D-15 shows the contribution to the constant term from the light output deficit originating from the finite attenuation length of green light in clear fibers. Figure D-16 is a similar plot where the light output deficit is now due to radiation damage assumed proportional to a 2 GeV electron shower longitudinal profile. Figure D-17 shows the effect on the mean energy deposited arising from varying the gap between scintillator tiles, keeping in mind that the absorber layers have no gaps within the confines of a module. All the effects studied to date result in small contributions to the resolution function of the calorimeter for the expected range of the parameters. We are still investigating the effects arising from the non uniformity of response across the tile.

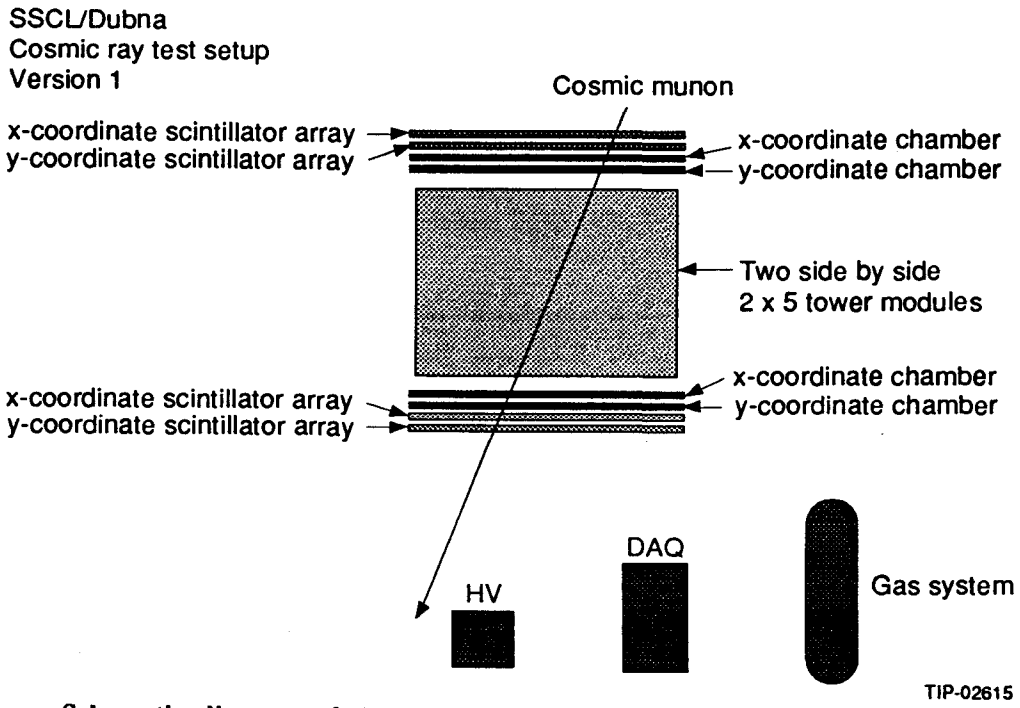

D-14: Schematic diagram of the planned cosmic ray test setup. Two side by side 2 × 5 tower modules expose 580 tiles to muons. The stacks can be disassembled and the scintillating tile-fiber-assemblies exchanged.

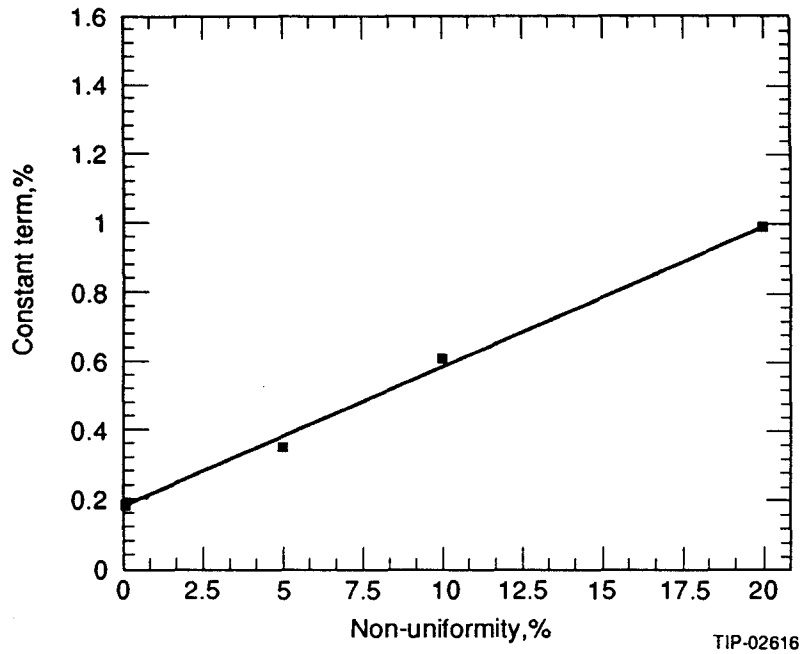

D-15: **Tile-to-tile gaussian non-uniformity contribution to the energy-constant term of the calorimeter resolution function.**

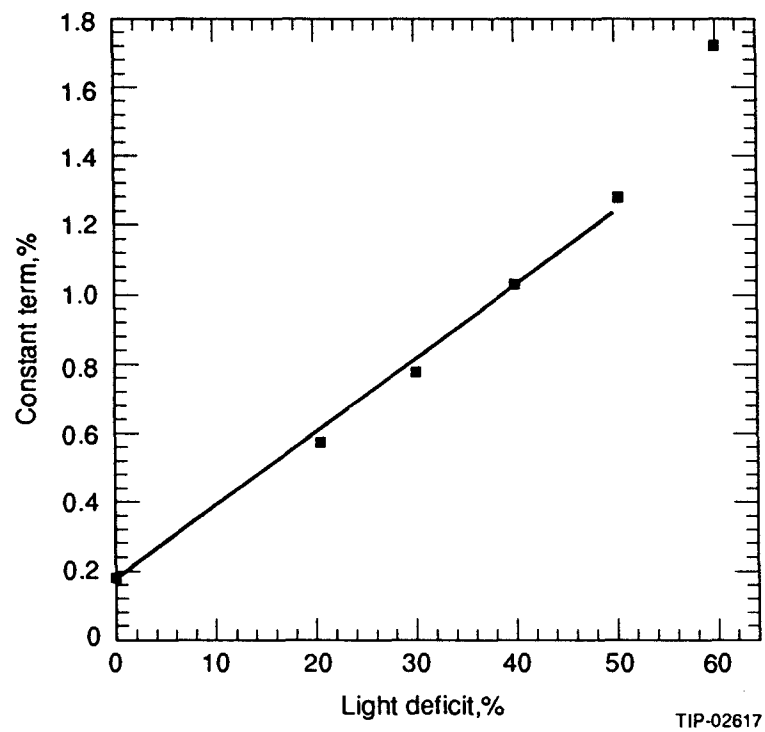

D-16: **Contribution to the constant term originating from the light output deficit due to the difference in length of clear fibers between the first and last tile of the stack.**

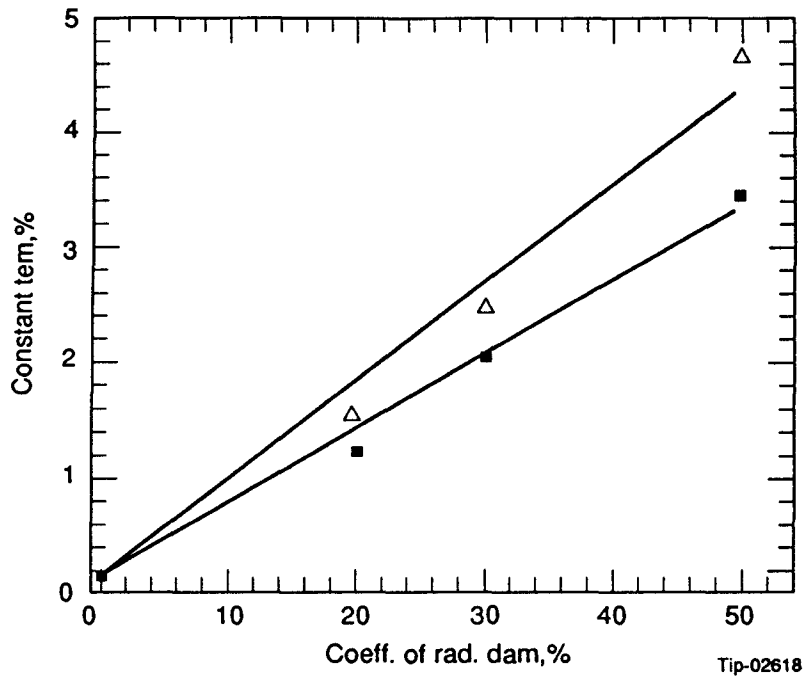

D-17: **Contribution to the energy-constant term of the electromagnetic resolution function arising from the light output deficit due to an assumed radiation damage profile from 2 GeV electron showers. The upper line is obtained by extracting the RMS from each distribution while the lower line, a better fit, is obtained from fitting Gaussians to the Gaussian part of the distributions.**

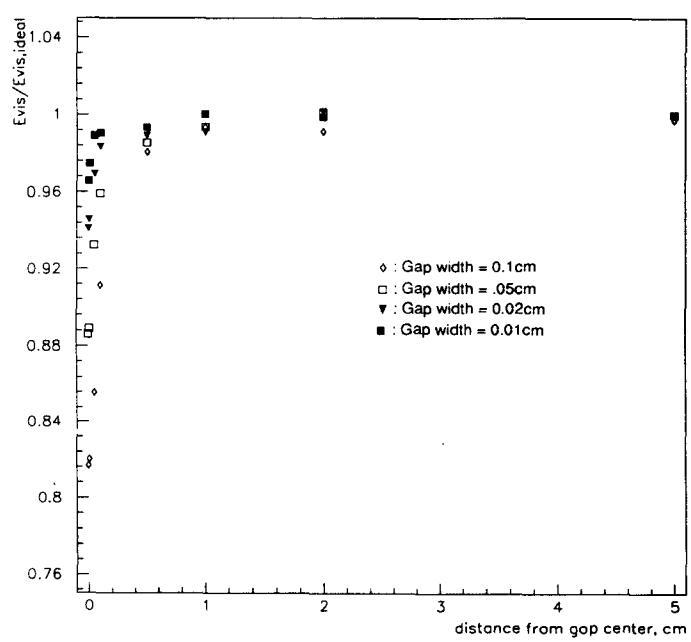

D-18: **Observed energy over ideal (no gap) energy ratio versus the half width of the tile-to-tile gap for a range of gap widths from 0.1 cm to 0.01 cm. The absorber layers have no gaps.**

Our group has continued and expanded electron acceptance studies begun in the context of the liquid-argon calorimeter. A phi-symmetric GEANT model of the scintillating-tile calorimeter has been coded in the SDC standards and was scanned along the eta-direction with 20 GeV transverse energy electrons developing full showers. This model includes a description of a realistic solenoidal coil assembly. The geometry studied to date is that of the reentrant end-cap concept as is shown on Figure D-18. In collaboration with physicists in Fermilab, a full magnetic field map was included in the simulation. Figures D-19 and 20 show the size of the stochastic term in the energy resolution function with the magnetic field "off" and "on" indicating a slight improvement in the complicated catcher to snout transition. Figures D-21 and 22 show this same resolution function (field-off and field-on) after applying a weight (eta-dependent and varying from 2.57 to 3.24) to the independently read-out first inner layer of the calorimeter, where possible. This massless gap correction restoring linearity of the energy response is shown to be very effective in recovering the resolution in the transition region between the barrel and the end-cap catcher. The first bump in the resolution function corresponds to this transition, while the second bump is due to the catcher to snout transition. In a recent design modification, the reentrant snout has been eliminated in favor of extending the catcher section in a flat end-cap wall all the way down to near η of 3. In addition, the effect of increasing the amount of projective overlap between the barrel and end-cap electromagnetic section has been studied favoring 10cm (one full tower) over 5cm.

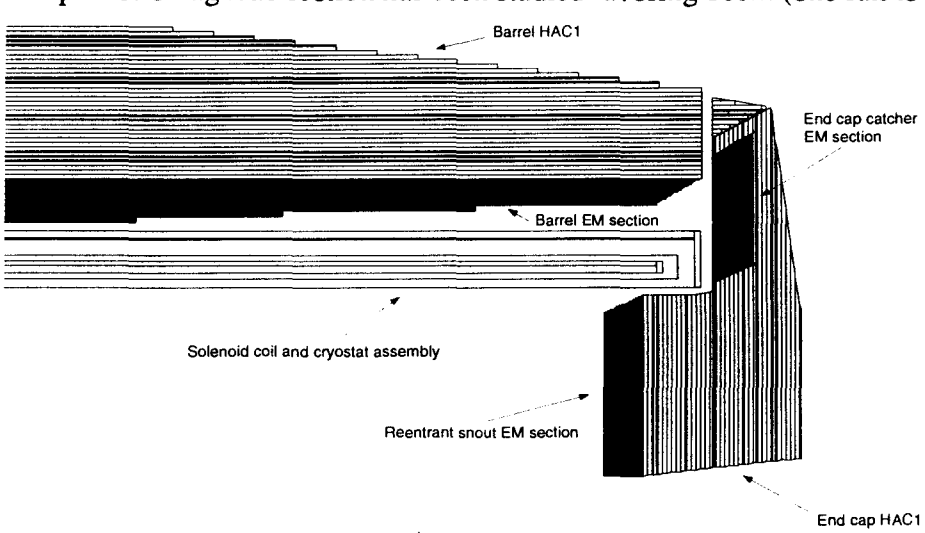

D-19: GEANT phi-symmetric model of the solenoidal coil plus cryostat assembly and of the electromagnetic EM and HAC1 sections of the barrel and end-cap calorimeters. The geometry of the end-cap is 15cm reentrant. The barrel-to-catcher transition model is close to the adopted geometry which has a flat end wall (non-reentrant).

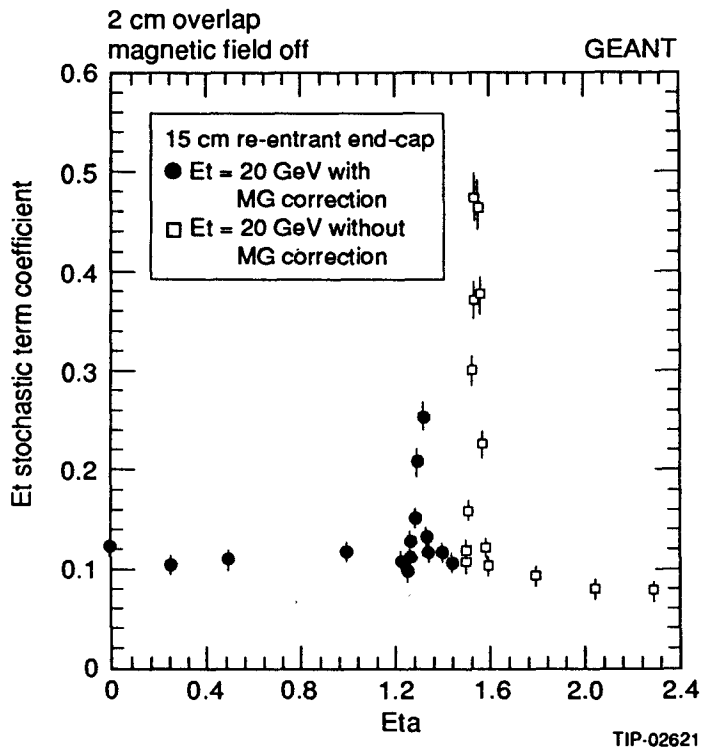

D-20: Stochastic term coefficient of the transverse energy resolution function versus pseudorapidity for electron showers of constant 20 GeV transverse energy. The magnetic field is off for this simulation.

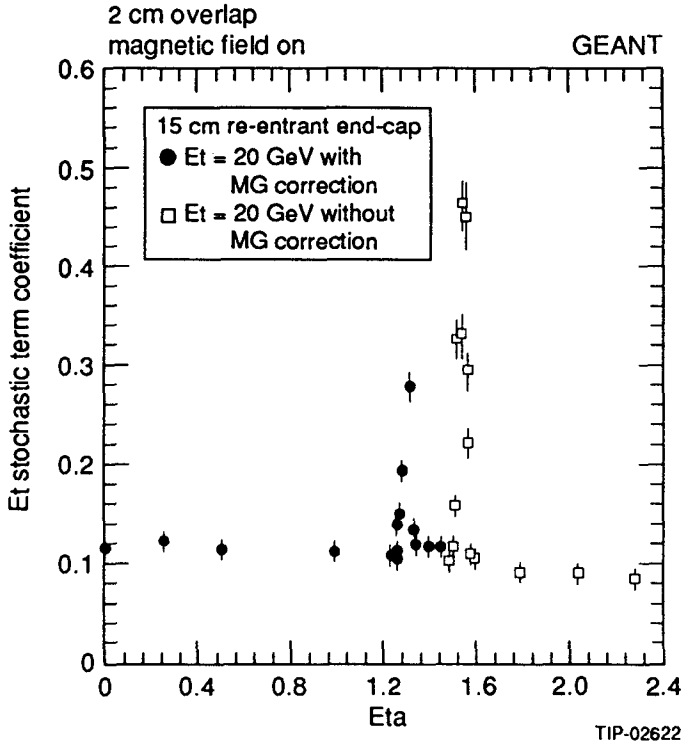

D-21: **Stochastic term coefficient of the transverse energy resolution function versus pseudorapidity for electron showers of constant 20 GeV transverse energy. The magnetic field is on for this simulation.**

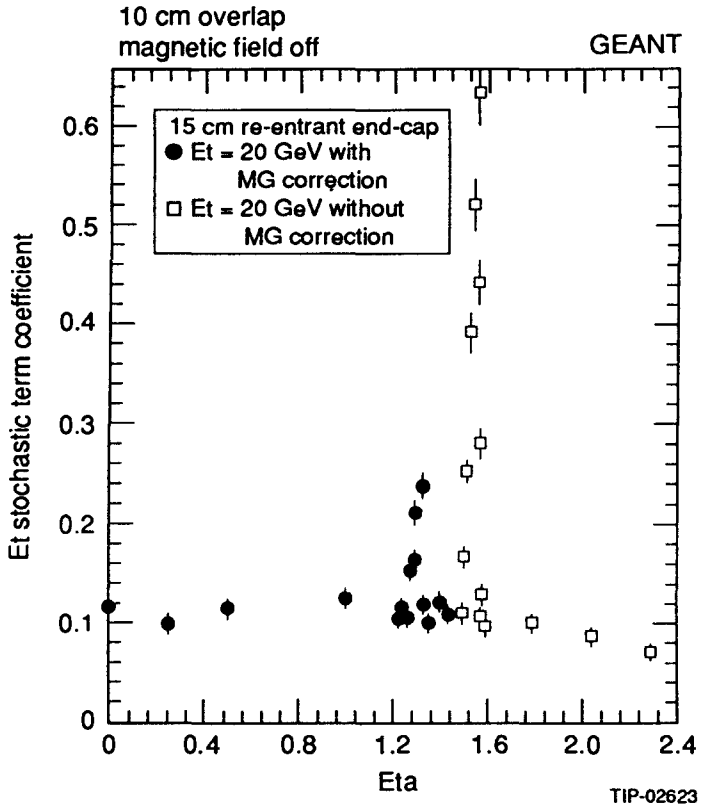

D-22: Stochastic term coefficient of the transverse energy resolution function versus pseudorapidity for electron showers of constant 20 GeV transverse energy. The magnetic field is off for this simulation.

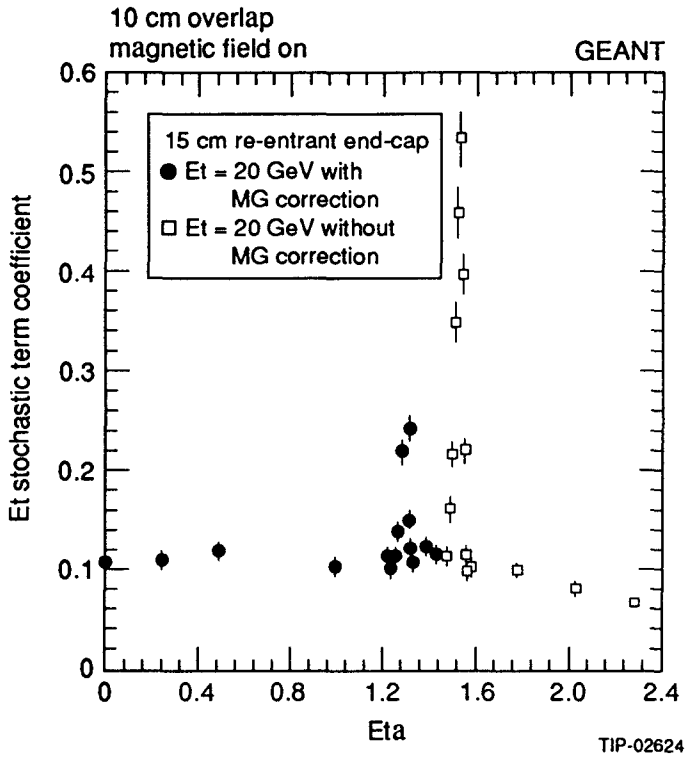

D-23: Stochastic term coefficient of the transverse energy resolution function versus pseudorapidity for electron showers of constant 20 GeV transverse energy. The magnetic field is on for this simulation.

We are in the process of pursuing these electron-acceptance studies and the following items are under immediate attention:

1) The effect of the phi-crack size between electromagnetic modules and the amount of non-projective rotation required to compensate for their inevitable presence.

2) The electromagnetic response in the barrel-to-end-cap region (and elsewhere) including the effects arising from:

   a) the solenoid coil and cryostat assembly (already included in the current model)

   b) the solenoid coil support structure and

   c) the tracker thickness causing bremsstrahlung and

   d) the tracker cabling material in the barrel-to-endcap transition.

3) The electron phi-acceptance and eta-acceptance, specially in the barrel-to-endcap transition.

These studies require a more realistic (detailed) GEANT model of the calorimeter in the SDC coding standards, reproducing the device at the plate level including individual modules and their associated non-projective rotations. Much of the code we have written for the liquid-argon

studies can be re-used with appropriate modifications and we expect to make full use of available code written elsewhere describing the various versions of the tracking detectors of the SDC.

APPENDIX E

PROGRESS IN THE USE OF AVALANCHE PHOTODIODES FOR READOUT OF CALORIMETERS

SSCL-552

SSCL-552

Superconducting Super Collider Laboratory

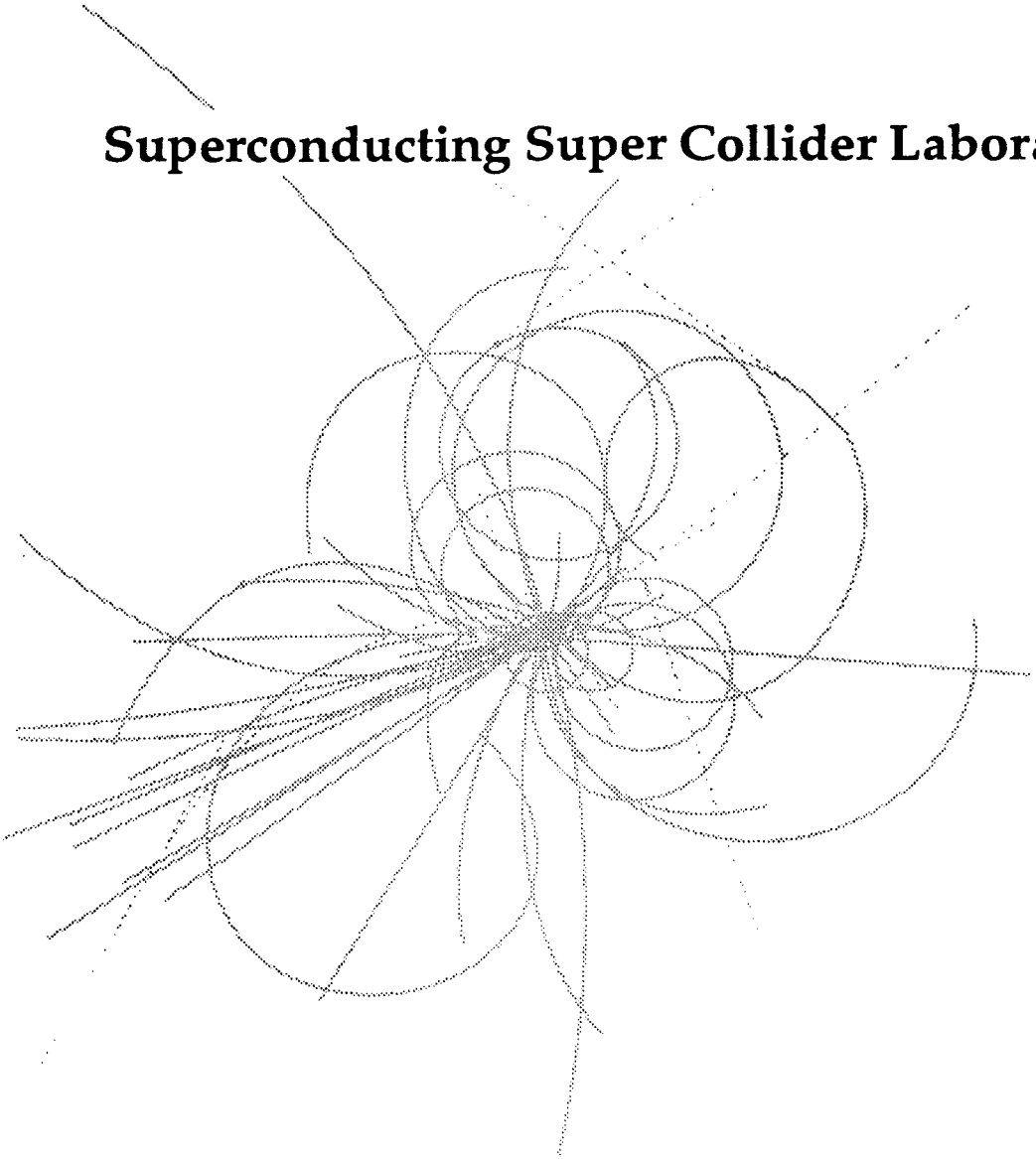

Progress in the Use of Avalanche Photodiodes for Readout of Calorimeters

H. Fenker, K. Morgan, and T. Regan

September 1991

SSCL-552

Progress in the Use of Avalanche Photodiodes for Readout of Calorimeters

H. Fenker, K. Morgan, and T. Regan

Physics Research Division
Superconducting Super Collider Laboratory†
2550 Beckleymeade Ave.
Dallas, TX 75237

September 1991

†Operated by the Universities Research Association, Inc., for the U.S. Department of Energy under Contract No. DE-AC35-89ER40486.

CONTENTS

FIGURES iv

1.0 INTRODUCTION 1

2.0 GENERAL CHARACTERIZATION OF APD OPERATION 1

3.0 SENSITIVE ELEMENT REQUIREMENTS FOR PRE-SHOWER/SHOWER-MAXIMUM DETECTORS 3

4.0 APD LINEAR CIRCUIT DEVELOPMENT 4

5.0 APD ARRAY SYSTEM DESCRIPTION 7

5.1 Electronic 7

5.2 Mechanical 12

5.3 Optical 15

5.4 System Test Results 18

6.0 SUMMARY 19

ACKNOWLEDGEMENTS 21

REFERENCES 23

FIGURES

1. Spectral response curves for two commercial APDs.....1
2. Oscilloscope trace showing the signal from an avalanche in an APD operated in Geiger mode. The same trace is shown at two different time scales. For this response the APD was discharging into 240 KΩ 2
3. Test circuit used for observing Geiger mode APD signals.....3
4. The DO charge-sensitive preamp circuit used in initial linear mode tests of APDs.....4
5. Block diagram of experimental arrangement for initial APD studies.....5
6. Early test results of an APD operating in linear mode and exposed to about 60 green (565 nm) photons. The electronic noise apparent in this figure was later reduced. 5
7. Response of an APD to varying amounts of incident light. The scatter of the data above and below the straight line was reduced by stabilizing the temperature of the APD.....6
8. Variation of APD response with time of day. Thermal stabilization of the APD eliminated this variation. Note that error bars indicate the statistical spread in the signals. The error on the mean is of order one ADC count.....7

9a. Charge-sensitive amplifier circuit implemented in the 96-channel APD system. 8

9b. Schematic diagram of a 16-channel APD/Amplifier/Driver circuit board. The three blocks at the top are the temperature monitoring circuits. 9

10 Photograph of the 96-channel array composed of six cards of 16 channels each. One card is shown with the RF shield removed. The APDs are imbedded in the bar at the front of each card. Optical connectors, one with fiber attached, are shown inserted in the topmost card. Thermal stability is provided by circulating water through the pipe attached to the front of the crate..... 11

11. The Pre-shower Detector. Scintillating fiber ribbons are in the middle and are read out by various test devices on either end. The entire assembly is enclosed in a light-tight box..... 12
12. Detail of the assembly of the electronic circuit board to the cooling system and crate. The avalanche photodiodes are mounted in the "isobar."..... 13
13. The Feed-Through Panel. Constructed of copper-clad black substrate, this panel provides light-tight bulkheads for eight ribbon cables, four gas or water lines, eight BNC cables, four SHV cables, and a multiconductor low-voltage connector. 14
14. Optical Alignment Procedure. The APD is mounted in a thermally stabilized brass bar. 15
15. Cross section of the APD Photodiode developed by EG&G Optoelectronics for use with 1-mm-diameter fibers. The APD itself is only 0.5 mm wide..... 16

16. Map of the response of the APD with and without the ball lens assembly. The response without the lens is indicated in the center of the figure. Although the APD itself has a diameter of only 0.5 mm, the lens collects light over about 1.2 mm..... 17
17. Variation in APD response as a function of temperature. The data were taken by monitoring the system for an extended period of time while the temperature went through its normal cycle. The line respresents a least-squares fit..... 18
18. The gain variation of three channels of APD as the global bias voltage supply is varied. The lines are the results of quadratic fits to the data. The error bars represent erros on the means of the distributions. 19

1.0 INTRODUCTION

During the past year the Superconducting Super Collider Tracking Group has progressed from acquisition of its first avalanche photodiode (APD) to installation of a 96-channel array of the devices. The work was motivated by the desire to learn how to use APDs as the sensitive elements in a fiber tracking detector, moderated by the presence of limited resources and the absence of activity within groups outside the SSC Laboratory on such a project. We chose, therefore, to team up with an ongoing research effort which intended to evaluate both pre-shower and shower-maximum detectors and various means of sensing the light produced.[1] The pre-shower detector is made of layers of scintillating fibers similar to a fiber tracker. The shower-maximum detector uses optical fibers to transmit the light from scintillating plates to the readout devices. Our contribution has been to develop the APD array for use in this test from concept to operation. Currently, the equipment is installed in Fermilab's MP beamline awaiting delivery of the final 36 APDs and exposure to the beam.

2.0 GENERAL CHARACTERIZATION OF APD OPERATION

An excellent review of avalanche photodiode operation and applications is given by Lightstone and McIntyre.[2] Here we provide a brief outline.

Avalanche photodiodes have been available on the market for many years, but have generally been considered uninteresting devices for high-energy physics because of their high cost and either low gain (~×200) or low repetition rate (few kHz). Without much effort, however, either a much higher repetition rate or a much higher gain can be achieved. At present the cost of APDs ranges from about $50 to about $200 per device, although this is anticipated to drop for large quantities. They possess excellent quantum efficiency, peaking around 80% for light in the 800-nm range and dropping to about half that in the blue. (Compare photomultiplier tubes, which are typically about 5-8% in the blue.) Figure 1 shows the spectral response curves for two different APDs.

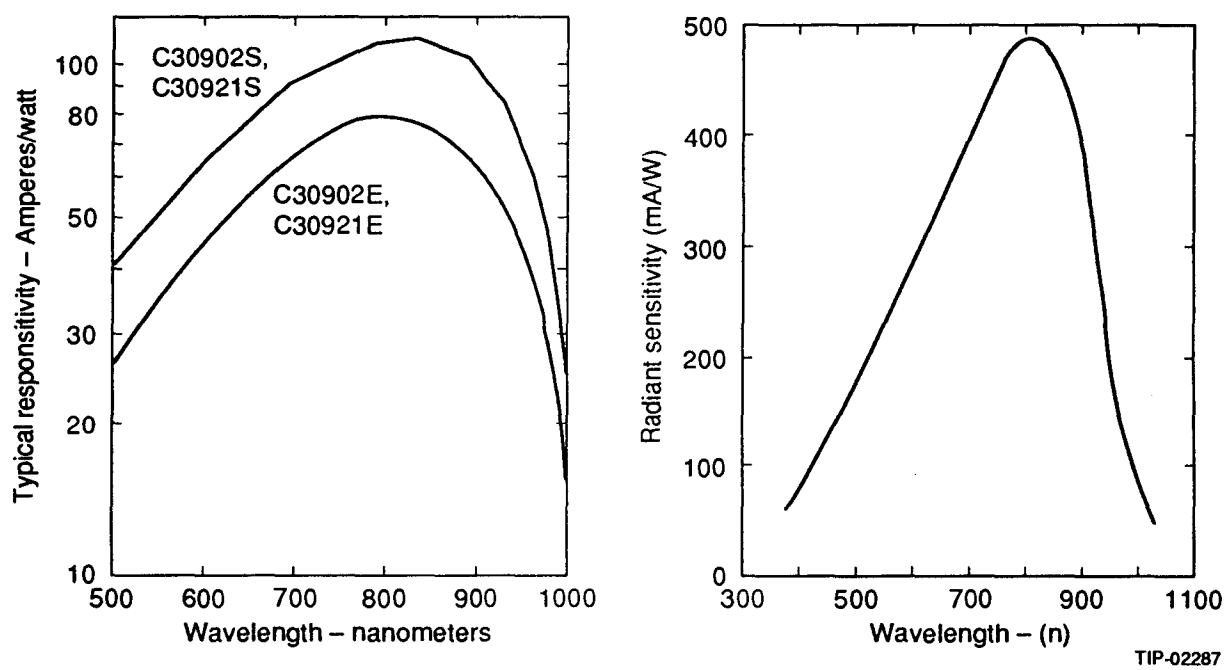

Figure 1. Spectral response curves for two commercial APDs.

The gain mechanism in APDs is an electron avalanche occurring in a high-field region of a thin silicon wafer. The high field develops in the depletion layer of the diode when a reverse bias is applied. As the reverse bias voltage is increased, the thickness of the depletion layer increases until it extends all the way through the diode. The external bias at that point is called the *depletion voltage*. An electron liberated by a photon striking a silicon atom in the P side of the diode will be accelerated toward the N side by the electric field in the depletion layer. Gain is developed as the electron is accelerated sufficiently to liberate additional electrons in collisions with the silicon lattice. The newly liberated electrons are also accelerated, strike atoms in the lattice, liberate more electrons, and so on.

If the electric field is increased above the *breakdown voltage*, then there is a significant probability that photons will be generated during the avalanche which will initiate independent avalanches in a different region of the APD, eventually involving the entire diode in the avalanche unless some external device limits it. This type of operation is referred to as *Geiger mode*. Below the breakdown voltage, the diode current increases linearly with increasing incident light, making it useful for measurements of light intensities as required for calorimetry. Figure 2 shows an oscilloscope trace from an APD operated in Geiger mode. The test circuit used to obtain this trace is given in Figure 3. The APD used in these tests is an EG&G 30902S.[3] In linear mode the gain is limited to a factor of a few hundred, so that the signal resulting from a single photoelectron is only a few hundred electrons. Observing such a tiny signal requires high-gain, low-noise electronics. The device manufacturer indicates that the total charge is collected in under 1 ns in this mode, but this is nontrivial to demonstrate because any observable signal is dominated by the associated electronics. Our experience with linear mode signals will be described more fully in the following sections.

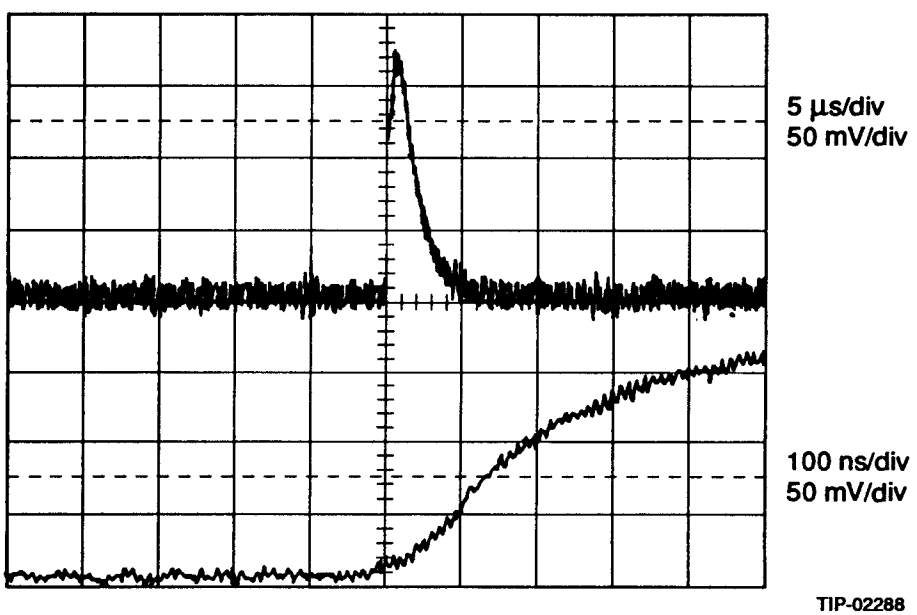

Figure 2. Oscilloscope trace showing the signal from an avalanche in an APD operated in Geiger mode. The same trace is shown at two different time scales. For this response the APD was discharging into 240 KΩ .

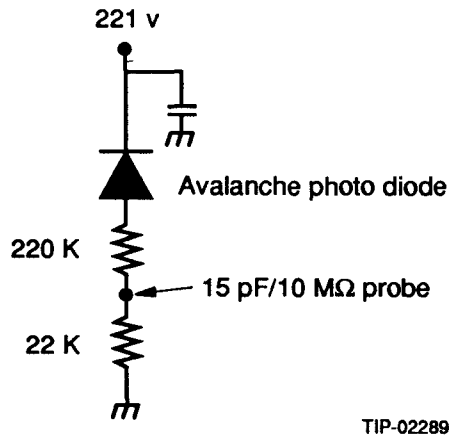

Figure 3. Test circuit used for observing Geiger mode APD signals.

3.0 SENSITIVE ELEMENT REQUIREMENTS FOR PRE-SHOWER/SHOWER-MAXIMUM DETECTORS

Pre-shower detectors are placed as the first layer in a calorimeter system and are intended to observe the incoming charged particle, if any, as well as the first stages of the electromagnetic shower. They are effectively a cross between a tracker and a calorimeter in that ideally they provide a precise measurement of the positions of charged particles as they enter the calorimeter without sacrificing undetected energy loss. Given the data collected by pre-shower and shower-maximum detectors, one can also make powerful cuts on particle identity: e/π; π^0/γ; e/γ. The spatial separation between identifiable particles can be as small as the segmentation of the detector, or down to ~500 μm.

In a pre-shower or shower-maximum detector built of scintillating fiber, then, the requirements on the sensitive elements are: 1) small size in order to mate naturally with the large number of small detector elements; 2) linear response to deposited energy in order to serve as part of a calorimeter; 3) sensitivity to typical minimum-ionizing particle energy deposits; 4) sufficient dynamic range to avoid saturation at shower maximum; and 5) speed consistent with the event rates expected in the experiment. It appears that certain ADPs may possess the necessary requirements for such detectors.

4.0 APD LINEAR CIRCUIT DEVELOPMENT

For detector development tests in a low-intensity test beam, it is not necessary to optimize the shaping time or repetition rate characteristics of the APD electronics. Therefore we chose to use a conventional charge-sensitive amplifier[4] utilizing low-noise FETs biased for optimum noise characteristics. Initial testing of this concept was performed using devices built for the D0 experiment at Fermilab.[5] The schematic is shown in Figure 4.

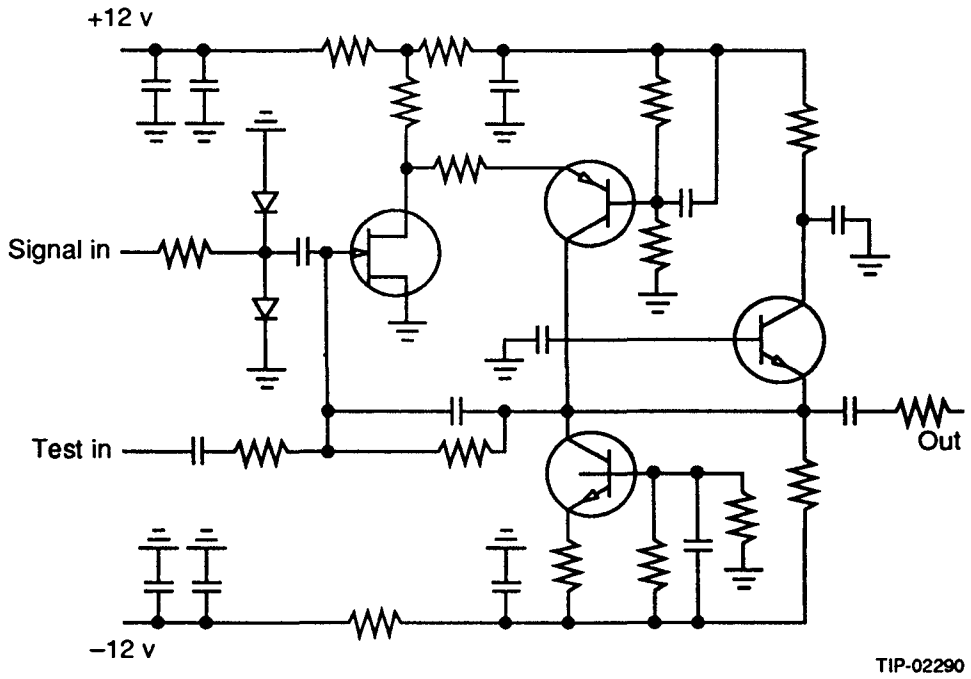

Figure 4. The DO charge-sensitive preamp circuit used in initial linear mode tests of APDs.

The tests of the APD and amplifier used a green LED (565 nm) to excite the photodetector, and a photomultiplier tube (PMT) preamp (LeCroy[6] 612) and a current-integrating analog-to-digital converter (LeCroy 2249A) to record the in-time output of the system. The LED was driven by short (~10 ns) pulses of ~175 v coupled to the LED through a capacitor. Some fraction of the light output of the LED was transmitted by a 1-mm-diameter plastic optical fiber to either the ADP (for testing) or to a PMT (for calibration of the light intensity). Because of their simplicity and low cost, AMP OPTIMATE series [7] connectors were used for the optical couplings in the system. It is also simple to fabricate mating optical sockets for these connectors (see below). The overall setup is shown in Figure 5.

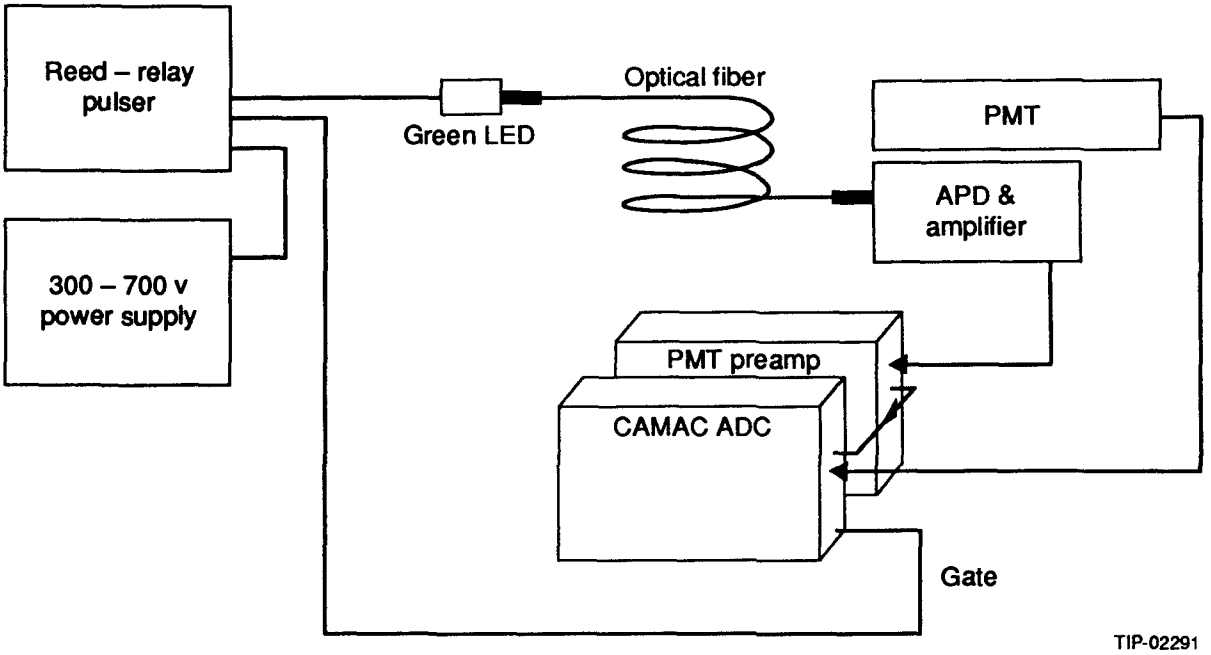

Figure 5. Block diagram of experimental arrangement for initial APD Studies.

Figure 6 shows two superposed histograms of the current integrated out of the electronics during a gate triggered by the light flasher. The lower histogram is the system response with no light flash; the upper histogram shows the response to a light flash determined later to be about 60 photons. This was the initial test of the system to determine whether it was at all sensitive to the test pulses of light.

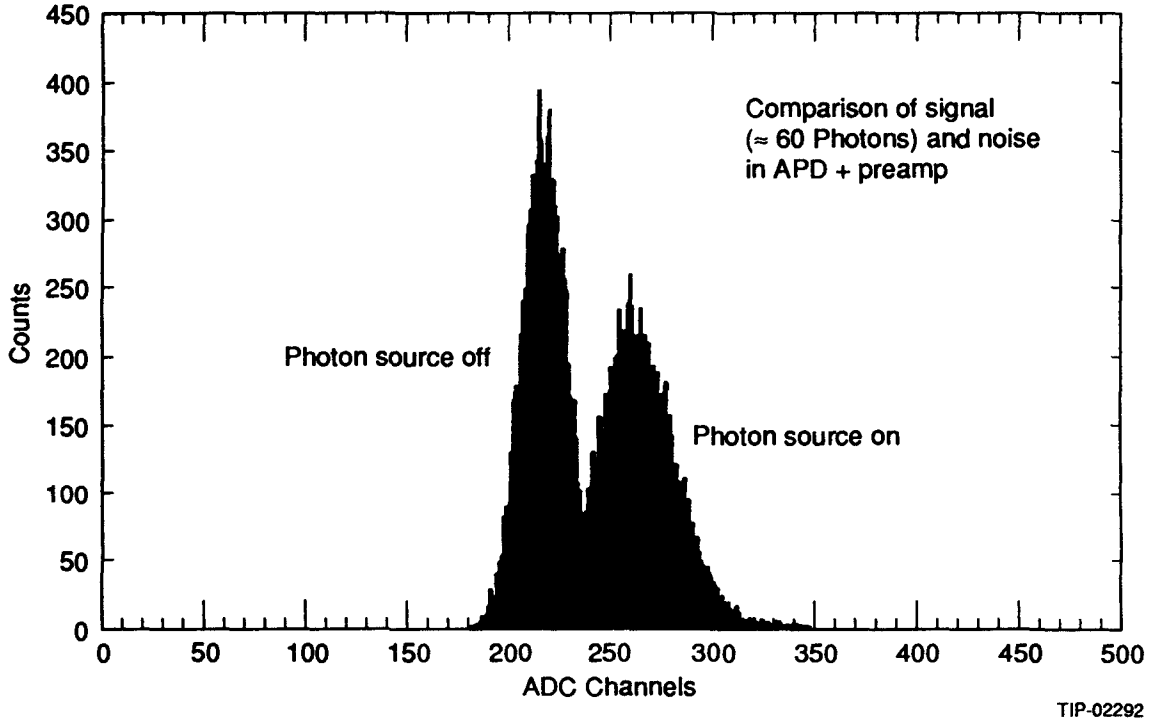

Figure 6. Early test results of an APD operating in linear mode and exposed to about 60 green (565 nm) photons. The electronic noise apparent in this figure was later reduced.

Further testing established the linearity of response of the system to differing light levels. To do this, the LED flasher supply voltage was varied over several hundred volts and the average APD/amplifier response was determined at each one. Then, data was taken at the same set of LED flasher voltages with the light input and signal output connected to a phototube instead of to the APD. In this way it was possible to estimate the number of photons incident on the surface of the APD (or PMT) at each LED flasher voltage. The PMT used for these tests was a Philips XP2020[8] with a quantum efficiency of ~6% at 565 nm. The APD under test has a circular sensitive area 0.5 mm in diameter, so that the APD sees at most 25% of the light emitted by the 1-mm-diameter fiber. When the fiber is attached to the PMT, all of the light strikes the PMT surface. (We determined that any reflection losses at the fiber-APD or fiber-PMT window interfaces must be small since no measurable change in the response of either detector was observed when optical grease was used at the interface. A fine polish was maintained on the end of the fiber, and all tests reported in this paper were made with dry optical contacts.) Thus, if N photoelectrons were produced in the phototube, there were $N/0.06$) photons at the PMT surface and at most $(0.25 \cdot N/0.06)$ photons incident on the APD surface. Figure 7 shows the APD system response to 565 nm light of intensity ranging from 0 photons to 1000 photons per pulse. In order to span this dynamic range of intensity we used two different LEDs having different coupling efficiencies to the optical fiber. The light intensity from each LED was calibrated as described above.

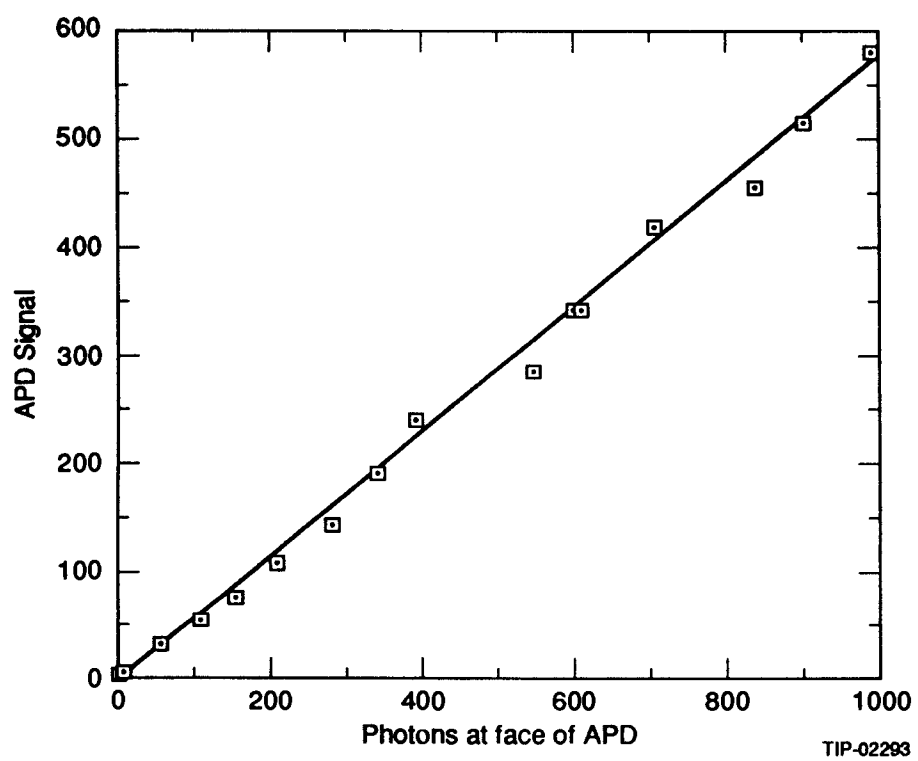

Figure 7. Response of an APD to varying amounts of incident light. The scatter of the data above and below the straight line was reduced by stabilizing the temperature of the APD.

It is apparent from Figure 7 that there is a linear relationship between the number of photons striking the APD and the integrated charge out of the APD electronics. The data are scattered around the best line fit, however, more than statistical errors alone would suggest. It is known that the breakdown voltage—and, therefore, the gain at constant bias voltage—varies with APD junction temperature. Typical specs give a voltage coefficient for constant gain of about 0.5 V/C°. When the linearity tests were repeated with the APD can inserted in a brass bar cooled by tap water (~20° C), the gain was observed to remain constant in time. Figure 8 shows the response as a function of time before thermal control was applied. From this work it became obvious that some form of temperature control or compensation would be required in order to make practical use of the APDs in the final system.

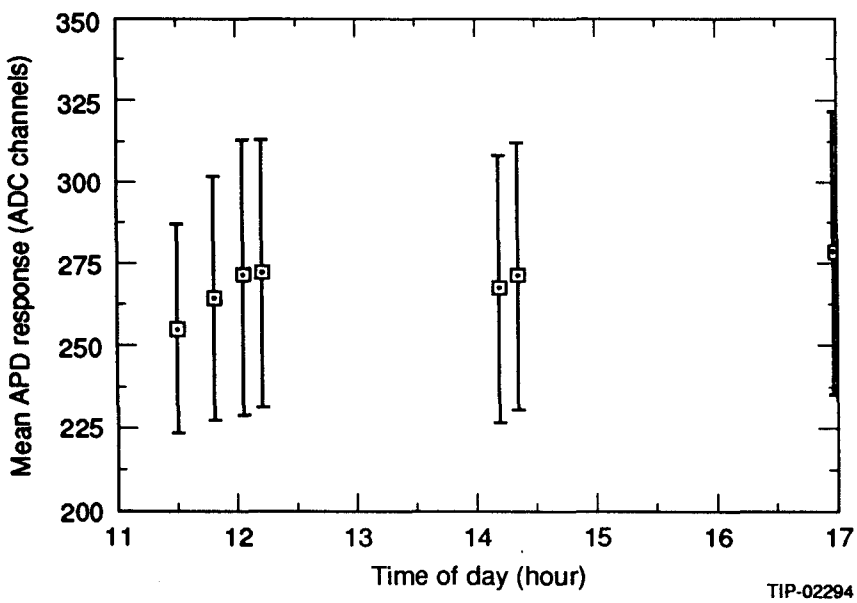

Figure 8. Variation of APD response with time of day. Thermal stabilization of the APD eliminated this variation. Note that error bars indicate the statistical spread in the signals. The error on the mean is of order one ADC count.

5.0 APD ARRAY SYSTEM DESCRIPTION

5.1 Electronic

A printed circuit board was fabricated implementing 16 copies of a charge-sensitive amplifier similar to the one studied initially. Provided as the final stage for each channel on the card is a differential ECL line driver (10216) used in the linear range. Bias voltage for each APD is adjustable over a range determined by a zener diode on the board, so that only one supply is necessary to bias all 16 channels even though they each may require different voltages. Temperature monitoring of the APDs is achieved by attaching an RTD to the metal assembly supporting the 16 devices. The RTD resistance, directly proportional to the

temperature, is converted to a voltage by a 1-mA current source. The voltage is amplified for noise immunity and sent out to a monitor panel along with a sample of the low-voltage power present on each card. The voltage monitors are necessary for practical system operation since safe engineering practices require fusing the power supply lines on each circuit board. The schematic of this circuit is shown in Figures 9a and 9b. Figure 10 is a photograph of one of the cards with the shielding removed.

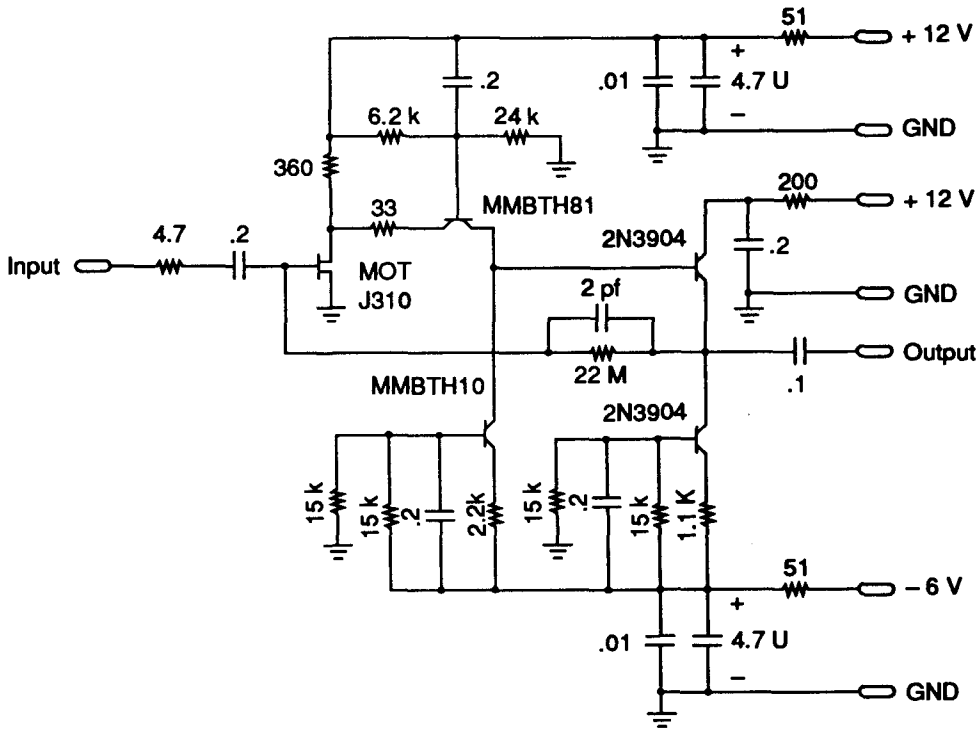

Figure 9a. Charge-sensitive amplifier circuit implemented in the 96-channel APD system.

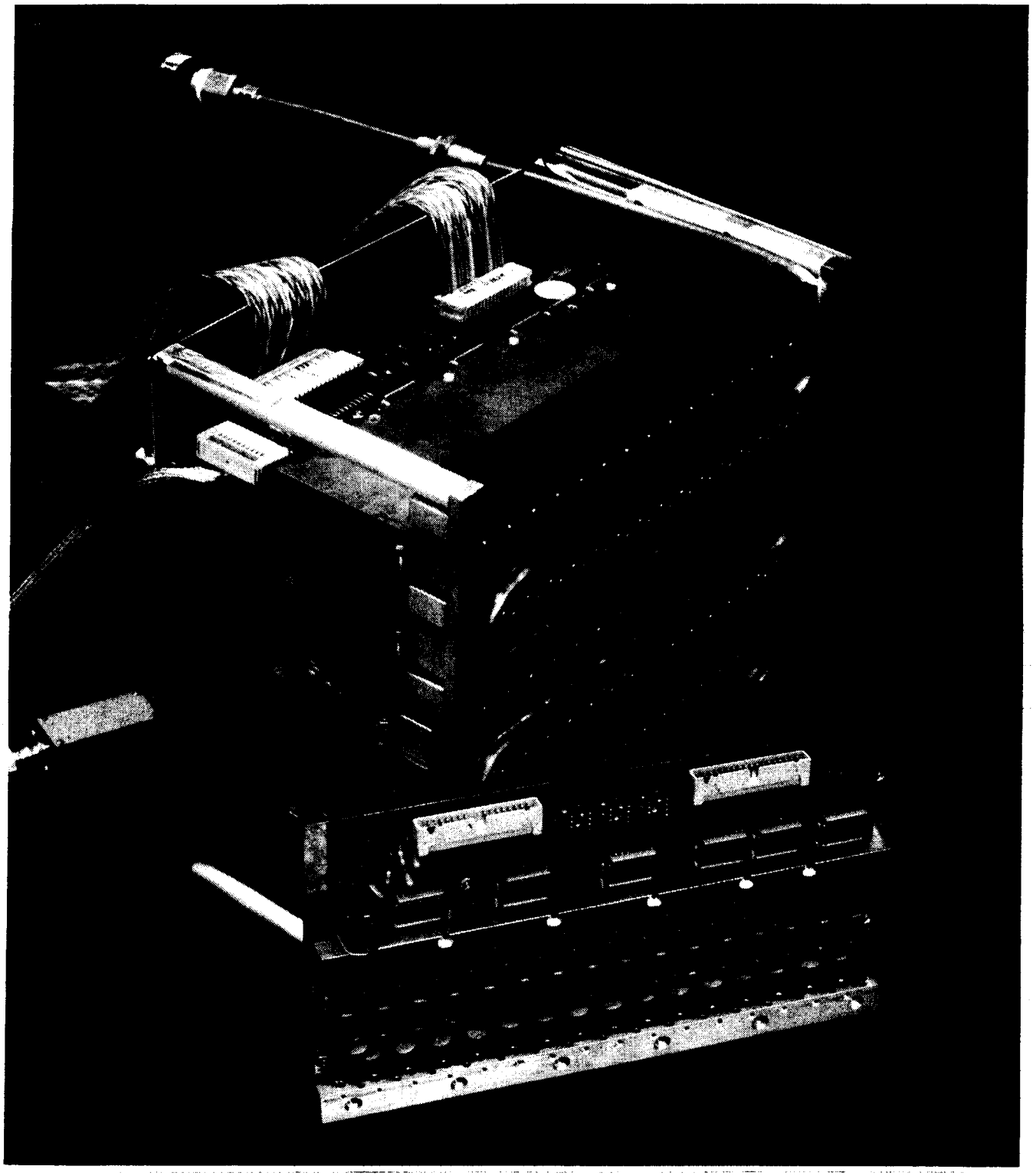

Figure 10. Photograph of the 96-channel array composed of six cards of 16 channels each. One card is shown with the RF shield removed. The APDs are imbedded in the bar at the front of each card. Optical connectors, one with fiber attached, are shown inserted in the topmost card. Thermal stability is provided by circulating water through the pipe attached to the front of the crate.

The resulting differential signals are transmitted over twisted-pair ribbon cables (about 30 m long) to the digitizing electronics. Truly isolated differential inputs are required at the receiving end to maintain acceptable noise levels in the test beam area and to ease the elimination of ground loops. This termination is provided by installing pulse transformers at the front panel of the LeCroy 1885F ADC, used in the data acquisition system.

5.2 Mechanical

Given that the system had to mate with an existing detector design, there were constraints imposed on overall size, net heat generation, RF noise production, layout and method of the optical connections, and means of communicating signals and utilities through the walls of the light-tight detector enclosure. Figure 11 is a working drawing of the entire detector and enclosure with APD system conceptual design shown in place.

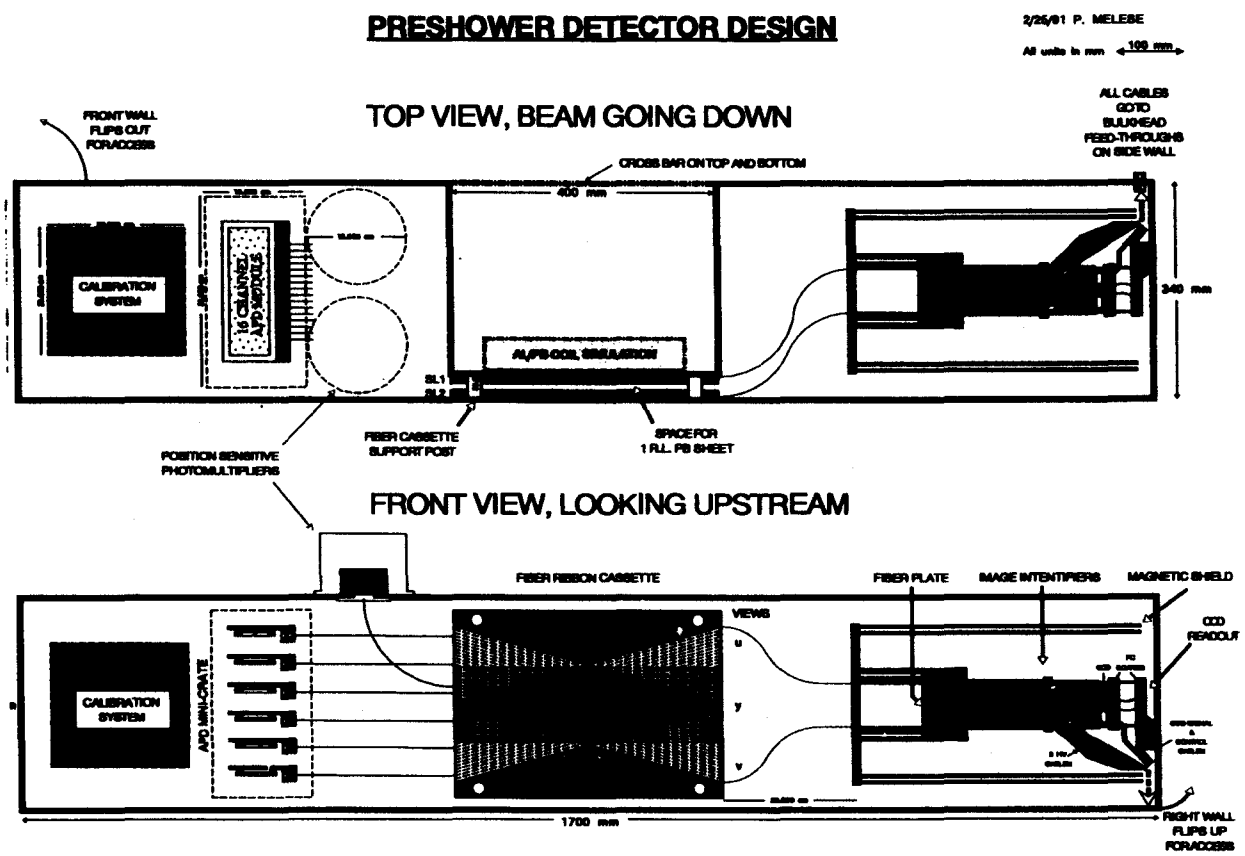

Figure 11. The Pre-shower Detector. Scintillating fiber ribbons are in the middle and are read out by various test devices on either end. The entire assembly is enclosed in a light-tight box.

Both to control the temperature of the APDs and to remove any heat generated by the electronics, chilled water was cycled through a copper pipe brazed to brass bars, which in turn were clamped in thermal contact with the metalwork surrounding the APDs. Figure 12 demonstrates this design. The metalwork was fabricated so as to accept the AMP optical connectors attached to the scintillating fibers and to align the fibers with the windows on the APDs. Also shown in this figure is the massive RF shielding incorporated on each circuit board. The circuits are inherently quiet, but quite sensitive to ambient RF noise because of the low APD signal levels.

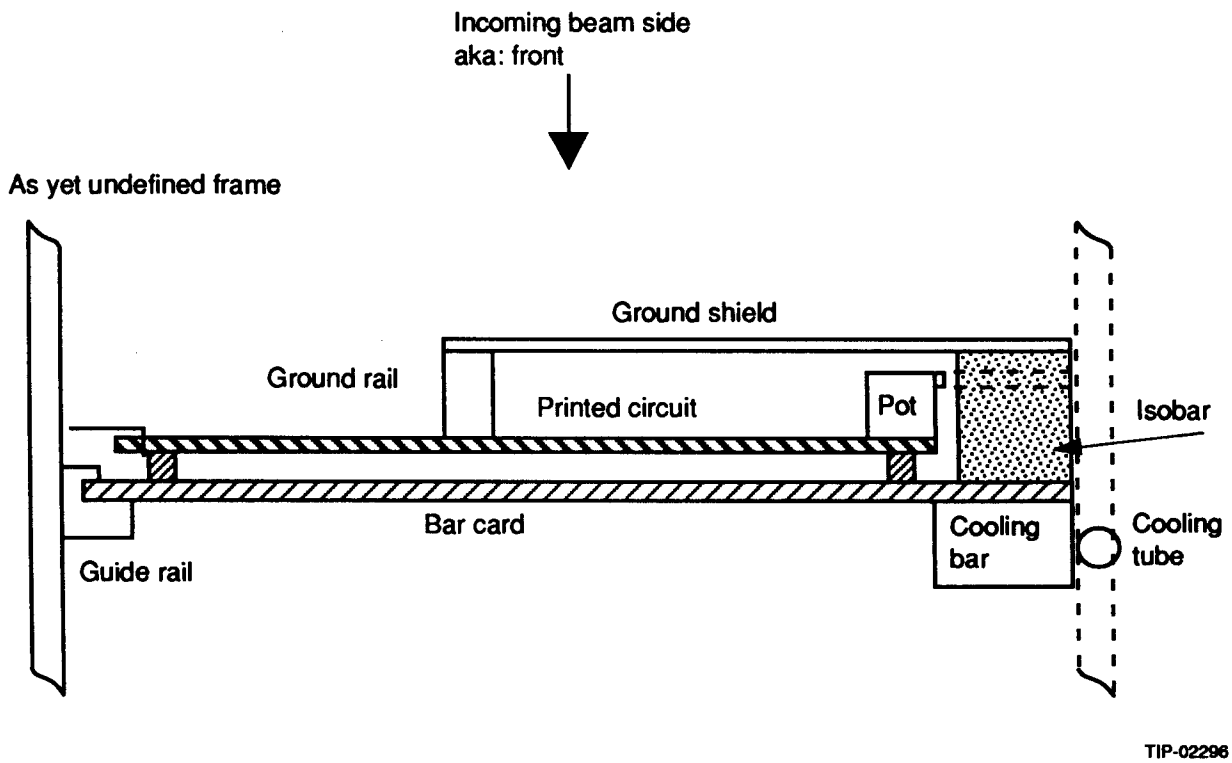

Figure 12. Detail of the assembly of the electronic circuit board to the cooling system and crate. The avalanche photodiodes are mounted in the "Isobar."

Feed-through connectors for chilled water, signals, power, and status monitoring were mounted on a special light-tight printed circuit board. Specifications for this panel were sent to the institution fabricating the detector enclosure so that a mating hole could be designed into it. This board is shown in Figure 13.

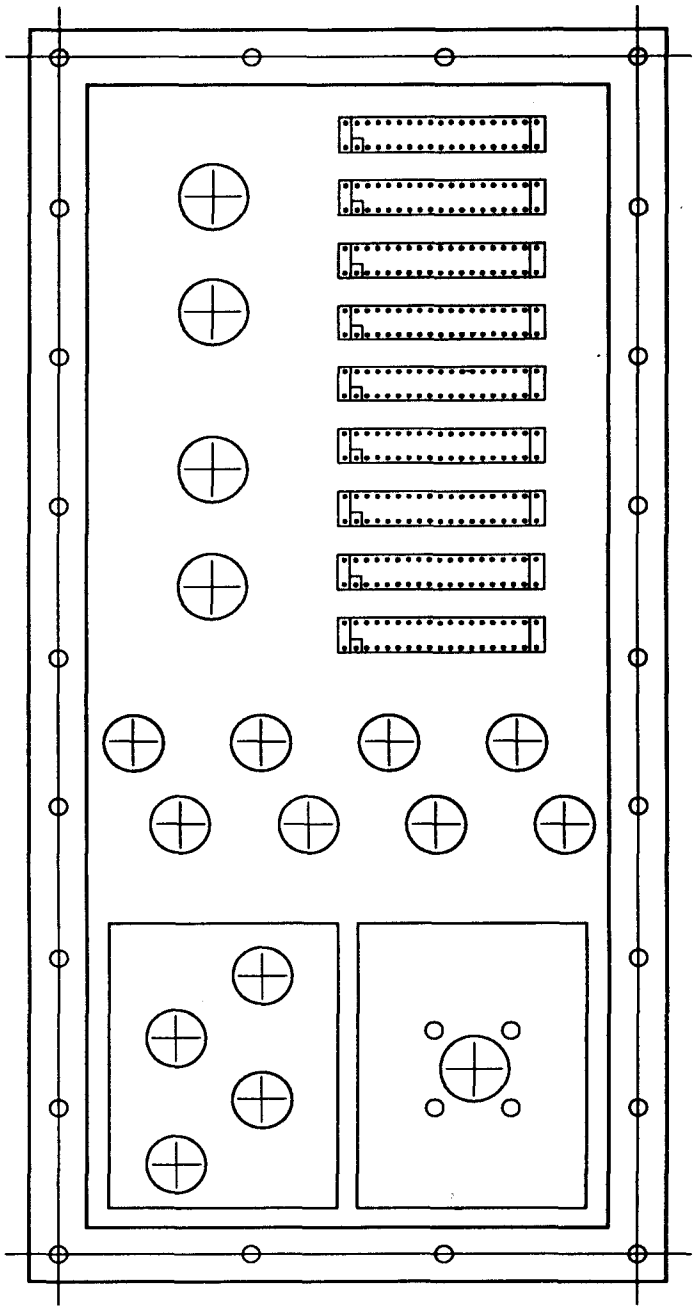

TIP-02297

Figure 13. The Feed-Through Panel. Constructed of copper-clad black substrate, this panel provides light-tight bulkheads for eight ribbon cables, four gas or water lines, eight BNC cables, four SHV cables, and a multiconductor low-voltage connector.

Six assemblies of circuit boards and APD mounting bars were fabricated. Spare circuit boards were prepared as well. The cards slide into slots in a custom-designed crate. One side of the crate is made up of heavy brass bars soldered to the chilled water pipe described above. The APD bars are clamped tightly to the chiller bars by commercial clamping fixtures to provide a secure thermal connection. Power, signal, and monitor cables are attached to each card by individual cables from the feedthrough panel. A photograph of the entire assembly is shown in Figure 10.

5.3 Optical

The same optical connectors used in the early bench tests of the APD were chosen for use in the full system. The AMP Optimate connector, shown with the mating hole, fiber, and APD in Figure 14, provides a convenient solution for a system of this size (96 channels total). The connectors are designed for 1-mm fibers having a large-diameter plastic sleeve around them, however. In order to attach them to fibers without a sleeve, the special plastic taper shown in the figure was developed.

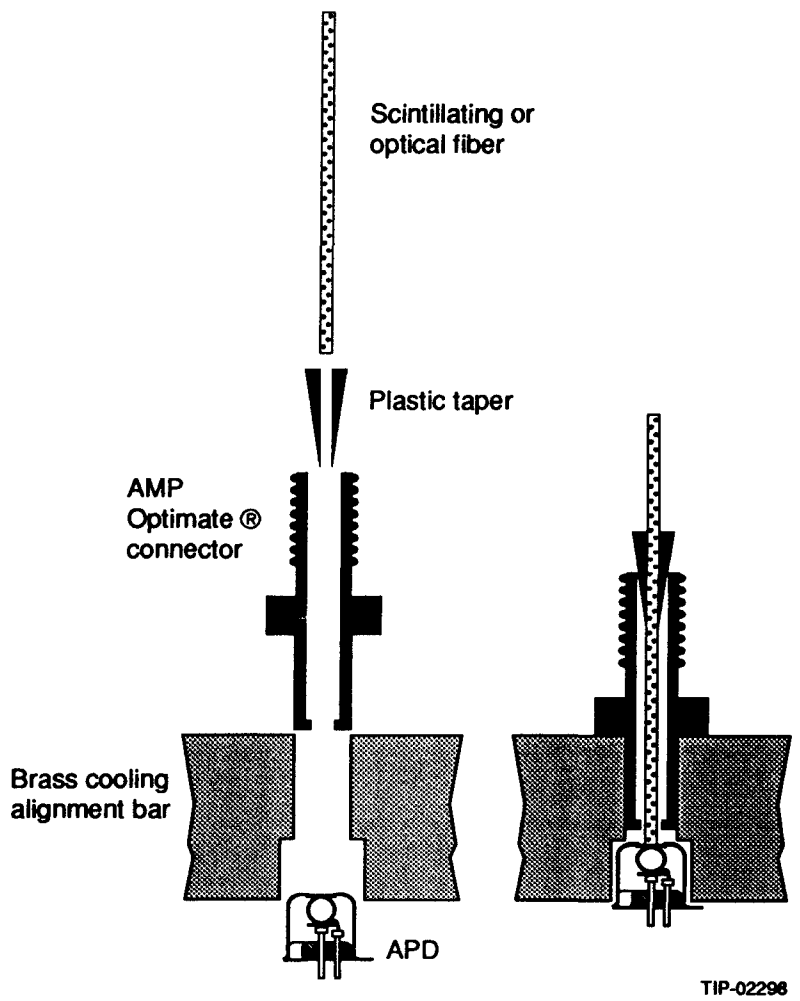

Figure 14. Optical Alignment Procedure. The APD is mounted in a thermally stabilized brass bar.

The standard APD assembly from EG&G is a metal can with a window in the center of the flat surface over the sensitive pn junction. Special devices were designed and fabricated by EG&G for this system to improve the optical coupling efficiency from the 1-mm-diameter scintillating fibers to the 0.5-mm-diameter diode. Figure 15 shows the solution. The photodiode and optical window are placed within 50 μm of the axis of the case to allow the outer diameter of the case to be used as an alignment reference. A spherical glass bead is mounted between the diode wafer and the window. This focuses light from the periphery of the fiber onto the APD surface, providing an effective sensitive area of diameter 1.2 mm. A map of the APD's response across the surface of the window is shown in Figure 16,[9] which is a composite of the results of two scans: one with the ball lens in place and one without the lens. It is clear from this figure that the lens both widens the effective aperture of the APD and provides a more nearly uniform response over the active area.

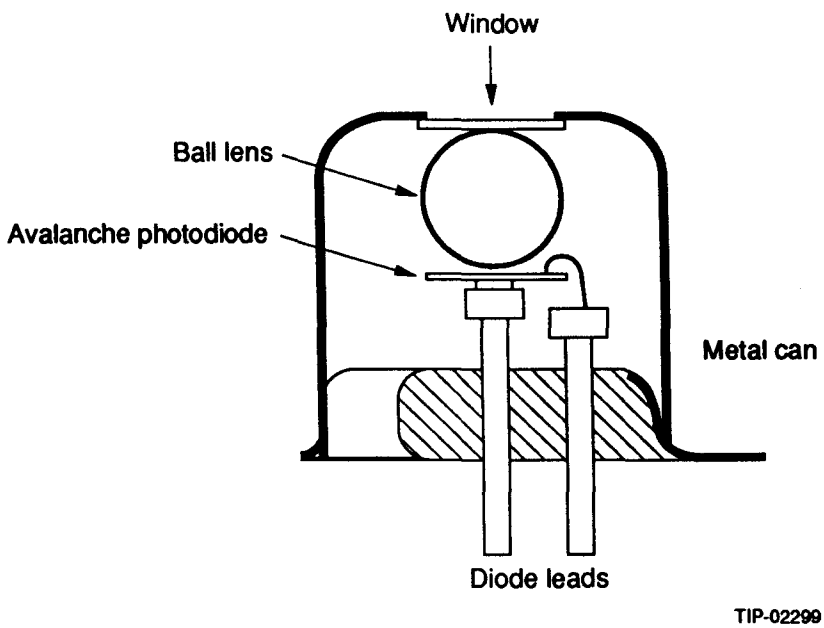

Figure 15. Cross section of the APD developed by EG&G Optoelectronics for use with 1-mm-diameter fibers. The APD itself is only 0.5 mm wide.

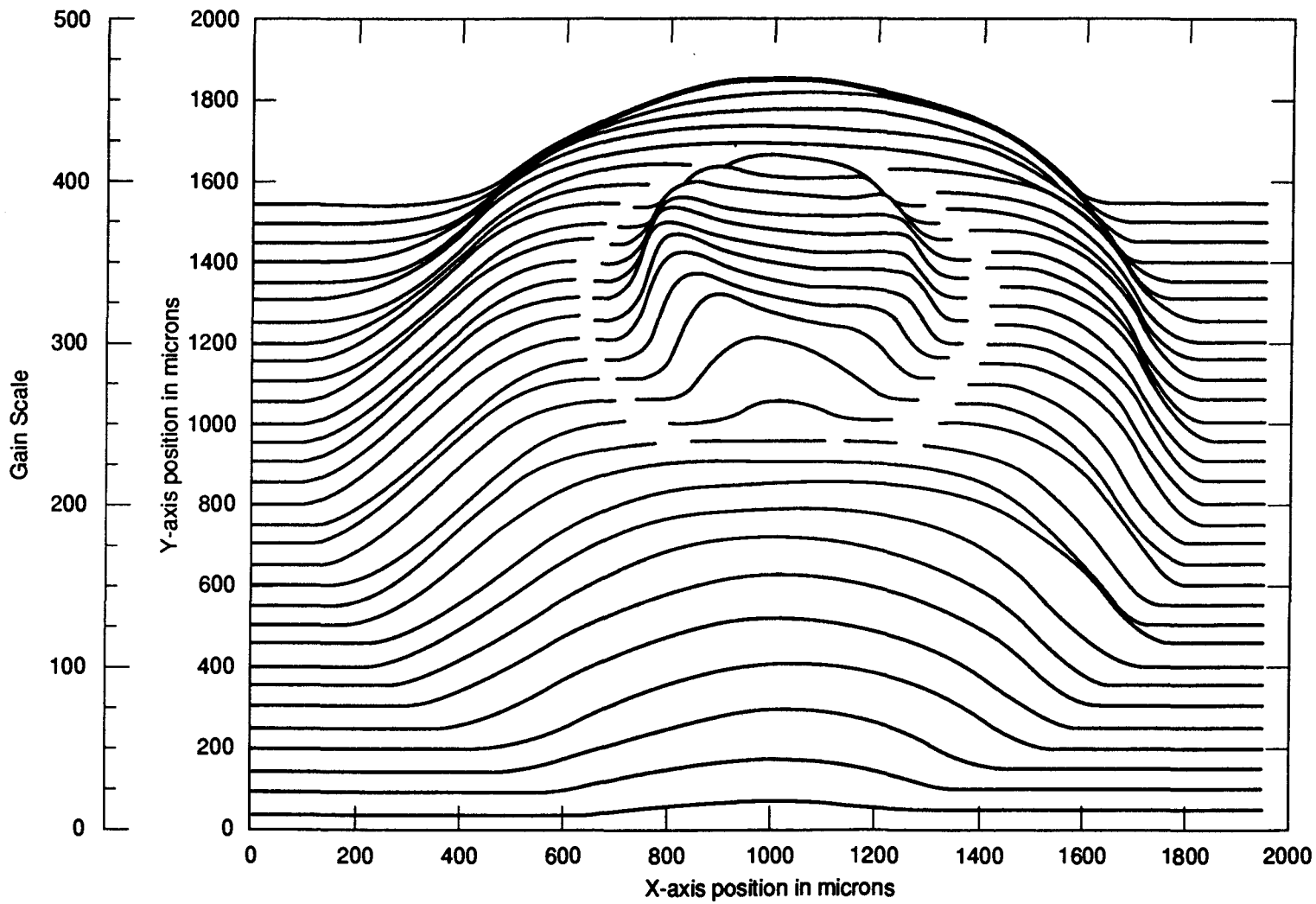

Figure 16. Map of the response of the APD with and without the ball lens assembly. The response without the lens is indicated in the center of the figure. Although the APD itself has a diameter of only 0.5 mm, the lens collects light over about 1.2 mm.

The fiber ends were prepared by cleaving them with a cutter designed to maintain a flat, perpendicular surface. They were then polished with the aid of a holding fixture, using a soft buffing surface. Finished fibers were inserted through the custom-tapered plugs and the plastic optical connectors. The tapers were driven home with the fiber-end protruding 250–500 μm from the end of the connector. This protrusion was chosen to ensure that the contact between the end of the fiber and the APD assembly window provided the mechanical stop, ensuring no gap in the light path. This system is very convenient to use because the optical connections are simple to make and are automatically light-tight.

5.4 System Test Results

As of this writing, the system is installed in the MP hall at Fermilab. It will be attached to the pre-shower detector and placed in the beam in the near future. Meanwhile, a number of system tests have been performed in preparation for actual data-taking.

It is necessary to set the gain of each channel in the entire assembly to an appropriate level. Although channel-to-channel gain variations could be accommodated at the time of off-line analysis, it is preferable to set all channels to the same value. In the present arrangement this is accomplished by adjusting the bias voltage of each APD so that the same signal is observed from all channels when each is excited by the same amount of light. The level of gain chosen for the pre-shower counter is such that the signal from a minimum-ionizing particle (no shower) can just be separated (1σ) from the baseline noise. In this way we should be sensitive to the incoming electron track as we measure the full shower energy deposited in each fiber. When the APD array is used with the shower-maximum detector, this gain will be reduced by about an order of magnitude in order to accommodate the larger signals without saturating the ADCs.

This channel balancing has been accomplished with one complication. The thermal control system as arranged while the crate is outside the detector box cycles approximately ±0.4 C° with a period of about 10 minutes. Over this 0.8 C° temperature range the gain of the APDs, at the setting required for detecting minimum ionizing particles, varies about 10%. Figure 17 shows the measured response of one channel as a function of APD temperature. As seen in the figure, the variation is quite linear over this range so that as the temperature of the devices is recorded along with the output signal level, this variation can be removed during analysis.

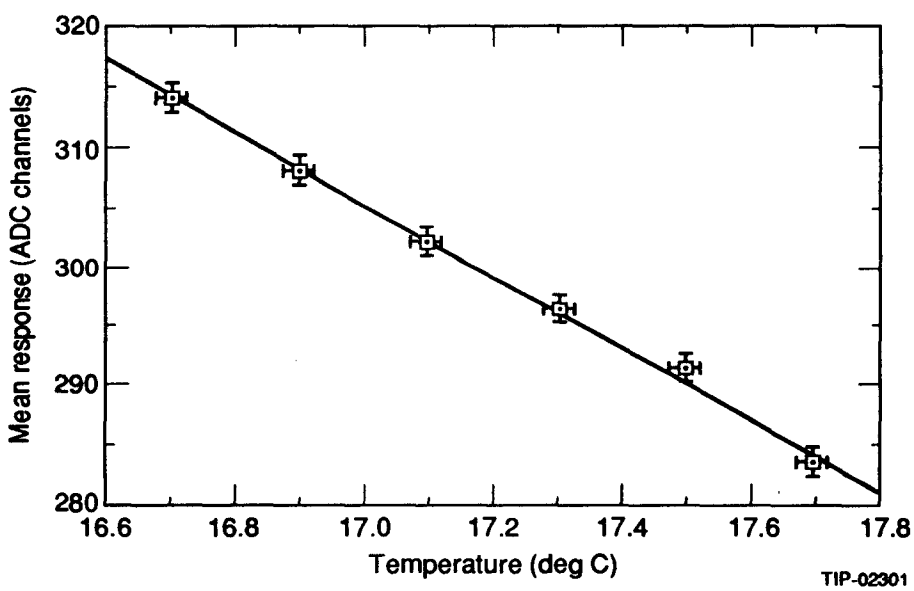

Figure 17. Variation in APD response as a function of temperature. The data were taken by monitoring the system for an extended period of time while the temperature went through its normal cycle. The line represents a least-squares fit.

When the APD system is moved from the pre-shower detector to the shower-maximum detector, the gains of all channels must be reduced uniformly. That this can be done without laboriously retuning each of the 96 channels is demonstrated by Figure 18, which shows the responses of a group of channels to the same light flash at three different global bias voltage settings. It appears that the gains of all of these channels track one another to within 5% over a change in average gain of at least a factor of two. Additional tests are needed to determine whether larger uniform gain variations can be achieved.

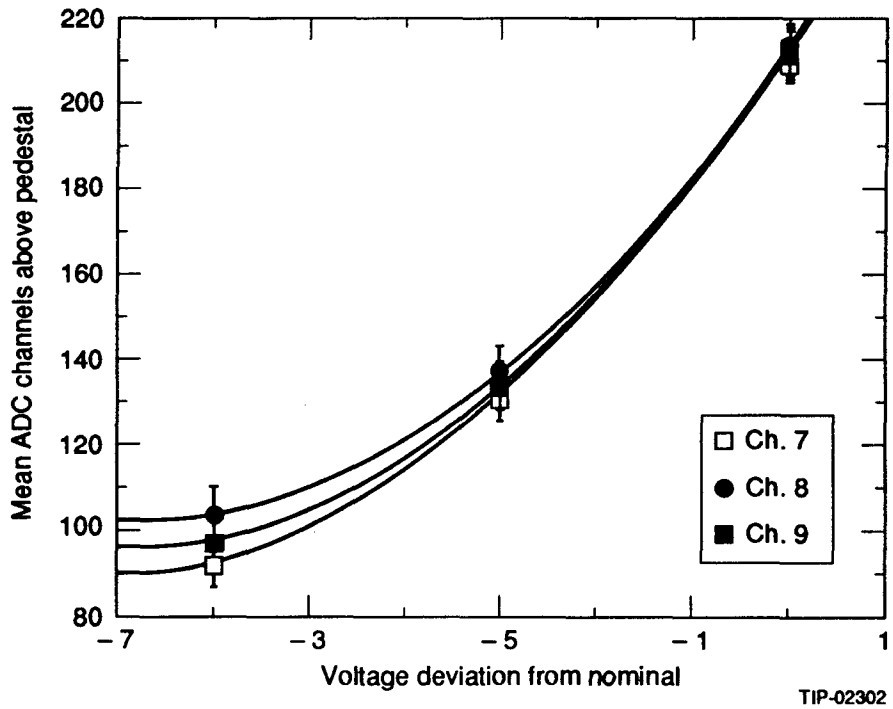

Figure 18. The gain variation of three channels of APD as the global bias voltage supply is varied. The lines are the results of quadratic fits to the data. The error bars represent errors on the means of the distributions.

6.0 SUMMARY

We have designed, built, and begun operation of a 96-channel array of avalanche photodiodes to detect the light produced in the scintillators of a pre-shower detector and a shower-maximum detector. In the process we have observed the relevant characteristics of APDs themselves and have developed practical ways to use them. Appropriate electronics, optical linkages, and environmental controls are necessary for such a system, but none imposes a serious obstacle. We anticipate that data collection in an electron beam will begin shortly and proceed smoothly, and that we will soon be able to report on the results from those tests.

ACKNOWLEDGEMENTS

The authors are deeply indebted to numerous researchers and diligent workers within a variety of organizations who have collaborated or provided advice and assistance during the course of this project. In particular, we wish to thank M. Esaili, G. Hale, and C. Mangene of the SSC Detector Physics Lab for their skill, patience, and diligence in developing and constructing the systems used in the tests described. For the pre-shower counter and arrangements for its use in these tests, we are grateful to researchers at Yale University and Rockefeller University. The development of the APDs by EG&G has been guided by Northeastern University, which provided the devices for this test. M. Hulbert of Northeastern, under the direction of I. Leedom and S. Reucroft, has taken the major responsibility for implementing the APD system in the beamline and for performing most of the system tests and calibration.

REFERENCES

1. L. price et al., Fermilab T841 Proposal, 1990.
2. A. W. Lightstone and R. J. McIntyre, *Proceedings of the Optical Society of America Meeting on Photon Correlation Techniques and Applications*, May 1988.
3. EG&G, Inc., Optoelectronics Division, Vaudreux, Quebec, Canada (formerly a division of RCA).
4. Paul Horowitz and Winfield Hill, *The Art of Electronics*, Cambridge University Press, 1990.
5. S. Aronson et al., D0 design report, Fermilab, November 1984.
6. LeCroy Corporation, 700 Chestnut Ridge Road, Chestnut Ridge, NY, 10977, U.S.A.
7. AMP Corporation, Harrisburg, PA, 17105, U.S.A.
8. Philips Components, 1755 North Collins Blvd., Richardson, TX, 75080, U.S.A.
9. Figure courtesy of R.J. McIntyre, EG&G Optoelectronics.

Disclaimer Notice

This report was prepared as an account of work sponsored by an agency of the United States Government. Neither the United States Government or any agency thereof, nor any of their employees, makes any warranty, express or implied, or assumes any legal liability or responsibility for the accuracy, completeness, or usefulness of any information, apparatus, product, or process disclosed, or represents that its use would not infringe privately owned rights. Reference herein to any specific commercial product, process, or service by trade name, trademark, manufacturer, or otherwise, does not necessarily constitute or imply its endorsement, recommendation, or favoring by the United States Government or any agency thereof. The views and opinions of authors expressed herein do not necessarily state or reflect those of the United States Government or any agency thereof.

Superconducting Super Collider Laboratory is an equal opportunity employer.

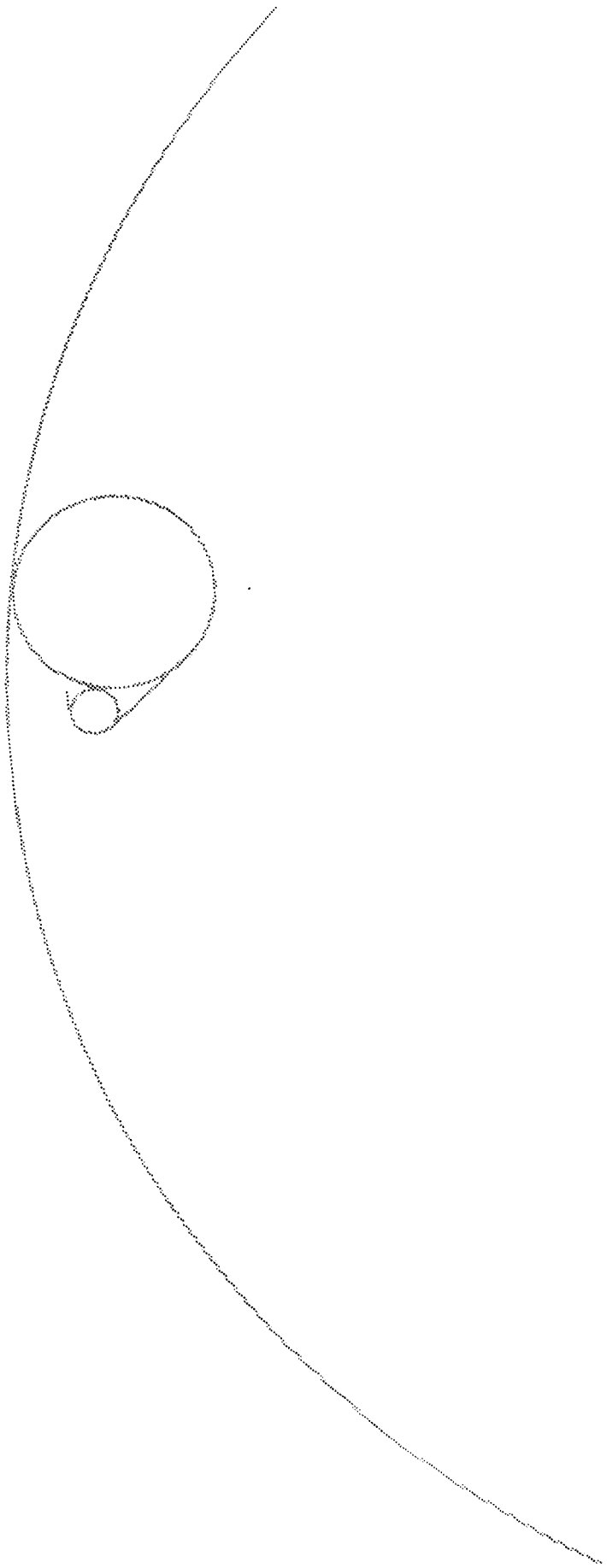

APPENDIX F

A STUDY OF AVALANCHE PHOTO DIODES IN GEIGER MODE

T. Regan and H. Fenker

for The SSC Tracking Group

March, 1992

Over the course of the last few months tests have been conducted on Avalanche Photo Diodes (APD's) in the linear and Geiger modes using the EG&G/RCA C3091S and the Hamamatsu S2383 devices.

A test module consisting of ninety six channels of electronics has been constructed to evaluate the behavior of APD's in the linear mode of operation. Six cards of sixteen channels each are being used in a test beam at Fermi National Accelerator Laboratory to study the APD's in a pre-shower calorimeter using scintillating fibers. The results of this are reported elsewhere[1]. An additional 128 channel test is planned to study the APD's in Geiger mode at that laboratory. One of the criteria to be studied is the behavior of these devices at rates approaching those to be found at the SSC Lab.

Following the results of previous studies by Brown et al.[2] it was first thought that the response speed of an APD might be increased by using some method to truncate the avalanche process. Since this mode of operation yields one to two volt signals, detecting them is a relatively simple process. Early studies demonstrated that the avalanche process was stopped because the voltage developed across the load resistor during avalanche, R1 Figure F-1, would reduced the voltage across the APD thereby bringing it below the breakdown voltage. From that, it seemed appropriate to think that if the avalanche could be quenched, or shortened, and not completely discharge the depletion region, that faster (higher rates) could be more easily achieved when combined with re-charging techniques.

The electrical properties of an inductor, coupled with the fast avalanche times of the APD would seem to be able to enhance that process. A 25 μH inductor was added, Figure F-2, in series with the bias supply and the cathode of the APD to cause an additional fast voltage drop, further reducing the voltage across the device as soon as any current began to flow into or out of it. In principle this would result in a lower amplitude signal but one which was still easily detectable and would inhibit the avalanche, at least somewhat.

Toward that end we designed and developed a test procedure whereby we would attempt to double pulse a green LED, 565 nm, driven by a Hewlett Packard pulse generator model 8082A, at pulse intervals of less than 300 nanoseconds (ns). The signal observed on the cathode of the APD, using a Tektronix 10X probe and an fast oscilloscope of like make, was negative going, in time with the pulse generator and was of approximately 200 mV in amplitude. This level would change as the bias voltage to the APD was varied. The anode signal was found to have an amplitude of ~ 2V, again depending on the bias voltage, and with a recharge time essentially unchanged from the first test. This recharge time is a simple RC time constant dependent on the current limiting resistor, R1, and the junction capacity of the depleted APD.

With the pulse generator set to deliver 200 ns pulse pairs, 20 ns wide, at 4 kHz repetition rate it is possible to re-pulse the APD when the high voltage is set carefully. (Figure F-3.) At this point we were uncertain of the number of photons being generated or converted. This soon proved to be very limiting since the LED simply would not respond quickly enough to the 5 volt, 20 ns pulses generated (Figure F-4). A fast, high voltage (Hg reed relay) pulser is needed to generate short high

---

[1] H. Fenker, et al., Progress in the Use of Avalanche Photodiodes for the Readout of Calorimeters, SSCL-552, 1991.

[2] R.G.W. Brown et al., Applied Optics / Vol 25, No.22 / 15 Nov. 1986 2 - OSA Proceedings May 31-June2 1988

voltage (~200V) pulses which will in turn create precise bursts of light to evaluate the APD's at a adequate quantitative level. A pulsed laser of the right frequency, ~450 nm, would be a far better solution to the problem if it could produce pulse pairs of the proper duty cycle.

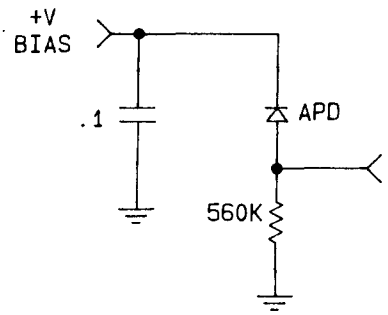

Figure F-1

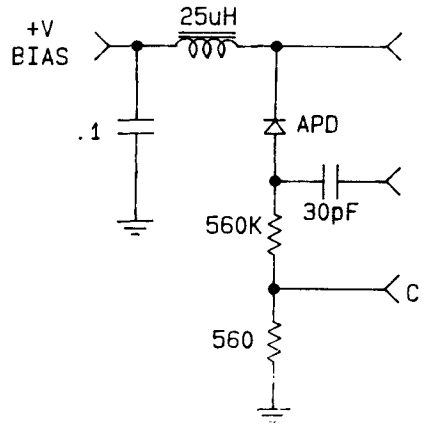

Figure F-2

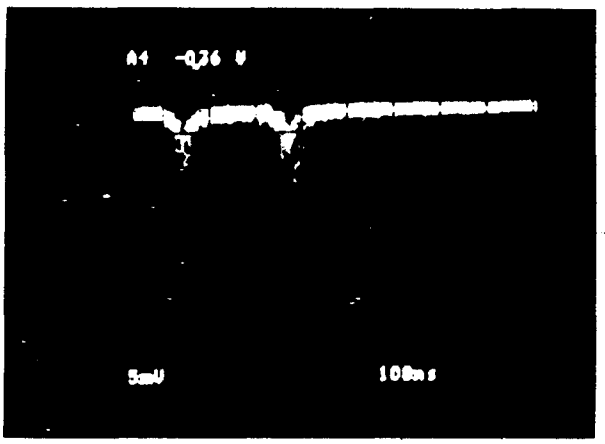

Figure F-3 Depicts Second Signal From APD on Order of 200ns

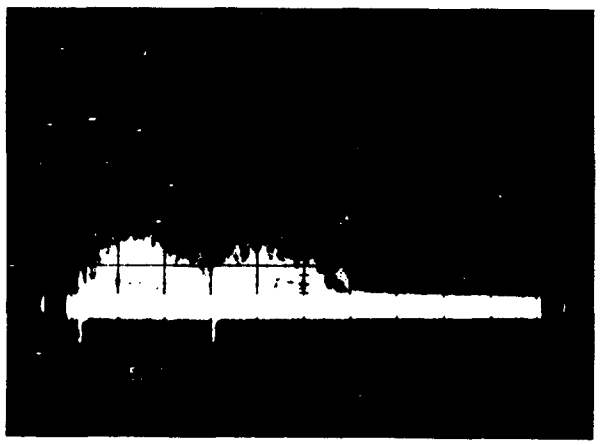

Figure F-4 Results of Low Exitation Voltage to DED Producing Excessive Time Smear from APD

While McIntyre et al [3] have mentioned the need to reduce stray capacitance, it was not at all clear that it must be almost totally eliminated. The anode of the APD is the high impedance point (electron collection point) in the system and any stray capacity to ground, ≥10pF, will completely bypass the high frequency component of the avalanche signal. This effect was observed when a probe was inserted to monitor the anode signal and the waveform at the divider, Figure F-3 test point "C", vanished. Since any silicon diode which is reverse biased behaves like a capacitor, it is

[3] A. W. Lightstone and R. J. McIntyre, Proceedings of the Optical Society of America Meeting on Photon Correlation Techniques and Applications; May, 1988.

apparent that the APD acts like a capacitor which is discharged into the load resistor at sub-nanosecond rise times. If any stray capacity to ground exists, the charge will be shunted around the divider network. While monitoring the cathode, a 15pF capacitor was connected between the anode of the APD and ground. The signal seen at the inductor-cathode junction increased markedly in amplitude suggesting an increase in signal current. Using this property, we coupled to the anode using a 30 pF capacitor into 51 ohms and observed fast signals, albeit differentiated, but in time with those at the cathode. Again the key to using these devices is to understand that they behave as a discharging capacitor does. If the charge is not totally depleted after one avalanche the device can be retriggered to produce another avalanche that is smaller but still easily detectable, Figure F-5.

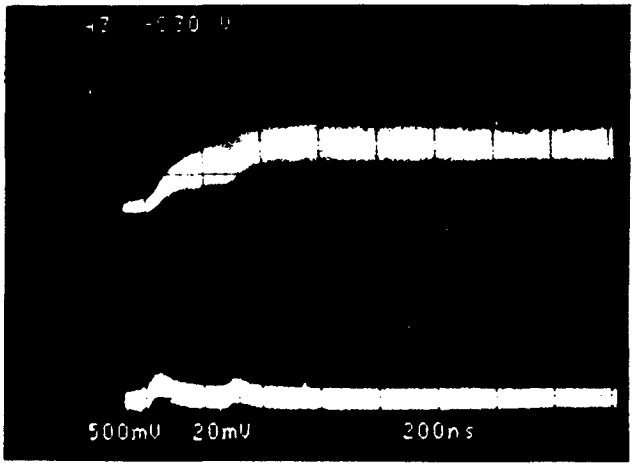

Figure F-5 Signal from Anode of APD Showing that Enough Charge Exists to Produce a Second Signal.

These results are encouraging, however there remains more work to be done. Certainly we need a faster and more accurate dual pulse generating system for more quantitative results at all light levels and at CW rates equal to at least 70 MHz. We need to evaluate the APD in different configurations where a negative bias supply is used in concert with the inductor at the anode and the output signal studied at both terminals of the APD. Different coupling methods need to be investigated and additionally, we need to study recharging methods using fast comparators and MOS switches.

APPENDIX G

INVOLVEMENT OF THE SSC TRACKING GROUP WITH VISIBLE LIGHT PHOTON COUNTERS

K. MORGAN, J. THOMAS, H. FENKER,

FOR THE SSC TRACKING GROUP

MARCH, 1992

Members of the Tracking Group at the Superconducting Supercollider Laboratory are pursuing a comparison of several different options for the light-sensitive elements of future scintillating fiber trackers. Visible Light Photon Counters (VLPCs) are very attractive devices which have recently been developed. The Group is setting up a test station to contribute to the evaluation of VLPCs. This report summarizes the hands-on experience with VLPCs gained by the authors in preparation for continuing this work.

Introduction

As part of our efforts toward developing readout systems for Scintillating Fibers we have established collaboration with Professor M. Atac from FNAL and UCLA. Dr. Atac is a pioneer in the development of cryogenic photo multipliers for scintillating fiber detectors. His original work with D. Petroff of the Rockwell International Science Center led to the application of Solid State Photo Multipliers (SSPM) to High Energy Physics detectors. Their success with the SSPM's led to the development of better optimized light counters which are less sensitive to the infra red components and more sensitive to visible light, Figure G-1. These newer devices are the Visible Light Photon Counters (VLPC)[4] Dr. Atac came to the the SSCL in July, 1991 to work on VLPC's and we progressed in two areas: 1) mechanical alignment and connections of VLPC's and 2) design of a VLPC support system for our further use here.

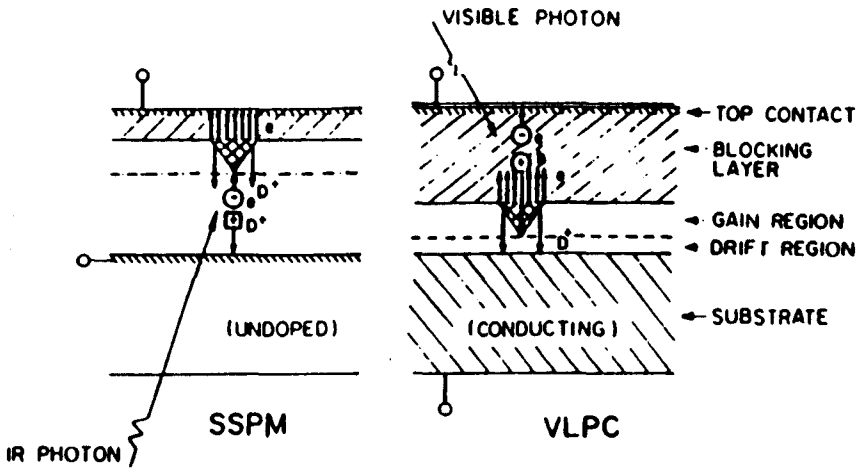

Figure G-1: Operation Principles of the SSPM and VLPC are indicated.

Mechanical Alignment and Connections of VLPC's

Rockwell International has cast the first arrays of VLPC's with 8 active channels on a single substrate. This small device is about 2 mm wide and 10 mm long with a center to center spacing of the eight active elements of less than 1 mm. In order to gain an understanding of the

---

[4]M. Atac et al., "Scintillating Fiber Tracking for the SSC Using Visible Light Photon Counters", prodeedings of the Fifth International Pisa Conference on Advanced Detectors, May, 1991.

technological difficulty of working with these arrays we mounted two of them into their cassette holders here at the SSCL, Figure G-2. Working under a microscope using parts fabricated at Fermilab which were then modified here, we mounted the arrays on small metal cassettes and soldered the output connections to stainless steel coaxial cables. Both operations were extremely delicate; jewelers screws were used to attach the VLPC mounting to the cassette holder and single strands of conductor were carefully cut to length and bent before being soldered into position on the output leads. Clear fibers were strung through the access rod of the cold finger cryogenic support with the intention of aligning them in near contact with each of the eight VLPC's. It was discovered that the spacing on the input holder did not match that of the array and this alignment step would not be adequate until the fiber holder was remade.

While we were not able to complete all of the tests, we accomplished our primary goal of gaining expertise in working with these tiny, delicate devices. We see some areas where the design of the current cassette can be improved and simplified. We have gained the knowledge necessary to fabricate our own cold finger/VLPC cassette holder in preparation for the delivery of VLPC's for testing here at the SSCL.

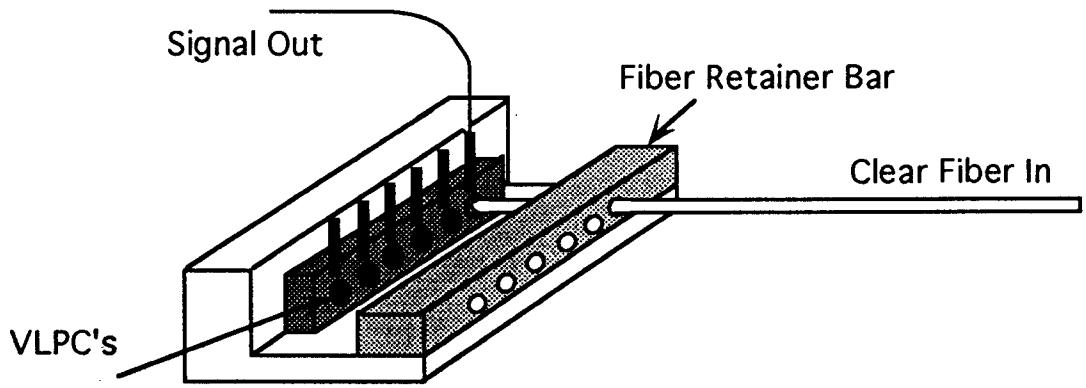

Figure G-2: VLPC Array with clear input fiber.

VLPC Support System

Operation of the VLPC requires a temperature of 7 degrees Kelvin. This is accomplished by using a cold finger in a liquid Helium cryostat and allowing the escaping gases to create a natural transition to room temperature along the support rod of the cold finger. Light signals and low voltage must be introduced via this support rod and the resultant electronic signals exited via the same rod. In order to understand the system and to help design our own version, we assembled the necessary components to make one VLPC work. Dr. Atac supplied the VLPC and the support rod/cold finger as well as a temperature monitor. We used a liquid helium cryostat borrowed from the Accelerator Division and our own test set-up for APD's to generate the input light, Figure G-3. The light was channeled into the VLPC on a clear fiber which was simply brought into contact with the input fiber of the VLPC. Since we could inject as much light as desired, no attempt was made to avoid light loss in connections; however this is a concern for future R & D work. In a matter of minutes from the moment we had cooled the cryostat we had injected light into the VLPC and photographed the resultant signals on our oscilloscope, Figure G-4. We were able to see traces from the multiple photoelectron pulses in well resolved bands.

The purpose of this exercise, to understand the difficulties of making VLPC's work, was easily accomplished. The operation of the device was much simpler than we had expected and we can now proceed to creating our own systems and design the experiments necessary to explore the performance of both the readouts and the detectors themselves.

Late in the summer of 1991, four members of our group traveled to UCLA to participate in tests of VLPC's and in measurements of attenuation lengths of scintillating fibers with different concentrations of dyes. The data collected in these measurements are published in a UCLA Preprint, and the paper has also been submitted to NIM[2]. We gained expertise in the operation of the cryogenic system for 16 channels of VLPC's and we also finalized the design of our own dipstick cryostat for continuing studies at the SSCL. Since that time we have constructed the dipstick assembly of high purity copper and low thermal expansion steel. We have purchased the necessary helium cryostat. We have acquired the necessary electronics to readout the VLPC's and we have developed the data acquisition system for making our measurements. These measurements await the arrival of the first restriction free VLPC's, the HISTE-3 model. We expect these to be available in the Spring of 1992.

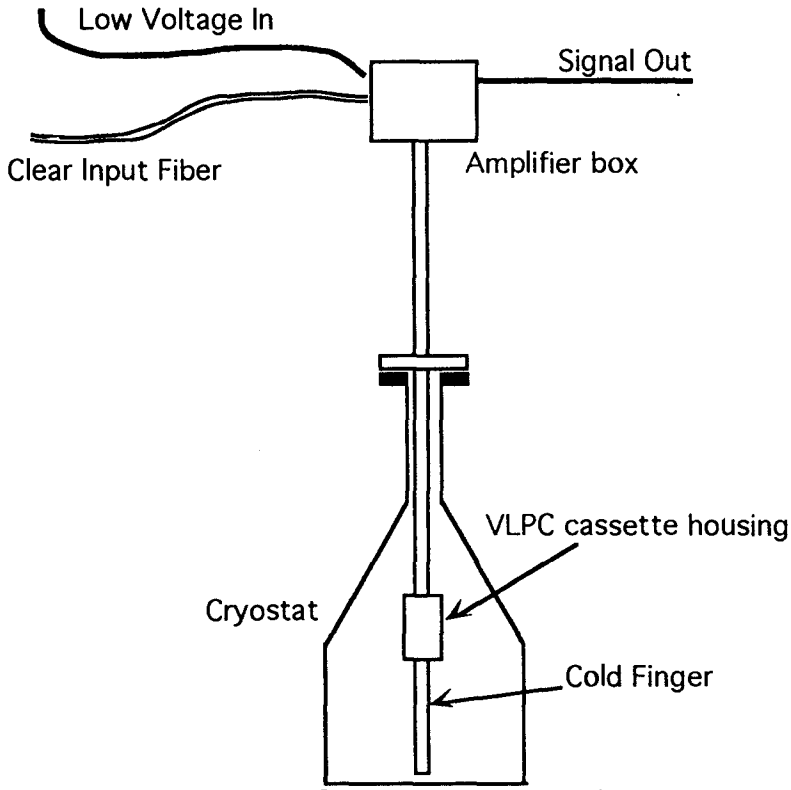

Figure G-3: VLPC Housing and Amplifier

2 Tracking with Scintillating Fibers and Visible Light Photon Counters, M. Atac, *et al.*, UCLA-PPH0040-2/92.

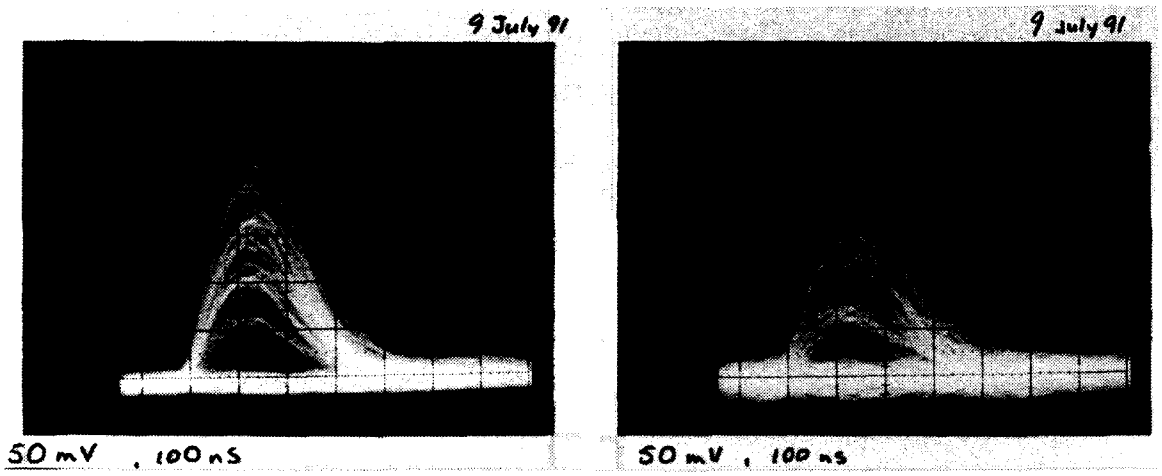

Figure G-4: Oscilloscope Pictures of Multiple Photoelectron Pulses from a VLPC.

APPENDIX H

PROGRESS ON TRACKING DETECTOR SIMULATIONS

F. BIRD AND D. COUPAL

FOR THE SSC TRACKING GROUP

MARCH, 1992

The goal of reconstructing charged particles in the SSC environment places critical demands on any tracking detector design. Physics goals require good efficiency and high resolution over large rapidity ($|\eta|<2.5$) for momenta of hundreds of MeV/c to hundreds of GeV/c. Any design must contend with hundreds of tracks due to overlapping events from in-time and prior beam crossings in the most robust but cost-effective way. Many physicists at SSCL and elsewhere are working hard to simulate the expected environment to evaluate various tracking schemes. The SSC Laboratory has become a center for these studies, with its Physics Detector Simulation Facility providing the essential computing power. Efforts within SSCL have focussed on SDC detector designs, but the results are generally applicable to detector options being considered by other collaborations.

A complete detector simulation requires a set of Monte Carlo event generators which provide physics input, a model of the detector under study, in this case a detector 'constructed' with the GEANT program, and some algorithms by which to reconstruct the events from the detector data. A set of routines to generate events for the SDC detector simulation was written and integrated into the SDC software package. These routines provide the capability for overlaying events from different generators to simulate backgrounds from multiple interactions over many beam crossings.

Examples of candidate designs for the SDC are shown in figures H-1 and H-2. Both designs have the same inner tracking detector, multiple layers of double-sided silicon strips with 50 micron pitch. The designs differ in their choice of outer tracker, one built with 4mm straw tubes and the other with 850 micron scintillating fiber. As an aid to the study of these (and other) designs, a set of fast simulation routines was also written for the SDC software package. The fast simulation calculates momentum resolution for Monte Carlo tracks given the positions, measurement errors, and radiation lengths (for the multiple scattering contribution) of the tracking detectors, for the central and forward regions. Figures H-3 and H-4 shows the results of such calculations for the two SDC alternatives.

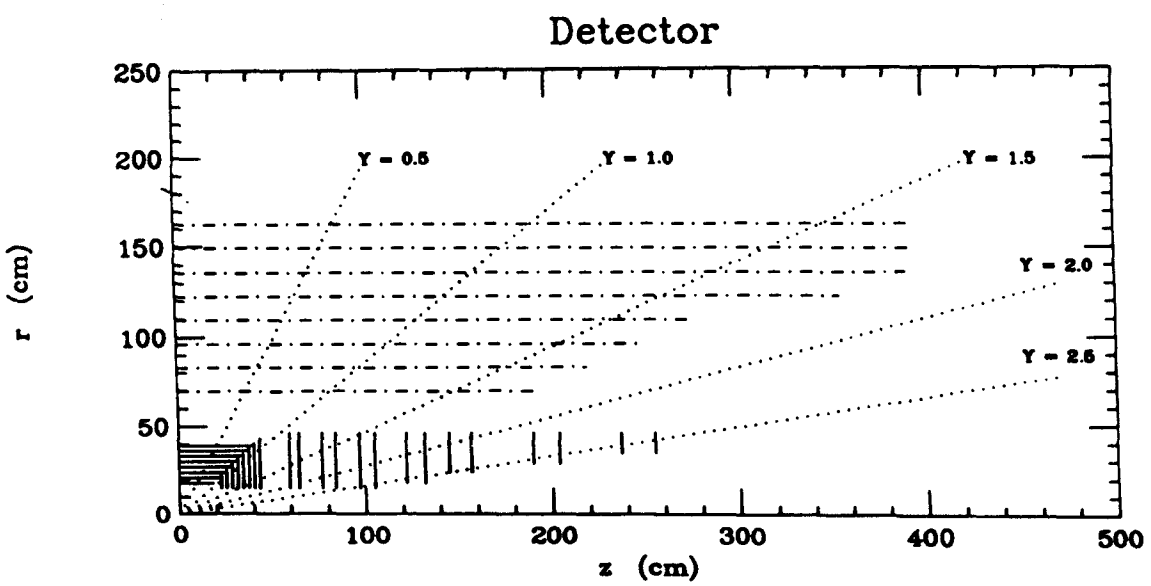

Figure H-1: The Straw Tube Outer Tracker and Silicon Inner Tracker Design Option for SDC

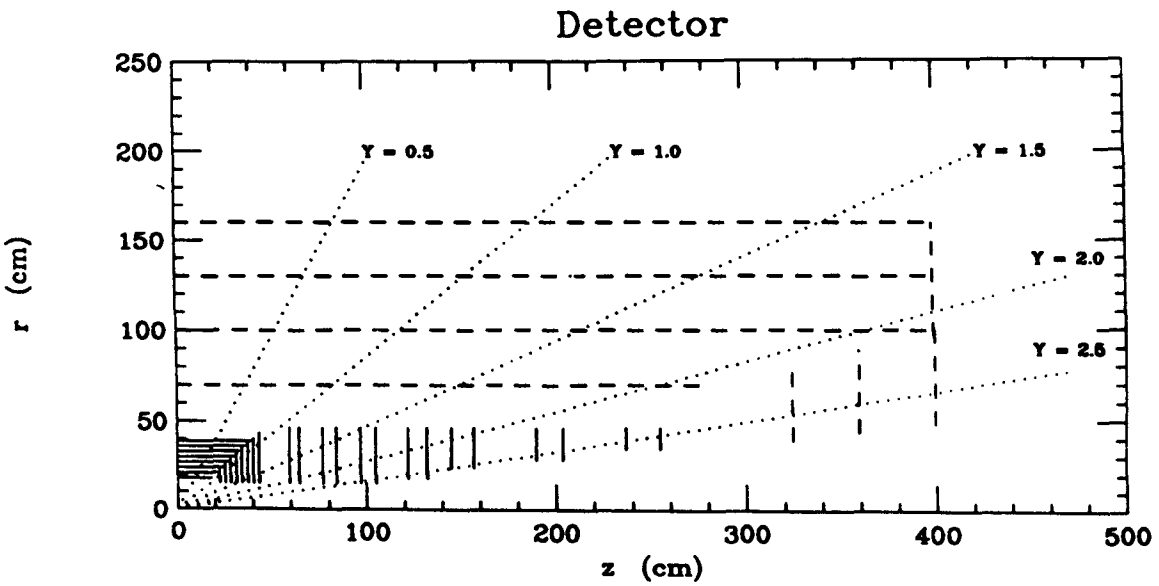

Figure H-2: The Scintillating Fiber Outer Tracker and Silicon Inner Tracker Design Option for SDC

The much more difficult issues of pattern recognition and track reconstruction efficiency require the complete detailed simulation of the detector and some means of finding and fitting tracks. The software tools for these studies have recently advanced to the point of providing preliminary answers to some of these hard questions. For example, Figure H-5 shows a sample event viewed along the beam direction –in this case a Higgs decaying to four muons with a background of minimum bias interactions appropriate for a luminosity of 10^{33} cm^2 sec^{-1}. Figure H-6 shows the results from a calculation of the channel occupancies for the silicon/outer tracking options of SDC as various ingredients in the simulation are "turned on". These initial studies will provide important information to help select between the SDC options, as they are based upon the most thorough simulation of the expected SSC environment available at present. Clearly, much work remains to develop and understand the optimal algorithms for track reconstruction and fitting, work that we intend to pursue in earnest at SSCL.

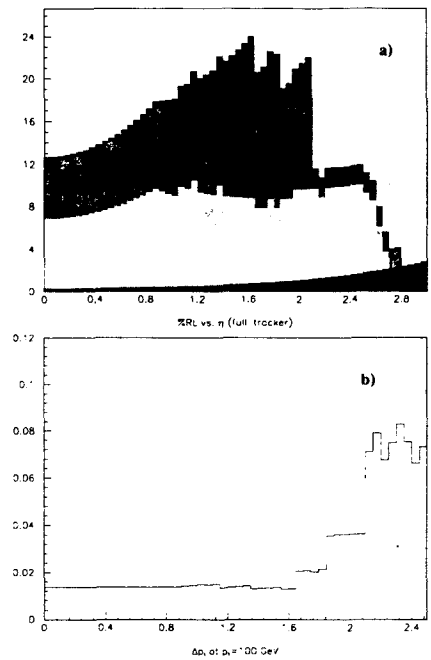

Figure H-3: a) Radiation length versus η for the scintillating fiber outer tracker option. The lower shaded area is the beam pipe, the middle area is the silicon tracker and the upper region is the fiber outer tracker. b) p_T resolution versus η for the total system.

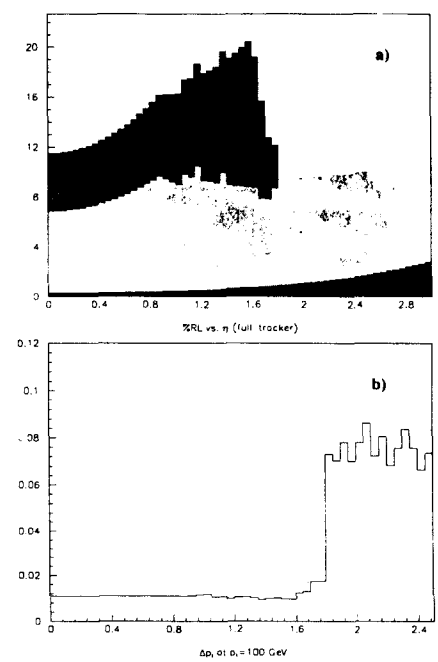

Figure H-4 a) Radiation length versus η for the straw tube outer tracker option. The lower shaded area is the beam pipe, the middle area is the silicon tracker and the upper region is the straw tube outer tracker. A forward outer tracker was not included in this study. b) p_T resolution versus η for the total system.

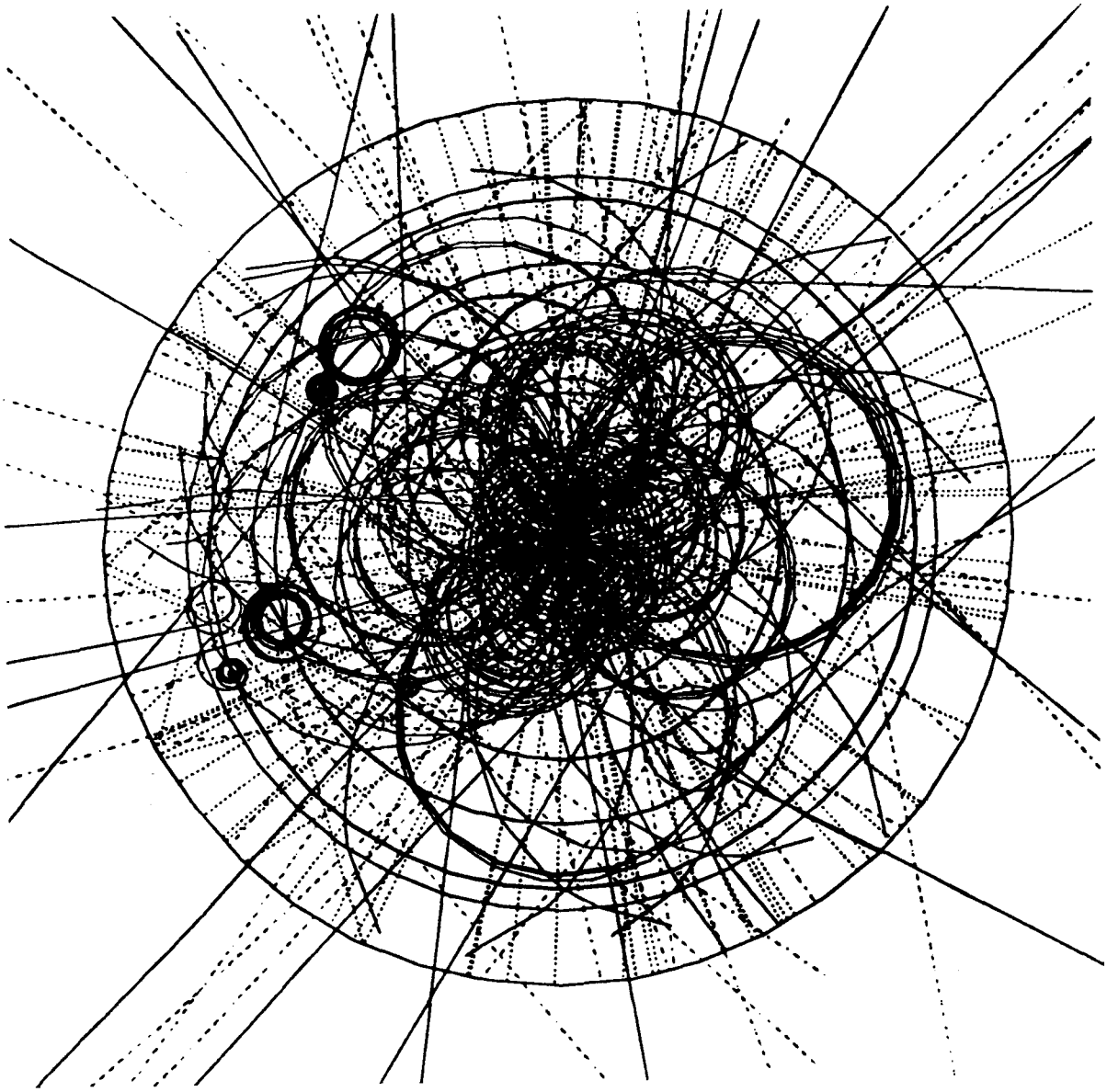

Figure H-5: Higgs decay to four muons plus minimum bias background in the SDC central tracker viewed along the beam direction. Only tracks in the barrel part of the silicon inner tracker ($|\eta| < .8$) are plotted. Charged tracks are shown as solid lines. Concentric rings indicate the eight layer silicon barrel, the four-layer fiber tracker and the solenoidal magnet coil.

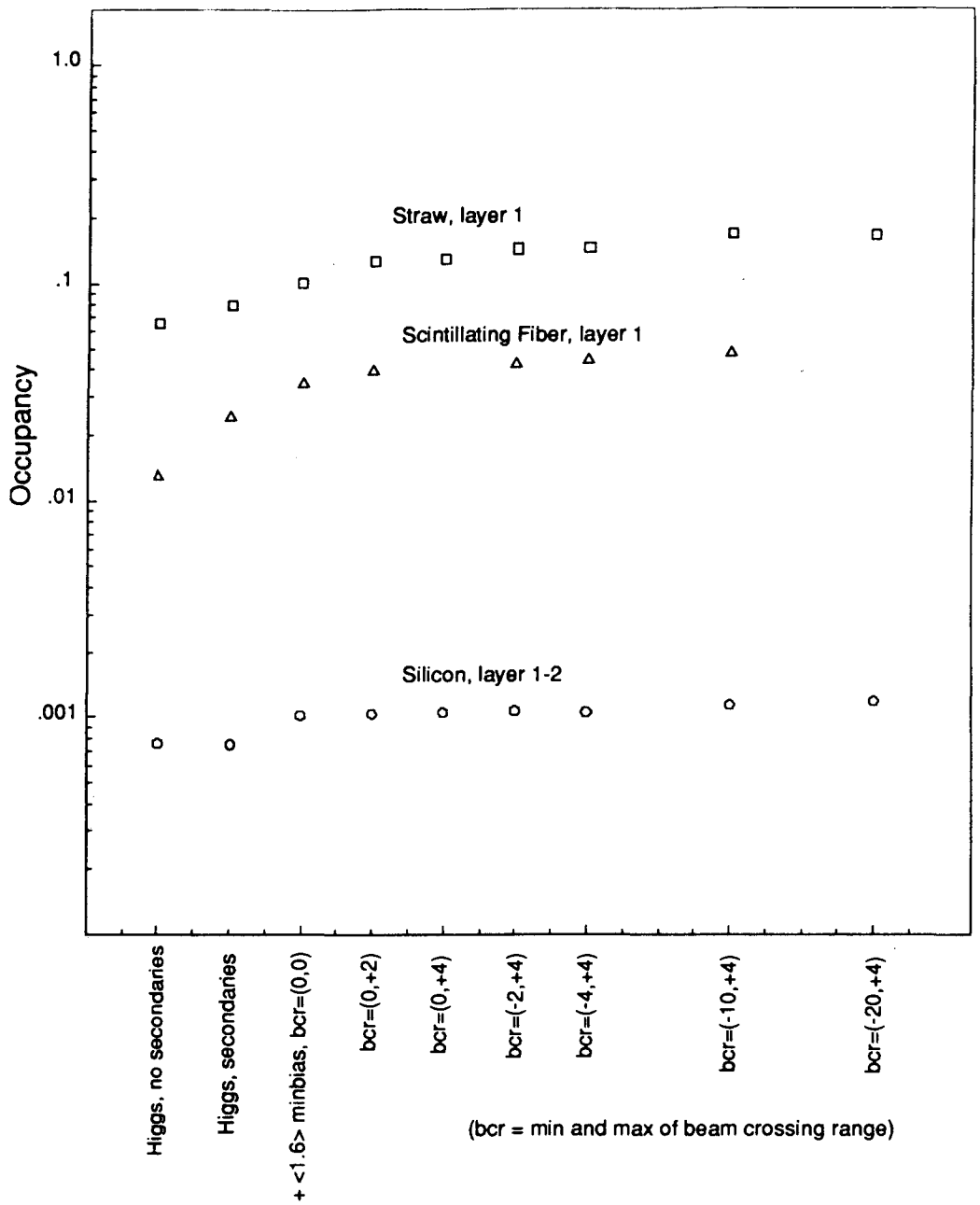

Figure H-6: Occupancy in the SDC Inner Silicon Layers and Innermost Layers of the Two Outer Tracker Options Under Various conditions in the simulation.

APPENDIX I

FRONT END FOR GAS MICROSTRIP DETECTORS

Guy Vanstraelen, Maher Abuzaid SSC Laboratory

System Configuration

Gas microstrip detectors are one of the tracking detector options for the forward region of the tracking volume. In collaboration with the SDC group we have designed a chip that meets the very stringent requirements of speed, low power consumption and high channel count.

The read-out system consists of 4 basic blocks shown in Figure I-1. The first block is analog, and consists of a preamp-comparator combination. The preamp is designed to provide sufficient amplification for the incoming signals to trip the comparator. The nominal input signal is $2.0\ 10^5\ e^-$ on a 5 pF strip capacitance. The rise and fall time of the signal are 10 ns, its pulse width is 20 ns. This is equivalent to an input current of $3.2\ 10^{-14}$ C/30 ns $\approx$ 1.07 μA. The comparator is designed to sense signals that have 1/20 the magnitude of the previously mentioned signal.

Further requirements or desires are a minimum power dissipation, slewing independent of the signal amplitude, minimum recovery time, and an input referred noise of less than 1000 e^-. The second block consists of a series of latches organized as shift register, that samples the comparator output and stores it during the level 1 trigger decision time, which is currently estimated to be around 4 μs. The shifting is synchronous with the SSC clock, running at 62.5 MHz. Because the pulse width of the comparator is longer than one clock period, a '1'-suppression circuit is build into the shift register. This circuit will pass only the first '1' in a series. Upon arrival of a level 1 trigger signal, data from the shift register is made available to the third block, an encoder circuit, which encodes the input data of the parallel channels into a centroid and a width code. The encoder should be able to handle multiple hits, represented by more than one group of activated channels. The final block is an 8 bit digital counter, which performs the task of local bunch counter (LBC). Its count is latched into a buffer, each time the encoder accepts new input, and is made available together with the encoded data. In this way relative timing information is provided.

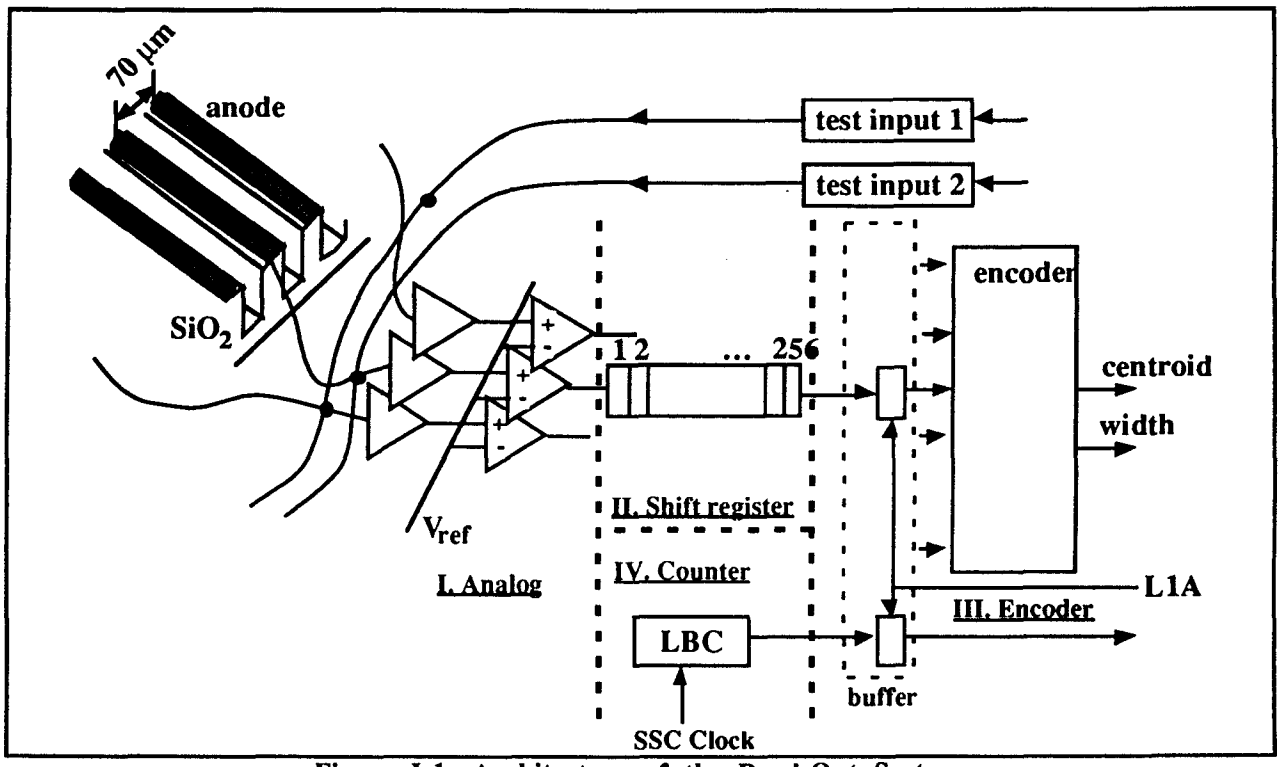

Figure I-1: Architecture of the Read-Out System.

Preamp-Comparator Combination.

The high detector capacitance makes a preamp with low input impedance a necessity. This can be accomplished by using a diode connected MOSFET to receive the signal, or by using of current sensitive amplifier. Both methods are explained next. To reach high speed and low power dissipation, a basic dilemma has to be solved. For a voltage sensitive amplifier, gain is given by $g_m r_o$, where g_m is the transconductance of the input transistor and r_o is the output impedance. The bandwidth (BW) is given by $1/(r_o C_L)$, with C_L the load capacitance. Achieving a BW of 10 MHz and a gain of 200 requires for $C_L = 50$ fF that $g_m > 625$ µS and that $r_o < 320$ kΩ. If the input transistor is biased in strong inversion, then $g_m = \sqrt{2\beta I_{ds}}$, with $\beta = \mu C_{ox} \frac{W}{L}$. In the latter formula, μ is the minority carrier surface mobility in $cm^2/(Vs)$, C_{ox} is the oxide capacitance in F/cm^2 and W/L is the width to length ratio of the MOS device. For a typical 1.2 µm CMOS process, $\beta \approx 47 \frac{W}{L}$ µS, resulting in the requirement $I_{ds} \frac{W}{L} > 4.2$ mA. If for example W/L = 100, then $I_{ds} > 42$ µA, which contradicts with the restrictions on power dissipation.

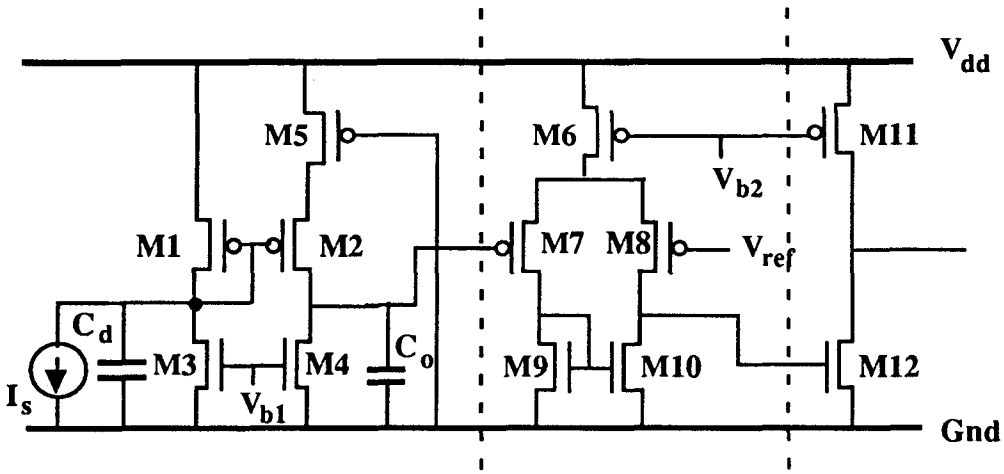

Figure I-2: Preamp With Diode Connected Input Transistor.

The first method to achieve low input impedance is illustrated in Figure I-2. The diode connected MOSFET M1 takes care of resetting the strip capacitance, M2 is the input transistor for the preamp. The gain for this configuration is limited to approximately 40. A problem with the circuit is the recovery of DC node voltages after applying an input pulse. The recovery time can only be shortened by increasing the bias current. This however decreases the gain. In order to have an input range of 0.05 to 1 μA, the preamp has to be followed by an additional amplifier stage and a high gain comparator. A further disadvantage of the current-mirror input is an increase in input referred noise due to the use of a current mirror.

The second solution is a current sensitive amplifier. Figure I-3 depicts the design in the Westinghouse n-well process. A half folded cascode (HFC) configuration is used as preamp. Table 1 gives the transistor dimensions corresponding to Figure I-3. The preamp-comparator combination uses ± 1.5 V as supply voltage. Only one additional bias voltage (V_b = 0.5 V) is needed. For stability reasons a small compensation capacitor C_c of 50 fF is needed in parallel with the feedback resistor. If this capacitor is eliminated, the ac response shows peaking around 10 MHz. The frequency response of the preamp, V_{out}/I_{in} and the phase shift, with and without C_c is shown in Figure I-4. The total power dissipation for the circuit is 181 μW. Figure I-5 illustrates the magnitude of the signals for a 0.05 μA input signal. Figure 6 shows the slewing, recovery time, double pulse resolution and width of the output pulse for the circuit. The double pulse resolution (DPR) is defined as the distance of two input pulses that appear as two separate pulses at the output. By increasing the size of M13 (increasing current) the slewing for small input signals can be improved. However, the DPR degrades. The recovery time and slewing can be changed by adapting the switching threshold voltage of the output inverter. By lowering the threshold voltage the slewing is decreased and the recovery time is increased. A version of the analog circuit suitable for fabrication in the UTMC p-well process is shown in Figure I-7. The circuit dissipates 100 μW. Its speed is reflected by Figure I-8. The transistor parameters are given in Table I-2. Notwithstanding the body effect for the input devices, the same comparator is used as for the Westinghouse n-well process. The reason being the fact that this type provides a convenient DC output voltage, putting the output inverter in a region of almost zero stand-by power. A p-channel device was chosen over an n-channel device to implement the feedback resistor because of its higher resistance. C_c had to be increased to 150 fF in this circuit.

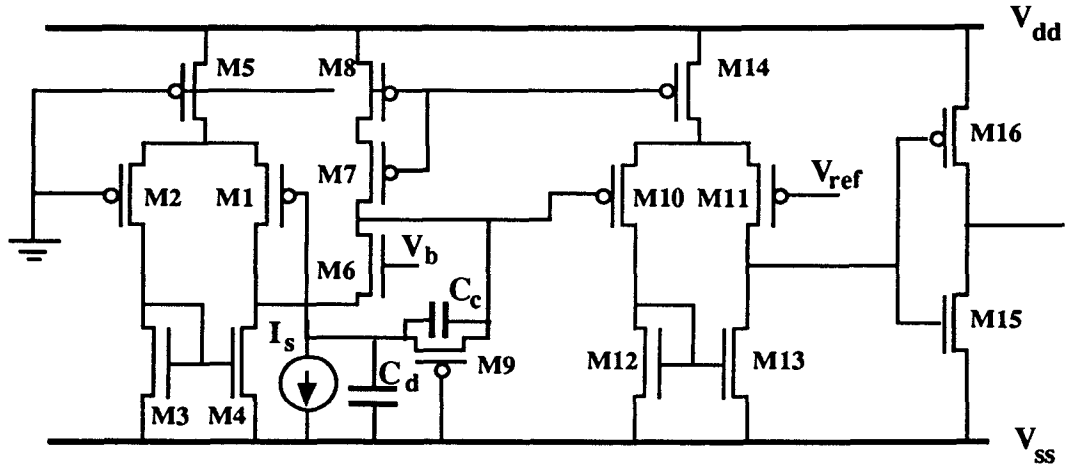

Figure I-3: Current sensitive amplifier combined with comparator and output buffer, and to be implemented in the 1.2 μm n-well Westinghouse process.

Table I-1: Transistor sizes and DC parameters for the HFC-comparator circuit

Transistor	W/L	I_{ds} [μA]	g_m [μS]	g_{ds} [μS]
M1 = M2	500/2	10.7	338.0	19.5
M3	20/1.2	10.7	133.6	0.1
M4	40/1.2	20.6	266.4	0.2
M5	10/2	21.4	59.0	4.2
M6	4/1.2	9.9	55.9	0.2
M7	4/1.2	9.9	36.2	1.1
M8	10/2	9.9	16.8	48.9
M9	3/40	0.0	0.0	0.93
M10 = M11	40/1.2	8.75	11.3	3.4
M12 = M13	5/1.2	8.75	59.1	0.15
M14	6/1.5	17.5	44.6	8.4
M15	4/1.2	11.9	9.5	71.3
M16	8/1.2	11.9	90.3	0.19

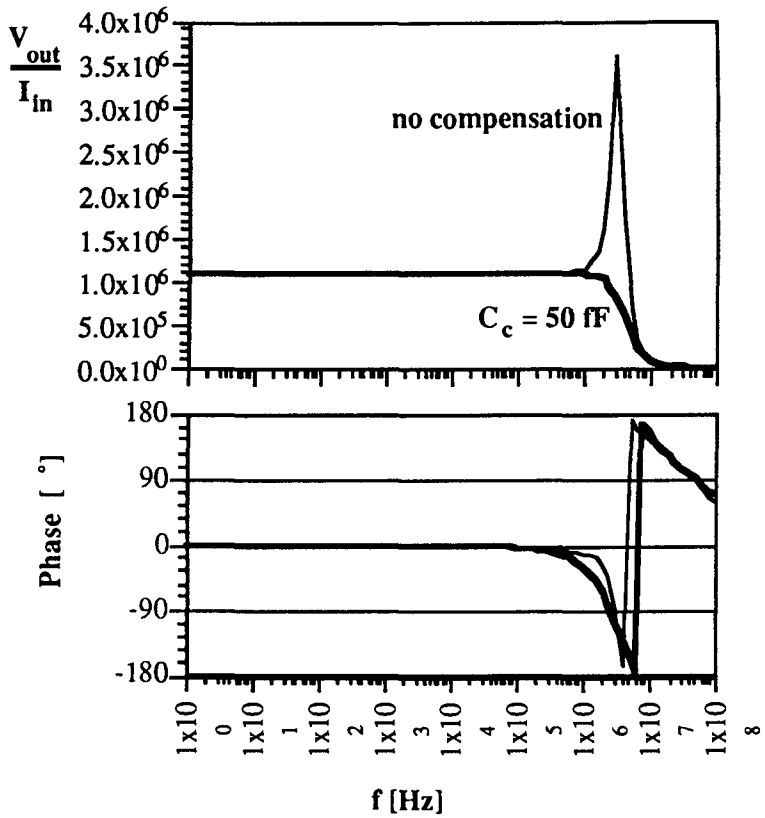

Figure I-4: Transresistance and Phase of the Preamp With and Without Compensation.

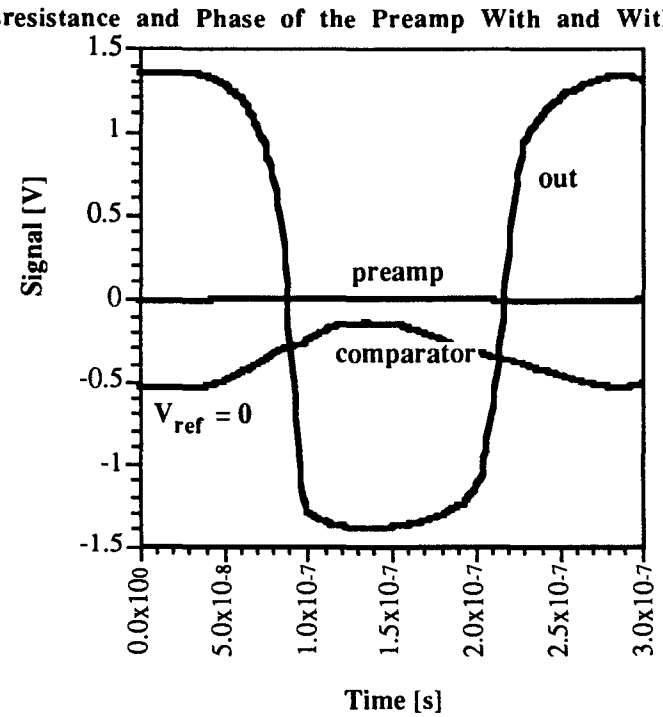

Figure I-5: Output signal of the preamp, comparator and buffer in response to a 0.05 μA input signal. The plot indicates how tiny the actual input signal is.

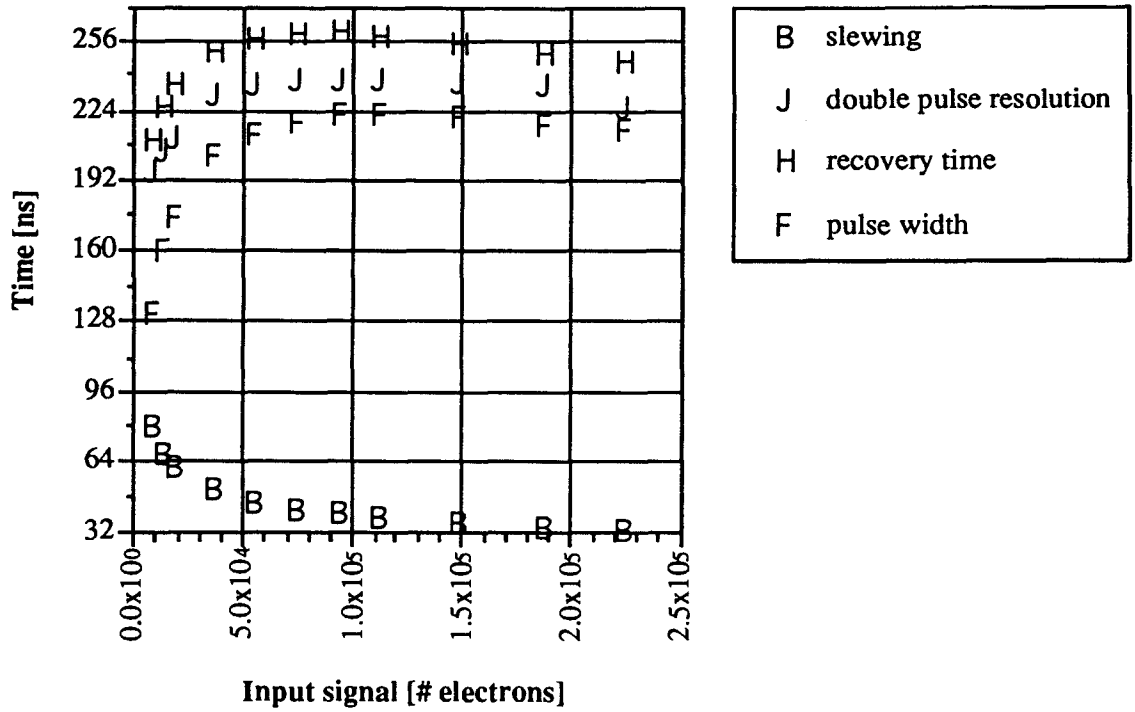

Figure I-6: Slewing, double pulse resolution, recovery time and output pulse width as a function of the input signal.

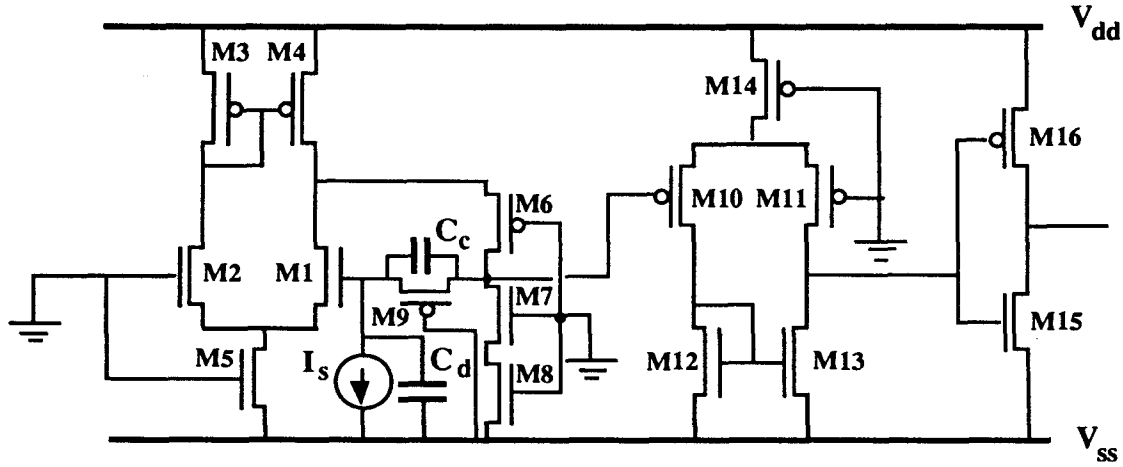

Figure I-7: Analog circuitry for the 1.2 μm p-well UTMC process.

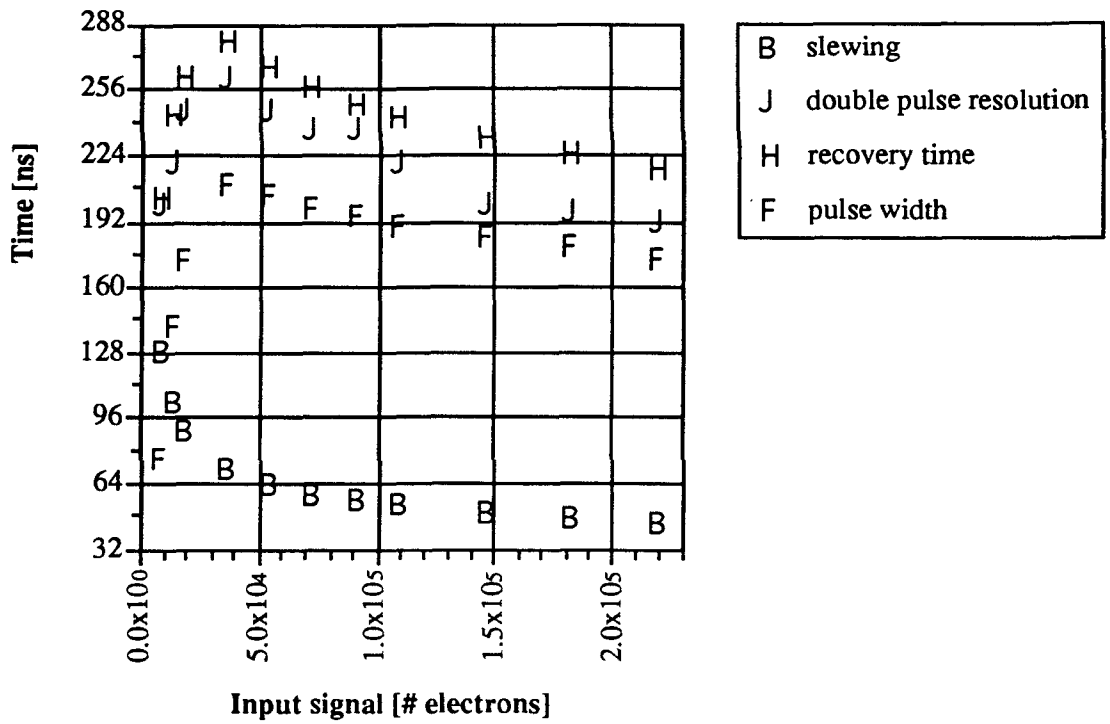

Figure I-8: Slewing, double pulse resolution, recovery time and output pulse width for the circuit of Figure 4.4.2-7.

Transistor	W/L	I_{ds} [μA]	g_m [μS]	g_{ds} [μS]
M1 = M2	250/2	3.6	235.0	0.17
M3	4/2	3.6	18.4	0.03
M4	11.2/2	10.8	53.7	0.09
M5	4/8	7.2	18.8	136 ps
M6	15/1.2	7.2	77.3	1.15
M7	15/1.2	7.2	109.4	0.59
M8	4/8	7.2	18.8	136 ps
M9	4/25	0.0	0.0	1.29
M10 = M11	40/1.5	9.1	119.5	0.59
M12 = M13	10/1.2	9.1	98.9	0.54
M14	6/2	18.2	38.0	15.7
M15	4/1.2	2.0	29.8	0.16
M16	4/1.2	2.0	1.35	170.9

Table I-2: Transistor sizes and DC parameters for the UTMC HFC-comparator circuit

The noise voltage due only to the amplifier and measured at the output, v_N^2, is given by:

$$v_N^2 \approx BW \left[2\, v_1^2 + 2 \left(\frac{g_{m3}}{g_{m1}}\right)^2 + \left(\frac{g_{m8}}{g_{m1}}\right)^2 v_8^2 + v_9^2 \right] \qquad (1)$$

where v_i^2 is the equivalent input noise voltage of transistor M_i

$$v_i^2 = \frac{8}{3} \frac{kT}{g_{mi}} [V^2/Hz\ ]\ i \neq 9$$

$$v_i^2 = 4\ \frac{kT}{g_{dsi}} [V^2/Hz\ ]\ i = 9$$

In equation (1) the noise due to the feedback resistor is dominant. For the preamp the transimpedance is determined by the feedback resistor:

$$\frac{V_{out}}{I_{in}} = \frac{1}{g_{ds9}} \qquad (2)$$

As a result the input referred noise current is given by:

$$i_N^2 = v_N^2\, g_{gs9}^2 \qquad (3)$$

This current is equivalent to an input noise charge with shape described in the introduction of this report. The magnitude of the noise is:

$$ENC = \frac{i_N \times 30\ ns}{1.6 \times 10^{-19}\ C}$$

$$\approx 56\ e^-\ rms \text{ for the Westinghouse design} \qquad (4)$$

$$\approx 24\ e^-\ rms \text{ for the UTMC design}$$

A second contribution to the total noise is the kTC noise caused by the input capacitance. The kTC input noise voltage is:

$$v_C = \sqrt{\frac{kT}{C_d}} \qquad (5)$$

which for $C_d = 5$ pF is equivalent to:

$$ENC_C = \frac{v_C\, C_d}{1.6 \times 10^{-19}\ C} \approx 899\ e^-\ rms \qquad (6)$$

A comparison between (4) and (6) shows that the amplifier noise is negligible.

Buffer with '1'-Suppression

The buffer is basically a simple shift register providing storage for the comparator output during the level 1 trigger decision time. This time is currently estimated to be 4 μs or 256 clock cycles, which is also the number of cells in the buffer. The buffer is built with 'David and Goliath' type latches (Figure I-9.a), where Goliath is the large inverter and David is the small feedback inverter. David restores the cell input, which is degraded by the use of a single pass transistor and refreshes it during the hold time. The single pass transistor configuration is chosen because it avoids the need for complementary pass transistors and two driving clocks. A drawback is the loss in speed. An n-channel transfer gate is known to be bad in passing a logic '1'. The speed of the n-DG can be increased by giving G a low threshold such that it already switches after a slight increase of the G input. Speed can be further optimized by making D switch at a high input voltage. In the same way the p-DG latch, which is affected by the bad characteristics of the p-channel device in passing a '0', is speeded up by giving G a high and D a low threshold voltage. The increased speed is illustrated in Figure I-9.b.

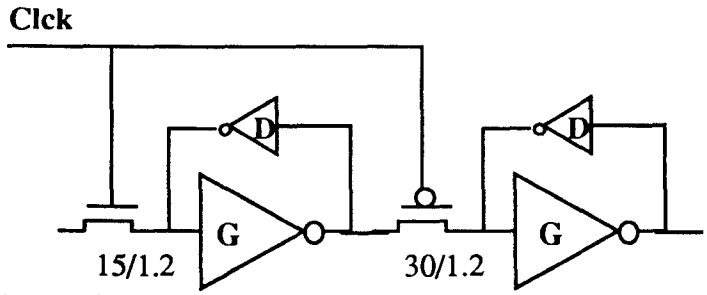

Figure I-9.a: D-latch, consisting of 'David & Goliath' type latches. The device sizes are for the UTMC process.

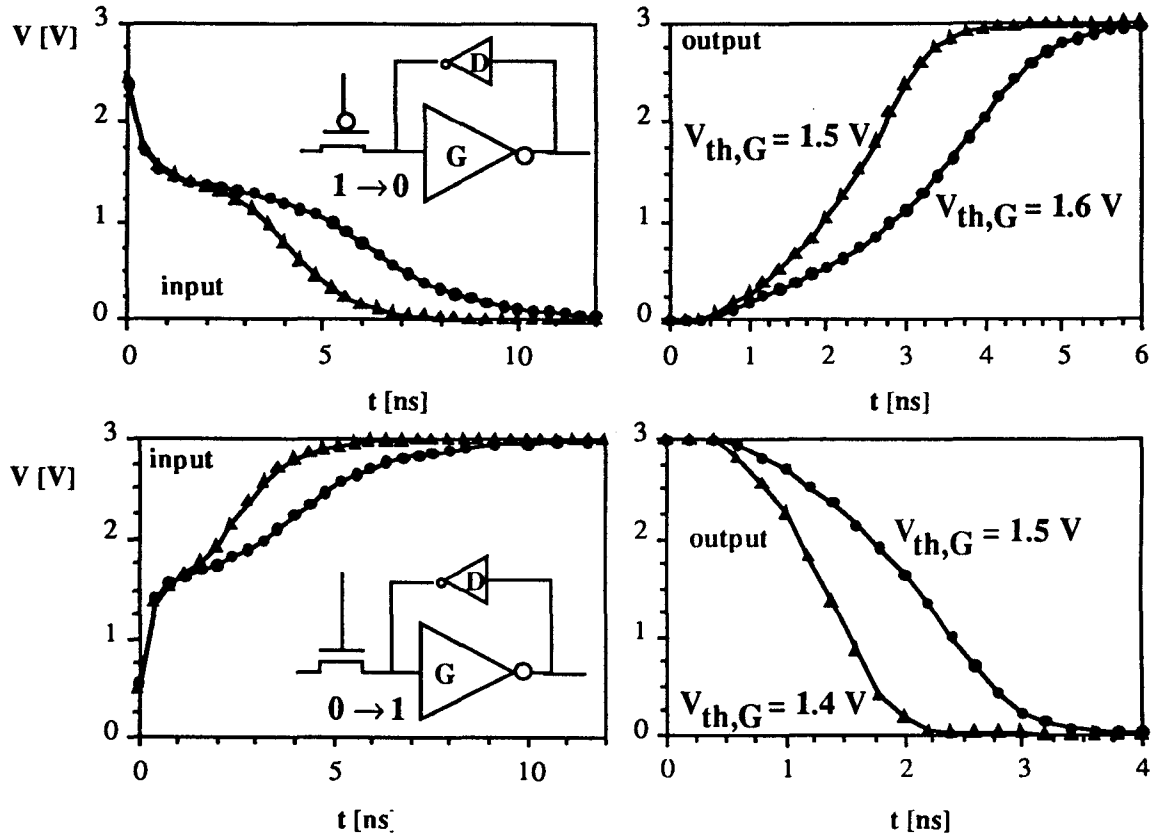

Figure I-9.b: Effect of optimizing the threshold levels on the speed.

The D and G transistors have to be dimensioned such that the driving capability of G is enough to force a logic level to the input of G in the next cell. This has to be done against the action of D in that cell, which tries to maintain the old value. Table I-3 gives the parameters for the latches to be implemented in the UTMC process. In this table, t_{dLH} and t_{dHL} are the delay time for switching low to high, and high to low. The values are measured from the moment the switch is opened.

Table I-3: Parameters for the D&G Cells.

	n-DG	p-DG
n-MOST-G	8/1.2	12/1.2
p-MOST-G	15/1.2	4/1.2
n-MOST-D	4/12	4/5
p-MOST-D	4/4	4/5
t_{dLH} [ns]	3.25	3.25
t_{dHL} [ns]	1.25	1.0

b. '1'-Suppression

The '1'-suppression circuit is designed to filter out successive '1' values in the buffer. Only a '1' following a '0' is passed. All succeeding '1' signals are replaced by a '0'. Figure I-10 shows a circuit that realizes this function. Table 4 reflects its operation based on the values of present and previous input value to the circuit.

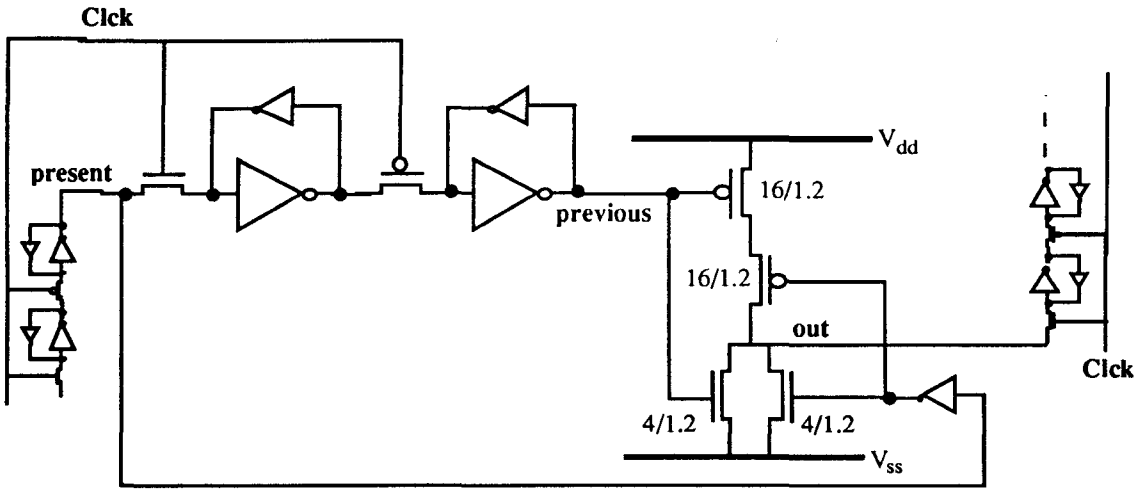

Figure I-10: '1'-Suppression Circuit.

Table I-4: Operation of the '1'-Suppression Circuit.

previous	present	out
0	0	0
0	1	1
1	0	0
1	1	0

Encoder

Each time a Level 1 trigger occurs the bit pattern at the end of the buffers should be given out in an encoded form. This is accomplished by the encoder, which puts out the width and the centroid of each group of consecutive activated channels ('1'-value). From two neighboring channels two signals are generated, a (01) signal indicating the leading edge of the group and a (10) signal indicating the trailing edge. Each channel has its address register. An address activated

by a (01) signal is put on the 'leading address' bus. A (10) signal causes the address to be put on the 'trailing address' bus. The width of the group is obtained by subtracting the contents of both buses. Problems occur if more than one group is hit. This is solved by scanning successive channels until an active (01) and corresponding (10) signal is found. Each time the addresses are transferred and subtracted. This approach is shown in Figure I-11.a. Because of the exponential increase in gate number if carry look ahead is used for a fast subtraction, a pipelined approach is used instead. Using a counter to scan all channels would mean that a number of clock cycles equal to the channel number is needed for the scan. This does not take into account the time needed for address transfer and subtraction. As a result of that, an unacceptable dead time will result. A much faster approach is to ripple a signal through an inverter chain, until it is stopped by a (01) or (10) signal. Hereafter the addresses are transferred and the scanning continues. This is shown in Figure I-11.b. The scanning is initiated by the clock going high. After the addresses are transferred, the corresponding latches are cleared and the scan signal will ripple through to the next (01) edge. The value of the last cell is used to initiate a reset of the scan circuit and to store new data in the encoder input latch. Using this method an unlimited number of activated groups can be handled. The maximum number of groups is intentionally limited to four, using a group counter. The dead time to read one group is given by the ripple-through time added to the time for the address transfer, which is half a clock period.

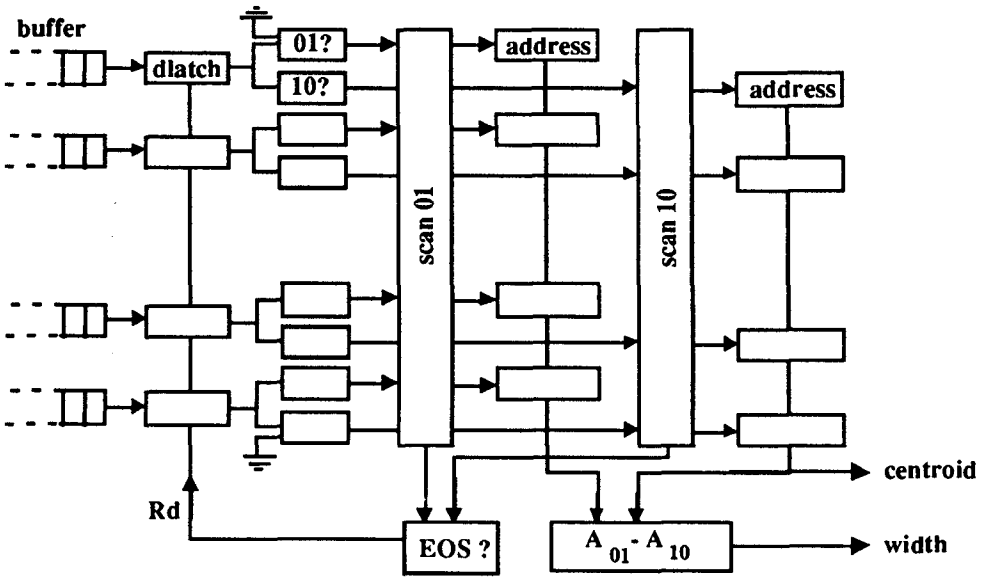

Figure I-11.a: Approach used for the width encoding.

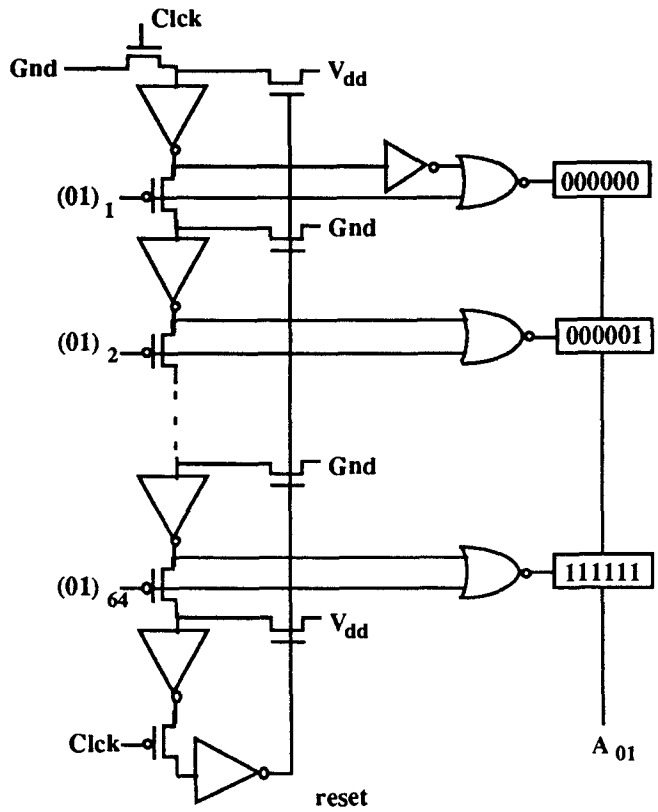

Figure I-11.b: Inverter chain used for the scanning.

Local Bunch Counter

An 8 bit counter operating at the 62.5 MHz SSC frequency gives timing information for successive outputs of the encoder. To obtain high speed and avoid the rippling through of carry information, the counter can either make use of a carry look ahead scheme with an exponential increase in the gate count, or it can be realized as a pipeline. The main disadvantage of existing binary counters is the fact that they are not modular, or an n bit counter can not be extended to an m bit counter by just adding (m-n) identical library cells. Here, a complete modular counter was designed by using a new counting code, which is illustrated in Table I-5. In this code all bit changes are defined or initiated by a low-to-high transition of the next lower order bit. This causes all carries to be known one clock period in advance of a bit change, hereby avoiding any carry delay. Because all bits are treated in the same way, their structure is identical and consequently extending a counter to any number of bits becomes straightforward.

Table I-5: New counting code.

0	0	0
0	0	1
0	1	0
1	1	1
1	0	0
1	0	1
1	1	0
0	1	1

The hardware implementation of this counting scheme is easy. Only three functional blocks are needed: a latch to retain the previous bit value, a '0' to '1' detection block which output signal, $(01)_{out}$, to allow the next bit to change, and finally, a circuit that generates the next bit value based on a $(01)_{in}$ signal and the present bit value. Figure I-12 shows a possible implementation. The counter designed for a 1.2 μm CMOS process has a simulated speed of 300 MHz. By using CMOS transmission gates and dynamic logic the speed can easily be increased to 0.5 GHz.

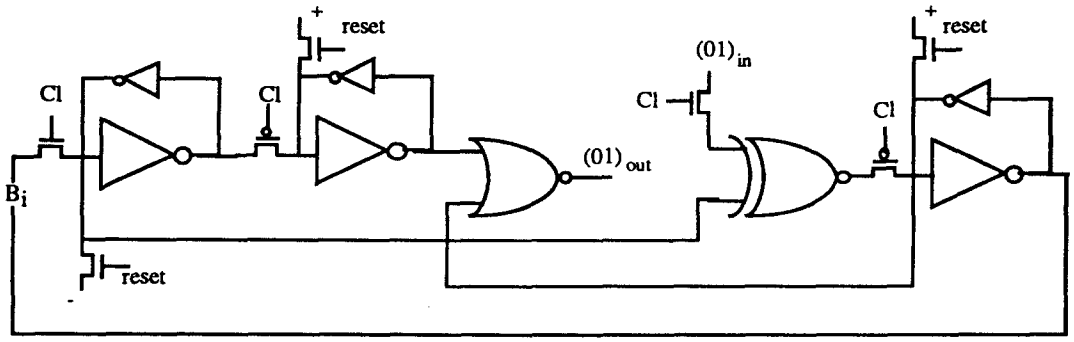

Figure I-12: Possible implementation of a counter cell.

APPENDIX J
TESTS OF TMC1004 TIME TO DIGITAL CONVERTER FOR SDC

Paschal Kibuule, Dario Crosetto, Wiyi Yang, Jheroen Dorenbosch

We report our findings on the TMC1004 chip, designed by Y. Arai of KEK, Japan. This design has been selected by the SDC collaboration for the readout of the straw tubes and the muon chambers. It is a Time to Digital Converter (TDC) with a least count of 1 ns. It provides on-chip pipelined storage for all hits in a 1 μs interval. The chip features continuous readout so that hits can be read out during digitization of subsequent data. In terms of power consumption, functionality and resolution it fulfills the requirements of the SDC experiment. Future versions will have sufficient memory depth to cover the required 4 μs storage time and will be radiation-hard.

We have investigated the behavior of this chip, concentrating our studies on the internal phase locked loop and on the time resolution. We have investigated the sensitivity to power supply variations and the clock frequency.

The TMC1004

The TMC1004 is a four channel, low-power, high-resolution multi-hit Time to Digital converter chip (Figure J-1). When operated at its nominal frequency of 31.25 MHz, it records the time difference between the leading edge of the input signal and the leading edge of the clock in time units 1 ns. An internal Phase Locked Loop (PLL) with 32 delay elements was used to subdivide the 32 ns clock into 32 equal 1 ns steps. The TDC dissipates only 7 mW per channel. Recorded data are encoded as a binary number to reduce the number of required output pins to 6 per channel.

Test Method Used

For testing a HP 82000 digital IC verification station is used. It allows for testing up to 100 MHz. It is turned on for 30 minutes before testing to reach a stable temperature. The continuity test is performed on the chip to check proper connections to the pins of the Device Under Test. We use test vectors corresponding to the normal operation mode of the chip. The first hundred cycles of the test sequence are required to allow the PLL to lock to the clock signal. After a few hundred cycles a signal is applied on the input of the TDC.

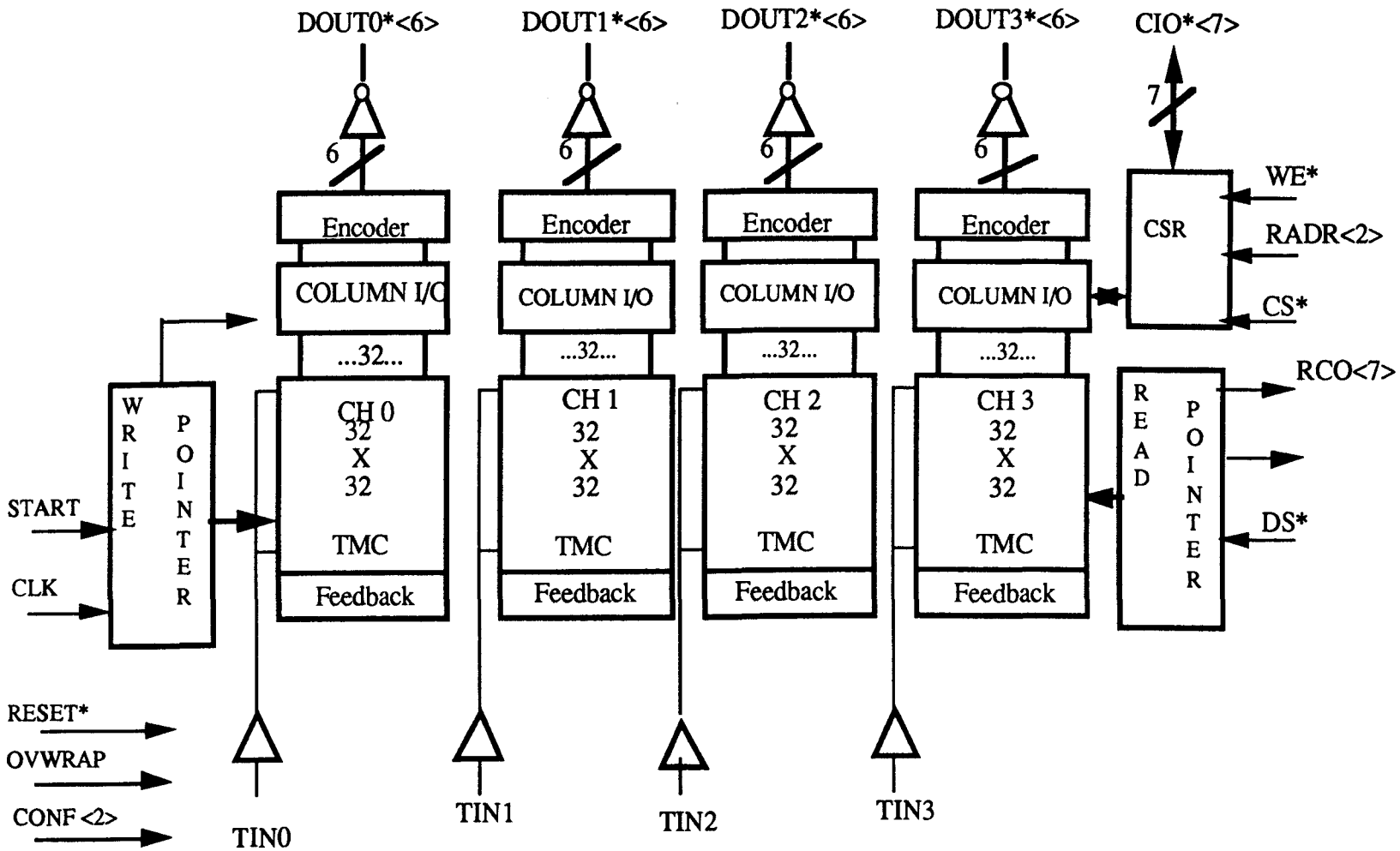

Figure J-1: TMC1004 Functional Block Diagram

Table J-1 Chip Properties

Table 1: Properties of the TMC1004 TDC chip	
• Time Resolution	1 ns/bit (0.8 ~ 1.6 ns/bit)
• Clock Frequency	31.25 MHz (40 - 20 MHz)
• Channels	4 channels
• Rows	32 Row/channel
• Bits	32 bit/Row
• pins	54 (I/O) + 34 (power/GND)
• Supply voltage	3 Volts
• I/O Level	CMOS level
• Chip Size	5 mm x 5.6 mm

The delay of the input signal relative to the clock is varied from 0 ns to 40 ns in steps of 100 ps. At each setting 20 measurements are made. The program "tmcRes" captures the results from the 82000. The program converts the individual output bits into a single integer and stores the result in a file for later processing. The spread sheet program Wingz is used to process these data.

Phase Locked Loop Studies

We examined the effect of the "OVR" pin, the way the measurements track the clock frequency and sensitivity of the chip to supply voltage variations. During earlier tests of this chip at the University of South Florida, we observed missing codes between the last bit of row N, and the first bit of row N+1 (Figure J-2). Later it was found that the control signal "OVR" was inadvertently set to zero instead of one. This reduced the number of delay elements from 32 to 31 which resulted in an increment of about 3% in the 1 ns quantization unit. This error caused the discontinuity in the data between rows. We repeated these measurements at the SSCL. Figure J-3 shows the averages of each set of 20 measurements as a function of the delay. We also show a fit to the averages for one row.

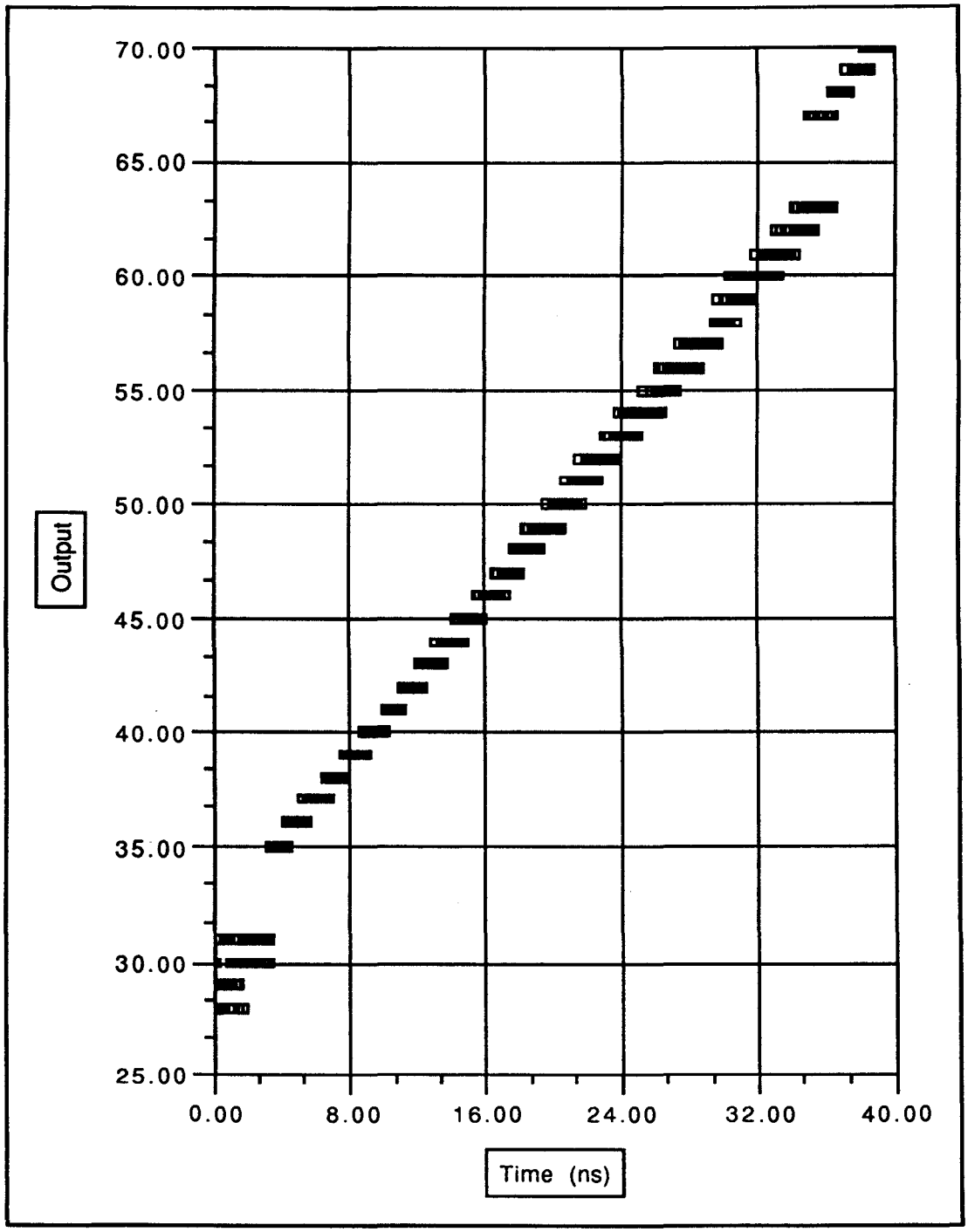

Figure J-2: TMC1004 response revealing missing codes. (OVR = 0)

The figure clearly shows the mismatch between neighboring rows. The large quantization unit translates in a reduced slope of the fitted curve. Ideally the slope is 1. However, the fitted slope of 0.92 is significantly smaller. When the "OVR" set to one, no missing code are observed

as seen from Figure J-4. It was obtained by performing the measurements at the nominal operation point with 3 supply voltage at 31.25 MHz.

Sensitivity to Supply Voltage

A number of tests were performed to probe the sensitivity of the chip to supply voltage variations. Figure J-5 shows two data sets where the chip was operated at 2.8, and 3.2 Volt. One can see that the curves practically fall on top of each other. This indicates a very low sensitivity of the PLL delay of power supply variations. This was further quantified by comparing the slopes obtained at different voltages. Figure J-6 gives the result of this comparison. Common mode rejection is better than 0.02% V.

It can be observed, however, that the slope is approximately 4% less the ideal slope of 1.0. It has been found that the slope varies between rows and is different for the four channels on the chip. This feature has been communicated to the designer of the chip. It is not yet fully understood, but changes will be made to future versions of the chip to avoid these variations. Later we estimate the contribution of the mismatched slopes to the overall resolution of the chip.

Tracking of Clock Frequency

To test the response of the chip to clock frequency variation, the supply voltage is kept at 3 Volts while the clock period is varied. For each setting we determine the slope. As the PLL locks to the clock, the quantization unit is expected to be proportionate to the clock period. Therefore the slope must be proportional to the clock frequency. Figure J-7 shows the appropriate linear relationship.

Resolution

To measure the overall resolution of the chip we calculate the difference between the data and the ideal behavior for a quantization unit of 1 ns. The standard deviation of these differences is 0.65 ns. Figure J-8 shows the differences between the averages at each delay setting and the ideal behavior.

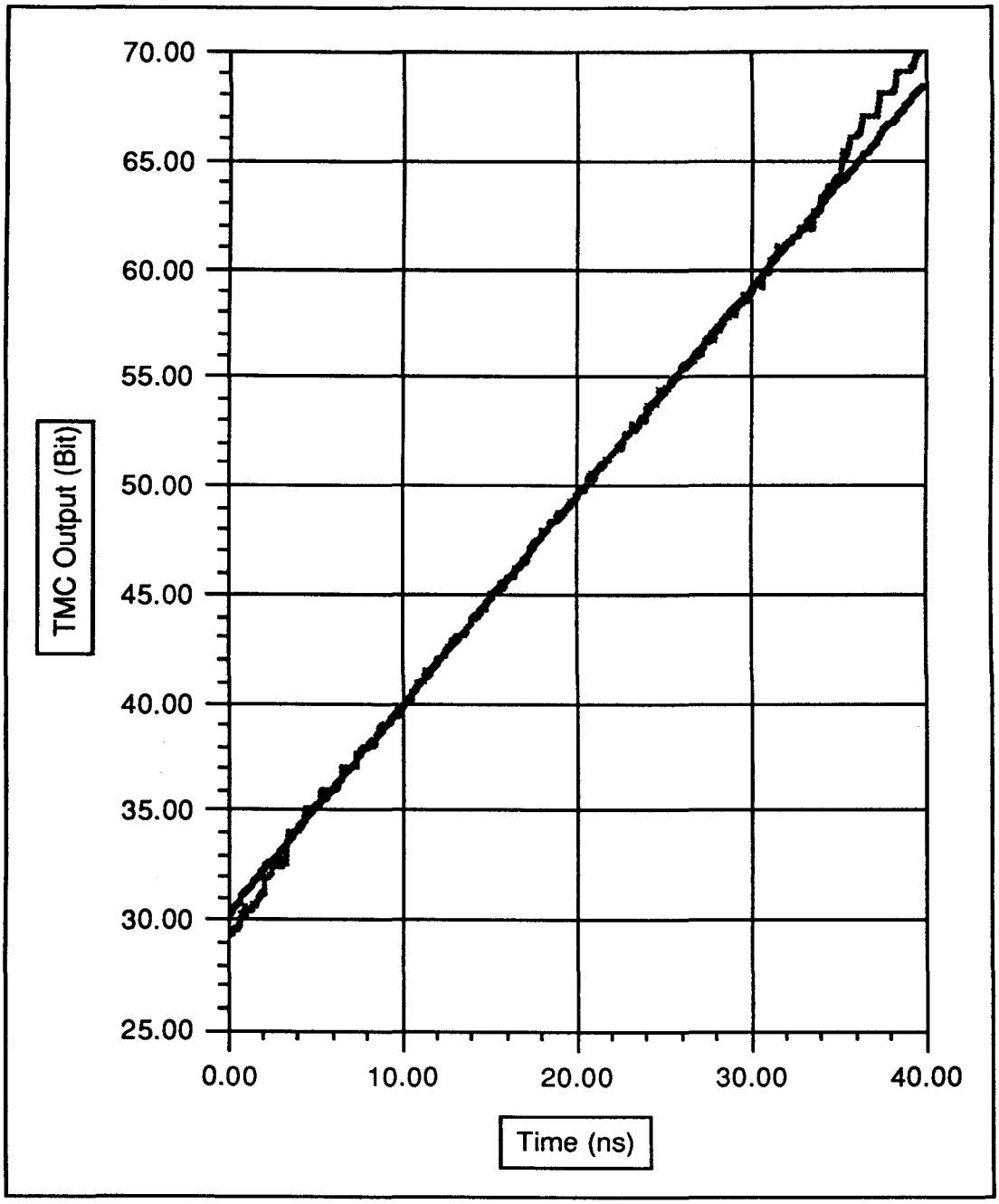

Figure J-3 : Average of 20 time measurement vs. input delay (OVR=0)

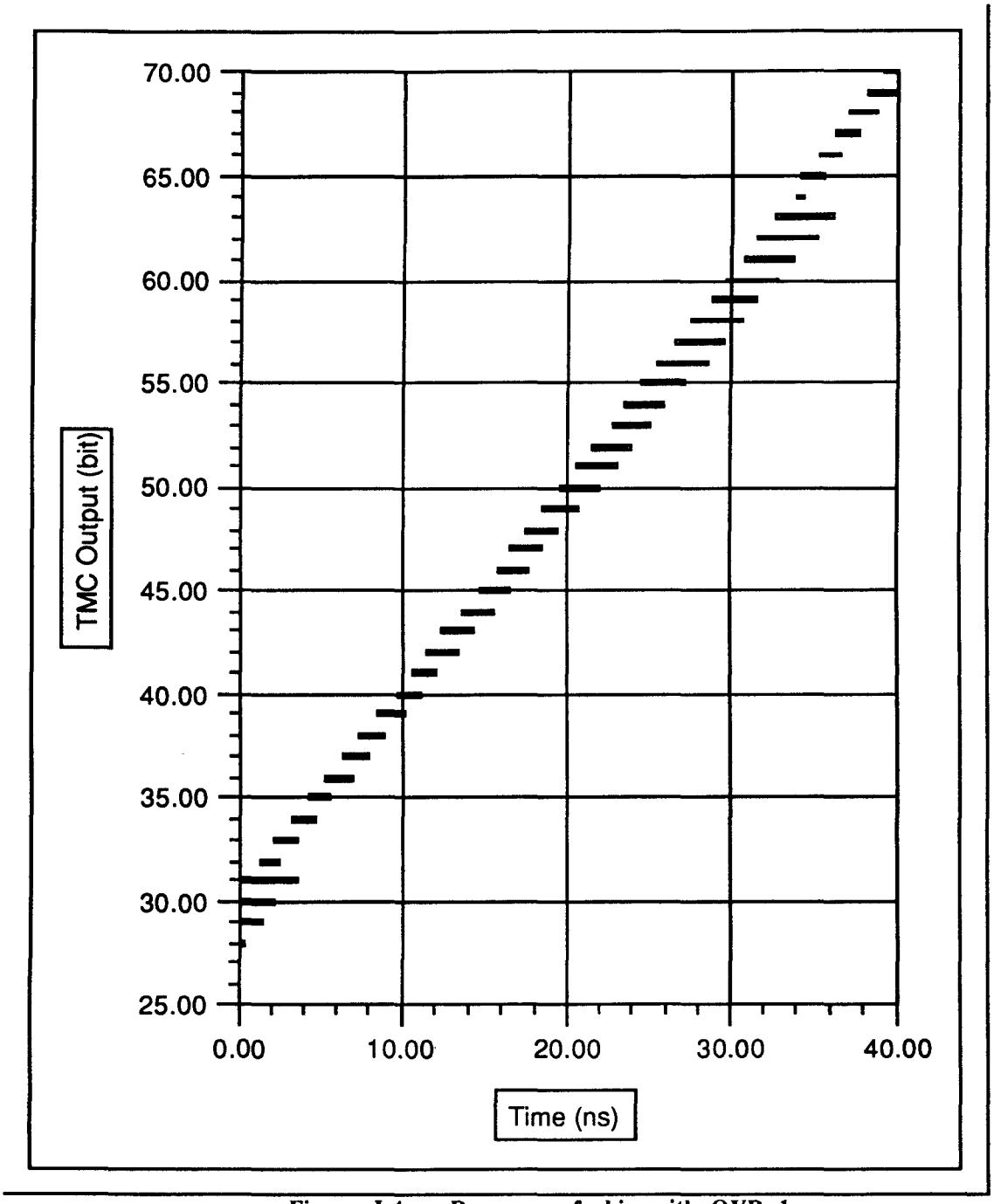

Figure J-4: Response of chip with OVR=1

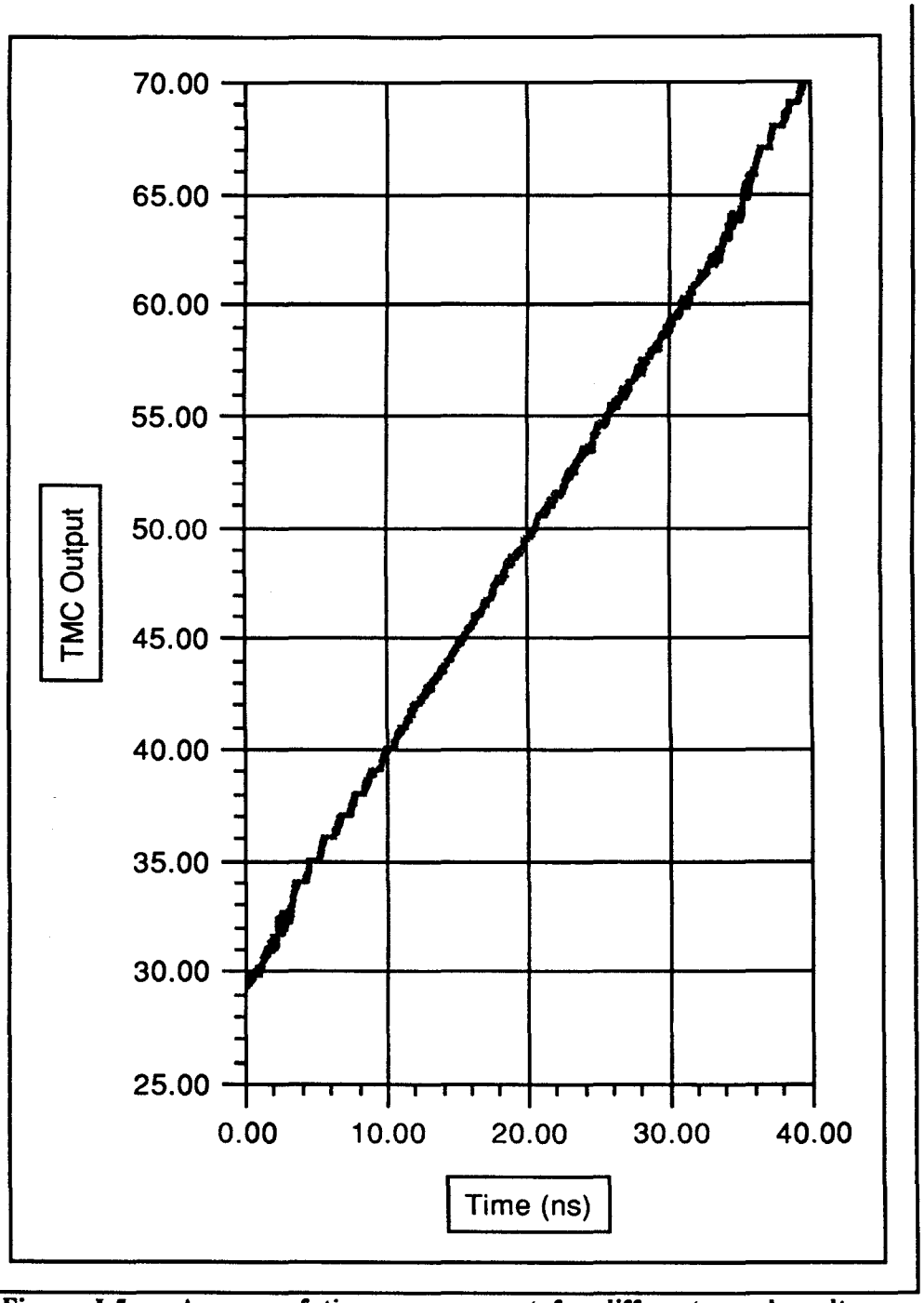

Figure J-5: Average of time measurement for different supply voltages

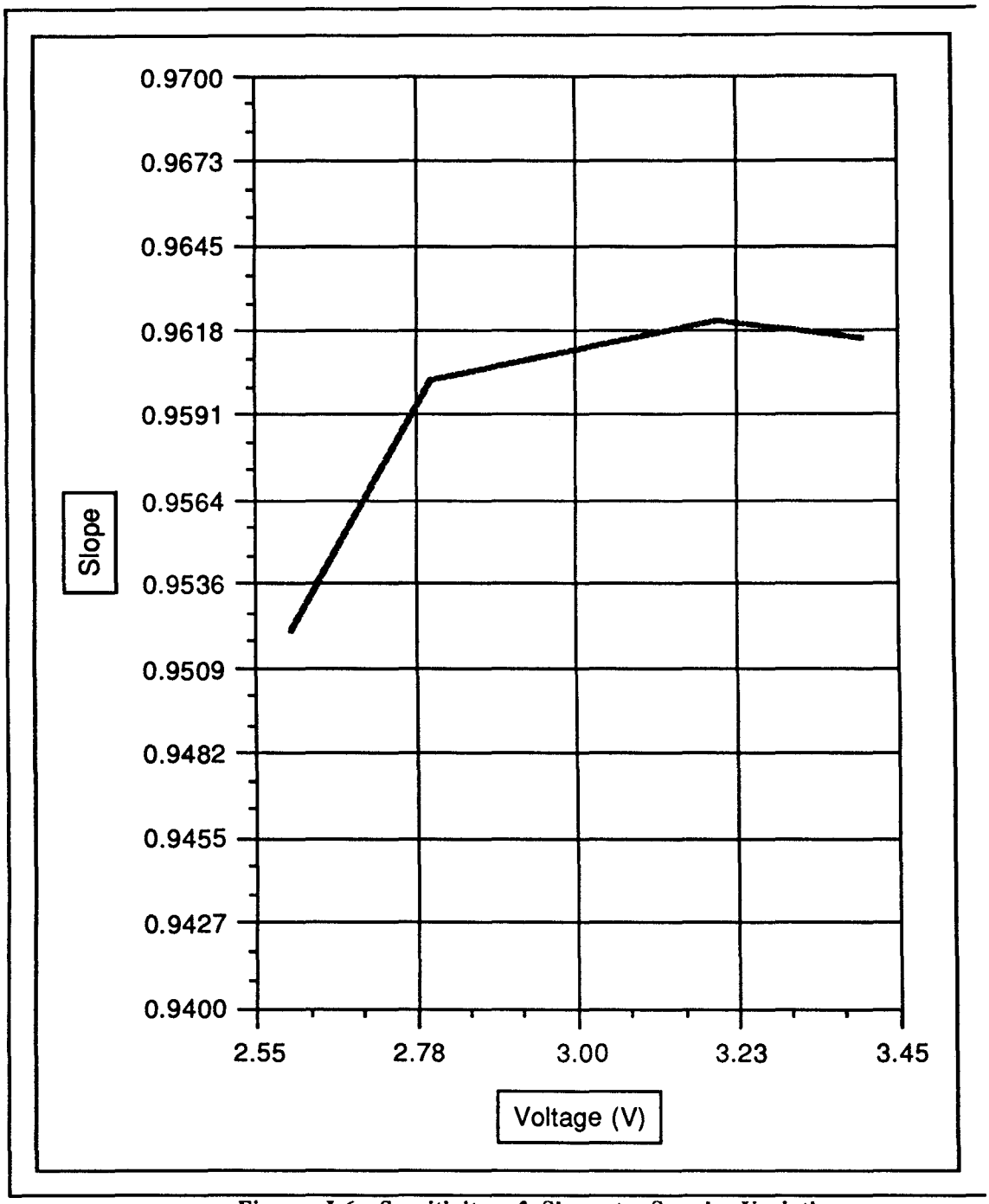

Figure J-6: Sensitivity of Slope to Supply Variations

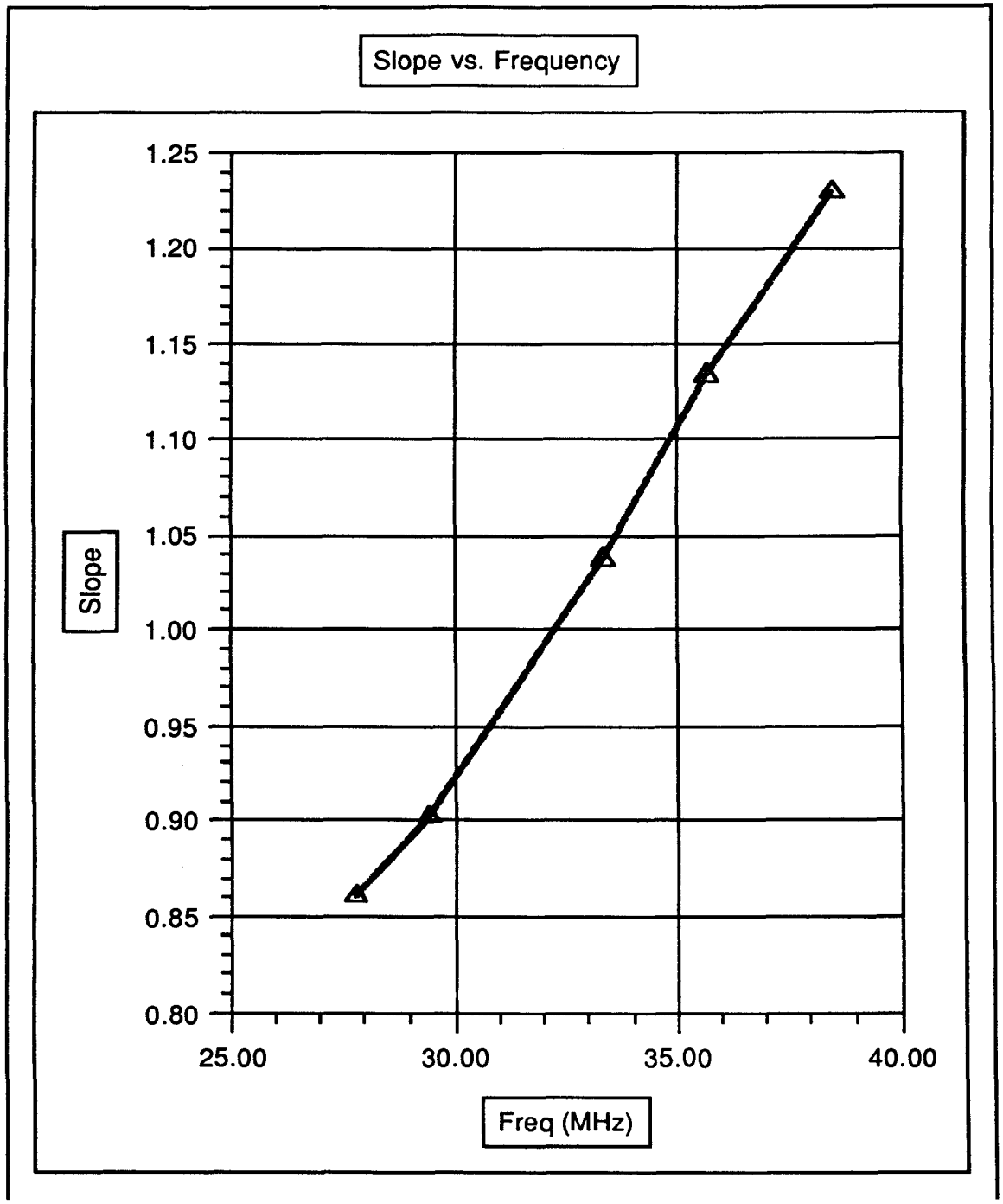

Figure J-7.: Slope as Function of Clock Frequency

The overall resolution can be decomposed into contributions from the quantization unit, the incorrect slope, and from the resolution at a fixed delay, caused by jitter in the internal 1 ns delay elements. The quantization error contributes 1 ns/$\sqrt{(12)}$ or 0.29 ns. The effect of the incorrect slope is 0.41 ns. The resolution due to jitter is shown in Figure 9. It increases with the delay, as more delay elements contribute to the jitter. The average sigma is 0.43 ns. The three contributions

can be combined quadratically to yield 0.66 ns, which corresponds to our measured resolution. One can estimate the overall resolution for a correct slope would improve to 0.52 ns.

Further Studies

The tests performed on this chip have shown some minor problems which we relayed to the designer for his attention. In order to fully characterize this chip we still have to probe its behavior under temperature changes. We will also quantify the slope variation with row and channel number. Suggestions for an improved encoding scheme will be communicated as well.

Conclusion

The tests performed on this chip have not shown any serious problems with the chip. It seems to satisfy most of the SSC specifications for use in the straw tube read out system. Small improvements in the resolution can be made by fixing slight deviations in the quantization unit. The design appears to be very robust. The chip functions correctly over a wide range of supply voltages and clock speeds.

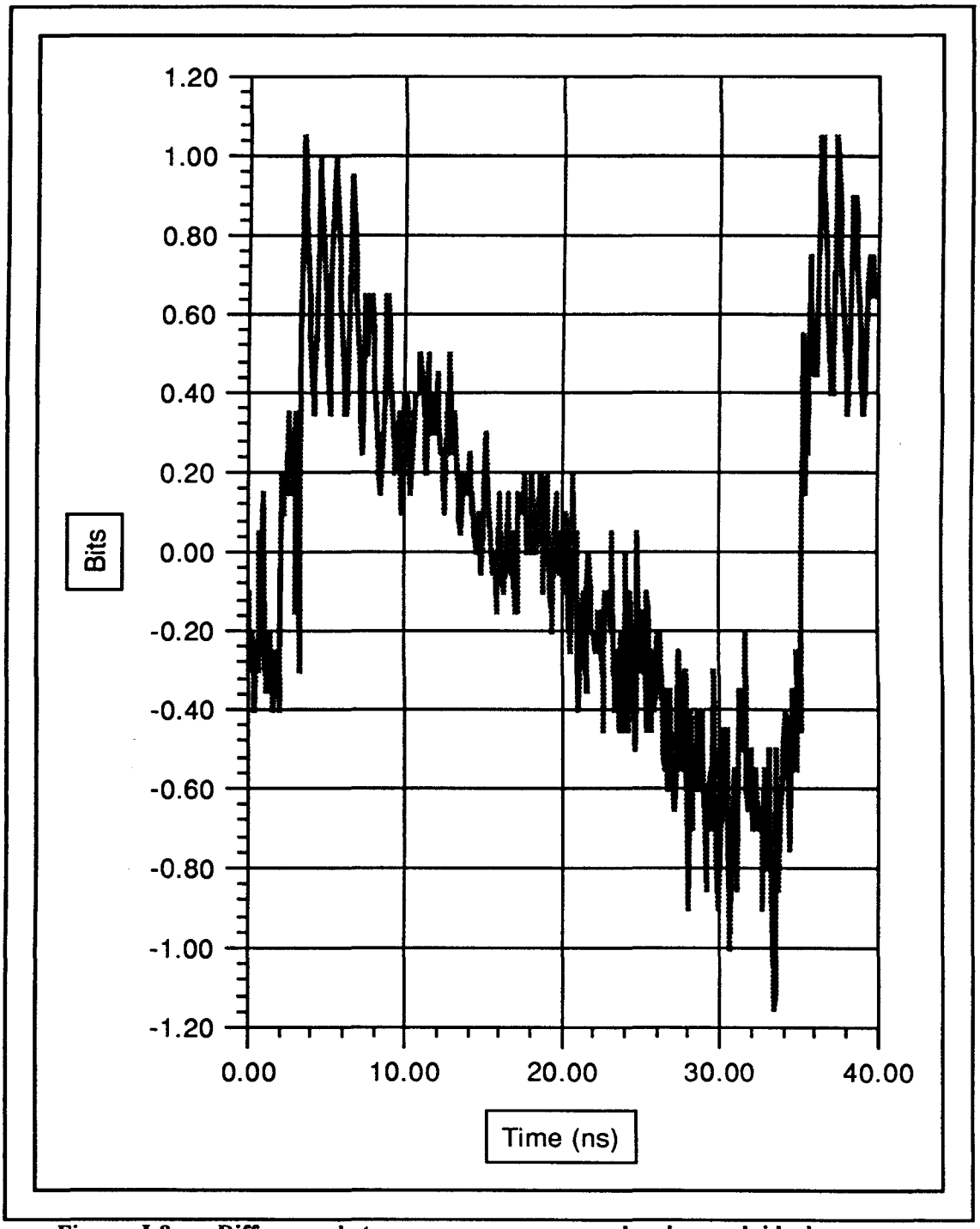

Figure J-8: Difference between average measured value and ideal response.

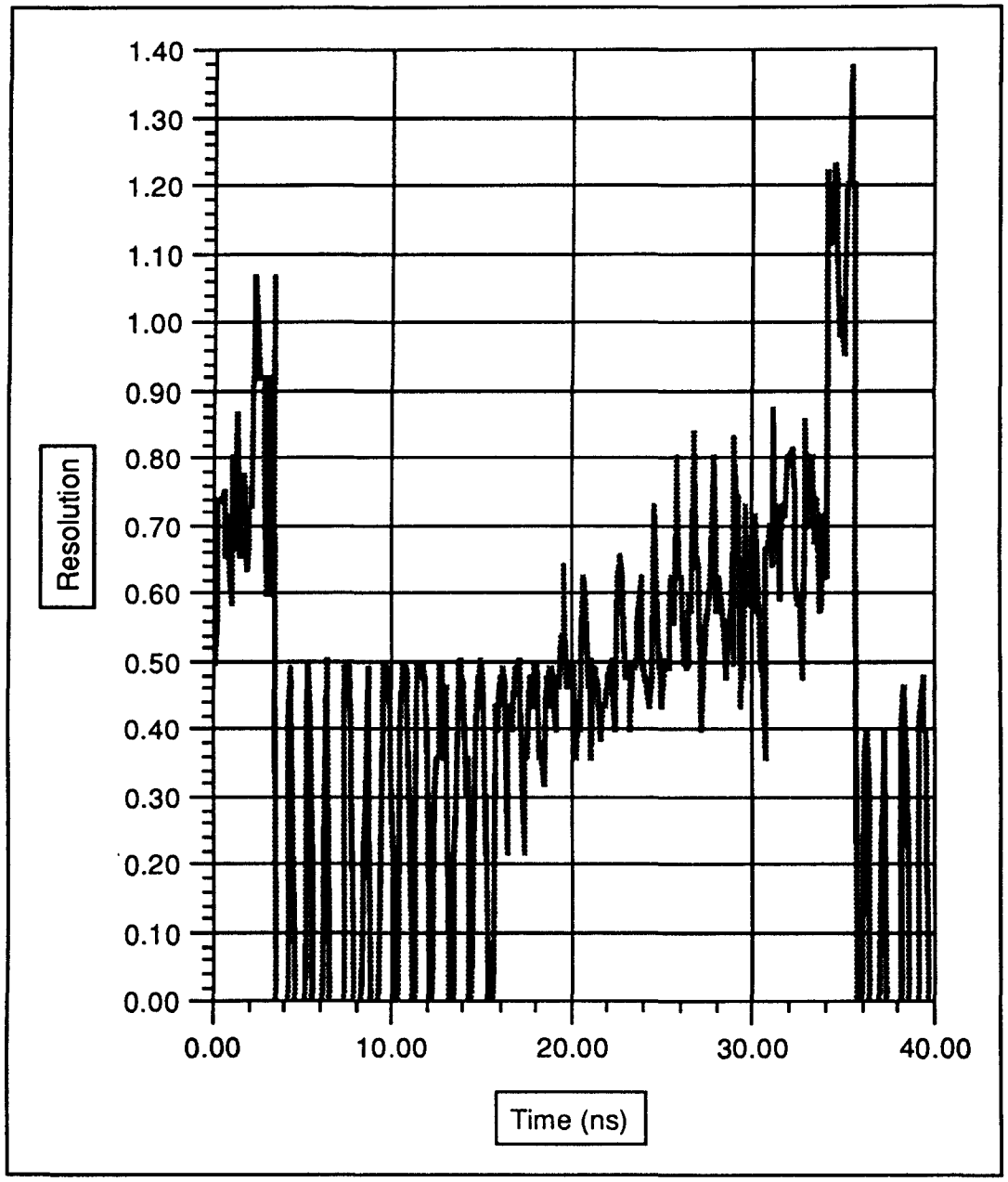

Figure J-9: Resolution as function of input delay.

APPENDIX K

DATA COLLECTION STUDIES FOR THE SUPERCONDUCTING SUPER COLLIDER

E.C. Milner, A.W. Booth, M. Botlo, J. Dorenbosch, E. M. Wang
Physics Research Division, Superconducting Super Collider Laboratory[§], 2550 Beckleymeade Avenue, Dallas, TX 75237 USA

and

R. V. Idate, V. S. Kapoor, V. K. Raj
The University of Texas at Arlington, Arlington, TX 76019 USA

Abstract

We report on simulations of data acquisition systems for experiments at the SSCL. Using the MODSIM II[1] object-oriented discrete-event simulation language, we have studied the behavior of various front-end circuits, data-collection chips, data-collecting networks, and multi-level triggers. Results include system deadtime, throughput, and efficiency, as they are influenced by data rates and system architecture.

Introduction

The Superconducting Super Collider Laboratory (SSC) is a new high energy physics laboratory where we expect to be performing experiments by the year 2000. We will search for new physics processes occurring in the collisions of two counter-rotating beams of 20-TeV protons in the 87-km long accelerator ring. The expected data rates, volume, and complexity will be unprecedented in the history of science. In this paper we discuss simulation studies of data acquisition (DAQ) systems for collecting these experimental data.

The typical experimental apparatus at the SSC will be a large, complex ensemble of five to ten distinct sub-systems: central tracking (Si micro-strips, straw tubes, scintillating fibers, etc.), calorimetry (electromagnetic and hadronic), muon tracking (wire chambers, timing detectors), triggering (multiple levels), and data acquisition. Sub-system channel counts will range from the small (about 1,000) to the large (about 5,000,000).

There will be differences in the data acquired from the sub-systems for each event. For example, it may be necessary to record for each calorimeter channel multiple samples of digitized data, while for Silicon micro-strips each channel gives only one bit of hit information.

The Collider will provide a beam crossing every 16 ns, with a mean of 1.6 collisions per crossing (100 mb cross section) occurring at the design luminosity of 10^{33} cm^{-2} s^{-1}, giving a 100 MHz interaction rate. We can expect data for each event to be about 0.4 MByte, giving a raw data rate of 40 TByte/s. Combined trigger rejection factors of 10^6 to 10^7 would reduce the data recording rate to 4 to 40 MBytes/s. Because of these high rates from large detectors, we anticipate the DAQ systems being more complex than those operating in present-day experiments.

§ Operated by the Universities Research Association, Inc., for the U.S. Department of Energy under Contract No. DE-AC02-89ER40486.

---

1 MODSIM II is a proprietary product of CACI Products Company, 3344, N. Torrey Pines Court, La Jolla, California 92037, USA.

Simulating Data Acquisition Systems

Since specifying any SSC DAQ system presents a challenging task of physics and engineering optimization, we decided from the beginning to incorporate behavioral simulation into our long-term design strategy. Many important design issues can be studied quickly at the behavioral level, without working in detail at the gate level. The emphasis in this technique is on understanding the essential functionality and interaction of system components. Comparing behavioral models for a variety of DAQ systems and components can lead to defining the optimum architecture.

Although there exist many interesting and imaginative variations, there are three prominent features of most concepts for SSC DAQ architectures: 1) data are buffered almost everywhere to derandomize input arrival sequences, to wait for a trigger decision, or to synchronize with other data or signals, 2) triggering is assumed to be done in increasingly complex stages, and 3) for events to be permanently stored, all data are collected together at some point in acquisition.

For a given system, the two most important measures of performance are throughput and deadtime. The throughput rate is dictated by the speed of data transfer technologies and the DAQ system network topologies. Deadtime can arise because of the complex interaction of many different system parameters including: buffer sizes, event sizes, trigger rates and processing times, channel bandwidth, cable delays, and error conditions. In addition, some of these parameters exhibit fluctuations with large correlations. A system can be optimized by measuring how changes in these parameters effect deadtime, throughput, and not incidentally, cost.

Each DAQ model embodies a set of assumptions, strategies, and design features that may be understood by critical testing in the simulation environment. Network issues include 'load' balancing, static and dynamic readout partitioning, multiplexing, system scalability, hardware redundancy, and routing. Another broad category concerning system control and monitoring includes issues of throttling (rejecting triggers when buffers are full), deadtime measurement, error detection and correction, and system-wide diagnostic strategies.

A Simulation Study: "Data Collection Network Buffer, Protocol, and Structure"

There exists in the high energy physics data acquisition community a conceptual DAQ architecture (Fig. K-1) featuring sub-system specific front end chips (FEC) to amplify, store, and transmit detector signals, a network of data collection chips (DCC), event builders (EB), a massive processing farm (FARM), and some means of data logging. Data are moved between these sub-systems in response to level 1 (L1), level 2 (L2), and level 3 (L3) trigger decisions. In addition, gating logic could monitor trigger operation, reduce the L1 or L2 trigger rate when buffers are full, and do deadtime accounting. We are modelling this system using an object-oriented simulation language called MODSIM II on SUN workstations.

The purpose of a data collection network in this system is to "funnel" data from the detector so that they can be collected in one location, analyzed, and recorded. This can be thought of as a simple parallel-to-serial data-flow conversion. This serialization process can begin on the detector near the front end chips, and continue in several layers or stages as signals are driven from the detector towards the counting house. In a typical design, data arriving at one of many input channels of a data collection chip are stored in input FIFO buffers. All data corresponding to an event are assembled in an output buffer for transfer to the next downstream DCC layer, or in the case of the final layer to the EB.

A difficulty arises because in general the parallel data arrive at input ports asynchronously. Since we want to serially order the data, effectively we wait for it all to arrive before transferring to the output buffer. But what happens if because some upstream buffer was full, some part of the

event was lost? Do we wait only some "time-out" period before discarding the event? Do we propagate "buffer full" signals or "data lost" signals throughout the system to flag the problem? Do we "throttle", reducing the trigger rates when we observe the buffers filling to prevent the problem from occurring in the first place? These questions are usually framed as a difference between two ways of controlling data flow: "push" versus "pull" (Fig.K-2).

In the pure-push style of data collection, data are sent to buffers without first verifying that space is available; if a receiving buffer is full the data are simply lost. In a modified-push system, when a sender needs to transmit data it polls the receiver to know when the data can be accepted. In a pull system, the receiver requests data be sent. Note that an optimized system may employ a mixture of these methods. In this report, we show results comparing the push techniques.

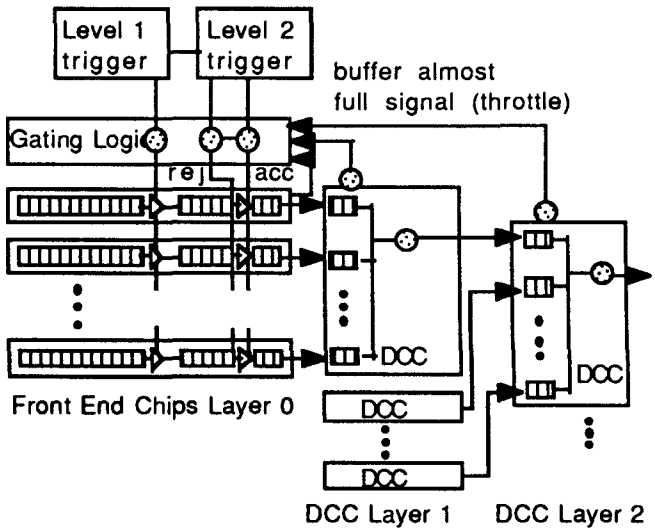

Figure K-1: Architecture of an example data acquisition system simulated for this report.

In response to level 1 and 2 trigger signals, detector data in the front end chips are transmitted to the data collection chips (DCC). Many DCCs are networked together so that after several DCC layers the detector data generated in parallel have been serialized and collected into the output buffer of the final layer DCC. The specific simulation configuration reported in this paper is 512 front end chips generating data feeding into 64 DCCs with 8 inputs each. In the second DCC layer, there are 8 DCCs with 8 inputs each, and in the third layer there is one DCC with 8 inputs.

DCC Operation

The DCC model consists of 'n' input ports, a processor, and one output port. Each of the input ports has a FIFO buffer. Data arriving at an input port of the DCC are put in the FIFO and the processor is notified that data have been stored. In MODSIM this is achieved by invoking a "method", but in hardware this could be implemented either by an interrupt or 'attention' register. The DC network is configured by connecting output ports in one "layer" to DCC input ports in the next downstream "layer". In a layer, DCCs are the same, with buffers of the same size and data-transfer lines running at the same speed. DCCs in layers near the front end will then have relatively smaller buffers and slower transfer rates than those near the end of the data stream.

The processor waits until data for a particular event have arrived at every port and then checks the level 2 identifier of each sub-event for consistency. The processor then removes the

sub-event from each input buffer, starting at buffer 0 and proceeding to buffer 'n-1' where n is the number of input ports on the DCC. These data are then transmitted to the DCC in the next layer or stage. The protocol for data transmission at this point is central to understanding the system behavior.

Data "Push" Techniques

In data "push" techniques when an event parcel has been assembled in an output buffer the processor sends it to a downstream buffer in another DCC. We term the simplest case "no-check push", in which the data transmitter always assumes the receiver has space available to store the data. If in fact there is no space, the data are lost and the transmitter is not informed, because there is no feedback connection between chips.

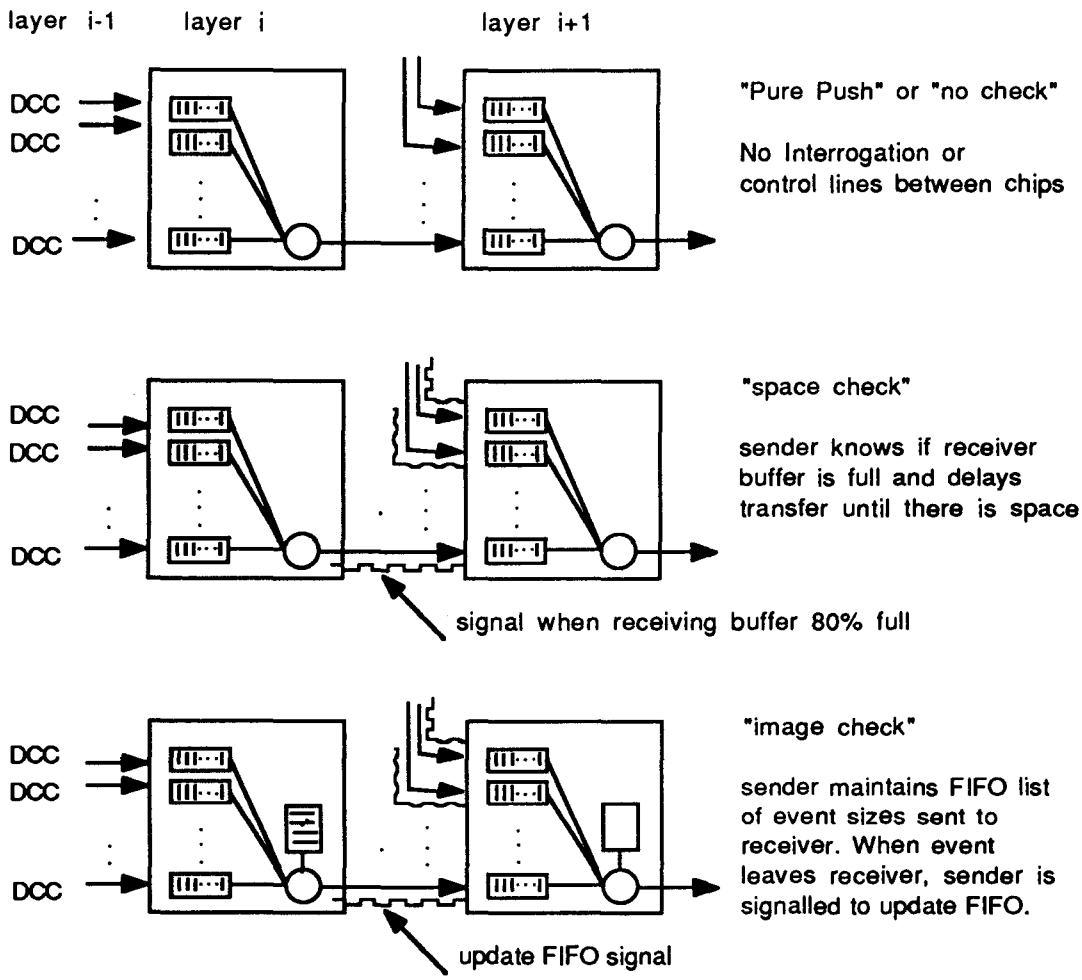

Figure K-2: Three different strategies for data transfer protocol between DCCs

Three different strategies for data transfer protocol between DCCs are shown: 1) pure push, in which no interrogation occurs between chips, and data are lost if no buffer space is available, 2) space check push, in which the sender initiates transfer to the receiver only when space is available, and 3) imaging push, in which the sender maintains a FIFO list of event sizes

sent. The FIFO is used to increment and decrement a counter recording the total amount of data stored in the receiving buffer. When an event leaves the receiving buffer the FIFO in the sending DCC is updated along with the total data count.

In "space-check push" the transmitting buffer queries the receiving buffer to find if there is sufficient space to hold the data. For example, when the receiving buffer is 80% full, its processor transmits a pulse to the transmitting buffer's processor to signal the "buffer almost full" condition, holdinK-off data sending. This requires a line between chips in the two layers, but if the two layers are near the front end, they may be on the same board, simplifying communication.

"Imaging push" is more clever, because it maintains a FIFO record (or image) of how much data have been stored in the receiving buffer. When an event part leaves the receiving buffer, a pulse is sent back to the original sending buffer so the FIFO image is updated. In this way the sending buffers know how much space is available in the receiving buffers, and send data only when it can be accepted. Buffer utilization is improved over the "space-check case", at the cost of a modest increase in complexity. The characteristic behavior of both space-check and imaging push at high rate is that the buffers "back up" and deadtime ultimately begins to occur in the most upstream layer. At lower rates they avoid deadtime and make efficient use of buffer space in all layers.

Data "Pull" Techniques

In data "pull" techniques the receiving DCC has no input buffers. When the processor finds data in upstream buffers it transfers the data into its own output buffer. This implies that it is physically close to the upstream buffers. Since the data for a given event are available in output buffers asynchronously, the essential point of study is the "pulling" algorithm. The simple scheme ("simple pull") would be to wait for each event parcel to arrive and assemble the parcels together in rigorous order in the output buffer. This could be refined by transferring each parcel when ready, but assembling them in general out of order in the output buffer. A pointer list would assist the downstream processor in assembling the parcels in order during subsequent transfer. This method is called "pointer pull", and would avoid the problem of waiting for event parcels to be ready for reading.

Global Control: Gating Logic

When the rate of data entering the data collection network is higher than the emptying rate, the buffers fill and deadtime occurs. This can be prevented by simply limiting the input rate. The technique we have modelled for doing this is called "throttling". When the buffers are almost full, the gating logic produces a "throttle" signal causing valid L2 triggers to be converted to L2 reject signals, so that the corresponding events do not enter the DC network. This means that DC buffers never fill completely, and deadtime occurs as a result of operation of the trigger gating logic. Since the gating logic is more accessible for monitoring, this may be preferable to creating and measuring deadtime within the DC network itself. However, the existence of latencies arising from transmitting "buffer almost full" signals to the gating logic imply that buffer utilization will be degraded. All of the "push" and "pull" techniques discussed above were simulated both with and without applying trigger gating logic throttling.

Simulation Parameters

The DC network topology for this study consisted of 512 front-end (FE) chips connected to 64 data collection chips (DCC) with eight input ports in the first layer of the DCC network, i.e. 8 FEs per DCC. In the second layer of the DCC network there were 8 DCCs, and in the third and final layer there was one DCC (see figure 1), so that data from 512 FEs were funnelled into one output DCC. With 30 FE channels per FE chip, 512 FE chips then correspond to 15360 FE

channels, or about one-quarter of a calorimeter with 64 thousand channels. The model therefore approximates a quadrant of the calorimeter readout.

Each DCC input buffer size was set to a depth of five events. The processor in the DCC transfers the event fragment assembled from it's input buffers to input buffers in a DCC in the next downstream layer. With a maximum of 120 units of data from each FE, the input buffer size in DCC layer one is then 600 units. The assembled event fragment form a layer 1 DCC is 960 units. Similarly, layer 2 buffer sizes are 4800 units input and the output event fragment is 7680 units. Layer 3 input buffers are 38400 units and output event size is 61440 units.

The time between each Level 2 trigger occurrence was generated randomly from a bounded exponential (from 16 ns to 100 μs) distribution. The mean of this distribution was set at 2, 4, 6, 8, or 10 kHz to study system behavior as a function of rate.

Two distributions were used to represent the input data sizes. The case with highest throughput would be no zero suppression, with each channel giving a fixed number of bytes per trigger. Specifically, each FE generated 120 units, corresponding to approximately 4 units of data for each of 30 FE channels. The reader may regard a "unit" as an arbitrary number of bits, but for the sake of realism, a byte is an appropriate "unit": 1 sample of 2 bytes plus 2 bytes of address information total to 4 bytes per trigger.

To represent the case where "zeroes" are suppressed in the FE chips, we use events generated from physics simulation with appropriate thresholds. Detector geometry (28,800 cells in both electromagnetic and hadronic compartments, with $\eta \times \phi$ segmentation of 0.05 x 0.05) and particle tracking were specified using GEANT. High-P_T QCD two-jet events were generated with ISAJET 6.43. The calorimeter was simulated using a custom fast shower parametrization, including shower fluctuations tuned with CDF test beam data [2]. Contributions were included from event pileup, though not from electronic noise. Electronic pulse shaping was 16-ns peaking bipolar. Level 2 trigger algorithms selected samples of single electrons (20 GeV threshold), QCD jets with P_T than 100 GeV, and jets $\not{E}_T$ greater than 100 GeV. These samples were written to separate disk files. These data are representative of topologies and kinematics expected at the SSC for Level-2 accepted events. For the work reported here the QCD 100 GeV jet sample (referred to as "physics data") was used directly as input to the MODSIM simulation. Using this input we studied the effect of physics correlations and fluctuations on the DC network behavior. The distribution maximum was 120 units, with a mean of 18.5 units, and a sigma of 15.7 units for the case where no energy threshold cut was applied to each cell. When a 60 MeV energy threshold is applied to each cell, the event size mean is reduced to 4.8 units, but the sigma is reduced relatively less to 6.4 units.

Throughput at the various levels was equalized by setting the data transfer rate as a function of how much data must be transmitted. A reasonable estimate for the rate of L2 accepted events entering the system is between 2 and 10 kHz. However, the transfer rates were tuned so that the bandwidth would saturate at 6 kHz.

Since the constant input size of 120 units will generate more data than the zero-suppressed physics case with a mean of 18.5 units, the transfer rates will of course be much higher. For the 120 unit fixed data-size case, the rate from the FE chips to layer 1 was 1388.88 ns/unit, from layer 1 to layer 2 it was 173.61 ns/unit, from layer 2 to layer 3 it was 21.70 ns/unit, and out of layer 3 it

---

2 Proceedings of the 1986 Summer Study on Physics of the Superconducting Super Collider, Snowmass, CO (1986), and Proceedings of the Summer Study on High Energy Physics in the 1990, Snowmass, CO (1988).

was 2.71 ns/unit. For the zero-suppressed physics distributions, the rate from the FE chips to layer 1 was 9009.01 ns/unit, from layer 1 to layer 2 it was 1126.13 ns/unit, from layer 2 to layer 3 it was 140.77 ns/unit, and out of layer 3 it was 17.60 ns/unit. Note that if the unit is one byte, then data must be transmitted out of layer 3 at 370 MB/s in the fixed event size case, but only at 55 MB/s in the zero-suppressed case. Each data transfer protocol simulation was done at 2, 4, 6, 8, and 10 kHz input rate for 1100 events. Statistics-gathering variables were reset after the first 100 events, so that the measurements were made on 1000 events occurring after buffer "warm-up." The warm-up period was defined after studying the effect on the stability of results of both larger and smaller warm-ups.

Results

For the fixed event size input data, Figure K-3 shows the throughput rate as a function of input rate for the protocols no check (NC), and image check (IC). These cases are shown both with and without trigger "throttling." In Figure K-4 the event transmission efficiency as a function of input rate is shown for no-check without throttling, and image check with throttling.

For the zero-suppressed, no threshold, physics input data, Figure K-5 shows the throughput rate as a function of input rate for IC protocol, comparing throttling to the case without throttling. In Figure K-6 the event transmission efficiency as a function of input rate is shown for image check without throttling.

The deadtime as a function of input rate for the NC and IC protocols was zero below 5 kHz input rate and at the percent level above 5 kHz. There were 512 FE chips, so if only one had a full buffer, the event became incomplete. This is an especially pronounced effect for the case of zero-suppressed physics input data, a distribution with large fluctuations in data size.

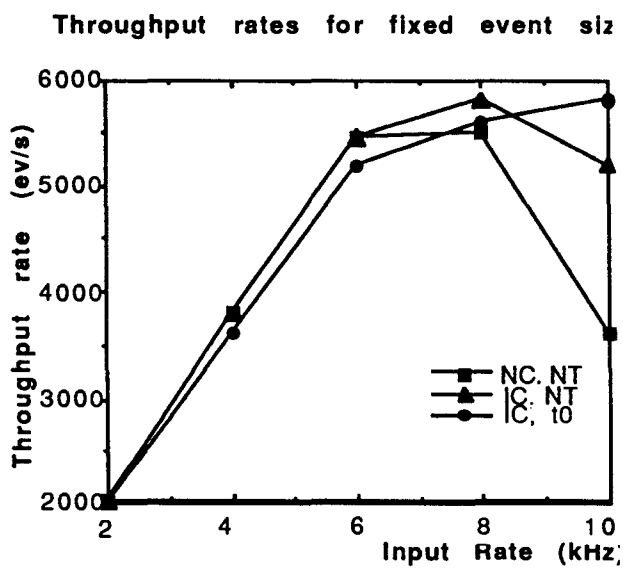

Figure K-3 Event Throughput Rates as a Function of Input Rate

Input event size fixed at 120 Units per front end chip for each L2 trigger. Results are shown for no-check, no throttle (NC, NT), image-check, no throttle (IC, NT), and image-check, throttle based on layer zero buffer usage (IC, TO).

Discussion

For a small DC network operating at modest rates and experiencing limited fluctuations, a simple pure-push (no check) protocol may be sufficient. System performance can be improved by implementing one of the strategies reported here.

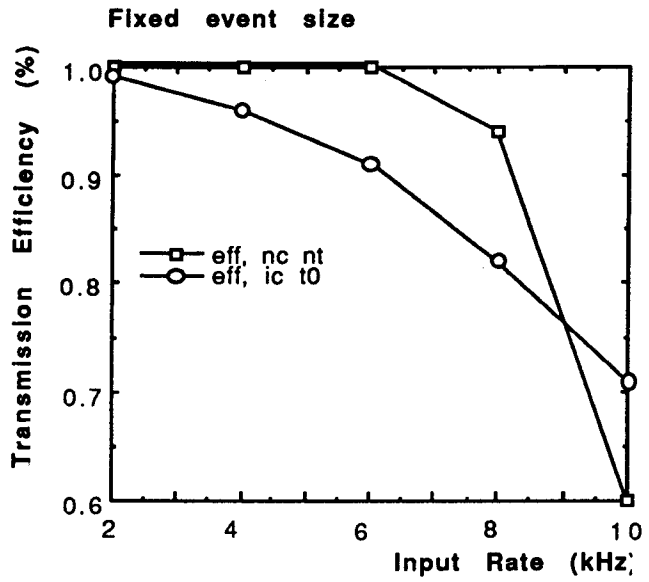

Figure K-5: Event transmission efficiency (nc,nt) and ic, t0)

Event transmission efficiency as a function of event input rate for no-check, no throttle (nc, nt), and image check, throttling based onlayer zero buffer usage (ic, t0).

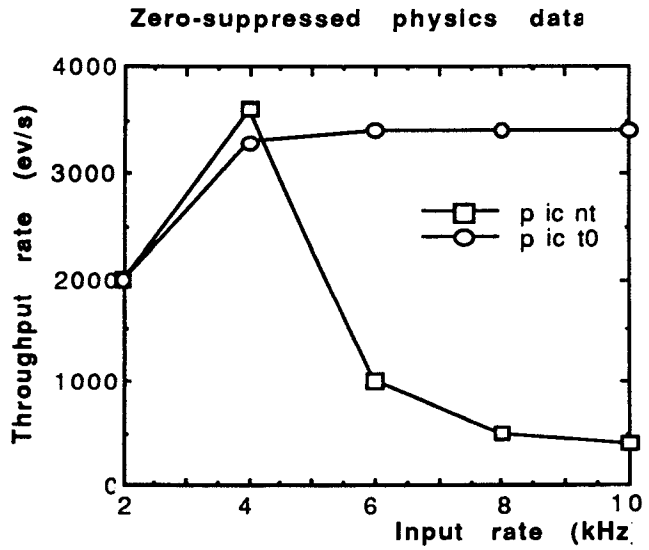

Figure K-5: Throughput rate as a function of input event rate using physics-generated data.

Results are shown for image check no throttle (ic, nt), and image check throttle (ic, t0).

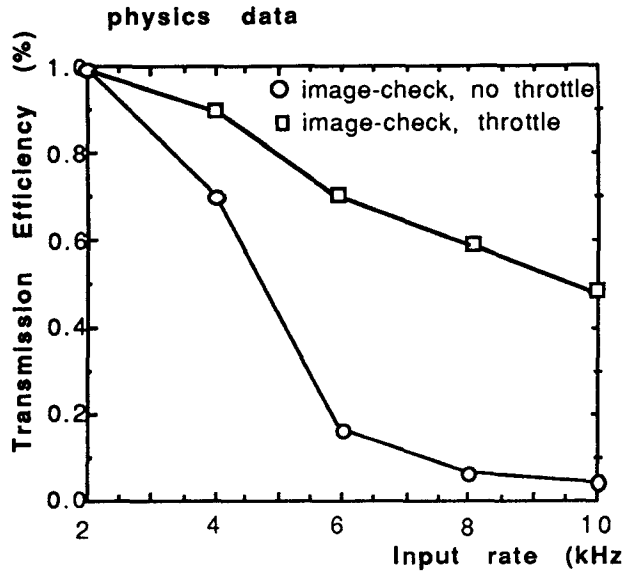

Figure K-6: Event transmission efficiency (ic,nt) and (ic,t0).

Event transmission efficiency as a function of input rate for zero-suppressed physics data using the image check protocol and no throttling (ic,nt), and with throttling (ic, t0).

The difference in behavior between pure-push or no-check protocol and image-checking is evident in Figure K-2. In no-check without trigger throttling, the network saturates near 6 kHz, but then a "logjam" develops at higher rates and the throughput falls precipitously. Image-checking without throttling (IC, NT) improves the failure rate somewhat. By imposing trigger throttling when the front end buffers (layer zero) begin to fill, the failure is a more slowly varying function of input frequency; it fails more "gracefully." This can be understood from the efficiencies shown in Figure K-3. In the case of no-check no throttling, all the transmission inefficiency arises from filling buffers; once they fill the "logjam" occurs, and the efficiency falls rapidly. In the image-checking case with throttling, the inefficiency arises in the gating logic because some good L2 triggers are converted to L2 reject signals. The buffers never fill, and the throughput "gracefully degrades."

In Figure K-4 and Figure K-5 we see a similar pair of plots, giving throughput and efficiency for zero-suppressed physics data input. Again, in the image-check throttling case, the throughput saturates at 6 kHz input and above. Without throttling the throughput falls to 5% at 10 kHz. In Figure K-5 we see that the throughput curve in Figure K-4 tracked the efficiency, because the buffers filled. However, with throttling the efficiency falls less dramatically.

In this respect buffer "imaging" is a promising strategy because it operates in the gating logic, thus avoiding some control signal transmission delays and improving buffer utilization.

Summary

We have presented a behavioral study comparing different techniques for operating a data collection network. For a variety of data transfer protocols we have calculated the throughput and efficiency as a function of input data rate. The results of our study show several ways for optimizing system performance, and the control features required. It will be possible now to make design judgments regarding system implementation based on the trade-offs between performance, buffering, transmission rate, and control complexity. Therefor, these studies provide guidance towards designing data collection chip sets and data collection networks.

APPENDIX L

OUTLINE OF SSCL TRIGGER STUDIES

Ed Wang

Introduction

The main physics goal (Electroweak symmetry breaking) of the SSC drive the design of the SSC accelerator. This in turn places demanding requirements on SSC detectors. In particular, we examine various issues in triggering and DAQ implied by these requirements. We already know that present day hadron collider and fixed target experiments already face fairly painful triggering and DAQ problems. It comes as no surprise that some problems may arise when we increase the energy by 20 and luminosity by 1000. while keeping the thresholds the same. We have embarked on a serious look into trigger and DAQ issues for SSC detectors and have developed a number of powerful tools in helping answer questions in a timely way.

Physics

If we were truly looking for the unknown, we would record every inelastic (and elastic for that matter) event at the SSC. This is impractical for the moment. We know (or at least we have declared) that we are interested in a number of physics processes. They are listed in the table below.

Table L-1: Physics Requirement

Process	σ	Lum. needed	Cuts needed
Higgs > 2γ	0.1 pb	10^{33}	2γ Et>20 GeV
Higgs > ZZ*	0.025 pb	10^{33}	2lep Et>20 GeV
Higgs > ZZ	0.05-0.005 pb	10^{33}	2lep Et>50 GeV
WWscatt	.0001 pb+	10^{33}	2lep Et>75 GeV
Top	20 nb	10^{32}	Et>20 GeV
SUSY	10 nb	10^{32}	
Z',W'	-	any	$M_{Z'}/4$
compositeness	-	any	jet Pt > Λ scale
CP violation	500 mb	10^{32}	lep. Pt>1.5 (?)

The table summarizes the physics requirements. It is not an exhaustive list. The 2γ decay mode of the Higgs sets the low energy threshold and luminosity requirements for high pt experiments. The triggering required for CP violation is still under study (do we need vertexing etc.?). We defer discussion of CP violation experiments for this present discussion.

Trigger Issues

Present Experience

We have begun an in depth survey of triggering of present and recent collider experiments (i.e. UA-1,UA-2, CDF,D0). We have tabulated rates for various level requirements. We have constructed a similar table for SSC experiments. The entries in the table at this point are only estimates based on fragmented analysis. We will systematically re-examine and document our findings.

SSC

We have begun to examine in detail trigger algorithms. This involves

- specifying the necessary observables (Et, isolation, ...)
- modeling the response of detectors that yield the observables (pulse shaping, shower shape and fluctuations, noise)
- definition of the algorithms which use the observables (trigger cell size, overlap?)
- tabulating the corresponding trigger rates and checking the efficiency for retaining a given signal.

From the table of trigger rates versus algorithms, we will then be able to assess how many trigger levels.are needed and derive the functionality of each trigger level. Some of the interesting detector variables are:

- segmentation
- electronics response
- noise
- precision (i.e. number of bits)

For example Figure L-1 shows trigger rates for a 1-electron / γ, trigger subject to various algorithms such as E_T cluster threshold only, E_T cluster and front/back, E_T cluster and isolation, E_T cluster and front/back plus isolation. We see that isolation is more powerful than front/back (though correlated). In addition, we can ask for track-shower match etc. (if we want electrons).

In addition, we wish to understand in more general terms:

- general trigger architectures
- interrelationship between trigger and data acquisition system

Much of this work is applicable to many SSC detectors.

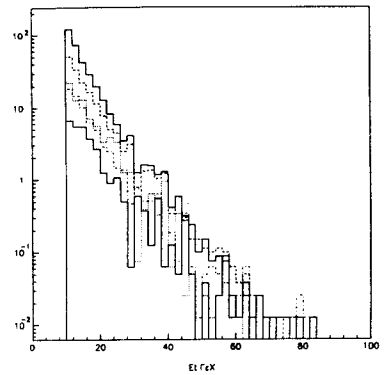

Figure L-1 E_t spectra for a single electromagnetic shower trigger for different trigger algorithms: upper solid curve - e. m. clusters, dash - front/back cut applied on clusters only, dots - isolation cuts only, dot dash - front/back and isolation applied, lower solid curve - front/back and wider isolation cut applied.

DAQ Issues

We recognize that an interplay between triggering and DAQ necessarily exists. We have used the output of our triggering algorithms as input to behavior simulation code written to simulate various DAQ architectures. In other words, we have the tools to start from first principles, simulate a detector, apply trigger algorithms and then simulate an entire DAQ system. We wish to :

- understand bandwidth requirements from physics identify bottlenecks in a given DAQ architecture
- tabulate throughput and efficiency
- understand error handling

A number of studies are in progress in order to provide some insight into issues concerning the trigger hardware architecture.

Data Volumes in Calorimeter Cells

A calculation of distributions of number of calorimeter cells above various thresholds (zero suppression) was performed under various noise conditions. The object is to understand how we might reduce data volumes. We imposed a trigger algorithm designed for a single electron trigger. Pileup events are superimposed weighted by a fast (16 ns peaking) bipolar shaping function and imposed electron trigger criteria of Ehad/Em<0.2 , E_t border/Em <0.2 and E_t >10 GeV on QCD 2 jet events. A general purpose detector like the SDC was modelled in GEANT and custom parametrized shower simulations for hadrons and electrons (including fluctuations tuned to CDF test data) were used. We checked the results using crude electron trigger criteria at Tevatron energies and find agreement both in E_t spectrum and overall rate.

Figure L-2 shows the number of calorimeter cells above threshold for 10^{33} running. for different thresholds and trigger cell sizes. We also investigated data volumes for 10^{34} running. We conclude that 10^{34} running with a 1 GeV E_t threshold will yield the same occupancy as 10^{33} without a threshold cut. Figure L-3 shows the effect of electronic noise (60 MeV EM and 630 MeV hadrons per 0.05 x 0.05) for 10^{33} running. One must go to a 1 GeV cell threshold in order to reduce the occupancies to the case where we have no electronic noise. What is the consequence of this cut? In a study concerning $\not{E}_T$ and missing jet E_t , we find that for $\not{E}_T$ >40 GeV, we can in fact take a 1 GeV cell cut, reconstruct jets and then from these jets, reconstruct $\not{E}_T$. One other issue affected by the suppression of data which has not been checked is the effect on background

rejection from isolation cuts (recall that isolation is based on demanding that a neighboring region around a candidate lepton be quiet of which a zero suppression cut will artificially make things look quieter).

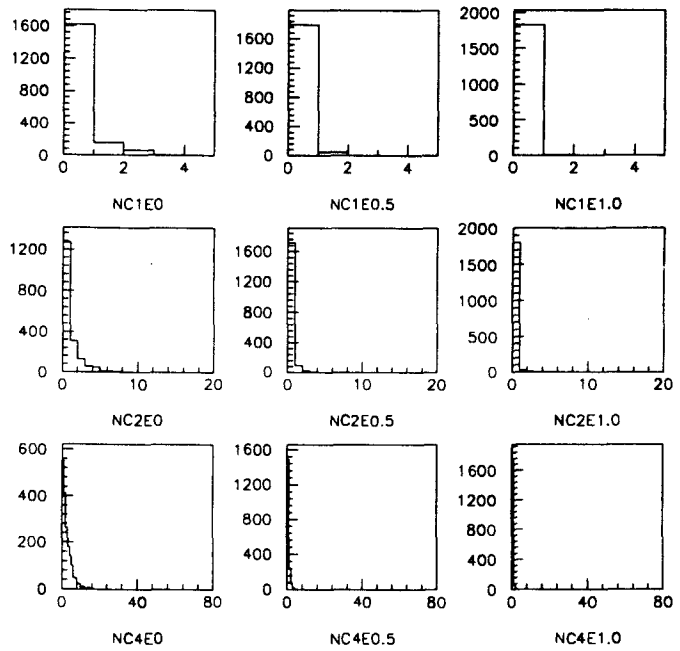

Figure L-2 Calorimeter data volumes for different single cell thresholds of 0, 0.5 and 1.0 GeV (column). A cell size of 0.5 * 0.5 in eta and phi is used. The luminosity if 10^{33} per cm per s. Different rows show the number of cell over theshold in areas of 2*2, 4*4 and 8*8 cells.

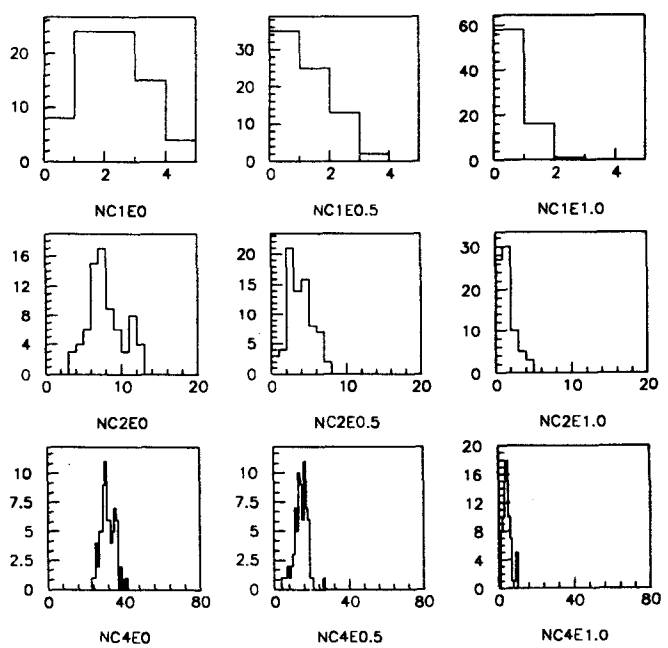

Figure L-3

Input Samples for Modsim

In order to proceed with behavioral simulation, we have generated 3 different samples of events which have passed what enough requirements to yield a 1-10 Khz rate. The table below summarizes the characteristics of each sample:

1-electron	E_T core > 10 GeV Front/Back<0.2 Border/Front<0.2
QCD jet	Pt [hard scatter]>100 GeV no jet algorithm applied.
$\not{E}_T$	Reconstruct jets and find vector sum jet E_T >100 GeV

These samples ought to reflect the types of correlations in a calorimeter cells for a wide variety of processes

APPENDIX M

DAQ DESIGN

M. BOTLO

In the following we will summarize ongoing activities in the areas of modular DAQ for test setups, behavioral simulations of DAQ systems and trigger studies performed in the electronics group of PRD. We also give a brief outlook towards future activities.

Present activities

Modular DAQ

In summer 1991 we started an effort towards the construction of a Data Acquisition Environment with the goal to provide the readout of detector components (Subdetectors, Front ends, DAQ) with the following characteristics:

- modularity (equipment can be added easily, different tasks can be executed in isolation)
- standardization (IEEE, POSIX, ...)
- scalability(size, speed, ...)
- cost effectiveness (publicly available software, industry standard hardware,...)
- adaptability (to different needs of test setups)
- transportability (between different HW platforms)

We decided to build two DAQ systems, namely MacDAQ and VMEDAQ.

MacDAQ

This setup is based on LabView II, a proprietary DAQ development tool set based on the Macintosh (Fig.M-1.). It has the advantage to be small, cheap, easy and modular. However it is not (yet) transportable to other computer platforms and is rather slow (few 10's Hz of 1 kB data) With this system we can acquire data from any front end which is connected to GPIB (CAMAC, VME, etc). The data are buffered in the Macintosh and stored on Exabyte 8500's. A subset of data are optionally written onto a large disk (1GB) which is connected to the Macintosh via SCSI. These data files can be accessed via FTP and transported to the UNIX environment. With the advent of MacOS-7 several Macintoshes can utilize the built in file sharing capability, thus forking off tasks like event display or online monitoring to other screens and cpu's. Applications for MacDAQ include stand-alone installation tests of hardware brought into the Laboratory, debugging of subsets of the equipment under test, the readout of auxiliary equipment such as scopes, high voltage supplies, the control of gas flow, etc.

VMEDAQ

After an evaluation phase of several real-time kernels (VxWorks, VRTX, LynxOS) we decided to build a system around VxWorks, provided by Wind River Systems [for details see: M. Botlo, J. Zalewski in CERN / MMCNL No.32 - 10/1991]. VMEDAQ is fast (several 100 Hz of 1 kB data), modular, standard and scalable (Fig. M-2.). It has the disadvantage to be large, more complicated and expensive. The real-time tasks run on Motorola 68030 CPU's (MVME147) in VME, data are transferred via the MXI-bus and/or Ethernet to a Sparc station, where they can be stored on large (2GB) SCSI-disks. These discs can also be mounted by other workstations, thus allowing a large number of users to have easy access to recently acquired data. Assynchrounosly, files containing a collection of events are dumped from these large disks to Exabyte 8500 tapes. The user interacts with the real-time environment through a graphical interface, based on

Openwindows. Functionalities such as event dumps with decoding of addresses, event display, tape operations and other offline operations are implemented.

From the point of DST production and analysis the event format in both DAQ systems is identical. Both systems will be documented and application tested in the GEM-TTR in summer 1992.

Future Developments

Modular DAQ

In summer '92 we will thoroughly test both systems in the GEM/TTR muon chamber tests at the SSCL. Furthermore, we plan to provide extensively documentation and upgrade our DAQ systems:

- provide interconnections to a larger variety of front end buses, notably to Fastbus.
- install faster crate interconnections. Evaluate, and if positive, implement VICbus
- continue the evaluation of various GUI's.
- evaluate Expert System packages. An expert system, integrated in the DAQ could improve reliability (and data taking capacity)
- evaluate LabView running in the UNIX environment. Our group was selected to be beta-site for this product.
- upgrade the real-time processors (currently MVME147) to 68040 based computers.

Figure M-3 shows how VMEDAQ can be expanded to read large amounts of channels. We will intensify our contacts with SDC, GEM, other divisions at SSCL, and with CERN groups in order to avoid duplications of efforts. We hope to be able to exercise the DAQ in other tests of Subdetectors and/or electronics applications. We will continue the evaluation of DAQ components (most notably real-time kernels, processors, GUI's, and storage technologies), and where appropriate, implement them into the DAQ.

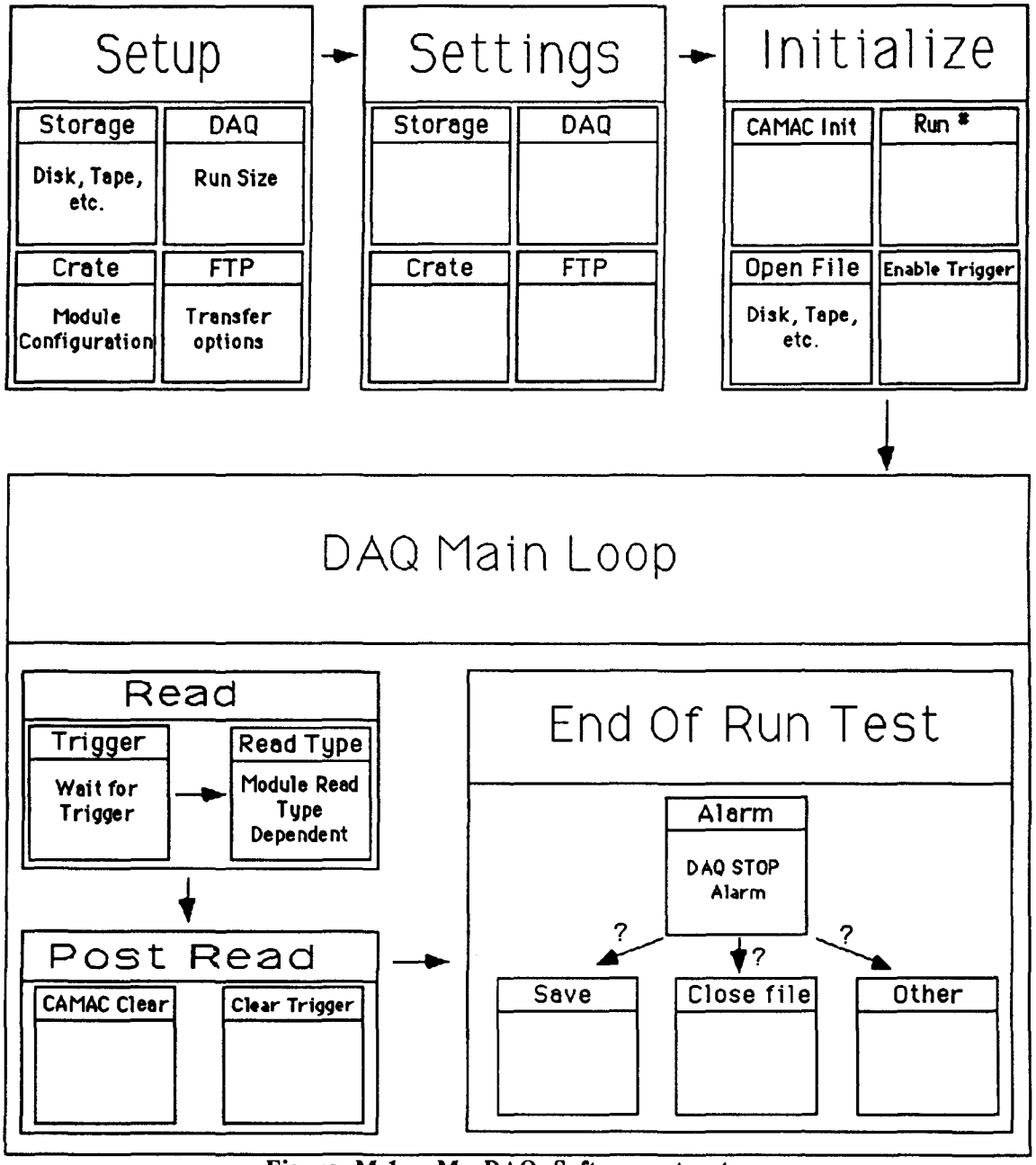

Figure M-1 MacDAQ Software structure

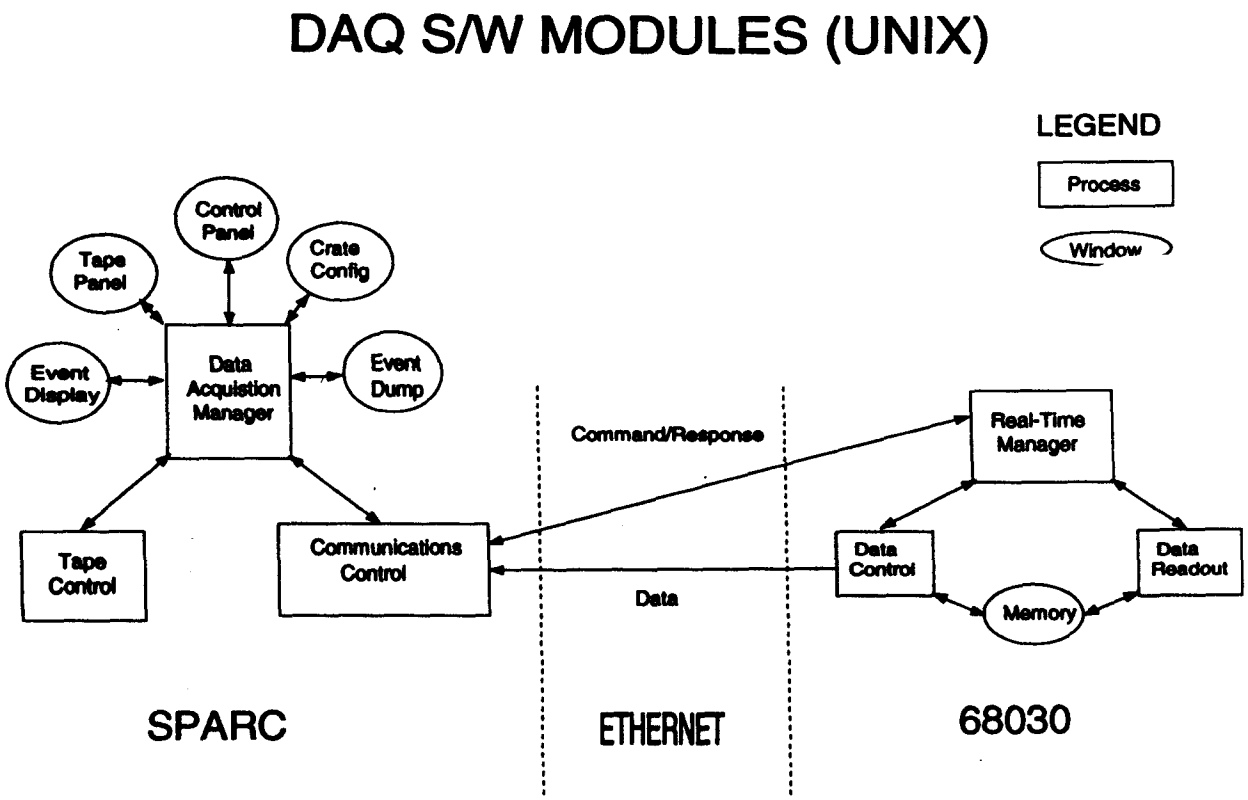

Figure M-2: VMEDAQ Layout.

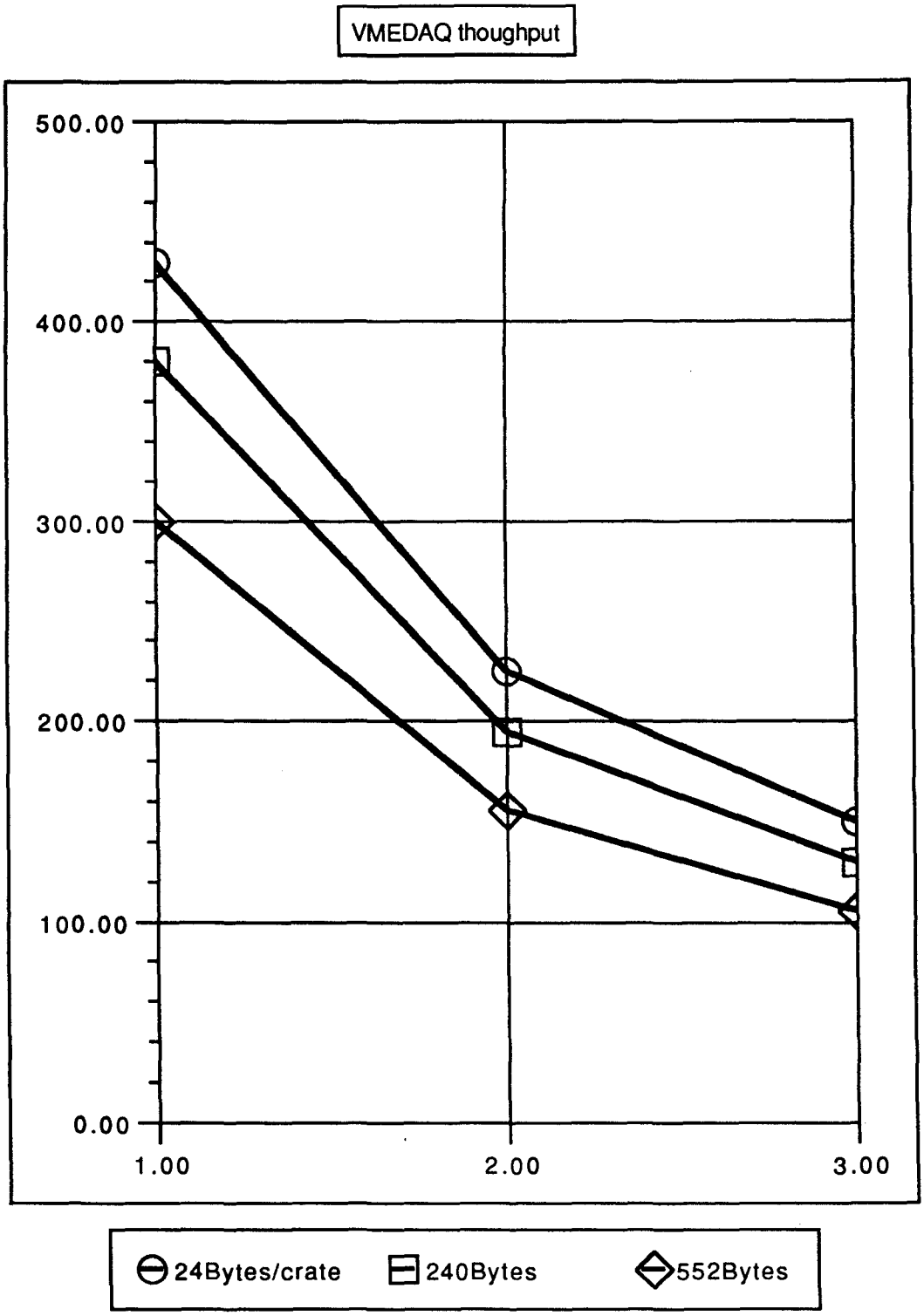

Figure M-3: VMEDAQ throughput for different numbers of crates.

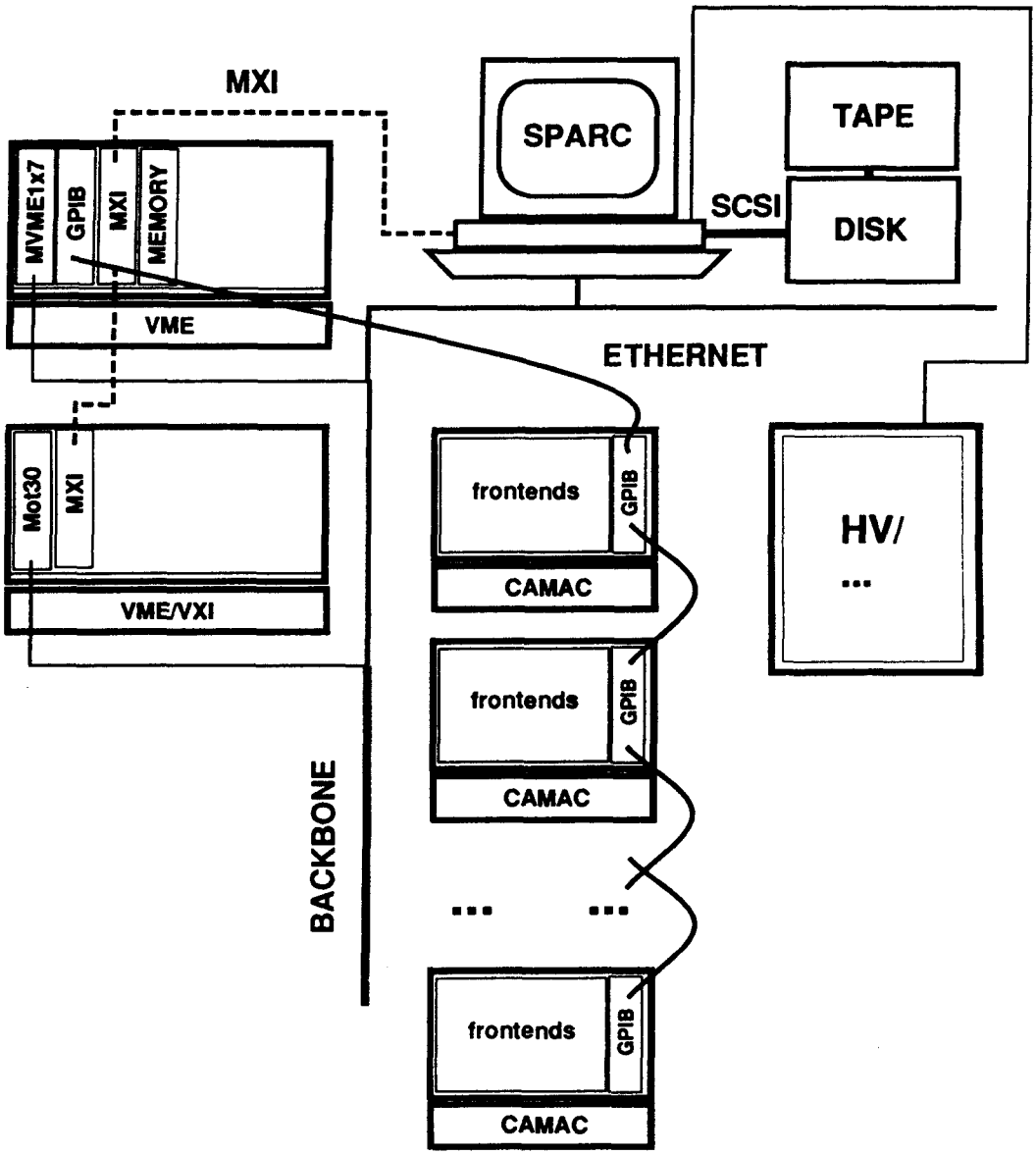

Figure M-4: Possible future implementation of VMEDAQ.

APPENDIX N
EVALUATION OF VXWORKS REAL-TIME KERNEL

Michi Botlo and Janusz Zalewski

(published in MMCNL32 / CERN, Oct 1991)

We understand the process of software evaluation as finding problems with software (code and its documentation) according to a number of criteria applicable to a particular application. Our evaluation criteria, for VxWorks 5.0, a proprietary real-time kernel from Wind River Systems (Alameda, CA, USA; European Office: Les Ulis, France) fall into 2 categories: general features and real-time features, appropriate for the data acquisition systems at the Physics Research Division of the SSC Laboratory.

Hardware used

First of all, it is crucial to realize that before starting the evaluation process itself, that the evaluator must have a good knowledge of the operating hardware installation.

We have tested VxWorks on a VME crate containing the following modules:

1 Processor #1, Motorola MVME147SA-2 module based on a 68030 microprocessor with 8 MB of memory and 32 MHz clock

2 Processor #2, Force SYS68K/CPU-30ZB(E) module based on a 68030 microprocessor with 4 MB of memory and 25 MHz clock

3 MVME224A-2 memory board with 8 MB address space

4 Home-made Four Channel Digitizer to sample analog signals with 12-bit 2 MHz ADC and 64 Kwords per channel.[1]

The host was a Sparc compatible workstation from Opus Systems, running under SunOS with Open Windows. We had also available a VME bus tracer module from VMETRO, which played a role in VME bus timing measurement. It should also be noted at this point, that:

- in the nearest future (fourth quarter of 1991) it is expected to have VxWorks ported to a 68030-based processor board from National Instrument (Austin, Texas, USA), running on VXI
- there is no known implementation of VxWorks for Intel 80x86 series, although there is one for Multibus II 680x0-based systems (made by Heurikon)
- three RISC processors are supported, Sparc, MIPS, and Intel 890.

General Features

1) Installation and Documentation

The installation is very simple. The software comes on at least two tapes (one with the kernel, binaries, configuration files, libraries, man pages, and another one with the GNU suite), accompanied by 2 manuals (Programmer's Guide, and Libraries), and a few pages of target-specific documentation (description of libraries). After extracting the tapes' contents onto a disk (what takes a few minutes), and installing the two ROM's on a processor board, the user needs to set interactively certain boot parameters, what takes also a couple of minutes. In this phase of installation we experienced many problems with finding respective information in VxWorks'

---

[1] A. Jones, ASD Division, Superconducting Super Collider

manuals, but this seems to be a result of our ignorance rather than some serious faults of the documentation itself. Nevertheless we found a few shortcomings. For example:

- while looking for functions performing cache enable/disable, we found a description of 'sysCacheEnable' for which no corresponding code existed; after a while of looking through the source code of configuration and header files, we found that calls have been changed to 'cacheEnable' but with a completely different semantics (arguments 0 and 1 mean now data cache and instruction cache rather than disable and enable, respectively)

- error codes are numbered in an inconsistent way, some in decimal, some in hexadecimal representation. An electronic documentation also exists in a form of a 'vwman' command. For this to work, one has to copy (or make a link) the file tmac.angen to /usr/lib/tmac for formatting (then remember to lower access permissions on this file to work properly).

2) Unix and Posix compliance

The general impression is that a 100% compliance is hard to achieve and VxWorks certainly is not Unix or Posix compliant to this extent. Even though the documentation tells something different, this is pure propaganda. Examples are:

- the most common command 'ls' does not work reliably under VxWorks, so that due to compatibility problems an official 'lsOld' command has been introduced.

- 'exit(1)' function works differently because it is supposed to work for tasks.

- 'fclose' must be used explicitly in each respective task before termination, because file descriptors in VxWorks are global

- several typical C functions are missing in VxWorks, for example 'atoi', 'atof', 'atol'

- code containing calls to 'getchar' function did not compile correctly because of 'stdargs.h' header file missing (in general, problems with header file were reported by all other users we got in touch with)

- I/O differences exist for 'printf' and 'scanf' function families (some of the are unbuffered and do not use the stdio facility). Honestly speaking Posix compliance cannot be resolved at this moment, because Posix.4 is only in its Draft form. What seems to the goal of most vendors is to achieve conformance with the smallest embedded systems AEP (Application Environment Profile).

3) Networking Capabilities

In general, networking is one of the strong and sometimes praised features of VxWorks, so we took a closer look at that. VxWorks comes initially without NFS installed, however a simple procedure allows this to do (see below). Then one can add hosts (hostAdd function) and mount their file systems (nfsMount function) to have remote access to them. Remote logins from VxWorks to Unix and vice versa are possible, full TCP/IP is supported. One serious problem we encountered, however, and spent many hours trying to fix it (unsuccessfully), was the "backplane network". Every controller (processor board) in a crate can work as a separate Ethernet node. This is OK if we have a few processor boards, but if there are more we run out of available Ethernet connections, since we need a separate Ethernet cable and interface for each processor. This complicates the TCP/IP access to the processors and also is a cost factor in building a system. Therefore it's much more convenient to have one board connected to Ethernet as a main node

(backplane master), acting as a router (gateway, in VxWorks terminology) between the external network and a subnet, created on the VME backplane. All processors in the crate receive individual Internet numbers of this new subnet and then communication with the outside world goes via the router (main node/processor). Thus all VxWorks-to-Unix network facilities normally available over Ethernet are also available over the backplane. Use of these facilities over the backplane is indistinguishable from use over any other medium. This is what VxWorks allows, however, due to an error in documentation (missing parameter 'net' in a 'route' command, for subnets only, on page 217 of the "VxWorks Programmer's Guide"), it was impossible to install the backplane network. With a help of the vendor's representatives, who worked on this remotely and finally found the error, we were able to run the backplane network after many hours of unsuccessful attempts.

4) Development Tools (languages, compilers, linkers, etc.)

The only language currently supported is C - the GNU implementation (although we have heard about the support for Ada under VADSworks from Verdix). It is also important that the VxWorks command interpreter is a C-shell, that is able to execute almost all C statements and functions, except of declarations, as its commands. You can run, however, only a single copy of a shell at a time (the reason is that the shell's parser is not reentrant). The central part of it is a global symbol table. Its basic characteristic is that it retains all global symbols after program termination, that is it's the responsibility of the programmer to remember and remove, if necessary, not only such objects as semaphores and mailboxes, but also global variables, whose values may influence subsequent executions of the program. Another feature of the shell is that it does not fully check module dependencies. For example, if modules are not loaded in a correct sequence initially, the loader finds that out and generates an error message. However, if modules are loaded in a correct sequence, and one of them is changed next and reloaded, other modules dependent on it do still preserve their former references to the old version, and no message indicates that this happens. The solution to this problem is a makefile, which keeps information on all dependencies, but to do so is the responsibility of the user.

5) Debugging Capabilities

We have checked very extensively only the shell's debugging capabilities. There were two reasons for this. First, our test programs were very short and did not need any sophisticated debugging. Second, shell debugging features seem to be very well suited for debugging C programs. This is due to the existence of a C-shell, and commands like:

- d display memory contents in 16-bit words
- m change the memory contents in 16-bit words
- i display information on all active tasks
- l disassemble and list the code
- s single stepping
- b set breakpoints, and some others.

These features allowed us to trace the state changes of every routine or task without difficulty. We found only one important drawback, namely, the 'd' and 'm' commands work only on 16-bit words and there is no way with them to work on single bytes, what is often necessary. The only remedy is to write your own routines to provide this capability if needed. We have had neither time nor need to use VxGDB, which is a VxWorks version of the GNU's GDB - debugger.

6) Vendor's support

After some initial struggles to overcome company's bureaucracy, we got enough support to solve all major problems. Some important points related to support are listed below:

- Software maintenance cost: $4000 (four thousand) for one year, one architecture, unlimited number of targets; in case of a site license purchased (see below for cost), this number grows to $10000 (ten thousand)
- Training courses are available for a separate fee, for example 4 days Device Drivers course: $1800.
- Software delivery is accompanied by a list of known problems (dated 29 November 1990 it contains 13 problems related mostly to VxGDB)
- Company's responding to our telephone calls was mostly prompt and helpful
- There exists a VxWorks users group affiliated at company's headquarters, meeting periodically a few times per year in different places (contact point: tina@wrs.com)
- There is a VxWorks software archive maintained at the National Center for Atmospheric Research, Boulder, CO. Ftp access is possible at thor.atd.ucor.edu (128.117.81.51).
- A listserver-like discussion group's mailing list is maintained at LBL. To subscribe, send a request to: vxwexplo-request@lbl.gov. The traffic is not overwhelming: during the period November '89 - March '91 there were 298 messages archived.

7) X-windows

We did not use this feature but it is stated, on one of the tapes, that with VxWorks a reentrant version of X-libraries must be used, which is different from the one in public domain, and provided for a separate fee.

8) Price

This is not necessarily related to VxWorks only but we believe that real-time kernels currently available on the market are highly overpriced. One possible reason for this situation is that there is no public domain kernel available. Here are some crazy prices we got during negotiations on site license for SSC:

- $150 k (one hundred fifty thousand) for unlimited development license for single architecture
- $500 k (yes, half a million) for unlimited development license for all architectures. Single license prices are as follows:
- about $20 k for one development license for one architecture, plus
- $600 one-time fee for each target.

Real-Time Features

1) Range of services

It seems that in the current version, VxWorks has a full range of services, including:

- tasking (5-state model assumed: executing, ready, pending, delayed, suspended; task spawn can be split into creation and activation; task restart possible)
- scheduling control (preemptive priority-based and round-robin; no option for user-defined policy))
- semaphores (binary, counting, mutexes; timed-out; prioritized or FIFO)
- message queues (timed out; prioritized)
- signals (no events, however this has been added by some of the users)
- interrupt control
- timers.

One thing which may be annoying is that in message passing only text messages are allowed. While it is not a serious limitation when using pointers, we find it rather inconvenient. In general, the basic functionality of both ORKID and POSIX.4 is achieved.

2) Kernel's size and configurability

It is relatively easy to reconfigure the kernel, that is to build a new VxWorks image. There are 3 basic files containing configuration data, which can be changed and adjusted by the user. After the changes are done, rebuilding the kernel requires only a single execution of the Unix 'make' command, which works on a Makefile submitted (with VxWorks) separately for each respective target.

It is not explicitly known what is the smallest possible size of the kernel, however, there are many configuration options to include or exclude certain services (libraries). For example, one can exclude all development facilities, the shell and network facilities, and create bootable applications or a ROM kernel.

3) Performance

We got the following numbers for selected simple benchmarks. No standard benchmarks (like Dr. Dobb's, etc.) were executed.

- Interrupt latency (see below) - <6 microseconds
- Semaphore shuffling time (give/take for the same task) - <8 microseconds
- Message send/receive (for the same task) - 84 microseconds
- Semaphore create - approx. 500 microseconds
- Deletion of 2 semaphores and 1 message queue - 44 microseconds
- Single task spawn (for minimal stack size) - 710 microseconds
- Task delete - 480 microseconds

We also believe that any benchmarks to be meaningful must be more comprehensive and refer to a particular applications architecture. Therefore we created our own but sufficiently general application benchmark for real-time applications, formed of 4 tasks:

- user interface (to enter parameters, activate and kill tasks, etc.)
- data acquisition (to read data, from inputs like ADCs, etc.)
- data handling (to preprocess input data in real time: simple averaging, etc.)
- data output (to write data onto a magnetic medium, send into a network, etc.)

For this kind of benchmark, no matter how fast the execution of a particular task was, we were able to achieve at most 1M word per second transfer speed for data acquisition via the VME bus: 64K 16-bit words were processed in about 70 milliseconds. This is much slower than the theoretical VME bus bandwidth. This number was measured by software and independently confirmed by VMETRO VME bus trace module. It also became clear that the use of semaphores and messages does not generate any significant overhead on the application.

The time to write onto a disk on a host (via Ethernet) was measured to be 12-14 milliseconds (file open, write a number, and file close). The write itself (append mode) took approximately 90 microseconds. To find these numbers we used mostly 'for' loops wherever possible, although the VxWorks-provided timex library could also be applied. One important characteristic of the kernel is the number of context switches per second without significant loss of performance. This is certainly related to the system clock rate, initially set to 60 Hz. The documentation states (the tickAnnounce() function's description; this routine informs the kernel of the passing of time) that clock frequencies in excess of 600 Hz are inefficient because the system will spend most of its time advancing the clock. What we found is that at clock speed 20 kHz the kernel crashes at all.

4) Interrupt Handling

The 'intConnect' function worked perfectly well, connecting a user-written handler (in C) to an auxiliary timer of the MVME147 module. We found that the value of approximately 6 microseconds, stated by different authors, for interrupt latency (the time it takes to execute the first instruction of an interrupt handler from when the interrupt occurs) is true and correct. However, we also noted that there is no way to measure it more accurately by software means, because MVME147 programmable clocks' resolution is 6.25 microsecond. Interrupt handling generated from the VME bus, which has lower priority than those generated internally, have not been tested.

5) Safety

This issue is often neglected and never mentioned in evaluations like this. While we understand that real-time kernels may not provide certain features (like protection, etc.) available from traditional operating systems, it must be clear that either error messages should be generated or respective information provided in manuals as warnings against all possible failures.

For example, one possible faulty situation we encountered (which was relatively easy to detect) was when user task's local variables size exceeded 20 KB, which is a default stack size. No warning message appeared on the screen and the program bombed. It took us quite a while to find out in the Programmer's Manual, in a chapter on debugging, under the Tips heading that: "VxWorks provides no protection against stack crashes. Such crashes occur when a task uses more stack than has been allocated for it, thus running into and writing over some other task or data. It generally manifests itself as a crash of some task other than the offending one, or other inexplicable behavior."

We believe that there are applications in which safety is so important that some additional overhead may be allowed to perform respective checks. We also found that the functions sysClkRateGet() and sysClkRateSet() work inconsistently. If we change the clock rate without using sysClkRateSet(), then the call to sysClkRateGet returns an old value. On the positive side, some measures against inadvertent task deletions and priority inversion are provided by means of mutexes. Infinite task lock (preemption lock) is possible without time-out, however with interrupts enabled.

6) Multiprocessor Capabilities

The interprocessor communication in real time is possible only via shared memory. Semaphores and messages can only work in a single address space. There are facilities, like pipes, sockets, remote procedure calls, etc., which allow interprocessor communication but certainly not in real time, when hard deadlines must be met.

7) Device Drivers' Support

i) Range of Devices Supported.

The official list contains drivers for the following devices:

- target-specific terminal (tyCoDrv.c), in our case for MVME147 on-board serial ports
- pseudoterminal (ptyDrv.c)
- network remote file I/O (netDrv.c), to access files transparently over the network via ftp or rsh
- NFS (nfsDrv.c)
- pipes (pipeDrv.c)
- pseudomemory (memDrv.c), high-level way to read/write absolute memory locations
- ram disk (ramDrv.c)
- Fujitsu SCSI Protocol Controller and Western Digital SCSI-Bus Interface Controller

ii) Ease of Modifying Existing Drivers.

There is source code for original drivers and a separate description of their functions provided (12 pages in a section of the Programmer's Guide), as well as a description of the internal driver's structure with extensive examples (21 pages in the same manual).

iii) Ease of Writing User Device Drivers.

Several libraries are mentioned in the Programmer's Manual that may be of assistance in writing device drivers. The list of all user-written VxWorks device-drivers worldwide is being compiled by Harvey Wong, Wind River Systems; to our knowledge, it has not been completed and made available yet. A 4-day "Writing Device Drivers" training course is offered once every couple of months (insufficient for writing SCSI drivers or Board Support packages).

iv) Porting Unix device drivers.

Unfortunately, this possibility has not been checked yet.